



isarc

INTERNATIONAL SCIENCE AND ART RESEARCH CENTER

<https://www.isarconference.org/>

3. INTERNATIONAL SCIENCES AND INNOVATION CONGRESS



EDITORS

Prof. Dr. Hasan SERİN

Dr. Muhammed Yaşar DÖRTBUDAK

CONGRESS BOOK

21 - 22 NOVEMBER 2021 / ANKARA



IKSAD
Publishing House



CONGRESS ID

CONGRESS TITLE

**3. INTERNATIONAL SCIENCES AND INNOVATION
CONGRESS**

DATE AND PLACE

21-22 NOVEMBER 2021, ANKARA/TURKEY ONLINE PRESENTATIONS

ORGANIZATION

ISARC

INTERNATIONAL SCIENCE AND ART RESEARCH CENTER

GENERAL COORDINATOR

Yasemin AĞAOĞLU

COORDINATOR

Gamze KÖYMEN

EDITOR

Prof. Dr. Hasan SERİN

Dr. Muhammed Yaşar DÖRTBUDAK

ORGANIZING COMMITTEE

Prof. Dr. Şefik TÜFENKÇİ

Assoc. Dr. Fatih ÇİĞ

Assoc. Dr. Reyhan DADAŞOVA

Assoc. Dr. Sevcan YILDIZ

Dr. Damezhan SADYKOVA

Dr. Serkan GÜN

İbrahim KAYA

Sefa Salih BİLDİRİCİ

PARCIPATING COUNTRIES

Algeria/ India/ Iran/ İtaly /Moldova /Morocco /Nigeria /Pakistan /Portekiz /Tunusie

Copyright © 2021 by iksad publishing house

All rights reserved. No part of this publication may be reproduced, distributed or transmitted in any form or by any means, including photocopying, recording or other electronic or mechanical methods, without the prior written permission of the publisher, except in the case of brief quotations embodied in critical reviews and certain other non-commercial uses permitted by copyright

law. Institution of Economic Development and Social
Researches Publications®

(The Licence Number of Publicator: 2014/31220)

TURKEY TR: +90 342 606 06 75

USA: +1 631 685 0 853

E mail: iksadyayinevi@gmail.com

www.iksadyayinevi.com

It is responsibility of the author to abide by the publishing ethics rules.

Iksad Publications – 2021©

ISBN: 978-625-8007-78-7

Cover Design: İbrahim KAYA

November / 2021

Ankara / Turkey

Size = 21x29,7 cm

SCIENCE AND ADVISORY COMMITTEE

- Prof. Dr. Abdullah ÖZTÜRK
Prof. Dr. Aparna SRIVASTA
Prof. Dr. Edip ÖRÜCÜ
Prof. Dr. Erdin BOZKURT
Prof. Dr. Hülya ÇİÇEK
Prof. Dr. Nilüfer PEMBEÇİOĞLU
Prof. Dr. Sevi ÖZ
Prof. Dr. Şefik TÜFENKÇİ
Doç. Dr. A. İnci SÖKMEN ALACA
Doç. Dr. Ahmet Umut HACİFEVZİOĞLU
Doç. Dr. Amıt ARORA
Doç. Dr. Arzu AKPINAR BAYİZİT
Doç. Dr. Bahadır KILCAN
Doç. Dr. Dinara FARDEEVA
Doç. Dr. Fatih ÇİĞ
Doç. Dr. Iqbal HOSSAIN
Doç. Dr. İsmail AKALTUN
Doç. Dr. Jasmin LATOVIÇ
Doç. Dr. K.A. TLEUBERGENOVA
Doç. Dr. Mehmet Ali AKKAYA
Doç. Dr. Mehmet Fırat BARAN
Doç. Dr. Murat DAL
Doç. Dr. Murat EYVAZ
Doç. Dr. Nebahat AKGÜN ÇOMAK
Doç. Dr. Neslihan ŞAHİN
Doç. Dr. Syed Ali Raza NAQVI
Doç. Dr. Yener Lütfü MERT
Dr. Öğr. Üyesi Aydın ÜNAL
Dr. Öğr. Üyesi Didem GÜVEN
Dr. Öğr. Üyesi Fatma HAYIT
Dr. Öğr. Üyesi Figen CERİTOĞLU
Dr. Öğr. Üyesi Hakan ALTUNAY
Dr. Öğr. Üyesi Merivan ŞAŞMAZ
Dr. Öğr. Üyesi Mubin KOYUNCU
Dr. Öğr. Üyesi Murat POLAT
Dr. Öğr. Üyesi Sema KAYAPINAR KAYA
Dr. Öğr. Üyesi Serkan ATMACA
Dr. Öğr. Üyesi Serkan GÜLDAL
Dr. Öğr. Üyesi Süleyman ADAK
Dr. Öğr. Üyesi Yasin YAKAR
Dr. Öğr. Üyesi Yaşar SUBAŞI
Dr. Babak SAFAEI
Dr. Ercan ÇATAK
Dr. Faisal SULTAN
Dr. Ghanshyam BARMAN
Dr. Hamdi DAĞISTANLI
Dr. Havva MEHTIEVA
Dr. Meryem GÖKTAŞ
Dr. Muhammad IMRAN
Dr. Sakıma BAYRAMOVA
Dr. Şükrü KALAYCI
Dr. Turan YANARDAĞ
- Orta Doğu Teknik Üniversitesi
Noida International University
Bandırma Onyediy Eylül Üniversitesi
Orta Doğu Teknik Üniversitesi
Gaziantep Üniversitesi
İstanbul Üniversitesi
Ankara Hacı Bayram Veli Üniversitesi
Van Yüzüncü Yıl Üniversitesi
İstanbul Arel Üniversitesi
Nişantaşı Üniversitesi
Shaheed Bhagat Singh State University
Uludağ Üniversitesi
Gazi Üniversitesi
Rusya Bilimler Akademisi
Siirt Üniversitesi
Bangladesh University
Gaziantep Dr. Ersin Arslan EAH.
Southern Federal University
Kazakh National Women's Pedagogical University
İzmir Kâtip Çelebi Üniversitesi
Siirt Üniversitesi
Munzur Üniversitesi
Gebze Teknik Üniversitesi
Galatasaray Üniversitesi
Cumhuriyet Üniversitesi
Government College University Faisalabad
İstanbul Galata Üniversitesi
Kırklareli Üniversitesi
Sabahattin Zaim Üniversitesi
Yozgat Bozok Üniversitesi
Siirt Üniversitesi
Süleyman Demirel Üniversitesi
Adıyaman Üniversitesi
İğdır Üniversitesi
Dicle Üniversitesi
Munzur Üniversitesi
Sivas Cumhuriyet Üniversitesi
Adıyaman Üniversitesi
Mardin Artuklu Üniversitesi
Harran Üniversitesi
Van Yüzüncü Yıl Üniversitesi
Tsinghua University
Eskişehir Osmangazi Üniversitesi
Hazara University
Uka Tarsadia University
MEV Koleji Özel İzmir Bornova Okulları
Moskova Tıp Akademisi
Bilecik Şeyh Edebali Üniversitesi
Government College University Faisalabad
AMEA
Gazi Üniversitesi
Ankara Üniversitesi



ISARC
3. INTERNATIONAL SCIENCES
AND INNOVATION CONGRESS
21-22 NOVEMBER 2021
ANKARA

CONGRESS PROGRAM

Join Zoom Meeting:

Meeting ID: 817 8292 1041

Passcode: 932346

<https://us02web.zoom.us/j/81782921041?pwd=VEtvYVc1eDRKcm5ZQ1IMRC9iaWgzUT09>

PARTICIPATING COUNTRIES

Algeria/ India/ Iran/ Italy /Moldova /Morocco /Nigeria /Pakistan /Portekiz /Tunisie

TOTAL NUMBER OF INTERNATIONAL PAPER: 42

PAPER FROM TURKEY: 38

zoom



Cloud Video Conferencing

Simple Online Meetings

Mobile Collaboration

Önemli, Dikkatle Okuyunuz Lütfen

- ❖ Kongremizde Yazım Kurallarına uygun gönderilmiş ve bilim kurulundan geçen bildirimler için online (video konferans sistemi üzerinden) sunum imkanı sağlanmıştır.
- ❖ Online sunum yapabilmek için <https://zoom.us/join> sitesi üzerinden giriş yaparak “Meeting ID or Personal Link Name” yerine ID numarasını girerek oturuma katılabilirsiniz.
- ❖ Zoom uygulaması ücretsizdir ve hesap oluşturmaya gerek yoktur.
- ❖ Zoom uygulaması kaydolmadan kullanılabilir.
- ❖ Uygulama tablet, telefon ve PC’lerde çalışıyor.
- ❖ Her oturumdaki sunucular, sunum saatinden 5 dk öncesinde oturuma bağlanmış olmaları gerekmektedir.
- ❖ Tüm kongre katılımcıları canlı bağlanarak tüm oturumları dinleyebilir.
- ❖ Moderatör – oturumdaki sunum ve bilimsel tartışma (soru-cevap) kısmından sorumludur.

Dikkat Edilmesi Gerekenler- TEKNİK BİLGİLER

- ◆ Bilgisayarınızda mikrofon olduğuna ve çalıştığına emin olun.
- ◆ Zoom’da ekran paylaşma özelliğine kullanabilmelisiniz.
- ◆ Katılım belgeleri kongre sonunda tarafınıza pdf olarak gönderilecektir
- ◆ Kongre programında yer ve saat değişikliği gibi talepler dikkate alınmayacaktır

IMPORTANT, PLEASE READ CAREFULLY

- ❖ To be able to attend a meeting online, login via <https://zoom.us/join> site, enter ID “Meeting ID or Personal Link Name” and solidify the session.
- ❖ The Zoom application is free and no need to create an account.
- ❖ The Zoom application can be used without registration.
- ❖ The application works on tablets, phones and PCs.
- ❖ The participant must be connected to the session 5 minutes before the presentation time.
- ❖ All congress participants can connect live and listen to all sessions.
- ❖ Moderator is responsible for the presentation and scientific discussion (question-answer) section of the session.

Points to Take into Consideration - TECHNICAL INFORMATION

- ◆ Make sure your computer has a microphone and is working.
- ◆ You should be able to use screen sharing feature in Zoom.
- ◆ Attendance certificates will be sent to you as pdf at the end of the congress.
- ◆ Requests such as change of place and time will not be taken into consideration in the congress program.

ÖNEMLİ NOT: SUNUMLARINIZI HEM TÜRKÇE HEM İNGİLİZCE HAZIRLAMANIZI RİCA EDERİZ.

ONLINE EXHIBITION

09:30-09:45



Sanatçı Adı Soyadı: Nur UYANIK ÇIRKIN

1986 yılında Çorum'da doğdu, 2009 yılında Gazi Üniversitesi plastik sanatlar seramik öğretmenliği lisans, 2013 yılında aynı üniversitenin seramik öğretmenliği yüksek lisans programından mezun oldu. 2021 yılında Süleyman Demirel Üniversitesi sanat ve tasarım sanatta yeterlik programını tamamladı. Bu süreçte sanat eğitimi veren kuruluşlarda öğretmenlik yaptı. Yükseköğretim kurumunda öğretim elemanı olarak çalıştı. Ulusal/uluslararası sempozyum/konferanslarda bildiriler sundu ve yerli/yabancı hakemli dergilerde makaleleri yayımlandı. Bir çok ulusal ve uluslararası sergi, sempozyum ve workshoplara katılan sanatçı sanat çalışmalarına kişisel atölyesinde devam etmektedir.

Artist Name Surname: Nur UYANIK ÇIRKIN

She was born in Çorum in 1986. She graduated from Gazi University plastic arts ceramics teaching undergraduate program in 2009 and from the same university's ceramics teaching graduate program in 2013. In 2021, she completed the Süleyman Demirel University art and design proficiency program. During this period, she worked as a teacher in institutions providing art education. She worked as a lecturer in a higher education institution. She has presented papers at national/international symposiums/conferences and his articles have been published in domestic/foreign peer-reviewed journals. The artist, who has participated in many national and international exhibitions, symposiums and workshops, continues her art works in his personal workshop.

21.11.2021

SUNDAY/ 10:00-12:00

MANAGEMENT

SESSION-1 HALL -1

MODERATOR: Dr. Bahar ALTUNOK

Algeria: 08:00-10:00 /India: 12:30-14:30/ Iran: 10:30-12:30 /İtaly: 08:00-10:00 /
Moldova: 09:00-11:00 / Morocco: 08:00-10:00 /Nigeria:08:00-10:00/ Pakistan: 12:00-14:00
/Portekiz: 07:00-09:00 / Tunisie: 08:00-10:00

AUTHORS	AFFILIATION	TOPIC TITLE
Dr. Musa DOĞRUER Assoc. Prof. Dr. Gürçan YILDIRIM Prof. Dr. Cabir TERZİOĞLU	Bolu Abant İzzet Baysal University	ROLE OF DIAVALENT Mn 2+ -SITES ON Ca 2+ -SITES ON FUNDAMENTAL ELECTRICAL QUANTITIES OF BULK Bi-2212 SYSTEMS
Dr. Musa DOĞRUER	Bolu Abant İzzet Baysal University	EFFECT of Sm/Sr PARTIAL REPLACEMENT ADDITION ON FUNDAMENTAL ELECTRICAL QUANTITIES OF Bi-2212 CRYSTAL STRUCTURE
Lect. Ahmet ÜNLÜ	Antalya Bilim University	DETECTION OF ELEMENTAL DIVERSITY IN TEETH IN THE BY IPAA METHOD
Lect. Ahmet ÜNLÜ	Antalya Bilim University	DETECTION OF IZOTOPES IN TOOTH SAMPLES USING THE IPAA METHOD
Saba SOHAİL Fakhar ud DİN Zakir ALİ	Quaid-i-Azam University, Pakistan	NEUROPROTECTIVE EFFECTS OF MELATONIN SLNs IN CEREBRAL ISCHEMIC INJURY MODEL
Sümeyye AKBULUT Elanur TUYSUZ Ahmet ADIGÜZEL Hakan ÖZKAN Mesut TAŞKIN	Atatürk University	ANTIMICROBIAL ACTIVITY OF FOOD-BORNE <i>Lactobacillus paracasei</i> subsp. <i>paracasei</i>
Asisst. Prof. Dr. Hamid CEYLAN	Atatürk University	DETECTION of SHARED CRITICAL SIGNATURES and PATHWAYS BETWEEN TYPE 2 DIABETES and HEART FAILURE
Veronica POZNEACOVA	Moldova State University, Faculty of Law, Moldova	THE PROTECTION AND GUARANTEEING OF THE RIGHTS TO HEALTH PROTECTION IN THE CONDITIONS OF THE COVID-19 EPIDEMIC
Asisst. Prof. Dr. İbrahim KONUK	Artvin Çoruh University	RISKS IDENTIFICATION FOR MINERARAL PROCESSING PLANTS
Emine TORAMAN Melike KARAMAN Ekrem SULUKAN Saltuk Buğrahan CEYHUN Harun BUDAK	Atatürk University	EFFECT of CHRONIC FLUORIDE ADMINISTRATION on ANTIOXIDANT ENZYMES in ZEBRAFISH LIVER
Assoc. Prof. Dr. Aysel GÜVEN Ertuğrul ALLAHVERDİ Tülay Diken ALLAHVERDİ	Başkent Üniversitesi Kafkas University	THE IMPORTANCE OF BIOCHEMICAL TESTS IN COVID-19 PATIENTS

21.11.2021

SUNDAY/ 10:00-12:00

MANAGEMENT

SESSION-1 HALL -2

MODERATOR: Prof. Dr. Aysegül GÜMÜŞ

Algeria: 08:00-10:00 /India: 12:30-14:30/ Iran: 10:30-12:30 /İtaly: 08:00-10:00 /
Moldova: 09:00-11:00 / Morocco: 08:00-10:00 /Nigeria:08:00-10:00/ Pakistan: 12:00-14:00
/Portekiz: 07:00-09:00 / Tunisie: 08:00-10:00

AUTHORS	AFFILIATION	TOPIC TITLE
Lect. Süleyman ŞÜKÜROĞLU Prof. Dr. Yaşar TOTİK Assoc. Prof. Dr. Ebru Emine ŞÜKÜROĞLU	Gümüşhane University Atatürk University	INVESTIGATION OF ELECTROLYTICAL SOLUTION OF THE SURFACE MORPHOLOGY AND COMPOSITION OF MgO, MgO:TiO ₂ , and MgO:TiO ₂ :C NANOCOMPOSITE COATINGS GROWED ON AZ91 MAGNESIUM ALLOY BY MAO METHOD
Lect. Süleyman ŞÜKÜROĞLU Prof. Dr. Yaşar TOTİK Assoc. Prof. Dr. Ebru Emine ŞÜKÜROĞLU	Gümüşhane University Atatürk University	MICROSTRUCTURAL CHARACTERIZATION OF MgO:TiO ₂ COATINGS GROWN BY MAO METHOD ON AZ91 Mg ALLOY
Prof. Dr. Ayşegül GÜMÜŞ Prof. Dr. Selçuk GÜMÜŞ	Van Yüzüncü Yıl University	SYNTHESIS AND COMPUTATIONAL STUDIES OF NOVEL QUINOLINE-SUBSTITUTED SCHIFF-BASE DERIVATIVES
Prof. Dr. Ayşegül GÜMÜŞ Prof. Dr. Selçuk GÜMÜŞ	Van Yüzüncü Yıl University	SYNTHESIS OF A FLUORESCENT TRIAZOLE DERIVATIVE AND THEORETICAL INVESTIGATION OF ITS METAL SENSOR PROPERTY
Resc. Assist. Dr. Nurşah KÜTÜK Sevgi DURNA DAŞTAN Sevil ÇETİNKAYA GÜRER	Sivas Cumhuriyet University	ANTIBACTERIAL ACTIVITY OF RGO/CLAY COMPOSITE AGAINST VARIOUS BACTERIA AND YEASTS
Resc. Assist. Dr. Nurşah KÜTÜK Sevil ÇETİNKAYA GÜRER	Sivas Cumhuriyet University	EFFECT OF OXIDATION ON METHYLENE BLUE PHOTOLYSIS
Assoc. Prof. Dr. Serkan ÖZTÜRK Ayhan YILDIRIM Gökhan GECE Hüsnü GERENGİ	Bursa Uludağ University/ Düzce University/University of Bergamo, İtalya	SYNTHESIS OF NEW TRI-CATIONIC SURFACTANTS AND ACTING AS CORROSION INHIBITOR IN ACIDIC ENVIRONMENT
Asisst. Prof. Dr. Gülşen TAŞKIN ÇAKICI	Sivas Cumhuriyet University	ADSORPTION OF RB FROM AQUEOUS SOLUTION WITH SODIUM ALGinate/HYDROXYPROPYMETHYLCELLULOSE COMPOSITE BEADS
Imen JENDOUBİ Mayssa ZOUAOUİ Chokri ISSAOUI Mohamed Faouzi ZİD Noura Fakhar BOURGUİBA	University of Tunis El Manar, Tunisia	INVESTIGATION OF THE OPTICAL PROPERTIES OF Na ₂ Ni ₂ (MoO ₄) ₃ NANOPARTICLES FOR PHOTOCATALYTIC APPLICATION POSTER PRESENTION
Imen JENDOUBİ Zaineb ABDELKAFI-KOUBAA Hammouda CHABBI Najet SRAIRI-ABID Mohamed Faouzi ZID	University of Tunis El Manar, Tunisia	PHYSICO-CHEMICAL AND BIOLOGICAL ACTIVITY OF A NEW VANADIUM COMPLEX
Melek YILGIN Neslihan DURANAY Dursun PEHLİVAN	Firat University	COMBUSTION BEHAVIOR OF BIOMASS IN FIXED BED

21.11.2021

SUNDAY/ 10:00-12:00

MANAGEMENT

SESSION-1 HALL -3

MODERATOR: Assist. Prof. Dr. Melih GÜZEL

Algeria: 08:00-10:00 /India: 12:30-14:30/ Iran: 10:30-12:30 /İtaly: 08:00-10:00 /
Moldova: 09:00-11:00 / Morocco: 08:00-10:00 /Nigeria: 08:00-10:00/ Pakistan: 12:00-14:00
/Portekiz: 07:00-09:00 / Tunisie: 08:00-10:00

AUTHORS	AFFILIATION	TOPIC TITLE
Dr. Olubunmi T. OLORUNPOMI Dr. Rabi S. DUWA	Nigeria Police Academy	VARIATION OF MOSQUITOES' GENERA AROUND POLAC ENVIRONMENT
ESWARI CHANDRA AKANKSHA.CH Dr. M. MEENA Ms. P. MALINI ANANDRAJ	RMK Engineering College, India	SMART FARMING - THE BACKBONE OF INDIAN ECONOMY
EWETOLA E. A. ISOLA J.O. BABATUNDE I. E.	Ladoke Akintola University/ Forest Research Institute of Nigeria	INFLUENCE OF GREEN MANURE FROM SPEAR GRASS ON SELECTED SOIL PHYSICAL PROPERTIES AND MAIZE GROWTH IN SOUTHERN GUINEA SAVANNA OF NIGERIA
Assist. Prof. Dr. R. ARUNKUMAR, M.Sc.(Ag.) Senior Research Fellow, V. BALAMURUGAN	SRS Institute of Agriculture and Technology, /Tamil Nadu Agricultural University,India	CLIMATE CHANGE AND ITS IMPACTS IN INDIAN HORTICULTURE
Resc. Assist. Ayşe Nur TANIŞ Assist. Prof. Dr. Fatma İLHAN Prof. Dr. İsmail KESKİN	Selçuk University	CANDIDATE GENES ASSOCIATED WITH YIELD TRAITS IN SHEEP
Havva Aybüke GÜVEN Assist. Prof. Dr. Feyza KIROĞLU ZORLUGENÇ	Nevşehir Hacı Bektaş Veli University	DETERMINATION OF QUALITY CHARACTERISTICS OF SOME COLOR POTATO CLONES WHICH WERE BREEDING IN NIGDE PROVINCE
K. GOMATHY S. Devisri MAHALAKSHMI Dr. G. Nixon Samuel VĪJAYAKUMAR Ms. M G. Meedphin RASI	RMK Engineering College, Kavaraipettai,India	SATELLITE CROP MONITORING
Assist. Prof. Dr. Melih GÜZEL Özlem AKPINAR	Gümüşhane University Gaziosmanpaşa University	ISOLATION AND IDENTIFICATION OF BACTERIA CAPABLE OF PRODUCING BACTERIAL CELLULOSE FROM VINEGARS PRODUCED FROM DIFFERENT FRUITS
G. RĪTHANYA Dr. G. Nixon Samuel VĪJAYKUMAR Dr. A. JAGADESAN Ms. V. NĪRMALA	RMK Engineering College, Kavaraipettai,India	ROLE OF ARTIFICIAL INTELLIGENCE IN SMART AGRICULTURE
A. ASWĪNĪ S. AISHWARYA Dr. A. VĪJAYALAKSHMI Dr. G. Nixon Samuel VĪJAYAKUMAR	RMK Engineering College, Kavaraipettai,India	NANOTECHNOLOGY IN FOOD SAFETY

21.11.2021

SUNDAY/ 12:00-14:00

MANAGEMENT

SESSION-2 HALL -1

MODERATOR: Dr. A. VIJAYALAKSHMI

Algeria: 08:00-10:00 / India: 12:30-14:30/ Iran: 10:30-12:30 / Italy: 08:00-10:00 /
Moldova: 09:00-11:00 / Morocco: 08:00-10:00 / Nigeria: 08:00-10:00/ Pakistan: 12:00-14:00
/Portekiz: 07:00-09:00 / Tunisie: 08:00-10:00

AUTHORS	AFFILIATION	TOPIC TITLE
Assist. Prof. A. SANJAIKANNAN Assist. Prof. R. LEENASREE	SRS Institute of Agriculture and Technology,INDIA	BAMBOO SHOOTS AND ITS BENEFITS
Chenna Kesavan K. Dr. M. MEENA Dr. A. VIJAYALAKSHMI Dr. S.D. Uma MAGESWARI	RMK Engineering College, India	SMART AGRICULTURE TECHNOLOGY USING IoT & RFID
Irene Adaeze KENNETH Luke Chinaru NWOSU	University of Port Harcourt, Nigeria	INVESTIGATIONS ON SOME IMPORTANT FACTORS THAT CAN INFLUENCE MAIZE GRAIN RESISTANCE TO MAIZE WEEVIL PEST IN STORAGE
R. Amara DEEPIKA Dr. A. VIJAYALAKSHMI Dr. G. Nixon Samuel VIJAYAKUMAR	RMK Engineering College, India	RESCUE FROM FOOD ADULTERATION BY SENSORS AND NANOTECHNOLOGY
Assist. Prof. Suyog A. BAGADE M.Sc. (Forestry) Scholar, Aditi A. BAGADE	Tamil Nadu Agricultural University/ College of Forestry,India	OVERVIEW OF BAMBOO DIVERSITY OF INDIA
T. Mohamed NADHIM Dr. M. MEENA Dr. Santhi M. GEORGE Dr. A. VIJAYALAKSHMI	RMK Engineering College, Kavaraipettai,India	AUTOMATED CULTIVATING AND HABITAT STABILIZER
AL. SAKTHI Dr. A. VIJAYALAKSHMI Dr. G. Nixon Samuel VIJAYAKUMAR	RMK Engineering College, Kavaraipettai,India	NANOTECHNOLOGY IN AGRICULTURE
B. KIRTHIKA Dr. A. VIJAYALAKSHMI Dr. G. Nixon Samuel VIJAYAKUMAR	RMK Engineering College, Kavaraipettai,India	NANO MATERIALS IN ANCIENT AND CURRENT SCENARIO – AN OVERVIEW

21.11.2021

SUNDAY/ 12:00-14:00

MANAGEMENT

SESSION-2 HALL -2

MODERATOR: Prof. Dr. Bilge ALBAYRAK ÇEPER

Algeria: 08:00-10:00 / India: 12:30-14:30/ Iran: 10:30-12:30 /İtaly: 08:00-10:00 /
Moldova: 09:00-11:00 / Morocco: 08:00-10:00/ Nigeria: 08:00-10:00/ Pakistan: 12:00-14:00
/Portekiz: 07:00-09:00 / Tunisie: 08:00-10:00

AUTHORS	AFFILIATION	TOPIC TITLE
Mert LÜYE Taner ERDOĞAN Ümit KARAHAN	Çukurova Makine İmalat Ve Ticaret A.Ş.	INVESTIGATION OF THE STRUCTURAL ANALYSIS OF THE STICK CYLINDER OF THE BACKHOE LOADER MACHINE WITH THE FINE ELEMENT METHOD AND THE DESIGN IMPROVEMENT STUDY
Hassan GUENDOZ	Mechanics Research Center (CRM), Algeria	CHROMIUM INSERTION INTO ZIRCONIUM WAFER SURFACE
Selin UĞURAL Prof. Dr. Bilge ALBAYRAK ÇEPER	Erciyes University	EXPERIMENTAL INVESTIGATION OF LPG-DIESEL COMBUSTION AT AN IGNITION ENGINE WITH REAGENT CONTROLLED COMPRESSION
Lahcene MEBARKİ Lamine GHALMİ Kamel FEDAOUI Mosbah ZİDANI	1Centre de Recherche en Mécanique/ 2Université A/MIRA Bejaia/ ISTA, University of Constantine/ University of Batna/ ALGERIA	EFFETS DE LA TENEUR EN Ni SUR LA MICROSTRUCTURE ET LES PROPRIÉTÉS MÉCANIQUES DES COMPOSITES TiC-Ni FABRIQUÉS PAR LA MÉTALLURGIE DES POUDRE (FRITTAGE EN PHASE SOLIDE)
Assist. Prof. Dr. Ali Can KAYA	Türk-Alman Üniversitesi Türkisch-Deutsche Universität	3-D QUANTITATIVE STRUCTURE INVESTIGATION OF GREY CAST IRON FOAMS BY MICRO-CT IMAGES
BOUTOUTA Aziza NAOUAL Handel GANDOUZ Hassen	Mechanics Research Center, Algeria/University of Mouhamed Cherif Messadia	MECHANICAL, STRUCTURAL AND CORROSION CHARACTERISATIONS OF ALUMINIUM MATRIX COMPOSITE AMCs Al-X m.% (α -Fe ₂ O ₃) ELABORATED BY LIQUID PHASE SINTERING
BOUTOUTA Aziza BLAOUİ Mohamed Mossaab HANDEL Naoual BOUARICHA Amor	Mechanics Research Center, Algeria/University of Mouhamed Cherif Messadia	STUDY OF THE GRAIN KINETIC DURING ISOTHERMAL HEATING IN WELD REGION OF PIPELINE STEEL X70
Mehmet Ali TUNALI Sercan KAYGISIZ	KBE Ar-Ge Merkezi	ALUMINYUM PROFİL ÖLÇÜM CİHAZI TASARIMI
Dr. Aissa LAOUISSI	Mechanics Research Centre. Algeria	MODELING AND OPTIMIZATION OF THE SURFACE ROUGHNESS AND MACHINING TIME WHEN MILLING THE PA6
Lect. Şevki KUTAY Bünyamin KAMAL	Recep Tayyip Erdoğan University	EVALUATION OF CAUSAL FACTORS OF MARINE DIESEL ENGINE CRANKSHAFT DAMAGES STEMMING FROM VESSEL CREW
Mehmet Ali TUNALI Rafet Emir BİRCAN	KBE Ar-Ge Merkezi	PRODUCTION MANAGEMENT SOFTWARE WITH REAL-TIME DATA AND INTEGRATION OF DESIGN DATA
Assist. Prof. Dr. Kemal Furkan SÖKMEN Ar-Ge Manager Emrah YÜRÜKLÜ Resc. Assist. Osman Bedrettin KARATAŞ	Bursa Technical University/ Uludag University	INVESTIGATION OF THE ELECTRONIC PERFORMANCE OF THE TOUCH CONTROL PANEL AND MULTIMEDIA SYSTEM USED IN THE NEW GENERATION VEHICLES WITH THE FINITE VOLUME METHOD IN THE THERMAL DIRECTION

21.11.2021

SUNDAY/ 12:00-14:00

MANAGEMENT

SESSION-2 HALL -3

MODERATOR: Dr. Aldemir Malveira de Oliveira

Algeria: 08:00-10:00 /India: 12:30-14:30/ Iran: 10:30-12:30 /Italy: 08:00-10:00 /
Moldova: 09:00-11:00 / Morocco: 08:00-10:00 /Nigeria: 08:00-10:00/ Pakistan: 12:00-14:00
/Portekiz: 07:00-09:00 / Tunisie: 08:00-10:00

AUTHORS	AFFILIATION	TOPIC TITLE
Abdelkader EL MAHI M'hammed ZIANE	Mohammed First Universty Morocco	ON THE TRIVIALITY OF IWASAWA MODULE OF THE CYCLOTOMIC Z_2 -EXTENSIONS OF CERTAIN REAL BIQUADRATIC FIELDS
Ahmet YÜCESAN	Süleyman Demirel University	ON THE CHARACTERIZATION OF SPHERICAL CURVES
Dr. Aldemir Malveira de Oliveira	Universidade do Minho/Portekiz	MACHINE LEARNING GOOGLE AS A TOOL IN THE EVALUATION PROCESS IN MATHEMATICS "AN EXPERIENCE IN THE AMAZON - NORTHERN BRAZIL"
Rebiai CHERİF Saidani NOUREDDİNE	University of Batna2, Algeria	FREE AND FORCED VIBRATION ANALYSIS OF SOLID STRUCTURES BY USING STRAIN BASED APPROACH"
Tunahan TURHAN Gözde ÖZKAN TÜKEL Ahmet YÜCESAN	Süleyman Demirel University/ Isparta University	ASSOCIATED PSEUDO-HYPERBOLIC SPACE PARTNER OF A SPACELIKE CURVE WITH TIMELIKE PRINCIPAL NORMAL
W. JBELİ M. F. ZİD	Université de Tunis El Manar, Tunisie	SYNTHÈSES, ÉTUDES STRUCTURALES ET CARACTÉRISATIONS PHYSICO-CHIMIQUES DE DEUX NOUVEAUX COMPOSÉS ORGANOMÉTALLIQUES À BASE DE COBALT
Carla Maria Lopes da Silva Afonso dos Santos Cristina Paula da Silva Dias Célia Maria Pinto Nunes João Tiago Praça Nunes Mexia	University of Beira Interior, Portugal/ New University of Lisbon	ORTHOGONAL BLOCK STRUCTURE, U-MATRICES AND UNIFORMLY BEST LINEAR UNBIASED ESTIMATORS

21.11.2021

SUNDAY/ 14:30-16:30

MANAGEMENT

SESSION-3 HALL -1

MODERATOR: Dr. Neslihan ŞAHİN

Algeria: 08:00-10:00 /India: 12:30-14:30/ Iran: 10:30-12:30 /İtaly: 08:00-10:00 /
Moldova: 09:00-11:00 / Morocco: 08:00-10:00 /Nigeria: 08:00-10:00/ Pakistan: 12:00-14:00
/Portekiz: 07:00-09:00 / Tunisie: 08:00-10:00

AUTHORS	AFFILIATION	TOPIC TITLE
Dr. Neslihan ŞAHİN Elvan ÜSTÜN	Cumhuriyet University/ Ordu University	SYNTHESIS AND CHARACTERIZATION OF A NEW CYCLOBUTYL SUBSTITUTED BENZIMIDAZOLIUM SALT
Ugochinyere Ihuoma NWOSU Chukwudi Paul OBITE Daniel Chinemeze OKOLIE	Federal University of Technology Owerri, Nigeria	STATISTICAL INVESTIGATIONS ON DISPARITY IN SPENDING HABITS OF ACADEMIC AND NON-TEACHING STAFF OF TERTIARY INSTITUTIONS IN IMO STATE, NIGERIA
Hasan YAKAN	Ondokuz Mayıs University	PREPARATION, STRUCTURE ELUCIDATION, AND ANTIOXIDANT ACTIVITY OF NEW ISATIN DERIVATIVES INCLUDING SCHIFF BASES
Assist. Prof. Dr. Mrs. Y. SUREKHA Assoc. Professor, K. Koteswara RAO Sr . Assist. Prof. Dr. G. Lalitha KUMARI Mr. A Srinath REDDY Ms. Kadiyala PUJITHA Assist. Prof. Dr. Mr. N Ramesh BABU	PVP Siddhartha Institute of Institute of Technology, RGKUT, INDIA /Srikakulam, Andhra Pradesh, INDIA	JOB MANAGER FOR JOB GROUPING ON COMPUTATIONAL GRIDS
Alireza MOGHADDASI Ph. D. Candidate Ramuna MİRHAJIANMOGHADDAM	Imamreza International University, Mashhad, Iran/ Yazd University, Iran	THE IMPACT OF CUSTOMER EXPECTED PERFORMANCE ON ONLINE WORD OF MOUTH WITH TRUST MEDIATOR
Talapaneni GEETHIKA Dr. M. MEENA Dr. Santhi M. GEORGE Dr. A.VIJAYALAKSHMI	RMK Engineering College, India.	HUMAN AUGMENTATION- AN OVERVIEW

21.11.2021

SUNDAY/ 14:30-16:30

MANAGEMENT

SESSION-3 HALL -2

MODERATOR: Prof. Dr. Hasan SERİN

Algeria: 08:00-10:00 /India: 12:30-14:30/ Iran: 10:30-12:30 /İtaly: 08:00-10:00 /
Moldova: 09:00-11:00 / Morocco: 08:00-10:00 /Nigeria: 08:00-10:00/ Pakistan: 12:00-14:00
/Portekiz: 07:00-09:00 / Tunisie: 08:00-10:00

AUTHORS	AFFILIATION	TOPIC TITLE
Prof. Dr. Hasan SERİN Assoc. Prof. Dr. Ferhat ÖZDEMİR	Kahramanmaraş Sütçü Imam University	FOREIGN TRADE ANALYSIS OF THE TURKISH FURNITURE INDUSTRY BY YEARS
Prof. Dr. Hasan SERİN Assoc. Prof. Dr. Ferhat ÖZDEMİR	Kahramanmaraş Sütçü Imam University	EVALUATION OF THE TURKISH FURNITURE INDUSTRY WITH SWOT ANALYSIS DURING THE PANDEMIC PERIOD
Mustafa RAFFEQ Serkan OZBAY	Gaziantep University	A REAL-TIME FALL DETECTION OF ELDERLY PEOPLE IN INDOOR ENVIRONMENTS
Aman MISHRA Assoc. Prof. Dr. Rahul DESAI Mr. G. M. WALUNJKAR	Alumni, Army Institute of Technology, Pune/India	PLM ENHANCEMENT DEVELOPMENT PORTAL
Naoual HANDEL Aziza BOUTOUTA Khalil BOUCHOUK	University of Mouhamed Cherif Messadia, Mechanics Research Centre. ALGERIA	CONTRIBUTION TO THE VALORIZATION OF CRYSTALLIZED AND GRANULATED SLAG IN CONCRETE MAKING
Assoc. Prof. Dr. Ferhat ÖZDEMİR Prof. Dr. Hasan SERİN	Kahramanmaraş Sütçü Imam University	RISK ANALYSIS EXAMPLE IN PARTICLE BOARD FACTORY
Assoc. Prof. Dr. Ferhat ÖZDEMİR Prof. Dr. Hasan SERİN	Kahramanmaraş Sütçü Imam University	INVESTIGATION OF THE SURFACE ROUGHNESS OF COMMERCIAL MDF BOARDS USED IN FURNITURE MANUFACTURING
Dounia KEDDARI Farah BOUTOUATOU	Territory Planning Research Center, University of Constantine 1, Algeria	MONITORING AND ASSESSMENT OF WATER QUALITY IN THE GUENITRA DAM, ALGERIA USING HYSICOCHEMICAL PARAMETERS AND POLLUTION ORGANIC INDEX
Ms. Radhika DALVI Mr. Devesh MORE Mr. Saket NIPHADE Assist. Prof. Dr. K. D. AHIRE	K.R.T. Arts, B.H. Commerce & A.M. Science (KTHM) College, India	STUDY OF NOISE LEVEL DURING DIWALI FESTIVAL 2021 AT SELECTED RESIDENTIAL AREAS IN NASHIK CITY OF INDIA

21.11.2021

SUNDAY/ 14:30-16:30

MANAGEMENT

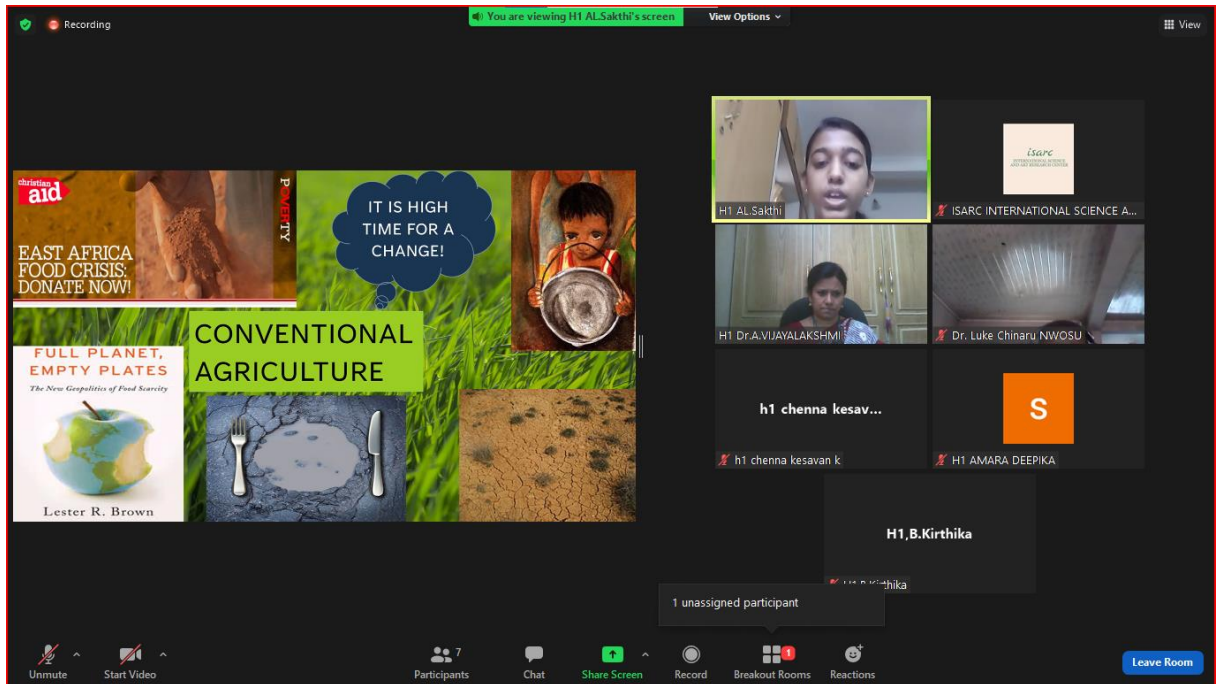
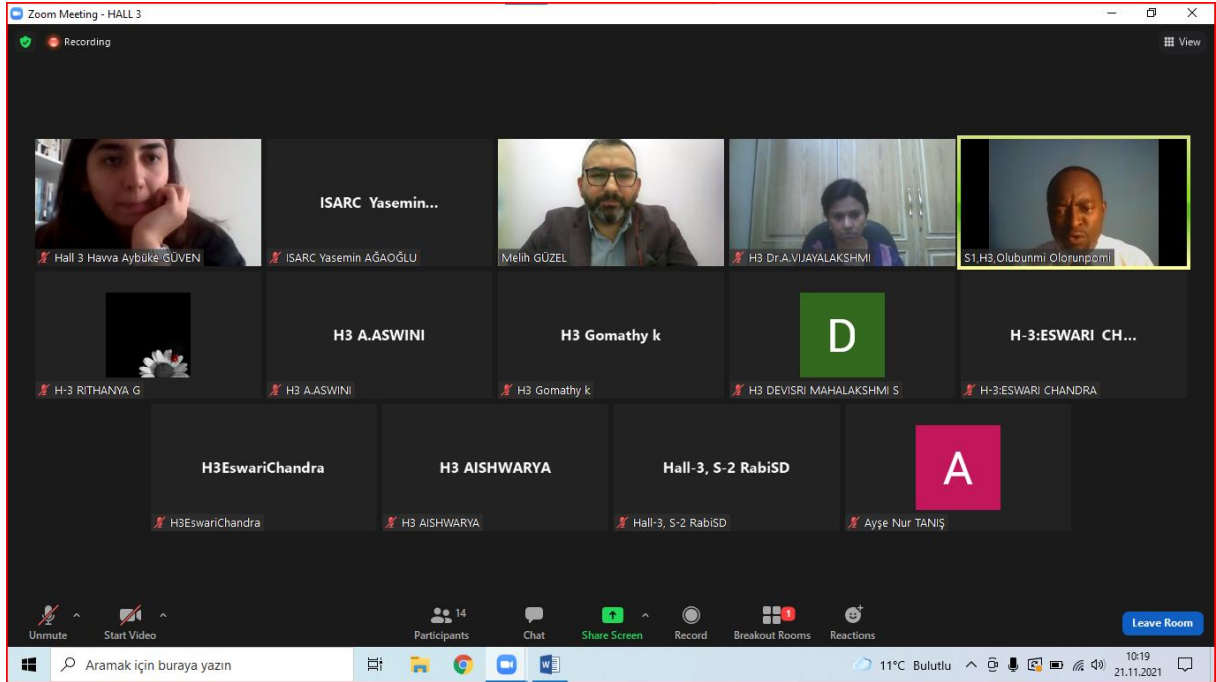
SESSION-3 HALL -3

MODERATOR: Dr. Bahar ALTUNOK

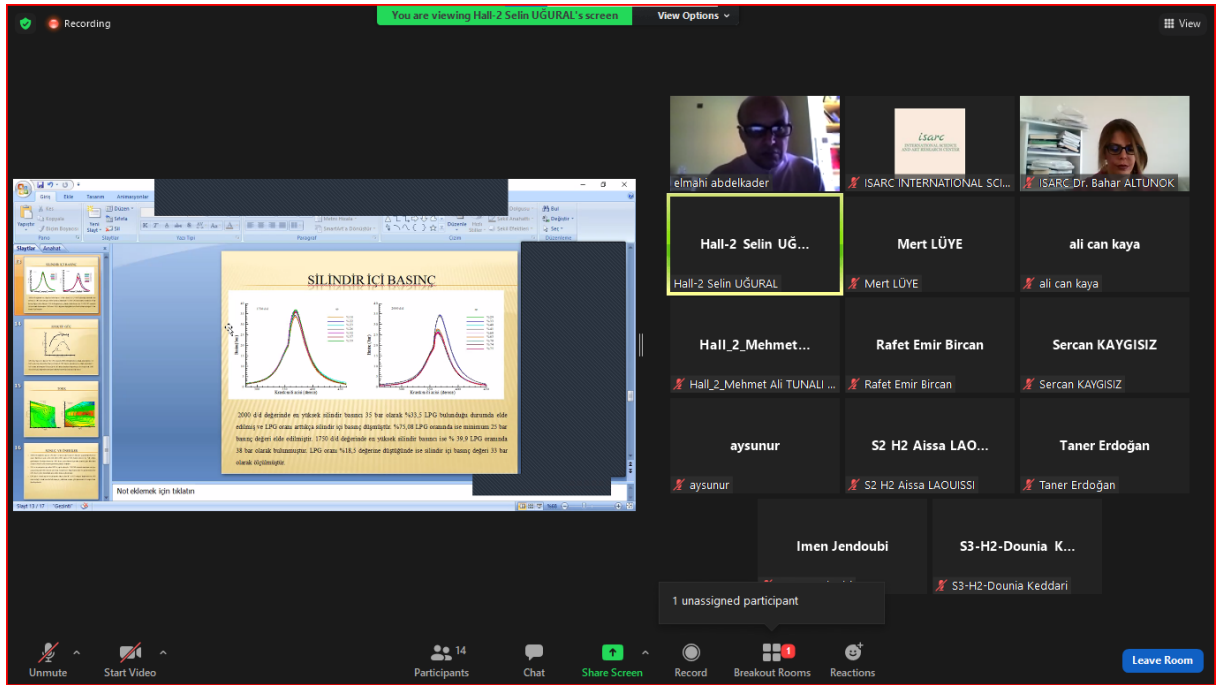
Algeria: 08:00-10:00 /India: 12:30-14:30/ Iran: 10:30-12:30 /İtaly: 08:00-10:00 /
Moldova: 09:00-11:00 / Morocco: 08:00-10:00 /Nigeria: 08:00-10:00/ Pakistan: 12:00-14:00
/Portekiz: 07:00-09:00 / Tunisie: 08:00-10:00

AUTHORS	AFFILIATION	TOPIC TITLE
Assoc. Prof. Dr. K. Koteswara RAO Sr . Assist. Prof. Dr. G. Lalitha KUMARI Assist. Prof. Dr. Mrs. Y. SUREKHA Ms . B. Kanaka APARNA Mukkapati ROHITH Assist. Prof. Dr. N Ramesh BABU	PVP Siddhartha Institute of Institute of Technology, RGKUT, INDIA /Srikakulam, Andhra Pradesh, INDIA	SIX SIGMA APPROACH TO ACHIEV THE STATISTICAL QUALITY ASSURANCE
A. GOPIKA Dr. A. VIJAYALAKSHMI Dr. G. Nixon Samuel VIJAYAKUMAR	RMK Engineering College, India.	SENSOR TECHNOLOGY IN FOOD INDUSTRY
Sr . Assist. Prof. Dr. G. Lalitha KUMARI Assoc. Prof. Dr. K. Koteswara RAO Assist. Prof. Dr. Mrs. Y. SUREKHA Ms. B. Chaitanya SREYA Kolli Pooja SRI Assist. Prof. Dr. Mr. N Ramesh BABU	PVP Siddhartha Institute of Institute of Technology, RGKUT, INDIA /Srikakulam, Andhra Pradesh, INDIA	EXPERIMENTAL AND EFFICIENT USAGE OF DATA MINING PRIMITIVES
Assist. Prof. Dr. Mr. N Ramesh BABU Assist. Prof. Dr. Mrs. Y. SUREKHA Assoc. Prof. Dr. K. Koteswara RAO Sr . Assist. Prof. Dr. G. Lalitha KUMARI Mr. G. Bhargav RAMUDU Monika Sai PINNINTI	PVP Siddhartha Institute of Institute of Technology, RGKUT, INDIA /Srikakulam, Andhra Pradesh, INDIA	EFFICIENT MONITORING OF THE PROJECTS THROUGH THE PERT AND MILESTONES
Assoc. Prof. Dr. K. Koteswara RAO Sr . Assist. Prof. Dr. G. Lalitha KUMARI Assist. Prof. Dr. Mrs. Y. SUREKHA Mr. CH. Rajesh CHANDRA Mounisha. RAAVI Assist. Prof. Dr. Mr. N Ramesh BABU	PVP Siddhartha Institute of Institute of Technology, RGKUT, INDIA /Srikakulam, Andhra Pradesh, INDIA	ARTIFICIAL VISION - MADE POSSIBLE BY MICRO MEDICAL ELECTRONICS
Hicret HOPOĞLU Prof. Dr. Ebru Şenadım TÜZEMEN	Sivas Cumhuriyet University	OPTICAL PROPERTIES OF NiO x THIN FILMS PRODUCED BY MAGNETRON SPUTTERING AT DIFFERENT PRESSURES
Hicret HOPOĞLU Hafize Seda AYDINOĞLU Prof. Dr. Ebru Şenadım TÜZEMEN	Sivas Cumhuriyet University	INFLUENCE of OXYGEN PRESSURE on OPTICAL PROPERTIES of RF MAGNETRON SPUTTERING Ga2O3 THIN FILMS
Dr. Gökhan KÜLEKÇİ	Gümüşhane Üniversitesi	THE STATISTICAL INVESTIGATION OF THE RELATIONSHIP BETWEEN SCHMİDT HARDNESS VALUES, POROSITY AND WATER APPROACH IN VOLCANIC ROCKS USING SPSS PROGRAM
Dr. Gökhan KÜLEKÇİ	Gümüşhane Üniversitesi	THE STATISTICAL RELATIONSHIP OF CURE TIME AND COMPRESSIVE STRENGTH IN PASTE BACKFILLING

PHOTO GALLERY



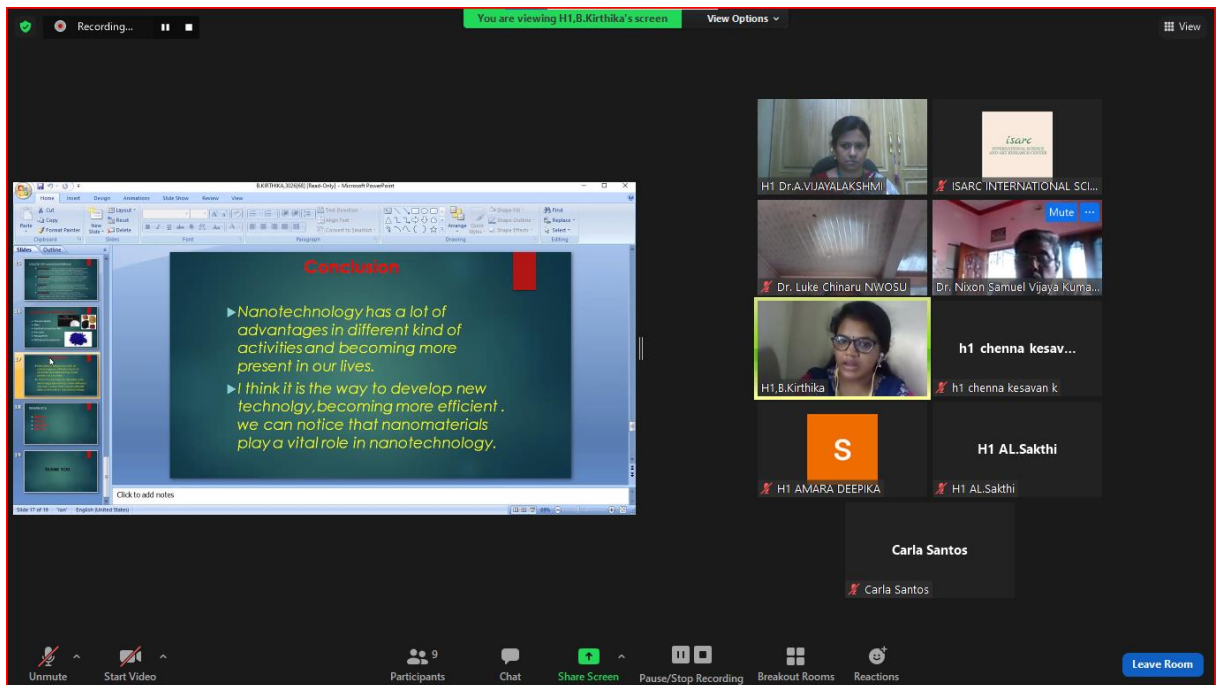
Recording... You are viewing Hall-2 Selin UĞURAL's screen View Options



The presentation slide displays two graphs showing pressure distribution. The text on the slide reads: "2000-44 değeriyle en yüksek silindirik basınç 33 bar olarak 7433,5 L/PD teknolojisi kullanılarak elde edilmiştir. 2000-44 değeriyle en yüksek silindirik basınç 33 bar olarak 7433,5 L/PD teknolojisi kullanılarak elde edilmiştir. 2000-44 değeriyle en yüksek silindirik basınç 33 bar olarak 7433,5 L/PD teknolojisi kullanılarak elde edilmiştir." Below the graphs, it states: "2000-44 değeriyle en yüksek silindirik basınç 33 bar olarak 7433,5 L/PD teknolojisi kullanılarak elde edilmiştir. 2000-44 değeriyle en yüksek silindirik basınç 33 bar olarak 7433,5 L/PD teknolojisi kullanılarak elde edilmiştir. 2000-44 değeriyle en yüksek silindirik basınç 33 bar olarak 7433,5 L/PD teknolojisi kullanılarak elde edilmiştir." At the bottom, it says "Not eklenen için tıklayın".

Participants in the grid include: elmhahi abdelkader, ISARC INTERNATIONAL SCI..., ISARC Dr. Bahar ALTUNOK, Hall-2 Selin UĞURAL, Mert LÜYE, ali can kaya, Hall_2_Mehmet..., Rafet Emir Bircan, Sercan KAYGISIZ, aysunur, S2 H2 Aissa LAO..., Taner Erdoğan, Imen Jendoubi, S3-H2-Dounia K..., and 1 unassigned participant.

Recording... You are viewing H1.B.Kirthika's screen View Options




The presentation slide is titled "Conclusion" and contains the following text: "► Nanotechnology has a lot of advantages in different kind of activities and becoming more present in our lives. ► I think it is the way to develop new technology, becoming more efficient, we can notice that nanomaterials play a vital role in nanotechnology." Below the text, it says "Click to add notes".

Participants in the grid include: H1 Dr.A.VIJAYALAKSHMI, ISARC INTERNATIONAL SCI..., Dr. Luke Chinaru NWOSU, Dr. Nixon Samuel Vijaya Kuma..., H1.B.Kirthika, h1 chenna kesav..., H1 AMARA DEEPIKA, H1 AL.Sakthi, and Carla Santos.

Recording... You are viewing Rafet Emir Bircan's screen View Options

Proje Konusu

- Proje kapsamında yaptığımız yazılım geliştirme çalışmalarıyla tasarım verileri kullanılarak malzeme listeleri hazırlanmaktadır.
- Ayrıca malzeme listesini oluşturacak parametrelerin düzenlenebilir olması sağlanacaktır.

www.kbe.com.tr Knowledge Based Engineering 

Participants: 13 Chat Share Screen Pause/Stop Recording Breakout Rooms Reactions Leave Room

Participants: Rafet Emir Bircan, ISARC INTERNATIONAL SCIENCE AND ART RESEARCH CENTER, ISARC Dr. Bahar ALTUN, H3-S2-REBIAI Cherif, Hall-2 Selin UĞURAL, Mert LÜYE, ali can kaya, Hall_2_Mehmet..., Sercan KAYGISIZ, aysunur, Taner Erdoğan, İmen Jendoubi

You are viewing Neslihan Şahin-Hall 1's screen View Options

Carbon and N-heterocyclic Carbene (NHC)

Carbon and N-heterocyclic Carbene (NHC) exist as a pair of isomers under ambient conditions in the gas phase and can react with a large number of transition-metal complexes. They are highly reactive. N-heterocyclic carbene (NHC) ligands are the most important group of organometallic chemistry due to their stability, high donor ability and unique steric and electronic properties.

The first complex of N-heterocyclic carbene with transition metals as ligands was carried out by Öfele and Wanzlick in 1968. Later, Arduengo et al. prepared the first crystalline free carbene by deprotonation of 1,3-bis(adamantyl) imidazolium chloride in 1991.

Öfele and Wanzlick, 1968

Arduengo, 1991

Participants: 5 Chat Share Screen Record Breakout Rooms Reactions Leave Room

Participants: Neslihan Şahin+Hall 1, ISARC INTERNATIONAL SCIENCE AND ART RESEARCH CENTER, Dr. Ugochinyere Ihuoma NWOSU, HASAN YAKAN, H1 GEETHIKA



İÇİNDEKİLER / CONTENTS

Sm/Sr KISMİ DEĞİŞTİRME İLAVELERİNİN Bi-2212 KRİSTAL YAPISININ TEMEL ELEKTRİK MİKTARLARINA ETKİSİ	30
Musa DOĞRUER	30
DIAVALENT Mn²⁺ TABAKASININ Ca²⁺ TABAKASINDA BULK Bi-2212 SİSTEMLERİNİN TEMEL ELEKTRİK MİKTARLARINDAKİ ROLÜ	36
Musa DOĞRUER	36
Gürcan YILDIRIM	36
Cabir TERZİOĞLU	36
DETECTION OF ELEMENTAL DIVERSITY IN TEETH IN THE BY IPAA METHOD	42
Öğr. Gör. Ahmet ÜNLÜ	42
DETECTION OF IZOTOPES IN TOOTH SAMPLES USING THE IPAA METHOD	43
Öğr. Gör. Ahmet ÜNLÜ	43
NEUROPROTECTIVE EFFECTS OF MELATONIN SLNS IN CEREBRAL ISCHEMIC INJURY MODEL	44
Saba SOHAİL	44
Fakhar ud DİN	44
Zakir ALİ	44
ANTIMICROBIAL ACTIVITY OF FOOD-BORNE <i>Lactobacillus paracasei</i> subsp. <i>paracasei</i>	45
Sümeyye AKBULUT	45
Elanur TUYSUZ	45
Ahmet ADIGÜZEL	45
Hakan ÖZKAN	45
Mesut TAŞKIN	45
DETECTION of SHARED CRITICAL SIGNATURES and PATHWAYS BETWEEN TYPE 2 DIABETES and HEART FAILURE	53
Hamid CEYLAN	53
THE PROTECTION AND GUARANTEENG OF THE RIGHTS TO HEALTHS PROTECTION IN THE CONDITIONS OF THE COVID-19 EPIDEMIC	63
Veronica POZNEACOVA	63

CEVHER HAZIRLAMA TESİSLERİNDE RİSKLERİN BELİRLENMESİ	70
İbrahim KONUK	70
KRONİK FLORÜR UYGULAMASININ ZEBRA BALIĞI KARACİĞERİNDEKİ ANTİOKSİDAN ENZİMLER ÜZERİNE ETKİSİ	81
Emine TORAMAN	81
Melike KARAMAN	81
Ekrem SULUKAN	81
Saltuk Buğrahan CEYHUN	81
Harun BUDAK	81
THE IMPORTANCE OF BIOCHEMICAL TESTS IN COVID-19 PATIENTS	88
Aysel GÜVEN	88
Ertuğrul ALLAHVERDİ	88
Tülay DİKEN ALLAHVERDİ	88
MAO YÖNTEMİYLE AZ91 MAGNEZYUM ALAŞIMI ÜZERİNE BÜYÜTÜLEN MgO, MgO:TiO₂ ve MgO:TiO₂:C NANOKOMPOZİT KAPLAMALARININ YÜZEY MORFOLOJİSİ VE BİLEŞİMİ ÜZERİNE ELEKTROLİTİK ÇÖZELTİNİN ETKİSİNİN İNCELENMESİ	90
Süleyman ŞÜKÜROĞLU	90
Yaşar TOTİK	90
Ebru EmineŞÜKÜROĞLU	90
AZ91 Mg ALAŞIMI ÜZERİNE MAO YÖNTEMİYLE BÜYÜTÜLEN MgO:TiO₂ KAPLAMALARIN MİKROYAPISAL KARAKTERİZASYONU	97
Süleyman ŞÜKÜROĞLU	97
Yaşar TOTİK	97
Ebru Emine ŞÜKÜROĞLU	97
SYNTHESIS AND COMPUTATIONAL STUDIES OF NOVEL QUINOLINE-SUBSTITUTED SCHIFF-BASE DERIVATIVES	103
Ayşegül GÜMÜŞ	103
Selçuk GÜMÜŞ	103

SYNTHESIS OF A FLUORESCENT TRIAZOLE DERIVATIVE AND THEORETICAL INVESTIGATION OF ITS METAL SENSOR PROPERTY	112
Ayşegül GÜMÜŞ	112
Selçuk GÜMÜŞ	112
ANTIBACTERIAL ACTIVITY OF RGO/CLAY COMPOSITE AGAINST VARIOUS BACTERIA AND YEASTS	119
Nurşah KÜTÜK	119
Sevgi DURNA DAŞTAN	119
Sevil ÇETİNKAYA GÜRER	119
EFFECT OF OXIDATION ON METHYLENE BLUE PHOTOLYSIS	123
Nurşah KÜTÜK	123
Sevil ÇETİNKAYA GÜRER	123
Yeni Tri-Katyonik Yüzey aktif Maddelerin Sentezi ve Asidik Ortamda Korozyon İnhibitörü Görevi üstlenmeleri	128
Serkan ÖZTÜRK	128
Ayhan YILDIRIM	128
Gökhan GECE	128
Hüsnü GERENGİ	128
SODYUM ALİNAT/ HİDROKSİPROPİLMETİSELÜLOZ KOMPOZİT BONCUKLARI İLE SULU ÇÖZELTİDEN RB'NİN ADSORPSİYONU	142
Gülşen TAŞKIN ÇAKICI	142
INVESTIGATION OF THE OPTICAL PROPERTIES OF NA₂Ni₂(MOO₄)₃ NANOPARTICLES FOR PHOTOCATALYTIC APPLICATION	152
Imen JENDOUBİ	152
Mayssa ZOUAOUİ	152
Chokri ISSAOUI	152
Mohamed Faouzi ZİD	152
Noura Fakhar BOURGUİBA	152
PHYSICOCHEMICAL AND BIOLOGICAL ACTIVITY OF A NEW VANADIUM COMPLEX	153
Imen JENDOUBI	153
Zaineb ABDELKAFI-KOUBAA	153
Hammouda CHABBI	153

<i>Najet SRAIRI-ABID</i>	153
<i>Mohamed Faouzi ZID</i>	153
<i>BİYOKÜTLENİN SABİT YATAKTA YANMA DAVRANIŞI</i>	154
<i>Melek YILGIN</i>	154
<i>Neslihan DURANAY</i>	154
<i>Dursun PEHLİVAN</i>	154
<i>TWO FACTOR ANALYSIS OF MOSQUITOES' GENERA AROUND POLAC ENVIRONMENT</i>	162
<i>Dr. Olubunmi T. OLORUNPOMI</i>	162
<i>Dr. Rabi S. DUWA</i>	162
<i>SMART FARMING - THE BACKBONE OF INDIAN ECONOMY</i>	174
<i>ESWARI CHANDRA AKANKSHA.CH.</i>	174
<i>Dr. M. MEENA</i>	174
<i>Ms. P. MALINI ANANDRAJ</i>	174
<i>SMART AGRICULTURE TECHNOLOGY USING IoT & RFID</i>	175
<i>Chenna Kesavan K.</i>	175
<i>Dr. M. MEENA</i>	175
<i>Dr. A. VIJAYALAKSHMI</i>	175
<i>Dr. S.D. Uma MAGESWARİ</i>	175
<i>INFLUENCE OF GREEN MANURE FROM SPEAR GRASS ON SELECTED SOIL PHYSICAL PROPERTIES AND MAIZE GROWTH IN SOUTHERN GUINEA SAVANNA OF NIGERIA</i>	176
<i>Ewetola E. A.</i>	176
<i>Isola J. O.</i>	176
<i>Babatunde, I. E.</i>	176
<i>CLIMATE CHANGE AND ITS IMPACTS IN INDIAN HORTICULTURE</i>	177
<i>Assist. Prof. Dr. Arunkumar R.</i>	177
<i>Senior Research Fellow, V. BALAMURUGAN</i>	177
<i>KOYUNLARDA VERİMİ ETKİLEYEN BAZI ADAY GENLER</i>	178
<i>Arş. Gör. Ayşe Nur TANIŞ</i>	178
<i>Dr. Öğr. Üyesi Fatma İLHAN</i>	178
<i>Prof. Dr. İsmail KESKİN</i>	178

NIĞDE İLİNDE ISLAH ÇALIŞMALARINI YAPILAN BAZI RENKLİ	189
PATATES KLONLARININ KALİTE ÖZELLİKLERİNİN BELİRLENMESİ	189
<i>Havva Aybüke GÜVEN</i>	189
<i>Dr. Öğr. Üyesi Feyza KIROĞLU ZORLUGENÇ</i>	189
SATELLITE CROP MONITORING	191
K. GOMATHY	191
<i>S. Devisri MAHALAKSHMI</i>	191
<i>Dr. G. Nixon Samuel VIJAYAKUMAR</i>	191
<i>Ms. M. G. Meedphin ARASI</i>	191
ISOLATION AND IDENTIFICATION OF BACTERIA CAPABLE OF PRODUCING BACTERIAL CELLULOSE FROM VINEGARS PRODUCED FROM DIFFERENT FRUITS	192
<i>Melih GÜZEL</i>	192
<i>Özlem AKPINAR</i>	192
ROLE OF ARTIFICIAL INTELLIGENCE IN SMART AGRICULTURE	193
G. RİTHANYA	193
<i>Dr. G. Nixon Samuel VIJAYKUMAR</i>	193
<i>Dr. A. JAGADESAN</i>	193
<i>Ms. V. NİRMALA</i>	193
NANOTECHNOLOGY IN FOOD SAFETY	194
<i>A. ASWINİ</i>	194
<i>Aishwarya S.</i>	194
<i>Dr. A. VIJAYALAKSHMI</i>	194
<i>Dr. G. Nixon Samuel VIJAYAKUMAR</i>	194
BAMBOO SHOOTS AND ITS BENEFITS	195
<i>Assist. Prof. Dr. Sanjaikannan A.</i>	195
<i>Assist. Prof. Dr. R. LEENASREE</i>	195
INVESTIGATIONS ON SOME IMPORTANT FACTORS THAT CAN INFLUENCE MAIZE GRAIN RESISTANCE TO MAIZE WEEVIL PEST IN STORAGE	196
<i>Irene Adaeze KENNETH</i>	196
<i>Luke Chinaru NWOSU</i>	196

RESCUE FROM FOOD ADULTERATION BY SENSORS AND NANOTECHNOLOGY	197
R. Amara DEEPIKA	197
Dr. A. VIJAYALAKSHMI	197
Dr. G. Nixon Samuel VIJAYAKUMAR	197
OVERVIEW OF BAMBOO DIVERSITY OF INDIA	198
Assist. Prof. Dr. Suyog A. BAGADE	198
M.Sc. (Forestry) Scholar, Aditi A. BAGADE	198
AUTOMATED CULTIVATING AND HABITAT STABILIZER	199
T. Mohamed NADHİM	199
Dr. M. MEENA	199
Dr. Santhi M. GEORGE	199
Dr. A. VIJAYALAKSHMI	199
NANOTECHNOLOGY IN AGRICULTURE	200
AL. SAKTHİ	200
Dr. A. VIJAYALAKSHMI	200
Dr. G. Nixon Samuel VIJAYAKUMAR	200
NANO MATERIALS IN ANCIENT AND CURRENT SCENARIO – AN OVERVIEW	201
B. KİRTHİKA	201
Dr. A. VIJAYALAKSHMI	201
Dr. G. Nixon Samuel VIJAYAKUMAR	201
SONLU ELEMANLAR METHODU İLE KAZICI YÜKLEYİCİ MAKİNEYE AİT STİK SİLİNDİRİN YAPISAL ANALİZİNİN İNCELENMESİ VE TASARIM İYİLEŞTİRME ÇALIŞMASI	202
Mert LÜYE	202
Taner ERDOĞAN	202
Ümit KARAHAAN	202
CHROMIUM INSERTION INTO ZIRCONIUM WAFER SURFACE	204
Hassan GUENDOZ	204
REAKTİF KONTROLLÜ SIKIŞTIRMA İLE ATEŞLEMELİ BİR MOTORDA	205
LPG-DİZEL YANMASININ DENEYSSEL İNCELENMESİ	205
Selin UĞURAL	205

<i>Prof. Dr. Bilge ALBAYRAK ÇEPER</i>	205
<i>Lahcene MEBARKİ</i>	213
<i>Lamine GHALMİ</i>	213
<i>Kamel FEDAOUİ</i>	213
<i>Mosbah ZİDANİ</i>	213
3-D QUANTITATIVE STRUCTURE INVESTIGATION OF GREY CAST IRON FOAMS BY MICRO-CT IMAGES	214
<i>Ali Can KAYA</i>	214
MECHANICAL, STRUCTURAL AND CORROSION CHARACTERISATIONS OF ALUMINIUM MATRIX COMPOSITE AMCs Al-X m.% (α-Fe₂O₃) ELABORATED BY LIQUID PHASE SINTERING	215
<i>BOUTOUTA Aziza</i>	215
<i>NAOUAL Handel</i>	215
<i>GANDOUZ Hassen</i>	215
STUDY OF THE GRAIN KINITIC DURING ISOTHERMAL HEATING IN WELD REGION OF PIPELINE STEEL X70	216
<i>BOUTOUTA Aziza</i>	216
<i>BLAOUİ Mohamed Mossaab</i>	216
<i>HANDEL Naoual</i>	216
<i>BOUARİCHA Amor</i>	216
ALÜMİNYUM PROFİL ÖLÇÜM CİHAZI TASARIMI	217
<i>Mehmet Ali TUNALI</i>	217
<i>Sercan KAYGISIZ</i>	217
GERÇEK ZAMANLI VERİLERLE ÜRETİM YÖNETİMİ YAZILIMI VE TASARIM VERİLERİNİN ENTEGRASYONU	219
<i>Mehmet Ali TUNALI</i>	219
<i>Rafet Emir BİRCAN</i>	219
MODELING AND OPTIMIZATION OF THE SURFACE ROUGHNESS AND MACHINING TIME WHEN MILLING THE PA6	221
<i>Aissa LAOUISSI</i>	221
GEMİ PERSONELİ KAYNAKLI GEMİ DİZEL MOTORU KRANKŞAFT HASARLARININ SEBEPSEL FAKTÖRLERİNİN DEĞERLENDİRİLMESİ	222
<i>Şevki KUTAY</i>	222
<i>Bünyamin KAMAL</i>	222

YENİ NESİL ARAÇLARDA KULLANILAN DOKUNMATİK KONTROL PANELİ VE MULTİMEDYA SİSTEMİNİN ELEKTRONİK PERFORMANSININ ISIL YÖNDEN SONLU HACİMLER METODUYLA İNCELENMESİ	224
Kemal Furkan SÖKMEN	224
Emrah YÜRÜKLÜ	224
Osman Bedrettin KARATAŞ	224
ON THE CHARACTERIZATION OF SPHERICAL CURVES	226
Ahmet YÜCESAN	226
MACHINE LEARNING GOOGLE AS A TOOL IN THE EVALUATION PROCESS IN MATHEMATICS "AN EXPERIENCE IN THE AMAZON - NORTHERN BRAZIL"	230
Prof. Dr. Aldemir MALVEİRA DE OLIVEİRA	230
FREE AND FORCED VIBRATION ANALYSIS OF SOLID STRUCTUES BY USING STRAIN BASED APPROACH	231
Rebiai CHERİF	231
Saidani NOUREDDİNE	231
ASSOCIATED PSEUDO-HYPERBOLIC SPACE PARTNER OF A SPACELIKE CURVE WITH TIMELIKE PRINCIPAL NORMAL	232
Tunahan TURHAN	232
Gözde ÖZKAN TÜKEL	232
Ahmet YÜCESAN	232
SYNTHESES, ETUDES STRUCTURALES ET CARACTERISATIONS PHYSICO-CHIMIQUES DE DEUX NOUVEAUX COMPOSES ORGANOMETALLIQUES A BASE DE COBALT	242
W. JBELI	242
M. F. ZID	242
ORTHOGONAL BLOCK STRUCTURE, U-MATRICES AND UNIFORMLY BEST LINEAR UNBIASED ESTIMATORS	243
Carla Maria Lopes da Silva AFONSO DOS SANTOS	243
Cristina Paula da SILVA DÍAS	243
Célia Maria PÍNTO NUNES	243
João Tiago Praça NUNES MEXÍA	243

SİKLOBÜTİL SÜBSTİTÜYE EDİLMİŞ BİR YENİ BENZİMİDAZOLYUM TUZUNUN SENTEZİ VE KARAKTERİZASYONU	244
<i>Neslihan ŞAHİN</i>	244
<i>Elvan ÜSTÜN</i>	244
STATISTICAL INVESTIGATIONS ON DISPARITY IN SPENDING HABITS OF ACADEMIC AND NON-TEACHING STAFF OF TERTIARY INSTITUTIONS IN IMO STATE, NIGERIA	251
<i>Ugochinyere Ihuoma NWOSU</i>	251
<i>Chukwudi Paul OBİTE</i>	251
<i>Daniel Chinemeze OKOLİE</i>	251
PREPARATION, STRUCTURE ELUCIDATION, AND ANTIOXIDANT ACTIVITY OF NEW ISATIN DERIVATIVES INCLUDING SCHIFF BASES	252
<i>Hasan YAKAN</i>	252
JOB MANAGER FOR JOB GROUPING ON COMPUTATIONAL GRIDS	260
<i>Sr. Assist. Prof. Dr. Mrs.Y. SUREKHA</i>	260
<i>Assoc. Prof. Dr. K. Koteswara RAO</i>	260
<i>Sr. Assist. Prof. Dr. G. Lalitha KUMARİ</i>	260
<i>Mr. A. Srinath REDDY</i>	260
<i>Ms. Kadiyala PUJİTHA</i>	260
<i>Assist. Prof. Dr. Mr. N. Ramesh BABU</i>	260
THE IMPACT OF CUSTOMER EXPECTED PERFORMANCE ON ONLINE WORD OF MOUTH WITH TRUST MEDIATOR	261
<i>Alireza MOGHADDASİ</i>	261
<i>Ramuna MİRHAJİANMOGHADDAM</i>	261
HUMAN AUGMENTATION- AN OVERVIEW	262
<i>Talapaneni GEETHİKA</i>	262
<i>Dr. M. MEENA</i>	262
<i>Dr. Santhi M. GEORGE</i>	262
<i>Dr. A. VİJAYALAKSHMİ</i>	262
TÜRKİYE MOBİLYA SEKTÖRÜNÜN YILLARA GÖRE DIŞ TİCARET ANALİZİ	263
<i>Hasan SERİN</i>	263
<i>Ferhat ÖZDEMİR</i>	263

PANDEMİ DÖNEMİNDE TÜRKİYE MOBİLYA SEKTÖRÜNÜN GZFT ANALİZİ İLE DEĞERLENDİRİLMESİ	269
<i>Hasan SERİN</i>	269
<i>Ferhat ÖZDEMİR</i>	269
A REAL TIME FALL DETECTION OF ELDERLY PEOPLE IN INDOOR ENVIRONMENTS	275
<i>Mustafa Hussain RAFEEQ</i>	275
<i>Serkan OZBAY</i>	275
PLM ENHANCEMENT DEVELOPMENT PORTAL	282
<i>Aman MISHRA</i>	282
<i>Assoc. Prof. Dr. Rahul DESAI</i>	282
<i>Assist. Prof. Dr. Mr. G. M. WALUNJKAR</i>	282
CONTRIBUTION TO THE VALORIZATION OF CRYSTALLIZED AND GRANULATED SLAG IN CONCRETE MAKING	283
<i>Naoual HANDEL</i>	283
<i>Aziza BOUTOUTA</i>	283
<i>Khalil BOUCHOUK</i>	283
YONGA LEVHA FABRİKASINDA RİSK ANALİZ ÖRNEĞİ	284
<i>Ferhat ÖZDEMİR</i>	284
<i>Hasan SERİN</i>	284
MOBİLYA ÜRETİMİNDE KULLANILAN TİCARİ MDF LEVHALARIN YÜZEY PÜRÜZLÜLÜKLERİNİN ARAŞTIRILMASI	291
<i>Ferhat ÖZDEMİR</i>	291
<i>Hasan SERİN</i>	291
MONITORING AND ASSESSMENT OF WATER QUALITY IN THE GUENITRA DAM, ALGERIA USING PHYSICOCHEMICAL PARAMERTS AND POLLUTION ORGANIC INDEX	297
<i>Dounia KEDDARI</i>	297
<i>Farah BOUTOUATOU</i>	297
STUDY OF NOISE LEVEL DURING DIWALI FESTIVAL 2021 AT SELECTED RESIDENTIAL AREAS IN NASHIK CITY OF INDIA	298
<i>R. A. DALVÍ</i>	298
<i>D. B. MORE</i>	298
<i>S. S. NIPHADE</i>	298

K. D. AHIRE	298
SIX SIGMA APPROACH TO ACHIEV THE STATISTICAL QUALITY ASSURANCE	299
Assoc. Professor, K. Koteswara RAO	299
Sr . Assist. Prof. Dr. G. Lalitha KUMARI	299
Assist. Prof. Dr. Mrs. Y. SUREKHA	299
Ms . B. Kanaka APARNA	299
Mukkapati ROHITH	299
Assist. Prof. Dr. Mr. N Ramesh BABU	299
ARTIFICIAL VISION - MADE POSSIBLE BY MICRO MEDICAL ELECTRONICS	300
Assoc. Professor, K. Koteswara RAO	300
Sr . Assist. Prof. Dr. G. Lalitha KUMARI	300
Assist. Prof. Dr. Mrs. Y. SUREKHA	300
Mr. CH. Rajesh CHANDRA	300
Mounisha RAAVI	300
Assist. Prof. Dr. Mr. N. Ramesh BABU	300
SENSOR TECHNOLOGY IN FOOD INDUSTRY	301
GOPIKA A.	301
Dr. A. VIJAYALAKSHMI	301
Dr. G. Nixon Samuel VIJAYAKUMAR	301
EXPERIMENTAL AND EFFICIENT USAGE OF DATA MINING PRIMITIVES	302
Sr . Assist. Prof. Dr. G. Lalitha KUMARI	302
Assoc. Professor, K. Koteswara RAO	302
Assist. Prof. Dr. Mrs. Y. SUREKHA	302
Ms. B. Chaitanya SREYA	302
Kolli Pooja SRI	302
Assist. Prof. Dr. Mr. N. Ramesh BABU	302
EFFICIENT MONITORING OF THE PROJECTS THROUGH THE PERT AND MILESTONES	303
Assist. Prof. Dr. Mr. N. Ramesh BABU	303
Assist. Prof. Dr. Mrs. Y. SUREKHA	303
Assoc. Professor, K. Koteswara RAO	303

<i>Sr . Assist. Prof. Dr. G. Lalitha KUMARI</i>	303
<i>Mr. G. Bhargav RAMUDU</i>	303
<i>Monika Sai PİNNİNTİ</i>	303
INFLUENCE of OXYGEN PRESSURE on OPTICAL PROPERTIES of RF MAGNETRON SPUTTERING Ga₂O₃ THIN FILMS	304
<i>Hicret HOPOĞLU</i>	304
<i>Hafize Seda AYDINOĞLU</i>	304
<i>Ebru Şenadım TÜZEMEN</i>	304
OPTICAL PROPERTIES OF NiO_x THIN FILMS PRODUCED BY MAGNETRON SPUTTERING AT DIFFERENT PRESSURES	305
<i>Hicret HOPOĞLU</i>	305
<i>Ebru Şenadım TÜZEMEN</i>	305
INVESTIGATION OF THE STATISTICAL RELATIONSHIP BETWEEN POROSITY, SCHMIDT HARDNESS AND WATER ABSORPTION RATES IN VOLCANIC ROCKS USING SPSS PROGRAM	306
<i>Gökhan KÜLEKÇİ</i>	306
THE STATISTICAL RELATIONSHIP OF CURE TIME AND COMPRESSIVE STRENGTH IN PASTE BACKFILLING	314
<i>Gökhan KÜLEKÇİ</i>	314
ON THE TRIVIALITY OF IWASAWA MODULE OF THE CYCLOTOMIC Z_2-EXTENSIONS OF CERTAIN REAL BIQUADRATIC	321
<i>ABDELKADER EL MAHI</i>	321
<i>M'HAMMED ZIANE</i>	321

Sm/Sr KISMİ DEĞİŞTİRME İLAVELERİNİN Bi-2212 KRİSTAL YAPISININ TEMEL ELEKTRİK MİKTARLARINA ETKİSİ

Musa DOĞRUER

ORCID ID: 0000-0002-4214-9159

Department of Medical Services and Techniques, Bolu Abant İzzet Baysal University

ÖZET

Bu çalışma, oda sıcaklığında özdirenç (ρ_{300K}), artık özdirenç (ρ_{res}), artık özdirenç oranları (RRR), ρ_{norm} , ρ_{90K} ve $\Delta\rho$ ile ilgili temel elektriksel özdirenç özellikleri üzerinde Sm/Sr değişiminin rolünü ele almaktadır. Bu çalışmada incelenen numunelerin süperiletkenlik özellikleri üzerinde Sm safsızlığının etkisini araştırmak için, sıcaklığın bir fonksiyonu olarak dc elektrik özdirenci 50 ila 110 K sıcaklık aralığında ölçülür. Mevcut çalışmada numuneler, 840 °C tavlama sıcaklığında 48 saat süreyle geleneksel katı hal reaksiyon yöntemiyle hazırlanmıştır. Ayrıca, bulk seramik bileşikler için dc elektrik özdirencinin sıcaklığa göre değişimine ait ölçümler, bir kriyojenik soğutma sisteminde geleneksel dört nokta yöntemi kullanılarak deneysel olarak gerçekleştirilmiştir. Ayrıca, yığın süperiletken numunelerin özdirenç eğrilerinde dramatik değişiklikler görülür. Deneysel sonuçlar, aliovalent Sm/Sr kısmi ikame mekanizmasının, safsızlık kalıntılarına dayanan yerel yapısal problemlerdeki arıtma/bozunma, gözeneklilik, bozulmalar, taneciklik derecesi, kısmi eriyen parçalar (tavlama sıcaklığının artırılması/azaltılması nedeniyle), tane hizalama dağılımları, mikroskobik çatlaklar, yüzey çatlağı başlatan her yerde mevcut kusurlar, tane birleştirme ve etkileşim problemlerinden dolayı Bi-2212 kristal yapısında yukarıda bahsedilen genel elektriksel nicelikleri ciddi şekilde etkilediğini göstermektedir.

Anahtar Kelimeler: $Bi_{1.7}Pb_{0.35}Sr_{1.9-y}Sm_yCa_{1.1}Cu_2O_x$, Sm/Sr ikamesi, Elektrik direnci.

EFFECT of Sm/Sr PARTIAL REPLACEMENT ADDITION ON FUNDAMENTAL ELECTRICAL QUANTITIES OF Bi-2212 CRYSTAL STRUCTURE

ABSTRACT

This study deals with the role of Sm/Sr replacement on the fundamental electrical resistivity properties as regards room temperature resistivity (ρ_{300K}), residual resistivity (ρ_{res}), residual resistivity ratios (RRR), ρ_{norm} , ρ_{90K} and $\Delta\rho$. In order to investigate the effect of Sm impurity on superconducting properties of the samples studied in this work, dc electrical resistivity as a function of temperature is measured in the temperature range from 50 to 110 K. In the current study, the samples are prepared by conventional solid-state reaction method at the annealing temperature of 840 °C for 48 h. Moreover, the measurements belonging to the change of dc electrical resistivity over temperature for the bulk ceramic compounds are experimentally performed by using the conventional four-point method in a cryogenic refrigeration system. Furthermore, there appears the dramatic changes in the resistivity curves of the bulk superconducting samples. The experimental results show that the aliovalent Sm/Sr partial

substitution mechanism affects seriously the general electrical quantities mentioned above due to the refinement/degradation in the local structural problems grounded on the impurity residues, porosity, distortions, degree of granularity, partial melting parts (because of the enhancement/reduction of annealing temperature), grain alignment distributions, microscopic cracks, surface crack-initiating omnipresent defects, grain coupling and interaction problems in the Bi-2212 crystal structure.

Key Words: Bi_{1.7}Pb_{0.35}Sr_{1.9-y}Sm_yCa_{1.1}Cu₂O_x, Sm/Sr substitution, Electrical resistivity.

1. INTRODUCTION

With the increment in the world population and especially development in the technological and industrial goods day by day, the humanbeings need much more energy. Thus, the contents related to the global energy problems including the energy efficient use, energy protection/production/saving and electricity demand based on the gradual enhancement in the energy consumption are required to be under control. Accordingly, the crucial reasons in the problems are arranged to be the energy efficiency, cost savings, resource conservation and climate protection. Of the main factors, the energy efficient use appears to be the first order. In this respect, the superconducting material which was initially discovered for the mercury heavy metal by Kamerlingh Onnes in 1911 [1] is one of the most preferred compounds for the potential application fields as regards the sensitive process control, advanced energy infrastructure, network systems, heavy-industrial technology, innovative engineering and large-scale application fields to overcome the global energy problems all over the world [2], [3], [4], [5], [6], [7], [8]. In the present work, we research the appropriate degree of aliovalent Sm/Sr partial substitute for the potential application fields of polycrystalline Bi-2212 superconducting ceramic structures with the aid of dc electrical resistivity measurements performed at 50 K-110 K. The dc electrical curves for the bulk Bi_{1.7}Pb_{0.35}Sr_{1.9-y}Sm_yCa_{1.1}Cu₂O_x superconducting compounds enable us to find the change in the resistivity features; namely, resistivity at 300 K temperature (abbreviated as ρ_{300K}), residual resistivity (ρ_{res}), ratio of residual resistivity (RRR), ρ_{norm} , ρ_{85K} , and $\Delta\rho$. The experimental results belonging to the electrical resistivity tests show that the aliovalent Sm/Sr replacement in the Bi-2212 ceramic matrix affects seriously the fundamental electrical features.

2. MATERIALS AND METHOD

In the current study, the pure and partial substitution of different Sm-sites at Sr-sites in the Bi_{1.7}Pb_{0.35}Sr_{1.9-y}Sm_yCa_{1.1}Cu₂O_x superconducting materials ($0 \leq x \leq 0.1$) are carried out in air by way of the solid-state reaction using high purity chemicals Bi₂O₃, PbO, SrCO₃, CaCO₃, CuO and Sm₂O₃ (Alfa Aesar Co., Ltd. 99.9% purity). These oxides and carbonates are weighed in stoichiometric proportion and further mixed in a grinding machine for 8 h. Then, the powder is calcined at 800 °C for 24 h in air with a heating/cooling rate of 5 °C/min. After the calcination, the powder is pressed into the rectangular bars with dimensions of 10x4x2 mm³ at the applied load of 200 MPa. The sintering is performed in two stages at 840 °C for 48 h. In the current study, the change in the dc

electrical features including the resistivity at 300 K temperature (abbreviated as ρ_{300K}), residual resistivity (ρ_{res}), ratio of residual resistivity (RRR), ρ_{norm} , ρ_{85K} , and $\Delta\rho$ of $\text{Bi}_{1.7}\text{Pb}_{0.35}\text{Sr}_{1.9-y}\text{Sm}_y\text{Ca}_{1.1}\text{Cu}_2\text{O}_x$ superconducting materials (where x is varied from 0, until 0.10) with the different aliovalent Sm/Sr partial replacement levels is examined. All the $\text{Bi}_{1.7}\text{Pb}_{0.35}\text{Sr}_{1.9-y}\text{Sm}_y\text{Ca}_{1.1}\text{Cu}_2\text{O}_x$ ceramic compounds will henceforth be shown as the Sm0, Sm1, Sm2, Sm3, Sm4 and Sm5 material. Differentiation of electrical resistivity against the environmental temperature changing in 50 K-110 K is determined with the aid of four-probe technique. Along with the experimental processes, 5 mA current is applied throughout the sample surface for $\text{Bi}_{1.7}\text{Pb}_{0.35}\text{Sr}_{1.9-y}\text{Sm}_y\text{Ca}_{1.1}\text{Cu}_2\text{O}_x$ superconducting materials. The experimental dc electrical resistivity findings are gathered by the programmable nano-voltmeter and current sources.

3. RESULTS AND DISCUSSION

3.1. Electrical resistivity findings founded on dc resistivity measurements

We examine the significant effect of Sm/Sr replacement in the polycrystalline $\text{Bi}_{1.7}\text{Pb}_{0.35}\text{Sr}_{1.9-y}\text{Sm}_y\text{Ca}_{1.1}\text{Cu}_2\text{O}_x$ crystal system on the electrical resistivity quantities (ρ_{300K} , RRR , ρ_{res} , ρ_{norm} , ρ_{90K} and $\Delta\rho$) by electrical measurements executed at the temperature range of 50 K-110 K. One can see the electrical resistivity evidence of bulk $\text{Bi}_{1.7}\text{Pb}_{0.35}\text{Sr}_{1.9-y}\text{Sm}_y\text{Ca}_{1.1}\text{Cu}_2\text{O}_x$ superconducting materials in Fig. 1. As seen from the figure, the Sm/Sr replacement in the bulk superconducting materials affects totally the electrical properties of superconducting materials. Moreover, Figure 1 reveals that each prepared compound displays standard metallic-like properties within the different dc electrical resistivity parameters. This is because, the Sm/Sr replacement level affects seriously the formation of super-electrons grounded on the coupling of electron-phonon interaction of adjacent multilayers in the Bi-2212 superconducting materials. Furthermore, Fig. 1 reveals that the existence of Sm impurity in the Bi-2212 compounds changes randomly the basic metallic properties because of the change in the permanent crystal structure problems related to the defects, lattice strains, microvoids/grain coalescences, omnipresent flaws, microscopic cracks, distortions, porosity and grain boundary coupling problems.

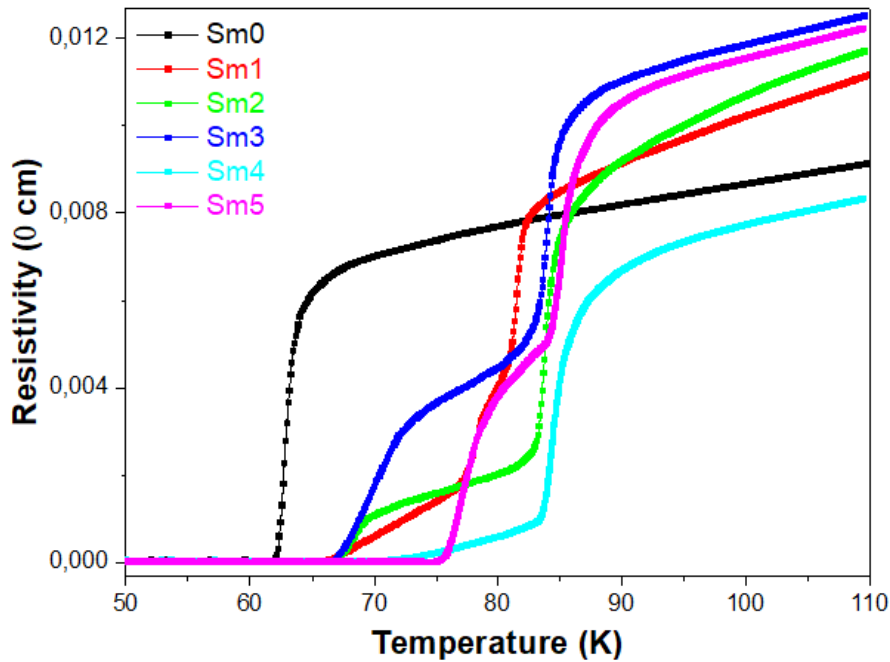


Fig. 1. Change of dc electrical curves of Sm/Sr substitution in bulk Bi-2212 materials

3.2. Resistivity at 300 K temperature

Like the metallic characteristics, when the Sm ions enhance in the superconducting matrix, the resistivity value at 300 K is measured to change randomly and the maximum value is obtained for the Sm1 sample. The ρ_{300K} parameters extracted from Fig. 1 for the polycrystalline $\text{Bi}_{1.7}\text{Pb}_{0.35}\text{Sr}_{1.9-y}\text{Sm}_y\text{Ca}_{1.1}\text{Cu}_2\text{O}_x$ superconducting materials can be seen from Table 1. Table 1 illustrates that the Sm4 compound possesses the smallest ρ_{300K} value of 22.23 mΩcm while the Sm1 material produced shows the highest ρ_{300K} of 23.3 mΩcm. The other Sm/Sr partially substituted materials have the moderate values. This means that the increase in the Sm impurity level in the bulk Bi-2212 superconducting material causes to deteriorate the itinerant charge carriers and is the formation of permanent crystal structure problems.

Table 1. Dc electrical resistivity results of Sm/Sr replaced Bi-2212 superconductors

Samples	ρ_{300K} (mΩcm)	ρ_{res} (mΩcm)	RRR (ρ_{300K}/ρ_{85K})	$\Delta\rho$ ($\rho_{300K}-\rho_{85K}$) (mΩcm)	ρ_{norm} ($\rho_{85}/\Delta\rho$)	ρ_{85K} (mΩcm)
Sm0	19.6	5.710	2.4623	11.64	0.683	7.96
Sm1	23.3	4.120	2.7476	14.82	0.572	8.48
Sm2	23.0	3.933	3.1165	15.62	0.472	7.38
Sm3	22.5	7.009	2.3437	12.90	0.744	9.60
Sm4	15.6	4.239	3.7956	11.49	0.357	4.11
Sm5	21.3	7.435	3.2819	14.81	0.438	6.49

3.3. Residual resistivity findings

The role of Sm additives on the ρ_{res} parameters of Bi-2212 materials is examined by Matthiessen's rule.

$$\rho(T) = \rho_i(T) + \rho_{res}$$

In the equation, the $\rho_i(T)$ resistance value is the temperature-varying parameter when at any temperature the total resistivity is identified as the $\rho(T)$ for a sample. Additionally, the value of ρ_{res} is temperature-independent parameter; in other words, the parameter is directly related to the dependence of crystallinity problems. One can see the ρ_{res} parameters for every material in Table 1. From the table, the Sm2 sample shows the smallest ρ_{res} value of 3.933 m Ω cm whereas the greatest ρ_{res} value of 7.435 m Ω cm is obtained for the Sm5 compound. The other compounds possess the moderate constants varying from 5.710 m Ω cm (for Sm0 material) until 4.239 m Ω cm (for Sm4 material).

3.4. ρ_{85K} parameter findings

The parameter ρ_{85K} results found are obviously illustrated in Table 1. According to the values in Table 1, the existence of Sm purity in the crystal structure leads to change randomly the value of ρ_{85K} parameter. On this basis, the Sm4 material shows the lowest ρ_{85K} parameter of 4.11 m Ω cm; on the other hand, the ρ_{85K} parameter has maximum point of 9.60 m Ω cm for the Sm3 compound. It is obvious from the experimental findings that the increment in the aliovalent Sm/Sr partial substitution affects significantly the impurity scattering and lattice strain.

3.5. RRR parameter findings

One can encounter the computed RRR parameters in Table 1. Based on the experimental findings, the material quality changes randomly with ascending the Sm/Sr replacement in the matrix. Thus, the parameter of RRR is observed to be 2.4623 for the pure sample when the value of 3.2819 is obtained for the Sm5 superconducting system. Therefore, the presence of excess manganese ions considerably deteriorates the superconducting crystal quality.

3.6. Experimental findings of $\Delta\rho$ and ρ_{norm} parameter

Differentiation of $\Delta\rho$ parameters of all the Sm/Sr partially substituted Bi-2212 superconducting materials is listed in Table 1. From the table, the substitution mechanism affects crucially the $\Delta\rho$ value as the Sm impurity level ascends in the crystal structure. On this basis, the Sm2 possesses the highest $\Delta\rho$ value of 15.62 m Ω cm; conversely, the Sm4 material has the smallest $\Delta\rho$ value (11.49 m Ω cm). The other compounds display the moderate parameters varying from 11.64 m Ω cm (Sm0 material) until 14.81 m Ω cm (for the Sm5 material). The experimental findings reveal that the increase of Sm additives in the polycrystalline Bi-2212 compounds leads to form permanent crystallinity problems. Moreover, the values of the ρ_{norm} parameter can be seen in Table 1. According to Table 1,

depending on the Sm purity level in the polycrystalline $\text{Bi}_{1.7}\text{Pb}_{0.35}\text{Sr}_{1.9-y}\text{Sm}_y\text{Ca}_{1.1}\text{Cu}_2\text{O}_x$ materials the ρ_{norm} parameter tends to change from 0.357 (for the Sm4) to 0.744 (for the Sm3).

CONCLUSION

In the present study, a relation between dc electrical resistivity features and permanent crystallinity problems is developed for $\text{Bi}_{1.7}\text{Pb}_{0.35}\text{Sr}_{1.9-y}\text{Sm}_y\text{Ca}_{1.1}\text{Cu}_2\text{O}_x$ crystal structure Sm/Sr replacement by dc electrical resistivity over environmental temperature measurements executed in range of 50 K-110 K. The pure and Sm/Sr partially replaced Bi-2212 materials are produced by the solid-state reaction method at the annealing temperature of 840 °C for duration of 48 h. According to the experimental results observed, we determine the ρ_{300K} , ρ_{res} , RRR , ρ_{norm} , ρ_{85K} and $\Delta\rho$ values for all the samples studied. It is obtained that the fundamental electrical properties seriously depend on the Sm impurity level. When the level of Sm nanoparticles enhances in the bulk $\text{Bi}_{1.7}\text{Pb}_{0.35}\text{Sr}_{1.9-y}\text{Sm}_y\text{Ca}_{1.1}\text{Cu}_2\text{O}_x$ materials, the electrical resistivity characteristics are found to randomly change because of the permanent crystallinity problems in the crystal system.

REFERENCES

- [1] H.K. Onnes, (1911). "Further experiments with Liquid Helium. D. On the change of Electrical Resistance of Pure Metals at very low Temperatures, etc. V. The Disappearance of the resistance of mercury", Koninklijke Nederlandsche Akademie van Wetenschappen Proc., 14, 113–115.
- [2] K.Y. Choi, I.S. Jo, S.C. Han, Y.H. Han, T.H. Sung, M.H. Jung, G.S. Park, S.I. Lee, (2011). "High and uniform critical current density for large-size $\text{YBa}_2\text{Cu}_3\text{O}_{7-y}$ single crystals," Curr. Appl. Phys., 11, 1020–1023.
- [3] B. Batlogg, (1998). "Cuprate superconductors: Science beyond high $T(c)$," Solid State Commun., 107, 639–647.
- [4] F.N. Werfel, U. Floegel-Delor, R. Rothfeld, T. Riedel, B. Goebel, D. Wippich, P. Schirrmeister, (2012). "Superconductor bearings, flywheels and transportation," Supercond. Sci. Technol., 25, 014007.
- [5] H.H. Xu, L. Cheng, S.B. Yan, D.J. Yu, L.S. Guo, X. Yao, (2012). "Recycling failed bulk YBCO superconductors using the NdBCO/YBCO/MgO film-seeded top-seeded melt growth method," J. Appl. Phys., 111, 103910.
- [6] A.T. Ulgen, U. Erdem, Y. Zalaoglu, T. Turgay, G. Yildirim, (2020). "Effect of vanadium addition on fundamental electrical quantities of Bi-2223 crystal structure and semi-empirical model on structural disorders-defects," J. Mater. Sci: Mater. El., 31, 13765–13777.
- [7] G. Yildirim, (2017). "Determination of optimum diffusion annealing temperature for Au surface-layered Bi-2212 ceramics and dependence of transition temperatures on disorders," J. Alloy. Compd., 699, 247–255.
- [8] S. Nagaya, N. Hirano, M. Naruse, T. Watanabe, T. Tamada, (2013). "Development of a high-efficiency conduction cooling technology for SMES coils," IEEE T. Appl. Supercond., 23, 5602804–5602807.

DIAVALENT Mn^{2+} TABAKASININ Ca^{2+} TABAKASINDA BULK Bi-2212 SİSTEMLERİNİN TEMEL ELEKTRİK MİKTARLARINDAKİ ROLÜ

Musa DOĞRUER

ORCID ID: 0000-0002-4214-9159

Department of Medical Services and Techniques, Bolu Abant İzzet Baysal University

Gürcan YILDIRIM

ORCID ID: 0000-0002-5177-3703

Department of Mechanical Engineering, Bolu Abant İzzet Baysal University

Cabir TERZİOĞLU

ORCID ID: 0000-0002-3944-0367

Department of Physics, Bolu Abant İzzet Baysal University

ÖZET

Mevcut çalışmada, polikristalin $Bi_{1.8}Sr_2Ca_{1.1-y}Mn_yCu_2O_x$ çok katmanlı süperiletken yapıdaki Ca-tabakaları (Ca^{2+}) üzerindeki farklı divalent Mn-tabakalarının (Mn^{2+}) etkisi belirlenmektedir. Oda sıcaklığı özdirenci, artık özdirenç, artık özdirenç oranları, ρ_{norm} , ρ_{85K} ve $\Delta\rho$ dahil olmak üzere bulk Bi-2212 süper iletken seramik sistemlerinin dc elektriksel direnç özelliklerinden saptırız. Her malzeme, farklı mol oranları $y = 0, 0.01, 0.03, 0.05, 0.07$ ve 0.1 ile tipik katı hal reaksiyon tekniği ile hazırlanır. Dc elektrik özdirencinin sıcaklık ölçümlerine karşı değişimi, 50 K ile 110 K sıcaklık aralığında deneysel olarak incelenmiştir. Gözlemlenen deneysel ölçüm sonuçlarına göre, temel elektriksel büyüklüklerin ikame seviyesi ile rastgele bir şekilde değiştiği gözlemlenmiştir. Bu çalışmada, taneler arası tane sınırı birleştirme bağlantı problemleri, homojen olmama, polarize edilebilir kafeslerdeki bipolaronlar, etkin ve dinamik elektron-fonon eşleşme olasılıklarının oluşumu, aşırı katkılıdan az katkılı duruma, yapısal bozukluklar-kusurlar, delik kapama enerjileri, uzun menzilli tutarlı durumda özdirenç/iletkenlik konumu ve özellikle termal dalgalanma enerjileri, yollardaki küçük homojen kümelerde süperiletkenliğin korunması, Josephson, enerji ve sızma eşiği parametreleri olmak üzere dc elektriksel büyüklüklerin temel yönlerindeki önemli değişiklikleri sistematik olarak inceliyoruz.

Anahtar Kelimeler: Elektriksel direnç, Bi-2212; Mn/Ca değişimi.

ROLE OF DIAVALENT Mn^{2+} -SITES ON Ca^{2+} -SITES ON FUNDAMENTAL ELECTRICAL QUANTITIES OF BULK Bi-2212 SYSTEMS

ABSTRACTS

In the current work, we determine the effect of different divalent Mn-sites on the Ca-sites in the polycrystalline $Bi_{1.8}Sr_2Ca_{1.1-y}Mn_yCu_2O_x$ multi-layered superconducting structure are investigated. we determine from the dc electrical resistivity features of bulk Bi-2212 superconducting ceramic systems including the room temperature resistivity, residual resistivity, residual resistivity ratios, ρ_{norm} , ρ_{85K} , and $\Delta\rho$. Every material is prepared by the typical solid-state reaction technique with the different mole-to-mole ratios of $y = 0, 0.01, 0.03, 0.05, 0.07$ and 0.1 .

The change of dc electrical resistivity versus temperature measurements is experimentally investigated in the temperature range from 50 K to 110 K. According to the experimental measurement results observed, it is found that the fundamental electrical quantities are observed to change randomly with the substitution level. In the present work, we systematically examine on the important changes in the fundamental aspects of dc electrical quantities including the intergranular grain boundary coupling link problems, inhomogeneity, bipolarons in the polarizable lattices, formation of effective and dynamics electron–phonon coupling probabilities, transition from inherit over-doped to under-doped state, structural disorders-defects, hole trap energies, location of resistivity/conduction in the long-range coherent state and especially energies of thermal fluctuation, maintenance of superconductivity in the small homogeneous clusters in the paths, Josephson coupled energy and percolation threshold parameters.

Key Words: Electrical resistivity, Bi-2212; Mn/Ca replacement.

1. INTRODUCTION

This Electrical resistivity is a significant problem for the application fields of superconducting material in the medical diagnosis, energy related sectors, industrial technology and application science. All issues completely are related to energy production, energy management policy and energy consumption. The advance in technology causes the acceleration with the exceeding of the resistivity in materials. The best way to reduce the resistance without any dissipation, power losses, energy consumption and ohmic losses is the phenomenon of superconductivity [1], [2], [3]. There are three different phases in the system which are called Bi-2201, Bi-2212 and Bi-2223 according to their chemical compositions ($\text{Bi}_2\text{Sr}_2\text{Ca}_{n-1}\text{Cu}_n\text{O}_x$) and they have critical temperatures in the regions of $\sim 20\text{K}$, $\sim 85\text{K}$ and $\sim 110\text{K}$, respectively. These phases are called very low T_c phase, low T_c phase and high T_c phase ([4]). In order to overcome or damage the problems encountered, we study the effect of various Mn/Ca substitution levels on the basic electrical properties of bulk Bi-2212 superconducting materials by temperature-dependent electrical resistivities obtained on the structural defects. It has been obtained that the purity of Mn in the superconducting system randomly changes the basic electrical properties.

2. MATERIALS AND METHOD

In the current study, the partial replacement of various Mn^{+2} sites at Ca-sites in the $\text{Bi}_{1.8}\text{Sr}_2\text{Ca}_{1.1-y}\text{Mn}_x\text{Cu}_2\text{O}_y$ materials are executed in air atmosphere by the solid-state reaction method using high purity chemicals Bi_2O_3 , SrCO_3 , CaCO_3 , CuO and MnO (Alfa Aesar Co., Ltd. 99.9% purity). These carbonates and oxides are weighed in stoichiometric percentage and then mixed in a grinding machine for 8 h. Then, the powder is calcined at $800\text{ }^\circ\text{C}$ for 24 h in air with a heating/cooling rate of $5\text{ }^\circ\text{C}/\text{min}$. The powder is pressed into rectangular bars with dimensions of $10 \times 4 \times 2\text{ mm}^3$ at 200 MPa applied load after the calcination. The sintering is exerted at $840\text{ }^\circ\text{C}$ for 48 h. Both voltage and current contacts are coated with silver paint to eliminate contact resistance. The variation of the resistivity is measured by passing 5 mA dc current through the superconducting material in the cryostat system

using a Keithley 220 current source and a Keithley 2182A nanovoltmeter. Using Labview software, the experimental indications are gathered with a correctness of about ± 0.1 K with a programmable nano voltmeter and current source. The superconductor materials created with various Mn stoichiometry such as; 0.00, 0.01, 0.03, 0.05, 0.07 and 0.1 will hereafter be indicated as Mn0, Mn1, Mn2, Mn3, Mn4, and Mn5, respectively.

3. RESULTS AND DISCUSSION

3.1. Results obtained on dc resistivity

In this current work, the basic metallic properties are obtained to change randomly with the enhancement in the Mn/Ca substitution up to a maximum concentration level of $x = 0.10$. In more detail, we examine the changes of ρ_{300K} , q_{res} , RRR , ρ_{norm} , ρ_{85K} and $\Delta\rho$ parameters by means of temperature-dependent resistivity measurements carried out temperature from 50 K to 110 K. Figure 1 shows that the dc electrical curves of Mn/Ca replacement in Bi-2212 superconducting material. From the curve, it is noticeable that the Mn/Ca partial replacement influences the basic electrical characteristic of $Bi_{1.8}Sr_2Ca_{1.1-y}Mn_xCu_2O_y$ materials. After the onset critical transition temperature, all samples demonstrate the standard metallic-like behavior as depicted in Fig. 1. In this respect, it is detected that the dc electrical resistivity results changed absolutely depending on the annealing temperature, confirming that the coupling electron-phonon interaction.

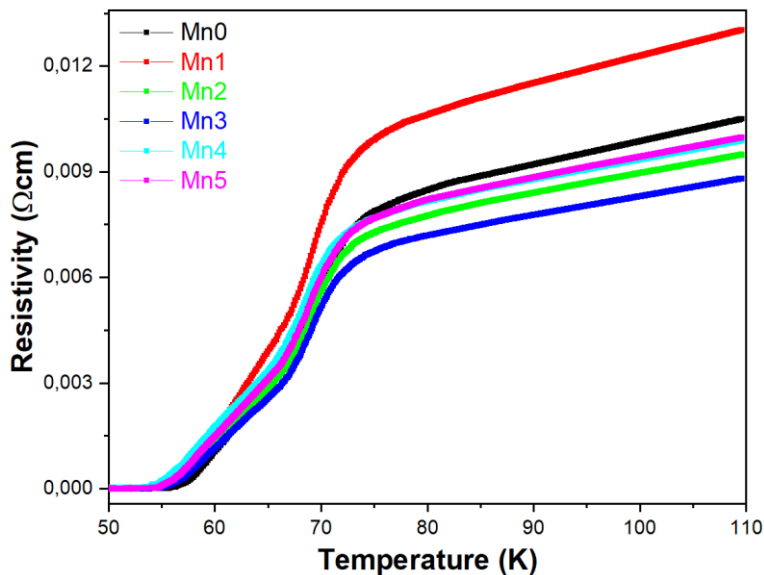


Fig. 1. Temperature-dependent dc electrical resistivity experimental findings for pure and Ca-site Mn substituted Bi-2212 superconducting materials.

3.2. Room temperature resistivity

The ρ_{300K} (room temperature resistivity) value change randomly as the Mn additive level increases in the

superconducting matrix and is found highest value for the Mn1 sample. In this regard, the ρ_{300K} results obtained are statistically depicted in Table 1. From the table, the Mn3 sample has the minimum ρ_{300K} value of 19.13 m Ω cm. Moreover, the value of Mn5 sample is found to be 21.88 m Ω cm, while the other samples of the ρ_{300K} parameters varied randomly with Mn/Ca replacement impurity level in the $\text{Bi}_{1.8}\text{Sr}_2\text{Ca}_{1.1-y}\text{Mn}_x\text{Cu}_2\text{O}_y$. This is due to the increased Mn purity concentration level in the polycrystalline superconducting system damaging the mobile hole carrier concentrations and the formation of structural problems. Further, it can be seen from the table that the existence of Mn additives damages tetragonal symmetry, hole trap energy, metastability, hybridization mechanism, inherently over-doped nature and truly metallic properties between the intergrain regions in the Bi-2212 systems ([5]).

Table 1. Dc electrical resistivity and superconducting parameters (ρ_{300K} , ρ_{85K} , ρ_{res} , RRR, ρ_{norm} and $\Delta\rho$) of pure and Ca-site Mn substituted Bi-2212 superconducting materials.

Samples	ρ_{300K} (m Ω cm)	ρ_{res} (m Ω cm)	RRR (ρ_{300K}/ρ_{85K})	$\Delta\rho$ ($\rho_{300K} - \rho_{85K}$) (m Ω cm)	ρ_{norm} ($\rho_{85}/\Delta\rho$)	ρ_{85K} (m Ω cm)
Mn0	24.56	4.888	2.759	15.66	0.568	8.90
Mn1	28.46	5.936	2.559	17.34	0.641	11.12
Mn2	20.14	4.449	2.477	12.01	0.676	8.13
Mn3	19.13	5.331	2.547	11.62	0.646	7.51
Mn4	20.82	6.062	2.443	12.30	0.692	8.52
Mn5	21.88	6.115	2.553	13.31	0.643	8.57

3.3. Residual resistivity findings

According to the literature, the Matthiessen's rule can be defined by the following equation

$$\rho(T) = \rho_i(T) + \rho_{res}$$

When the parameter $\rho_i(T)$ gives the resistivity depending on the temperature value, $\rho(T)$ is associated to the total resistivity at any temperature. Moreover, the ρ_{res} parameter is totally independent of temperature owing to the dependence of crystallinity difficulties [6]. One can see all the ρ_{res} values determined from the Fig. 1 curves in Table 1. It can be seen from the table that the Mn2 sample demonstrates the lowest ρ_{res} value of 4.449 m Ω cm while the highest ρ_{res} value of 6.115 m Ω cm is found for the Mn5 sample. The other samples have the intermediate values ranging from 4.888 m Ω cm (for the Mn0) 6.062 m Ω cm (for the Mn4).

3.4. ρ_{85K} parameter findings

We also analyze the change of ρ_{85K} parameters with the Mn/Ca substitution in the $\text{Bi}_{1.8}\text{Sr}_2\text{Ca}_{1.1-y}\text{Mn}_x\text{Cu}_2\text{O}_y$ superconducting crystal system. It is evident from the table that the ρ_{85K} value is in the range of about 8.13 m Ω cm to 11.12 m Ω cm. In addition, the presence of Mn nanoparticles in the Bi-2212 superconducting samples leads to the random change in the lattice strain and purity scattering in the crystal structure.

3.5. RRR parameter findings

The residual resistivity ratio (ρ_{300K}/ρ_{85K}) allows us to evaluate the difference in the sample attributes of the Mn/Ca replacement in the polycrystalline Bi-2212 materials. According to the table, the RRR values is observed to be about 2.759 for the Mn0 sample while the least value of 2.443 is found for the Mn4 material. In this regard, the existence of Mn influence harms the related characteristics and crystallinity quality ([7]).

3.6. ρ_{norm} and $\Delta\rho$ parameter findings

For the $\text{Bi}_{1.8}\text{Sr}_2\text{Ca}_{1.1-y}\text{Mn}_x\text{Cu}_2\text{O}_y$ materials, ρ_{norm} and $\Delta\rho$ parameters are examined with the assistance of dc electrical resistivity measurements. The $\Delta\rho$ values is related to the variation of resistivity between ρ_{300K} and ρ_{85K} values whereas the constant of ρ_{norm} is calculated from the ratio $\rho_{85K}/\Delta\rho$. These parameters give information about the variation in the defects in the Bi-2212 superconducting structure with the Mn/Ca replacement. According to the experimental results, every result is noticed to be clearly dependent on the Mn impurity level. Besides, the minimum $\Delta\rho$ are calculated about 11.62 m Ω cm for the Mn3 sample while the maximum $\Delta\rho$ are computed about 17.34 m Ω cm for the Mn1 compound. Further, the maximum ρ_{norm} value is calculated about the 0.692 for the Mn4 sample. To sum up, the electrical resistivity measurement findings demonstrate that the Mn impurity damages the electrical properties of materials.

CONCLUSION

In conclusion, we examine the effect of Mn impurities on the basic electrical and superconducting characteristics with the assistance of temperature dependent electrical resistivity experimental studies. Every material is prepared with various molar Mn purity content level of $x=0.00, 0.01, 0.03, 0.05, 0.07$ and 0.10 by the solid-state reaction method at 300 K in atmospheric air. The experimental dc electrical resistivity curves enable us to describe the ρ_{300K} , ρ_{res} , RRR , ρ_{norm} , ρ_{90K} and $\Delta\rho$ parameters. It is obtained that the dc electrical properties considerably depend on the Mn nanoparticles level. As the Mn additives level enhances in the Bi-2212 superconducting materials, the electrical resistivity features are obtained to randomly change because of the permanent local structural problems in the crystal matrix.

REFERENCES

- [9] J.D. Hodge, H. Muller, D.S. Applegate, Q. Huang, (1995). "A resistive fault current limiter based on high temperature superconductors," *Appl. Supercond.*, 3, 469–482.
- [10] S.Y. Oh, H.R. Kim, Y.H. Jeong, O.B. Hyun, C.J. Kim, (2007). "Joining of Bi-2212 high-Tc superconductors and metals using indium solders," *Phys. C*, 463, 464–467.
- [11] M. Chen, W. Paul, M. Lakner, L. Donzel, M. Hoidis, P. Unternaehrer, R. Weder, M. Mendik, (2002). "6.4 MVA resistive fault current limiter based on Bi-2212 superconductor," *Phys. C*, 372, 1657–1663.
- [12] S.E. Mousavi Ghahfarokhi, M. Zargar Shoushtari, (2010). "Structural and physical properties of Cd-doped $\text{Bi}_{1.64}\text{Pb}_{0.36}\text{Sr}_2\text{Ca}_{2-x}\text{Cd}_x\text{Cu}_3\text{O}_y$ superconductor," *Phys. B*, 405, 4643–4649.
- [13] Y. Zalaoglu, U. Erdem, F.C. Bolat, B. Akkurt, T. Turgay, G. Yildirim, (2021). "Improvement in fundamental electronic properties of Bi-2212 electroceramics with trivalent Bi/Tm substitution: a combined experimental and empirical model approach," *J. Mater. Sci: Mater. Electron*, 32, 19846–19858.
- [14] B. Akkurt, U. Erdem, Y. Zalaoglu, A.T. Ulgen, T. Turgay, G. Yildirim, (2021). "Evaluation of crystallographic and electrical superconducting features of Bi-2223 advanced ceramics with vanadium addition," *J. Mater. Sci: Mater. Electron*, 32, 5035–5049
- [15] X. Xu, J.H. Kim, S.X. Dou, S. Choi, J.H. Lee, H.W. Park, M. Rindfleisch, M. Tomsic, (2009). "A correlation between transport current density and grain connectivity in MgB_2/Fe wire made from ball-milled boron," *J. Appl. Phys.*, 105, 103913.

DETECTION OF ELEMENTAL DIVERSITY IN TEETH IN THE BY IPAA METHOD

Öğr. Gör. Ahmet ÜNLÜ

Antalya Bilim Üniversitesi, Sağlık Hizmetleri Meslek Yüksek Okulu, Tıbbi Hizmetler ve Teknikleri Programı, Tıbbi Görüntüleme Teknikleri Bölümü, Antalya, Türkiye

ORCID ID: 0000-0001-6246-1046

ABSTRACT

There are many element analysis methods for substances whose element diversity is unknown. One of them is the photon activation analysis method (IPAA). In this study, photon activation analysis method(IPAA), which is a technique developed for analytical results, was used. A linear accelerator was used for the detection of the mother and daughter nuclei in the teeth, and therefore for the determination of the element diversity in the teeth. The tooth samples used in the study were supplied by Akdeniz University Faculty of Dentistry. The conditions that determine the diversity of the data to be obtained in this study are due to the age, gender and environmental factors of the samples. The tooth has gone through various physical stages before being stimulated into the specimens. After these procedures, cLINAC is ready to be excitement. The 18 MeV tip emitted from cLINAC was exposed to bremsstrahlung photons. γ -rays emitted from tooth samples exposed to these bremsstrahlung tip exit photons were obtained using high resolution γ spectrometry. As a result of this γ spectrometry, mother and daughter nuclei were detected in the teeth. Factors that provide this difference, age, gender, nutrition types and external factors that develop depending on geographical conditions are the most important reasons for this diversity. Elements such as Sr, Ca, Co, Mg, Na, N were determined from different tooth samples examined in this study. As a result, the elements identified here help us to have very detailed information about the characteristic features of the tooth sample.

Keywords:Photo activation analysis, Nuclear Physics, γ spectrometry, Element diversity of teeth.

DETECTION OF IZOTOPES IN TOOTH SAMPLES USING THE IPAA METHOD

Öğr. Gör. Ahmet ÜNLÜ

Antalya Bilim Üniversitesi, Sağlık Hizmetleri Meslek Yüksek Okulu, Tıbbi Hizmetler ve Teknikleri Programı, Tıbbi Görüntüleme Teknikleri Bölümü, Antalya, Türkiye

ORCID ID: 0000-0001-6246-1046

ABSTRACT

With the IPAA method, which has a very important place among the element analysis methods, many substances with unknown element concentrations can be shed light on. The particular preference of the IPAA method has an important and unique place not only in elemental analysis, but also in the detection of isotopes of elements. In this study, we determined the isotopes of the elements in tooth samples using the IPAA method. Thanks to the reaction processes it went through, we were able to determine where the detected element actually came from, that is, its isotopes. Isotopes here actually mean the essence of the detected element, which is possible thanks to the detection of isotopes in the reactions of the detected element. In addition, the natural abundance ratios of the detected isotopes were discovered in this way. The isotopes of some of the dental samples examined in this study are included. The data analyzed here are the characteristic gamma rays emitted after stimulation. Characteristic gamma rays emitted from matter in the excited state were detected by gamma spectroscopy, which consists of HpGe detectors. The measured characteristic gamma-ray fingerprint is similar. While determining the isotopes, a nuclear data analysis program called Gf3 was used. In addition, Nuclear data center (NUDAT) was used for the possible reactions of the samples. Thanks to the possible reactions of the element whose main nucleus was detected, its isotopes could be determined. Thanks to the detection of the possible reaction, the daughter nucleus, hence the mother nucleus, could be detected. As a result, isotope atoms detected in dental samples have an important role in both the reactions and the determination of the main nucleus.

Keywords: IPAA, Nuclear Physics, Determine İsope, γ spectrometry

NEUROPROTECTIVE EFFECTS OF MELATONIN SLNS IN CEREBRAL ISCHEMIC INJURY MODEL

Saba SOHAIL

Department of Pharmacy, Quaid-i-Azam University, Islamabad, Pakistan

Fakhar ud DİN

Department of Pharmacy, Quaid-i-Azam University, Islamabad, Pakistan

Zakir ALI

Department of Pharmacy, Quaid-i-Azam University, Islamabad, Pakistan

ABSTRACT

The objective of this research was to formulate and characterize lipid nanoparticles (NPs) loaded with a lipophilic drug melatonin (MLT) in order to resolve its poor solubility. The method of nanotemplate engineering was used to prepare (MLT- SLNs). The prepared formulation was characterized for particle size through zeta sizer and morphology by scanning electron microscopy (SEM) and transmission electron microscopy (TEM), thermal behaviour with differential scanning calorimetry (DSC) and polymorphic changes by using powder X-ray diffraction (PXRD). In vitro

release study was conducted using dialysis bag diffusion technique while in vivo pharmacologic studies were conducted on rats. In vivo neuroprotective effects of MLT-SLNs were evaluated in cerebral ischemia induced by permanent middle cerebral artery occlusion (p-MCAO) in rats. The infarct volume in brain was measured by staining with 2,3,5-triphenyltetrazolium chloride after 48 h of cerebral ischemia. The results showed that MLT-SLNs were spherical and uniform with size ranging in nanometers. Comparative assessment of MLT dispersion by DSC and PXRD against MLT-SLNs showed significant changes in thermal behaviour as it changed from crystalline to amorphous form. In addition, the release of MLT from MLT-SLNs over 24 h was found to occur in a sustained fashion. Also, in the case of MLT-SLNs, in vivo tests for neuroprotective effects showed improved effects in infarct percentage, neurobehavioural studies, biochemical test, oxidative enzyme analysis, ELISA, immunohistochemistry and H & E staining as compared to MLT dispersion, thus enhancing the suitability of NPs to carry poorly soluble lipophilic drugs such as MLT. Further to determine the critical role of Nrf2 involved in melatonin mediated neuroprotection, we antagonized Nrf2 by All-trans retinoic acid (ATRA), and such treatment abrogated the protective effects of melatonin accompanied with exaggerated neuronal toxicity as demonstrated by increased infarction and hyper expressed inflammatory biomarkers. These findings clearly indicate that MLT-SLNs may be a promising neuroprotective pharmaceutical formulation for the treatment of cerebral ischemia, mainly by activating the Nrf2/HO-1 pathway. However, extensive exploration is still required in order to delineate the underlying protective mechanisms of MLT-SLNs. To sum up in a nutshell the findings of this study in relation to MLT-SLNs, provided a compelling argument for use of this approach in the treatment of ischemic stroke.

Key Words: Melatonin; Solid Lipid Nanoparticles; Neuroprotective; ischemic stroke

ANTIMICROBIAL ACTIVITY OF FOOD-BORNE

Lactobacillus paracasei subsp. *paracasei*

Sümeyye AKBULUT

Atatürk Üniversitesi, Fen Fakültesi, Moleküler Biyoloji ve Genetik Bölümü
ORCID ID:0000-0001-6326-5266

Elanur TUYSUZ

Atatürk Üniversitesi, Fen Fakültesi, Moleküler Biyoloji ve Genetik Bölümü
ORCID ID: 0000-0001-6052-930X

Ahmet ADIGÜZEL

Atatürk Üniversitesi, Fen Fakültesi, Moleküler Biyoloji ve Genetik Bölümü
ORCID ID: 0000-0001-8848-6647

Hakan ÖZKAN

Atatürk Üniversitesi, Fen Fakültesi, Moleküler Biyoloji ve Genetik Bölümü
ORCID ID: 0000-0003-0048-8248

Mesut TAŞKIN

Atatürk Üniversitesi, Fen Fakültesi, Moleküler Biyoloji ve Genetik Bölümü
ORCID ID:0000-0002-9350-9628

ABSTRACT

It is known that the microflora of LAB generally consists of milk and dairy products, plants, plant wastes, human and animal intestinal mucous membranes. Lactic acid bacteria found especially in dairy products (cheese, yoghurt, butter, kefir, kumiss, etc.); Since they produce antimicrobial substances such as lactic acid, diacetyl, hydrogen peroxide and bacteriocin, they have been used as a preservative culture (GRAS) in food production for many years. Therefore, these bacteria are of great importance for the food industry. The most powerful way to obtain beneficial strains for the food industry and to produce medically important products is the isolation and screening of LAB from these foods. In our present study; 26 isolates were obtained from 8 feta cheese samples obtained from Erzurum province and its districts and these isolates were phenotypically characterized at the first stage. Isolates, whose morphological and physiological analyzes were made, were then distinguished from each other on the basis of species by genomic fingerprint analysis [rep-PCR (GTG₅ and BOX PCR)]. As a result of the analysis; antimicrobial properties of 6 isolates, which are thought to be different, were tested against *Salmonella typhi*, *Staphylococcus aureus*, *Listeria monocytogenes*, *Bacillus cereus*, *Escherichia coli*, *Yersinia enterocolitica* and *Candida albicans*. The isolate showing strong antimicrobial effect was first analyzed biochemically with API 50 CHL System (bioMérieux, France) and then genomically identified by 16S rRNA sequence analysis.

Keywords: Feta cheese, lactic acid bacteria, antimicrobial effect, molecular identification

1. INTRODUCTION

The general definition of lactic acid bacteria, which constitutes a group of Gram-positive bacteria combined with their morphological, metabolic and physiological characters, is as follows: Lactic acid bacteria; They are Gram-positive, non-spore forming, catalase-negative, cytochrome-free, non-aerobic, aerotolerant, acid-tolerant, strongly fermentative, cocci or rod-shaped bacteria that produce lactic acid as the main end product during sugar fermentation. These bacteria, which are almost never encountered in water and soil; It is possible to encounter in milk and dairy products, fermented foods, some plants, intestinal systems of humans and some living things. (Jabbari *et al.* 2017, Mirzaei *et al.* 2018). They cause pH decrease by producing organic acids such as lactic acid from carbohydrate sources in their environment. lactic acid bacteria; they produce acid at these low pHs. Lactic acid bacteria have been used for many years in the production of various fermented foods. It is known that some foods subjected to lactic acid fermentation in this way have a longer shelf life due to the organic acids produced. (Nebbia *et al.* 2021). However, it has been determined that lactic acid bacteria also produce inhibitory substances such as hydrogen peroxide, free fatty acids, ammonia, diacetyl and bacteriocin, which have antagonistic effects against other microorganisms, apart from organic acids. Lactic acid bacteria are of great industrial importance as they are used as starters in the production of various foods, produce antimicrobial substances such as bacteriocin, and are included in the composition of probiotic products. Fermented products produced naturally by traditional methods or used as starter cultures and offered to consumers in the markets are a good source for lactic acid bacteria strains. Isolated strains of lactic acid bacteria; They have great potential in different fermented product production stages in terms of taste, smell, bacteriocin production. (Cholakov,*et al.* 2021). To this end; Isolation and identification of lactic acid bacteria is of great importance. Among the foods produced as a result of fermentation, the most important foods that have an important history and importance are fermented milk products. Among the fermented milk products, which have great microbiological importance, products such as cheese, yogurt, butter, kefir and kumiss are very important. Cheese is the most consumed fermented milk product, which contains the richest group in terms of microflora.

The factor that gives the cheese its unique taste and aroma is the addition of lactic acid bacteria, which is lost by pasteurization, as pure culture. The most important genera of lactic acid bacteria are; *Lactobacillus*, *Lactococcus*, *Enterococcus*, *Streptococcus*, *Pediococcus*, *Leuconostoc*, *Weissella*, *Carnobacterium*, *Tetragenococcus* and *Bifidobacterium*. In particular, it has been proven by studies that *Lactobacillus* bacteria are quite dominant in cheese microflora (Zaidi *et al.* 2017).

In our current study; Lactic acid bacteria were isolated from white cheese samples collected from Erzurum province and its districts. Obtained isolates were characterized and identified with all their phenotypic and genotypic characteristics. Among these isolates, it was aimed to detect bacteria belonging to the genus *Lactobacillus*, which is responsible for a very dominant flora in cheese. As a result of the phenotypic and genotypic characterizations, the antimicrobial activity of food-borne *Lactobacillus paracasei* subsp *paracasei*,

which was determined as suitable for the purpose, was tested as a result of the studies carried out.

2. RESEARCH AND FINDINGS

2.1. Experimental Studies

1. Sample Collection

A total of 8 white cheese samples taken from Erzurum province and its districts were brought to the laboratory environment under aseptic conditions and stored at +4°C until they were studied (Adıgüzel *et al.* 2008).

2. Isolation of Lactic Acid Bacteria

25 g of test sample was taken under aseptic conditions and homogenized in stomacher by adding 225 ml of sterile physiological water (0.85% NaCl (Merck 1.06404.1000)). Sharpe) and M17 Agar media were spread-cultivated from the appropriate dilutions and incubated for 48 hours at 35 °C. Typical-looking colonies that developed as a result of incubation were selected and placed in the prepared stock cultures for long-term preservation. They were coded (- 86°C) stored (Adıgüzel *et al.* 2008, Bin Masalam *et al.* 2018).

3. Determination of Gene Profiles of Bacteria by Rep-PCR Method

GTG₅ and BOX-PCR methods were applied for genomic fingerprint analysis of test isolates. GTG₅ and BOX universal primers were used in these methods, which were performed using specific PCR analysis. (Sáez *et al.* 2017) .

4. Phenotypic Characterization

For phenotypic characterization of test isolates; The isolates transferred to MRS and M17 agar medium were incubated at 35 °C for 24-48 hours. For phenotypic characterization, isolates were subjected to morphological (cocci, bacillus etc.) and physiological (Gram staining, catalase production test, oxidase production test, gas production test from glucose, determination of growth at different pH, temperature and salt concentrations) tests. (Sáez *et al.* 2017, Baker *et al.* 2019).

5. Determination of Antimicrobial Activity of Lactic Acid Bacteria Isolates

The antimicrobial activities of the isolates, which were differentiated on the basis of species by rep-PCR analysis, were tested against various food pathogens such as *Salmonella typhi*, *Staphylococcus aureus*, *Listeria monocytogenes*, *Bacillus cereus*, *Escherichia coli*, *Yersinia enterocolitica* and *Candida albicans* using disc diffusion method (Sanpa *et al.* 2019).

6. Biochemical Characterization

The isolate, which gave positive results from the isolates analyzed for antimicrobials, was then biochemically

characterized. The API 50 CHL System (bioMérieux, France) was used for the determination and identification of the carbon sources used by the isolate and the results obtained were APILAB Plus Ver. 3.3 (BioMérieux Diagnostic A, Istanbul).

7. Genotypic Characterization

For genotypic characterization; DNA of the isolate, which gave a positive result as a result of antimicrobial activity analysis, was isolated by applying the Promega WizardR Genomic DNA Purification kit (A2360) protocol. Then, 16S rRNA sequence analysis was performed using 27F,1492R universal primers and pGEM-T-Easy vector system (Promega, UK). The 16S rRNA gene sequences of the isolate sequence analyzed; Determined using Applied Biosystems Model 373A DNA Sequencer and ABI PRISM Cycle Sequencing Kit (Macrogen, The Netherlands). GenBank and EzTaxon (<http://blast.ncbi.nlm.nih.gov/blast.cgi> and <http://www.eztaxon.org>) servers were used to evaluate the sequence analysis results. (Ashrethalatha *et al.* 2016).

2.2. Experimental Results

In the study, 8 white cheese samples were collected from Erzurum province and its districts, and lactic acid bacteria were isolated from these samples. A total of 26 isolates were handled. Phenotypic and genotypic characterization of the isolates (Figure 1 and Figure 2), which were distinguished from each other on the basis of species by genomic fingerprint analysis, was then performed. rep-PCR (GTG₅ and BOX) method was used for genomic fingerprint analysis. According to the results of the analysis, it was determined that there were 6 different species.

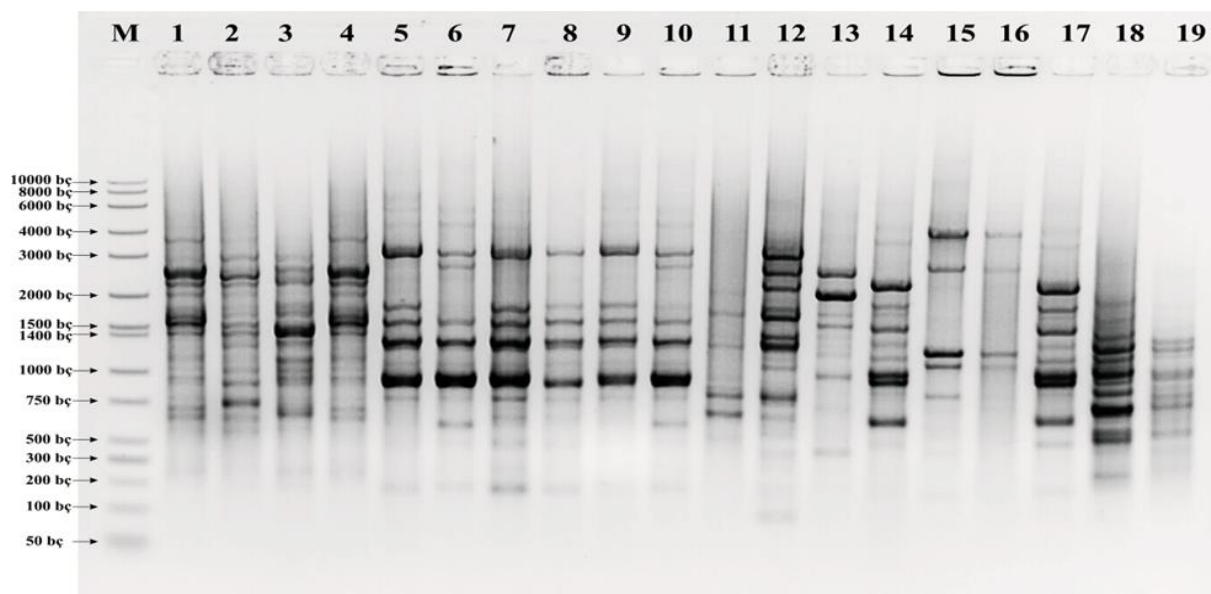


Figure 1. GTG₅-PCR band profiles of some isolates

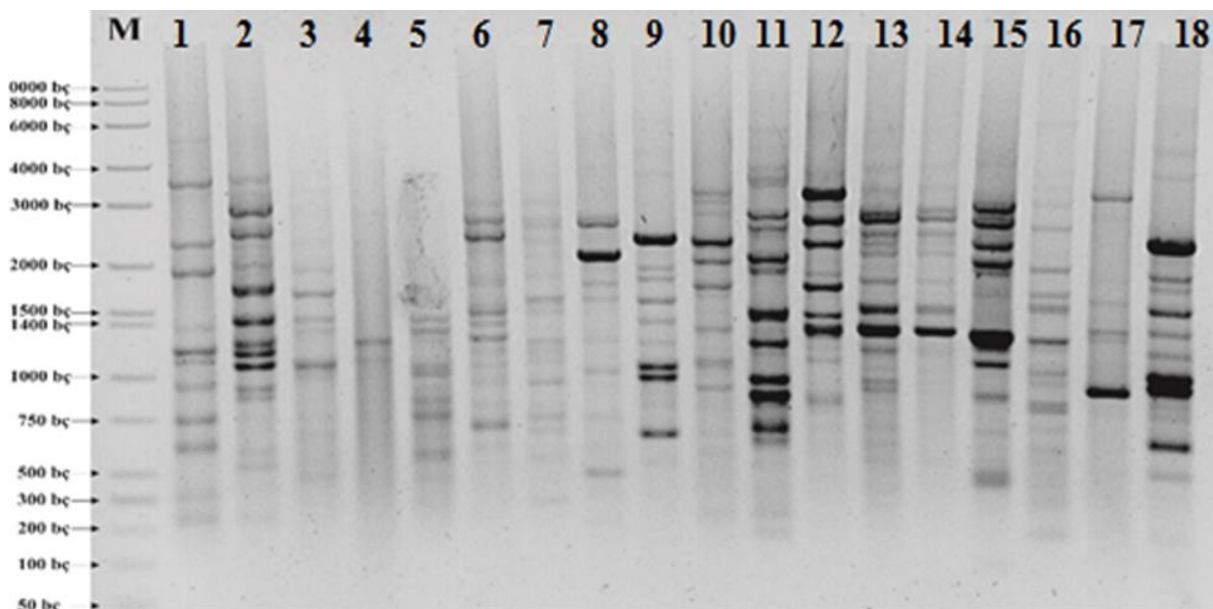


Figure 2. BOX-PCR band profiles of some isolates

According to conventional analyzes on different species; ES2, ES17 and ES24 coded isolates were morphologically bacillus; ES8, ES12 and ES20 coded isolates were determined to be cocci morphologically. In addition, it was determined that all isolates were Gram (+), oxidase (-), catalase (-) and endospore (-). In addition, as a result of the motility test, it was concluded that all isolates were immobile except for the ES2 coded isolate. When the gas production potentials of the test isolates were investigated, both homofermentative and heterofermentative isolates were found.

As a result of the tests performed to analyze which pH, temperature and salt concentrations the isolates show the best development; ES2, ES12, ES20 and ES24 coded isolates at 15-45 °C; It was determined that ES8 and ES17 coded isolates showed growth at 30-37 °C. Again, as a result of the pH analysis; ES2, ES8, ES12 and ES24 coded isolates showed the best growth at pH 4-6, ES17 and ES20 coded isolates showed the best growth at pH 5-6. As a result of salt analysis; It was determined that ES17 coded isolate 2-5%, ES2 coded isolate 2-9%, ES20 coded isolate 2-10%, ES8 and ES12 coded isolates 2-11%, ES24 coded isolate 2-12% salt concentration showed the best growth. Ni *et al.* (2015) when lactic acid bacteria were analyzed conventionally; They determined that these bacteria generally grow in an acidic environment such as pH=3 at 35-45 °C and at a salt concentration of 6.5%. Considering such literature data, it was seen that the conventional analysis results we obtained in our study were compatible with the literature data. The antimicrobial properties of 6 different isolates were tested against *Salmonella typhi*, *Staphylococcus aureus*, *Listeria monocytogenes*, *Bacillus cereus*, *Escherichia coli*, *Yersinia enterocolitica* and *Candida albicans* by disk diffusion method. As a result of the disc diffusion method, it was observed that the ES24 isolate had a strong antimicrobial effect against *Staphylococcus aureus*, *Escherichia coli*, *Candida albicans* (Table 1). Overall, the isolate with an average inhibition power of 8.01 mm was found to have a good capacity to inhibit pathogenic bacteria. Islam *et al.* (2012) investigated the

antimicrobial effect of *Lactobacillus paracasei* strain isolated from local yoghurts against pathogenic microorganisms and found that this strain had the best antimicrobial activity among the isolates and other strains. Again, Verdenelli *et al.* (2009) investigated the probiotic properties of *Lactobacillus rhamnosus* and *Lactobacillus paracasei*, which they isolated from human feces in their study; reported that these two strains have antimicrobial and antioxidant effects and can be used as probiotic organisms. In our study, it was determined that the strain with the best antimicrobial effect belonged to *Lactobacillus paracasei* subsp *paracasei* species, and it is aimed to investigate the probiotic potential of this species in future studies.

Table 1. Antimicrobial activity

Isolate	<i>Staphylococcus aureus</i>	<i>Escherichia coli</i>	<i>Candida albicans</i>
ES24	+++	++	++

zone of inhibition (mm) > 10 mm = +++, >5 mm = ++, <5 mm = +

The isolate, coded ES24, with strong antimicrobial activity was analyzed biochemically by API 50 CHL System (bioMérieux, France) (Table 2).

Table 2. API 50 CHL Results

ES24 API 50 CHL RESULTS	
<i>L-Arabinose</i>	+
<i>Ribose</i>	+
<i>Xylose</i>	+
<i>Adonitol</i>	-
<i>Galactose</i>	+
<i>D-Glucose</i>	+
<i>D-Fructose</i>	+
<i>D-Mannose</i>	-
<i>Rhamnose</i>	-
<i>Dulcitol</i>	-
<i>Mannitol</i>	-
<i>Sorbitol</i>	-
<i>Met-D-Gluc.</i>	+
<i>NAG</i>	+
<i>Amygdaline</i>	-
<i>Arbutine</i>	-
<i>Esculine</i>	-
<i>Salicine</i>	-
<i>Cellobiose</i>	-
<i>Maltose</i>	+
<i>Lactose</i>	+
<i>Melibiose</i>	+

Saccharose
 Trehalose
 Melezitose
 D-Raffinose
 Gentiobiose
 D-Turanose
 D-Tagatose
 D-Arabitol
 L-Arabitol

-
-
-
-
-
-
-
-
-

As a result of this analysis, considering that the API test kit alone was not sufficient for diagnosis, it was decided that the results should be supported by 16S rRNA sequence analysis, and then it was identified genomically by 16S rRNA sequence analysis. As a result of 16S rRNA sequence analysis, it was determined that the ES24 coded isolate was 99% similar to *Lactobacillus paracasei* subsp *paracasei*.

3. CONCLUSION

1. In our study; A total of 26 isolates were obtained from 8 white cheese samples obtained from Erzurum province and its districts.
2. The isolates, whose morphological and physiological analyzes were performed, were distinguished from each other by genomic fingerprint analysis [rep-PCR (GTG5 and BOX PCR)]. As a result of the analysis; It was concluded that 6 isolates were different from each other.
3. Antimicrobial properties of 6 isolates thought to be different; Tested against *Salmonella typhi*, *Staphylococcus aureus*, *Listeria monocytogenes*, *Bacillus cereus*, *Escherichia coli*, *Yersinia enterocolitica* and *Candida albicans*. ES24 coded isolate; It has been found to have a strong antimicrobial effect against *Escherichia coli*, *Staphylococcus aureus*, *Candida albicans*.
4. The ES24-encoded isolate was first biochemically analyzed with the API 50 CHL System (bioMérieux, France), and then genomically identified by 16S rRNA sequence analysis. As a result of 16S rRNA sequence analysis; *Lactobacillus paracasei* subsp. It was determined that it was similar to *paracasei*.

REFERENCES

1. Adıgüzel, G., Fermente Türk Sucuğundan İzole Edilen Laktik Asit Bakterilerinin Fenotipik ve Genotipik Yöntemlerle Karakterizasyonu. 2008.
2. Ashrethlatha, A., Aarthy, U., Poonkodi, T. and Narayanan, R.B. 2016. Identification and molecular characterization of Lactic Acid Bacteria (LAB) species from the medicinal plant *Cissus quadrangularis* (Pirandai). *International Food Research Journal* 23(6): 2695-2701.

3. Baker, D., Basondwah, S., Jambi, E., Rahimuddin, S.A., Abuzaid, M. and Aly, M. Molecular Identification, Characterization and Antioxidant Activities of Some Bacteria Associated with Algae in the Red Sea of Jeddah. 2019. *Pakistan Journal of Biological Sciences*. 22:467-476.
4. Bin Masalam, M.S., Bahieldin, A., Alharbi, M.G., Al-Masaudi, S., Al-Jaouni, S.K., Harakeh, S.M and Al-Hindi, R.R. 2018. Isolation, Molecular Characterization and Probiotic Potential of Lactic Acid Bacteria in Saudi Raw and Fermented Milk. *Evidence-Based Complementary and Alternative Medicine*. Volume 2018, Article ID 7970463, 12 pages.
5. Cholakov, R., Tumbarski, Y., Yanakieva, V., Dobrev, I., Salim, Y., & Denkova, Z. (2021). Antimicrobial activity of *Leuconostoc lactis* strain BT17, isolated from a spontaneously fermented cereal beverage (Boza). *Journal of Microbiology, Biotechnology and Food Sciences*, 2021, 47-49.
6. Jabbari, V., Khiabani, M. S., Mokarram, R. R., Hassanzadeh, A. M., Ahmadi, E., Gharenaghadeh, S., ... & Kafil, H. S. (2017). *Lactobacillus plantarum* as a probiotic potential from kouzeh cheese (traditional Iranian cheese) and its antimicrobial activity. *Probiotics and antimicrobial proteins*, 9(2), 189-193.
7. Mirzaei, E. Z., Lashani, E., & Davoodabadi, A. (2018). Antimicrobial properties of lactic acid bacteria isolated from traditional yogurt and milk against *Shigella* strains. *GMS hygiene and infection control*, 13.
8. Nebbia, S., Lamberti, C., Lo Bianco, G., Cirrincione, S., Laroute, V., Coccagn-Bousquet, M., ... & Pessione, E. (2021). Antimicrobial Potential of Food Lactic Acid Bacteria: Bioactive Peptide Decrypting from Caseins and Bacteriocin Production. *Microorganisms*, 9(1), 65.
9. Ni K, Wang Y, Li D, Cai Y, Pang H. 2015. Characterization, Identification and Application of Lactic Acid Bacteria Isolated from Forage Paddy Rice Silage. *PLoS ONE* 10(3): e0121967. doi:10.1371/ journal.pone.0121967.
10. Sáez, G.D., Hébert, E.M., Saavedra, L., Zárate, G. 2017. Molecular identification and technological characterization of lactic acid bacteria isolated from fermented kidney beans flours (*Phaseolus vulgaris* L. and *P. coccineus*) in northwestern Argentina. *Food Research International*. 102, 605–615.
11. Sanpaa, S., Sanpaa, S. and Suttajitb, M. 2019. Lactic acid bacteria isolates from Pla-som, their antimicrobial activities and fermentation properties in Pla-som. *Journal of Food Health and Bioenvironmental Science*. 12(1): 36-43.
12. Zaidi, N. A., Hamid, A. A., & Hamid, T. A. T. H. (2017). Lactic acid bacteria with antimicrobial properties isolated from the intestines of japanese quail (*Coturnix Coturnix Japonica*). *Galeri Warisan Sains*, 1(1), 10-12.
13. T. Islam, F. Sabrin, E. Islam, M. Billah, K.M.D. Islam, —Analysis of antimicrobial activity of *Lactobacillus paracasei* ssp. *paracasei*-1 isolated from regional yogurt, *Int. Res. J. Applied Life Sci*, vol. 1, no. 4, pp. 66-72, 2012.
14. Verdenelli MC, Ghelfi F, Silvi S, Orpianesi C, Cecchini C, Cresci A. Probiotic properties of *Lactobacillus rhamnosus* and *Lactobacillus paracasei* isolated from human faeces. *Eur J Nutr*. 2009 Sep;48(6):355-63. doi: 10.1007/s00394-009-0021-2. Epub 2009 Apr 14. PMID: 19365593.

DETECTION of SHARED CRITICAL SIGNATURES and PATHWAYS BETWEEN TYPE 2 DIABETES and HEART FAILURE

Hamid CEYLAN

Atatürk University, Faculty of Science, Department of Molecular Biology and Genetics

ORCID ID: 0000-0003-3781-4406

ABSTRACT

Diabetes mellitus (DM) has become one of the important health problems and it has been rising more rapidly. On the other hand, heart failure (HF), which is known to be associated with DM, is highly prevalent in patients with diabetes. Although they are known to be related, the common underlying critical drivers for these two diseases remain blurry. This study aims to investigate mRNA regulation in the hearts of non-diabetic HF (nD-HF) and diabetic HF (D-HF) patients. Differently expressed genes (DEGs) were identified using a transcriptome profile (GSE26887) retrieved from the Gene Expression Omnibus (GEO) database. Furthermore, gene ontology annotation, pathway enrichment analysis, protein-protein interaction (PPI) network analysis of the coexpression genes, and the module analysis of the PPI network were performed using DAVID online tool and Cytoscape software plugins (NetworkAnalyzer, MCODE, and Cytohubba) respectively. A total of 149 (88 upregulated and 61 downregulated) intersection genes were identified, whose expression is similarly altered in both non-diabetic and diabetic heart failure patients. Finally, by the PPI network analysis results, five genes (*SOCS3*, *IL6*, *MYC*, *CD274*, and *TNFSF10*) were determined as hub genes. In summary, through integrative analysis of gene expression, molecular drivers, pathways and potential therapeutic targets shared in both nD-HF and D-HF patients were identified.

Keywords: Bioinformatics, Diabetes, Heart failure, Hub genes

1. INTRODUCTION

The incidence of diabetes mellitus (DM), which has become one of the most important health problems of today, is increasing day by day. According to the World Health Organization (WHO) and International Diabetes Federation (IDF) reports, almost half a billion people worldwide have diabetes, and 1.5 million deaths each year are directly related to this health problem (van Herpt et al. 2020).

Cardiovascular diseases (CVDs) are another public health problem that has an increasing prevalence and causes an average of 18 million deaths each year (Gerc et al. 2020). Heart failure (HF), which is known to be associated with DM, is highly prevalent in patients with diabetes mellitus (Kenny and Abel 2019). It is known that the heart failure developing risk is more than 2 times higher in patients with diabetes (Dunlay et al. 2019). Although they are known to be related, the common underlying drivers critical for these two diseases remain blurry.

Increased morbidity and mortality associated with heart failure (HF) in diabetic patients underscore the need for a better understanding of the underlying molecular events (Greco et al. 2012; Rorth et al. 2018). Indeed, effective HF therapy in diabetic patients requires a complex strategy encompassing the development of improved diagnostic and prognostic markers and innovative pharmacological approaches (Inamdar and Inamdar 2016).

Given the complexity observed in polygenic or multifactorial diseases pathophysiology including DM and HF, alterations in the whole genome should be taken into account for effective treatment. Therefore, transcriptome analysis and the identification of core genes through a bioinformatics-based approach provide a molecular basis for relevant biological questions. The goal of this study was to investigate shared regulation in the hearts of diabetic HF (D-HF) and nondiabetic HF (ND-HF) patients.

2. MATERIAL AND METHODS

2.1. Data Retrieval and Differential Gene Expression Analysis

Gene expression profile (GSE26887) which includes 6 D-HF, 11 nD-HF, and 2 control individuals retrieved from Gene Expression Omnibus (GEO) database. Only male samples were analyzed. Then, differentially expressed genes were identified using the GEO2R web tool (Barrett et al. 2013). $|\logFC| > 1.0$ and $p < 0.05$ was regarded as the cut-off criteria to screen for significant DEGs. Then, the Venn diagram was drawn using the Multiple List Comparator online tool (<https://www.molbiotools.com/listcompare.php>) for screening overlapping genes between the samples. A schematic representation of the methodology used in the present study is shown in Fig. 1.

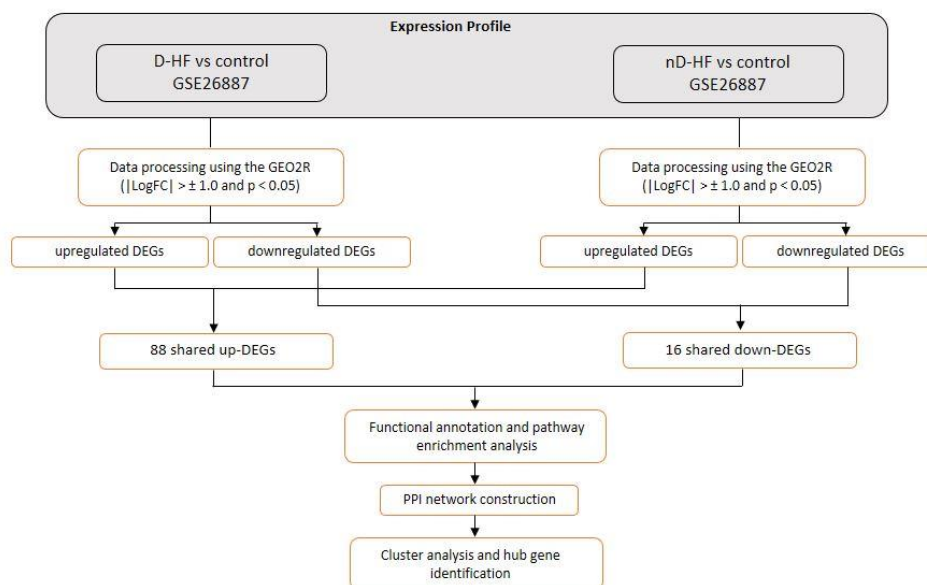


Figure 1. A schematic representation of the methodology used in the present study

2.2. Functional annotation and pathway enrichment analysis

To identify DEGs at the biologically functional level, GO (gene ontology) and KEGG (Kyoto Encyclopedia of Genes and Genomes) pathway analysis was conducted using DAVID (The Database for Annotation, Visualization, and Integrated Discovery) online tool (Huang da et al. 2009).

2.3. Protein-protein interaction network construction and selecting the hub genes

Protein-protein interaction (PPI) network was firstly mapped by STRING (The Search Tool for the Retrieval of Interacting Genes) online tool (Szklarczyk et al. 2015), and then visualized and analyzed using Cytoscape software (Shannon et al. 2003). MCODE (Molecular Complex Detection) plug-in of the Cytoscape was applied to identify significant clusters in the PPI network. Cytohubba plug-in of Cytoscape was used to screen the hub genes based on the Maximal Clique Centrality (MCC) calculation algorithm. To narrow down the number of hub gene candidates in the PPI network, the first 5 genes were ranked.

3. RESULTS

3.1. Identification of DEGs

A total of 149 (88 upregulated and 61 downregulated) intersection genes were identified, whose expression is similarly altered in both diabetic and non-diabetic heart failure patients (Figure 2a and 2b).

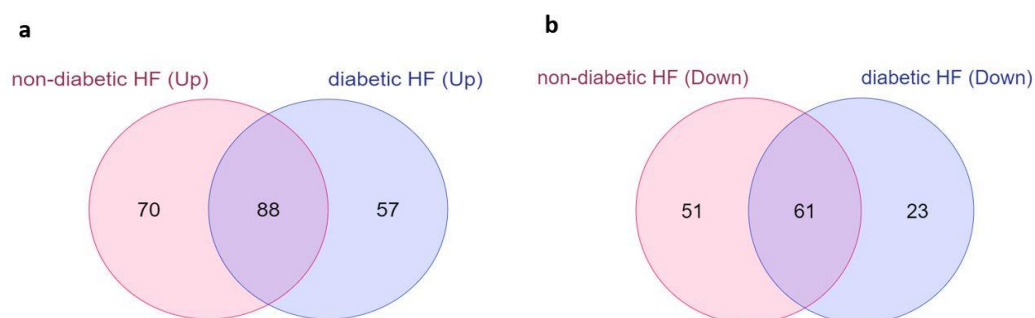


Figure 2: Venn diagram showing the overlapping DEGs between samples. 2a; overlapped upregulated genes, 2b; overlapped downregulated genes. HF; heart failure.

3.2. GO term and pathway enrichment analyses

GO analysis classified both upregulated and downregulated DEGs into three categories: molecular function (MF), biological processes (BP), and cellular components (CC). The results showed that the identified genes are involved in many critical processes and pathways, such as cellular response, regulation of blood pressure, inflammatory response, cardiac conduction system development, and TNF signaling pathway (Table 1 and 2).

Table 1. GO and KEGG pathway enrichment analysis results of the upregulated DEGs. GO; Gene Ontology, KEGG; Kyoto Encyclopedia of Genes and Genomes, BP; Biological Process, MF; Molecular Function, CC; Cellular Component.

Category	Term	Value
	negative regulation of cell differentiation	1.0E-08
	cellular defense response	1.0E-05
	positive regulation of cell proliferation	1.0E-03
	skeletal system development	1.0E-03
	regulation of blood pressure	1.0E-03
	negative regulation of transcription, DNA-templated	1.0E-03
	mRNA splicing	1.0E-03
	RNA processing	1.0E-03
	negative regulation of apoptotic process	1.0E-03
	cardiac conduction system development	1.0E-02
	cell adhesion	1.0E-02
	extracellular fibril organization	1.0E-02
	extracellular region	1.0E-03
	proteinaceous extracellular matrix	1.0E-03
	extracellular matrix	1.0E-03
	extracellular space	1.0E-02
	integral component of plasma membrane	1.0E-02
	cell-cell junction	1.0E-02
	RNA binding	1.0E-02
	extracellular matrix structural constituent	1.0E-02
	nucleotide binding	1.0E-02
	protein coupled purinergic nucleotide receptor activity	1.0E-02
KEGG_PATHWAY	neuroactive ligand-receptor interaction	1.0E-02

Table 2. GO and KEGG pathway enrichment analysis results of the downregulated DEGs. GO; Gene Ontology, KEGG; Kyoto Encyclopedia of Genes and Genomes, BP; Biological Process, MF; Molecular Function, CC; Cellular Component.

Category	Term	Value
	inflammatory response	1.0E-05
	microtubule-based process	1.0E-04
	platelet degranulation	1.0E-03
	cell cytokine production	1.0E-03
	G1/S phase response	1.0E-03
	cellular iron ion homeostasis	1.0E-02
	negative regulation of cell proliferation	1.0E-02
	positive regulation of fibroblast proliferation	1.0E-02
	immune response	1.0E-02

	positive regulation of epithelial cell proliferation	0E-02
	positive regulation of T cell proliferation	0E-02
	oskeleton organization	0E-02
	lular response to drug	0E-02
	lular response to interleukin-1	0E-02
	positive regulation of inflammatory response	0E-02
	gative regulation of cell adhesion mediated by integrin	0E-02
	und healing	0E-02
	ponse to toxic substance	0E-02
	ate inflammatory response	0E-02
	ponse to organonitrogen compound	0E-02
	colemma	0E-04
	rotubule	0E-03
	racellular space	0E-03
	inuclear region of cytoplasm	0E-02
	ernal side of plasma membrane	0E-02
	racellular membrane-bounded organelle	0E-02
	losome	0E-02
	rotein binding	0E-03
	uctural constituent of cytoskeleton	0E-03
	TP binding	0E-03
	AGE receptor binding	0E-02
	TPase activity	0E-02
	agosome	0E-04
EGG_PATHWAY	p junction	0E-03
EGG_PATHWAY	F-1 signaling pathway	0E-02
EGG_PATHWAY	IF signaling pathway	0E-02
EGG_PATHWAY	gionellosis	0E-02

3.3. PPI network and hub gene analysis

The PPI network of DEGs with combined scores greater than 0.4 was constructed by STRING online tool (Fig. 3) and visualized through Cytoscape software. According to acquired information from the STRING database, a total of 84 nodes and 113 edges were mapped in the PPI network (Fig. 4).

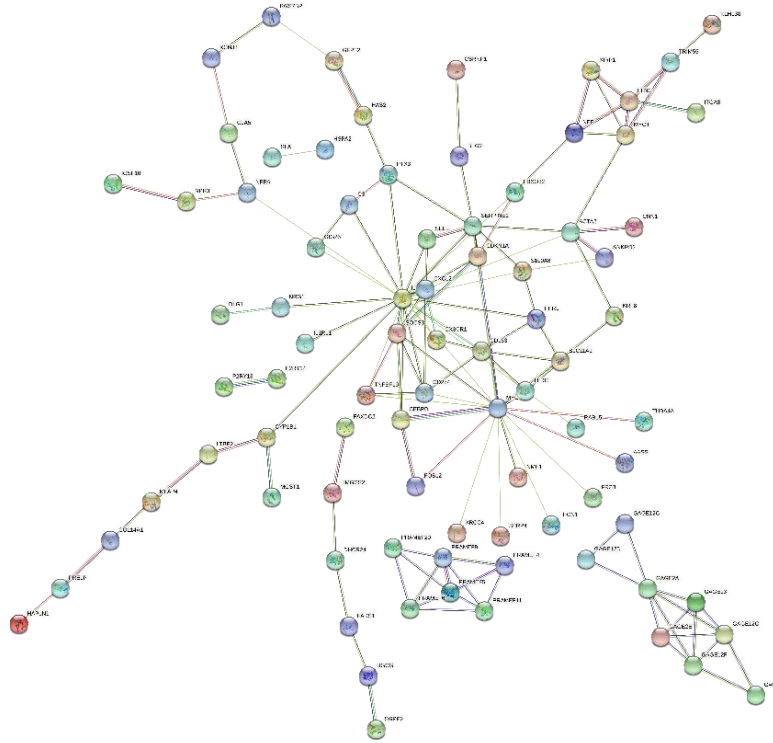


Figure 3. PPI network connectivity map generated via STRING database.

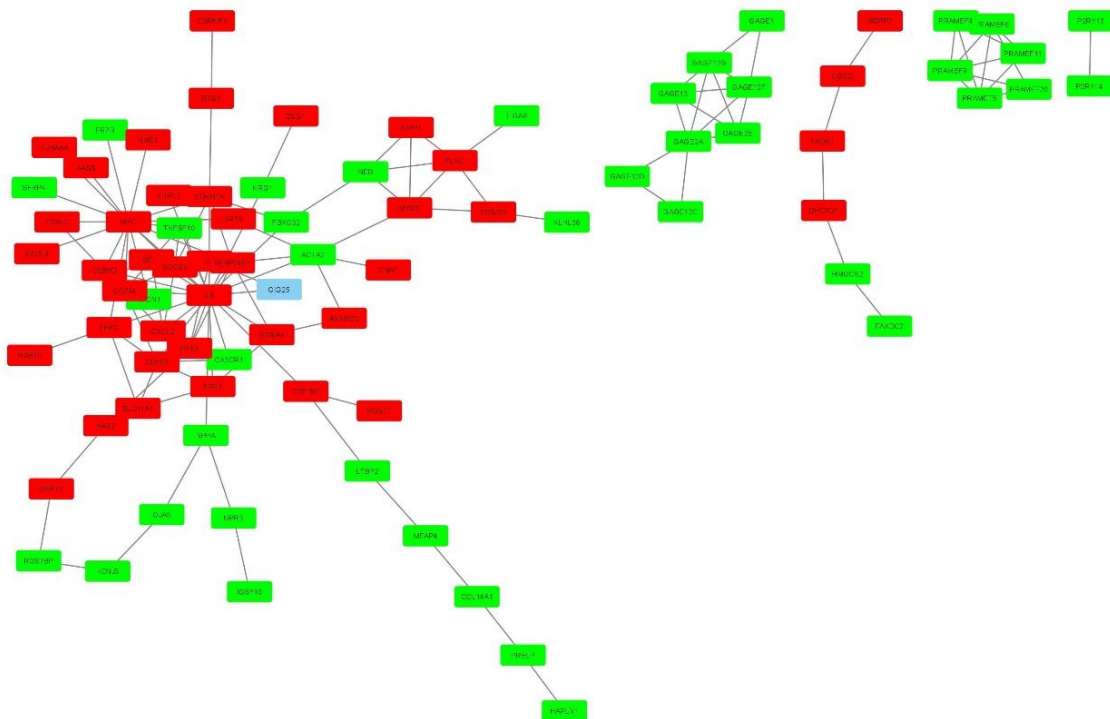


Figure 4. The whole PPI network of DEGs visualized via Cytoscape (red nodes represent downregulated DEGs and green nodes represent upregulated DEGs). PPI; protein-protein interaction.

Based on the degree of importance, one cluster (score > 5), which was composed of upregulated and downregulated genes, was then screened from the PPI network using the MCODE plug-in (Fig. 5a). It was observed that the first 5 genes ranked according to the MCC score overlapped with the cluster obtained by MCODE (Fig. 5b). Finally, by the PPI network analysis results, these five genes (*SOCS3*, *IL6*, *MYC*, *CD274*, and *TNFSF10*) were determined as hub genes.

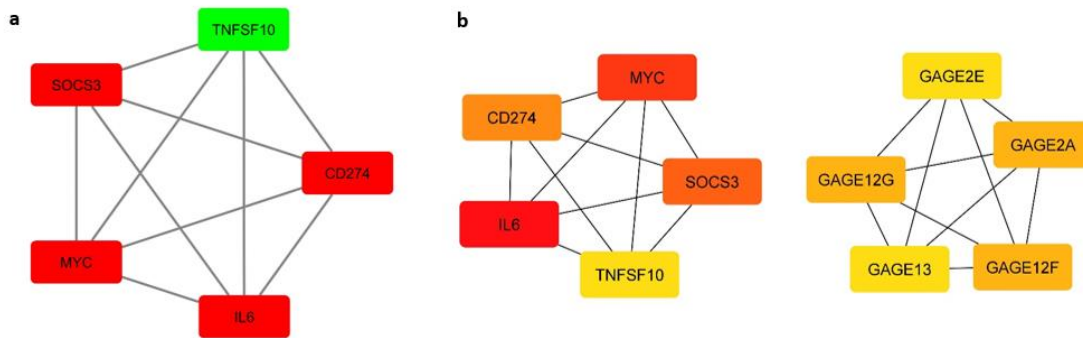


Figure 5. a: The functional sub-network analysis of PPI network. **a:** The sub-module from the PPI network of DEGs. **b:** The top-ranked DEGs according to MCC score. PPI; protein-protein interaction, MCC; Maximal Clique Centrality.

4. DISCUSSION

T2D and HF are well correlated polygenic and complex diseases and have many common risk factors. These multiple drivers, independently or together, may contribute to the pathogenesis of the disease and disrupt related pathways (Shu et al. 2017). However, an effective treatment strategy for patients suffering from these health problems has not been fully developed. Therefore, new perspectives are needed to identify molecular targets that cause disease or aggravate disease pathology. In the present study, bioinformatics analysis was engaged to explore key biomarkers and the pathological processes in myocardial tissues, acquired from nD-HF and D-HF patients and control groups. Analyzes showed that there are 5 key genes (*SOCS3*, *IL6*, *MYC*, *CD274*, and *TNFSF10*) involved in both diabetic and non-diabetic heart disease.

SOCS (suppressor of cytokine signaling) family proteins (*SOCS1–7* and *CIS*) are intracellular proteins (Yasukawa et al. 2012). Among them, *SOCS3* directly interacts with gp130, a common β -receptor component of the IL-6 (another hub gene identified in this study) cytokines, which regulates downstream signaling pathways that play pathological roles in the development of cardiac hypertrophy and HF, such as JAK/STAT and PI3K/AKT (Fischer and Hilfiker-Kleiner 2007). Clinical and experimental studies have shown reduced *SOCS3* expression in the failing human myocardium and knockout of *SOCS3* results in cardiac hypertrophy, chamber dilatation, and dysfunction (Mann et al. 2010; Yajima et al. 2011). These findings suggest that *SOCS3* and *IL6* may be new potential therapeutic targets for the treatment of cardiac hypertrophy and HF. Consistent with previous studies, our results confirmed that *SOCS3* expression was markedly downregulated in both D-HF and nD-HF patients.

MYC (*MYC* proto-oncogene, BHLH transcription factor) is a transcription factor that influences and regulates the expression of thousands of genes (Bywater et al. 2020). Previous studies have shown that *MYC* directly modulates mitochondrial biogenesis in cardiac myocytes and responds to pathological stress by regulating energy metabolism in the heart (Ahuja et al. 2010). In addition, several separate reports have revealed that *MYC* expression is significantly reduced in the failing human heart tissue (Wolfram et al. 2011; Wang et al. 2020). These results

suggest that transcription factor MYC plays critical role in heart failure developmental progress, and is a potential therapeutic target.

As a type 1 transmembrane protein, CD274 (or programmed death-ligand 1; PD-L1), plays a major role in suppressing the adaptive arm of immune systems. Although CD274 is mainly expressed on T, B, and antigen-presenting cells, it is also expressed in some non-hematopoietic tissues, including the heart (Qin et al. 2019). Expression of PD-L1 in normal tissues suggests that the PD-1/PD-L1 signaling pathway protects against tissue inflammation and helps homeostasis maintenance (Chinai et al. 2015). A study by Juchem et al. showed that cardiac pathology characterized by cardiomyocyte necrosis occurs in the absence of PD-L1 (Juchem et al. 2018). Other studies also suggest that PD-L1 expression is central to autoimmune heart disease, and reported that PDL-1 blockade cause repeated pericardial and pleural effusions that may contribute to pericarditis (Lucas et al. 2008).

The proapoptotic protein encoded by *TNFSF10* (Tumor necrosis factor-related apoptosis-inducing ligand; TRAIL), another gene identified in this study, exhibits broad biological functions (Kakareko et al. 2021). Currently, there is not enough information about the effect of TRAIL on the heart, although it is released from cardiac myocytes (Eom et al. 2016). Available evidence suggests that elevated TRAIL is associated with multiple forms of heart failure and cardiomyocyte apoptosis processes (Liao et al. 2005; Tanner and Grisanti 2021).

In summary, through integrative bioinformatics-based analysis of gene expression, key drivers that can be further investigated to determine the molecular mechanisms shared in both D-HF and nD-HF patients were identified in the present study. The limitations of our study need to be noted, such as sample size and *in vivo* validation of our findings.

REFERENCES

- Ahuja P, Zhao P, Angelis E, Ruan H, Korge P, Olson A, Wang Y, Jin ES et al (2010). Myc controls transcriptional regulation of cardiac metabolism and mitochondrial biogenesis in response to pathological stress in mice. *J Clin Invest* 120:1494-505. <https://doi.org/10.1172/JCI38331>
- Barrett T, Wilhite SE, Ledoux P, Evangelista C, Kim IF, Tomashevsky M, Marshall KA, Phillippy KH et al (2013). NCBI GEO: archive for functional genomics data sets--update. *Nucleic Acids Res* 41:D991-5. <https://doi.org/10.1093/nar/gks1193>
- Bywater MJ, Burkhart DL, Straube J, Sabo A, Pendino V, Hudson JE, Quaiife-Ryan GA, Porrello ER et al (2020). Reactivation of Myc transcription in the mouse heart unlocks its proliferative capacity. *Nat Commun* 11:1827. <https://doi.org/10.1038/s41467-020-15552-x>
- Chinai JM, Janakiram M, Chen F, Chen W, Kaplan M and Zang X (2015). New immunotherapies targeting the PD-1 pathway. *Trends Pharmacol Sci* 36:587-95. <https://doi.org/10.1016/j.tips.2015.06.005>
- Dunlay SM, Givertz MM, Aguilar D, Allen LA, Chan M, Desai AS, Deswal A, Dickson VV et al (2019). Type 2 Diabetes Mellitus and Heart Failure: A Scientific Statement From the American Heart Association and the Heart Failure Society of America: This statement does not represent an update of the 2017 ACC/AHA/HFSA heart failure guideline update. *Circulation* 140:e294-e324. <https://doi.org/10.1161/CIR.0000000000000691>
- Eom YW, Jung HY, Oh JE, Lee JW, Ahn MS, Youn YJ, Ahn SG, Kim JY et al (2016). Isoproterenol Enhances Tumor Necrosis Factor-Related Apoptosis-Inducing Ligand-Induced Apoptosis in Human Embryonic Kidney Cells through Death Receptor 5 up-Regulation. *Korean Circ J* 46:93-8. <https://doi.org/10.4070/kcj.2016.46.1.93>
- Fischer P and Hilfiker-Kleiner D (2007). Survival pathways in hypertrophy and heart failure: the gp130-STAT3 axis. *Basic Res Cardiol* 102:279-97. <https://doi.org/10.1007/s00395-007-0658-z>
- Gerc V, Masic I, Salihefendic N and Zildzic M (2020). Cardiovascular Diseases (CVDs) in COVID-19 Pandemic Era. *Mater Sociomed* 32:158-164. <https://doi.org/10.5455/msm.2020.32.158-164>
- Greco S, Fasanaro P, Castelveccchio S, D'Alessandra Y, Arcelli D, Di Donato M, Malavazos A, Capogrossi MC et al (2012). MicroRNA dysregulation in diabetic ischemic heart failure patients. *Diabetes* 61:1633-41. <https://doi.org/10.2337/db11-0952>
- Huang da W, Sherman BT and Lempicki RA (2009). Systematic and integrative analysis of large gene lists using DAVID bioinformatics resources. *Nat Protoc* 4:44-57. <https://doi.org/10.1038/nprot.2008.211>
- Inamdar AA and Inamdar AC (2016). Heart Failure: Diagnosis, Management and Utilization. *J Clin Med* 5. <https://doi.org/10.3390/jcm5070062>
- Juchem KW, Sacirbegovic F, Zhang C, Sharpe AH, Russell K, McNiff JM, Demetris AJ, Shlomchik MJ and Shlomchik WD (2018). PD-L1 Prevents the Development of Autoimmune Heart Disease in Graft-versus-Host Disease. *J Immunol* 200:834-846. <https://doi.org/10.4049/jimmunol.1701076>
- Kakareko K, Rydzewska-Rosolowska A, Zbroch E and Hryszko T (2021). TRAIL and Cardiovascular Disease-A Risk Factor or Risk Marker: A Systematic Review. *J Clin Med* 10. <https://doi.org/10.3390/jcm10061252>
- Kenny HC and Abel ED (2019). Heart Failure in Type 2 Diabetes Mellitus. *Circ Res* 124:121-141. <https://doi.org/10.1161/CIRCRESAHA.118.311371>
- Liao X, Wang X, Gu Y, Chen Q and Chen LY (2005). Involvement of death receptor signaling in mechanical stretch-induced cardiomyocyte apoptosis. *Life Sci* 77:160-74. <https://doi.org/10.1016/j.lfs.2004.11.029>
- Lucas JA, Menke J, Rabacal WA, Schoen FJ, Sharpe AH and Kelley VR (2008). Programmed death ligand 1 regulates a critical checkpoint for autoimmune myocarditis and pneumonitis in MRL mice. *J Immunol* 181:2513-21. <https://doi.org/10.4049/jimmunol.181.4.2513>

- Mann DL, Topkara VK, Evans S and Barger PM (2010). Innate immunity in the adult mammalian heart: for whom the cell tolls. *Trans Am Clin Climatol Assoc* 121:34-50; discussion 50-1.
- Qin W, Hu L, Zhang X, Jiang S, Li J, Zhang Z and Wang X (2019). The Diverse Function of PD-1/PD-L Pathway Beyond Cancer. *Front Immunol* 10:2298. <https://doi.org/10.3389/fimmu.2019.02298>
- Rorth R, Jhund PS, Mogensen UM, Kristensen SL, Petrie MC, Kober L and McMurray JJV (2018). Risk of Incident Heart Failure in Patients With Diabetes and Asymptomatic Left Ventricular Systolic Dysfunction. *Diabetes Care* 41:1285-1291. <https://doi.org/10.2337/dc17-2583>
- Shannon P, Markiel A, Ozier O, Baliga NS, Wang JT, Ramage D, Amin N, Schwikowski B and Ideker T (2003). Cytoscape: a software environment for integrated models of biomolecular interaction networks. *Genome Res* 13:2498-504. <https://doi.org/10.1101/gr.1239303>
- Shu L, Chan KHK, Zhang G, Huan T, Kurt Z, Zhao Y, Codoni V, Tregouet DA et al (2017). Shared genetic regulatory networks for cardiovascular disease and type 2 diabetes in multiple populations of diverse ethnicities in the United States. *PLoS Genet* 13:e1007040. <https://doi.org/10.1371/journal.pgen.1007040>
- Szklarczyk D, Franceschini A, Wyder S, Forslund K, Heller D, Huerta-Cepas J, Simonovic M, Roth A et al (2015). STRING v10: protein-protein interaction networks, integrated over the tree of life. *Nucleic Acids Res* 43:D447-52. <https://doi.org/10.1093/nar/gku1003>
- Tanner MA and Grisanti LA (2021). A Dual Role for Death Receptor 5 in Regulating Cardiac Fibroblast Function. *Front Cardiovasc Med* 8:699102. <https://doi.org/10.3389/fcvm.2021.699102>
- van Herpt TTW, Ligthart S, Leening MJG, van Hoek M, Lievever AG, Ikram MA, Sijbrands EJJ, Dehghan A and Kavousi M (2020). Lifetime risk to progress from pre-diabetes to type 2 diabetes among women and men: comparison between American Diabetes Association and World Health Organization diagnostic criteria. *BMJ Open Diabetes Res Care* 8. <https://doi.org/10.1136/bmjdr-2020-001529>
- Wang H, Wang X, Xu L and Cao H (2020). Identification of transcription factors MYC and C/EBPbeta mediated regulatory networks in heart failure based on gene expression omnibus datasets. *BMC Cardiovasc Disord* 20:250. <https://doi.org/10.1186/s12872-020-01527-9>
- Wolfram JA, Lesnefsky EJ, Hoit BD, Smith MA and Lee HG (2011). Therapeutic potential of c-Myc inhibition in the treatment of hypertrophic cardiomyopathy. *Ther Adv Chronic Dis* 2:133-44. <https://doi.org/10.1177/2040622310393059>
- Yajima T, Murofushi Y, Zhou H, Park S, Housman J, Zhong ZH, Nakamura M, Machida M et al (2011). Absence of SOCS3 in the cardiomyocyte increases mortality in a gp130-dependent manner accompanied by contractile dysfunction and ventricular arrhythmias. *Circulation* 124:2690-701. <https://doi.org/10.1161/CIRCULATIONAHA.111.028498>
- Yasukawa H, Nagata T, Oba T and Imaizumi T (2012). SOCS3: A novel therapeutic target for cardioprotection. *JAKSTAT* 1:234-40. <https://doi.org/10.4161/jkst.22435>

THE PROTECTION AND GUARANTEEING OF THE RIGHTS TO HEALTH PROTECTION IN THE CONDITIONS OF THE COVID-19 EPIDEMIC

Veronica POZNEACOVA

3rd year student, Moldova State University, Faculty of Law, Chisinau, Republic of Moldova

ORCID ID: 0000-0003-0762-5049

ABSTRACT

Human rights represent the subject of regulation of several international and national acts. The right to health protection is a fundamental right regulated in the international acts. Constitutional regulations guarantee the observance of this right by enshrining it at the constitutional level. The importance of the right to health cannot be denied, especially starting from the link between this right and the right to life. However, in the conditions of the pandemic situation, the state confronts with certain difficulties in the aspects related to guaranteeing and ensuring the right to health protection. This right is restricted in some aspects, including the access of people with chronic diseases to healthcare, the treatment of people with Covid-19 by all doctors without regard to their specialty. This article examines the content of the right to health protection and its restriction during the pandemic. In this context, we analyzed the international and national regulation of this right, its place in the context of human rights and violation of this right in the period of the epidemic situation.

Keywords: *right to health protection, human rights, international treaties, limitation of rights*

Introduction The pandemic situation that began in the Wuhan region of China in the December 2019 and spread around the world generated the economic, social, political and medical crisis. We can claim that the emergency bans related to coronavirus changed our lives as a consequence, we were limited in the exercising of our essential rights. The purpose of this research is to determine the influence of the pandemic situation on the exercising of the right to health protection. For achieving this goal, it is important to analyze the right to health protection as a component part of a human inalienable right and to determine if the pandemic situation causes some damages on our right to health protection or this right is completely respected by the state.

Results and discussions

The legal nature of that right can be determined by analyzing the right to health protection and by establishing the role of that right in the context of fundamental human rights. We would like to begin analyze of these topic with consideration that human's rights are those rights that belong to a person from birth, are inherent and universally recognized. [Buga L., 2013, p. 19] Speaking about the right to health protection, we would like to highlight that this right is linked to the human condition at the level of current life requirements, thanks to its content, ensuring that citizens maintain and develop their physical and mental qualities, which would allow them to participate effectively in political, economic, social and cultural life and events. Health protection contains obligations for public authorities. This consideration refers to the state's obligation to take the measures

that are necessary to ensure hygiene and public health.[Vieriu E., Vieriu D., p 307] It should be noted that this right is very complex and includes more mutual obligations of the state. To ensure this right, the state should take all measures to reduce the mortality of newborns and infant mortality, as well as it should guarantee the healthy development of the children; the state should improve all aspects of environmental and industrial hygiene; it should prevent and treat epidemic diseases and professional diseases and fight against these diseases; the state should guarantee citizens access to medical services, the possibility to be treated in the good conditions. So, the state should guarantee the treatment of illness for people that life in this state. [Cârnaț T., 2010 p. 302]

We would like to mention the history of this right that was proclaimed after the Second World War.[Ionescu C., p. 122] This fundamental right was established for the first time in 1946 in the Constitution of the World Health Organization, whose preamble proclaims that “*the enjoyment of the highest attainable standard of health is one of the fundamental rights of every human being without distinction of race, religion, political belief, economic or social condition*”. [WHO BASIC DOCUMENTS,2014,p.1] Subsequently, the right to health has been enshrined in numerous international acts: The Universal Declaration of Human Rights (art. 25); International Covenant on Economic, Social and Cultural Rights (art.12); The Universal Declaration on the Eradication of Hunger and Malnutrition; The Declaration of the United Nations Conference on the Human Environment; United Nations Conference on Environment and Development (adopted at the 1992 Rio conference). In continuation, we would like to analyze the more important articles from these international acts.

According to article 25 of Universal Declaration of Human Rights “*Everyone has the right to a standard of living adequate for the health and well-being of himself and of his family, including food, clothing, housing and medical care and necessary social services, and the right to security in the event of unemployment, sickness, disability, widowhood, old age or other lack of livelihood in circumstances beyond his control*” [Universal Declaration of Human Rights,1948, article 25 (1)]. According to this article, the state must guarantee to its citizens a good life level, free access to medical treatment and unemployment benefits. According to the second paragraph “*motherhood and childhood are entitled to special care and assistance. All children, whether born in or out of wedlock, shall enjoy the same social protection*”. [Universal Declaration of Human Rights,1948, article 25 (2)] This legal norm refers to the necessity of providing some additional support for the most socially vulnerable categories. These obligations are included in the characteristic of the social state. The Republic of Moldova rectified this convention, so our state should respect them.

According to another international convention International Covenant on Economic, Social and Cultural Rights adopted and opened for signature, ratification and accession by General Assembly resolution 2200A (XXI) of 16 December 1966 entry into force 3 January 1976 “*The States Parties to the present Covenant recognize the right of everyone to the enjoyment of the highest attainable standard of physical and mental health*”. [International Covenant on Economic, Social and Cultural Rights, 1976, art. 12 (1)] So, every person has a

right to prove his or her physical and psychical health and to do things that can help him or her in self-development. We would like to highlight the fact that everyone has right to health protection and no one can be limited in this right. *“The steps to be taken by the States Parties to the present Covenant to achieve the full realization of this right shall include those necessary for: (a) The provision for the reduction of the stillbirth-rate and of infant mortality and for the healthy development of the child; (b) The improvement of all aspects of environmental and industrial hygiene; (c) The prevention, treatment and control of epidemic, endemic, occupational and other diseases; (d) The creation of conditions which would assure to all medical service and medical attention in the event of sickness”.*[*International Covenant on Economic, Social and Cultural Rights, 1976, art. 12 (2)*] So, according to this document the state must take measures to prove the people's living conditions and health. At the global level, the issues of the right to health fall within the competence of the World Health Organization (WHO), whose main purpose is to ensure the necessary conditions for all peoples to achieve the highest degree of people's health.[Negru B., Osmochescu N., Smochină A., Gurin C., Creangă I., 2012 p. 155]

Another document that refers to the right to health protection is the Charter of fundamental rights of the European Union, which was officially proclaimed in Nice in December 2000 by the European Parliament, the Council and the European Commission. In December 2009, with the entry into force of the Treaty of Lisbon, the Charter of fundamental rights was awarded the same binding legal force as the treaties. The Charter combines into a single document the rights previously found in various legislative instruments, such as national and European laws, as well as international conventions of the Council of Europe, The United Nations (UN) and the International labor organization (ILO). Section IV "Solidarity" includes the right of workers to information and consultation within the enterprise, the right to negotiate and collective action, the right to access services for accommodation, protection, in causes that refers to unjustified dismissal from work, working conditions equal and fair and correct, the prohibition of child labor and the protection of young people at work, in family life and work life, social protection and social security, health protection, access to services or economic interests, environmental protection, consumer protection.[Safta M., 2018, p 188] So, we would like to highlight the fact that in this international Charter is included the right to health protection.

In the legal system of the Republic of Moldova the right to health protection has been applied, for the first time on the territory of actual Republic of Moldova, in 1978, being included in the Constitution of the Moldovan Soviet Socialist Republic, which extended the number of the rights and liberties adding the right to health protection, right to housing, the right to participate in public administration and the right to file complaints against state bodies and public organizations.[Rusu V., 2013, p. 37] Constitution of the Republic of Moldova in the article 36 claims that *“the right to health protection is guaranteed”* [*Constituția Republicii Moldova, 1994, art.36 paragraph (1)*]. This means that the state guarantees that the right to health protection will be respected

by the government authority and by the other people. It also means that the person cannot be limited in this right. We would like to highlight the importance of the right to health protection and to show that the public authority realizes the importance of this right in our life. The state is entrusted with several positive, complex obligations that refer to the regulation of the legal and institutional framework for compulsory health insurance, implementation of state programs to inform the population, construction of hospitals, training of personnel, medical, etc. [Safta M., 2018, p 264] According to the second paragraph of this article “*the minimum health insurance offered by the state shall be free of charge*” [Constituția Republicii Moldova, 1994, art. 36 paragraph (2)]. This means that the state must give to people the possibility to be treated without payment. “*The structure of the National Health Protection System and the means of protecting the physical and mental health of the person shall be established according to the Organic Law*” [Constituția Republicii Moldova, 1994, art. 36 paragraph (3)]. This paragraph refers to the procedure that should be respected in the process of passing the law that refers to health protection.

Speaking about of the classifications developed by the doctrine that refers to the human's rights, we will briefly outline the classification criteria developed by researchers and determine the place of the right to health protection in the context of natural human's rights. Romanian professor Ion Deleanu classifies human's rights in rights and freedoms that protect a person as a value in itself, as a biological being, rights that protect a person as a "person", as social or "molecular social relations" that can be divided into human rights and the rights of collectives of people. [Deleanu I., 1996, p. 92] According to his classification, the right to health protection is the part of the rights and liberties that refer to a person's relationship within the society or state that are exercised individually. [Deleanu I., 1996, p. 95] Professor Tudor Drăganu classifies human rights into individual freedoms, socio-economic rights, political rights, socio-political rights, public freedoms, positioning the right to health protection as a component part of the social-economic right. [Drăganu T., 1998, p. 164]

Another classification developed by legal doctrine is based on the geographical scope of the right's regulation. Within this classification, we distinguish universal protection systems, or more precisely, with a universal vocation, and regional systems that are based on so-called regional spaces, usually with a continent-wide vocation. [Bîrsan C., 2005, p. 30] The right to health protection is part of the rights with the universal protection.

Using the criterion of recipients, reporting to recipients of established protection, we can distinguish general human rights that apply to all persons and rights recognized by certain categories of persons as specific rights, such as children, women, employed persons, etc. [Bîrsan C., 2005, p. 30] According to this category, we can claim that the right to health protection as a general right, because this right is assigned to all people.

Using the same criterion, it is possible to distinguish individual rights recognized to each person individually, regardless of whether they are exercised or right that refers to the collectives of people such as the right to

association. [Law no. 212 of 24-06-2004 on the state of emergency, siege and war regime, p. 31] According to this classification, the right to health protection can be located within the framework of rights exercised individually, recognized by each person.

The Covid-19 epidemic caused the crisis of the medical system and had many other adverse social, economic and political consequences. The COVID-19 pandemic meant a great problem for the entire medical system that needed an urgent adaptation to the current situation. The first-line medical workers who entered the fight against the disease exhausted every resource available, so it was necessary to train other medical professionals besides infectious diseases or those in intensive care, due to the fact that some incorrect estimates of the duration of the pandemic were made. Another limit of our right to health protection represents the fact that the state could not take the measures that are necessary to ensure public health. The number of doctors that are sick of COVID-19 were in the permanent growth prior to vaccination of medical workers. The statistics says that the 1/3 of all sick patients were medical worker. This shows that the state could not guarantee to them a good health condition during their work and they should risk with their health for treating other people. Another limitation of our right to health is that COVID 19 is treated by all doctors who are not ill, without paying any attention to medical specialties. For example, a surgeon should work with the patients that suffer from COVID-19. This fact causes the high mortality rate of these patients. Our medical system, as well as the medicine of other countries, was not prepared for this epidemic situation, doctors did not have any protective equipment at the beginning of the epidemic that provoked the disease of many medical workers. It should be noted that for the Republic of Moldova, this COVID-19 pandemic came, first of all, with dramatic infection statistics, as well as with an unprecedented medical and economic crisis.

On the other hand, the people who have chronic diseases and must undergo outpatient treatment every 6 months did not have this possibility. This caused aggravation of symptoms of their diseases. These people are in the group of risk and all patients that died because of COVID-19 had chronic diseases. So, the health of these people is at risk. Also, we know some cases when a person was hospitalized with other illness or had surgery and was infected by COVID-19 in the hospital.

Some patients are forced to have their treatment at home, so they are treated by themselves without any medical treatment. Their health is in the risk because a person who does not have the medical training cannot understand exactly if there is nothing wrong with his health or there are reasons for concern. This situation could lead to complications of COVID-19 disease.

Speaking about the violation of the right to health protection, we should mention article 15 of the ECHR, which we consider appropriate to quote in full. *“It provides the possibility of non-compliance with the norms established by the Convention in the in the state of emergency: 1. In time of war or other public emergency*

threatening the life of the nation any High Contracting Party may take measures derogating from its obligations under this Convention to the extent strictly required by the exigencies of the situation, provided that such measures are not inconsistent with its other obligations under international law. 2. No derogation from Article 2, except in respect of deaths resulting from lawful acts of war, or from Articles 3, 4 (paragraph 1) and 7 shall be made under this provision. 3. Any High Contracting Party availing itself of this right of derogation shall keep the Secretary General of the Council of Europe fully informed of the measures which it has taken and the reasons therefor. It shall also inform the Secretary General of the Council of Europe when such measures have ceased to operate and the provisions of the Convention are again being fully executed.”

In accordance with the Decree on declaring a State of emergency No. 1 (No. 1).55 of 17-03-2020, “*the Parliament of the Republic of Moldova will inform the Genera-Secretary of The United Nations and the General- Secretary of the Council of Europe within three days of this decree and the reasons for its adoption*” (Article 5). So, we note that all the legal procedures that had to be followed were respected in accordance with the norms of national and international law.

Conclusion We can conclude that in this period people are limited in the right to health protection. This situation is common for majority of states that are fighting the COVID-19 epidemic. State can limit people in the exercising of their right during the state of emergency according to international legislation. We can claim that the pandemic situation, in general, the declaring a state of emergency, in particular, restricts, even in some cases, deprives people of one of the most important rights-the right to health protection, but the limitation of this right is absolutely legal, since all procedures of national and international legislation have been respected. It is clear that the COVID-19 pandemic has taken all of humanity by surprise, destroying the health systems, the global economy, and the social agendas of all nations. So, the only thing that we can do is to detect the violation of the right to health protection, in order to prevent it from the future violation if the state of emergency being declared.

References

- BASIC DOCUMENTS (2014). Forty-eighth edition Including amendments adopted up to 31 December 2014 World Health Organization <http://apps.who.int/gb/bd>
- Bîrsan C. (2005). *European Convention on human rights Commentary on articles* Vol. I. Rights and freedoms, All Beck Publishing House Bucharest
- Buga L., (2013). *Book on constitutional law for students of the first year* Chisinau. [Online] <https://old.criminology.md/curricula/cur2.pdf>
- Cârnaț T. (2010). *Constitutional law*, 2nd edition, Chisinau, "PRINT-CARO" publishing house.
- Constitution of the Republic of Moldova* (2016) published: 29.03.2016 in Official Monitor No. 78 art No : 140 date of entry into force: 27.08.1994 Online:<http://parlament.md/CadruLegal/Constitution/tabid/151/language/ro-RO/Default.aspx>
- Deleanu I. (1996). *Constitutional law and political institutions*, vol.II, "Chemarea" Publishing House, Iasi
- Drăganu T. (1998). *Constitutional law and political institutions-elementary treaty*. Bucharest, Lumina Lex Publishing House,

file:///D:/c%4%83r%C8%9Bi%20de%20drept/c%4%83r%C8%9Bile%20de%20drept%20constitu%C8%9Bional/CAIET%20la%20disciplina%20DREPT%20CONSTITU%C5%A2IONAL.pdf

European Convention on Human Rights (1950) as amended by Protocols Nos. 11, 14 and 15 supplemented by Protocols Nos. 1, 4, 6, 7, 12, 13 and 16 Online: [European Convention on Human Rights \(coe.int\)](http://www.coe.int)

International Covenant on Economic, Social and Cultural Rights (1966) Adopted and opened for signature, ratification and accession by General Assembly resolution 2200A (XXI) of 16 December 1966 entry into force 3 January 1976, in accordance with article 27 Online: <https://www.ohchr.org/EN/ProfessionalInterest/Pages/CESCR.aspx>

Ionescu C. *Constitutional law and political institutions*. [Online] file:///D:/c%4%83r%C8%9Bi%20de%20drept/c%4%83r%C8%9Bile%20de%20drept%20constitu%C8%9Bional/drept-constitutional-si-institutii-politice_compress.pdf

Law no. 212 of 24-06-2004 on the state of emergency, siege and war regime in the Oficial Monitor Nr. 132-137 art. 696 6666 Online: https://www.legis.md/cautare/getResults?doc_id=27024&lang=ro

Negru B., Osmochescu N., Smochină A., Gurin C., Creangă I.. (2012). *Constitution of The Republic Of Moldova. Comment*, Chisinau, Arc Publishing House

Rusu V. (2013). *Constitutional law course notes*. (Cycle I). Chisinau, USEM, [Online] https://elibrary.ceiti.md/files/12/Televca/Juridica/003_-_Dreptul_constitutional.pdf

Safta M., (2018). *Constitutional law and political institutions* Vol. I. General Theory of constitutional law. Rights and freedoms 4th edition, revised. Bucharest, Ed.: Hamangiu

Universal Declaration of Human Rights (1948) proclaimed by the United Nations General Assembly in Paris (General Assembly resolution 217 A) <https://www.un.org/en/universal-declaration-human-rights/>

Vieriu E., Vieriu D. *Constitutional law and political institutions*. [Online] https://www.academia.edu/25905820/DREPT_CONSTITU%C5%A2IONAL_%C5%9EI_INSTITU%C5%A2II_POLITICE

CEVHER HAZIRLAMA TESİSLERİNDE RİSKLERİN BELİRLENMESİ

İbrahim KONUK

Artvin Coruh University, Faculty of Health Sciences, Department of Occupational health and Safety
Cayağzı-campus

ORCID ID: 000-003- 4082-2570

Yeraltından veya açık ocaklardan çıkarılan ham cevherin işlenmeden kullanılması ekonomik değildir. Cevher zenginleştirme işlemleri, çıkarılan mineralin ekonomik olarak kullanılmasını sağlar. Cevher zenginleştirme tesisleri birçok prosesi bünyesinde barındırmaktadır, aynı zamanda zenginleştirme prosesleri sırasında kimyasalların üretildiği entegre tesislerdir. Büyük ve tehlikeli makinelerin kullanılması bu işyerlerinde iş kazalarına neden olmaktadır. Maden işleme faaliyetleri, işin doğası gereği birçok tehlike içermektedir. Günümüzde iş kazalarını ve meslek hastalıklarını önlemeye yönelik reaktif yaklaşımlar yerini koruyucu bakış açısına bırakmıştır. . Bunu başarmanın en önemli aracı ise risk değerlendirmesidir. İşyerinde risklerin belirlenmesini ve önleyici tedbirlerin alınmasını içerir. . Zenginleştirme tesisinin çalışma koşulları, çalışanların ve çevredeki toplulukların sağlığını olumsuz etkiler, solunum sisteminde rahatsızlık, gürültüye bağlı işitme kaybı ve zihinsel stres belirtileri, ağır metallerin absorpsiyonu, zararlı kimyasal gazların varlığı ve içme suyu kaynaklarının kirlenmesi gibi. Bu çalışma, maden zenginleştirme tesisinin çalışma koşullarının, çevre ve maruz kalan işçilerin ve çevredeki toplulukların sağlığı üzerindeki etkisini araştırmaktadır. Ayrıca tehlikeyi ve iş kazasını azaltmaya yönelik riskleri de tanımlar, ayrıca maden zenginleştirme tesisindeki çalışma koşulları ve toz, gürültü vb. risk faktörleri ile maden zenginleştirme işlemleri için yasal gereklilikler ve iş sağlığı ve güvenliği standartlarına odaklanmaktadır.

Anahtar Kelimeler: Zenginleştirme, Risk, Cevher, Kaza, Tehlike

RISKS IDENTIFICATION FOR MINERARAL PROCESSING PLANTS

ABSTRACT

It is not economical to use the run of mine extracted from underground or open pit mines without being processed. The processes of ore beneficiation provides the use of the mined mineral economically. Ore enrichment plants contain many processes, at the same time they are integrated facilities where chemicals are produced during the enrichment processes. The use of large and dangerous machinery makes these workplaces bring about occupational accidents. Mineral processing activities contain many dangers due to the nature of the business. Nowadays reactive approaches to prevent work accidents and occupational diseases are replaced by terms of preventive point of view. The most important tool to achieve this, the risks assessment that include the identification of risks and the taking preventive measures in the workplace. The working condition of beneficiation plant also affect the health of employees and has negative impact on the health of surrounding communities, such as disturbance in respiratory system, noise induced hearing loss and mental stress symptoms,

absorption of heavy metal, existence of harmful chemical gases and contamination of drinking water resources. This study investigates the impact of mineral enrichment plant's working condition on the environment and health of exposed workers and surrounding communities. It also describes risks for reducing danger and occupational accident and also focuses on working conditions and risk factors such as dust and noise etc in the mineral enrichment plant, legal requirements and standards of occupational health and safety for mineral enrichment processes.

Keywords : Enrichment, Risk, Ore, Accident, Danger

1. INTRODUCTION

Mining is the main industrial sector that has existed since the most primitive times and has developed at a dizzying pace in the last few decades, becoming the main sector of the industry. All of the processes carried out to turn various minerals into the most valuable raw material for the industry's needs and to separate those with economic value are called mineral processing. While rapid technological developments serve human welfare, on the other hand also brings dangers to human life and the environment. Every new material, every new machine, tool and equipment that enters the production process, if necessary precautions are not taken, poses a threat to human health, workplace safety and environmental health. A healthy working environment is the prerequisite for work peace. Because occupational accidents and diseases threaten human life and health as a result of their consequences, as well as impose heavy costs on businesses (Baradan, 2006). Considering the amount of fatal occupational accidents in the Turkish mining sector between 1996 and 2012 investigated by the International Labor Organization, although it has been observed that there has been a decrease in the number of accidents in recent years, especially in the Soma and Ermenek mine disasters in 2014 reveals that occupational health and safety practices in the mining sector should be implemented more effectively. (Grossman, 2014). Although the sector with the highest number of occupational accidents in Turkey is the construction sector, considering the frequency of occupational accidents among employees, the mining sector ranks first (TÜİK, 2013). A significant part of the ore preparation facilities in Turkey are operated with low performance. This situation is caused by the fact that the technology in the facilities is very old, as well as the lack of ore preparation information and the scarcity of trained personnel. (Onal, 2014).

In this study, possible hazardous risks are identified in terms of OHS (Occupational Health and Safety) and the measures to be taken in terms of OHS are summarized with a simple risk analysis. . The management of the possible risks is important especially in the mineral processing plant. The aim of this study is also to find out identification of risks that can stop or delay mineral processing activities and results in extra cost. Perceiving of these determined risks by employees are also other subject of this study. Risk identification is process that determines the importance of risks associated mineral processing activities. It should be part of processes, but

can be applied at any time as new risks emerges. (Okwiri, 2017).

Risk and Hazard in the Occupational Health and Safety Law No. 6331 is the danger that means the potential for harm or damage that exists in the workplace or may come from outside, that may affect the employee or the workplace; Risk refers to the possibility of loss, injury, or other harmful result resulting from the hazard. The valuable economic minerals are separated from gangue (no value) material according to their physical properties such as hardness, brittleness, structure, fracture shape, color, brightness, fluorescence, phosphorescence, magnetic susceptibility, electrical conductivity, radioactivity, in the mineral processing plant. It can be separated with the help of chemical properties such as thermal properties and different solubility and physico-chemical properties based on surface and interface properties. Flotation process is one of the most economical and efficient processes today for the selective recovery of fine sized minerals (Habashi, 2005; 2006; Willse., Napier, 2006). The main operational steps in mineral processing are as follows:

Raw ore (the ore out of mine).

Pre-Enrichment Operations (Crushing, grinding, sizing).

Enrichment Processes (Physical, chemical or physico-chemical methods).

Final step (Concentrated products and tailings).

Jaw Crusher-Cone Crusher-Rotary Crusher-Hammer Crusher-Roll Crusher-Impact Crusher-Disc Crusher- Others are used for crushing process.

Ball mill- Rod mill-Mixed Mill-Planetary Mill-Others are used for grinding process.

Grill-Fixed Screen-Vibrating Screen-Tromel Screen-Others are used for screening process. Spiral Classifier-Log Washer-Hydro cyclone-Others are used for hydraulic classification. Classification of mineral enrichment methods are as follows:

Physical (Hand picking, Gravity Separation-Jig-Shaking Table-Gemini Table-Humprey Spiral-MGS-Falcon Concentrator-Knelson Concentrator-Hydrocyclones)

Float and-Immersion Tanks.

Heavy Media Drums.

Magnetic Separation, Wet magnetic Separator-Dry Magnetic Separator-Electrostatic Separator-Others.

Chemical (Metallurgical processes-Hydrometallurgical).

Leach Tanks, In situ Leaching.

Pyrometallurgy, Smelting Furnaces.

Physical Metallurgical- Electrolysis processes.

Solvent Extraction-Cementation-Others (S. Top, H. Vapur, 2015).



Figure.1. Murgul Copper Concentrator.

2.MATERIALS AND METHOD

In this study, it is aimed to evaluate the operations of mineral processing plant in terms of OHS (Occupational Health and Safety). Identifying risks in order to take safety measures before undesired accidents happen during the activities of mineral concentrator is important with the prepared guide related with OHS. In the basis of the research, the literature review being made in books, articles, magazines found at Artvin Coruh University's library and internet media. It has been determined that very few studies have been carried out in our country related to the subject. The information and data obtained from various domestic and foreign sources have been synthesized. Identified risks are also related with working condition, equipment, machinery, physical and chemical hazards such as noise, illumination, gas, chemicals, electrical magnetic field, dust, vibration and management system, ergonomic inconveniences, human (skill and behavior of workers, inadequate training) and environmental external factors etc. In the risks identification, many hazards were observed but the probabilities and severity of risks were not determined. After the risks identification, necessary measures are applied to reduce possible hazards and occupational accidents.

3. RESULTS AND DISCUSSION

3.1. Identified hazardous risks in mineral processing activities and measures against dangers

3.1.1. Noise.

Noise affect the hearing health and sense of people negatively, disturbs physiological and the psychological balance, reduces or completely destroy work performance (efficiency), silences and quality of the environment. It is an important environmental pollution consisting of unwanted sounds (www.rsham.saglik.gov.tr). The most important effect of noise that needs to be emphasized is the hearing loss. This loss may be temporary or permanent. Temporary hearing, also called auditory fatigue. Loss may disappear after a while away from the noisy environment (this time depends on the level of the affected sound, the frequencies and the duration of the effect). It can last from a few hours to a few days. However, in a noisy environment, as a result of years of exposure, permanent hearing loss occurs. The noise level is given in dB (decibels). Decibel is not a unit in the real sense, but is the logarithm of the ratio. dB (A).

Noise measurement values of ETİ Silver Mine in dB (A).

Cone crusher floor	93-94
Ccone crusher feeder floor	101-102
Panel room	68-69
Rest room	57-58
Jaw crusher side	90-91
Grinding unit (inlet)	95-96
Grinding unit rest room	70-71
Mill floor	97-98
Mill upper floor	97-98
Grinding unit ground floor	98-99
Mill ground floor	107-108
Compressor room	89-90
Generator room	107-108
Smelting furnace	92-93
Regulator	90-91
Rest room	78-79
Resting room	47-48

Noise values should be determined in the mineral processing plant on the basis of working personnel. It should be determined whether it exceeds the value (80 dB) specified in the safety regulation. This measurement and the analyzes are repeated in 6-month periods and the noise statistics are obtained. Daily working hours for personnel should be adjusted accordingly.

In the light of these findings, it is aimed to protect and improve the health levels of employees.

The following precautions need to be taken.

1. Technical Measures: Selecting processes and programming with as little noise as possible, regular maintenance of noise sources should be performed and noise should not affect the employees in other departments by surrounding noise source with special sound absorbing partitions. It is necessary to ensure the operation of the machines in this scope.

Precautions for Workers: Those who will work in workplaces with high noise levels

should undergo regular health check-ups. The use of ear protectors (ear plug) and ear protection helmets should be ensured effectively. (S. Top, H. Vapur, 2015).



Figure.2. Ear Protectors and Helmets for Noise Protection.

Workplace noise exposure causes decreased coordination, concentration and work performance, temporary hearing loss, permanent hearing loss, stress causes heart, stomach and nervous system disorders (Ediz, et al)

3.1.2. Ergonomic Inconveniences

Ergonomic nonconformities are one of the most important issues to be considered in the ore preparation processes. Keeping employees in a fixed or inappropriate position all the time can cause musculoskeletal disorders, as well as disperse concentration and invite other hazards. Repeating the same operations thousands of times in a monotonous way, especially during manual sorting, is one of the most important factors that trigger stress. Shifting shifts to other processes at regular intervals and giving more rest time to workers dealing with tiring jobs such as manual sorting can be provided.



Figure.3. Hand sorting in Bigadic Borate Concentrator Plant Turkey, (Strauss. 2016).

3.1.2. Dust.

The run off mine ore undergoes crushing, grinding, drying cleaning, and product classification operations to become marketable commodity in mineral processing plants . These operations are highly mobile and mechanized and generate large amounts of dust. both individually and collectively.If dust control methods are inadequate, hazardous levels of respirable dust can be released into the working environment, potentially endanger the workers. In order to prevent this risk, there are occupational health and safety (OHS) regulations to limit the respirable dust being exposed by concentrator workers. Engineering controls are conducted in the operations of mineral plant to reduce dust generation and limit worker exposure. Dust collector systems are generally cooperated with operating machines for dust removal purpose. Each hoods are assambled above the opearating crusher, screens. conveyor etc and connected to suction and filtration unit through pipes in the dust collector system.



Figure.4.Dust suction and filtration unit (Tech flow, 2002).

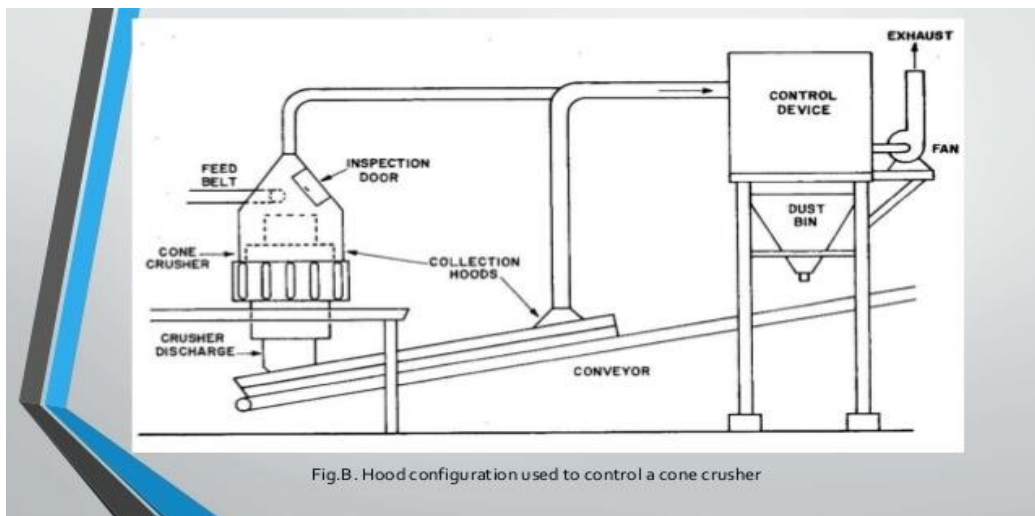


Fig.B. Hood configuration used to control a cone crusher

Figure.5. Hood configuration used to control a cone crusher (Tech flow,2002).

Water spraying,, electrostatic separator and fan ventilation are another methods for dust supression. By preferring wet processes, the problem can be eliminated at the source. Alternatively, the use of dust masks as PPE (Personnel Protective equipment) or dust collectors can be provided. Otherwise, diseases such as quartz-

induced silicosis, iron-induced siderosis and coal-borne anthracosis appear related with dust exposed workers. Briefly dust exposure in the workplace causes occupational respiratory diseases, Irritation of eyes, ears, nose, throat and skin, damage to machinery and equipment, weakening of vision distance and undesirable odors.(Official Gazette, 2013)

3.1.3. Chemical hazards.

Various types of organic or inorganic chemicals are used to separate valuable minerals from gangue materials efficiently in mineral processing plant. Complex minerals such as lead-zinc, copper-zinc, copper-zinc-lead enriched by separating them from each other with the help of control reagents and collector reagents in the flotation process. Large amounts of collector, frother, suppressor and control reagents (suppressants, promoter, pH adjusters, dispersants, and foam inhibitors etc) are needed in flotation units. Solid particles of water used in mineral processing plant contaminated with poisonous flotation reagents, metal ions (copper, lead, zinc, nickel) and arsenic, fluoride, mercury, antimony and chloride ions. In order to prevent the contamination of water tanks with these particles, conditioning of circulated water is required to accelerate the settling of fine particles in thickeners and residue pools. Flocculating and coagulating reagents are used for this purpose.

While working with chemical substances, only authorized persons should work with and prepare chemicals and must use the necessary PPE (Personnel Protective Equipment) when using the chemical substance. Chemicals should not be stored anywhere other than the storage area. Material safety document form before using any chemical substance should be examined. Safety showers and eye care washing stations should be available and their layout should be hung (NSW, 2002).



Figure.6. Eye washing station (Helvacioğlu, 2016).

Chemicals containing cyanide have been used efficiently and safely for more than 125 years for gold and silver recovery. The average cyanide concentration in cyanide leaching applications is around 250 ppm. The lethal dose for hydrogen cyanide is 50 mg, and 200-300 mg for sodium and potassium salts. Since cyanide can easily evaporate at low pH, it should be used in processes at high pH, between pH 9.3 and 9.5 (Renklidağ , Karaman, 2003).

Extreme care should be taken when processing radioactive minerals such as uranium and thorium and boron ores containing poisonous arsenic such as realgar and orpiment. Xanthates are reagents, commonly used in flotation processes for enrichment of metallic minerals such as copper, lead, zinc, gold etc. in the flotation unit of mineral processing plant. They evolve carbon disulphide gas on combustion or on water mixing. Suspected acute carbon disulphide toxicity has been reported during xanthate reagent preparation at gold mine (Donoghue, 1998).

3.1.4. Working in confined spaces.

It can be any space of an enclosed nature where there is a risk of death or serious injury from hazardous substances or dangerous conditions (eg lack of oxygen). Some confined spaces are identified as enclosures with limited openings which are storage tanks, silos, reaction vessels, enclosed drains, sewers and unventilated or poorly ventilated rooms.

Hazards in confined spaces are divided into atmospheric and physical.

Atmospheric hazards; Suffocating atmospheres, toxic gases, oxygen deficiency/excess, flammable and explosive atmospheres, toxic atmospheres, irritant or corrosive atmospheres.

Physical hazards; Material collapse and falling objects, mechanical equipment, working at height, electric shock and decreased vision.

Safe working conditions should be maintained in confined spaces and the people responsible for these areas should be determined, the suitability of the health status of the people who will work in these areas should be checked, confined spaces entry permits should be issued and only authorized persons should enter these areas. All emergency procedures in confined spaces should be prepared (HSE, 1997).

3.1.5. Mechanical hazards.

Machine parts may do linear, rotary or oscillating motion individually or in combination. In many cases, moving parts can exert a force that cause injury to workers working with the machine.

In order to avoid mechanical hazards necessary precautions should be taken given below.

Raising awareness of employees about mechanical hazards and safe working through training.

It is possible to prevent unauthorized persons from working with machines inappropriately.

Appropriate clothing when working closely with machines with moving parts must be worn,

Machine guards should be placed around all moving machinery parts. All electrical appliances and hand tools should be regularly checked and maintained. Do not allow someone else to operate the machine during

maintenance and repair work. Appropriate machine labeling should be done to prevent that danger. Emergency stop button should be placed on the machines to be used in dangerous situations.

3.1.6. Electricity

It is not possible to work in the facilities without electricity. Employees using electricity

face with threatening conditions. Faults and unsafe working with electricity causes closure of the entire processes, fires in the work area and destruction of machines. It can also cause serious injury and death to workers.

The precautions that can be taken in the workplace are as follows:

Performing electrical work only by trained and authorized personnel and the use of plastic gloves and appropriate shoes during the electrical occupation. Use of earth leakage circuit breaker in all circuits in the workplace. Putting insulated mats for works on distribution panels and main switch. Pay attention to grounding, care should be taken not to stay wet while working in an electrical environment. In addition, a fire extinguisher should be used instead of water in a fire that may arise from electricity due to conductivity. In processes where mineral separation is made with the help of magnetic field, pacemaker, metal prosthesis, etc. users should not be operated (S. Top, H. Vapur, 2015).

Inadequate training

Periodic OHS trainings are given once a year for very dangerous workplaces, once every 2 years for hazardous workplaces, and once every 3 years for less hazardous workplaces. Duration of that training is at least 16 hours in very dangerous workplaces, at least 12 hours in hazardous workplaces, and at least 8 hours in less hazardous workplaces and is arranged for each employee.

All of the employees are obliged to perform the task assigned to them at the working place to maintain the necessary safety conditions.

5. CONCLUSION

Within the scope of the study, the risks identification and the basic measures to be taken against the risks that may occur in terms of OHS (Occupational health and safety) in the mineral processing plant were examined. An empirical risk analysis has not been outlined. Mineral processing vary depending on the properties of the minerals to be enriched. It should not be forgotten that different hazards in mineral processes come together and increase the degree of risk and cause worse results. Therefore, it is important to provide safe working environment. Stress is also another important factor to be considered. It is of great importance that the

institutions and organizations that provide technical support on OHS which are currently implemented, regardless of interest and objectively taking into account the issues specified in the regulation. Considering that Turkey is partially rich in mineral reserves, it is in the first place in terms of boron reserves and second in terms of thorium reserves, and the OHS culture has just begun to settle; Turkey needs to set world standards in terms of OHS methods to be applied in processing these ore and the other ores. When the sources of risks are examined, maintenance-repair works result in higher risk. This result emergence that mineral processing is one of the most dangerous sector. Taking measures regarding employee health and safety in enrichment processes are the most important factors for the prevention of work accidents and occupational diseases. In this case the risk identification and assessment that are vital and important tools.

4. REFERENCES

- Baradan, S., 2006. Türkiye İnşaat Sektöründe İş Güvenliğinin Yeri ve Gelişmiş Ülkelerle Kıyaslanması, DEÜ Mühendislik Fakültesi Fen ve Mühendislik Dergisi, S. 87-100.
- Donoghue , A. M., 1998. Carbon disulphide absorbtion during xanthate reagant mixing in a mineral concenrator, Occup Med, Issue 48, p. 469-478.
- Ediz İ. G. ve ark, Madencilikte Gürültüye Bağlı İşitme Kayıplarının İncelenmesi, Türkiye 13. Kömür Kongresi Bildiriler Kitabı (TMMOB Maden Mühendisleri Odası), (Birinci Baskı), Sayfa: 14-15, Zonguldak, 2002.
- Grossman, L., 2014. Rescue Robots Could Help in Next Turkey Mine Disaster, New Scientist, 222, Issue 2970, S. 24.
- Habashi, F., 2005. A Short History of Hydrometallurgy, Hidrometallurgy, Issue79, p. 15-22.
- Habashi, F., 2006. A Short History of Mineral Processing Proceedings of XXIII International Mineral Processing Congress, p. 3-8
- (HSE) Health and Safety Executive, Confined spaces 1997. A brief guide to working safely, Sayfa:1- 5, <http://www.hse.gov.uk/pubns/indg258.pdf>, (Access date: 17.11.2021)
- http://www.rshm.saglik.gov.tr/bolumler/bolumdetaylari/cevresagligi/guruItu_calisma.htm. (Access date: 18.11.2021)
- NSW., 2002. Department of Mineral Resources, Minerals Industry Safety Handbook. Part-4. P. 90-92,
- Okwiri, A. L., 2017. Risk assesment and risk modelling in geothermal drilling, MSc thesis. Iceland School of Energy School of Science and Engineering Reykjavik University.
- Önal, G., (Önal, G., Ateşok, G., Tahsin, K.), 2014. Cevher Hazırlama El Kitabı, Yurt Madenciliğini Geliştirme Vakfı Yayınları, İstanbul, S. 632.
- Renklidağ, T., Karaman, A.G., 2003. Siyanür Zehirlenmesi , Sürekli Tıp Eğitimi Dergisi, 12, 9, S. 350-353.
- Official gazette., 2013(Resmi Gazete, Tozla Mücadele Yönetmeliği, Resmi Gazete Sayısı: 28812, Ankara.
- S. Top, H. Vapur., 2015. İSG Yönünden Cevher Hazırlama Proseslerindeki Problemler ve Önerilen Çözümler. Maden İşletmelerinde İşçi Sağlığı ve İş Güvenliği Sempozyumu, Adana.
- Strauss. T., 2016. Ore sorting in mining. Ore sorting-www.merlyn-consulting.com/wp-content/upload (Access date: 18.11.2021).
- Tech flow.,2002. https://techflow.net/mineral_grinding.html (Access date: 19.11.2021).
- TÜİK, 2013. İş Kazaları ve İşe Bağlı Sağlık Problemleri Araştırma Sonuçları Raporu, S. 26.
- Wiils. B. A, TJ Napier-Munn ., 2006, Mineral Processing Technology 7th Edition, Elsevier Science & Technology Books, p. 444.
- Helvacıoğlu.M., 2016. Bakır cevherlerinin zenginleştirilmesi işletmesinde iş sağlığı ve güvenliğinin değerlendirilmesi (İş Sağlığı ve Güvenliği Uzmanlık Tezi).

KRONİK FLORÜR UYGULAMASININ ZEBRA BALIĞI KARACİĞERİNDEKİ ANTIOKSİDAN ENZİMLER ÜZERİNE ETKİSİ

Emine TORAMAN

Atatürk University, Science Faculty, Department of Molecular Biology and Genetics
ORCID ID: 0000-0001-7732-6189

Melike KARAMAN

Atatürk University, Science Faculty, Department of Molecular Biology and Genetics
ORCID ID: 0000-0002-0973-2561

Ekrem SULUKAN

Atatürk University, Fisheries Faculty, Aquaculture Department
ORCID ID: 0000-0002-4414-9873

Saltuk Buğrahan CEYHUN

Atatürk University, Fisheries Faculty, Aquaculture Department
ORCID ID: 0000-0003-1808-5041

Harun BUDAK

Atatürk University, Science Faculty, Department of Molecular Biology and Genetics
ORCID ID: 0000-0002-7371-8959

ÖZET

Florür, kimyasal formülü F⁻ olan inorganik ve mono-atomik bir anyondur. Suda, havada ve toprakta doğal olarak bulunur. Halk sağlığı üzerinde nörotoksik, genotoksik, oksidatif hasar ve bilişsel becerilerin bozulması gibi etkileri vardır. Florür; içme suyu, yiyecekler, ilaçlar, sınaî ve kozmetik ürünler gibi çeşitli kaynaklardan vücuda alınabilmektedir. Piyasada bulunan diş macunları ve ağız temizleme ürünleri de mevcut florür kaynaklarıdır ve vücuttaki florür konsantrasyonunu artırmaktadır. Diş macunları ve ağız temizleme solüsyonlarındaki florür konsantrasyonları 230-1500 mg/L arasındadır. Okul öncesi çağındaki çocukların yutma refleksinin yetersizliği, daha fazla miktarda florür alımına neden olmaktadır. Yapılan çalışmada belirli dozlara alınan florürün zebrafish karaciğer dokusundaki antioksidan enzim aktiviteleri üzerindeki etkisi araştırılmıştır. Çalışmada yetişkin zebra balıklarına, kullanımına izin verilen dozlar dikkate alınarak 6 hafta boyunca 1.5, 5 ve 100 ppm florür uygulaması gerçekleştirilmiştir. Kronik maruziyet sonrasında balıklar disekte edilerek karaciğer dokuları alınmıştır. Daha sonra bu dokulardaki SOD, CAT ve GPx enzim aktiviteleri incelenmiştir. Elde edilen sonuçlar değerlendirildiğinde; kontrol grubuna göre kıyaslandığında SOD aktivitesinin 1.5 ve 5 ppm'de anlamlı bir değişim göstermediği fakat 100 ppm'de anlamlı bir azalma gösterdiği bulunmuştur. CAT aktivitesi değerlendirildiğinde; 1.5, 5 ve 100 ppm dozlarında aktivitede kontrol grubuna kıyasla istatistiksel olarak anlamlı bir artış görülürken, GPx aktivitesinde ise uygulanan üç dozun da aktivitede anlamlı bir değişim göstermediği tespit edilmiştir. Elde edilen tüm sonuçlar göz önüne alındığında düşük dozlarda kronik florür uygulamasının zebra balığında oksidatif hasar oluşturarak antioksidan enzim sistemini etkilediği görülmüştür.

Anahtar Kelimeler: Flor, zebra balığı, antioksidan enzim

EFFECT of CHRONIC FLUORIDE ADMINISTRATION on ANTIOXIDANT ENZYMES in ZEBRAFISH LIVER

ABSTRACT

Fluoride is an inorganic and monoatomic anion with the chemical formula F^- . It occurs naturally in water, air and soil. It has effects such as neurotoxic, genotoxic, oxidative damage and deterioration of cognitive skills on public health. Fluoride can be taken into the body from various sources such as drinking water, food, drugs, industrial and cosmetic products. Commercially available toothpastes and mouthwashes are also sources of fluoride and increase the fluoride concentration in the body. Fluoride concentrations in toothpastes and mouthwash solutions range from 230-1500 mg/L. Insufficiency of swallowing reflex in preschool children causes higher fluoride intake. In the study, the effect of fluoride taken at certain doses on antioxidant enzyme activities in zebrafish liver tissue was investigated. In the study, 1.5, 5 and 100 ppm fluoride solutions were applied to adult zebrafish for 6 weeks, taking into account the allowed doses. After chronic exposure, fish were dissected and liver tissues were taken. Then, SOD, CAT and GPx enzyme activities in these tissues were examined. When the results obtained are compared with the control group, it was found that SOD activity did not show a significant change at 1.5 and 5 ppm, but showed a significant decrease at 100 ppm. When CAT activity is evaluated, while a statistically significant increase was observed in the activity at 1.5, 5 and 100 ppm doses compared to the control group. Also, it was determined that the three doses applied did not show a significant change in the GPx activity. Considering all the results obtained, it has been observed that chronic fluorine application at low doses affects the antioxidant enzyme system by creating oxidative damage in zebrafish.

Key words: Fluoride, zebrafish, antioxidant enzyme

1. INTRODUCTION

Fluorine is an essential trace element for proper organism function. Due to its high reactivity, it is only found in a bound state in the natural environment. En elektronegatif element ve en güçlü oksidanlardan biridir. It has the lowest molecular mass and smallest ion radius among all halogens, so it easily penetrates cells and changes its chemical properties by binding with other elements and compounds. In conditions exceeding the toxic dose, fluorine shows harmful effects on the organism. Fluoride ions can affect the enzyme system. They can directly or indirectly modulate enzyme activity by forming complexes with metals incorporated into enzyme molecules (Zhang et al. 2013). In this way, it interferes with the course of metabolic processes involving carbohydrates, lipids and proteins. Fluorine inhibits or, less frequently, activates important enzymes involved in many metabolic pathways. These are enzymes that are mainly involved in glycolysis and Krebs. In addition, it inhibits fatty acid oxidation and reduces the activity of pyruvate dehydrogenase, which reduces the amount of acetyl-

CoA in cells and reduces cholesterol synthesis. Sodium fluoride (NaF) negatively regulates the concentration of Na⁺, K⁺ and ATPase activity, which is an important enzyme in the polymerization of amino acids, thus inhibiting the binding process of amino acids to peptides and blocking DNA synthesis (Stawiarska-Pieta et al. 2012). Prolonged exposure to fluorine compounds produces morphological changes in many organs, resulting in dysfunction. Organs particularly susceptible to the effects of fluoride are the liver and kidneys. Pathological changes also occur in the heart, pancreas and lungs. Previous studies have shown that disturbances in redox processes play an important role in the pathomechanism of the observed changes. Fluoride ions exhibit the ability to initiate a process called respiratory burst and stimulate superoxide radical production. By interacting with reactive oxygen components, it disrupts cell function, oxidizes enzymes and other structural and transmembrane proteins, changing the structure and permeability of cell membranes (Caglayan et al. 2021).

Fluoride is often classified as a trace element. However, there is much more to the environment than the term 'trace' implies. People can be exposed to high levels of fluoride from natural (drinking water and vegetables and fruits from endemic areas) or industrial (fluorine emission) sources and from the misuse of dental care products containing fluoride. When fluoride is digested, it accumulates in calcifying tissues such as bone, cartilage and dental tissues. There are many studies showing that the appropriate amount of fluoride is beneficial for health to prevent dental caries. However, if ingested in excessive amounts, it can adversely affect health. Chronic fluorosis results from excessive fluoride ingestion over a long period of time. In humans, mottled teeth are an obvious clinical manifestation of dental fluorosis when the fluoride level in drinking water exceeds 1.5 ppm. Dental fluorosis can develop in permanent teeth at the age of 6-8 years (Guner et al. 2016). Pathological changes in enamel are dose dependent. At higher amounts, ingested fluoride is retained in bone, but there is an ongoing debate as to whether chronic fluorosis causes metabolic, functional, and structural damage to soft tissues. The liver is one of the target organs attacked by excess fluoride. Prolonged exposure to fluoride leads to disruption of many metabolic processes and reduced detoxification abilities of that organ. Histopathological examinations showed that the liver of animals exposed to fluoride had increased degrees of hepatocellular necrosis, degenerative changes, hepatic hyperplasia, centrilobular necrosis, inflammation, and hepatocyte infiltration (Dec et al. 2018). Fluorine also exacerbates amino acid deamination processes and inhibits the conversion of sorbitol to fructose. Oxidative stress is a common mechanism by which chemical toxicity can occur in the liver. Excessive fluoride intake causes oxidative stress, DNA damage, modifications of membrane lipids, apoptosis and cell cycle changes in hepatocytes (Błaszczuk et al. 2011). Studies have shown that high fluoride plays an important role in oxidative stress caused by active oxygen and free radicals. However, the consequences of chronic exposure to low doses of fluoride have not been clarified. In our study, the effect of low doses of fluoride exposure on antioxidant enzymes in liver tissue in zebrafish was investigated.

2. RESEARCH AND FINDINGS

2.1. Experimental Studies

2.1.1 Experimental Materials

In the study, 6 months old and healthy AB genotype zebra fish obtained from Atatürk University Fisheries Experimental Research Unit were used. Acrylic tanks measuring 35 cm x 20 cm x 23 cm (length x width x height) were used in the experiment. NaF obtained from a commercial company was used as fluoride source in the study.

2.1.2. Formation of Experimental Groups and Fluoride Exposure

A total of 4 groups were used in the study. For each group, 20 fish (10 males: 10 females) were placed in the tanks. The water temperature was maintained at approximately 28 °C with the aid of the heater. Animals were acclimated for at least one week prior to experiments and fed twice daily with a standard diet (artemia and flake food). The tanks of the treatment and positive control groups were adjusted to 1.5 mg/L, 5 mg/L and 100 mg/L with fluoride prepared by dissolving them in distilled water. During the 6-week exposure period, 2/3 of all tank water was replenished daily with freshly prepared water of the same concentrations and temperature. The fluoride concentration determined in the study was chosen considering the amount that can be taken daily and the acceptable fluorine concentrations in drinking water. After 6 week exposures, the fish were dissected and liver tissues were taken.

2.1.3. Determination of Antioxidant Enzyme Activities

Liver samples from zebrafish chronically exposed to fluoride were weighed and washed three times with 0.9% isotonic solution, and then 1/5 phosphate buffer (50 mM, pH: 7.4, containing 10mM EDTA) was added. After the tissue was homogenized, it was centrifuged at 10000 g for 30 minutes at 4°C. The supernatant was used for enzyme activity. SOD activity determination, Sun et al. (1998) according to the method specified. SOD activity was measured according to xanthine-xanthine oxidase and nitroblue tetrazolium method. One SOD unit was defined as the amount of enzyme that inhibited the NBT reduction rate by 50%. CAT activity determination, Aebi et al. (1984) according to the method. Specific enzyme activity was expressed as EU/mg protein. GPx activity determination, Beutler et al. (1984) according to the method. Specific enzyme activity was expressed as EU/mg protein.

2.1.4. Statistical analysis

Data from all experiments were analyzed by one-way analysis of variance (ANOVA), followed by post hoc comparisons between experimental groups. Significance was determined as $P < 0.05$. Data are presented as

mean \pm SEM.

2.2. Experimental Results

Fluoride has a known therapeutic effect against dental caries, but any element can cause side effects if taken in overdose. In this context, high levels of F in water sources cause endemic fluorosis in humans. In animal models, chronic treatment with high doses of F has been shown to effect several tissues. Many proteins and enzymatic systems have been shown to undergo changes when exposed to high levels of F (Pereira et al. 2013). Fluoride is important for the growth and development of living organisms. The fluoride concentration in uncontaminated fresh water ranges from 0.01 to 0.3 mg/L and is quite low. Additionally industrialization, use of agricultural pesticides and fluoride-containing fertilizers, discharge of fluoridated municipal water, decomposition of fluoride minerals, anthropogenic and natural activities such as volcanic eruption contribute to the increased fluoride load in surface waters and groundwater reserves.

Oxidative stress is generally recognized as one of the most common effects of fluoride. Fluoride causes toxicity to organisms. Because it can catalyze excessive radical production, which can cause cell death and tissue damage by disrupting the activities of antioxidant enzymes, lipid peroxidation, and modification of nucleic acids. Many studies have shown that fluoride can inhibit antioxidant enzymes such as superoxide dismutase (SOD), catalase (CAT) and glutathione peroxidase (GSH-Px), alter the glutathione level (GSH) and induce the formation of excessive reactive oxygen species (ROS). Fish liver is the main detoxification organ, especially sensitive to exogenous toxic substances. It can metabolize and transform toxic substances taken into the body through various mechanisms of action. Therefore, it has a powerful detoxification function, making the liver a target organ for toxic substances (Cao et al. 2020).

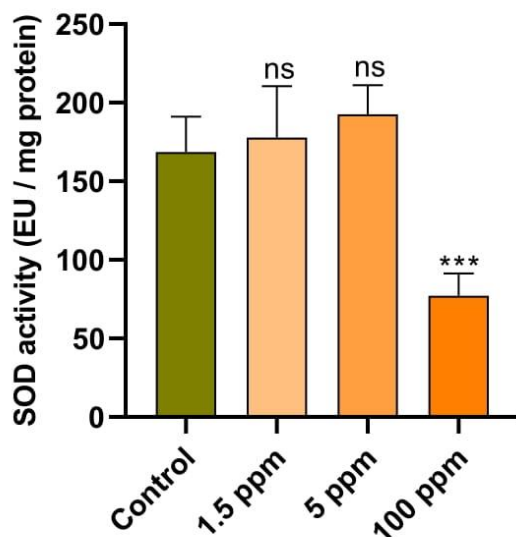


Figure 2.2.1. SOD specific activity in liver tissue

When the studies in the literature are examined, it is seen that fluoride may cause structural and functional abnormalities in the liver. In our study, when the change in SOD activity in the liver was examined; when compared to the control group, there was no significant change in the 1.5 and 5 ppm groups, while a statistically significant decrease was observed in the 100 ppm group. This indicates that 100 ppm is extremely toxic to the cell and may inhibit SOD activity by inhibiting antioxidant capacity.

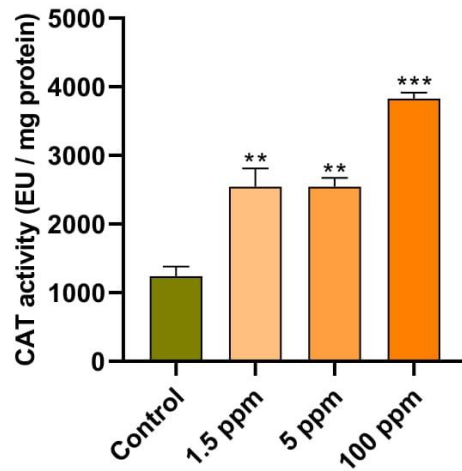


Figure 2.2.2. CAT specific activity in liver tissue

When the change in CAT activity is examined; a statistically significant increase was observed in all three treatment groups compared to the control group. This shows that fluoride works to prevent oxidative stress by activating antioxidant system enzymes.

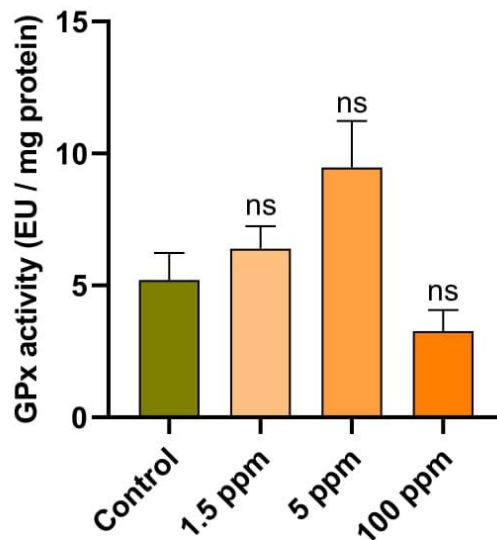


Figure 2.2.3. GPx specific activity in liver tissue

When the GPx activity in the liver after fluoride treatment was examined, there was no statistically significant change in all three fluoridated groups compared to the control group.

3. CONCLUSION

Fluorine is an extremely reactive chemical element that forms compounds with almost all other elements. The molecular mechanism of fluoride toxicity is mainly related to the destruction of the delicate oxidant/antioxidant balance, which can lead to liver damage through oxidative damage. Many studies have shown that exposure to fluoride can cause oxidative stress by generating excess superoxide radicals and their derivatives including peroxynitrite, hydrogen peroxide, hydroxyl radicals. Oxidative stress in aquatic organisms can be reflected in the antioxidant system. Antioxidant enzymes such as SOD, CAT, GPx are important defense enzymes against ROS and are generally considered as oxidative stress biomarkers. Many studies have shown that fluoride can induce excessive ROS generation and decrease SOD, CAT and GPx activities in the liver of experimental animals. In our study, it was observed that excessive amounts of ROS were produced after fluoride exposure and inhibited and decreased SOD activity in zebrafish liver, while significantly increasing CAT activity.

KAYNAKÇA

- Blaszczyk, I., Birkner, E. and Kasperczyk, S., 2011. "Influence of Methionine on Toxicity of Fluoride in the Liver of Rats", *Biological Trace Element Research*, 139 (3), 325-331.
- Caglayan, C., Kandemir, F. M., Darendelioglu, E., Kucukler, S. and Ayna, A., 2021. "Hesperidin protects liver and kidney against sodium fluoride-induced toxicity through anti-apoptotic and anti-autophagic mechanisms", *Life Sciences*, 281
- Cao, J. L., et al., 2020. "Sesamin attenuates histological alterations, oxidative stress and expressions of immune-related genes in liver of zebrafish (*Danio rerio*) exposed to fluoride", *Fish & Shellfish Immunology*, 106 715-723.
- Dec, K., et al., 2018. "Pre-and postnatal exposition to fluorides induce changes in rats liver morphology by impairment of antioxidant defense mechanisms and COX induction", *Chemosphere*, 211 112-119.
- Guner, S., Uyar-Bozkurt, S., Haznedaroglu, E. and Menten, A., 2016. "Dental Fluorosis and Catalase Immunoreactivity of the Brain Tissues in Rats Exposed to High Fluoride Pre- and Postnatally", *Biological Trace Element Research*, 174 (1), 150-157.
- Pereira, H. A. B. D., et al., 2013. "Proteomic Analysis of Liver in Rats Chronically Exposed to Fluoride", *Plos One*, 8 (9),
- Stawiarska-Pieta, B., Bielec, B., Birkner, K. and Birkner, E., 2012. "The influence of vitamin E and methionine on the activity of enzymes and the morphological picture of liver of rats intoxicated with sodium fluoride", *Food and Chemical Toxicology*, 50 (3-4), 972-978.
- Zhang, S., et al., 2013. "Fluoride-elicited developmental testicular toxicity in rats: Roles of endoplasmic reticulum stress and inflammatory response", *Toxicology and Applied Pharmacology*, 271 (2), 206-215.

THE IMPORTANCE OF BIOCHEMICAL TESTS IN COVID-19 PATIENTS

Aysel GÜVEN

Pathology Laboratory Technician, Vocational School of Healthcare Services, Basket University

ORCID ID: 0000-0001-7511-7105

Ertuğrul ALLAHVERDİ

Kafkas University Department of Orthopedics and Traumatology

ORCID ID: 0000-0001-5830-4662

Tülay DİKEN ALLAHVERDİ

Kafkas University Department of General Surgery

ORCID ID: 0000-0001-7723-7338

ABSTRACT

In this study, 189 patients with positive PCR tests who applied to the Covid 1,2,3 services of Kafkas University Faculty of Medicine between November 1 and November 16, 2020 were included in the study. The relationship between the Covid-19 pathogen and blood biochemical parameters was investigated. The relationship between the Covid-19 pathogen and blood biochemical parameters was investigated. For this purpose, demographic characteristics of patients and some biochemical parameters (creatinine, albumin, total bilirubin, PT-INR, HDL-cholesterol, LDL-cholesterol, very low-density lipoprotein (VLDL)-cholesterol, triglyceride, total cholesterol, WBC (Leukocyte count), HGB (hemoglobin), HCT (Hematocrit), RDW (red cell Distribution Width), NEU (Neutrophil), LYM (Lymphocyte Count), MON (Monocytes), Bas (Basophil), EOS (Eosinophile), NEU % (% Neutrophil), LYM % (Lymphocyte), MON % (% Monocyte), BAS % (% Basophil), EOS % (% Eosinophile), PCT (Platelet Crit), MPV (Mean Platelet Volume), PLT (Platelet count) laboratory results were evaluated. Based on the results obtained, it was examined whether there was a significant relationship between the biochemical levels of the patients and compensation, and whether these parameters could be used as prognostic indicators could be used as prognostic indicators.

Keywords: Covid-19, biochemical parameters, prognosis.

COVID-19 HASTALARDA BİYOKİMYASAL TESTLERİN ÖNEMİ

ÖZET

Bu çalışmaya 1 Kasım -16 Kasım 2020 zaman aralığında Kafkas Üniversitesi Tıp Fakültesi Covid 1-2-3 servislerinde başvuran PCR testleri pozitif çıkan 189 hasta çalışmaya dahil edildi. COVID-19 Patojenin kan biyokimyasal parametrelerle ilişkisi araştırıldı. Bu amaçla hastaların demografik özellikleri ve bazı biyokimyasal parametreler (kreatinin, albumin, total bilirubin, PT-INR, HDL-kolesterol, LDL-kolesterol, Çok düşük dansiteli lipoprotein (VLDL)-kolesterol, trigliserid, total kolesterol, WBC (Lökosit sayısı), HGB (Hemoglobin) (Hgb), HCT (Hematokrit), RDW (Red cell Distribution Width) (Eritrosit sayısı), NEU (Nötrofil),



LYM (Lenfosit Sayımı), MON (Monositler), BAS (Bazofil), EOS (Eozonofil), NEU% (% Nötrofil), LYM% (% lenfosit), MON % (% Monosit), BAS% (%Bazofil), EOS % (%Eozonofil), PCT (Platelet Crit), MPV (Mean Platelet Volume), PLT (Trombosit sayısı) laboratuvar sonuçları değerlendirildi.

Elde edilen sonuçlar üzerinden hastaların biyokimyasal düzeyleri ile ve kompanzasyon arasında anlamlı bir ilişki olup olmadığına ve bu parametrelerin prognoz göstergesi olarak kullanıp kullanılmayacağına bakıldı.

Anahtar Kelimeler: Covid-19, biyokimyasal parametreler, prognoz.

MAO YÖNTEMİYLE AZ91 MAGNEZYUM ALAŞIMI ÜZERİNE BÜYÜTÜLEN MgO, MgO:TiO₂ ve MgO:TiO₂:C NANOKOMPOZİT KAPLAMALARININ YÜZEY MORFOLOJİSİ VE BİLEŞİMİ ÜZERİNE ELEKTROLİTİK ÇÖZELTİNİN ETKİSİNİN İNCELENMESİ

Süleyman ŞÜKÜROĞLU
Gümüşhane University, Faculty of Health Sciences, Department of Occupational Health and Safety
ORCID ID: 0000-0003-4291-6378

Yaşar TOTİK
Atatürk University, Faculty of Engineering, Department of Mechanical Engineering
ORCID ID: 0000-0003-2620-1989

Ebru Emine ŞÜKÜROĞLU
Gümüşhane University, Faculty of Engineering, Department of Mechanical Engineering
ORCID ID: 0000-0001-8638-5471

ÖZET

Mikro ark oksidasyonu (MAO), magnezyum alaşımlarının yüzey özelliklerini iyileştirebilen umut verici yüzey işleme yöntemlerinden biridir. Bununla birlikte, gözeneklerin ve mikro çatlakların varlığı, Mg Alaşımlarının kullanım alanlarını önemli ölçüde kısıtlamaktadır. Bu çalışmada, AZ91 Mg alaşımları üzerindeki MAO kaplamanın yüzey özelliklerini geliştirmekle birlikte gözenekleri ve mikro çatlakları kapatmak için TiO₂ ve C kombinasyonlu ve kombinasyonsuz MgO nanokompozit kaplamalar büyütülmüştür. Ayrıca bu çalışmada MAO yöntemi ile çok fonksiyonlu kompozit kaplamalar üretilmiştir. Kaplamanın mikro yapısı ve bileşimi SEM, EDS ve XRD teknikleri ile karakterize edilmiştir. Sonuçlar, partikül ilaveli kaplamaların yüzeylerinde gözeneklerin ve mikro çatlakların azaldığını, daha homojen ve yoğun kaplamaların büyütüldüğünü göstermektedir.

Anahtar Kelimeler: MAO yöntemi, MgO kaplama, MgO:TiO₂ kaplama, MgO:TiO₂:C kaplama, AZ91 Mg alaşımı, kaplama mikroyapısı.

INVESTIGATION OF ELECTROLYTICAL SOLUTION OF THE SURFACE MORPHOLOGY AND COMPOSITION OF MgO, MgO:TiO₂, and MgO:TiO₂:C NANOCOMPOSITE COATINGS GROWN ON AZ91 MAGNESIUM ALLOY BY MAO METHOD

ABSTRACT

Micro-arc oxidation (MAO) is one of the promising surface treatment methods that can enhance the surface properties of magnesium alloys. However, the existence of pores and microcracks significantly restricts the further advancement of Mg Alloys. In this study, effective materials, TiO₂ and C, with and without combination of MgO nanocomposite coatings, were employed to seal the pores and micro-cracks in order to enhance the surface properties of the MAO coating on AZ91 Mg alloys. Also in this study, a multi-functional composite coatings are fabricated by micro-arc oxidation method. The microstructure, and composition of the coating were

characterized by SEM, EDS and XRD. The results show that the pores and microcracks on the surfaces of the particle addition coatings are reduced, and more homogeneous and dense coatings are enlarged.

Keywords: MAO method, MgO coating, MgO:TiO₂ nanocomposite coating, MgO:TiO₂:C nanocomposite coating, AZ91 Mg alloy, coating microstructure.

1. GİRİŞ

Teknolojinin hızlı ilerlemesiyle birlikte insanoğlu gerek askeri gerekse havacılık sektöründe; üretimden kontrole, kontrolden kullanım ve bakıma kadar bütün aşamalarda malzeme biliminin önemini farketmektedir. Endüstrinin birçok alanı için hafiflik çok önemli bir yer tutsa da yüksek dayanımlardan ödün vermeden hafif ve uzun ömürlü malzemelerin seçimi sürekli gelişime açık bir nokta olmaktadır. Özellikle havacılık ve savunma sanayisinde kullanılan araç ve ekipmanların; metalik yapı malzemelerinde korozyona karşı yüksek direnç, hafiflik, yüksek dayanım, titreşim ve şok sönmüleyebilme gibi özelliklere sahip olmaları aranan en temel özelliklerdir (Çağan vd., 2017; Kaçar vd., 2006). Magnezyum ve alaşımları hafif olmaları, yüksek mukavemete sahip olmaları, şok ve titreşimlere karşı dirençli olmaları nedeni ile hava araçlarının, hidrolik depoları, yakıt depoları gibi yük binmeyen parçalarında, şanzıman ve dişli kutularında, egzoz gazı çıkış sistemlerinde ve oturma yerlerinde; Roket ve füzelerin, füze ve dümen gövdesinde; ateşli silahların, alıcıları, şarjör, silah gövdesi, silah dipçiğinde; askeri kara araçlarında ise, tanklarda, araç vites kutularında, yağ pompası gövdesi vb. ekipmanlarında tercih edilmektedir. Bu malzemelerde hafiflik; yakıt tüketimini azaltmak amacıyla istenmektedir, Ancak hız ve güç ihtiyaçlarının artması ile hafif parçaların kullanımının yanında bu parçaların daha dayanıklı olması gereksinimi de ortaya çıkmaktadır. Bu ihtiyaçları karşılayabilmek amacıyla Alüminyum (Al), Magnezyum (Mg), Titanyum (Ti), Bakır (Cu) gibi hafif metalik malzemeler ve alaşımları, havacılık ve savunma sanayisinde yapı elemanlarının üretiminde tercih edilmektedir (Öztürk ve Kaçar 2012; Zhang vd., 2018).

Yapı malzemesi olarak kullanılan magnezyum ve alaşımlarının hafifliği yoğunluklarının azaltılması ile sağlanmaktadır. Ancak bu metallerin saf hallerinin yanıcı olması, düşük mukavemet özelliği göstermeleri, aşınma ve korozyon dirençlerinin zayıf olması, gerilme korozyon çatlamasına maruz kalmaları ve yüksek aktifliğe sahip olduklarından galvanik korozyona sebep olmalarından dolayı havacılık ve savunma sanayisinin özel ihtiyaçlarını karşılamada da yetersiz kalmaktadır. Ayrıca bu malzemelerden yapılan sistem ve/veya parçaların; yüksek sıcaklıklara dayanabilmesi ve yüksek enerjili partiküllerin çarpma etkisinde dirençli olabilmeleri de geliştirilmesi gereken özelliklerinin başında gelmektedir. Bu olumsuz etkileri giderebilmek amacıyla alaşımlama yöntemi kullanılmakta ve yeni magnezyum alaşımları geliştirilmektedir. Bu durum yüksek maliyetlerinden dolayı ekonomiye olumsuz olarak yansımaktadır. Oysa sınırlı malzeme rezervlerine sahip olan ülkemizde gelişen teknoloji paralelinde alternatif yöntem olan yüzey kaplama işlemlerinin Magnezyum ve

alaşımına uygulanarak sektörün istediği özel ihtiyaçların karşılanması sağlanabilmektedir

Yüzey kaplama yöntemleri arasında en etkililerinden birisi mikro ark oksidasyon (MAO) yöntemidir. MAO yöntemi bazik bir çözelti içerisinde gerçekleşen elektrokimyasal bir anodik oksidasyon işlemidir ve son yıllarda hem akademik hem de endüstriyel alanlarda kullanımını artmaktadır. MAO yöntemi diğer kaplama yöntemleri ile kıyaslandığında çevreci bir yöntemdir. Mg, Ti ve Al gibi farklı fiziksel ve mekanik özelliğe sahip aynı zamanda yüksek miktarda kullanılan metallerde uygulanabilmesi tercih sebeplerindedir (Demirci, 2013). Yöntemin temeli arzu edilen yüzeye göre oluşturulan elektrolite daldırılan numunenin yüksek gerilim ile üzerinde oksit tabakası ile oluşmasıdır (Arslan vd. 2013; Yang vd. 2020). Oluşan oksit tabakası sert, kalın, aşınma ve korozyon direncini yükseltmektedir.

MAO yöntemi le kaplanmış magnezyum alaşımlarında seramik yüzey oldukça porlu yapıya ve yer yer mikro çatlaklara sahip olması nedeniyle agresif ortamlarda yeterli korozyon direnci gösterememektedir.

Bu çalışmada, AZ91 Mg alaşımları üzerindeki MAO kaplamanın yüzey özelliklerini geliştirmekle birlikte gözenekleri ve mikro çatlakları kapatmak için TiO_2 ve C kombinasyonlu ve kombinasyonsuz MgO nanokompozit kaplamalar büyütülmüştür. Kaplamanın mikro yapısı ve bileşimi SEM, EDS ve XRD teknikleri ile karakterize edilmiştir.

2. ARAŞTIRMA VE BULGULAR

2.1. Deneysel Çalışmalar

Altlık malzemesi olarak, 20*20*3 mm boyutlarında kimyasal bileşimleri Tablo 2.1 de verilen AZ91 alaşımları kullanılmıştır. Taban malzemeler, kaplama işleminden önce farklı tane boyutlu SiC zımparalar ile $Ra \approx 0,1 \mu m$ pürüzlülük değerine parlatılmıştır. Daha sonra numuneler aseton, etanol ve saf su ile temizlenmiştir.

Tablo 2.1. AZ91 altlık malzemelerin kimyasal bileşimleri (% ağırlık)

Bileşim (% Ağırlık)								
Alaşım	Mg	Al	Zn	Si	Cu	Ni	Fe	Mn
%	Kalan	8,30-9,70	0,30-1,00	0,01	0,03	0,002	0,005	0,20

MAO işlemi Faraday Elektronik tarafından büyütülen sisteminde, KOH, Na_2HPO_4 ve Na_2SiO_3 sulu çözeltisi ve aynı çözeltiye TiO_2 ilave edilerek elektrolit olarak kullanılmıştır. MAO oksidasyon işlemi AC güç kaynağı kullanılarak bipolar modda gerçekleştirildi. Kaplama parametreleri Tablo 2.2 de gösterilmektedir.

Tablo 2.2. MAO kaplama işlemi parametreleri

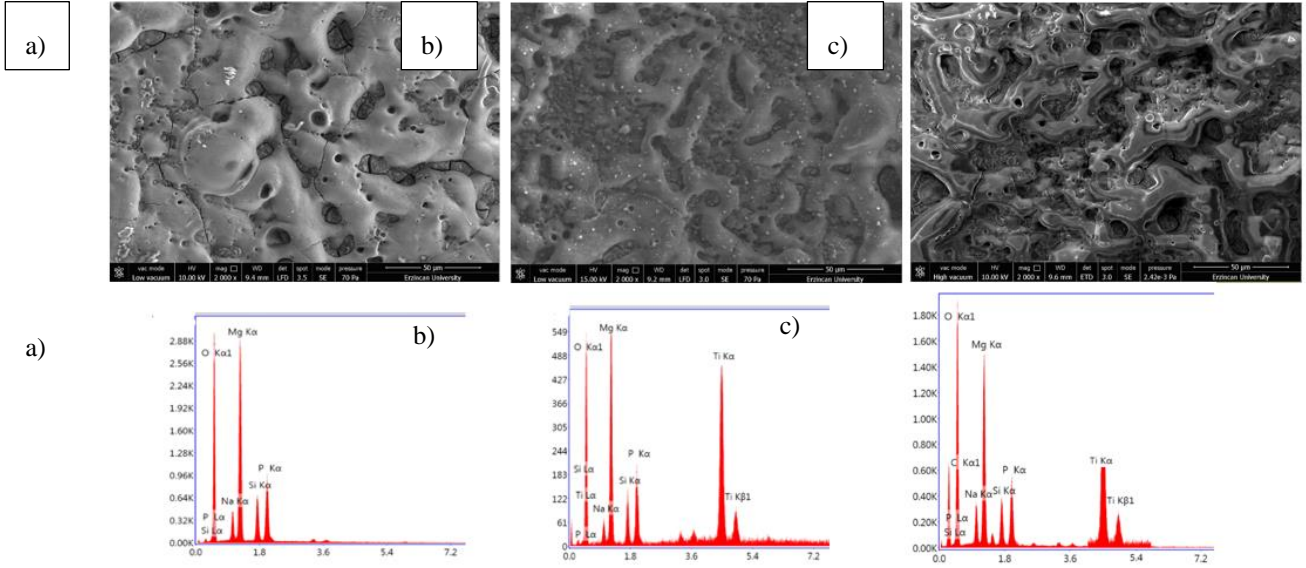
Frekans	300 Hz	
Voltaj	500/-100	
% duty	% 15/-% 1	
İşlem süresi	15	
Çözelti içerikleri		
1. Çözelti	2. Çözelti	3. Çözelti
KOH	KOH	KOH
Na ₂ HPO ₄	Na ₂ HPO ₄	Na ₂ HPO ₄
Na ₂ SiO ₃	Na ₂ SiO ₃	Na ₂ SiO ₃
-	TiO ₂ patikülü	TiO ₂ patikülü
-	-	C patikülü

Kaplama işlemi sonrası taban malzemeler üzerinde büyütülen kaplamaların kalınlığı, kaplanmış numunelerin kesit görüntüleri, yüzey topografyası Taramalı Elektron Mikroskobu (SEM-zeis 6400) ile faz analizleri ise XRD cihazıyla tespit edildi.

2.2. Deneysel Sonuçlar

MAO işlemi sonrası oluşan yüzeylerin karakteristik özellikleri yüzeylerin porlar içermesinden kaynaklanan pürüzlü bir yapıya sahip olmasıdır. Bu porlar deşarj kanalları olarak adlandırılmaktadır (Ozkara, 2009). Yüzeyde oluşan bu porların boyutları ve genel yapıları uygulanan kaplama parametrelerine bağlı olarak değişebilmektedir (Kucukosman, 2020). Kaplama parametreleri arasında en etkin olanlar akım ve voltaj değerlerinin değişimi olarak söylenebilir (Ozkara, 2009). Bu değerlerin artmasıyla büyütülen Kaplamaların yüzeylerinde daha pürüzlü ve gözenekli yapı görülebilmektedir. Bu durumun nedeni olarak uygulanan akım yoğunluğunun artmasıyla kaplama esnasında meydana gelen deşarj kanallarının sayısının artmasıyla birlikte bu kanallar etrafında meydana gelen yüksek ısı değişiminin sebep olduğu amorf bir katılaşmanın gerçekleşmesi olarak gösterilebilir. (Kucukosman, 2020, Kucukosman, 202; Dzhurinskiy). Katılaşan bölgeler krater yapıya benzer bir morfoloji gösterebilmektedir. Kaplama işlemi devam ettiği sürece bu süreç kendini sürekli tekrarlamakta ve yüzeyde pürüzlü ve gözenekli bir yapı meydana gelmektedir. Dolayısıyla açılan deşarj kanalları sayesinde altlık malzemeden gelen iyonlar elektrolit çözeltisi ile reaksiyona girerek yeni katmanları oluşturmaktadır (Kucukosman,2020). Mikro ark oksidasyon prosesinde, gözlemlenen süreç basitçe Faraday elektroliz kanunlarına bağlanabilir. İşlem süresince deşarj kanalları, mevcut reaksiyonların oluşmasıyla elektrolit ile sürekli etkileşim halindedir. Katılaşan yapının çapı ve kalınlığı, literatürdeki çalışmalar ışığında bir çok parametreye bağlıdır (Córdoba, 2016; Kucukosman,2020). Örneğin kaplama süresi veya uygulanan voltaj değeri bu parametrelerin en etkinleri arasında gösterilebilir. Ancak Kaplama işleminin gerçekleştiği elektrolitin içeriğinde son derece önemlidir. Elektrolit içerisine ilave edilen katkılar çözeltinin iletkenliğini değiştirebilmektedir. Şekil 2.1 de gösterilen yüzey SEM görüntülerinden anlaşıldığı üzere elektrota ilave edilen

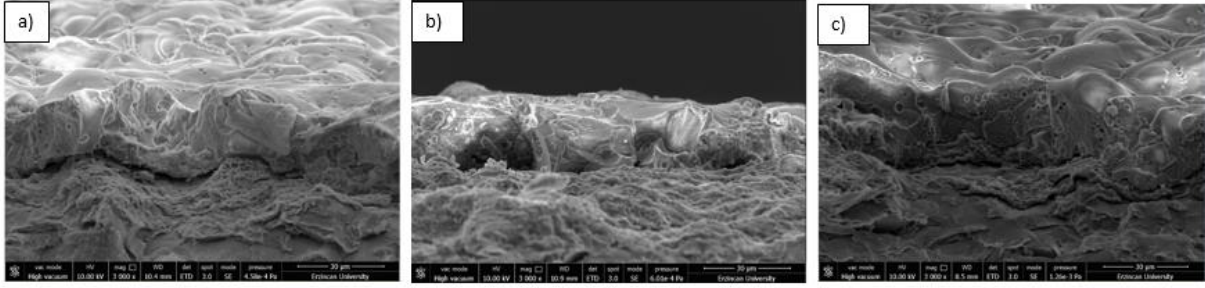
katkılarının çeşitliliğinin artmasıyla yüzeydeki por sayısı azalmış ve beraberinde çapları büyümüştür. Deşarj kanalının ve çevresinde oluşan yapının çap artışı deşarj kanalının yoğunluğundaki azalmayla dengelenmektedir. Farklı içerikli çözeltiler içinde kaplanan numunelere ait yüzey SEM fotoğrafları incelendiğinde, katkı ilave edilmeyen çözelti içinde (Şekil 2.1-a) kaplanan örneklerin daha gözenekli ve kaba olduğu; termal gerilmelerden kaynaklanan çatlakların ise daha kısa sürede oluştuğu görülmektedir. Ayrıca bu çatlakların yüzeyin bir çok yerinde bulunduğu da söylenebilir.



Şekil 2.1. a) TiO_2 ilavesiz elektrolit içerisinde büyütülen kaplamanın SEM görüntüsü ve EDX analizi **b)** TiO_2 ilaveli elektrolit içerisinde büyütülen kaplamanın SEM görüntüsü ve EDX analizi **c)** TiO_2 ve C ilaveli elektrolit içerisinde büyütülen kaplamanın SEM görüntüsü ve EDX analizi

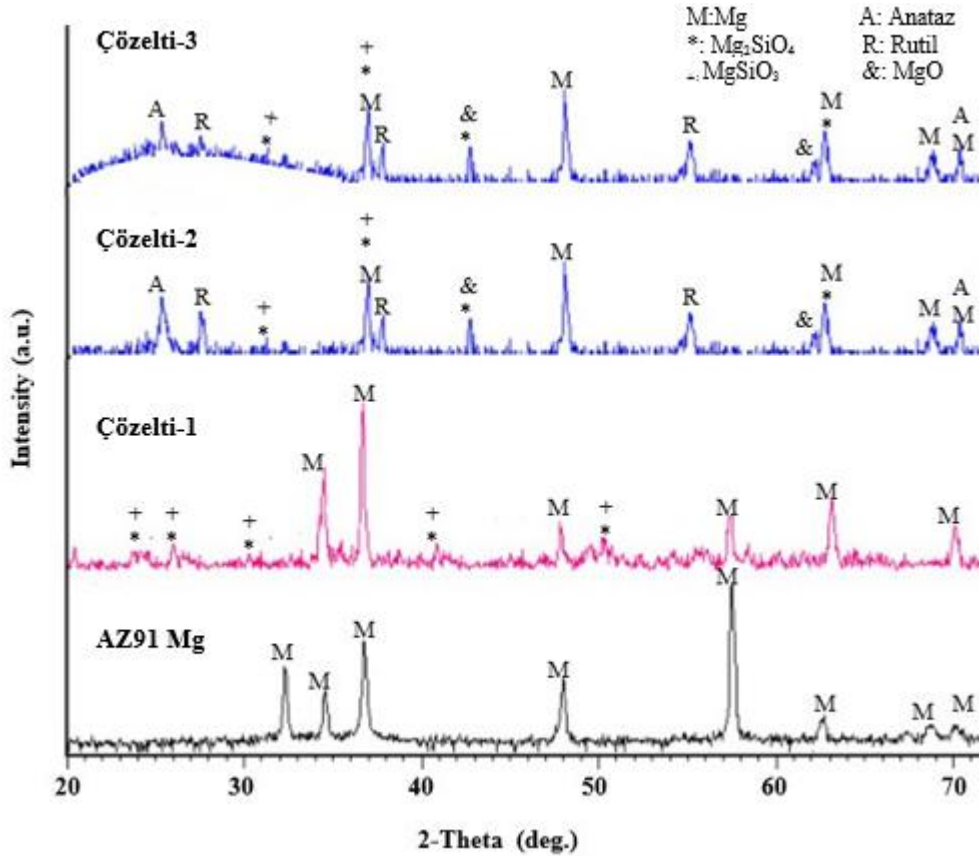
Katkı içeren elektrolit çözeltileri içerisinde büyütülen kaplamalar için poroz yapının arttığı; altlık metal ile oluşan kaplama arasındaki arayüzey bölgesinin ise daha düz ve belirgin hale geldiği Şekil 2.3 de gösterilen kesit SEM fotoğraflarından görülmektedir. Ayrıca kaplamaların; altlık malzemeye iyi tutunduğu, poroz bir yapıya sahip olduğu ve kaplama kalınlığı, yüzey pürüzlülüğü ve porozite miktarının katkı çeşitliliği artışıyla arttığı da görülmektedir. Kaplama içerisindeki katkı malzemelerinin çeşitliliğinin artması, altlık malzemeye yakın bölgelerde daha yoğun bir kaplama oluşmasına sebep olmuştur (Kucukosman, 2021; Sankara Narayanan 2014). Bu artışla açık ve kapalı porlar daha da büyümektedir. Çözelti 3 ve 2 ile yani çözelti içerisinde TiO_2 ve TiO_2 ile beraber C partiküllerinin ilavesiyle büyütülen kaplamalar Çözelti 1 ile yani dışarıdan herhangi bir partikül ilave edilmeden büyütülen kaplamalara göre daha porozdur ve SEM fotoğraflarında görüldüğü gibi daha girintili çıkıntılıdır. Fakat kaplama kalınlığında gözle görülür bir artış meydana gelmiştir

Yüzeyden alınan EDX analizine göre TiO_2 katkılı Çözelti-2 ile büyütülen Kaplamaların yüzeylerinde Ti elementine rastlanmıştır. Bununla birlikte Çözelti-3 ile büyütülen kaplamalarda ise Ti elementi ile birlikte yüzeyde C elementinde rastlanmıştır.



Şekil 2.3. a) TiO₂ ilavesiz elektrolit içerisinde büyütülen kaplamaya ait kesit görüntüsü b) TiO₂ ilaveli elektrolit içerisinde büyütülen kaplamaya ait kesit görüntüsü

XRD grafikleri incelendiğinde tüm kaplamalı örneklerde yüzeyde Mg₂SiO₄, MgSiO₃ ve MgO oluştuğu görülmektedir. TiO₂ katkılı yüzeylerde Anataz ve rutil fazlara rastlanmıştır. TiO₂'nin termodinamik olarak en kararlı yapısı rutile fazıdır. MAO ile büyütülen kaplamalar düşük sıcaklıklarda yarı kararlı faz olan anataz ve yüksek sıcaklıklarda kararlı rutil fazından oluşabilmektedir. Çözelti içerisinde ilave edilen katkıların başlangıç voltaj değerini düşürerek kaplama oluşumunu uzun süreye yaydığı literatürden bilinmektedir (Córdoba; 2016). Bu bilgi doğrultusunda rutil fazın ve MgO kararlı fazının TiO₂ ilave edilen çözeltide kaplanan kaplamalarda büyüdüğü görülmektedir. C ilave edilen kaplamalarda yani Çözelti 3 ile kaplanan örneklerde XRD grafikleri Çözelti 2 ile hemen hemen aynı görünmektedir bu durumun C nun amorf yapısından kaynaklandığı düşünülmektedir.



Şekil 2.4. Kaplanmamış ve Kaplanmış örneklerin XRD paternleri

3. SONUÇ

- ✓ TiO₂ ve C ilaveleri ile AZ91 alaşımı üzerine MAO yöntemiyle kaplamalar başarılı bir şekilde büyütülmüştür.
- ✓ MgO, MgO:TiO₂ ve MgO:TiO₂:C nanokompozit kaplamalarının karşılaştırıldığında katkılı yüzeylerde daha homojen ve daha az gözeneklere sahip yüzeyler elde edilmiştir.
- ✓ XRD analizine göre yüzeyde Mg₂SiO₄, MgSiO₃ ve MgO oluştuğu görülmektedir ancak TiO₂ ilave edilen kaplamalarda bu fazlara ilave olarak TiO₂'nin Rutil ve Anataz fazlarında rastlanmıştır.

KAYNAKÇA

- Çağan, S.Ç., Uğurlu, M., Buldum, B.B., Sevim, İ. 2017. “Magnezyum ve Alaşımlarının Savunma Sanayisi için Üretilen Araçlardaki Uygulamaları”, II. Uluslararası Savunma Sanayi Sempozyumu (IDEFIS 2017) Bildiri Kitabı, 395-401.
- Kaçar, İ., Zile, M., Öztürk, F. 2006. “Havacılık Sanayinde Magnezyum Alaşımları”, I. Havacılık ve Uzay Konferansı (UHUK 2006).
- Öztürk, F., Kaçar, İ. 2012. “Magnezyum Alaşımları ve Kullanım Alanlarının İncelenmesi”, Niğde Üniversitesi Mühendislik Bilimleri Dergisi, Cilt 1, Sayı 1, 12-20.
- Zhang, X., Chen, Y., Hu, J. 2018. “Recent advances in the development of aerospace materials”, Progress in Aerospace Sciences, 97, 22-34.
- Arslan E., Totik Y., Demirci E.E., Efeoglu I., 2013. “Wear and adhesion resistance of duplex coatings deposited on Ti6Al4V alloy using MAO and CFUBMS”, Surface & Coatings Technology 214, 1–7.
- Yang W., Gao Y., Peng G. Dapeng X., Hua L., Wang A., 2020. “Adhesion, biological corrosion resistance and biotribological properties of carbon films deposited on MAO coated Ti substrates”, Journal of the Mechanical Behavior of Biomedical Materials, 101, 103448.
- Demirci, Ebru Emine Şüküroğlu, Ersin Arslan, Kadri Vefa Ezirmik, Özlem Baran Acımert, Yaşar Totik, İhsan Efeoglu, 2013. Investigation of wear corrosion and tribocorrosion properties of AZ91 Mg alloy coated by micro arc oxidation process in the different electrolyte solutions, Thin Solid Films. <http://dx.doi.org/10.1016/j.tsf.2012.07.145>.
- Dzhurinskiy D., Y. Gao, W.K. Yeung, E. Strumban, V. Leshchinsky, P.J. Chu, A. Matthews, A. Yerokhin, R.G. Maev, 2015. Characterization and corrosion evaluation of TiO₂:n-HA coatings on titanium alloy formed by plasma electrolytic oxidation, Surf. Coat. Technol, 269, 258-265.
- Córdoba L.C., M.F. Montemor, T. Coradin, 2016. Silane/TiO₂ coating to control the corrosion rate of magnesium alloys in simulated body fluid, Corros. Sci., 104, 152-161.
- Sankara Narayanan T.S.N., S. Park., M. H. Lee., 2014. Strategies to improve the corrosion resistance of microarc oxidation (MAO) coated magnesium alloys for degradable implants: Prospects and challenges, Prog. Mater Sci. 60, 1-71.
- Özkara, İsa Metin, 2009. 2024 Alüminyum Alaşımının Mikro Ark Oksidasyon Yöntemiyle Kaplanması Ve Yüzey Özelliklerinin Geliştirilmesi, İstanbul Teknik Üniversitesi- Fen Bilimleri Enstitüsü, İstanbul.
- Kucukosman R, EE Sukuroglu, Y Totik, S Sukuroglu, 2020. Effects of graphene oxide addition on wear behaviour of composite coatings fabricated by plasma electrolytic oxidation (PEO) on AZ91 magnesium alloy Journal of Adhesion Science and Technology 35 (3), 242-255
- Kucukosman R, E Şüküroğlu, Y Totik, S Şüküroğlu, 2021. Investigation of wear behavior of graphite additive composite coatings deposited by micro arc oxidation-hydrothermal treatment on AZ91 Mg alloy, Surfaces And Interfaces, Cilt.22, 2021

AZ91 Mg ALAŞIMI ÜZERİNE MAO YÖNTEMİYLE BÜYÜTÜLEN MgO:TiO₂ KAPLAMALARIN MİKROYAPISAL KARAKTERİZASYONU

Süleyman ŞÜKÜROĞLU
Gümüşhane University, Faculty of Health Sciences, Department of Occupational Health and Safety
ORCID ID: 0000-0003-4291-6378

Yaşar TOTİK
Atatürk University, Faculty of Engineering, Department of Mechanical Engineering
ORCID ID: 0000-0003-2620-1989

Ebru Emine ŞÜKÜROĞLU
Gümüşhane University, Faculty of Engineering, Department of Mechanical Engineering
ORCID ID: 0000-0001-8638-5471

ÖZET

Mg ve alaşımlarının yüzey özelliklerini iyileştirmek için kullanılan yöntemlerden birtanesi de MAO yöntemidir. Bu yöntem yüksek voltajlarda malzeme yüzeyine seramik bir kaplama oluşturmaktadır. Bu yöntem ile büyütülen kaplamaların pürüzlü ve gözenekli yapıya sahip olması bu kaplamaların korozyon direncini olumsuz etkilediği için kaplamaların kullanım alanlarını sınırlamaktadır. Yapıdaki gözenekliği azaltarak nihai özellikleri iyileştirmek için uygulanan yöntemlerden en etkin olanı mikro ve nano partiküllerin varlığına bağlı olarak değişen elektrolit koşullarıdır. Bu çalışmada, elektrolite ilave edilen TiO₂ partiküllerinin, AZ91 Mg alaşımı üzerine büyütülen seramik kaplamanın mikroyapısına etkisi araştırılmıştır.

Anahtar Kelimeler: MAO yöntemi, MgO:TiO₂ kaplama, AZ91 Mg alaşımı.

MICROSTRUCTURAL CHARACTERIZATION OF MgO:TiO₂ COATINGS GROWN BY MAO METHOD ON AZ91 Mg ALLOY

ABSTRACT

One of the methods used to improve the surface properties of Mg and its alloys is the MAO method. This method creates a ceramic coating on the material surface at high voltages. The rough and porous structure of the coatings grown with this method limits the usage areas of the coatings as it negatively affects the corrosion resistance of these coatings. The most effective of the methods applied to improve the final properties by reducing the porosity in the structure is the electrolyte conditions that change depending on the presence of micro and nano particles. In this study, the effect of TiO₂ particles added to the electrolyte on the microstructure of the ceramic coating grown on AZ91 Mg alloy was investigated.

Keywords: MAO method, MgO:TiO₂ coating, AZ91 Mg alloy.

1. GİRİŞ

Biyolojik implant malzemesi olarak kullanılan Mg ve alaşımları sahip oldukları biyouyumluluk ve çok iyi mekanik özelliklerinden dolayı sürekli olarak geliştirilmektedir. Ayrıca Mg ve alaşımları, biyolojik açıdan bakıldığında ise kemik oluşumu ve kalsiyum fosfat birikiminde temel bir rol oynamaktadır. Ek olarak, magnezyumun insan kemiğine yakın (3-20 GPa) ve kemikle uyum gösteren bir elastisite modülü vardır (41-45 GPa) (Guan, 2013; Staiger, 2006). Buna karşılık titanyum alaşımlarının elastisite modülleri (110–117 GPa) veya kobalt-krom alaşımlarının elastisite modülü (230 GPa), kemiğinkinden oldukça yüksektir (Bakhsheshi-Rad,2016). Bu durum, implant malzemelerin uygulandıkları kemik için stres korumasına yol açabilmektedir. Ancak bu biyolojik, fiziksel ve mekanik özellikler açısından avantajlara rağmen, Cl^- iyonu içeren çözeltilerdeki yüksek korozyon oranları göstermeleri bu alaşımların tıbbi uygulamalarda uzun süre kullanımlarını sınırlayabilmektedir (Witte, 2008; Hermawan, 2010). Ek olarak, Mg^{2+} iyonlarının oluşumuyla sonuçlanan hızlı bozunma, hidrojen evrimi ve ardından kanda birikimin yanı sıra yerel pH'ın artması hücre ölümüne ve doku iltihabına yol açabilmektedir (Bakhsheshi-Rad, 2017). Mg ve alaşımlarının bozunma oranını azaltmak için son birkaç yılda yüzey modifikasyonu teknikleri önerilmektedir. Bu bağlamda, yapılan literatür araştırmalarında; kaplamaların Mg alaşımı altlık yüzeyini çevreleyen agresif çözeltiden ayırabildiği ve dolayısıyla bozunma hızını azalttığı bildirmiştir. Mg alaşımları üzerine uygulanabilen birçok kaplama yöntemi bulunmaktadır ancak mikro ark oksidasyon (MAO) yöntemi, genellikle kalın ve sert olmakla birlikte Mg altlıkları ile iyi bir bağlanma kuvvetine sahip olan gözenekli oksit tabakalarını imal etmek için en umut verici yöntemler arasında gösterilmektedir. MAO yönteminde, kullanılan alkali elektrolitlerin PH'ı 8-12 arasında olduğu için çevre dostu olması, taban malzemede çarpılma olmaması, kullanılan Alternatif Akım Güç Kaynağının kendine özgü avantajlar sağlaması, yüksek adezyon kuvvet elde edilmesi ve gerek mekanik, gerekse tribolojik olarak diğer yöntemlerden daha iyi özellikler göstermesi prosesin son yıllarda alternatif bir yöntem olarak tercih edilmesine neden olmuştur (Demirci; 2013). Bu bağlamda çok sayıda çalışma elektrolite kalsiyum ve fosfor gibi elementlerin eklenmesinin biyoaktiviteyi artırabileceğini ve Mg alaşımlarının korozyon direncinin artmasına yol açan gözeneklerin boyutunu ve sayısını azaltabileceğini göstermektedir. MAO yöntemiyle elde edilen kaplamaların sahip oldukları gözenekli yüzeyler MAO yöntemi ile kaplanan altlıkların uzun vadeli korozyon önleyici performansını sınırlamaktadır. Bu nedenle, MAO kaplamalarının gözeneklerinin kapatılması, bu kaplama yönteminin uygulamalarını geliştirmek için esastır.

Bu çalışmada; MAO kaplamalarının uygulamalarını geliştirmek için gözeneklerinin kapatılması amaçlanmıştır. Bu bağlamda bu çalışmada, gözenekliliği ve gözenek boyutunu azaltmak ve böylece uygulamalardaki korozyon direncini iyileştirmek için MAO yöntemiyle büyütülen MgO kaplamalara titanyum dioksit (TiO_2) dahil edilmiştir.

2. ARAŞTIRMA VE BULGULAR

2.1. Deneysel Çalışmalar

Altlık malzemesi olarak, 20*20*3 mm boyutlarında kimyasal bileşimleri Tablo 2.1 de verilen AZ91 alaşımları kullanılmıştır. Taban malzemeler, kaplama işleminden önce farklı tane boyutlu SiC zımparalar ile $Ra \approx 0,1 \mu\text{m}$ pürüzlülük değerine parlatılmıştır. Daha sonra numuneler aseton, etanol ve saf su ile temizlenmiştir.

Tablo 2.1. AZ91 altlık malzemelerin kimyasal bileşimleri (% ağırlık)

Bileşim (% Ağırlık)								
Alaşım	Mg	Al	Zn	Si	Cu	Ni	Fe	Mn
%	Kalan	8,30-9,70	0,30-1,00	0,01	0,03	0,002	0,005	0,20

MAO işlemi Faraday Elektronik tarafından üretilen sisteminde, KOH, Na_2HPO_4 ve Na_2SiO_3 sulu çözeltisi ve aynı çözeltiye TiO_2 ilave edilerek elektrolit olarak kullanılmıştır. MAO oksidasyon işlemi AC güç kaynağı kullanılarak bipolar modda gerçekleştirildi.

Tablo 2.2. MAO kaplama işlemi parametreleri

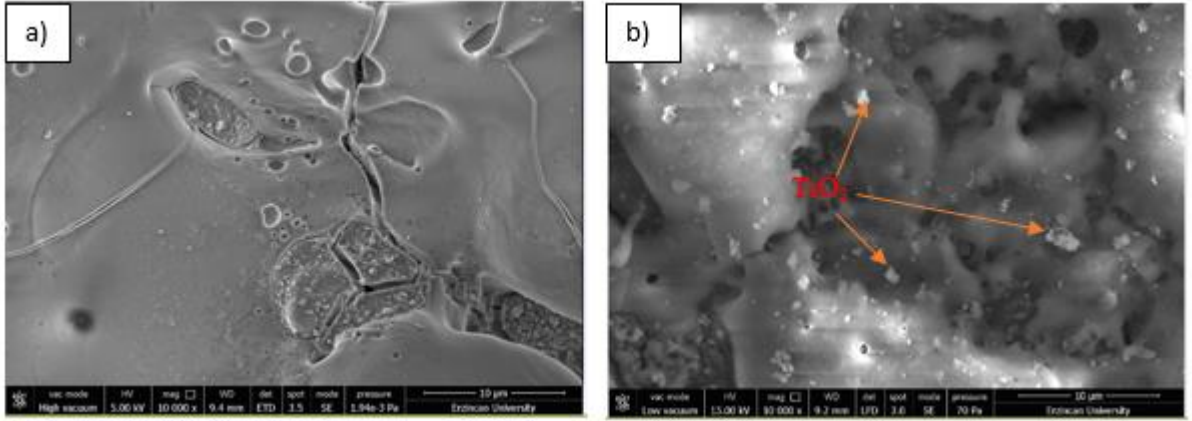
Frekans	300 Hz
Voltaj	500/-100
% duty	% 15/-% 1
İşlem süresi	15

Kaplama işlemi sonrası taban malzemeler üzerinde büyütülen kaplamaların kalınlığı, kaplanmış numunelerin kesit görüntüleri, yüzey topografyası Taramalı Elektron Mikroskopu (SEM-zeis 6400) ile faz analizleri ise XRD cihazıyla tespit edildi.

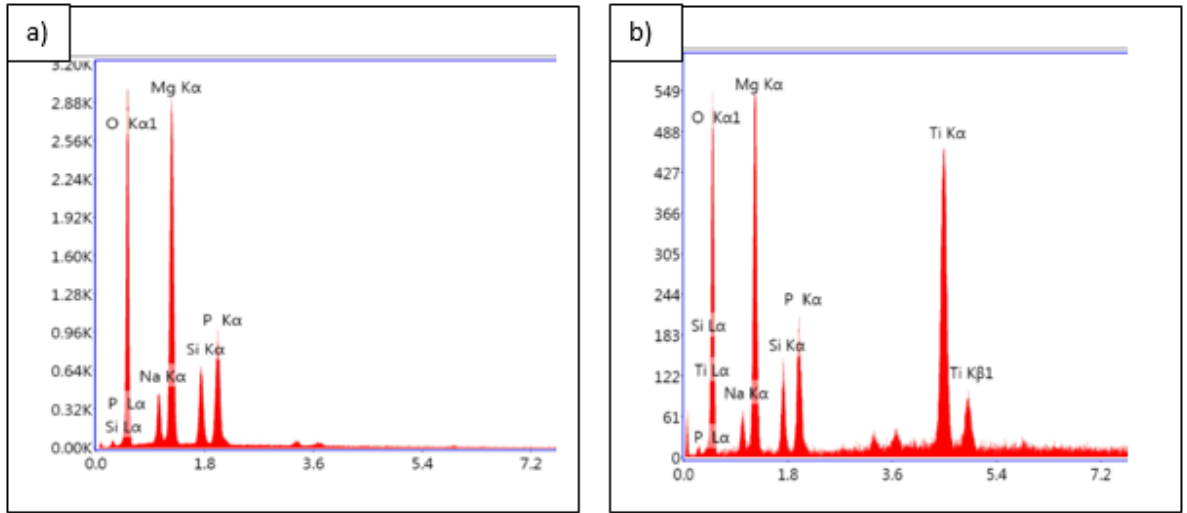
2.2. Deneysel Sonuçlar

Şekil 2.1 de gösterilen SEM görüntüleri incelendiğinde taban malzeme üzerine büyütülen kaplamaların pürüzlü bir yüzeye, çok sayıda değişik boyutlarda mikro ergimelerin neden olduğu volkan görünümlü oluşumlara ve bazı büyük oluşumların uçlarında çok sayıda dairesel mikro gözeneklere sahip olduğu gözlemlenmiştir. Şekil 2.1-a elektrolit içerisine TiO_2 ilave edilmeyen Şekil 2.1-b ise elektrolit içerisine TiO_2 ilave edilen kaplamalara ait yüzey görüntüleridir. Şekiller incelendiğinde TiO_2 ilave edilen elektrolit içerisinde büyütülen kaplamanın yüzeyinin daha uniform olduğu görülmektedir (Córdoba, 2016; Dzhurinskiy, 2015). Gözeneklerin uniform ve uniform olmayan yapıdaki farklı dağılımlarının nedeni ark kanalları içerisinde meydana gelen lokal ergimeler ve bu erimiş malzemenin dağılımından kaynaklandığı düşünülmektedir (Narayanan, 2014). Şekil 2.2 de ise EDX analizi verilmiştir. Kaplanmış örneklerin yüzeylerinden alınan EDX analizine göre bütün kaplamalarda Si, Na ve O elementleriyle birlikte Mg elementine rastlanmıştır. Bu elementlerin kaplama çözeltisi içerisindeki elementlerden kaplama içerisine nüfuz ettiği düşünülmektedir (Lin, 2013, . TiO_2 ilave edilen kaplamanın

yüzeyinden alınan EDX analizinde ise Ti elementine rastlanmıştır. Bu durum kaplamanın gerçekleştirileceği elektrolit içerisine ilave edilen TiO₂ partiküllerinin kaplama içerisine nüfuz ettiği ve yüzeyde büyütülen MgO Kaplamalara TiO₂ katkısının yapılabildiğini göstermektedir.



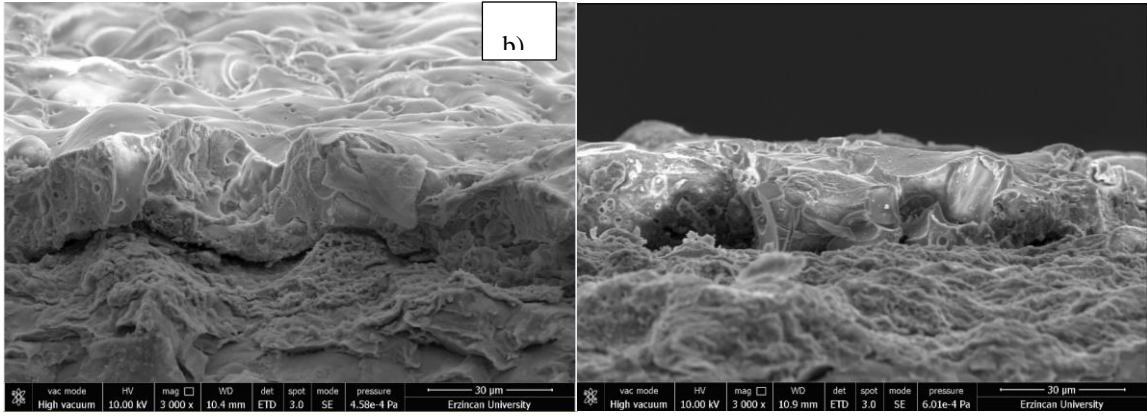
Şekil 2.1. a) TiO₂ ilavesiz elektrolit içerisinde büyütülen kaplamanın SEM görüntüsü ve b) TiO₂ ilaveli elektrolit içerisinde büyütülen kaplamanın SEM görüntüsü



Şekil 2.2. a) TiO₂ ilavesiz elektrolit içerisinde büyütülen kaplamaya ait EDX ve b) TiO₂ ilaveli elektrolit içerisinde büyütülen kaplamaya ait EDX

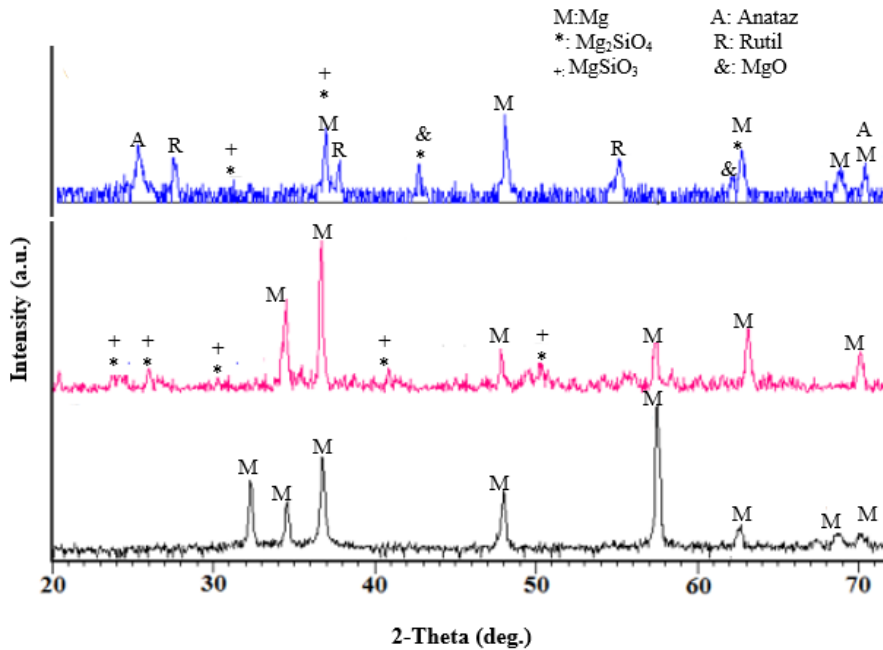
TiO₂ ilave edilen elektrolitlerde kaplanan örneklerin kalınlıklarında bir fark olduğu gözlenmiştir. Şekil 2.3 de gösterildiği gibi, TiO₂ ilave edilen çözeltide büyütülen kaplamaların kalınlıkları (~25µm), TiO₂ ilave edilmeyen çözeltide büyütülen kaplama kalınlığından (~20 µm) daha fazla olduğu görülmektedir. Bu durumun çözelti içerisine ilave edilen TiO₂ ilavesinin kaplama başlangıç voltaj değerini düşürdüğü ve aynı süre içerisinde daha kalın bir kaplama büyütülebildiğini göstermektedir. Ayrıca kaplama ile yüzey arasındaki uyum kesit görüntülerinden açıkça gösterilmektedir. Kaplama yüzeye oldukça adeziv olarak büyümüş ve herhangi bir kopma veya ayrılmaya rastlanılmamıştır. Oysa Şekil 2.3-a da gösterilen TiO₂ ilave edilmeyen elektrolit içerisinde büyütülen kaplamalarda, kaplama ve taban malzeme arasında kopma ve ayrılmalara rastlanmıştır.

a)



Şekil 2.3. a) TiO_2 ilavesiz elektrolit içerisinde büyütülen kaplamaya ait kesit görüntüsü b) TiO_2 ilaveli elektrolit içerisinde büyütülen kaplamaya ait kesit görüntüsü

Şekil 2.4 de gösterilen XRD verileri incelendiğinde hem TiO_2 ilave edilmeyen elektrolitte hem de TiO_2 ilave edilen elektrolitte kaplanan örneklerin yüzeylerinde Mg_2SiO_4 , $MgSiO_3$ ve MgO oluştuğu görülmektedir. TiO_2 ilave edilen elektrolit içerisinde büyütülen kaplamalarda TiO_2 ye ait Anataz ve rutil fazlara rastlanmıştır. TiO_2 'nin termodinamik olarak en kararlı yapısı rutile fazıdır. MAO ile büyütülen kaplamalar düşük sıcaklıklarda yarı kararlı faz olan anataz ve yüksek sıcaklıklarda kararlı rutil fazından oluşabilmektedir (Stanić, 2010; Huang, 2016). Çözelti içerisine ilave edilen katkıların başlangıç voltaj değerini düşürerek kaplama oluşumunu uzun süreye yaydığı literatürden bilinmektedir. Bu bilgi doğrultusunda rutil fazın ve MgO kararlı fazının TiO_2 ilave edilen çözeltide kaplanan kaplamalarda büyüdüğü görülmektedir.



Şekil 2.4. Kaplanmamış ve Kaplanmış örneklerin XRD paternleri

3. SONUÇ

- TiO₂ ilavesiyle AZ91 magnezyum alaşımı üzerine MgO:TiO₂ katkılı oksit tabakası başarıyla büyütülmüştür.
- Katkılı ve katkısız kaplanmış yüzeyler karşılaştırıldığında TiO₂ katkılı yüzeylerde daha homojen ve daha küçük gözeneklere sahip yüzeyler elde edilmiştir.
- Kaplama çözeltisi içerisine ilave edilen TiO₂'nin yüzeyden alınan EDX analizi sonrasında yüzeyin birçok yerinde bulunduğu tespit edilmiştir.
- XRD analizine göre yüzeyde Mg₂SiO₄, MgSiO₃ ve MgO olduğu görülmektedir ancak TiO₂ ilave edilen kaplamalarda bu fazlara ilave olarak TiO₂'nin Rutil ve Anataz fazlarına da rastlanmıştır.

KAYNAKÇA

- Guan R.-G., A.F. Cipriano, Z.-Y. Zhao et al.,2013. Development and evaluation of a magnesium–zinc– strontium alloy for biomedical applications: Alloy processing, microstructure, mechanical properties, and biodegradation, *Mater. Sci. Eng. C*, 33, 3661-3669.
- Staiger M. P., A. M. Pietak., J. Huadmai. and G. Dias.,2006. Magnesium and its alloys as orthopedic biomaterials: A review, *Biomaterials* 27, 1728–1734.
- Bakhsheshi-Rad H.R., E. Hamzah, M. Daroonparvar et al.,2016. Enhancement of corrosion resistance and mechanical properties of Mg–1.2Ca–2Bi via a hybrid silicon-biopolymer coating system, *Surf. Coat. Technol.* 301, 133-139.
- Witte F., Hort N.,2008. Degradable Biomaterials Based on Magnesium Corrosion, *Curr. Opin. Solid State Mater. Sci.*, 12, 63-72.
- Hermawan H., D. Dubé, D. Mantovani,2010. Developments in metallic biodegradable stents. *Acta Biomaterialia*, vol. 6, no. 5, pp. 1693-1697 *Acta Biomater.* 5, 1693–1697.
- Bakhsheshi-Rad H.R., E. Hamzah, A.F. Ismail, M. Aziz, M. Daroonparvar, E. Saebnoori, A. Chami2017. In vitro degradation behavior, antibacterial activity and cytotoxicity of TiO₂-MAO/ZnHA composite coating on Mg alloy for orthopedic implants. The address for the corresponding author was captured as affiliation for all authors. Please check if appropriate. *Sct*(2017), doi:10.1016/j.surfcoat.2017.11.027
- Demirci, Ebru Emine Şüküroğlu, Ersin Arslan, Kadri Vefa Ezirmik, Özlem Baran Acimert, Yaşar Totik, İhsan Efeoğlu, 2013. Investigation of wear corrosion and tribocorrosion properties of AZ91 Mg alloy coated by micro arc oxidation process in the different electrolyte solutions, *Thin Solid Films*. <http://dx.doi.org/10.1016/j.tsf.2012.07.145>
- Dzhurinskiy D., Y. Gao, W.K. Yeung, E. Strumban, V. Leshchinsky, P.J. Chu, A. Matthews, A. Yerokhin, R.G. Maev, 2015. Characterization and corrosion evaluation of TiO₂:n-HA coatings on titanium alloy formed by plasma electrolytic oxidation, *Surf. Coat. Technol*, 269, 258-265.
- Córdoba L.C., M.F. Montemor, T. Coradin, 2016. Silane/TiO₂ coating to control the corrosion rate of magnesium alloys in simulated body fluid, *Corros. Sci.*, 104, 152-161.
- Lin X., L. Tan., Q. Zhang, et al., 2013. The in vitro degradation process and biocompatibility of a ZK60 magnesium alloy with a forsterite-containing micro-arc oxidation coating, *Acta Biomater.*, 9, 8631-8642.
- Sankara Narayanan T.S.N., S. Park., M. H. Lee.,2014. Strategies to improve the corrosion resistance of microarc oxidation (MAO) coated magnesium alloys for degradable implants: Prospects and challenges, *Prog. Mater Sci.* 60, 1-71.
- Stanić V., S. Dimitrijević, J. Antić-Stanković et al., 2010. Synthesis, characterization and antimicrobial activity of copper and zinc-doped hydroxyapatite nanopowders, *Appl. Surf. Sci.*, 256, 6083- 6089.
- Huang Y., X. Zhang, H. Qiao, M. Hao, H. Zhang et al.,2016. Corrosion resistance and cytocompatibility studies of zinc-doped fluorohydroxyapatite nanocomposite coatings on titanium implant, *Ceram. Int.*, 42, 1903-1915.



SYNTHESIS AND COMPUTATIONAL STUDIES OF NOVEL QUINOLINE-SUBSTITUTED SCHIFF-BASE DERIVATIVES

Ayşegül GÜMÜŞ

Van Yüzüncü Yıl University, Department of Chemistry, Faculty of Science, Campus, Van
ORCID ID: 0000-0002-1613-7074

Selçuk GÜMÜŞ

Van Yüzüncü Yıl University, Department of Chemistry, Faculty of Science, Campus, Van
ORCID ID: 0000-0002-8628-8943

ABSTRACT

Schiff bases are some of the most widely used organic compounds. They are used as pigments and dyes, catalysts, intermediates in organic synthesis, and as polymer stabilisers. The nitrogen atom of azomethine C=N double bond in Schiff base exhibits a strong affinity for transition metal ions. Schiff base derivatives incorporating a fluorescent moiety are appealing tools for optical sensing of metal ions. In this study, 8-hydroxyquinoline derivative was reacted with benzyl bromide by one-pot triazole synthesis method to obtain 1,4-disubstituted triazole compound. Fluorescent Schiff base derivatives were synthesized by reacting triazole-linked quinolinealdehyde derivative with aminopyrene and aminoanthracene, which are very good fluorophores. Molecular probes containing pyrene or anthracene framework were well suited for the development of chemosensors due to their extended π -conjugation property, chemical stability, high quantum yields and effective photoluminescence features. These compounds have high potential to be used as metal chemosensors. Detection of a specific type of a metal is very important in terms of biouse of the related compound. After the synthesis, the metal coordination characteristics of the new compounds were investigated theoretically at the level of Density Functional theory with the application of B3LYP/6-31++G(d,p), which is a combination of hybrid exchange function and basis set.

Keywords: Anthracene, Pyrene, Triazole, Schiff Bases, Structural And Electronic Properties

1. INTRODUCTION

The evolution of fluorescence sensing has been known as an essential and fascinating research field of analytical chemistry at present, due to its simplicity in measurements, low detection limit, low cost, real-time analysis and quantified applications in the environment, biological systems and molecular catalysis [1-6].

Molecular probes containing pyrene or anthracene framework were well suited for the development of chemosensors due to their extended π -conjugation property, chemical stability, high quantum yield and effective photoluminescence features [7-10].

Schiff bases are known to be good ligand for metal ions [11] and used to develop chemosensors since the nitrogen atom of azomethine C=N double bond in Schiff base exhibits a strong affinity for transition metal ions.

Schiff base metal complexes have numerous applications like antitumor properties [12], antioxidative activities [13], and attractive electronic and photophysical properties [14]. In addition, Schiff base derivatives incorporating a fluorescent moiety are appealing tools for optical sensing of metal ions. Tetradentate ligands such as salen- or pyridine-type symmetrical Schiff bases are capable of forming complexes with certain metal ions which can exhibit unusual coordination, high thermodynamic stability, good fluorescent properties and biological activities [15].

Triazole-containing compounds show various biological activities including antimicrobial [16], anti-inflammatory [17], antidepressant [18], anticonvulsant [19], antifungal [20], enzyme inhibition [21] activities. 1,2,3-Triazoles have also a wide range applications in industry as anticorrosive agents, dyes, photostabilizers, photographic materials, and agrochemicals [22–24]. Remarkable stability toward metabolic transformations, H-bonding capability, and high dipole moment make triazoles attractive building components [25–27].

Motivated by these studies, Schiff base structure was built between benzyl substituted salicylaldehyde and amino anthracene. Triazole bridge connecting benzyl and salicylaldehyde could furnish an extra binding site. Salicylaldehyde was connected with anthracene by C=N structure. Anthracene and pyrene were employed as fluorophore due to their outstanding photophysical properties and easy modification [28]. The C=N structure might provide another binding state, which could improve the selectivity.

2. RESULTS AND DISCUSSION

2.1. Experimental

General

All experiments were carried out in pre-dried glassware in an inert atmosphere of argon. All the chemicals used in the biologic assay studies were purchased from Sigma (Sigma-Aldrich GmbH, Sternheim, Germany). ^1H NMR and ^{13}C NMR spectra were recorded in CDCl_3 on a Agilent NMR spectrometer (400 MHz). ^1H (400 MHz) and ^{13}C NMR (100 MHz) were recorded in CDCl_3 and the chemical shifts are expressed in ppm relative to CDCl_3 (δ 7.26 and 77.0 for ^1H and ^{13}C NMR, respectively) as the internal standard.

Flash column chromatography was performed by using thick-walled glass columns and silica gel (60-mesh; Merck). The reactions were monitored by thin-layer chromatography (TLC) using Merck 0.2-mm silica gel 60 F254 analytical aluminium plates, visualized by UV light.

Synthesis of 8-(prop-2-yn-1-yloxy)quinoline-2-carbaldehyde, 1.

8-hydroxyquinoline-2-carbaldehyde (1.7 g, 10 mmol) was dissolved in 30 mL THF. K_2CO_3 (4.14 g, 30 mmol) was added and the mixture was refluxed for 30 min. Then propargyl bromide (1.7 mL, 12 mmol) was added

slowly. The mixture was refluxed overnight and cooled. After filtration solvent was evaporated. Crude product was purified by column chromatography (EtOAc: Hexane 1:4).

Yellow solid. (1.03 g, 86% yield); ^1H NMR (CDCl_3 , 400 MHz): δ 10.28 (s, 1H), 8.27 (dd, $J=0.7$ ve 8.5 Hz, 1H), 8.04 (d, $J=8.5$ Hz, 1H), 7.63-7.59 (m, 1H), 7.50 (dd, $J=1.2$ ve 8.3 Hz, 1H), 7.34 (dd, $J=1.2$ ve 7.8 Hz, 1H), 5.08 (d, $J=2.4$ Hz, 2H), 2.57 (t, $J=2.4$ Hz, 1H); ^{13}C NMR (CDCl_3 , 100 MHz): δ 193.6, 153.7, 151.6, 140.0, 137.3, 131.4, 129.4, 120.6, 117.9, 111.0, 77.8, 76.6, 56.9.

Synthesis of 2-((1-benzyl-1H-1,2,3-triazol-4-yl)methoxy)benzaldehyde, 2.

A mixture of benzyl bromide (1 mmol), 2-(prop-2-ynyloxy), 8-(Prop-2-iniloksi)kinolin-2-karbaldehit (211 mg, 1 mmol), L-proline (24 mg, 0.2 mmol), Na_2CO_3 (24 mg, 0.2 mmol), NaN_3 (65 mg, 1 mmol), sodium ascorbate (20 mg, 0.1 mmol), DMSO/ H_2O (18:2, 2.0 mL), and $\text{CuSO}_4 \cdot 5\text{H}_2\text{O}$ solution (1 M, 0.05 mL) in a 20 mL scintillation vial was stirred overnight at 65°C . The crude mixture was poured into cold dilute NH_4OH solution (30 mL) and extracted with ethyl acetate (3×20 mL). The collected organic layer was washed with brine, dried over MgSO_4 , and concentrated in *vacuo*. The crude product was purified by flash column chromatography.

Yellow solid. ^1H NMR (CDCl_3 , 400 MHz): δ 10.22 (s, 1H), 8.25 (dd, $J=3.3$ ve 8.5 Hz, 1H), 8.02 (dd, $J=4.0$ ve 8.4 Hz, 1H), 7.70 (s, 1H), 7.60-7.55 (m, 1H), 7.46 (dd, $J=2.0$ ve 8.2 Hz, 1H), 7.41 (dd, $J=1.8$ ve 7.8 Hz, 1H), 7.35-7.33 (m, 3H), 7.26-7.24 (m, 2H), 5.56 (d, $J=2.8$ Hz, 2H), 5.52 (d, $J=1.9$ Hz, 2H); ^{13}C NMR (CDCl_3 , 100 MHz): δ 193.6, 154.6, 151.4, 144.1, 140.1, 137.3, 134.3, 131.3, 129.7, 129.1, 128.8, 128.2, 123.2, 120.3, 117.8, 111.2, 63.4, 54.3.

General procedure for the synthesis of Schiff Bases, SB-1 and SB-2.

8-((1-benzyl-1H-1,2,3-triazol-4-yl)methoxy)quinoline-2-carbaldehyde **2** (170 mg, 0.5 mmol) and aryl amine (0.5 mmol) were dissolved in 5 mL ethanol. Reaction mixture was mixed at room temperature overnight. Solid was filtered and dried.

(E)-N-((8-((1-benzyl-1H-1,2,3-triazol-4-yl)methoxy)quinolin-2-yl)methylene)anthracen-1-amine, SB-1.

Yellow solid. ^1H NMR (CDCl_3 , 400 MHz): δ 9.00 (s, 1H), 8.95 (s, 1H), 8.67 (d, $J=8.5$ Hz, 1H), 8.46 (s, 1H), 8.32 (d, $J=8.5$ Hz, 1H), 8.08-8.02 (m, 2H), 7.95 (d, $J=8.5$ Hz, 1H), 7.69 (s, 1H), 7.56-7.46 (m, 5H), 7.38 (dd, $J=6.7$ ve 2.1 Hz, 1H), 7.33-7.22 (m, 5H), 7.16 (d, $J=7.0$ Hz, 1H), 5.60 (s, 2H), 5.50 (s, 2H); ^{13}C NMR (CDCl_3 , 100 MHz): δ 161.2, 154.3, 154.0, 148.4, 144.5, 136.7, 134.3, 132.1, 132.0, 131.6, 130.2, 129.1, 128.8, 128.7, 128.2, 128.1, 128.0, 127.7, 127.1, 126.1, 125.7, 125.4, 125.4, 123.1, 122.8, 120.4, 119.5, 111.6, 111.0, 63.6, 54.3.

(E)-N-((8-((1-benzyl-1H-1,2,3-triazol-4-yl)methoxy)quinolin-2-yl)methylene)pyren-1-amine, SB-2.

Yellow solid. ^1H NMR (CDCl_3 , 400 MHz): δ 9.11 (s, 1H), 8.79 (d, $J=9.2$ Hz, 1H), 8.67 (d, $J=9.5$ Hz, 1H), 8.27 (d, $J=8.5$ Hz, 1H), 8.21-8.17 (m, 3H), 8.14 (d, $J=9.2$ Hz, 1H), 8.08-7.99 (m, 3H), 7.90 (d, $J=8.2$ Hz, 1H), 7.70 (s, 1H), 7.53-7.46 (m, 2H), 7.38-7.22 (m, 6H), 5.61 (s, 2H), 5.49 (s, 2H); ^{13}C NMR (CDCl_3 , 100 MHz): δ 161.2, 154.2, 154.2, 144.5, 144.1, 140.2, 136.6, 134.3, 131.5, 131.4, 130.4, 130.2, 129.1, 128.8, 128.1, 128.1, 127.4, 127.3, 127.2, 126.2, 126.1, 125.6, 125.3, 125.2, 124.8, 123.2, 123.1, 120.4, 119.3, 115.3, 111.0, 63.5, 54.3.

Computational Method

The three-dimensional ground state (S_0) geometry of the compound was geometry optimized using Density Functional Theory (DFT) by using the Gaussian 16W package program and the hybrid functional B3LYP. The B3LYP is composed of Becke's three parameter exchange functional (B3) and the nonlocal correlation functional by Lee, Yang, and Parr (LYP). The basis set used for all atoms was 6-31++G(d,p) in both DFT and time-dependent density functional theory (TD-DFT) method. We have applied default G16 grid for computations.

For the novel compound, vibrational analyses were carried out using the same basis set employed in the corresponding geometry optimizations. The frequency analysis of none of the compounds yielded any imaginary frequencies, indicating that the structure of each molecule corresponds to at least a local minimum on the potential energy surface. The normal mode analysis was performed for $3N-6$ vibrational degrees of freedom, N being the number of atoms in the molecule.

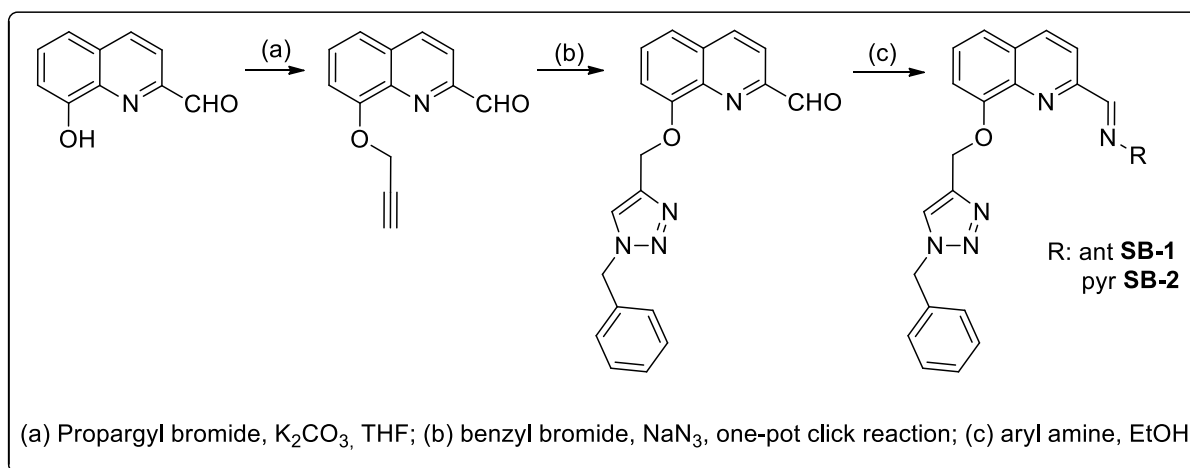
The low-lying triplet (T) and singlet excited states (S) of the compounds were relaxed to obtain their minimum energy geometries using the TD-DFT as implemented in Gaussian 16W package program. The vertical excitation energies and oscillator strengths were obtained for the lowest triplet and singlet transitions at the optimized ground state equilibrium geometries by using TD-DFT at the same hybrid functional and basis set. Optimized ground state structures were utilized to obtain the electronic absorption spectra, including maximum absorption wavelengths, oscillator strengths, and main configuration assignment by using TD-DFT.

2.2. Experimental Results

The key substrate 8-(prop-2-yn-1-yloxy)quinoline-2-carbaldehyde **1** was synthesized by the addition of propargyl bromide to commercially available 8-hydroxyquinoline-2-carbaldehyde by O-propargylation method (Scheme 1)

Terminal acetylene unit on 8-(prop-2-yn-1-yloxy)quinoline-2-carbaldehyde **1** make it a valuable candidate for one-pot synthesis of the target triazole structure **2**. Aliphatic and aromatic azides from corresponding halides

can easily be generated as intermediates in one-pot synthesis method and converted to desired triazole derivatives without isolation. The operational simplicity of this method makes it attractive for wide variety of applications. Initially, 8-(prop-2-yn-1-yloxy)quinoline-2-carbaldehyde was employed in one-pot, two-step procedure by reacting with sodium azide and benzyl bromide (Scheme 1).



Scheme 1. Synthesis of Schiff-base derivatives

The Schiff bases **SB-1** and **SB-2** were prepared by the condensation reaction of triazole-substituted hydroxyquinoline-2-carbaldehyde with the corresponding amino anthracene and amino pyrene as illustrated in Figure 1 below.

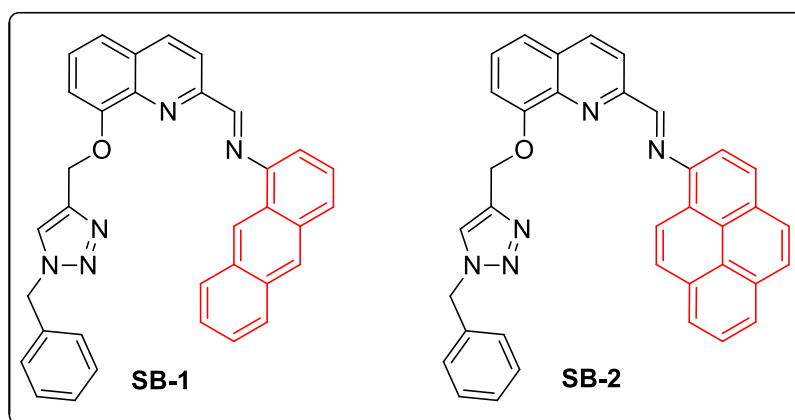


Figure 1. Synthesized Schiff bases

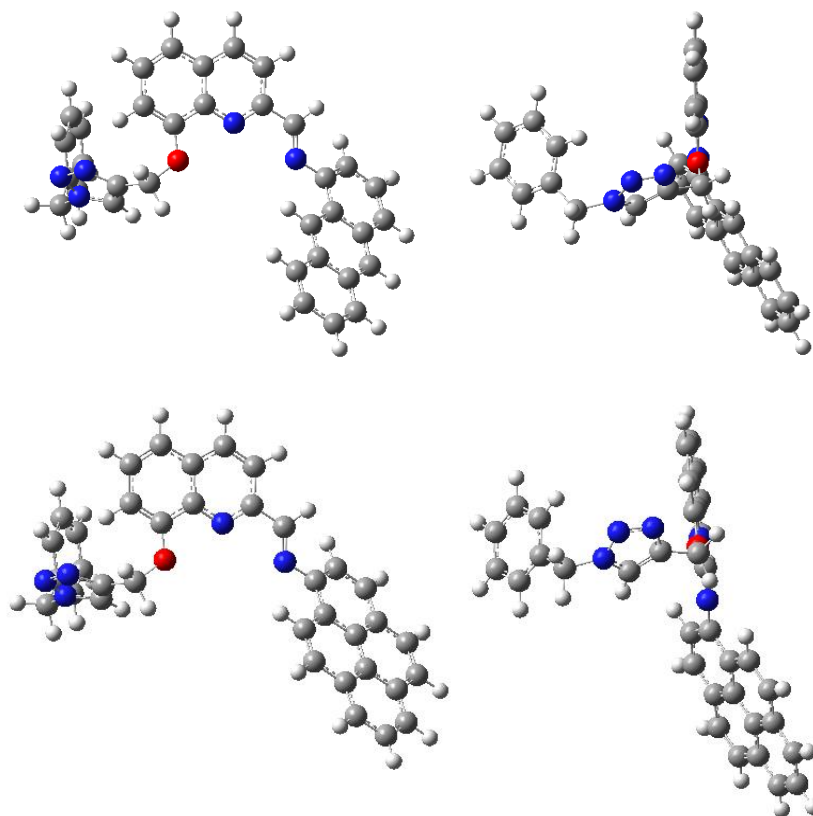


Figure 2. Geometry optimized structures of Schiff bases

The geometry optimized structures of the anthracene and pyrene Schiff base compounds have been obtained by the application of B3LYP/6-31++G(d,p) method. The front and side view of the geometries are given in Figure 2. Although triazole units are located towards outside the coordination center, there are still a few heteroatoms to form successful complexes with metals. The results of the TDDFT studies can be seen in Figure 3. For anthracene derivative (**SB-1**), non-metal structure possessed three bands at 260 nm, 390 nm and 520 nm whereas Zn^{2+} metal complex had only two strong bands at 380 nm and 580 nm. The band at 260 nm had disappeared. For the pyrene derivative (**SB-2**) (Figure 4) no peak lose is observed but peaks at 210, 290, 310 and 470 nm shifted to red in Zn^{2+} complex.

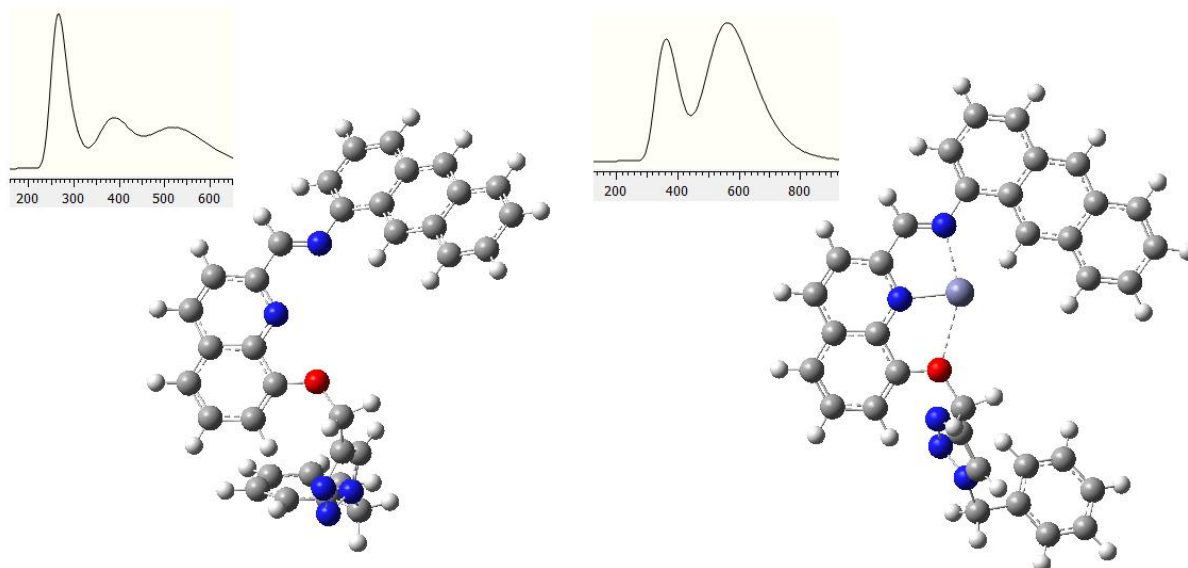


Figure 3. Geometry optimized structures and corresponding UV-Vis spectra of SB-1.

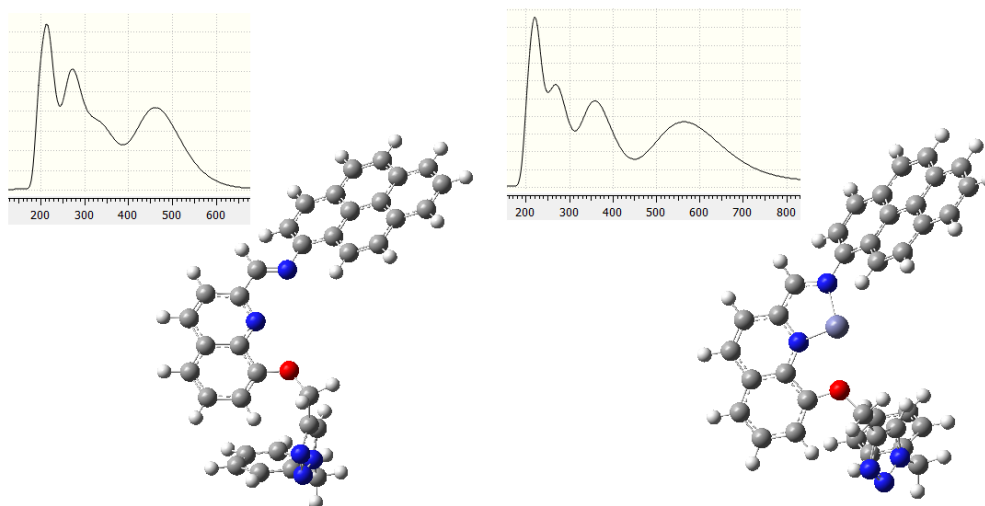


Figure 4. Geometry optimized structures and corresponding UV-Vis spectra of SB-2.

3. CONCLUSION

In conclusion, propargyl unit was attached to quinoline-aldehyde by O-propargylation and alkyne derivative was obtained. Then, triazole-substituted quinoline-aldehyde **2** was synthesized with high yield by one-pot method. Target fluorescent Schiff-bases were isolated from the reaction of aldehyde group on quinolinealdehyde ring with amino anthracene and amino pyrene successfully.

Theoretical calculation on the coordination ability of the compounds showed that the UV-Vis spectra of the compounds indicate high sensitivity to Zn²⁺ coordination. TDDFT computations of the metal coordinated Schiff bases yielded red-shifted bands.

Acknowledgement

We are grateful to Presidency of Scientific Research Projects of Van Yuzuncu Yil University for financial support (FDP-2019-7847).

References

- [1] Silva, A. P. Gunaratne, H. Q., Gunnlaugsson, T., Huxley, A. J. M., McCoy, C. P., Rademacher, J. T., Rice, T. E. (1997). Signaling Recognition Events with Fluorescent Sensors and Switches, *Chem. Rev.* 97, 1515-1566.
- [2] Hu, R., Feng, J., Hu, D. H., Wang, S.Q., Li, S., Li, Y., Yang, G. O. (2010). A Rapid Aqueous Fluoride Ion Sensor with Dual Output Modes, *Angew. Chem., Int. Ed.* 49, 4915-4918.
- [3] Fan, J., Hu, M., Zhan, P., Peng, X. (2013). Energy transfer cassettes based on organic fluorophores: construction and applications in ratiometric sensing, *Chem. Soc. Rev.* 42, 29-43.
- [4] Yang, Y., Zhao, Q., Feng, W., Li, F. (2013). Luminescent Chemodosimeters for Bioimaging, *Chem. Rev.* 113, 192-270.
- [5] Lim, X. (2016). The Nanoscale Rainbow, *Nature.* 531, 26.
- [6] Gao, M., Tang, B.Z. (2017). Fluorescent Sensors Based on Aggregation-Induced Emission: Recent advances and perspectives, *ACS Sens.* 2, 1382-1399.
- [7] Demirel, G.B., Daglar, B., Bayindir, M. (2013). Extremely fast and highly selective detection of nitroaromatic explosive vapours using fluorescent polymer thin films, *Chem Commun.* 55, 6140-6142.
- [8] (a) Ding, L., Fang, F. (2010). Chemically assembled monolayers of fluorophores as chemical sensing materials, *Chem Soc Rev.* 11, 4258-4273. (b) Sivaraman, G., Gulyani, A. (2018). Chemically diverse small molecule fluorescent chemosensors for copper ion. *Coord. Chem rev.*, 357, 50-104.
- [9] Shanmugaraju, S., Jadhav, H., Karthik, R., Mukherjee, P. S. (2013). Electron rich supramolecular polymers as fluorescent sensors for nitroaromatics, *RSC Adv.* 15, 4940-4950.
- [10] Pandey, R., Reddy, L., Ishihara, S., Dhir, A., Krishnan, V. (2013). Conformation induced discrimination between picric acid and nitro derivatives/anions with a Cu-pyrene array: the first decision making photonic device, *RSC Adv.* 3, 21365-21368.
- [11] Epstein, D. M., Choudhary, S., Churchill, M. R., Keil, K. M., Eliseev, A.V., Morrow, J. R. (2001). Chloroform-Soluble Schiff-Base Zn(II) or Cd(II) Complexes from a Dynamic Combinatorial Library, *Inorg. Chem.* 40, 1591-1596.
- [12] Da Silveira, V. C., Luz, J. S., Oliveira, C. C., Graziani, I., Ciriolo, M. R., Ferreira, A. M. (2008). Double-strand DNA cleavage induced by oxindole-Schiff base copper(II) complexes with potential antitumor activity, *J. Inorg. Biochem.* 102, 1090-1103.
- [13] Li, Y., Yang, Z. Y. (2009). DNA binding affinity and antioxidative activity of copper(II) and zinc(II) complexes with a novel hesperetin Schiff base ligand, *Inorg. Chim. Acta* 362, 4823-4831.
- [14] Kasselouri, S., Garoufis, A., Katehanakis, A., Kalkanis, G., Perlepes, S. P., Hadjiliadis, N. (1993). 1:1 Metal complexes of 2-(2'-pyridyl)quinoxaline, a ligand unexpectedly formed by the reaction between 2-acetylpyridine and 1,2-phenylenediamine, *Inorg. Chim. Acta* 207, 255-258.
- [15] Morris, G. A., Zhou, H., Stern, C. L., Nguyen, S. T., (2001). A General High-Yield Route to Bis(salicylaldimine) Zinc(II) Complexes: Application to the Synthesis of Pyridine-Modified Salen-Type Zinc(II) Complexes, *Inorg. Chem.* 40, 3222-3227.
- [16] Esvaran, S., Adhikari, A. V., Shetty, N. S. (2009). Synthesis and antimicrobial activities of novel quinoline derivatives carrying 1,2,4-triazole moiety, *Eur. J. Med. Chem.* 44, 4637-4647.
- [17] Kumar, S. S., Kavitha, H. P. (2013). Synthesis and biological applications of triazole derivatives, *Mini-Rev. Org. Chem.* 10, 40-65.
- [18] Radhika, C., Venkatesham, A., Sarangapani, M. (2012). Synthesis and antidepressant activity of disubstituted-5-aryl-1,2,4-triazoles, *Med. Chem. Res.* 31, 3509-3513.

- [19] Plech, T., Luszczki, J. J., Wujec, M., Flieger, J., Pizon, M. (2013). Synthesis, characterization and preliminary anticonvulsant evaluation of some 4-alkyl-1,2,4-triazoles, *Eur. J. Med. Chem.* 60, 208–215.
- [20] Chaudhary, P. M., Chavan, S. R., Shirazi, F., Razdan, M., Nimkar, P., Maybhate, S. P., Likhite, A. P., Gonnade, R., Hazara, B. G., Deshpande, S. R. (2009). Exploration of click reaction for the synthesis of modified nucleosides as chitin synthase inhibitors, *Bioorg. Med. Chem. Lett.* 17, 2433–2440.
- [21] Zhou, J. P., Zhang, H. B., Qian, H., Lin, L., Huang, W. L., Ni, S. J. (2009). Synthesis and biological evaluation of aromatase inhibitors, *Lett. Drug Design Discov.* 6, 181–185.
- [22] Holla, B. S., Mahalinga, N. S. (2005). Synthesis, characterization and antimicrobial activity of some substituted 1,2,3-triazoles, *Eur. J. Med. Chem.* 40, 1173–1178.
- [23] Elmorsi, M. A., Hassanein, A. M. (1999). Corrosion inhibition of copper by heterocyclic compounds, *Corros. Sci.* 41, 2337–2352.
- [24] Kim, D. K., Kim, J., Park, H. J. (2004). Synthesis and biological evaluation of novel 2-pyridinyl-[1,2,3]triazoles as inhibitors of transforming growth factor beta 1 type 1 receptor, *J. Bioorg. Med. Chem. Lett.* 14, 2401–2405.
- [25] Seo, T. S., Li, Z., Ruparel, H., Lu, J. (2003). Click chemistry to construct fluorescent oligonucleotides for DNA sequencing, *J. Org. Chem.* 68, 609–612.
- [26] Sivakumar, K., Xie, F., Cash, B. M., Long, S., Barnhill, H. N. A (2004). Fluorogenic 1,3-dipolar cycloaddition reaction of 3-azidocoumarins and acetylenes, *Org. Lett.* 6, 4603–4606.
- [27] Dondoni, A., Marra, A. (2006). “Click chemistry” inspired synthesis of *pseudo*-oligosaccharides and amino acid glycoconjugates, *J. Org. Chem.* 71, 364–367.
- [28] Chan, J., Dodani, S. C., Chang, C. J. (2012). Reaction-based small-molecule fluorescent probes for chemoselective bioimaging, *Nature Chemistry* 4, 973–984.



SYNTHESIS OF A FLUORESCENT TRIAZOLE DERIVATIVE AND THEORETICAL INVESTIGATION OF ITS METAL SENSOR PROPERTY

Ayşegül GÜMÜŞ

Van Yüzüncü Yıl University, Department of Chemistry, Faculty of Science, Campus, Van

ORCID ID: 0000-0002-1613-7074

Selçuk GÜMÜŞ

Van Yüzüncü Yıl University, Department of Chemistry, Faculty of Science, Campus, Van

ORCID ID: 0000-0002-8628-8943

ABSTRACT

Fluorescent sensor is one of the most important chemical sensors and is a powerful tool for imaging target molecules and ions in the living organism. Because it has high sensitivity and simultaneous imaging. 8-Hydroxyquinoline is one of the widely used chelating moieties for metal ion coordination, and quite a number of chemically modified 8-hydroxyquinoline derivatives have been used as metal binding probes. Triazole substituted 8-HQ could furnish an extra binding site, and might inhibit the possible excited-state intramolecular proton transfer (ESIPT) event.

In this work, fluorescence chemosensor was designed based on ionophore-bridge-fluorophore approach. In the structure of the designed chemosensor, anthracene unit was used as fluorophore. The receptoric hydroxy quinoline group to interact with the metal ion were incorporated into the structure by the triazole bridge which has high coordination properties. Detection of a specific type of a metal is very important in terms of biouse of the related compound. In addition to the synthetic approach, the metal coordination properties of the novel chemosensor was investigated theoretically at the level of Density Functional theory with the application of B3LYP/6-31++G(d,p), which is a combination of hibrit exchange function and basis set.

Keywords: Anthracene, Triazole, Quinoline, Structural And Electronic Properties

1. INTRODUCTION

In recent years, more and more attentions have been drawn to devise ingenious fluorescent sensors capable of selective recognition and effectively detecting the presence of alkali, alkaline earth and transition metal ions because of their importance in biological systems as well as to environmental concerned [1,2]. However, among different chemosensors, fluorescence-based ones present many advantages as fluorescence measurements are usually very sensitive, low cost, easily performed and versatile, offering subnanometer spatial resolution with submicron visualization and submillisecond temporal resolution [3,4].

8-Hydroxyquinoline is one of the widely used chelating moieties for metal ion coordination, and quite a number of chemically modified 8-hydroxyquinoline derivatives have been used as metal binding probes [5-9]. 8-HQ

was introduced into fluorescent probes acting as a metal ion chelating agent for metal ions detection. Triazole substituted 8-HQ could furnish an extra binding site, and might inhibit the possible excited-state intramolecular proton transfer (ESIPT) event.

The chemistry of 1,2,3-triazole derivatives has gained interest over the past few years due to their wide range of applications in chemical, biological, medicinal, and materials science. The Huisgen 1,3-dipolar cycloaddition of azides and alkynes is the most efficient pathway for the synthesis of substituted 1,2,3-triazoles as chemotherapeutic agents [10-11], synthetic intermediates for bioactive compounds, agrochemicals, optical brighteners, photostabilizers, anticorrosive agents, and metal chelators [12-14]. The extraordinary stability toward metabolic transformations and aromatic nature of the triazole ring along with its high dipole moment and H-bonding capability, makes it an important functionality as a connecting group [15-18].

In the present study, the synthetic typical motif consist of a core fluorescent signaling unit of anthracene, which is well connected with oxyquinoline through triazole bridge, to generate a suitable ionophore site that has great affinity to coordinate with a metal ion.

2. RESULTS AND DISCUSSION

2.1. Experimental

General

All experiments were carried out in pre-dried glassware an inert atmosphere of argon. All the chemicals used in the biologic assay studies were purchased from Sigma (Sigma-Aldrich GmbH, Sternheim, Germany). ^1H NMR and ^{13}C NMR spectra were recorded in CDCl_3 on a Agilent NMR spectrometer (400 MHz). ^1H (400 MHz) and ^{13}C NMR (100 MHz) were recorded in CDCl_3 and the chemical shifts are expressed in ppm relative to CDCl_3 (δ 7.26 and 77.0 for ^1H and ^{13}C NMR, respectively) as the internal standard.

Flash column chromatography was performed by using thick-walled glass columns and silica gel (60-mesh; Merck). The reactions were monitored by thin-layer chromatography (TLC) using Merck 0.2-mm silica gel 60 F254 analytical aluminium plates, visualized by UV light.

Synthesis of Fluorescent Sensor

8-(prop-2-ynyloxy)quinoline-2-carbaldehyde, **2**.

8-hydroxyquinoline-2-carbaldehyde **1** (1.0 g, 5.7 mmol) was dissolved in 30 mL THF. K_2CO_3 (2.0 g, 15 mmol) was added and the mixture was refluxed for 30 min. Then, propargyl bromide (1 mL, 6.8 mmol) was added slowly. Reaction mixture was refluxed overnight. After TLC control, reaction mixture was cooled and filtered.

Solvent was evaporated under vacuum and crude product was purified by flash column chromatography (EtOAc: Hexane 1:4).

White solid. (1.03 g, 86% yield); ^1H NMR (CDCl_3 , 400 MHz): δ 10.28 (s, 1H), 8.27 (dd, $J=0.7$ and 8.5 Hz, 1H), 8.04 (d, $J=8.5$ Hz, 1H), 7.63-7.59 (m, 1H), 7.50 (dd, $J=1.2$ and 8.3 Hz, 1H), 7.34 (dd, $J=1.2$ and 7.8 Hz, 1H), 5.08 (d, $J=2.4$ Hz, 2H), 2.57 (t, $J=2.4$ Hz, 1H); ^{13}C NMR (CDCl_3 , 100 MHz): δ 193.6, 153.7, 151.6, 140.0, 137.3, 131.4, 129.4, 120.6, 117.9, 111.0, 77.8, 76.6, 56.9.

(8-(prop-2-yn-1-yloxy)quinolin-2-yl)methanol, **3**.

8-(prop-2-ynyloxy)quinoline-2-carbaldehyde **2** was dissolved in 10 mL methanol. NaBH_4 was added to reaction mixture and stirred at room temperature. After the reaction completed, 1 mL of water was added and extracted with EtOAc. Solvent was evaporated under vacuum and crude product was purified by flash column chromatography (EtOAc: Hexane 1:4).

Pale yellow solid. (1.81 g, 85% yield); ^1H NMR (CDCl_3 , 400 MHz): δ 8.11 (d, $J=8.5$ Hz, 1H), 7.46 (d, $J=1.2$ Hz, 1H), 7.44 (s, 1H), 7.38 (d, $J=8.5$ Hz, 1H), 7.28-7.26 (m, 1H), 4.99 (d, $J=2.4$ Hz, 2H), 4.94 (s, 2H), 2.54 (t, $J=2.4$ Hz, 1H); ^{13}C NMR (CDCl_3 , 100 MHz): δ 158.6, 152.7, 138.9, 136.9, 128.8, 126.2, 120.8, 119.1, 111.5, 78.4, 76.1, 64.8, 57.0.

9-(azidomethyl)anthracene, **4**.

9-(Chloromethyl)anthracene (227 mg, 1 mmol) ve NaN_3 (130 mg, 2 mmol) were dissolved in 20 mL CH_3CN and refluxed overnight at 85 °C. After all starting compounds were consumed, reaction mixture was filtered and solvent was evaporated under vacuum. Crude product was purified by flash column chromatography by EtOAc:Hexane mixture (1:15).

Yellow solid. (228 mg, 98% yield); ^1H NMR (CDCl_3 , 400 MHz): δ 8.51 (s, 1H), 8.32-8.28 (m, 2H), 8.07-8.06 (m, 1H), 8.05-8.04 (m, 1H), 7.62-7.58 (m, 2H), 7.54-7.50 (m, 2H), 5.33 (s, 2H); ^{13}C NMR (CDCl_3 , 100 MHz): δ 131.4, 130.7, 129.3, 129.0, 126.8, 125.8, 125.2, 123.5, 46.3.

8-((1-(anthracen-9-ylmethyl)-1H-1,2,3-triazol-4-yl)methoxy)quinoline-2-carbaldehyde, **5**.

(8-(prop-2-yn-1-yloxy)quinolin-2-yl)methanol, **3** (213 mg, 1 mmol) and 9-(azidomethyl)anthracene, **4** (233 mg, 1 mmol) were dissolved in 5 mL $\text{THF}:\text{H}_2\text{O}$ (4:1). $\text{CuSO}_4\cdot 5\text{H}_2\text{O}$ (25 mg, 0.1 mmol) and sodium ascorbate (40 mg, 0.2 mmol) were added and reaction mixture was mixed overnight at room temperature. After the reaction was complete, water was added and extracted with EtOAc. Product was purified by flash column chromatography by EtOAc:Hexane (2:1).

Yellow solid. (300 mg, 67% yield); ^1H NMR ($\text{CDCl}_3/\text{DMSO}$, 400 MHz): δ 8.54 (s, 1H), 8.41 (d, $J=8.9$ Hz, 2H), 8.07 (d, $J=8.5$ Hz, 1H), 8.02 (d, $J=8.4$ Hz, 2H), 7.68 (s, 1H), 7.56-7.52 (m, 3H), 7.48-7.44 (m, 2H), 7.33-7.25 (m, 2H), 7.16-7.14 (m, 1H), 6.53 (s, 2H), 6.21 (s, 2H), 4.62 (s, 2H); ^{13}C NMR (DMSO, 100 MHz): δ 160.9, 153.5, 143.4, 138.9, 136.6, 131.4, 130.7, 129.6, 129.4, 128.5, 127.5, 126.1, 125.5, 124.8, 123.8, 123.6, 120.4, 119.6, 111.1, 65.3, 62.8, 46.1.

Computational Method

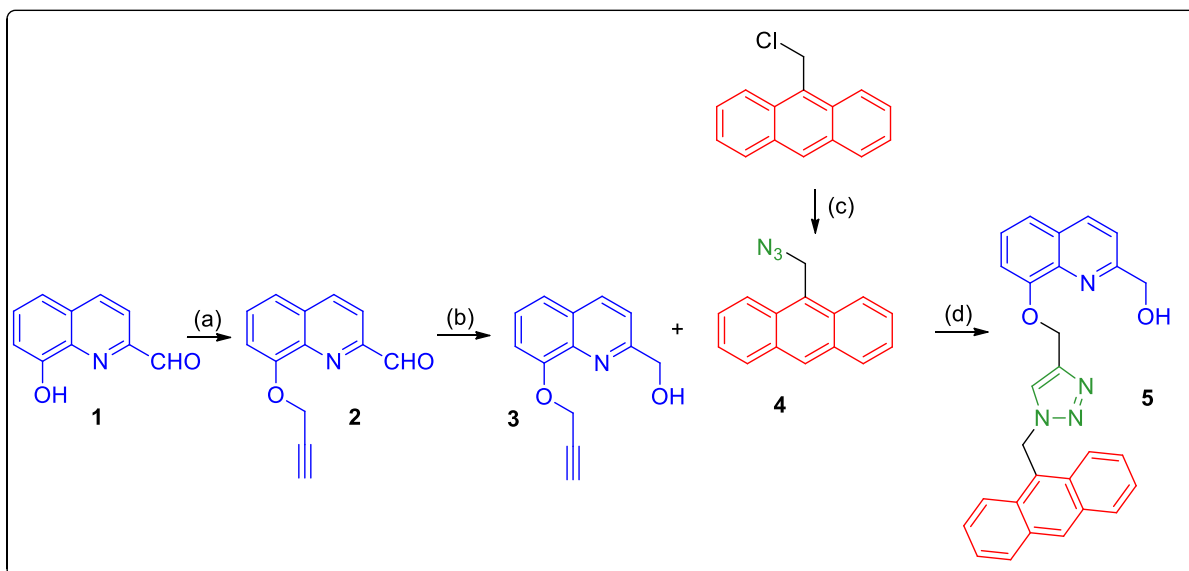
The three-dimensional ground state (S_0) geometry of the compound was geometry optimized using Density Functional Theory (DFT) by using the Gaussian 09W package program and the hybrid functional B3LYP. The B3LYP is composed of Becke's three parameter exchange functional (B3) and the nonlocal correlation functional by Lee, Yang, and Parr (LYP). The basis set used for all atoms was 6-31++G(d,p) in both DFT and time-dependent density functional theory (TD-DFT) method. We have applied default G09 grid for computations.

For the nonel compound, vibrational analyses were carried out using the same basis set employed in the corresponding geometry optimizations. The frequency analysis of none of the compounds yielded any imaginary frequencies, indicating that the structure of each molecule corresponds to at least a local minimum on the potential energy surface. The normal mode analysis was performed for $3N-6$ vibrational degrees of freedom, N being the number of atoms in the molecule.

The low-lying triplet (T) and singlet excited states (S) of the compounds were relaxed to obtain their minimum energy geometries using the TD-DFT as implemented in G09 package program. The vertical excitation energies and oscillator strengths were obtained for the lowest triplet and singlet transitions at the optimized ground state equilibrium geometries by using TD-DFT at the same hybrid functional and basis set [22]. Optimized ground state structures were utilized to obtain the electronic absorption spectra, including maximum absorption wavelengths, oscillator strengths, and main configuration assignment by using TD-DFT.

2.2. Experimental Results

The present molecular probe containing quinoline and anthracene fluorophores has been synthesized. The synthetic route adopted for preparation of **5** is shown in Scheme 1. Click chemistry, serving as a linking strategy for the 1, 3 dipolar cycloaddition of alkyne and azide by generating 1, 2, 3-triazoles, has been exploited in the wide variety of areas including bio conjugation, drug design and material chemistry. Meanwhile, the 1,2,3-triazole linker could be exploited for the binding of cations which might be useful in the recognition of metal ions. Based on this statement, the probe **5** was designed (Scheme 1). This could be easily synthesized using the anthracene azide **4** and alkyne of 8-oxyquinoline, **2** in the presence of CuSO_4 as a catalyst.



Scheme 1. (a) Propargyl bromide, K_2CO_3 , THF; (b) $NaBH_4$, MeOH; (c) NaN_3 , THF; (d) $CuSO_4$, sodium ascorbate.

2.3. Computational Results

First of all, geometry optimization of the quinoline based anthracene derivative and its complex with Zn^{2+} have been performed to obtain the ground state structure. The structures after geometry optimization can be seen in Figure 1. As can be observed the triazole moiety is directed out of the coordination center which was unfortunate for us since the triazole nitrogen units had been thought to be a very well coordination part of this potential chemosensor. However, hydroxyl groups formed a very nice coordination with the metal. The UV-VIS spectra of the compounds have been obtained by the same method of computation. The non-metal triazole compound has got two major peaks at around 200-250 nm and a non-intense peak at 390 nm. Zn complex possesses a new band at around 720 nm which is the intensified band of the parent structure that shifted red.

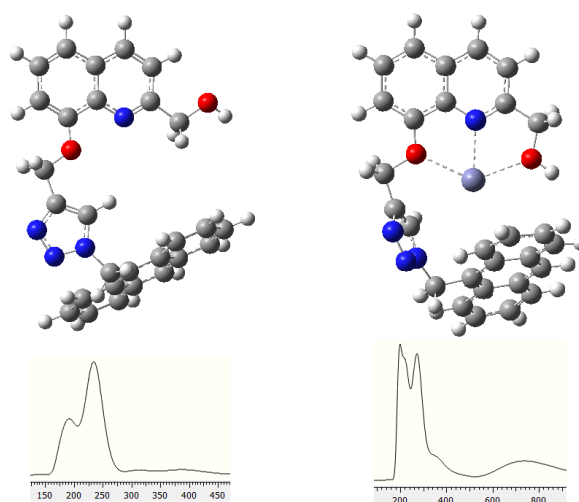


Figure 1. Geometry optimized structures and corresponding UV-VIS spectra of the compound 5

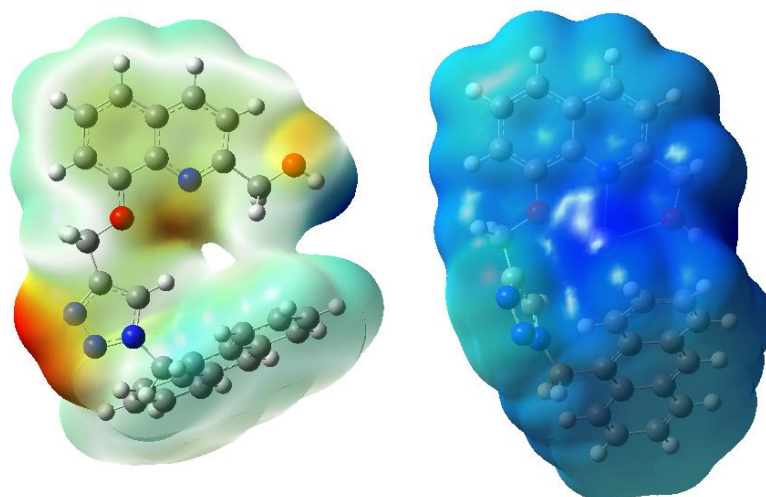


Figure 2. 3D electrostatic potential maps for triazole compound **5**

When the electrostatic potential maps of the structures are examined, it is seen that the region where coordination is expected is rich in electrons. Therefore, cationic structures have a high potential to approach this region and form a coordination complex. However, the nitrogens of the triazole ring also carry a significant negative charge. It is important how this will affect the interaction of cations and anthracene-triazole-quinoline structures. As can be seen from Figure 2, upon coordination of the metal the electron distribution throughout the system has completely changed due to electron donation from the main structure to the central metal cation.

3. CONCLUSION

In conclusion, propargyl unit was attached to 8-OH of quinoline by O-propargylation and alkyne derivative was obtained. Then, aldehyde group on quinoline ring was reduced to alcohol unit. In the last step, anthracene azide was coupled with this quinoline-alkyne derivative in the presence of Cu(I) catalyst by forming triazole bridge and a novel fluorescent sensor was isolated in good yield. Theoretical calculation on the coordination ability of this quinoline derivative showed that the UV-Vis spectrum of the compound changed upon metal coordination. TDDFT computations of the metal coordinated compound yielded red-shifted bands.

Acknowledgement

We are grateful to the Turkish Scientific and Technical Research Council for the Grant (No. 118Z421).

References

- [1] Krämer, R. (1998). Fluorescent Chemosensors for Cu²⁺ Ions: Fast, Selective, and Highly Sensitive. *Angew. Chem. Int. Ed.* 37, 772–773.
- [2] Uauy, R., Olivares, M., Gonzalez, M. (1998). Essentiality of copper in humans. *Am. J. Clin. Nutr.* 67, 952–959.

- [3] de Silva, A. P., Gunaratne, H. Q. N., Gunlaugsson, T., Huxley, A. J. M., McCoy, C. P., Rademacher, J. T., Rice, T. E. (1997). Signaling Recognition Events with Fluorescent Sensors and Switches. *Chem. Rev.* 97, 1515–1566.
- [4] Czarnik, A.W. (1992). *Fluorescent Chemosensors for Ion and Molecule Recognition*, first ed., A.C.S, Washington.
- [5]. Chen, Y., Wan, L., Yu, X., Li, W., Bian, Y. and Jiang, J. (2011). Rational Design and Synthesis for Versatile FRET Ratiometric Sensor for Hg²⁺ and Fe²⁺: A Flexible 8-hydroxyquinoline Benzoate Linked Bodipy-Porphyrin Dyad. *Org. Lett.*, 13, 5774-5777.
- [6]. Jotterand, N., Pearce, D. A. and Imperiali, B. (2001). Asymmetric Synthesis of a New 8-Hydroxyquinoline-Derived α -Amino Acid and Its Incorporation in a Peptidylsensor for Divalent Zinc. *J. Org. Chem.*, 66, 3224-3228.
- [7]. Zhao, Y., Lin, Z., Liao, H., Duan, C. and Meng, Q. (2006). A highly selective fluorescent chemosensor for Al³⁺ derived from 8-hydroxyquinoline. *Inorg. Chem. Commun.*, 9, 966-968.
- [8]. Li, Z., Xi, P., Huang, L., Xie, G., Shi, Y., Liu, H., Xu, M., Chen, F. and Zeng, Z. (2011). A highly selective fluorescent chemosensor for Cd(II) based on 8-hydroxyquinoline platform. *Inorg. Chem. Commun.*, 2011, 14, 1241-1244.
- [9]. Tian, H., Li, B., Wang, H., Li, Y., Wang, J., Zhao, S., Zhu, J., Wang, Q., Liu, W., Yao, X. and Tang, Y. (2011). A nanocontainer that releases a fluorescence sensor for cadmium ions in water and its biological applications. *J. Mater. Chem.*, 21, 10298-10304.
- [10] Huisgen, R. (1984). 1,3-Dipolar Cycloaddition—Introduction, Survey, Mechanism. In *1,3-Dipolar Cycloaddition Chemistry*. Padwa, A., Ed. Wiley: New York.
- [11] Agalave, S. G., Maujan, S. R., Pore, V. S. (2011). Click chemistry: 1,2,3-triazoles as pharmacophores. *Chem. Asian J.*, 6, 2696–2718.
- [12] Krivopalov, V. P., Shkurko, O. P. (2005), 1,2,3-Triazole and its derivatives. Development of methods for the formation of the triazole ring. *Russian Chem. Rev.*, 74, 339–379.
- [13] Yet, L. (2004). *Progress in Heterocyclic Chemistry*; Elsevier, Oxford, UK.
- [14] Katritzky, A. R., Zhang, Y., Singh, S. K. (2003). 1,2,3-Triazole formation under mild conditions via 1,3-dipolar cycloaddition of acetylenes with azides. *Heterocycles*, 60, 1225–1239.
- [15] Seo, T. S., Li, Z., Ruparel, H., Lu, J. (2003). Click chemistry to construct fluorescent oligonucleotides for DNA sequencing. *J. Org. Chem.*, 68, 609–612.
- [16] Sivakumar, K., Xie, F., Cash, B. M., Long, S., Barnhill, H. N. (2004). A fluorogenic 1,3-dipolar cycloaddition reaction of 3-azidocoumarins and acetylenes. *Org. Lett.* 6, 4603–4606.
- [17] Dondoni, A., Marra, A. (2006). C-Glycoside clustering on calix[4]arene, adamantane, and benzene scaffolds through 1,2,3-triazole linkers. *J. Org. Chem.*, 71, 7546–7557.
- [18] Hota, S., Kashyap, S. (2006). “Click chemistry” inspired synthesis of *pseudo*-oligosaccharides and amino acid glycoconjugates. *J. Org. Chem.* 71, 364–367.

ANTIBACTERIAL ACTIVITY OF RGO/CLAY COMPOSITE AGAINST VARIOUS BACTERIA AND YEASTS

Nurşah KÜTÜK

Sivas Cumhuriyet University, Department of Chemical Engineering

Sevgi DURNA DAŞTAN

Sivas Cumhuriyet University, Department of Biology

Sevil ÇETİNKAYA GÜRER

Sivas Cumhuriyet University, Department of Chemical Engineering

ABSTRACT

Graphene has become the most popular material in recent years due to its high mechanical and thermal strength, large surface area, lightness and many other unique properties. It is used in various application areas such as drug release, sensors, photocatalytic removal. In addition, graphene and its modified composites are used in many biomedical applications such as drug release, bioimaging, anticancer agent, biosensor development, photothermal therapy, tissue engineering and photocatalytic activity. For this reason, there is an increasing trend for the supply of materials with low toxicity and antibacterial properties. In this study, the antibacterial activity of reduced graphene oxide (RGO)/clay composite, in which graphene, reduced graphene oxide and sodium bentonite (NaB) was modified, was analyzed in different yeasts and bacteria. The antibacterial analysis of the samples were made according to the Minimum Inhibition Broth method. *Staphylococcus aureus* (ATTC 29213), *Pseudomonas aeruginosa* (ATCC 27853), *Escherichia coli* (ATCC 25922) and *Bacillus cereus* (ATCC 11778) bacteria and *Candida albicans* (ATCC 10231), *Candida tropicalis* (DSM 11953) yeasts were used during the analysis. The antibacterial properties of the samples were determined according to the minimum inhibition concentration (MIC).

Keywords: Graphene, clay, antibacterial activity, *Escherichia coli*, RGO

INTRODUCTION

Graphene, which is a two-dimensional and crystalline material, has properties such as very good strength, elasticity, thermal and electric conductivity (Zhong et al., 2017). Various methods such as micromechanical method, chemical vapor method, epitaxis growth are used for graphene synthesis (Kavinkumar et al., 2017). Reduced GO synthesized by reduction of graphene oxide is a cheap technique to obtain graphene (Gupta et al., 2017). Graphene-based materials are attracting attention among nanomaterials due to their many unique properties. Graphene oxide and reduced graphene oxide have been reported to have antibacterial properties against many bacteria (Guo et al., 2017). Graphene is used in various biomedical applications such as bioimaging, drug release, antibacterial agent, biomolecule detection (Kavinkumar et al., 2017). In addition, it is used as a drug carrier especially in cancer treatment due to its biocompatibility, large surface area and

physicochemical properties (Huang et al., 2018).

In this study, antibacterial activity of RGO/NaB and RGO/NaB/PEG composites was investigated according to microdilution broth method. The effect of adding sodium bentonite and PEG to RGO on antibacterial activity was investigated.

MATERIALS AND METHOD

Antibacterial Activity

The GO used in the study was characterized in our previous published study (Kütük et al. 2019). Microdilution Broth method against microorganisms was used to determine the minimum inhibition concentration (MIC) of GO, NaB, RGO/NaB and RGO/NaB/PEG samples [Eloff, 1998]. *Staphylococcus aureus* (ATCC 29213), *Pseudomonas aeruginosa* (ATCC 27853), *Escherichia coli* (ATCC 25922), *Bacillus cereus* (ATCC11778), *Candida albicans* (ATCC 10231) and *Candida tropicalis* (DSM11953) microorganisms were used in the study. The chemicals could not be dissolved in the distilled water solvent in the ultrasonic water bath. Ethanol was added to dissolve it, in this case the dissolution process is achieved, but since ethyl alcohol is already cytotoxic on microorganisms, the effect of chemicals dissolved in ethyl alcohol-water solvent on microorganisms could not be investigated. Therefore, stock solutions were prepared by dissolving the chemicals in 20% dimethyl sulfoxide (DMSO). (DMSO is a frequently preferred substance since it has no effect on microorganisms) Stock solutions were prepared at a concentration of 100 mg/ml. PEG used in the preparation of chemicals is not cytotoxic on microorganisms. For control purposes, PEG was also applied on microorganisms. Since PEG is in liquid form, serial dilutions of 1/5, 1/10, 1/20 etc... were applied to the wells. Mueller Hinton Broth (Accumix® AM1072) for bacteria, Saboraud Dextrose Broth (Himedia ME033) media for *Candida albicans* and *Candida tropicalis* were used. 90 µl of medium was added to the wells in the first row of the microtiter plates and 50 µl of medium was added to the other wells. 11th the wells in the row were used as sterility control and 100 µl of medium was added (CLSI, 2012; CLSI, 2002). Wells in the 12th row were used as growth control. 10 µl of extract was added to the first row of wells and serial dilution was made. A suspension of McFarland 0.5 turbidity was prepared from microorganisms grown on blood agar medium, by extracting loops. 50 µl of microorganism suspension was added to each well at 5×10^5 CFU/mL for bacteria and $0.5-2.5 \times 10^3$ CFU/mL for *Candida albicans*. Plates with bacteria added were incubated at 37 °C, plates with *Candida albicans* added at 35 °C for 16-24 hours. Here, the first wells with reduced bacterial colony appearance were considered as the MIC value. The test was repeated 3 times and the same results were obtained.

RESULTS AND DISCUSSION

Substances are reported as significant when their antimicrobial activity values are 0.1 mg/ml or less, moderately effective in the range of $0.1 < MIC \leq 0.625$ mg/ml, and weakly effective when the MIC value is more than 0.625 mg/ml (Awouafack et al., 2013; Kuete, 2010). The antimicrobial activity values of the analyzed chemicals were found to be 2.5 mg/ml for RGO/NaB composite and 5 mg/ml for RGO/NaB/PEG composite on only *E. coli* bacteria. This may be due to the fact that *E. coli*, as a gram-negative bacterium, have a thin cell wall (Pourbeyram et al., 2017). It is seen in Table 1 that the antimicrobial activities of other materials on microorganisms are >5 mg/ml. Researchers reported that GO has the strongest antibacterial activity among nanomaterials containing graphite, GO and RGO, and both GO and RGO can be a potential antibacterial agent. The physical and chemical interaction between the cells of microorganisms and GO is the main reason why GO is antibacterial (Nanda et al., 2016). However, this situation is variable depending on the particle size, surface area, oxygen-containing groups and number of layers (Gurunathan & Kim, 2016). It is seen that all the materials used and prepared in this study (Table 1) have weak antimicrobial effects on 6 different microorganisms. However, its antimicrobial effect on different microorganisms has not been studied yet and it is planned to examine the antimicrobial properties of different materials and microorganisms for future research.

Table 1. Antibacterial activity of RGO/NaB, RGO/NaB/PEG, GO and NaB, PEG 400 samples against *E.coli*, *S. Aureus*, *P. Aeruginosa*, *B. Cereus*, *C. Albicans*, *C.tropicalis* microorganisms

		E.coli	S.aureus	P.aeruginosa	B.cereus	C.albicans	C.tropicalis
Sample name	Stock Concentration	ATCC 25922	ATCC 29213	ATCC 27853	ATCC11778	ATCC10231	DSM11953
RGO/NaB	100 mg/ml (DMSO)	2.5 mg/ml	>5 mg/ml	>5 mg/ml	>5 mg/ml	>5 mg/ml	>5 mg/ml
RGO/NaB/PEG	100 mg/ml (DMSO)	5 mg/ml	>5 mg/ml	>5 mg/ml	>5 mg/ml	>5 mg/ml	>5 mg/ml
GO	100 mg/ml (DMSO)	>5 mg/ml	>5 mg/ml	>5 mg/ml	>5 mg/ml	>5 mg/ml	>5 mg/ml
(PEG 400)	Pure	$>1/5$	$>1/10$	$>1/20$	$>1/40$	$>1/80$	$>1/160$

CONCLUSION

Graphene modified materials are frequently used in the biomedical field. Therefore, its antibacterial properties are important. In this study, antibacterial properties of RGO-based composites were found to be weak. This value was determined as 2.5 mg/ml against *Escheria coli* for the RGO/NaB composite. The antibacterial properties of GO improved with the addition of PEG and NaB after reduction.

References

- Awouafack, M. D., McGaw, L. J., Gottfried, S., Mbouangouere, R., Tane, P., Spiteller, M., & Eloff, J. N. (2013). Antimicrobial activity and cytotoxicity of the ethanol extract, fractions and eight compounds isolated from *Eriosema robustum* (Fabaceae). *BMC Complementary and Alternative Medicine*, 13.
- CLSI, (2012). *Methods for Dilution Antimicrobial Susceptibility Tests for Bacteria that Grow Aerobically*, Approved Standard, 9th ed., CLSI document M07-A9. Clinical and Laboratory Standards Institute, 950 West Valley Road, Suite 2500, Wayne, Pennsylvania 19087, USA.
- CLSI, (2002). *Reference Reference Method for Broth Dilution Antifungal Susceptibility Testing of Yeasts*, Approved Standard, 2nd ed., NCCLS document M27- A2. CLSI, 940 West Valley Road, Suite 1400, Wayne, Pennsylvania 19087- 1898, USA.
- Eloff, JN., (1998). A sensitive and quick microplate method to determine the minimal inhibitory concentration of plant extracts for bacteria. *Planta Med*, 64, 711–713
- Guo, Z., Xie, C., Zhang, P., Zhang, J., Wang, G., He, X., Ma, Y., Zhao, B., & Zhang, Z. (2017). Toxicity and transformation of graphene oxide and reduced graphene oxide in bacteria biofilm. *Science of the Total Environment*, 580, 1300–1308.
- Gupta, V., Sharma, N., Singh, U., Arif, M., & Singh, A. (2017). Higher oxidation level in graphene oxide. *Optik*, 143, 115–124.
- Gurunathan, S., & Kim, J. H. (2016). Synthesis, toxicity, biocompatibility, and biomedical applications of graphene and graphene-related materials. *International Journal of Nanomedicine*, 11, 1927–1945.
- Huang, C., Wu, J., Jiang, W., Liu, R., Li, Z., & Luan, Y. (2018). Amphiphilic prodrug-decorated graphene oxide as a multi-functional drug delivery system for efficient cancer therapy. *Materials Science and Engineering C*, 89(March), 15–24.
- Kavinkumar, T., Varunkumar, K., Ravikumar, V., & Manivannan, S. (2017). Anticancer activity of graphene oxide-reduced graphene oxide-silver nanoparticle composites. *Journal of Colloid and Interface Science*, 505(July), 1125–1133.
- Kuete, V. (2010). Potential of Cameroonian plants and derived products against microbial infections: A review. *Planta Medica*, 76(14), 1479–1491.
- Kütük, N., Boran, F., Çetinkaya Güner, S. (2019). Green Reduction of Graphene Oxide By Using Kombucha Tea. *Eskişehir Technical University Journal of Science and Technology A - Applied Sciences and Engineering*, December.
- Nanda, S. S., Yi, D. K., & Kim, K. (2016). Study of antibacterial mechanism of graphene oxide using Raman spectroscopy. *Scientific Reports*, 6(June).
- Pourbeyram, S., Bayrami, R., & Dadkhah, H. (2017). Green synthesis and characterization of ultrafine copper oxide reduced graphene oxide (CuO/rGO) nanocomposite. *Colloids and Surfaces A: Physicochemical and Engineering Aspects*, 529(May), 73–79.
- Zhong, Y., Zhen, Z., & Zhu, H. (2017). Graphene: Fundamental research and potential applications. *FlatChem*, 4, 20–32.

EFFECT OF OXIDATION ON METHYLENE BLUE PHOTOLYSIS

Nurşah KÜTÜK

Sivas Cumhuriyet University, Department of Chemical Engineering

Sevil ÇETİNKAYA GÜRER

Sivas Cumhuriyet University, Department of Chemical Engineering

Abstract

In recent years, paint, pharmaceutical, toxic and carcinogenic by-product chemicals have polluted the nature. Removal of dyes in wastewater resulting from industrial applications is important in terms of preventing environmental pollution and harm to human health. Some of dyes as cationic and anionic such as methylene blue (MB), methyl orange (MO), malachite green (MG) and rhodamine B lead to environmental pollution owing to the existence in polluted water. Photodegradation technique for dye removal from wastewater has been applied in the presence of various photocatalysts. Among these materials, inorganic materials such as bentonite, kaolin or zeolite, graphene and its derivatives, metal and metal oxide nanoparticles and composite materials modified with various polymers can be listed. Methylene blue (MB) is an organic and cationic dye and is an industrial waste harmful to human health and nature. Methylene blue has been decomposed under UV light by photolysis and achieved removal from waste water. In this study, photolysis of MB under 366 nm UV lamp in the presence of H₂O₂ with time was investigated. The photolysis process was studied in MB-contaminated water for 180 min and analyzed at 664 nm in UV/vis spectroscopy.

Keywords: Methylene blue, degradation, photolysis, oxidation

INTRODUCTION

Today, environmental pollution is the biggest and most serious problem in the world with its harmful consequences (Natarajan et al., 2018). Water pollution occurs with organic compounds (dyes) and inorganic elements (metals) (Nabi et al., 2020). Dye waste is a negative result of the developing industry. Cause serious harm to human health and aquatic life (Soto-Robles et al., 2021). Their structure is quite stable and they are difficult to decompose in nature. In addition, many have carcinogenic effects (Chahar et al., 2021). Various techniques such as advanced oxidation, ozonation, adsorption, sedimentation and filtration are used to remove waste (Abdelrahman et al., 2019). Photodegradation technique is the best way to remove organic compounds from water (Nabi et al., 2020). Advanced oxidation techniques are frequently used in wastewater treatment. The hydroxyl groups formed increase the degree of oxidation and ensure the degradation of organic impurities (Soto-Robles et al., 2021). Methylene blue (C₁₆H₁₈ClN₃S.3H₂O) (3,7-bis(dimethylamino)-phenazothionium chloride) is a dark blue dye (Bağdat Yaşar & Özcan, 2004). Methylene blue is used for dyeing in the cotton and leather industry and in the pharmaceutical field. It causes serious harm to human health (Acedo-Mendoza, 2020; Jawad

et al., 2020). In this study, the removal of methylene blue dye from aqueous media by photolysis technique and the effect of hydrogen peroxide on the process were investigated.

EXPERIMENTAL

Materials

The methylene blue used in the study was purchased from Isolab. Hydrogen peroxide (H₂O₂) was purchased from Tekkim. The molecular structure of methylene blue is given in Figure 1.

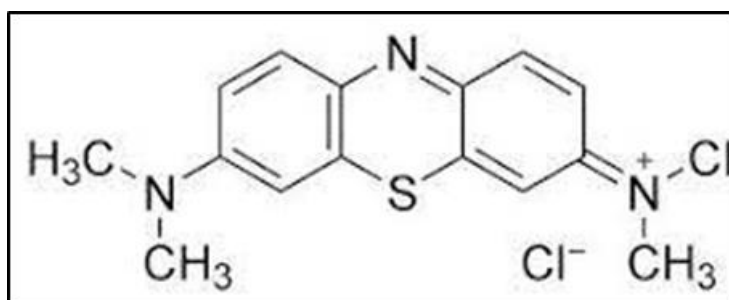


Fig.1 Molecule formula of methylene blue

Photocatalytic degradation

To start the photolysis process, first, 2 mL of H₂O₂ was added to a 200 ml MB solution at a concentration of 10 ppm and mixed. The UV lights were then turned on and the solution was irradiated with UV light for 180 minutes during which time a 4 mL sample was taken every 30 min. Photolysis studies were performed using a 366 nm UV lamp (Merck). The absorption intensity was measured with a UV/vis Lamp 2600 spectrophotometer to determine the MB concentration. The wavelength at which methylene blue gives maximum absorbance is 664 nm. Percent degradation was calculated according to Equation 1.

$$\text{Degradation (\%)} = \frac{(C_0 - C)}{C_0} \times 100 \quad (1)$$

C₀ is the initial dye concentration (t = 0) and C is the dye concentration after irradiation for the selected time point.

RESULTS AND DISCUSSION

The calibration chart in Figure 2 was used to calculate the removal amount of methylene blue in the photolysis process and the concentration amounts were calculated. For this purpose, the dye was prepared at various concentrations in the range of 2-12 mg/L and absorbance values were determined at 664 nm.

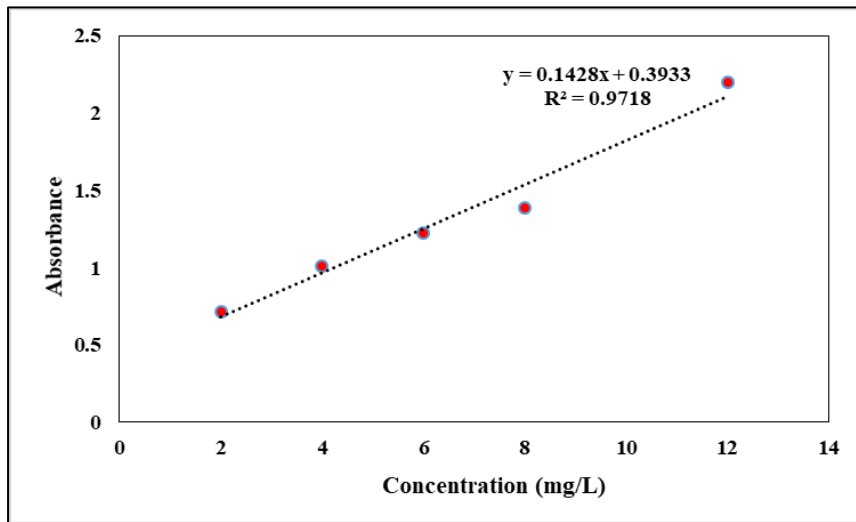


Fig 2. Calibration graph of methylene blue

In Figure 3, UV/vis spectra of methylene blue for 180 minutes are given. It is seen that the characteristic peak of the dye at 664 nm gradually decreases over time. Photolysis is slow as there is no catalyst in the process. After 180 min, 20% of the methylene blue was removed from the aqueous solution.

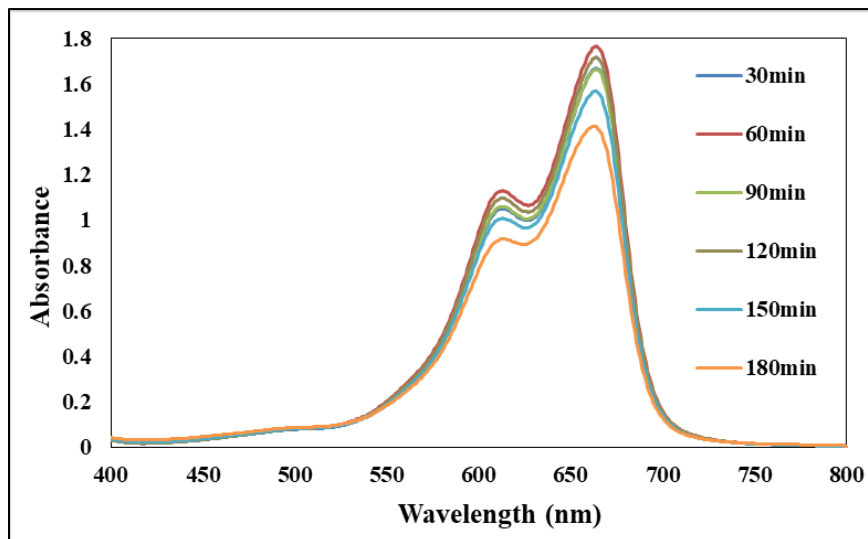


Fig.3 UV-vis spectrum showing degradation of MB solution under UV light irradiation

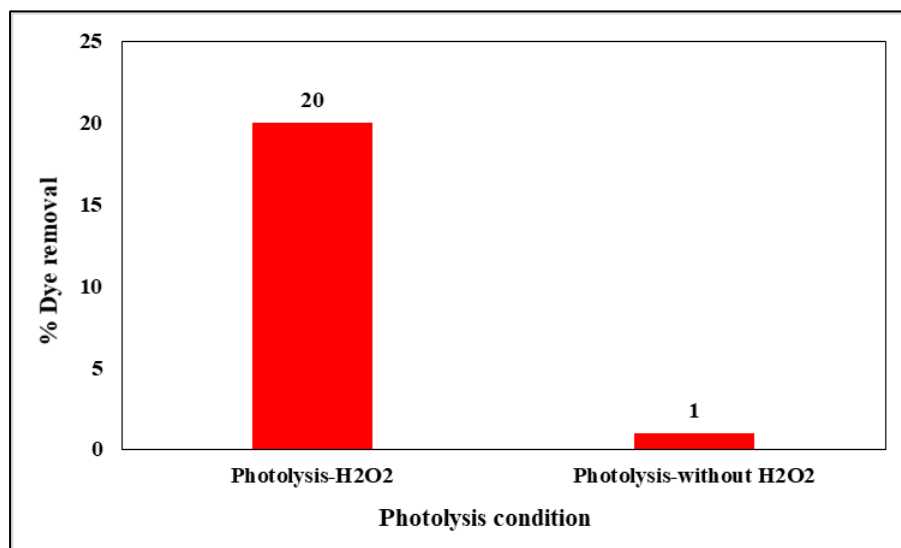


Fig.4 Dye removal results

To measure the effect of the presence of hydrogen peroxide on photolysis, experiments were performed without hydrogen peroxide under the same experimental conditions. It was determined that the dye removal was 1% at the end of 180 min. In the presence of hydrogen peroxide, 20% was achieved in dye removal. This result shows that in the photolysis of methylene blue, which is a cationic dye, hydroxyl ions from hydrogen peroxide interact with the dye electrostatically and have a positive effect on dye degradation.

CONCLUSION

Removal of waste in water has become one of the most studied subjects of scientists in recent years. As in this study, photolysis and photodegradation are the most popular methods used. As a result of the study, it is seen that hydrogen peroxide positively affects the photolysis process and affects dye removal. It is seen that hydrogen peroxide positively affects the photolysis process and affects dye removal. This may indicate to the catalyst that its use is not necessary. As the photolysis time increases, dye removal also increases.

References

- Abdelrahman, E. A., Hegazey, R. M., Kotp, Y. H., & Alharbi, A. (2019). Facile synthesis of Fe₂O₃ nanoparticles from Egyptian insecticide cans for efficient photocatalytic degradation of methylene blue and crystal violet dyes. *Spectrochimica Acta - Part A: Molecular and Biomolecular Spectroscopy*, 222, 117195.
- Acedo-Mendoza. (2020). *Materials Science in Semiconductor Processing* Photodegradation of methylene blue and methyl orange with CuO supported on ZnO photocatalysts : The effect of copper loading and reaction temperature. 119(June).
- Bağdat Yaşar, S., & Özcan, M. (2004). BAÜ Fen Bil. Enst. Dergisi (2004).6.2 Metilen Mavisinin Çözücü Ekstraksiyonu İle Sulu Çözeltilerden Geri Kazanımı, BAÜ Fen Bil. Enst. Dergisi, 6(2), 50–58.
- Chahar, D., Taneja, S., Bisht, S., Kesarwani, S., Thakur, P., Thakur, A., & Sharma, P. B. (2021). Photocatalytic activity of cobalt substituted zinc ferrite for the degradation of methylene blue dye under visible light irradiation. *Journal of Alloys and Compounds*, 851, 156878.
- Jawad, A. H., Abdulhameed, A. S., & Mastuli, M. S. (2020). Acid-factionalized biomass material for methylene blue dye removal: a



- comprehensive adsorption and mechanism study. *Journal of Taibah University for Science*, 14(1), 305–313.
- Nabi, G., Ain, Q. U., Tahir, M. B., Nadeem Riaz, K., Iqbal, T., Rafique, M., Hussain, S., Raza, W., Aslam, I., & Rizwan, M. (2020). Green synthesis of TiO₂ nanoparticles using lemon peel extract: their optical and photocatalytic properties. *International Journal of Environmental Analytical Chemistry*, 00(00), 1–9.
- Natarajan, S., Bajaj, H. C., & Tayade, R. J. (2018). Recent advances based on the synergetic effect of adsorption for removal of dyes from waste water using photocatalytic process. *Journal of Environmental Sciences (China)*, 65, 201–222.
- Soto-Robles, C. A., Nava, O., Cornejo, L., Lugo-Medina, E., Vilchis-Nestor, A. R., Castro-Beltrán, A., & Luque, P. A. (2021). Biosynthesis, characterization and photocatalytic activity of ZnO nanoparticles using extracts of *Justicia spicigera* for the degradation of methylene blue. *Journal of Molecular Structure*, 1225, 129101.

Yeni Tri-Katyonik Yüzey aktif Maddelerin Sentezi ve Asidik Ortamda Korozyon İnhibitörü Görevi üstlenmeleri

Serkan ÖZTÜRK

Bursa Uludağ University, Faculty of Arts and Sciences, Department of Chemistry, Görükle Campus
ORCID ID: 0000-0002-9396-1403

Ayhan YILDIRIM

Bursa Uludağ University, Faculty of Arts and Sciences, Department of Chemistry, Görükle Campus
ORCID ID: 0000-0002-2328-9754

Gökhan GECE

Bursa Technical University, Faculty of Engineering and Natural Sciences, Department of Chemistry
ORCID ID: 0000-0001-9310-5407

Hüsnü GERENGİ

Düzce University, Faculty of Engineering, Department of Mechanical Engineering, Corrosion Research Laboratory
University of Bergamo, Department of Engineering and Applied Sciences, BG, Italy
ORCID ID: 0000-0002-9663-4264

ÖZET

Korozyon özellikle metal endüstrisinin en önemli sorunlarından birisidir. Korozyon sebebiyle metal yüzeyi deforme olur ve böylece metalik özellikler git gide kaybolur. Metal yüzeyini korozyona karşı önlemeye yönelik kullanılan yöntemlerden biri uygun inhibitör kullanımımıdır. Asidik ortamda hızlı bir şekilde meydana gelen metal korozyonuna karşı mücadelede kullanılan etkin inhibitörlerden biri de katyonik yüzey aktif maddelerdir. Bu düşünceden yola çıkarak, 1.0 M HCl çözeltisi ortamında meydana gelen metal korozyonunu önlemek amacıyla yapısında üç pozitif yüklü azot atomu içeren, farklı karbon zincir uzunluklu iki adet tri-katyonik yüzey aktif madde sentezlenmiştir. Yapıları NMR spektroskopisi yöntemi (¹H-NMR ve ¹³C-NMR) ile aydınlatıldıktan sonra bu bileşiklerin asidik korozif ortamda korozyon inhibisyon etkinlikleri kütle kaybı yöntemiyle incelenmiştir. Bunun için değişik konsantrasyonlarda inhibitör içeren 1.0 M HCl çözeltileri hazırlanmış ve bu çözeltilere metal kuponlar oda sıcaklığında 24 saat süre ile daldırılarak inhibitör konsantrasyonunun korozyonu önlemedeki etkisi araştırılmıştır. Kütle kaybı yöntemiyle yapılan korozyon testleri sonucunda, sentezlenen tri-katyonik yüzey aktif maddelerin düşük karbon çeliğinin asidik ortamdaki korozyonuna karşı etkin oldukları tespit edilmiştir. Her iki bileşiğin farklı konsantrasyonlarında gerçekleşen testlerde hem yüksek (> % 92) hem de birbirine çok yakın korozyon inhibisyon etkinliği sonuçları elde edilmiştir. Her iki bileşiğin inhibisyon etkinliği sonuçları birbirine yakın olmasına rağmen, daha uzun karbon zincirli yüzey aktif maddenin kısa zincirli olana göre daha iyi koruma gösterdiği belirlenmiştir. İnhibitör etkinliği sonuçları gereği, asidik ortamda metal yüzeyini korozyona karşı koruduğunu desteklemek adına taramalı elektron mikroskobu (SEM) ile metal yüzeyi görüntüleri alınmıştır.

Anahtar Kelimeler: Sentez, Tri-Katyonik Yüzey Aktif Madde, Korozyon İnhibitörü, Asidik Ortam, SEM

SYNTHESIS OF NEW TRI-CATIONIC SURFACTANTS AND ACTING AS CORROSION INHIBITOR IN ACIDIC ENVIRONMENT

ABSTRACT

Corrosion is one of the most important problems of the metal industry. Due to corrosion, the metal surface is deformed and thus the metallic properties are gradually lost. One of the methods used to prevent the metal surface against corrosion is the use of an appropriate inhibitor. One of the effective inhibitors used in the fight against metal corrosion that occurs rapidly in an acidic environment is cationic surfactants. Based on this idea, two tri-cationic surfactants with different carbon chain lengths, containing three positively charged nitrogen atoms, were synthesized in order to prevent metal corrosion occurring in the 1.0 M HCl solution environment. After their structures were elucidated by NMR spectroscopy method ($^1\text{H-NMR}$ and $^{13}\text{C-NMR}$), the corrosion inhibition activities of these compounds in acidic corrosive medium were investigated by weight loss method. For this purpose, 1.0 M HCl solutions containing different concentrations of inhibitor were prepared and metal coupons were immersed in these solutions at room temperature for 24 hours to investigate the effect of inhibitor concentration on corrosion prevention. As a result of the corrosion tests performed by the weight loss method, it was determined that the synthesized tri-cationic surfactants were effective against the corrosion of low carbon steel in acidic environment. In the tests performed at different concentrations of both compounds, both high (> 92%) and very close corrosion inhibition efficiency results were obtained. Although the inhibition efficiency results of both compounds were close to each other, it was determined that the longer carbon chain surfactant showed better protection than the short chain one. According to the results of inhibitor activity, metal surface images were taken with scanning electron microscope (SEM) to support that it protects the metal surface against corrosion in acidic environment.

Keywords: Synthesis, Tri-cationic surfactant, Corrosion Inhibitor, Acidic Environment, SEM

1. GİRİŞ

Teknolojinin gelişimi ile beraber metal ve alaşımlarının kullanımı her alanda artış göstermiştir. Bu artış, özellikle metal endüstrisi için önemli bir sorun olan korozyon olayını meydana getirmekte ve bu olumsuz soruna karşı önlem alınmasını gerektirmektedir. Çünkü korozyon sayesinde metaller, buldukları ortamda elektrokimyasal ya da kimyasal reaksiyonlara girerek metalik özelliklerini kaybetmektedir (Bereket ve Gerengi, 2006). Metalin ortam ile elektrokimyasal reaksiyonuna örnek olarak, çeliğin ana bileşeni olan demirin, çeşitli türler oluşturmak üzere su, oksijen ve hidrojen iyonları ile etkileşimi verilebilir. Özellikle, asit çözeltisinden gelen hidrojen iyonlarının, demir metali korozyonuna sebebiyet veren zararlı bir etken olmaktadır (Zhu, Free, Woollam ve Durnie, 2017). Ancak endüstride, metal yüzeylerdeki pasın ve yabancı maddelerin temizlenmesi

için asitle temizleme sıklıkla kullanılmaktadır. Bu amaç için de en çok HCl ve H₂SO₄ çözeltileri kullanılmaktadır (Bereket ve Pinarbasi, 2008). Asitle yapılan bu yıkama sonucunda ilgili metal yüzeyinde metal korozyonu olayı meydana gelmektedir.

Korozyona karşı mücadelede, birçok yöntem bilinmektedir. Bunların içerisinde en önemli olanlarından biri, özellikle asidik korozif ortamda, inhibitör kullanmaktır. Korozyon inhibitörü, ortama düşük konsantrasyonlarda eklendiğinde korozyon hızını önemli ölçüde azaltan maddedir. Metal yüzeyine tutunarak koruyucu bir film tabakası oluşturan bu maddeler korozif çözelti ortamında yeterince iyi çözünmesi gerekmektedir (Öztürk, 2018).

Son yıllarda, literatürde, asidik ortamda meydana gelen korozyona karşı korozyon inhibitörü olarak görev yapan bileşikler arasında katyonik yüzey aktif maddeler önemli bir yer tutmuştur. Bu bileşiklerin, yapısına bağlı olarak, korozif ortamda iyi çözümleri, metal yüzeyine fiziksel ve kimyasal yollarla iyi tutunmaları korozyon hızını azaltmalarında ve böylece metal korozyonuna karşı mücadele vermelerinde etkili olmuştur (Hegazy, El-Etre, El-Shafaie, ve Berry, 2016; Öztürk, 2017; Yıldırım, Öztürk ve Çetin, 2013; Shalabi, Helmy, El-Askalany ve Shahba, 2019). Yapısında tek bir pozitif grup içeren mono-katyonik yüzey aktif maddelerin dışında, iki adet pozitif yüklü grup içeren di-katyonik gemini tipi (simetrik ikiz yapıda) (Feng, Yin, Zhang, Li, Song, Chen ve Liu, 2018; Abd El-Lateef, Abo-Riya ve Tantawy, 2016; Asefi, Arami ve Mahmoodi, 2010) ve gemini tipi olmayan (Hegazy, Azzam, Kandil, Badawi ve Sami, 2016; Öztürk, 2019) yüzey aktif maddelerin korozyon inhibitörü olarak kullanıldığı çalışmalar da mevcuttur. Bu çalışmaların tamamında sentezlenen yüzey aktif maddelerin anti-korozyon etkisi gravimetrik ölçümlere dayalı kütle kaybı testleriyle araştırılmıştır.

Literatürde, yapısında üç adet pozitif grup içeren ve asidik ortamda korozyon inhibitörü olarak kullanılan tri-katyonik yüzey aktif maddeler ile ilgili az sayıda çalışma vardır. Bu çalışmalardan Bensajjay ve ark. 2011 düz zincirli amonyum tuzunun 1.0M HCl ortamındaki korozyona karşı inhibitör performansını araştırmışlardır. Bir başka çalışmada ise EldougDoug ve ark. 2018, setil-2-kloroasetatin di-amid ile reaksiyonu sonucu tri-katyonik yüzey aktif maddeyi sentezlemiş ve kütle kaybı ile potansiyodinamik polarizasyon yöntemleri kullanılarak hidroklorik asit çözeltilerinde karbon çeliği için korozyon inhibitörü olarak incelemişlerdir.

Bu araştırmada, yapısında üç adet pozitif yüklü azot atomu içeren iki adet farklı karbon zincir uzunluklu yeni tri-katyonik yüzey aktif maddelerin sentezlenmesi hedeflenmiştir. Bu bileşiklere ilişkin, değişik inhibitör konsantrasyonlarında, kütle kaybı yöntemi kullanılarak, 1.0 M HCl asidik ortamında düşük karbon çeliği üzerinde oluşacak korozyona karşı etkinliklerinin incelenmiştir.

2. DENEYSEL KISIM

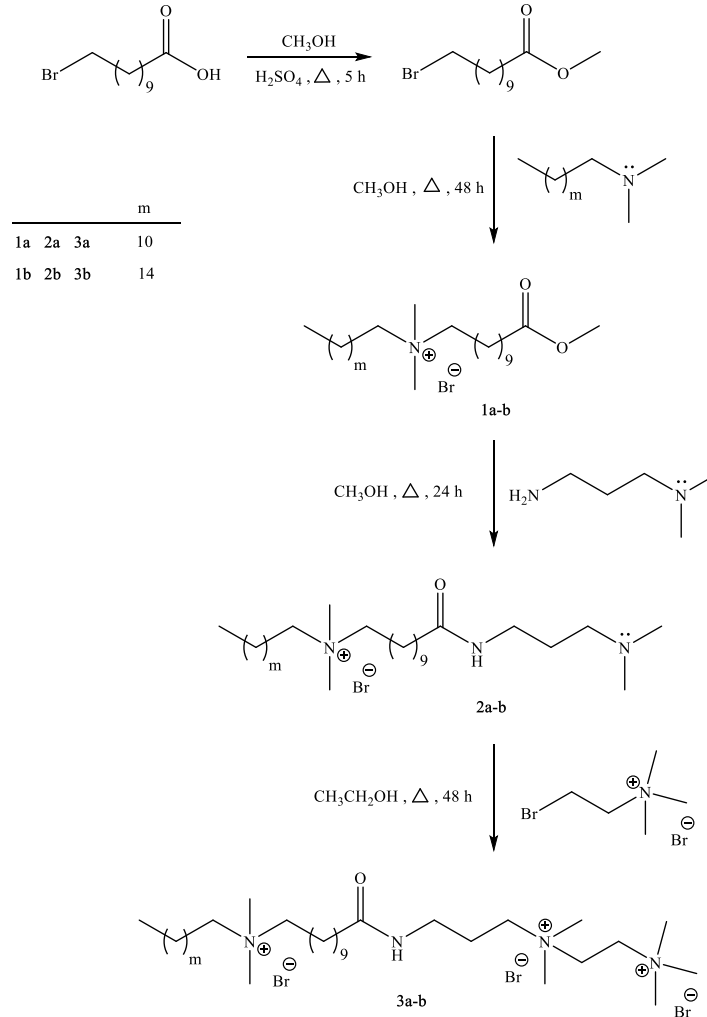
2.1. Deneysel Çalışmalarda Kullanılan Materyaller

Sentezlerde kullanılan reaktif ve solvent kimyasalları Merck ve Sigma-Aldrich şirketlerinden temin edilmiştir.

Son ürün olarak sentezlenen tri-katyonik yüzey aktif madde bileşiklerinin NMR spektrumları (^1H NMR ve ^{13}C -NMR), DMSO (Dimetilsülfoksit) içinde Agilent 600 MHz Premium Kompakt NMR spektrometresi kullanılarak elde edildi. Metal kuponların sabit tartıma gelene kadar kurutulması için NUVE EV 018 vakumlu fırın kullanılmıştır.

2.2. Bileşiklerin Sentezi

Reaksiyon serisinin ilk aşaması, katalizör olarak sülfürik asidin kullanıldığı metanol bileşiği ile 11-bromoundekanoik asidin etkileşimi ile gerçekleştirilen Fisher esterleşme reaksiyonudur. İkinci aşamada, metil-11-bromoundekanoat bileşiği, Şekil 1'deki reaksiyon şemasında gösterilen koşullar altında ilgili uzun zincirli üçüncül amin ile reaksiyona sokuldu ve **1a-b** bileşikleri sentezlendi. Daha sonra, **1a-b** bileşikleri, **2a-b** bileşikleri verecek şekilde N,N-dimetilamino-1-propilamin ile metanol varlığında 150 °C'de 24 saat geri soğutucu altında ısıtıldı. Metanol buharlaştırıldı ve **2a-b** bileşikleri, iyi verimlerle kahverengimsi yağ olarak elde edildi. Son aşamada, yapısında 12 ile 16 karbonlu uzun zincir içeren tri-katyonik yüzey aktif maddeler (**3a-b**), bileşik **3a** için açıklanan prosedürle sentezlendi.



Şekil 1. Bileşiklerin sentez şeması

2.2.1. N¹-(3-(11-(dodesildimetilamonio)undekanamido)propil)-N¹,N¹,N²,N²,N²-pentametiletan-1,2-diaminyum tribromür (3a)

Reaksiyon için bileşik **2a** (10.13 mmol) ve (2-bromoetil) trimetilamonyum bromür (10.13 mmol) kullanıldı. İki reaktif ve 30 ml etanol, bir geri soğutucuya takılmış 100 mL'lik yuvarlak tabanlı bir reaksiyon şişesine yerleştirildi. Reaksiyon karışımı, 48 saat boyunca geri soğutucu altında ısıtıldı. Bu süreden sonra etanol, indirgenmiş basınç altında buharlaştırıldı ve elde edilen tortu, sıcak aseton ile yıkandı. Çöken katı, vakum altında süzülerek ayrıldı ve süzüntüden aseton buharlaştırıldı. Koyu kahverengi yağlı mum ürünü % 81 verimle elde edildi.

2.2.2. N¹-(3-(11-(hegzadesildimetilamonyo)undekanamido)propil)-N¹,N¹,N²,N²,N²-pentametiletan-1,2-diaminyum tribromür (3b)

Reaksiyon için bileşik **2b** (10.12 mmol) ve (2-bromoetil) trimetilamonyum bromür (10.12 mmol) kullanıldı. **3a** bileşiğinin sentez prosedürünün aynısı kullanıldı (Verim: % 78).

2.3. Asidik Ortamda Gerçekleştirilen Korozyon Testleri

Asidik ortamda gerçekleştirilen korozyon testlerinde düşük karbon içerikli soğuk haddelenmiş çelikten hazırlanan metal plakalar kullanılmıştır. Bu çelik malzeme DIN EN 10130 (DIN Standardı, 2007) normuna uygundur ve kimyasal bileşimi Tablo 1'de verilmiştir. Metal plakalar, 0.1 cm kalınlığında, 2.2 cm genişliğinde ve 5.0 cm uzunluğunda dikdörtgen şeklinde kesilmiştir.

Tablo 1. Kullanılan çelik malzemenin kimyasal bileşimi

Bileşim (%)				
C	Mn	P	S	Fe
0.07	0.35	0.015	0.015	geri kalan

Gravimetrik ölçümlere dayalı korozyon testlerinin hazırlık aşaması literatürde daha önce bildirilen yöntemle yapılmıştır (Öztürk, 2018). Bunun için 0,1 cm kalınlığında, 2,2 cm genişliğinde ve 5,0 cm uzunluğunda kesilen metal plakalar, pas lekelerinin ve oksit tabakalarının çıkması için %15'lik HCl çözeltisinde 5 dakika bekletildi. Plakalar daha sonra destile su ile temizlendi. Kuruyan metal plakaların yüzeyi zımpara kağıdı (180) ile zımparalanmış ve bir süre asetonda tutulmuştur. Asetondan çıkarılan plakalar, bir vakum fırınında ve daha sonra sabit tartıma kadar kısa bir süre açık havada kurutuldu ve test öncesi metal plakanın kütlesi tartıldı.

Asidik sulu ortamda gerçekleştirilen korozyon testlerinden önce 1.0 M HCl çözeltisi taze olarak hazırlanmıştır. Teste tabi tutulan tri-katyonik yüzey aktif maddeler belirli oranlarda tartılarak 100 mL 1.0 M HCl içinde çözüldü ve 150 mL'lik kapaklı cam kaplara yerleştirildi. Bu şekilde yüzey aktif maddelerin asidik ortamda 10, 25, 50, 100 ve 250 ppm çözeltileri hazırlanmıştır. Diğer taraftan kontrol testi ve karşılaştırma için 100 mL 1.0 M HCl

başka bir cam kaba konuldu ve içerisine inhibitör eklenmedi. Hazırlanan inhibitörsüz ve inhibitörlü asidik çözeltilere ön test tartımı yapılan metal plakalar ip ile bağlanarak daldırıldı ve karıştırılmadan 24 saat oda sıcaklığında bekletildi. 24 saatlik test süresinden sonra aşındırıcı ortamdan çıkarılan metal plakalar, bir piset kullanılarak damıtılmış su ile durulanmıştır. Plakalar daha sonra aseton ile temizlendi; önce bir vakumlu fırında, daha sonra kısaca açık havada kurutuldu ve testten sonra metalin kütlesi tartıldı.

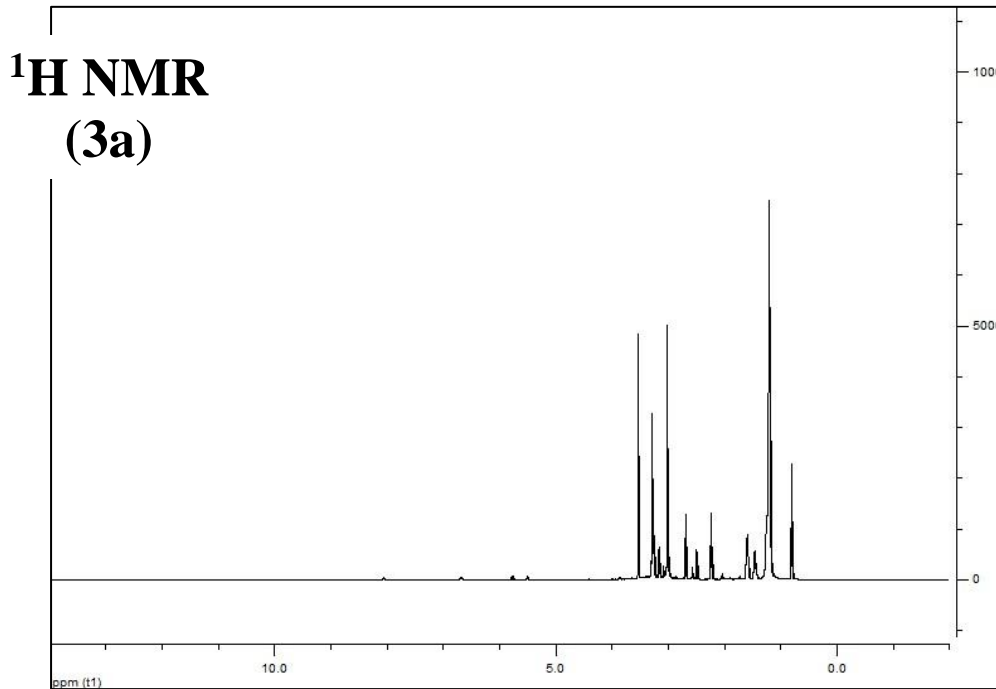
2.4. Taramalı elektron mikroskobu (SEM) ile metal yüzey görüntüsü

Metal yüzeyin SEM görüntüsü, 0.1 cm kalınlığında, 2.0 cm genişliğinde ve 2.0 cm uzunluğunda kareler halinde kesilmiş metal plakalar üzerinde alınmıştır. Asidik ortamda gerçekleştirilen korozyon testlerinden sonra metal plakalar aseton ile yıkayıp vakumlu desikatörde kurutuldu ve taramalı elektron mikroskobu cihazı (Carl Zeiss EVO 40) ile yüksek vakum altında 1000 kez büyütülen metal yüzeylerin SEM görüntüleri elde edildi.

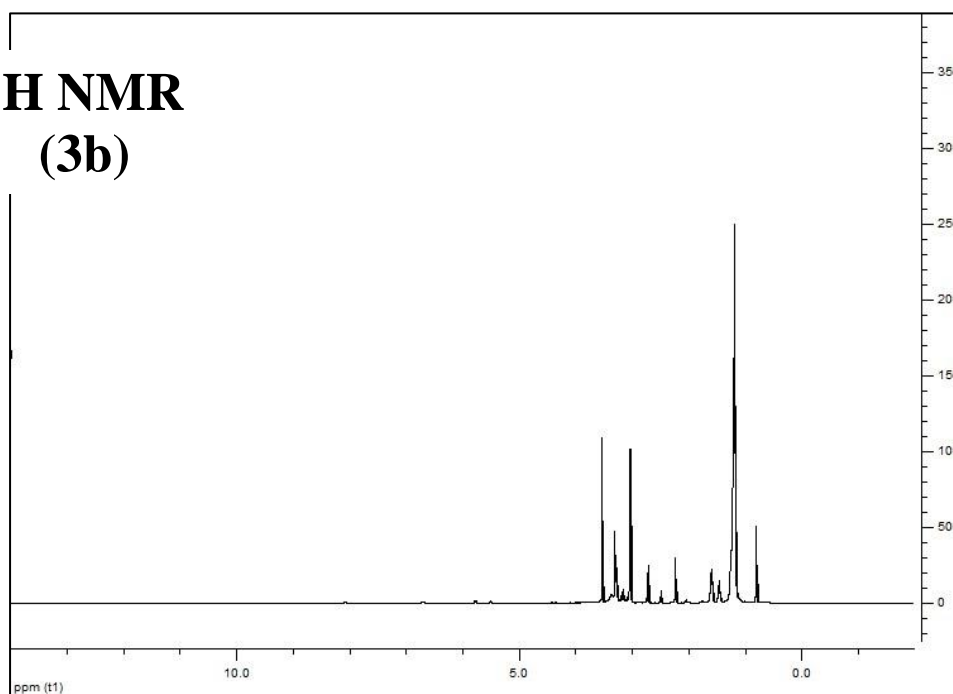
3. SONUÇLAR ve TARTIŞMA

3.1. Tri-Katyonik Yüzey aktif maddelerin NMR Spektrumları

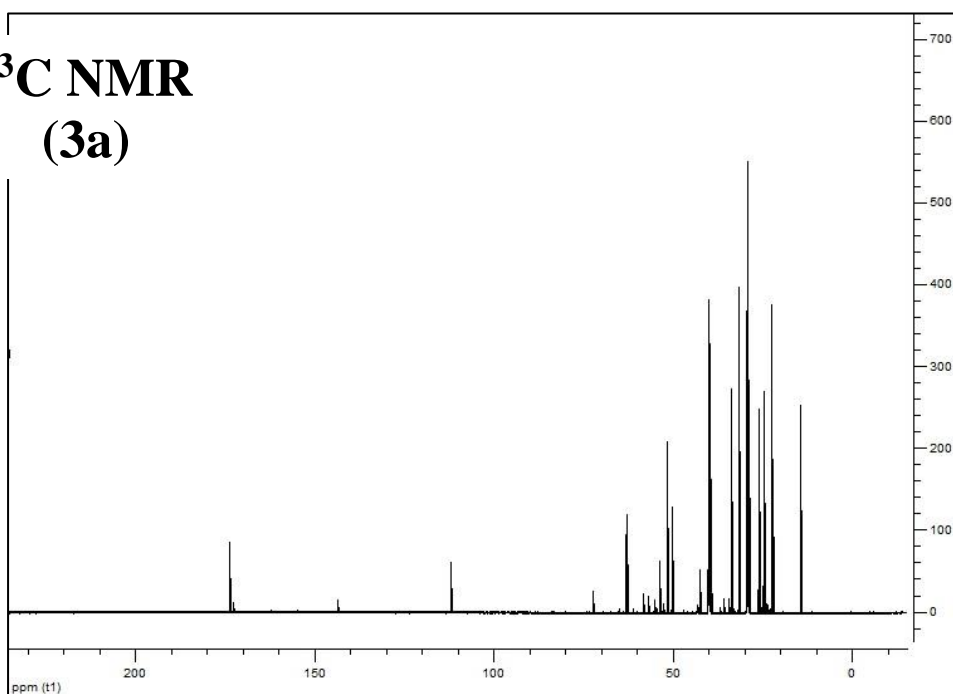
Sentezlenen tri-katyonik yüzey aktif maddelerin (**3a**, **3b**) ^1H NMR ile ^{13}C NMR spektrumları Şekil 2’de görülmektedir. Ayrıca bileşiklerin NMR pik değerleri de Tablo 2’de verilmiştir.



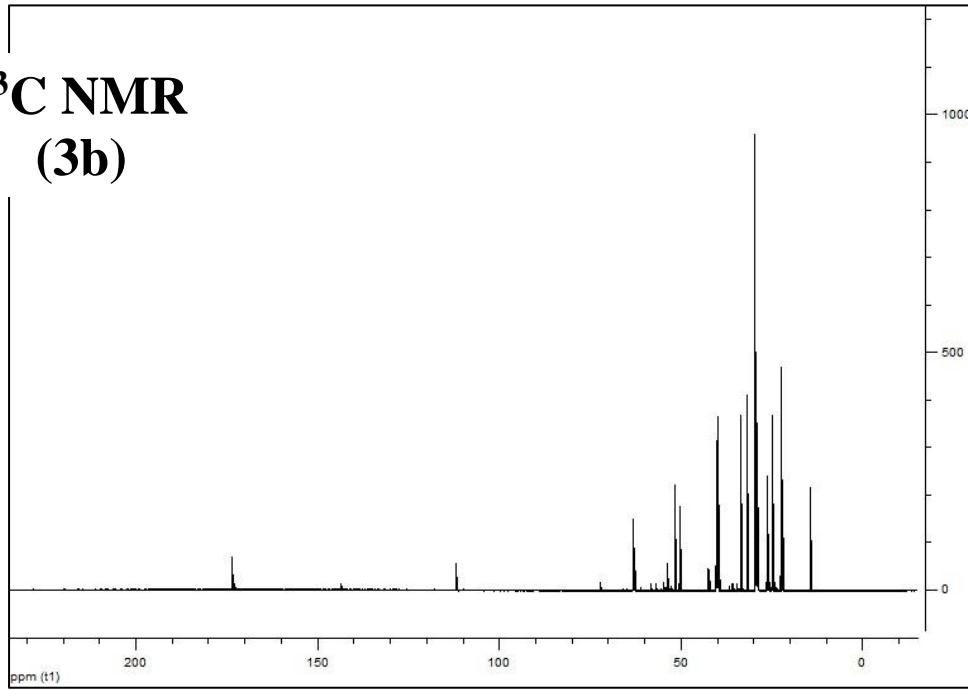
^1H NMR (3b)



^{13}C NMR (3a)



¹³C NMR (3b)



Şekil 2. Tri-katyonik yüzey aktif maddelerin ¹H NMR ile ¹³C NMR spektrumları

Tablo 2. Tri-katyonik yüzey aktif maddelerin NMR pik değerleri

NMR Pik Değerleri	
3a	<p>¹H NMR (600 MHz, DMSO-d₆): δ (ppm) = 8.06 (t, 1H, O=C-NH), 3.54 [s, 4H, (CH₃)₂N⁺-CH₂-CH₂-N⁺(CH₃)₃], 3.30 [s, 6H, O=C-NH-CH₂-CH₂-CH₂-N⁺(CH₃)₂], 3.27 [t, 6H, -CH₂-N⁺(CH₃)₂-CH₂-], 3.02 [s, 9H, -N⁺(CH₃)₃], 2.24 (t, 2H, -CH₂-CO-NH-), 1.60 [quint, 4H, -CH₂-CH₂-N⁺(CH₃)₂-CH₂-CH₂], 1.47 (quint, 2H, -CH₂-CH₂-CO-NH-), 1.29–1.16 (m, 38H, -CH₂-), 0.81 (t, 3H, CH₃-)</p> <p>¹³C NMR (150 MHz, DMSO-d₆): δ (ppm) = 173.71 [CO-NH], 63.07 [-CH₂-N⁺(CH₃)₂-CH₂-], 53.82 [CO-NH-CH₂-CH₂-CH₂-N⁺], 51.61 [CO-NH-(CH₂)₃-N⁺(CH₃)₂-CH₂-CH₂-N⁺(CH₃)₃], 50.36 [CO-NH-(CH₂)₃-N⁺(CH₃)₂-CH₂-CH₂-N⁺(CH₃)₃], 42.48 [-N⁺(CH₃)₂-CH₂-CH₂-N⁺(CH₃)₃], 33.69 [-N⁺(CH₃)₂-CH₂-CH₂-N⁺(CH₃)₃], 31.77 [-CH₂-N⁺(CH₃)₂-CH₂-], 14.38 [CH₃-].</p>
3b	<p>¹H NMR (600 MHz, DMSO-d₆): δ (ppm) = 8.08 (t, 1H, O=C-NH), 3.53 [t, 4H, (CH₃)₂N⁺-CH₂-CH₂-N⁺(CH₃)₃], 3.31 [t, 6H, O=C-NH-CH₂-CH₂-CH₂-N⁺(CH₃)₂], 3.28 [t, 6H, -CH₂-N⁺(CH₃)₂-CH₂-], 3.04 [s, 9H, -N⁺(CH₃)₃], 2.23 (t, 2H, -CH₂-CO-NH-), 1.60 [quint, 4H, -CH₂-CH₂-N⁺(CH₃)₂-CH₂-CH₂], 1.47 (quint, 2H, -CH₂-CH₂-CO-NH-), 1.34–1.12 (m, 38H, -CH₂-), 0.80 (t, 3H, CH₃-)</p> <p>¹³C NMR (150 MHz, DMSO-d₆): δ (ppm) = 173.62 [CO-NH], 63.00 [-CH₂-N⁺(CH₃)₂-CH₂-], 53.81 [CO-NH-CH₂-CH₂-CH₂-N⁺], 51.57 [CO-NH-(CH₂)₃-N⁺(CH₃)₂-CH₂-CH₂-N⁺(CH₃)₃], 50.39 [CO-NH-(CH₂)₃-N⁺(CH₃)₂-CH₂-CH₂-N⁺(CH₃)₃], 42.52 [-N⁺(CH₃)₂-CH₂-CH₂-N⁺(CH₃)₃], 33.69 [-N⁺(CH₃)₂-CH₂-CH₂-N⁺(CH₃)₃], 31.80 [-CH₂-N⁺(CH₃)₂-CH₂-], 14.32 [CH₃-].</p>

Bileşiklerin ^1H NMR spektrumlarında net bir şekilde görülmesi de, **3a** bileşiği için 8.06 ppm'de, **3b** bileşiği için ise 8.08 ppm'de amit NH bağına ait triplet pikler elde edilmiştir. Tablo 2'de özellikle pozitif yüklü azotlara bağlı metil grubu hidrojenlerine ait karakteristik pik değerleri verilmiştir. Sadece NMR spektrumlarından elde edilen bu karakteristik pik değerlerinden bile tri-katyonik yüzey aktif maddelerin başarıyla sentezlendiği söylenebilmektedir.

3.2. HCl Çözeltilerinde Korozyon Testleri

1.0 M HCl sulu çözeltisinde gravimetrik yöntemle belirlenen yüzde inhibisyon etkinlikleri (% IE) Tablo 3'te verilmiştir. Yüzde inhibisyon etkinliği değerleri aşağıdaki eşitlikten (1) hesaplanmıştır:

$$\% IE = \frac{W_0 - W}{W} \times 100 \quad (1)$$

Burada;

$\% IE$: yüzde inhibisyon etkinliği

W_0 : inhibitör içermeyen ortamdaki metal kuponun kütle kaybı (mg)

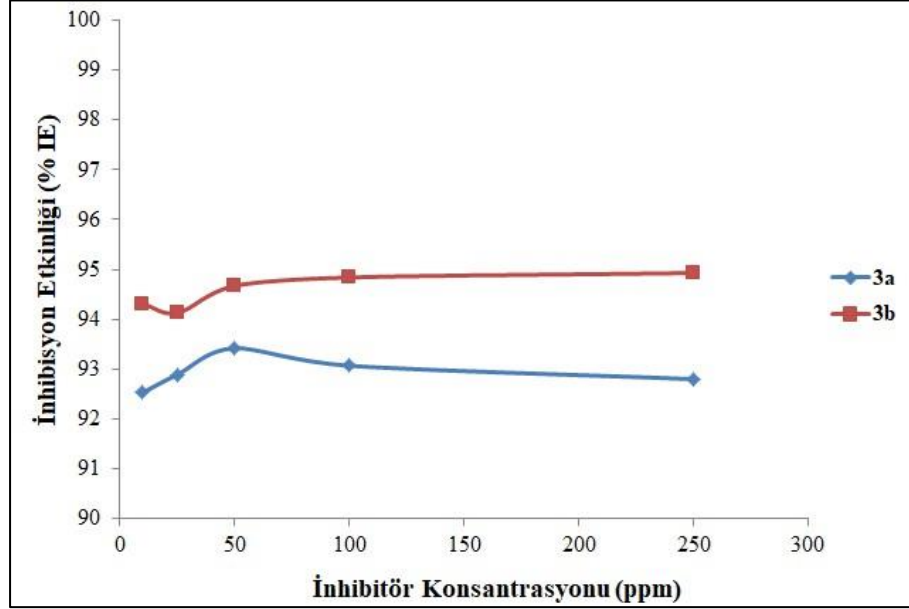
W : inhibitör içeren ortamdaki metal kuponun kütle kaybı (mg)

Tablo 3. Oda sıcaklığında 24 saat süreyle 1.0 M HCl ortamında farklı yüzey aktif madde konsantrasyonları için hesaplanan korozyon inhibisyon etkinlikleri (% IE)

Yüzey aktif madde	Korozyon inhibisyon etkinlikleri (% IE)				
	10 ppm	25 ppm	50 ppm	100 ppm	250 ppm
3a	92.53	92.89	93.42	93.07	92.80
3b	94.31	94.13	94.67	94.84	94.93

Korozyon testleri oda sıcaklığında (25 °C) 1.0 M HCl çözeltisinde, farklı inhibitör konsantrasyonlarında (10, 25, 50, 100 ve 250 ppm) yapılmıştır. Tablo 3'deki değerler incelendiğinde, her bir yüzey aktif madde için korozyon testine tabi tutulan konsantrasyon arttıkça (10 → 250 ppm) inhibisyon etkinliklerinin genellikle birbirine çok yakın çıktığı görülmüştür. Normalde, inhibitör konsantrasyonunun artmasıyla inhibisyon etkinliğinin arttığı bilinmektedir (Öztürk, 2017; Qiu, Xie ve Shen, 2005; Aiad, Riya, Tawfik ve Abousehly, 2016). Ancak, bir yüzey aktif madde için, kritik misel konsantrasyonuna ulaşana kadar konsantrasyonu artırıldığında metal yüzeyine adsorbe olacak madde miktarı arttığından, metal yüzeyi korozif ortama karşı daha korunaklı olacaktır. Böylece metaldeki kütle kaybının azalmasına bağlı olarak inhibitörün inhibisyon etkinliği artacaktır.

Yüzey aktif maddeler kritik misel konsantrasyona ulaştıktan sonra ise inhibitör konsantrasyonu artışı ile korozyon inhibisyon etkinliğinin çok değişmediği bilinmektedir. Burada inhibitör etkinliklerinin birbirine çok yakın çıkması tri-kasyonik yüzey aktif maddelerin kritik misel konsantrasyonlarına ulaşmış olabileceklerini göstermektedir. Yüzey aktif maddelerin konsantrasyonlarına bağlı olarak inhibisyon etkinliğindeki bu değişimleri, Şekil 3'te grafiksel olarak görmek mümkündür.



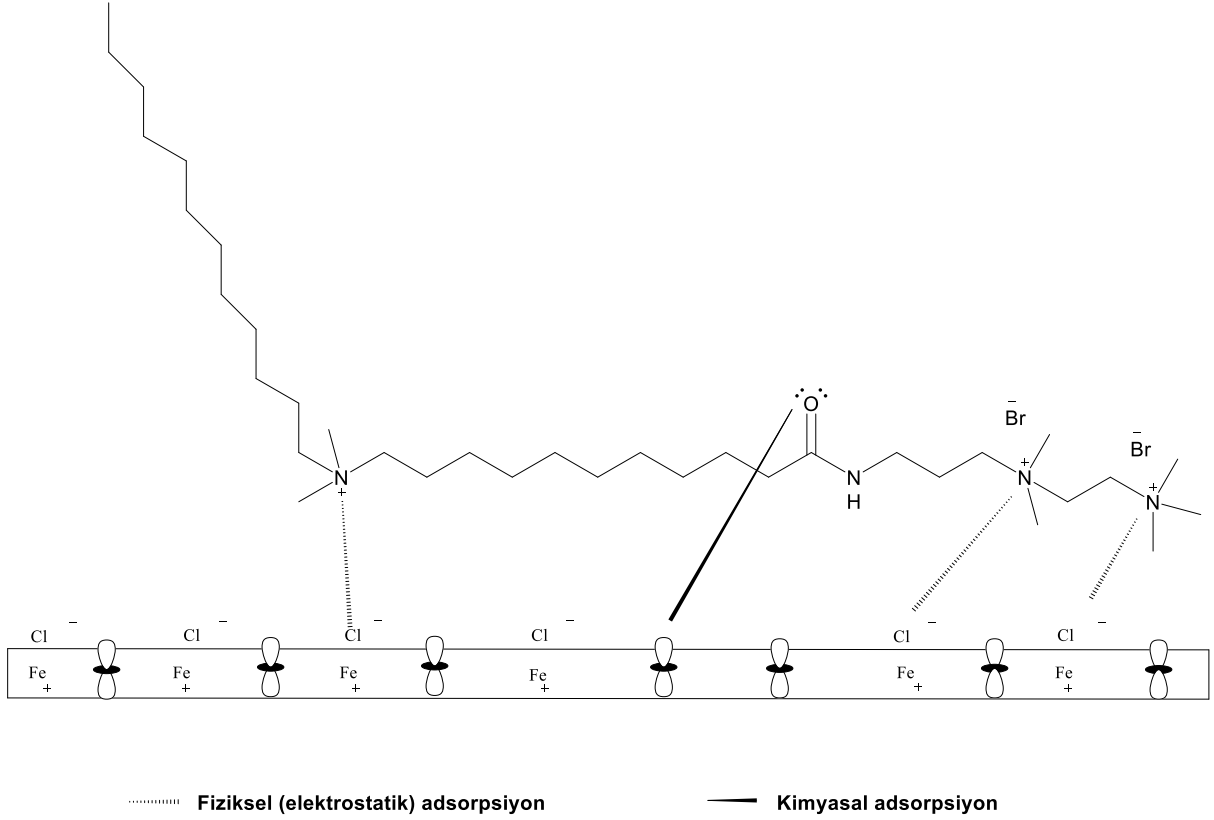
Şekil 3. İnhibitör konsantrasyona bağlı olarak inhibisyon etkinliğindeki değişimlerin grafiksel görünümü

İnhibitör olarak kullanılan yüzey aktif madde metale tutunduktan sonra, asidik ortamda korozyon olayına sebebiyet veren yarı reaksiyonların (anot: metaldeki demirin 2+ yükseltgenme basamağına yükseltgenmesi ve katot: HCl'den gelen H⁺ iyonunun H₂'e indirgenmesi) her birine ya da ikisine de engel olarak metal yüzeyini korozyonun zararlı etkilerine karşı dayanıklı kılar. Bu elektrokimyasal reaksiyonların engellenmesi hem korozyon hızının düşmesine bağlı olarak inhibitörün inhibisyon etkinliğinin artmasına, hem de metal yüzeyinin korozyona karşı korunmasına neden olmaktadır.

Sentezlenen tri-kasyonik yüzey aktif maddelerin yapılarını karşılaştırdığımızda, maddelerdeki tek yapı farkı, farklı karbon sayılı zincir uzunluklarıdır. **3a** bileşiğinin uzun karbon zincirinde 12 karbon atomu, **3b** bileşiğinde ise 16 karbon atomu bulunmaktadır. Her iki bileşiğin Şekil 2'de verilen inhibisyon etkinliği değerlerine bakıldığında birbirine yakın sonuçlar elde edilmiş olsa da **3b** bileşiğinin inhibisyon etkinliklerinin **3a** bileşiğinden biraz daha fazla olduğu görülmektedir. Bu beklenen bir sonuçtur, çünkü uzun zincirdeki karbon sayısı arttıkça inhibisyon etkinliği de artmaktadır (Yıldırım, Öztürk ve Çetin, 2013; Öztürk, 2017). Van der Waals kuvvetleri nedeniyle moleküllerin uzun alkil zincirleri arasındaki polar olmayan etkileşimler, korozif ortama karşı daha iyi bir koruyucu tabaka sağlar ve korozif ortamın metal yüzeyine yaklaşımına engel olmaktadır.

3.3. Korozyon İnhibisyon Mekanizması

Metalik korozyonun önlenmesi veya metalik korozyon hızının azalması, inhibitör moleküllerin metal yüzey üzerine adsorpsiyonuna bağlıdır. Sentezlenen tri-katyonik yüzey aktif maddelerin metal yüzeyine olası adsorpsiyonu Şekil 4'te gösterilmektedir.



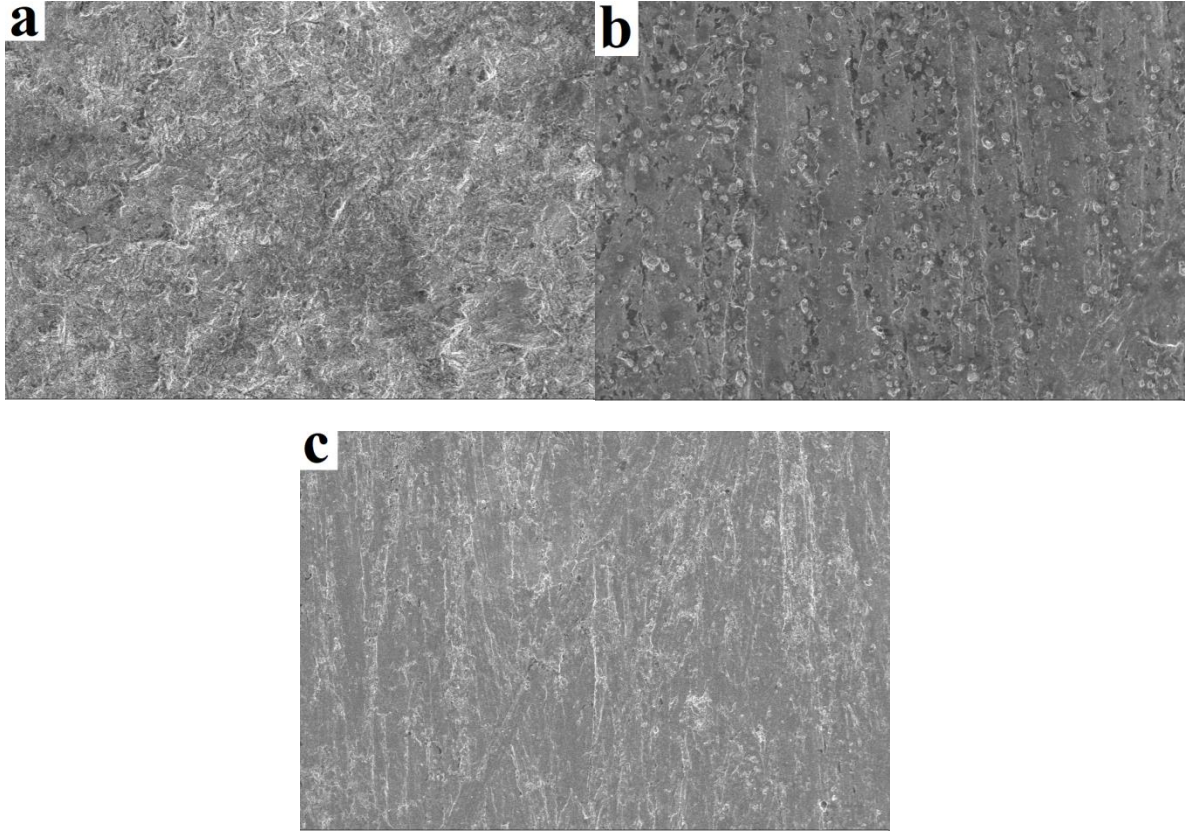
Şekil 4. Tri-katyonik yüzey aktif maddelerin metal yüzeyine adsorpsiyon mekanizması

Şekil 4'de verilen adsorpsiyon mekanizmasında görüldüğü üzere, korozyon olayının anot reaksiyonunda demirin +2 yükseltgenme basamağına yükseltgenmesi sonucu pozitif yüklenen metal yüzeyi, asitten gelen Cl⁻ iyonlarının etkisiyle dipol oluşturarak negatif hale dönüşmüştür (Yıldırım, Öztürk ve Çetin, 2013; Öztürk, 2017). Negatif yüklü dipole, inhibitörlerin pozitif yüklü azot atomları elektrostatik etkileşimle metal yüzeyine adsorbe olmaktadır. Ayrıca, bileşiklerin yapısında yer alan oksijen atomlarındaki ortaklanmamış elektron çiftleri, metal plakalardaki Fe elementinin boş d orbitalleriyle etkileşerek kimyasal yolla metal yüzeye tutunmaktadır. Hem kimyasal, hem de fiziksel yolla adsorpsiyon sonucu asidik korozif ortamın metal yüzeyine olan olumsuz etkisine engel olunmaktadır.

3.4. SEM

Organik bileşiklerin asidik ortamdaki metal yüzeyinin korozyonuna karşı koymasının bir ölçüsü olan inhibisyon etkinliği sonuçlarının desteklenmesi yönünde taramalı elektron mikroskobu analizi önem arz etmektedir. Yirmi dört saat süreyle, inhibitörlü ve inhibitörsüz asit çözeltisine daldırılan metal kupon yüzeylerinin, taramalı

elektron mikroskobu cihazı ile çekilen 1000 kat büyütülmüş yüzey görüntüleri Şekil 5'te görülmektedir.



Şekil 5. Metal yüzeylerine ait SEM görüntüleri

Taramalı elektron mikroskobu (SEM), metal yüzeyi üzerindeki morfolojik değişimleri görmemizi ve yorumlamamızı sağlamaktadır (Öztürk, 2018). Şekil 5–a'daki görüntüde, inhibitörsüz asit çözeltisine daldırılan metal yüzeyi görülmektedir. İnhibitörsüz asit ortamına maruz kalan metal yüzeyinin tümünde aşınma gözlenirken, yüzeyin girintili çıkıntılı ve pürüzlü bir hal aldığı görülmektedir. Bu da, metal yüzeyinde korozyon olayının gerçekleştiğini ve yüzeyde korozyon ürünlerinin oluştuğunu göstermektedir. Şekil 5–b ve Şekil 5–c 'de verilmiş olan yüzey görüntüleri ise sırasıyla **3a** ve **3b** nolu tri-katyonik yüzey aktif maddeleri içeren asit ortamında 24 saat bekletilmiş metal yüzeylerine aittir. İnhibitörlü asit ortamına maruz kalan metal yüzeylerinde herhangi bir aşınma ve pürüzlülüğün olmadığı ve daha düz bir görünüm aldığı görülmektedir. Metal yüzeylerinde görülen çizik izleri test öncesi yapılan zımparalama işleminden kaynaklanmaktadır. Tri-katyonik yüzey aktif maddeleri için elde edilen bu metal yüzeyi SEM görüntüleri, yüzey aktif maddelerin yüzeye adsorbe olarak metali korozyona karşı koruduğunu desteklemiştir.

4. SONUÇ

- Üç adet pozitif azot atomu içeren farklı karbon zincirli 2 adet tri-katyonik yüzey aktif madde sentezlenmiş ve yapıları NMR spektroskopisi (^1H NMR ve ^{13}C NMR) ile aydınlatılmıştır.

- Sentezlenen yüzey aktif maddelerin asidik ortamda gerçekleşen metal korozyonunu engelledikleri, iyi inhibisyon etkinliği sergilemelerinden, anlaşılmıştır.
- Her iki bileşiğin farklı konsantrasyonlarında gerçekleşen testlerde birbirine çok yakın korozyon inhibisyon etkinliği sonuçları elde edilmiştir.
- Daha uzun karbon zincirli yüzey aktif maddenin (**3b**) kısa zincirli olana göre (**3a**) biraz daha iyi koruma gösterdiği belirlenmiştir.
- İnhibitörlerin asidik ortamda metal yüzeyini korozyona karşı koruduğu, taramalı elektron mikroskobu (SEM) ile metal yüzeyi görüntüleri alınarak, desteklenmiştir.

TEŞEKKÜR

Bu çalışma, Bursa Uludağ Üniversitesi Bilimsel Araştırma Projeleri Birimi tarafından Proje Numarası: OUAP(F)-2019/15 kapsamında desteklenmiştir.

KAYNAKÇA

- Abd El-Lateef, H. M., Abo-Riya, M. A. & Tantawy, A. H. (2016). Empirical and quantum chemical studies on the corrosion inhibition performance of some novel synthesized cationic gemini surfactants on carbon steel pipelines in acid pickling processes. *Corrosion Science*, 108, 94-110.
<http://dx.doi.org/10.1016/j.corsci.2016.03.004>
- AIad, I., Riya, M. A., Tawfik, S. M. & Abousehly, M. A. (2016). Protection of carbon steel against corrosion in hydrochloric acid solution by some synthesized cationic surfactants. *Protection of Metals and Physical Chemistry of Surfaces*, 52, 339–347.
DOI:10.1134/S2070205116020027
- Asefi, D., Arami, M. & Mahmoodi, N. M. (2010). Electrochemical effect of cationic gemini surfactant and halide salts on corrosion inhibition of low carbon steel in acid medium. *Corrosion Science*, 52, 794-800. doi:10.1016/j.corsci.2009.10.039
- Bensajjay, F., Alehyen, S., El Achouri, M., Hajjaji, N., Bellaouchou, A., Perez, L., & Infante, M. R. (2011). Inhibition of the corrosion of iron in acidic solution by the oligomeric surfactant N,N,N',N',N"-pentamethyl diethyleneamine-N,N"-di-[tetradecylammonium bromide]. *Anti-Corrosion Methods and Materials*, 58(5), 258-266.
<http://dx.doi.org/10.1108/00035591111167730>
- Bereket, G. & Gerengi, H. 2006. Harmonic Analysis For Corrosion Monitoring. X. International Corrosion Symposium, November 1-4 Adana, 403-405.
- Bereket, G. & Pinarbasi, A. (2008). Inhibition effect of some heterocyclic compounds on pure aluminium in 0.1 M hydrochloric acid solution. *Corrosion*, 16, 17-22.
- DIN Standard 2007. Cold rolled low carbon steel flat products for cold forming—Technical delivery conditions; German version EN 10130:2006. Berlin, Germany: DIN Deutsches Institut für Normung e.V., 14s.
- EldougDoug, W. I., Ali, A. I., Elaraby, A. & Mabrouk, E. M. (2018). Corrosion inhibition of Tri-cationic surfactant on carbon steel in hydrochloric acid solution. *Journal of Basic and Environmental Sciences*, 5, 289-300.
- Feng, L., Yin, C., Zhang, H., Li, Y., Song, X., Chen, Q. & Liu, H. (2018). Cationic Gemini Surfactants with a Bipyridyl Spacer as Corrosion Inhibitors for Carbon Steel. *ACS Omega*, 3, 18990-18999.
<https://doi.org/10.1021/acsomega.8b03043>
- Hegazy, M. A., El-Etre, A. Y., El-Shafaie, M. & Berry, K. M. (2016). Novel cationic surfactants for corrosion inhibition of carbon

- steel pipelines in oil and gas wells applications. *Journal of Molecular Liquids*, 214, 347-356.
<http://dx.doi.org/10.1016/j.molliq.2015.11.047>
- Hegazy, M. A., Azzam, E. M. S., Kandil, N. G., Badawi, A. M. & Sami, R. M. (2016). Corrosion Inhibition of Carbon Steel Pipelines by Some New Amphoteric and Di-cationic Surfactants in Acidic Solution by Chemical and Electrochemical Methods. *Journal of Surfactants and Detergents*, 19, 861-871.
<https://doi.org/10.1007/s11743-016-1824-9>
- Öztürk, S. (2017). Synthesis and Corrosion Inhibition Effects of Quinazolin-(3H)-4-One Derivatives Containing Long-Chain Pyridinium Salts on Carbon Steel in 1.5 M HCl, *Protection of Metals and Physical Chemistry of Surfaces*, 53(5), 920-927.
<https://doi.org/10.1134/S2070205117050161>
- Öztürk, S. (2018). Düşük Karbon Çeliğinin Asidik Ortamdaki Korozyonuna Karşı İnhibitör Özelliği Gösteren 4-Okso-Kinazolin Türevi Katyonik Yüzey Aktif Maddelerin Sentezi. *Sakarya Üniversitesi Fen Bilimleri Enstitüsü Dergisi*, 22 (3), 986-1000.
10.16984/saufenbilder.350569
- Öztürk, S., (2019). Synthesis of Quinazoline Derivative Di-Cationic Surfactants and Their Corrosion Protection of Mild Steel in Acidic Media. *Russian Journal of Organic Chemistry*, 55(2), 245-249.
<https://doi.org/10.1134/S1070428019020179>
- Qiu, L. G., Xie, A. J. & Shen, Y. H. (2005). A novel triazole-based cationic gemini surfactant: synthesis and effect on corrosion inhibition of carbon steel in hydrochloric acid. *Materials Chemistry and Physics*, 91, 269–273.
<https://doi.org/10.1016/j.matchemphys.2004.11.022>
- Shalabi, K., Helmy, A.M., El-Askalany, A.H., Shahba, M.M. (2019). New pyridiniumbromidemono-cationic surfactant as corrosion inhibitör for carbon steel during chemical cleaning: Experimental and theoretical studies. *Journal of Molecular Liquids*, 293, 111480. <https://doi.org/10.1016/j.molliq.2019.111480>
- Yıldırım, A., Öztürk, S. & Çetin, M. (2013). Novel Amide-Based Cationic Surfactants as Efficient Corrosion Inhibitors for Carbon Steel in HCl and H₂SO₄ media, *Journal of Surfactants and Detergents*, 16, 13–23. <https://doi.org/10.1007/s11743-012-1356-x>
- Zhu, Y., Free, M. L., Woollam, R., Durnie, W. (2017). A review of surfactants as corrosion inhibitors and associated modeling, *Progress in Materials Science*, 90:159–223.
<http://dx.doi.org/10.1016/j.pmatsci.2017.07.006>

SODYUM ALJİNAT/ HİDROKSİPROPİL METİLSELÜLOZ KOMPOZİT BONCUKLARI İLE SULU ÇÖZELTİDEN RB’NİN ADSORPSİYONU

Gülşen TAŞKIN ÇAKICI

Sivas Cumhuriyet University, Yıldızeli Vocational School, Chemistry and Chemical Process Technology

ORCID ID: 0000-0001-7564-9777

ÖZET

Suyun kirlenmesi, ekosistemlerin dengesini ve insan sağlığını ciddi şekilde etkileyen bir sorundur. Tekstil endüstrisi tarafından atılan suların renklendiricilerin giderilmesi için yıllar içinde çeşitli teknikler uygulanmış; yine de elde edilen bazı atıkların işlenmesi zor ve zehirlidir. Bu çalışmanın amacı, endüstride yaygın olarak kullanılan katyonik bir boyar madde olan rodamin B'nin (RB) sulu çözeltiden adsorpsiyon yoluyla giderilmesinde adsorban olarak çevre dostu biyobozunur polimerler ile hazırlanan boncukların kullanımını araştırmaktır. Bu nedenle sodyum aljinat (NaAlg) ve hidroksipropilmetilselüloz (HPMC) ile çapraz bağlı sodyum aljinat/hidroksipropilmetilselüloz (NaAlg/HPMC) kompozit boncukları hazırlandı. Çapraz bağlayıcı olarak kalsiyum klorür (CaCl_2) kullanılmış ve çapraz bağlama süresinin şişme yüzdesine etkisi araştırılmıştır. Çapraz bağlama süresi ile şişmenin azaldığı belirlendi. Ayrıca adsorban miktarı, RB başlangıç derişimi, sıcaklık ve pH'ın RB adsorpsiyon kapasitesi üzerine etkileri değerlendirildi. Sonuçlar pH 4,25 sıcaklık 25°C ve adsorban miktarı 0,5 mg/mL olduğunda maksimum adsorpsiyon kapasitesi 10,24 mg/g elde edildi. Sıcaklık arttığında adsorpsiyon kapasitesi azaldı.

Anahtar Kelimeler: Sodyum Aljinat, Hidroksipropil Metil Selüloz, Rodamin-B, Adsorpsiyon

ADSORPTION OF RB FROM AQUEOUS SOLUTION WITH SODIUM ALGINATE/ HYDROXYPROPYMETHYLCELLULOSE COMPOSITE BEADS

ABSTRACT

Pollution of water is a problem that seriously affects the balance of ecosystems and human health. Various techniques have been applied over the years to remove colorants from the waters discharged by the textile industry; however, some of the resulting wastes are difficult to process and toxic. This study aims to investigate the use of beads prepared with environmentally friendly biodegradable polymers as an adsorbent in the removal of rhodamine B (RB), a widely used cationic dye, from aqueous solution by adsorption. Therefore, cross-linked sodium alginate/ hydroxypropylmethylcellulose (NaAlg/HPMC) composite beads were prepared by sodium alginate (NaAlg) and hydroxypropylmethylcellulose (HPMC). Calcium chloride (CaCl_2) was used as a crosslinker and, the effect of crosslinking time was investigated on the swelling percentage. It was determined that swelling decreased with crosslinking time. In addition, the effects of adsorbent amount, RB initial

concentration, temperature, and pH were evaluated on RB adsorption capacity. The maximum adsorption capacity of 10.24 mg/g was obtained when the pH was 4.25, the temperature was 25°C, and the amount of adsorbent was 0.5 mg/mL. As the temperature increased, the adsorption capacity decreased.

Keywords: Sodium Alginate, Hydroxypropyl Methyl Cellulose, Rhodamine-B, Adsorption

1. GİRİŞ

Son zamanlarda endüstriyel atıklardan kaynaklanan artan kirlilik nedeniyle saf su kaynaklarının kıtlığı hem toplum hem de araştırmacılar tarafından yoğun ilgi görmüştür (Godiya, Xiao ve Lu, 2019).

Sentetik boyalar; kağıt yazıcılar ve tekstil boyacılar dahil olmak üzere birçok endüstride yaygın olarak kullanılmaktadır. Sentetik boyaların önemli bir kısmı, tekstil işleme sırasında çevreye giren atık sular içerisinde bulunmaktadır. Şimdiye kadar boyaların sudan uzaklaştırılması için boyanın cinsi, ortamdaki boya miktarı, uzaklaştırılması için gereken kimyasal ve malzeme maliyetleri birer etken olarak incelenmiş ve bunun sonucunda basınçlı kum ve benzeri birçok yöntem incelenmiştir. Aktif karbon filtreleri, membran teknolojileri, ileri oksidasyon prosesleri, adsorpsiyon-biyodegradasyon prosesleri, elektrokoagülasyon, biyolojik arıtma ve kimyasal oksidasyon kullanılmıştır (Liu ve ark., 2007; Fayazi, Ghanei-Motlagh ve Taher, 2015; Han ve ark., 2016). Bunlar arasında adsorpsiyon yöntemi baskındır, çünkü adsorpsiyonun endüstriyel atık suların arıtılması için mükemmel bir yol olduğu kanıtlanmıştır. Adsorpsiyon düşük maliyet, kullanılabilirlik, karlılık, kullanım kolaylığı ve verimlilik gibi önemli avantajlar sunmaktadır (Demirbas, 2008). Ayrıca alternatif adsorbanların geliştirilmesi son araştırmaların odak noktası olmuştur.

Bazik menekşe olarak da adlandırılan Rodamin B (RB), sentetik floresan keton heterosiklik bir boyadır. Rodamin B (RB), baskı, tekstil, kağıt yapımı, boya ve deri gibi endüstrilerde boyar madde olarak yaygın kullanılma sahiptir (Lops ve ark., 2019; Arami ve ark., 2005; Pourreza, Rastegarzadeh ve Larki, 2008). Önemli miktarda RB çevreye salınarak suyu kirletmekte ve biyolojik sistemler ile insan yaşamı için tehlikeye neden olmaktadır (Madhav ve ark., 2018; KaurRajvir ve Kaur, 2014). Bununla birlikte, RB'nin uygulanması, toksisitesi ve kanserojenlik özellikleri nedenleriyle sınırlıdır. RB'nin özellikleri, suda yüksek çözünürlüğü nedeniyle sudan zor elimine edilen ve ışık, sıcaklık, kimyasallar ve mikroplar tarafından zor bozunması diğer sentetik aromatik boyalarla benzerdir (Lacerda ve ark., 2015; Li ve ark., 2015). RB'nin uzaklaştırılması atık su arıtımı için önemlidir. Günümüzde endüstriyel atık sulardan RB'yi uzaklaştırmak için kimyasal flokülasyon, iyon değiştirme teknikleri, elektrokimyasal prosesler, membran filtrasyon, adsorpsiyon gibi çeşitli yöntemler denenmekte olup, bunların arasında adsorpsiyon en verimli ve pratik bir yöntemdir (Yang ve ark., 2019; Thakur ve Kaur, 2017). Tang ve ark. (2015), Rodamin B'nin sodyum aljinat aşısı poli(akrilik asit-ko-akrilamid)/kaolin kompozit hidrojel üzerindeki sorpsiyon davranışı üzerine detaylı bir çalışma yapmışlardır. Adsorban olarak aktive edilmiş karbonlarda, RB'yi uzaklaştırmak için yaygın olarak uygulanmaktadır (Abdolrahimi ve

Tadjarodi, 2019). Ancak aktif karbon, gelişmekte olan ülkeler için uygun olmayan yüksek maliyetli bir malzemedir (Inyinbor, Adekola ve Olatunji, 2017). Bu nedenle, birçok bilim insanı düşük maliyetli adsorbanların geliştirilmesine daha fazla dikkat etmektedir.

Sodyum aljinat (NaAlg), mannuronik asit ve guluronik asitten oluşan çevre dostu bir doğal karbonhidrat polimeridir (Su ve Chen, 2018). Ucuz, toksik olmaması, biyoyumluluğu, biyobozunabilirliği, bol karboksil ve hidroksil grupları nedeniyle atık sudaki boya ve ağır metalleri uzaklaştırmak için yaygın olarak kullanılır (Lv ve ark., 2013; Ma ve ark., 2018). NaAlg, iki değerlikli veya çok değerlikli katyonlarla (Ca^{+2} , Ba^{+2} ve Fe^{+3} gibi) iyonik bağlanma yoluyla çapraz bağlanabilir ve üç boyutlu ağlara sahip boncukları oluşturabilir (Shan ve ark., 2019; Sun ve ark., 2012). Ancak çapraz bağlı NaAlg'nın etkin adsorpsiyon sahasının, çapraz bağlama sırasında karboksil gruplarının tüketimi nedeniyle önemli ölçüde azaldığı bulunmuştur. Bu nedenle, yüksek verimli adsorban elde etmek için NaAlg'nın diğer bazı malzemelerle kompoziti oluşturulmaktadır. Sodyum aljinat, adsorpsiyon kapasitesini, mekanik stabilitesini ve dayanıklılığını arttırmak için daha fonksiyonel grupları dahil etmek için fizikokimyasal işlemlerle kolayca değiştirilebilir. Örneğin, Bahrami ve ark. (2019) sudaki metilen mavisi boyasının ortadan kaldırılması için çapraz bağlayıcı olarak N,N'-metilen-bis(akrilamid) (MBA) kullanarak çapraz bağlı NaAlg/PAAm bazlı hidrojel üretmişlerdir ve bu da metilen mavisi için tatmin edici adsorpsiyon kapasitesini ortaya koymaktadır Hidroksipropil metilselüloz (HPMC), kozmetikte (Lochhead, 2017), farmasötiklerde (Kaur ve ark., 2018) ve gıda (Burdock, 2007) formülasyonunda yaygın olarak uygulanan suda çözünür selüloz eterlerin bir ailesidir. HPMC zincirleri kolayca çapraz bağlanabilir ki bu da ilaç salımı (Marani, Bloisi ve Petri, 2015) veya kirleticilerin adsorpsiyonunda (Martins, Toledo ve Petri, 2018; Toledo, Marques ve Petri, 2019; Toledo ve ark., 2019) kullanılabilirliğini ortaya koymaktadır. Yukarıda bahsedilen potansiyel uygulamalara rağmen, mekanik özellikler üzerindeki sonuçlar, bu tür malzemelerdeki suyun durumları ve bunların boyalara olan afiniteleri üzerindeki sonuçlar yeterince araştırılmamıştır. Bu zamana kadar yapılan çalışmalarda NaAlg ve HPMC'den oluşan karışımlar yaygın olarak ilaç salımlarında kullanılmıştır (Nochos, Douroumis ve Bouropoulos, 2008; Prabu ve ark., 2016).

Bu çalışmada sodyum aljinat (NaAlg) ve hidroksipropilmetilselüloz (HPMC) ile çapraz bağlı sodyum aljinat/hidroksipropilmetilselüloz (NaAlg/HPMC) kompozit boncukları hazırlandı. Çapraz bağlama süresinin hazırlanan boncukların şişme yüzdesine etkisi araştırıldı. NaAlg/HPMC boncukları ile rodamin B boyar maddesinin sudan uzaklaştırmak için kolay ve ekonomik adsorpsiyon yöntemi incelendi. Adsorpsiyon koşullarının (adsorban miktarı, RB başlangıç derişimi, sıcaklık ve pH gibi) adsorpsiyon kapasitesi üzerine etkisi değerlendirildi. NaAlg ve HPMC ile hazırlanan boncukların adsorpsiyon yönteminde kullanımı ilk olacaktır.

2.MATERYAL VE METOD

2.1. Kimyasallar

Sodyum aljinat (NaAlg) polimeri (orta viskozite) ve hidroksipropil metil selüloz (HPMC) Sigma- Aldrich'den (Almanya) temin edildi. Merck firmasına ait rodamin-b (RB) adsorpsiyon araştırmasında, CaCl₂ ise çapraz bağlama işleminde kullanıldı.

2.2. Polimerik Boncuk (Adsorban) Formülasyonu

1:1 oranında NaAlg/ HPMC polimer karışımı toplam polimer miktarı %1 (m/V) olacak şekilde hazırlandı. Boncuklar CaCl₂ (%3 m/V) çapraz bağlayıcı çözeltisine belirli uzaklıktan enjektör ile damlatılarak oluşturuldu. Değişen sürelerde (15-60 dk.) çapraz bağlayıcı çözelti içerisinde sabit hızda karıştırılarak çapraz bağlanması sağlandı. Çapraz bağlı boncuklar süzülüp saf su ile yıkandı. 40°C sıcaklıkta kurutulup oda koşullarında saklandı (Şekil 1).



Şekil 1. NaAlg/HPMC boncuklar

2.3. % Şişme Değerlerinin Belirlenmesi

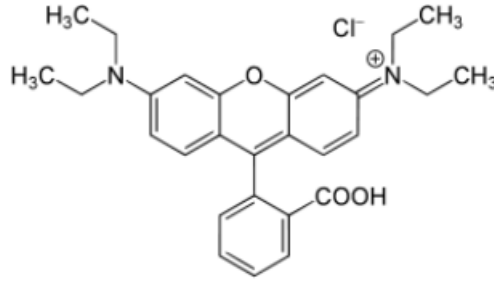
Çapraz bağlı boncukların yüzde şişme değerleri 24 saat (25 °C) suya daldırılarak belirlendi. Etüvde kurutulan ve sabit tartıma getirilen boncukların şişme yüzdeleri (%SD) denklem (1) ile hesaplandı.

$$SD\% = \frac{M_{ıslak} - M_{kuru}}{M_{kuru}} \times 100 \quad (1)$$

M_{ıslak} ve M_{kuru} sırasıyla suda bekletilen ve etüvde kurutulan boncukların tartım değeri(g).

2.4. RB Çözeltisi Hazırlanma

C₂₈H₃₁ClN₂O₃ molekül formülüne sahip RB stok çözeltisinden (200 mg/L) 50 mg/L, 100 mg/L, 150 mg/L derişimlerinde RB çözeltileri hazırlandı.



Şekil 2. RB kimyasal yapısı

2.5. RB Adsorpsiyon Çalışması

Hazırlanan NaAlg/HPMC boncukları ile RB adsorpsiyonu çalışmaları, 25 mL RB çözeltisi belirli miktarda adsorban ile 200 rpm karıştırma hızında 2 saat süre ile gerçekleştirildi. RB adsorpsiyonu çalışmalarında adsorpsiyon kapasitesi üzerine; adsorban miktarı (0,5-3 mg/mL), RB derişimi (50-200 mg/L), pH (3-9) ve sıcaklığın (25-45°C) etkileri incelendi. Adsorplanan RB konsantrasyonu 553 nm'de spektrofotometrik (Thermoscientific, Genesys 150- UV visible spektrofotometre) yöntem ile belirlendi. Adsorpsiyon kapasitesi aşağıdaki denklem ile belirlendi:

$$q = \frac{(C_0 - C) \times V}{m} \quad (2)$$

q; Adsorpsiyon kapasitesi (mg/g), C_0 ve C ; sırasıyla RB'nin başlangıç ve son derişimi (mg/mL), V ; hacim (mL); m ; adsorban miktarı (g).

3.SONUÇLAR VE TARTIŞMA

3.1. NaAlg/HPMC Boncukların Şişme Yüzdeleri

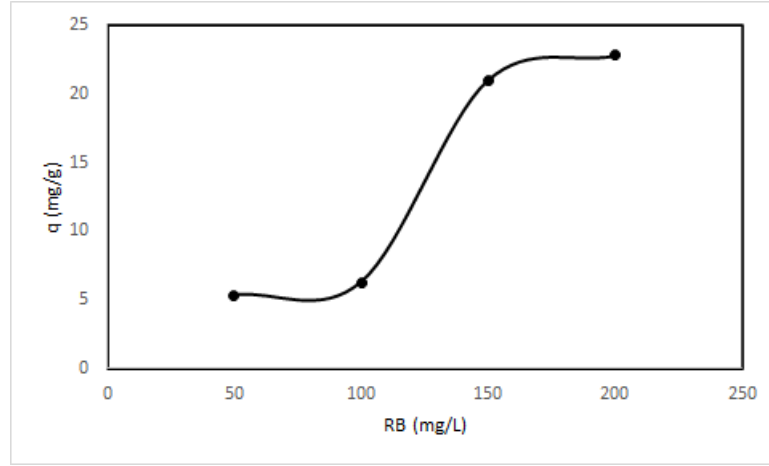
$CaCl_2$ çapraz bağlama çözeltisinde 15 dk, 30 dk ve 60 dk sürelerle çapraz bağlanmış NaAlg/ HPMC boncukların şişme yüzdeleri Eşitlik 1 kullanılarak hesaplandı. Tablo 1'de değişen çapraz bağlama sürelerine karşılık hazırlanan boncukların şişme yüzdeleri verildi.

Tablo 1. Değişen çapraz bağlama süresindeki çapraz bağlı NaAlg/HPMC boncukların %şişme değerleri

Çapraz bağlama süresi (dk)	%Şişme
15	256,9
30	205,4
60	140,1

Tablo 1'de artan çapraz bağlama süresi ile % şişme değerinin azaldığı görülmüştür. Polimerlerin şişme davranışları ile polimerik zincirde çapraz bağlanma derecesi ve serbest hacim gibi özellikler açıklanmaktadır. Çalışmada en yüksek şişme yüzdesine sahip boncuklar adsorpsiyon çalışmalarında kullanıldı.

3.2. Boya Çözeltilerinin Başlangıç Konsantrasyonunun Adsorpsiyon Üzerine Etkisi Başlangıç RB konsantrasyonunun adsorpsiyon kapasitesi üzerindeki etkisi Şekil 3'de gösterilmektedir. 50-200 mg/L aralığında RB derişimi ile yapılan adsorpsiyon deneylerinde 3mg/mL boncuk kullanıldı.

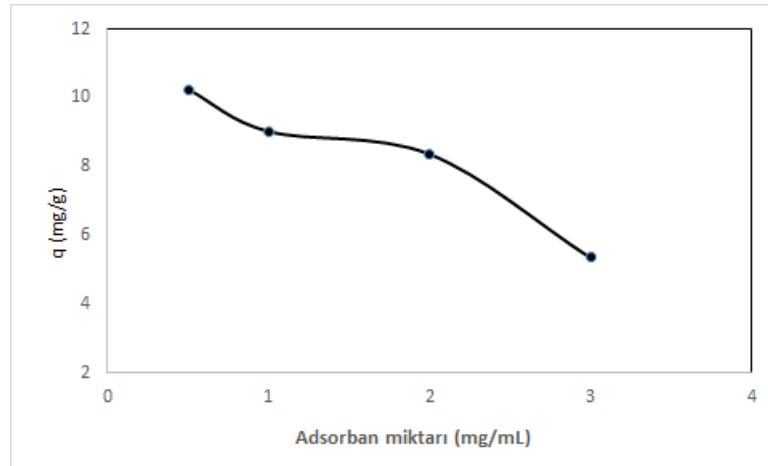


Şekil 3. RB başlangıç derişiminin adsorpsiyon kapasitesi üzerine etkisi [25°C, pH=4,25, 3 mg/mL adsorban]

Şekil 3'de görüldüğü gibi, RB'nin başlangıç konsantrasyonu arttıkça adsorpsiyon kapasitesinde doğrusal bir artış vardır. Maksimum adsorpsiyon kapasitesi 22,8 mg/g olarak 200 mg/L RB çözeltisinde elde edildi. Boya konsantrasyonunun artması, boya moleküllerinin çözeltiden adsorban yüzeyine difüzyonunu hızlandırmıştır. Katyonik boyalar için, kompozitteki -COO⁻ iyonu gibi negatif yüklü gruplar ile boya molekülleri üzerindeki pozitif yüklü gruplar arasında güçlü elektrostatik kuvvetler vardır (Zhu ve ark., 2017). Ayrıca artan başlangıç boya konsantrasyonu ile konsantrasyon gradyanının itici gücünde artış olmuştur (Kaushal ve Tiwari, 2010). Bu nedenle, boya konsantrasyonları arttıkça adsorpsiyon kapasitesi büyük ölçüde artar.

3.3. Adsorban Miktarının Adsorpsiyon Üzerine Etkisi

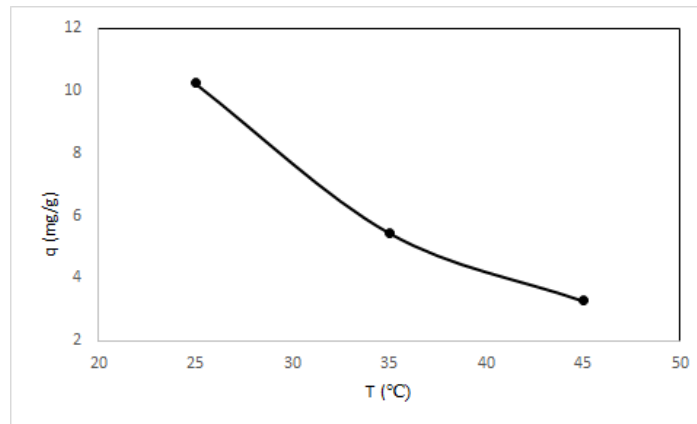
Adsorban miktarının adsorpsiyon kapasitesi üzerine etkisi Şekil 4'de gösterilmiştir. Adsorban miktarı 0,5'den 3mg/mL'e yükseldikçe RB adsorpsiyon kapasitesi 10,24 mg/g'dan 5,4 mg/g'a azalmıştır. Adsorban miktarının artması, adsorbanın birim yüzey alanı üzerindeki aktif adsorpsiyon noktalarının azalmasına yol açması ile adsorpsiyon kapasitesi azalmıştır. Zou ve ark. (2019) poliakrilamid/aljinat mikroküreleri ile metilen mavisi adsorpsiyon çalışmalarında da benzer sonuçlar elde etmiştir.



Şekil 4. Adsorban miktarının adsorpsiyon kapasitesi üzerine etkisi [25°C, pH=4,25, [RB]=50mg/L]

3.4. Sıcaklığın Adsorpsiyon Üzerine Etkisi

NaAlg/HPMC'nin farklı sıcaklıklarda adsorpsiyon kapasitesi Şekil 5'de verilmiştir. Sıcaklık 25'ten 45°C'ye yükseldiğinde adsorpsiyon kapasitesinin kademeli olarak azaldığı grafikten görülmektedir. NaAlg/HPMC yapısında hidrojen bağ oluşumunu arttıran çok sayıda hidroksil ve karboksil grubu bulunmaktadır. Sıcaklığın artması, hidrojen bağlarının oluşumunu olumsuz etkilemektedir. Moleküler zincirlerin kıvrılma derecesi büyüyerek ve adsorbanların adsorpsiyon bölgelerinin azalmasına, dolayısıyla sıcaklığın artışı ile adsorpsiyon kapasitesinde azalış söz konusu olmuştur (Zou ve ark., 2019).

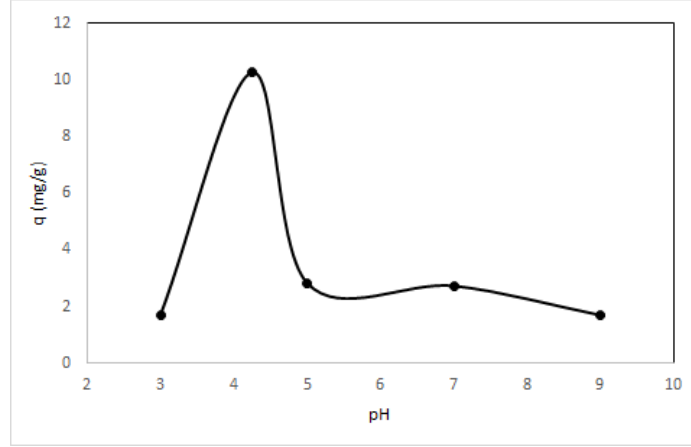


Şekil 5. Sıcaklığın adsorpsiyon kapasitesine etkisi [pH=4,25, [RB]=50mg/L, 0,5 mg/mL NaAlg/HPMC]

3.5. pH'ın Adsorpsiyon Üzerine Etkisi

pH'ın RB adsorpsiyon kapasitesi üzerine etkisini incelemek için pH= 3 – 9 arasında değiştirilmiş, elde edilen sonuçlar Şekil 6'da verilmiştir. pH adsorbanın aktif bölgelerini ve yüzey yükünü etkilediği için, organik boyar maddelerin adsorpsiyonunda oldukça önemlidir (Sharma, Rekha ve Mohanty, 2016). En yüksek adsorpsiyon kapasitesi pH= 4,25'de elde edilmiştir (Şekil 6). Daha yüksek pH değerlerinde ise adsorpsiyon kapasitesi düşmüştür. pH değerlerinin değişmesiyle RB'nin yapısının değiştiği bilinmektedir. Asidik ortamda RB katyonik formunu gösterirken, bazik ortamda zwitteriyonik haldedir (Tang ve ark., 2015). Temel ortamda, bir RB

molekülünün ksanten grubunun, elektrostatik etkileşimler yoluyla başka bir RB molekülünün karboksil grubu ile birleştirilmesi kolaydır. Sonuç olarak, adsorban yüzeyinde adsorpsiyon büyük ölçüde engellenir (Eftekhari, Habibi-Yangjeh ve Sohrabnezhad, 2010; Tsai, Lai ve Hsien, 2003). Bununla birlikte, asidik koşullar altında karboksil gruplarının ayrışması geciktirilir. Böylece RB molekülleri ile NaAlg/HPMC boncukları yüzeyi arasındaki elektrostatik çekim artar ve düşük pH değerinde yüksek adsorpsiyon kapasiteleri elde edilir.



Şekil 6. pH'nin adsorpsiyon kapasitesine etkisi [25°C, [RB]=50mg/L, 0,5 mg/mL NaAlg/HPMC]

4. SONUÇLAR

Bu çalışmada 1:1 oranında NaAlg ve HPMC ile hazırlanan ve CaCl₂ ile çapraz bağlanan NaAlg/HPMC boncukları ile RB boyarmaddesinin adsorpsiyonu incelenmiştir. Farklı sürelerde çapraz bağlanmış boncukların şişme değerlerine bakıldığında en yüksek şişmenin 15 dk çapraz bağlanmış NaAlg/HPMC boncuklarında elde edilmiştir. 15 dk. çapraz bağlı NaAlg/HPMC boncuklarının RB adsorpsiyonunda kullanılmasında; RB başlangıç derişimi, adsorban miktarı, sıcaklık ve pH'nin adsorpsiyon kapasitesi üzerine önemli etkileri olan parametreler olduğu görülmüştür. Yapılan deneyler sonucunda pH 4,25'de 0,5 mg/mL NaAlg/HPMC boncukları, 200 mg/L RB derişiminde en yüksek adsorpsiyon kapasitesi elde edildi. Bu çalışmada, toksik katyonik boya olan RB'nin sulu ortamdan uzaklaştırılması için çevre dostu, ekonomik, pratik ve kolay temin edilebilen bir adsorban başarıyla elde edilmiş oldu. Bu nedenle, çalışılan materyal, sulu çözeltilerden katyonik boyaların uzaklaştırılması için potansiyel bir adsorban olarak önerilebilir.

KAYNAKLAR

- Abdolrahimi N. and Tadjarodi A. (2019). Adsorption of Rhodamine-B from Aqueous Solution by Activated Carbon from Almond Shell. *Proceedings*, 41, 51-54.
- Arami M., Limaee N. Y., Mahmoodi N. M., and Tabrizi N. S. (2005). Removal of Dyes From Colored Textile Wastewater By Orange Peel Adsorbent: Equilibrium and Kinetic Studies. *Journal of Colloid and Interface Science*, 288, 371–376.
- Bahrami Z., Akbari A., Eftekhari-Sis B. (2019). Double Network Hydrogel Of Sodium Alginate/Polyacrylamide Cross-Linked With POSS: Swelling, Dye Removal And Mechanical Properties. *International Journal of Biological Macromolecules*, 129,187–197.

- Burdock G.A. (2007). Safety Assessment Of Hydroxypropyl Methylcellulose As A Food Ingredient. *Food Chemistry and Toxicology*, 45, 2341-2351.
- Demirbas A. (2008). Heavy Metal Adsorption onto Agro-Based Waste Materials: A Review. *Journal of Hazardous Materials*, 157, 220–229.
- Eftekhari S., Habibi-Yangjeh A., and Sohrabnezhad S. (2010). Application of AIMCM-41 for Competitive Adsorption Of Methylene Blue And Rhodamine B: Thermodynamic And Kinetic Studies. *Journal of Hazardous Materials*, 178, 349–355.
- Fayazi M., Ghanei-Motlagh M., Taher M.A. (2015). The Adsorption of Basic Dye (Alizarin red S) from Aqueous Solution onto Activated Carbon/ γ -Fe₂O₃ Nano-Composite: Kinetic and Equilibrium Studies. *Materials Science in Semiconductor Processing*, 40, 35–43.
- Godiya C.B., Xiao Y., Lu X. (2019). Amine Functionalized Sodium Alginate Hydrogel for Efficient and Rapid Removal of Methyl Blue in Water. *International Journal of Biological Macromolecules*, 144, 671–681.
- Han H., Wei W., Jiang Z., Lu J., Zhu J., Xie J. (2016). Removal of Cationic Dyes from Aqueous Solution by Adsorption onto Hydrophobic/Hydrophilic Silica Aerogel. *Colloid Surface A*, 509(20), 539–549.
- Inyinbor A. A., Adekola F. A., and Olatunji G. A. (2017). Liquid Phase Adsorptions of Rhodamine B Dye Onto Raw And Chitosan Supported Mesoporous Adsorbents: Isotherms And Kinetics Studies. *Applied Water Science*, 7, 2297–2307.
- Kaur G., Grewal J., Jyoti K., Jain U.K., Chandra R., Madan J. (2018). Oral Controlled And Sustained Drug Delivery Systems: Concepts, Advances, Preclinical, And Clinical Status, A.M. Grumezescu (Ed.), *Drug targeting and stimuli sensitive drug delivery systems*, William Andrew, pp. 567-626.
- KaurRajvir H. and Kaur K. (2014). Removal of Rhodamine-B Dye From Aqueous Solution onto Pigeon Dropping: Adsorption, Kinetic, Equilibrium and Thermodynamic Studies. *Journal of Materials and Environmental Science*, 5, 1830–1838.
- Kaushal M. & Tiwari A. (2010). Removal of Rhodamine-B from Aqueous Solution by Adsorption onto Crosslinked Alginate Beads, *Journal of Dispersion Science and Technology*, 31(4), 438-441.
- Lacerda V. S., López-Sotelo J. B., Correa-Guimarães A., Hernández-Navarro S., Sánchez-Báscones M., Navas-Gracia L. M., Martín-Ramos P., Martín-Gil J. (2015). Rhodamine B Removal With Activated Carbons Obtained from Lignocellulosic Waste. *Journal of Environmental Management*, 155, 67–76.
- Li F., Chen Y., Huang H., Cao W., and Li T. (2015). Removal of Rhodamine B and Cr(VI) from Aqueous Solutions by a Polyoxometalate Adsorbent. *Chemical Engineering Research and Design*, 100, 192–202.
- Liu C-H., Wu J-S., Chiu H-C., Suen S-Y., Chu K.H. (2007). Removal of Anionic Reactive Dyes From Water Using Anion Exchange Membranes as Adsorbers. *Water Research*, 41(7), 1491–1500.
- Lochhead R.Y. (2017). The Use Of Polymers In Cosmetic Products, In *Cosmetic Science And Technology*, K. Sakamoto, R.Y. Lochhead, H.I. Maibach, Y. Yamashita (Eds.). *Cosmetic science and technology: Theoretical principles and applications*, Elsevier, pp. 171-221.
- Lops C., Ancona A., Cesare K. D., Dumontel B., Garino N., Canavese G., Hernández S., Cauda V. (2019). Sonophotocatalytic Degradation Mechanisms of Rhodamine B Dye Via Radicals Generation by Micro- and Nano-Particles of ZnO. *Applied Catalysis B: Environmental*, 243, 629–640.
- Lv X., Jiang G., Xue X., Wu D., Sheng T., Sun C., Xu X., (2013). Fe(0)-Fe₃O₄ Nanocomposites Embedded Polyvinyl Alcohol/Sodium Alginate Beads For Chromium(VI) Removal. *Journal of Hazardous Materials*, 262, 748-758.
- Ma Y., Wang J., Xu S., Feng S., Wang J. (2018). Ag₂O/Sodium Alginate-Reduced Graphene Oxide Aerogel Beads For Efficient Visible Light Driven Photocatalysis. *Applied Surface Science*, 430, 155-164.
- Madhav S., Ahamad A., Singh P., and Mishra P. K. (2018). A Review of Textile Industry: Wet Processing, Environmental Impacts, and Effluent Treatment Methods. *Environmental Quality Management*, 27, 31–41.
- Marani P.L., Bloisi G.D., Petri D.F.S. (2015). Hydroxypropylmethyl Cellulose Films Crosslinked With Citric Acid For Control

- Release Of Nicotine. *Cellulose*, 22, 3907-3918.
- Martins B.F., Toledo P.V.O., Petri D.F.S. (2017). Hydroxypropyl Methylcellulose Based Aerogels: Synthesis, Characterization And Application As Adsorbents For Wastewater Pollutants. *Carbohydrate Polymers*, 155, 173-181.
- Nochos A., Douroumis D., and Bouropoulos N. (2008). In Vitro Release Of Bovine Serum Albumin From Alginate/HPMC Hydrogel Beads, *Carbohydrate Polymers*, 74, 451-457.
- Pourreza N., Rastegarzadeh S., and Larki A. (2008). Micelle-mediated Cloud Point Extraction and Spectrophotometric Determination of Rhodamine B Using Triton X-100. *Talanta*, 77, 733-736.
- Prabu D., Majdalawieh A. F., Abu-Yousef I. A., Inbasekaran K., Balasubramaniam T., Nallaperumal N., and Gunasekar C. J. (2016). Preparation And Characterization Of Gatifloxacin-Loaded Sodium Alginate Hydrogel Membranes Supplemented With Hydroxypropyl Methylcellulose And Hydroxypropyl Cellulose Polymers For Wound Dressing, *International Journal of Pharmaceutical Investigation*, 6(2), 86-95.
- Shan S., Tang H., Zhao Y., Wang W., Cui F. (2019). Highly Porous Zirconium-Crosslinked Graphene Oxide/Alginate Aerogel Beads For Enhanced Phosphate Removal. *Chemical Engineering Journal*, 359, 779-789.
- Sharma, V., Rekha, P., Mohanty, P. (2016). Nanoporous Hypercrosslinked Polyaniline: An Efficient Adsorbent For The Adsorptive Removal Of Cationic And Anionic Dyes. *Journal of Molecular Liquids*, 222, 1091-1100.
- Su X., Chen B. (2018). Tough, Resilient And pH-Sensitive Interpenetrating Polyacrylamide/Alginate/Montmorillonite Nanocomposite Hydrogels. *Carbohydrate Polymers*, 197, 497-507.
- Sun J.Y., Zhao X., Illeperuma W.R., Chaudhuri O., Oh K.H., Mooney D.J., Vlassak J.J., Suo Z. (2012). Highly Stretchable and Tough Hydrogels, *Nature*, 489, 133-136.
- Tang Y., Wang Q., Zhou B., Ma D., Ma Z., and Zhu L. (2015). College of Chemical and Environmental Engineering, Shandong University of Science and TechSynthesis of Sodium Alginate Graft Poly (acrylic acid-co-acrylamide)/ Kaolin Composite Hydrogel and the Study on its Sorption of Rhodamine B, *Polymers & Polymer Composites*, 23, No. 7.
- Tang Y., Wang Q., Zhou B., Ma D., Ma Z., and Zhu L. (2015). Synthesis of Sodium Alginate Graft Poly(Acrylic Acid-Co-Acrylamide)/Kaolin Composite Hydrogel and The Study on Its Sorption of Rhodamine B. *Polymers & Polymer Composites*, 23(7), 467-474.
- Thakur A. and Kaur H. (2017). Response surface optimization of Rhodamine B dye removal using paper industry waste as adsorbent. *International Journal of Industrial Chemistry*, 8, 175-186.
- Toledo P.V.O., Marques L.R., Petri D.F.S. (2019). Recyclable xanthan/TiO₂ Composite Cryogels Towards The Photodegradation Of Cr(VI) Ions And Methylene Blue Dye. *International Journal of Polymer Science*, 1-13, 10.1155/2019/8179842.
- Toledo P.V.O., Martins B.F., Pirich C.L., Sierakowski M.R., Teixeira-Neto E., Petri D.F.S. (2019). Cellulose Based Cryogels As Adsorbents For Organic Pollutants. *Macromolecular Symposia*, 383, Article 1800013.
- Tsai W. T., Lai C. W., Hsien K. J. (2003). Effect of Particle Size Of Activated Clay On The Adsorption Of Paraquat From Aqueous Solution. *Journal of Colloid and Interface Science*, 263, 29-34
- Yang J., Yu S., Chen W., and Chen Y. (2019). Rhodamine B Removal from Aqueous Solution by CT269DR Resin: Static and Dynamic Study. *Adsorption Science & Technology*, 37, 709-728.
- Zhu L., Guan C., Zhou B., Zhang Z., Yang R., Tang Y., and Yang J. (2017). Adsorption of Dyes onto Sodium Alginate Graft Poly(Acrylic Acidco-2-Acrylamide-2-Methyl Propane Sulfonic Acid)/ Kaolin Hydrogel Composite, *Polymers & Polymer Composites*, 25 (8), 627-634.
- Zou X., Zhang H., Chen T., Li H., Meng C., Xia Y., Guo J. (2019). Preparation and Characterization Of Polyacrylamide / Sodium Alginate Microspheres And Its Adsorption of MB Dye. *Colloids and Surfaces A: Physicochemical and Engineering Aspects*, 567, 84-192.

INVESTIGATION OF THE OPTICAL PROPERTIES OF $\text{Na}_2\text{Ni}_2(\text{MoO}_4)_3$ NANOPARTICULES FOR PHOTOCATALYTIC APPLICATION

Imen JENDOUBI

Laboratory of Materials, Crystallochemistry and Applied Thermodynamics, Faculty of Sciences of Tunis, University of Tunis El Manar, Tunisia.

Mayssa ZOUAOUÏ

Laboratory of Materials, Crystallochemistry and Applied Thermodynamics, Faculty of Sciences of Tunis, University of Tunis El Manar, Tunisia.

Chokri ISSAOUI

Laboratory of Materials, Crystallochemistry and Applied Thermodynamics, Faculty of Sciences of Tunis, University of Tunis El Manar, Tunisia.

Mohamed Faouzi ZID

Laboratory of Materials, Crystallochemistry and Applied Thermodynamics, Faculty of Sciences of Tunis, University of Tunis El Manar, Tunisia.

Noura Fakhra BOURGUÏBA*

Laboratory of Materials, Crystallochemistry and Applied Thermodynamics, Faculty of Sciences of Tunis, University of Tunis El Manar, Tunisia.

ABSTRACT

In this paper, $\text{Na}_2\text{Ni}_2(\text{MoO}_4)_3$ was prepared by sol-gel method. Structural, vibrational and optical properties have been investigated. X-ray powder diffraction analysis revealed that the titled compound crystallizes in the orthorhombic system with Pnma space group. Vibrational study by means FTIR spectroscopy confirms the existence of the $(\text{MoO}_4)_2$ - functional group. Optical properties were recorded at room temperature using UV–visible spectroscopy in the spectral range (200–1500) nm. The UV–Vis absorption bands are attributed to the charge transfer from the oxygen ligands to the central molybdate atom inside the $(\text{MoO}_4)_2$ - groups. The optical absorbance was measured also to determinate the optical band gap using Kubelka–Munk function. The photocatalytic properties were evaluated by the degradation of methylene blue under UV lamps. The highest photodegradation efficiency was 89 %. Therefore, $\text{Na}_2\text{Ni}_2(\text{MoO}_4)_3$ can be a potential photocatalyst for the removal of dye wastewater pollution driven by visible-light.

Keywords: band gap; photocatalytic activity; photodegradation; UV light; methylene blue



PHYSICOCHEMICAL AND BIOLOGICAL ACTIVITY OF A NEW VANADIUM COMPLEX

Imen JENDOUBI *

Laboratory of Materials, Crystallochemistry and Applied Thermodynamics, Faculty of Sciences, University of Tunis El Manar, Tunis, Tunisia

Zaineb ABDELKAFI-KOUBAA

Laboratory of Venoms and Therapeutic Molecules, Institut Pasteur de Tunis, University of Tunis El Manar Tunis 1002, Tunisia.

Hammouda CHABBI

Laboratory of Materials, Crystallochemistry and Applied Thermodynamics, Faculty of Sciences, University of Tunis El Manar, Tunis, Tunisia

Najet SRAIRI-ABID

Laboratory of Venoms and Therapeutic Molecules, Institut Pasteur de Tunis, University of Tunis El Manar Tunis 1002, Tunisia.

Mohamed Faouzi ZID

Laboratory of Materials, Crystallochemistry and Applied Thermodynamics, Faculty of Sciences, University of Tunis El Manar, Tunis, Tunisia

ABSTRACT

Nowadays, with the growing problem of water contamination from discharged effluents by the increasing expansion of textile, leather, paper and ink industries and the problems related to pathogenic microorganisms causing diseases, the need for a substance with antimicrobial, anticancer and photocatalytic activity is very high. Decavanadate compounds have attracted the attention of several research groups due to their application in a variety of fields ranging from environmental to medicinal applications, which include wastewater treatment [1] and cancer therapy [2]. During the last decades, a significant number of the new decavanadates have been synthesized and explored intensively. In the present work, the compound $(C_5H_8N_2)_6V_{10}O_{28} \cdot 2H_2O$ was prepared by slow evaporation from an aqueous solution. The structural, vibrational and optical properties have been studied. X-ray diffraction analysis revealed that the compound $(C_5H_8N_2)_6V_{10}O_{28} \cdot 2H_2O$ crystallized in the triclinic system with the space group P-1. The vibrational study by confirms the existence of functional groups. The diffuse reflectance was recorded to determine the band gap. The material studied has been used for the main areas of research which include photocatalytic materials for wastewater treatment and biological applications in the development of anticancer drugs. The prepared compound acts as a photocatalyst for the removal of methylene blue (MB) dye under visible light irradiation. It also demonstrated a highly selective anticancer effect against U87 cells compared to other cell lines (IGR39,MDA-MB-231).

Keywords: Decavanadate, Synthesis, Infrared spectroscopy, Band gap, Photocatalytic activity, Anticancer activity.

BİYOKÜTLENİN SABİT YATAKTA YANMA DAVRANIŞI

Melek YILGIN

Fırat Üniversitesi, Mühendislik Fakültesi, Kimya Mühendisliği Bölümü

Neslihan DURANAY

Fırat Üniversitesi, Mühendislik Fakültesi, Kimya Mühendisliği Bölümü

Dursun PEHLİVAN

Fırat Üniversitesi, Mühendislik Fakültesi, Kimya Mühendisliği Bölümü

ÖZET

Bu çalışmada -8+ 16 mesh tane boyutundaki fındık kabuğu, ay çekirdeği küspesi, pamuk kozası, Antep fıstığı kabuğu ve badem yeşil kabuğu gibi tarımsal biyokütle atıklarının uçucu madde ve karbon yanma davranışları içinden doğal konveksiyonla hava geçen ve üzerinde yanmanın gerçekleştiği elek sepet bulunduran bir sabit yatak yakma sisteminde incelendi. Tutuşma zamanı, uçucu madde ve karbon yanma hızları ve süreleri üzerine fırın başlangıç sıcaklığının (550, 600 ve 650°C) etkisi incelendi.

Uçucu madde yanma periyodunda her bir biyokütlenin tutuşma süresinin fırın başlangıç sıcaklığı ile kısaldığı, uçucu madde yanma süresinin düzenli bir değişim göstermediği ve yanma hızı ile yanma süresi arasında ilişki olmadığı belirlendi. Karbon yanma periyodunda ise yanma süresinin fırın başlangıç sıcaklığı ile kısaldığı ve karbon yanma süresi ile yanma hızı arasında ilişki olmadığı görüldü. Sadece biyokütle türünün yanma davranışı üzerinde etkili olduğu sonucuna varıldı.

Anahtar Kelimeler: Biyokütle, Sabit yatak, Yanma

COMBUSTION BEHAVIOR OF BIOMASS IN FIXED BED

ABSTRACT

In this study, the volatile matter and carbon combustion behaviours of a number of domestic and industrial biomass wastes (-8+ 16 mesh particle size), namely hazelnut shell, sunflower seed pulp, boll, pistachio shell and almond husk were investigated in a fixed bed combustion system, along which air flowed by natural convection and incorporated a wire mesh basket on which combustion was taken place. Effect of initial furnace temperature (550, 600 and 650°C) on ignition times, volatiles and carbon combustion rates and times were investigated. It was determined that ignition times of all the biomasses decreased with initial furnace temperature, combustion times didn't show a regular change and there was no relationship between combustion rates and times. In the carbon combustion period, however, it was observed that combustion times decreased with the initial furnace temperature and there was no relationship between combustion rates and times. It was concluded that only kind of biomass have effected notably the combustion behaviour.

Keywords: Biomass, Fixed bed, Combustion

1. GİRİŞ

Küresel ısınmanın bir sonucu olarak ortaya çıkan bölgesel ve küresel iklim değişikliği tehdidi başta CO₂ olmak üzere sera gazı emisyonlarında önemli ölçüde bir azalma gerektirmektedir (Lu vd., 2008). Fosil yakıtların sadece sürdürülebilirliği değil, aynı zamanda yanma ürünleri de sorunludur. Sera gazlarının atmosferde birikmesi nedeniyle ortaya çıkan olumsuzluklar fosil yakıtların yerini alabilecek alternatif enerji kaynakları ile giderilebilir. Bu nedenle, evsel ve endüstriyel fırınlarda kullanılan yakıtların yenilenebilir yakıtlarla değiştirilme olanakları araştırılmaktadır (Panahi ve diğ., 2016). Biyokütle, bol olması, doğal olarak yetişmesi ve hasattan sonra aynı yerde yeniden yetiştirilebilmesi nedeniyle yenilenebilir enerji kaynağı olarak sınıflandırılmaktadır. Biyokütle büyürken atmosferik karbondioksiti tükettiği ve daha sonra yandığında atmosfere geri verdiği için kapalı bir karbon döngüsü yaratır. Biyokütlenin, özellikle atık biyokütlenin termal kullanımı, diğer yenilenebilir enerji kaynaklarıyla birlikte elektrik üretimi için uygun maliyetli, çevreye duyarlı bir seçenek olabilir (McKendry, 2002; Panahi ve diğ., 2016). Biyokütle, odun artıkları, tarımsal artıklar (ekinlerden, gıda işlemeden ve hayvan besiciliğinden), özel enerji mahsulleri ve biyo-tabanlı belediye katı atıkları olarak dört kategoriye ayrılabilir (Yang ve diğ., 2007). Bu artıkların temel biyokütle bileşenleri (selüloz, hemiselüloz ve lignin) yönünden içerikleri değişkendir. Bu bileşenlerin biyokütle yanma davranışı üzerinde belirgin etkileri olduğu bilinmektedir (Lang ve Hurt, 2002; Biagini ve diğ., 2009).

Katı yakıtların piroliz, gazlaştırma ve yakma gibi termo-kimyasal işlemleri artık yaygın olarak kabul gören süreçlerdir. Katı yakıt yakma, herhangi bir ek kimyasal işlem olmaksızın oksijen varlığında gerçekleşen, iyi bir şekilde kurgulanabilen ve oldukça güvenilir bir enerji üretim teknolojisidir. Bir katı yakıtın yanması esas olarak oksidatif piroliz (alevlenme) ve heterojen yükseltgenme olmak üzere iki aşamadan oluşur (Sharma ve diğ., 2015; Varunkumar ve diğ., 2011; Mahapatra ve Dasappa, 2011). Katı fazda yanma (char yanması), reaksiyon hızı yönünden gaz faz reaksiyonundan (alevli yanma) çok daha yavaştır. Katı yakıtların fiziksel ve kimyasal özelliklerine bağlı olarak yanma süreci önemli ölçüde farklılık gösterir. Biyokütlenin reaktivitesi uçucu bileşenlerin hızlı çıkışı nedeni ile düşük ranklı kömürlerden daha yüksektir (Wang ve diğ., 2020; Das ve diğ., 2020). Biyokütle yakıtları, tıpkı düşük ranklı kömürlerin yanma mekanizmalarında olduğu gibi, piroliz ile uçucu madde çıkışı ve yanma sırasını takip eder. Bununla birlikte, kömür ve biyokütlenin yanması arasında bazı önemli farklılıklar vardır. Kömür yoğunlukları tipik olarak düşük ranklı kömürler için 1100 kg/m³ ile yüksek yoğunluklu pirolitik grafit için 2330 kg/m³ arasında değişmektedir. Buna karşılık biyokütle yoğunlukları saman için 100 kg/m³ ile orman odunu için 500 kg/m³ arasında değişmektedir. Biyokütle uçucu madde oranı genellikle %70-80, kömürlerinki ise %10-50 aralığındadır. Biyokütle yakıtlarının ısı değerleri, kömürlerinkinden kayda değer ölçüde daha düşüktür. Yakma uygulamalarında biyokütle ya tek başına (tek kaynak yakıt olarak) ya da birincil yakıtla birlikte (birlikte ateşleme) yakılır. Ayrıca, biyokütle yakıtlarındaki yüksek nem ve kül içeriği

tutuşma ve yanma sorunlarına neden olabilir (Sami ve diğ., 2001).

Günümüzde, enerji talebindeki artış, azalan enerji kaynakları ve fosil yakıtların küresel ölçüde atmosferik kirlenici özellikleri göz önüne alındığında, daha verimli ve minimum çevresel etki sunan yeni teknolojilere ihtiyaç duyulmaktadır. Biyokütle yakıtları bu talebi karşılamada dikkate değer bir potansiyele sahiptir. Bu yakıtların bolluğu, özellikle düşük maliyeti ve temel olarak küresel iklimi etkileyen sera gazı emisyonlarının azaltılmasıyla ilgili önemli çevresel özellikleri nedeniyle gelecekte ısı ve elektrik üretimi için kullanımlarının artacağı beklenmektedir (Vamvuka ve diğ., 2011). Katı biyokütle yakıtlar için başlıca yakma teknolojileri sabit yatak ve akışkan yatak yakma sistemleridir. Sabit yatak yakma sistemleri genellikle düşük maliyet ve çalışma kolaylığı nedeniyle daha küçük ölçekli elektrik üretiminde tercih edilirler.

Biyokütlenin tek başına yanma davranışı ile ilgili pek çok çalışma bulunmaktadır. Kömür ile birlikte ikincil yakıt olarak kullanılması açısından tek başına yanma davranışlarının bilinmesi önemlidir. Biyokütle ile kömürün pelet halinde ve çoklu taneler halinde sabit yatakta yanma davranışının tutuşma süresi, uçucu madde yanma periyodu ve karbon yanma periyodu yönünden ele alındığı çalışmalar sınırlıdır (Duranay ve diğ., 2008; Yilgin ve diğ., 2021). Bundan dolayı, laboratuvar ölçekli bir sabit yatak yakma sisteminde farklı biyokütle türlerinin yanma davranışlarının incelenmesi bu çalışmanın amacını oluşturmaktadır.

2. MATERYAL VE YÖNTEM

2.1. Örneklerin Hazırlanması ve Proximate (Kısa) Analiz

Çalışmada, Antep fıstığı kabuğu (AFK), fındık kabuğu (FK), badem yeşil kabuğu (BYK), pamuk kozası (PK) ve ay çekirdeği küspesi (AÇK) olmak üzere beş biyokütlenin yanma davranışı incelendi. Örnekler havanda küçük parçalar haline getirilip elendikten sonra-100 mesh büyüklüğündeki kısım proximate analizlerde (nem, uçucu madde ve kül), -8+16 mesh büyüklüğündeki kısım ise yakma deneylerinde kullanıldı.

Örneklerin nem oranı Mettler LJ 16 nem tayin cihazı ile belirlendi. Uçucu madde ve kül içerikleri ASTM D standartlarına göre, sabit karbon miktarı ise farktan belirlendi.

2.2. Yakma deneyleri

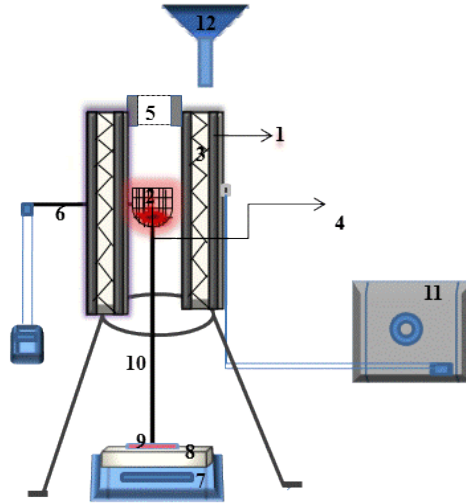
Biyokütle örnekleri Şekil 1’de görülen sabit yatak yakma sisteminde yakıldı. Yakma sistemi 105 mm dış çaplı, 42 mm iç çaplı ve 120 mm yüksekliğinde, içinde direnç telleri taşıyan refrakter tuğla döşenmiş silindirik kesitli dikey bir kamaradır. Fırın üzerine ısı kaybını önlemek amacıyla 20 mm yüksekliğinde ortası delik bir refrakter kapak yerleştirildi. Paslanmaz çelikten yapılmış 30 mm çaplı bir elek sepet 250 mm uzunluğundaki çelik cubuğun ucuna takılmış ve altta bir destek üzerine sabitlenmiş şekilde kamara içerisine yerleştirilmiştir. Sepet sistemini taşıyan destek yanma sırasındaki kütle değişimlerinin kaydedilmesi amacı ile hassas bir terazi ($\pm 0,001$ g) üzerine yerleştirildi. Fırın değişik voltaj transformatörü yardımı ile çalışma sıcaklığına ısıtıldı. Fırın başlangıç

sıcaklığı elek sepet yakınına yerleştirilen termoçift ile kontrol edildi.

Belirli bir yakma deneyinde, ön ısıtılmış fırın içerisindeki sepet üzerine yoğunluklarına bağlı olarak 0,600-1.000 g biyokütle besleme hunisi yardımıyla boşaltıldığı anda kronometre çalıştırıldı. Tanelerin uçucu madde yanması sırasındaki tutuşma yani alev görünme anı ve alev sönme zamanı ayna yardımı ile kaydedildi. Bu süreler arasındaki fark uçucu madde yanma süresidir. Alev söndükten sonraki karbon yanma periyodunda ise akkor halinde yanmaya devam eden tanelerin kararına zamanı kaydedildi. Karbon yanma süresi, bu zaman ile alevin söndüğü zaman arasındaki süreyi belirtmektedir. Örneklerin uçucu madde yanma hızı ile karbon yanma hızlarının belirlenmesi amacı ile yanma sırasında her 5 saniyede bir kütle değişimi kaydedildi. Örneklerin yanma davranışları 500, 550 ve 600°C'lik fırın başlangıç sıcaklıklarında incelendi. Yanma hız verileri her bir örneğin belirtilen sıcaklıklarda en az iki defa yakılması ile elde edildi.

Uçucu madde ve karbon yanma hızları, yanma sırasında kaydedilen kütle değişimi eğrilerinin ortalama eğimleri ve başlangıç miktarları dikkate alınarak (1) denklemi ile hesaplandı. Burada W_0 örneğin uçucu madde veya sabit karbon miktarını temsil etmektedir (Yilgin ve Pehlivan, 2009).

$$R = \left(\frac{1}{W_0} \right) \left(\frac{dW}{dt} \right) \quad (1)$$



Şekil 1. Deneysel sabit yatak yakma sistemi: 1. Refrakter tuğla; 2. Sepet; 3. Direnç teli; 4. Biyokütle; 5. Fırın kapağı; 6. Termoçift; 7. Terazi; 8. Destek; 9. Ayna; 10. Sepet çubuğu; 11. Gerilim değiştirici; 12. Besleme hunisi

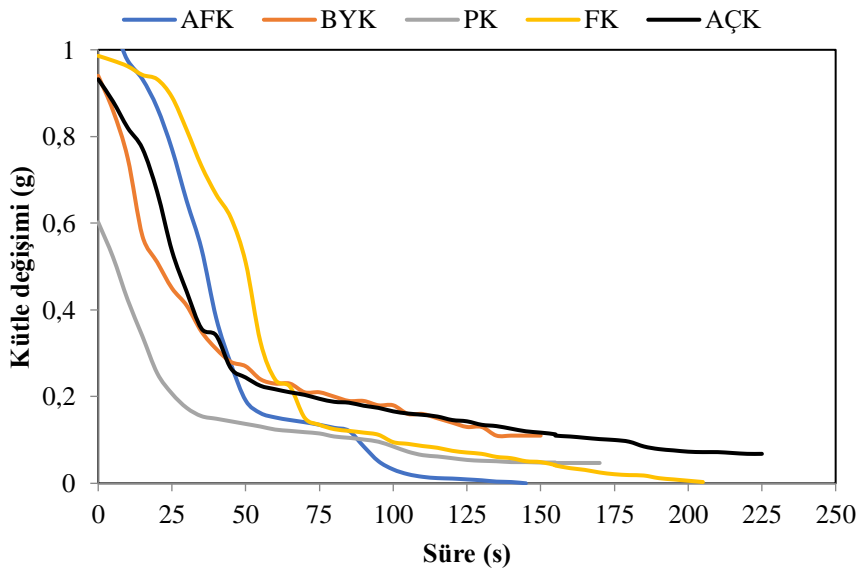
3. SONUÇLAR VE TARTIŞMA

Antep fıstığı kabuğu (AFK), fındık kabuğu (FK), badem yeşil kabuğu (BYK), pamuk kozası (PK) ve ay çekirdeği küspesinin (AÇK) proximate analiz sonuçları Tablo 1'de verilmiştir. Biyokütle örneklerinin kül içerikleri %1-11 arasında sabit karbon içerikleri %15-26 arasında değişmektedir. Biyokütle için külün kaynağını oluşturan inorganik maddelerin yumuşak odunda %1'den az, sert odun ve tarımsal atıklarda ise %15'e kadar değiştiği bildirilmektedir (Yaman, 2004).

Biyokütle örneklerinin 500°C fırın başlangıç sıcaklığı için kütlelerinin zamanla değişimi Şekil 2' de görülmektedir. Şekildeki eğrilerde örneklerin yanması sırasında uçucu madde ve karbon yanma periyodu olmak iki üzere farklı yanma bölgesi bulunmaktadır.

Tablo 1. Biyokütle örneklerinin Proximate analiz sonuçları (%kütle) (*: Farktan belirlendi.)

Örnek	Nem	Uçucu madde	Kül	Sabit karbon*
FK	6,2	69,4	1,0	23,4
AFK	3,4	77,2	2,5	16,9
AÇK	4,3	71,5	5,9	18,3
BYK	5,3	67,7	10,9	16,1
PK	6,0	74,2	4,0	15,8



Şekil 2. Örneklerin 500°C'deki yanma sırasında kütle değişimi

Biyokütle örneklerinin 500, 550 ve 600°C fırın başlangıç sıcaklıklarında uçucu madde yanma periyoduna ait tutuşma zamanı, uçucu madde yanma süresi ve uçucu madde yanma hızları Tablo 2'de verilmiştir. Tabloda BYK örneğinin 500°C ve 550°C fırın başlangıç sıcaklıklarında tutuşmadığı gözlemlendi. Bunun nedeni bu sıcaklıklarda BYK tanelerinin ısınması ve bozunması sonucu ortaya çıkan yanıcı uçucu maddelerin tane çevresinde yeterli bir konsantrasyona ulaşmamasıdır. Bu sıcaklıklarda tutuşma süreleri belirlenen diğer örneklerin ise alevlerinin zayıf olduğu gözlemlendi. Örneğin Tablo 1'de FK ve AÇK'nin uçucu madde miktarları biri birine yakın olmasına rağmen tutuşma süreleri ve uçucu madde yanma süreleri farklıdır. Bu durum biyokütle nemi, temel biyopolimer bileşenleri ve fiziksel yapısından kaynaklanabilir. Literatürde fındık kabuğunun holoselüloz içeriğinin %56,6 lignin içeriğinin %40 ve ay çekirdeği kabuğunun holoselüloz içeriğinin %67,1 ve lignin içeriğinin ise %27,1 olduğu belirtilmiştir (Bilgic ve diğ., 2016). Bu durum ay çekirdeği küspesinde hemiselüloz ve selüloz içeriklerinin yüksek olması nedeniyle düşük yakma sıcaklığında

bu bileşenlerin parçalanma sıcaklıklarına hızlı bir şekilde ulaşması ve uçucu bileşenlerin taneden hızla salınmasıyla yeterli konsantrasyona geldiğini göstermektedir. Biyokütle 300°C'nin altında parçalanabilen bir yakıttır. Biyokütle başlıca hemiselüloz, selüloz ve ligninden oluşmaktadır. Odunun yapısını oluşturan hemiselülozun 225-325°C, selülozun 305-375°C ve ligninin ise 250-500°C sıcaklık aralığında parçalandığı bildirilmektedir (Prins ve ark., 2006). BYK 'nın 500 ve 550°C fırın başlangıç sıcaklıklarında tutuşmaması bu bileşenlerin daha düşük olmasından kaynaklanabilir. Bu sıcaklık aralıklarından ligninin parçalanma sıcaklık aralığının hemiselüloz ve selüloza göre daha geniş olduğu görülmektedir. Uçucu madde yanma süresinin biyokütleyle bağlı olarak değiştiği, FK ve AFK örneklerinde 550°C 'de arttığı 600°C 'de ise azaldığı tablodan görülmektedir. Bu durum örneklerdeki uçucu bileşenlerin 550°C 'de yapıdan tamamen uzaklaştığını gösterebilir. Fırın başlangıç sıcaklığının 600°C olduğu yakma sıcaklığında tutuşma ve uçucu madde yanma sürelerinin belirgin olarak kısılması bunu doğrulamaktadır. Yanma sırasında kaydedilen kütle değişim eğrilerinin eğimi ve 1 nolu denklemden hesaplanan hız değerlerinin uçucu madde yanma süresi ile ilişkili olmadığı görülmektedir. Bu durum alev görülmeden önce tanelerden uçucu madde çıkışı olduğunu göstermektedir (Yilgin, 2009).

Tablo 2. Biyokütle örneklerinin uçucu madde yanma süreleri ve uçucu madde yanma hızları

Örnek	Sıcaklık (°C)	Tutuşma zamanı (s)	Uçucu madde yanma süresi (s)	Uçucu madde yanma hızı (s ⁻¹).10 ²
FK	500	48	17	1,7
AFK		27	33	2,0
AÇK		35	19	1,8
BYK		-	-	-
PK		14	16	3,4
FK	550	17	47	1,7
AFK		19	45	1,8
AÇK		29	21	2,1
BYK		-	-	-
PK		11	16	2,8
FK	600	8	25	2,4
AFK		10	21	1,6
AÇK		7	29	1,8
BYK		19	8	1,7
PK		5	6	5,2

Tablo 3. Biyokütle örneklerinin karbon yanma hızları ve süreleri (*: BYK örneğinin toplam yanma sürelerini göstermektedir.)

Örnek	Sıcaklık (°C)	Karbon yanma süresi (s)	Karbon yanma hızı (s ⁻¹).10 ³
FK	500	328	4,2
AFK		301	5,9
AÇK		171	5,6
BYK		326*	-
PK		157	9,9
FK	600	282	3,9
AFK		291	5,6

AÇKÜ	550	228	4,9
BYK		307*	-
PK		133	10,2
FK		235	6,8
AFK		202	10,5
AÇK	600	166	6,9
BYK		236	11,9
PK		74	15,4

Biyokütle örneklerinin 500, 550 ve 600°C fırın başlangıç sıcaklıklarında karbon yanma periyoduna ait yanma hızları ve süreleri Tablo 3'de verilmektedir. FK' nın karbon yanma süresi diğer örneklerden daha yüksektir. Bu durum, Tablo 1'de görüldüğü gibi, sabit karbon içeriğinin diğer örneklerden yüksek olmasından kaynaklanmaktadır. Örneklerin karbon yanma süreleri yakma sıcaklığı ile beklenildiği gibi kısalmıştır. Biyokütleyle bağlı olarak karbon yanma süresi arasında belirgin bir değişim gözlenemediği bunun da örneklerin karbon içeriklerinin yakın olmasından kaynaklandığı söylenebilir. Tablodan uçucu maddenin taneleri tamamen terk etmediği durumda karbon yanma hızlarında artış olduğu ve karbon yanma periyodunda geride kalan uçucu bileşenlerin salımının yanma hızını etkilediği söylenebilir. Burada yanma süresi ile yanma hızları arasında bir ilişki görülmemektedir.

SONUÇLAR

Biyokütlenin sabit yatakta yanması üzerine biyokütle çeşidinin ve sıcaklığın etkisinin incelendiği çalışmada aşağıdaki sonuçlara varıldı:

- Biyokütlenin yapısı ve temel bileşenleri tutuşma süresi üzerinde etkilidir.
- Biyokütlelerin karmaşık biyopolimer yapısı uçucu madde yanma hızları ile sürelerinin ilişkilendirilmesini engellemektedir.
- Karbon yanma süresi sıcaklık ile azalmakta ancak, yanma hızı ile süresi arasında bir ilişki bulunmamaktadır.
- Karbon yanma periyodunda uçucu bileşenlerin varlığının karbon yanma hızı üzerinde etkilidir.

KAYNAKLAR

- Biagini, E., Simone, M., Tognotti, L. (2009). Characterization of High Heating Rate Chars of Biomass Fuels. Proceedings of the Combustion Institute, 32 (2009), 2043-2050.
- Bilgic, E., Yaman, S., Haykiri-Acma, H., Kucukbayrak, S. (2016). Is torrefaction of polysaccharides-rich biomass equivalent to carbonization of lignin-rich biomass?. *Bioresource Technology*, 200, 201-207.
- Das, S., Sarkar, P.K., Mahapatra, S. (2021). Single Particle Combustion Studies of Coal/Biomass Fuel Mixtures. *Energy*, 217, 119329.
- Duranay, N., Yilgin, M., Pehlivan, D. (2008). Co-combustion of Pellets from Soma Lignite and Waste Dusts of Furniture Works. *International Journal of Green Energy* 5 (6), 456-465.
- Lang, T., Hurt, R.T. (2002). Char Combustion Reactivities for a Suite of Diverse Solid Fuels and Char-forming Organic Model Compounds. Proceedings of the Combustion Institute, 29, 423-431.
- Lu, H., Robert, W., Peirce, G., Ripa, B., Baxter, L.L. (2008). Comprehensive Study of Biomass Particle Combustion. *Energy & Fuels*,

22, 2826-2839.

- Mahapatra, S., Dasappa, S. (2014). Influence of Surface Area to volume Ratio of Fuel Particles on Gasification Process in a Fixed Bed. *Energy for Sustainable Development*, 19,122-129.
- McKendry, P. (2002). Energy Production from Biomass (part 1): Overview of Biomass. *Bioresource technology*, 83, 37-46.
- Panahi , A., Levendis , Y.A., Vorobiev, N., Schiemann, M. (2017). Direct observations on the combustion characteristics of Miscanthus and Beechwood biomass including fusion and spheroidization. *Fuel Processing Technology*, 166,41-49.
- Prins, M.J., Ptasinski, K.J., and Janssen, F.J.J.G., (2006). Torrefaction of Wood Part 1. Weight Loss Kinetics. *Journal of Analytical and Applied Pyrolysis* , 77, 28-34.
- Sami, M., Annamalai, K., Wooldridge, M. (2001). Co-firing of coal and biomass fuel blends. *Progress in Energy and Combustion Science*, 27, 171-214.
- Sharma, M., Attanoor, S., Dasappa, S. (2015). Investigation into Co-gasifying Indian Coal and Biomass in a Down draft Gasifier – Experiments and Analysis. *Fuel Processing Technology*, 138, 435-444.
- Vamvuka, D., Sfakiotakis, S., Mourouzidis, T., Bandelis, G. (2011). Development of a Biomass-Fired Combustion Unit for Residential Heating *Combustion Science and Technology*, 183, 764–778.
- Varunkumar, S., Rajan, N.K.S., Mukunda, H.S. (2011). Single Particle and packed bed Combustion in Modern Gasifier Stoves- Density Effects. *Combustion Science and Technology*, 183, 1147-1163.
- Wang, M., Shen, Y., Guo, P. Konga, J., Wu, Y., Chang, L., Wanga, J. Xie, W. (2020). A Comparative Study on the Intrinsic Reactivity and Structural Evolution During Gasification of Chars from Biomass and Different Rank Coals. *Journal of Analytical and Applied Pyrolysis*, 149,104859.
- Yaman, S. (2004). Pyrolysis of biomass to produce fuels and chemical feedstocks. *Energy Conversion and Management*, 45, 651–671.
- Yang, Y.B., Sharifi, V.N., Swithenbank, J., Ma, L., Darvell, L.I., Jones, J.M., Pourkashanian, M., Williams, A. (2007). Combustion of a Single Particle of Biomass. *Energy & Fuel*, 22, 306-316.
- Yilgin, M., Pehlivan, D. (2009). Volatiles and char combustion rates of demineralised lignite and wood blends. *Applied Energy*, 86, 1179-1186.
- Yilgin, M., Yildirim, S., Pehlivan, D. (2021). Combustion of Hazelnut Shell-Lignite Blends in Poly-particulate Beds. *Biomass Conversion and Biorefinery*, Basımda.

TWO FACTOR ANALYSIS OF MOSQUITOES' GENERA AROUND POLAC ENVIRONMENT

Dr. Olubunmi T. OLORUNPOMI

Nigeria Police Academy, Faculty of Science, Department of Computer Science and Mathematics, Wudil Kano State, Nigeria.

ORCHID ID: 0000-0002-4886-7880

Dr. Rabi S. DUWA

Nigeria Police Academy, Faculty of Science, Department of Biological Sciences, Nigeria Police Academy, Wudil, Kano, Nigeria

ORCHID ID: 0000-0001-5886-7537

ABSTRACT

The survey of adult mosquitoes in four selected sites in Nigeria Police Academy (Polac), Wudil, Kano, Nigeria in September, 2019 was subjected to a two-factor analysis model in order to test for significance differences among sample means. A total of one thousand and sixty (1060) mosquitoes comprising of 3 genera; Anopheles, Aedes and Culex were identified in the girls' hostel, girls' hostel staircase, quarter guard, and clinics. Anopheles mosquitoes was higher in terms of abundance with a total number of 632 samples, about 36.79% followed by Culex mosquitoes with a total number of 223 samples, about 21.04% and Aedes mosquitoes with a total number of 214 samples, about 20.19%. Also, 170 of the mosquitoes were males; about 16.04% and 890 of the mosquitoes were females; about 83.96%. The population of mosquitoes in girls' hostel was 228, about 21.51%; the staircase of the girls' hostel is 454, about 42.83%; the quarter guard 340, about 32.08%; and the clinic is 38, about 3.58%; thus, abundance of mosquitoes is prevalent in the staircase of the girls' hostel followed by the girls' hostel, quarter guard and the clinic. The interaction plot publicized that the differences between levels of one factor for Aedes will depend on the level of the other factors of Anopheles and Culex mosquitoes. Fishers' significant difference test disclosed that the mean of observation of the staircase is significantly different from the mean of observation of the clinics and girls' hostel; but, not significantly different from the means of the observation of the quarter guard. The Tukey's honestly significant difference test showed that no significant differences were observed between site surveyed sample means of girls' hostel and clinic, quarter guard and girls' hostel, girls' hotel staircase and girls' hostel as well as girls' hotel staircase and quarter guard; but significant differences transpired between site surveyed sample means of quarter guard and clinic, girls' hotel staircase and clinic. Also; significant differences transpired between sample means of Anopheles and Aedes. Mosquito nips cause a considerable health risk to the cadets, with mosquito-borne diseases causing millions of deaths a year global; as such, disincentive procedures to keep them at anchorage are indispensable.

Keywords: Disease, Polac Environment, Human health, Infections, Mosquitoes-Genera, Two-Factor Model

INTRODUCTION

Mosquitoes are the most important vectors of public health due to their roles in the transmission of diseases such as Malaria, Lymphatic filariasis and others. Apart from their role in the transmission of diseases, the sound they make to announce their presence is also annoying. Different species of this insect have been identified as

the vector transmitting these diseases. The females of most species have piercing and sucking mouth parts for sucking blood. Malaria is a life-threatening disease caused and spread by *Plasmodium* parasite and female mosquito vectors, respectively with 92% of malaria cases and 93% of malaria deaths occurring in the African region (WHO, 2018). According to WHO, 2015 the transmission of diseases by mosquitoes is more intense in places where the mosquito life span is longer (so that the parasite has time to complete its development inside the mosquito) and where it prefers to bite humans rather than animals. According to WHO, 2019 World Malaria Report, Nigeria had the highest number of global malaria cases (25 % of global malaria cases) in 2018 and accounted for the highest number of deaths (24 % of global malaria deaths). The mature female anopheles mosquito needs a blood meal for its reproduction.

Two-way analysis of variance enables us to look at the individual and joint effects of two independent variables on one dependent variable; thus, it tells us about the main effect and the interaction effect. Regularly, ANOVA is used to test equality among several means by comparing variance among groups relative to variance within groups (random error). Moreover, the design affords natural replications that result from overlapped factors. Tests of main effects are tests of one factor averaged over levels of the other factors (Bland & Altman, 1996c; Fisher, 1925; Fujikoshi, 1993). Absence of interaction between two factors implies that the additive effect of one factor is identical across all levels of the other factor. In that situation, tests and interpretation of main factors are straightforward. If interactions exist, one must interpret main effects carefully, because relations among mean levels of one factor differ according to levels of the second factor (Fisher, 1925; Kleinbaum, et al., 1988; Winer et al., 1991; Fujikoshi, 1993; Bland & Altman, 1995c; Zar, 1999; Gelman, 2005; Sit, 2007; Kass, 2011).

MATERIALS AND METHODS

Study Area and Sites

Nigeria Police Academy, Wudil Kano, Nigeria lies on latitude 11°49`N and longitude 8°51` E and falls within the semi-arid Sudan savannah zone of West Africa about 840 kilometers from the edge of the Sahara Desert as shown in figure 1. Kano has a mean height of about 472.45m above sea level. The temperature of Kano usually ranges between a maximum of 33°C and a minimum of 15.8°C although sometimes during the harmattan, it falls down to as low as 10°C. Kano has two seasonal periods, which consist of four to five months of wet season and a long dry season lasting from October to May. The rainfall in this area ranges between 1016mm and 1524mm with a relative humidity between 60% and 80%. The guinea savannah is divided into two vegetation zone; the northern and southern guinea savannah. The temperature of this area is highly influenced by the Niger Benue trough where heat is trapped.



Figure 1: Map of Nigeria Police Academy Wudil Kano, Nigeria

Study Design

The study was carried out in four selected sites in some parts of the Nigeria Police Academy, Wudil Kano, Nigeria. These sites are Girls' hostel, staircase, Quarter guard (a building used mainly for the detention of offenders in the Academy premises), and the clinic.

Sample Collection

In the month of September, 2019 mosquitoes were collected indoors between 05:30pm and 06:00am using the pyrethrum-base aerosol spray (Raid). Mosquitoes were collected on white clothes spread on the floors of the four (4) selected sites: Girls hostel, staircase, quarter guard, and clinic. All knocked down mosquitoes were collected into sample bottles and taken to the laboratory for morphological identification as described by (Amusan, et al., 2007; Gillies & Coetzee, 1987).

Mosquitoes were picked with forceps, dropped on a clean slide and then observed under a light microscope with $\times 40$ objectives. Features such as size of antennae, color and size of the maxillary palps, length of proboscis, colour and shape of abdomen, colour and length of legs, colour of wings etc., were observed and compared. Individual mosquitoes were identified into species level, counted and recorded.

Statistical Analysis Technique

The dataset comprises of three insects (mosquito); Anopheles, Culex, and Aedes being surveyed at different sites (Girls Hostel, Girl's hostel staircase, Quarter Guard, and Clinic) of Nigeria Police Academy, Wudil, Kano State. The insects have male and female as interaction.

A two-way ANOVA test analyzes the effect of the independent variables on the expected outcome along with their relationship to the outcome itself (Yates, 1934; Kass, 2011). All these variables are varying independently and normally around a mean. Let Y_{ijk} denote the response random variable in k-th measure for treatment (i,j); $k = 1, \dots, n_{ij}$, $i = 1, \dots, I$ indexes the levels of the first factor, and $j = 1, \dots, J$ indexes the levels of the second

factor, then:

$$Y_{ijk} = \mu_{ij} + \varepsilon_{ij} \quad (1)$$

Besides the variation explained by the factors, there remains some amount of unexplained variation ε_{ijk} , random error. The mean of the response variable is modeled as a linear combination of the explanatory variables (Gelman, 2005; Gelman and Hill, 2006):

$$\mu_{ij} = \mu + \alpha_i + \beta_j + v_{ij} \quad (2)$$

where μ is the population group means, α_i is the additive main effect of level i from the first factor (i -th row in the contingency table), β_j is the additive main effect of level j from the second factor (j -th column in the contingency table) and v_{ij} is the non-additive interaction effect of treatment (i,j) from both factors (cell at row i and column j in the contingency table) (Fujikoshi, 1993).

A two-way ANOVA partitions the total sum of squares into within sum of squares and between sum of squares. Carrying out hypothesis test on an appropriate test statistic requires the assumption of normality for the ANOVA model that is; $Y_{ijk} \sim N(\mu_{ij}, \sigma^2)$ (homoscedasticity) or equivalently $\varepsilon_{ijk} \sim N(0, \sigma^2)$ and the homogeneity of variance among groups being compared is expected to be similar across all groups. If one of these assumptions is not met, we might need to transform the data using a logarithmic or exponential transformation to reduce the variability in the data, or you may be able to use a non-parametric alternative.

The mean corresponds to mosquitoes (Anopheles, Culex, Aedes) by gender groups (female, male) that are defined by the combination of the two independent variables surveyed at girls hostel, girls' hostel staircase, quarter guard, and clinics has the following hypotheses adopted at 0.05 level of significance. The dataset was analyzed using R programming language.

Hypothesis (I): Main effect insects

H_0 : insect group means are all equal versus

H_A : at least one insect group mean is different from the others

Hypothesis (II): Main effect of site surveyed

H_0 : surveyed site group means are all equal versus

H_A : at least one surveyed site group mean is different from the others

RESULTS AND DISCUSSION

Descriptive statistics of table 1 revealed that, a total of one thousand and sixty (1060) mosquitoes comprising of 3 genera; Anopheles, Aedes and Culex were identified during the month of September, 2019 in the girls' hostel, girls' hostel staircase, quarter guard, and clinics. The population of mosquitoes in girls' hostel is 228, about 21.51%; the staircase of the girls' hostel is 454, about 42.83%; the quarter guard 340, about 32.08%; and the clinic is 38, about 3.58%; thus, abundance of mosquitoes is prevalent in the staircase of the girls' hostel followed by the girls' hostel, quarter guard and the clinic. Also, Anopheles mosquitoes was higher in terms of abundance with a total number of 632 samples, about 36.79% followed by Culex mosquitoes with a total number of 223 samples, about 21.04% and Aedes mosquitoes with a total number of 214 samples, about 20.19%. More so, 170 of the mosquitoes were males, about 16.04% and 890 of the mosquitoes were females, about 83.96% in Nigeria Police Academy.

Table 1: Descriptive Statistics

Sites surveyed	Anopheles		Culex		Aedes		Total(mean)
	Male	Female	Male	Female	Male	Female	
Girls' hostel	15	182	4	22	1	4	228
Staircase	45	111	28	74	39	157	454
Quarter guard	17	223	14	74	2	10	340
Clinic	4	26	1	6	0	1	38
Total (mean)	81	542	47	176	42	172	1060

The F test on table 2 for the main effect of insect with p -value=0.163 indicates that the insects group means are all equal. Also, the F test for the main effect of the sites surveyed with p -value=0.237 indicates that surveyed site group means are all equal.

Table 2: Analysis of Variance for the month of September (original data)

Response data	df	SS	MS	F-value	Pr(>F)
insect	2	13640	6820	2.012	0.163
Sites_surveyed	3	15707	5236	1.545	0.237
residuals	18	61002	3389		

To validate the inferences made for the ANOVA in table 2, we need to check for normality and homogeneity of variances assumptions of its residuals.

Normality Assumption of the Dataset

It can be seen in figures 2 below that the residuals of the original data are not distributed symmetrically around the centre of all scores.

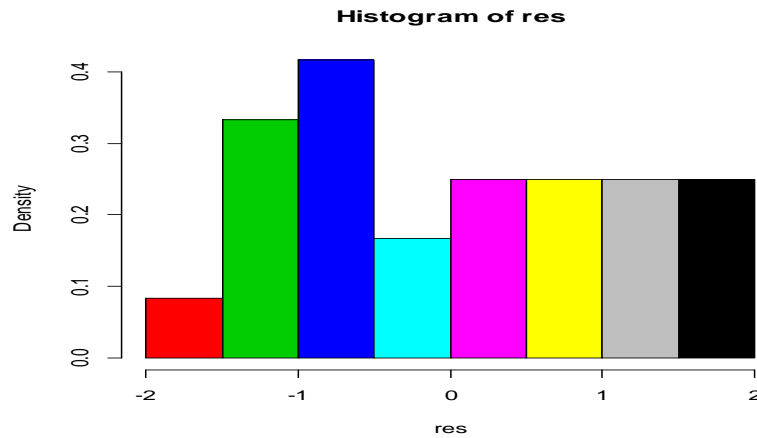


Figure 2: Histogram of the original data

It can be seen from the plot of sample quantiles in figure 3 that the datasets are not normally distributed since the points seem to deviate markedly away from the straight line with outliers' points at the ends of the line, distanced from the bulk of the observations.

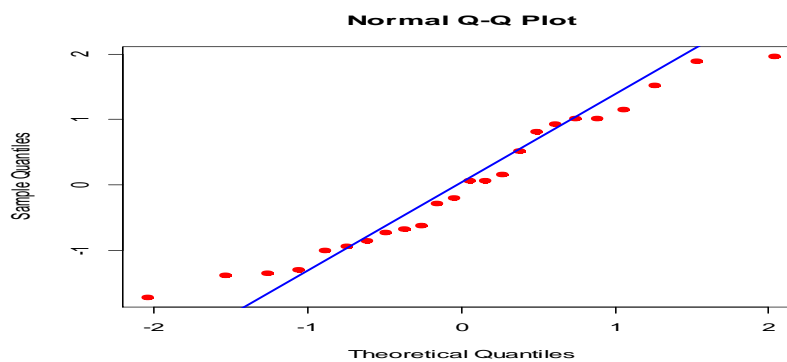


Figure 3: Quantile to quantile plot

Table 3: Normality test for the month of September (original data)

Tests	Statistics	P-value
Shapiro-Wilk	0.8746	0.00649
Jarque-Bera	14.2451	0.0008067

Shapiro-Wilk and Jarque-Bera tests revealed that the residuals of the model are not normally distributed with p-values of 0.00649 and 0.0008067 less than significance level, 0.05.

Homogeneity of Variances Assumption

The results of table 4 revealed that variances are not equal across groups or samples, since the p-value of 0.00265 is less than significance level, 0.05.

Table 4: Homogeneity of Variances test for the month of September (original data)

K-squared	df	p-value
14.1959	3	0.00265

The residual of the original data did not satisfy the assumptions of normality and homogeneity of variance; so, the inferences made from table 2 are not valid. We have to transform the data using a logarithmic transformation. The F test on table 5 for the main effect of insect with p-value=0.00946 indicates that the insects group means are all not equal. Also, the F test for the main effect of the sites surveyed with p-value=0.00195 indicates that surveyed site group means are all not equal, that is, they are different from the others.

Table 5: Analysis of Variance for the month of September (transformed data)

Response data	df	SS	MS	F-value	Pr(>F)
insect	2	16.44	8.218	6.105	0.00946
Sites_surveyed	3	29.96	9.986	7.418	0.00195
residuals	18	24.23	1.346		

To validate the inferences made for the ANOVA in table 5, we check for normality and homogeneity of variances assumptions of its residuals as done previously. The null-hypothesis that the population residuals are normally distributed in table 6 cannot be rejected for Shapiro-Wilk and Jarque-Bera tests with p-values of 0.1764 and 0.518 greater than significance level, 0.05.

Table 6: Normality test for the month of September (transformed data)

Tests	Statistics	P-value
Shapiro-Wilk	0.9415	0.1764
Jarque-Bera	1.3156	0.518

The results of table 7 revealed that variances are equal across groups or across samples, since the p-value of 0.2301 is greater than significance level of 0.05. Thus, after the transformation of the data the basic assumptions of ANOVA were satisfied. Hence, the inferences made about table 5 are valid and we conclude that insect group means and the surveyed site group means are all not equal, that is, they are different from the others.

Table 7: Homogeneity of Variances test for the month of September (transformed data)

K-squared	df	p-value
4.3074	3	0.2301

The design plot of figure 4 showed that Aedes mosquitos' has a low mean of yields; Culex mosquitos' mean of yields is slightly below the overall mean, while Anopheles mosquitos' mean of yields is above the overall mean of the samples. Thus, Anopheles mosquito is more in Polac for the month of September. Furthermore, the staircase and quarter guard have the highest mean of yields for mosquitoes, while the girls hostel's and the

clinics' mean of yields fall below overall mean of the sample. Thus, the staircase and quarter guard are breeding places for mosquitoes in Polac for the month of September.

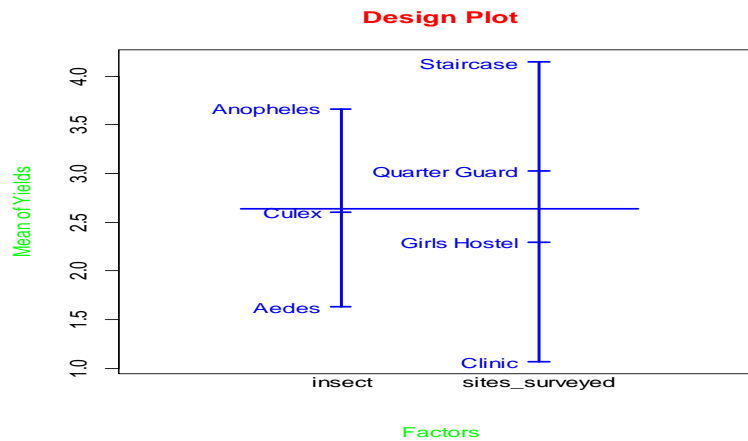


Figure 4: Design plot for mean of yields against the factors

The line that connects the means of data in figure 5 for Culex and Anopheles are quite parallel; thus, the interaction effects are very small compared to main effects or they are only apparent in a small number of treatments; so, they are probably unimportant. Also, the mean of data for Aedes crisscross the mean of data for Anopheles and Culex; thus, the differences between levels of one factor for Aedes will depend on the level of the other factors of Anopheles and Culex mosquitoes.

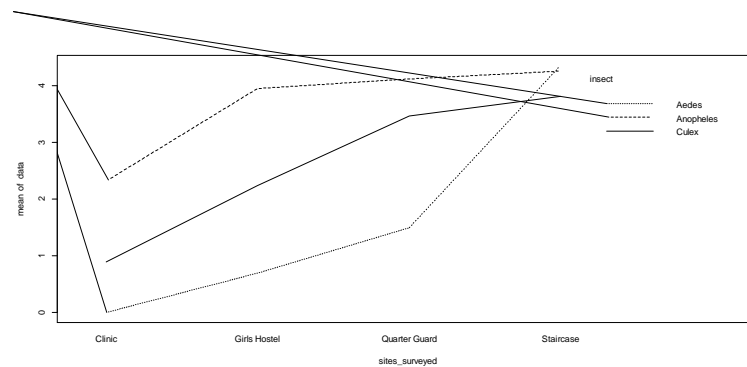


Figure 5: Interaction plot for mean of data against site surveyed

In figure 6 below, the interaction plots' lines for staircase, quarter guard, girls hostel and clinic are close to parallel; thus, the interaction effects will be very small compared to main effects or only apparent in a small number of treatments; so, they are probably unimportant.

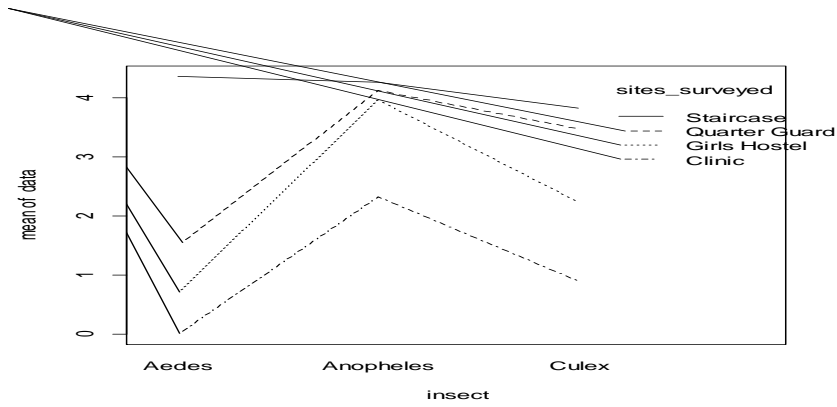


Figure 6: Interaction plot for mean of data against the insects

It can be seen from table 8 that, the mean of observation of the girls’ hostel is not significantly different from the mean of observation of the clinics. Also, the mean of observation of quarter guard is significantly different from the mean of observation of the clinic; but, insignificantly different from the mean of the observation of the girls’ hostel. More so, the mean of observation of the staircase is significantly different from the mean of observation of the clinics and girls’ hostel; but, not significantly different from the means of the observation of the quarter guard.

Table 8: Fisher’s Least Significant Different (LSD) Test

	Clinic	Girls Hostel	Quarter Guard
Girls Hostel	0.1529	-----	-----
Quarter Guard	0.0275	0.3833	-----
Staircase	0.0013	0.0361	0.1905

Tukey's honestly significant difference (HSD) test is used to test differences among sample means for significance. It tests all pairwise differences while controlling the probability of making one or more Type I errors; i.e., the probability of rejecting the null hypothesis (no significance difference) given that the null hypothesis is true. This post-hoc analysis will provide greater insight into the differences or similarities between specific groups. In figure 7; the between groups of all insects sample means’ plots for Culex and Aedes as well as Culex and Anopheles crossed the boundary line to the left; thus, no significant differences between groups of their sample means. But, significant differences transpired between sample means of Anopheles and Aedes.



Figure 7: Tukey HSD confidence interval plot of insects

In figure 8 below, the plots of the 95% confidence interval for the differences in the sample means of site surveyed. It can be seen that the girls' hostel and clinic, as well as the girls' hostel staircase and quarter guard crossed the boundary line to the left, while the remaining site surveyed did not cross the boundary line and remained at the right side. Thus, no significant differences were observed between site surveyed sample means of girls' hostel and clinic, quarter guard and girls' hostel, girls' hotel staircase and girls' hostel as well as girls' hotel staircase and quarter guard. Succinctly, significant differences between site surveyed sample means of quarter guard and clinic, girls' hotel staircase and clinic were detected.

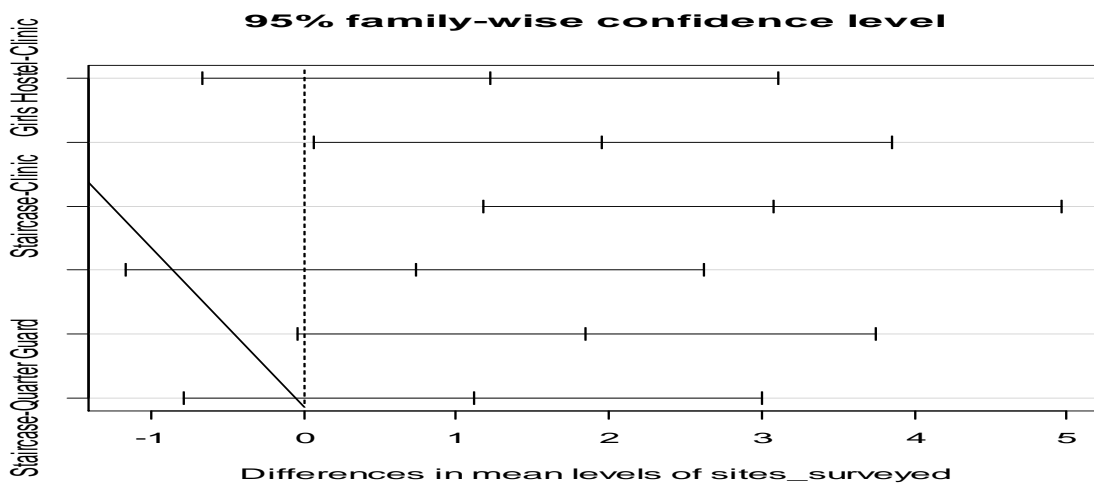


Figure 8: Tukey HSD confidence interval plot of sites surveyed

CONCLUSION

The survey of adult mosquitoes in four selected sites in Nigeria Police Academy (Polac), Wudil, Kano, Nigeria in September, 2019 was subjected to a two-factor analysis model in order to test for significance differences among sample means. A total of one thousand and sixty (1060) mosquitoes comprising of 3 genera; Anopheles,

Aedes and Culex were identified in the girls' hostel, girls' hostel staircase, quarter guard, and clinics. Anopheles mosquitoes was higher in terms of abundance with a total number of 632 samples, about 36.79% followed by Culex mosquitoes with a total number of 223 samples, about 21.04% and Aedes mosquitoes with a total number of 214 samples, about 20.19%. Also, 170 of the mosquitoes were males; about 16.04% and 890 of the mosquitoes were females; about 83.96%. The population of mosquitoes in girls' hostel was 228, about 21.51%; the staircase of the girls' hostel is 454, about 42.83%; the quarter guard 340, about 32.08%; and the clinic is 38, about 3.58%; thus, abundance of mosquitoes is prevalent in the staircase of the girls' hostel followed by the girls' hostel, quarter guard and the clinic. The interaction plot publicized that the differences between levels of one factor for Aedes will depend on the level of the other factors of Anopheles and Culex mosquitoes. Fishers' significant difference test disclosed that the mean of observation of the staircase is significantly different from the mean of observation of the clinics and girls' hostel; but, not significantly different from the means of the observation of the quarter guard. The Tukey's honestly significant difference test showed that no significant differences were observed between site surveyed sample means of girls' hostel and clinic, quarter guard and girls' hostel, girls' hotel staircase and girls' hostel as well as girls' hotel staircase and quarter guard; but significant differences transpired between site surveyed sample means of quarter guard and clinic, girls' hotel staircase and clinic. Also; significant differences transpired between sample means of Anopheles and Aedes. Mosquitoes transfer diseases that afflict human health, and communicate quite a few illnesses and parasites; as such, operative mosquito control tools that they can use without posing unreasonable risk to human health and the environment are indispensable.

REFERENCES

- Amusan, A.A.S., Mafiana, C.F. & Oke, O.A. (2007). A survey of adult mosquitoes in the hostels of the University of Agriculture, Abeokuta, Ogun State, Nigeria. *The Nigerian Journal of Parasitology*, 24:167-172.
- Altman, D. G. & Bland, J. M. (1996). Comparing several groups using analysis of variance. *British Medical Journal*, 312: 1472-1473.
- Bland, J. M. & Altman, D. G. (1995c). Multiple significance tests: the Bonferroni method. *British Medical Journal*, 310: 170.
- Bland, J. M. & Altman, D. G. (1996c). The use of transformation when comparing two means. *British Medical Journal*, 312: 1153.
- Fisher, R.A. (1925). *Statistical Methods for Research Workers*. Edinburgh, United Kingdom: Oliver & Boyd.
- Fujikoshi, Y. (1993). "Two-way ANOVA models with unbalanced data". *Discrete Mathematics*. 116 (1): 315–334. DOI:10.1016/0012-365X(93)90410-U.
- Gelman, A. (2005). "Analysis of variance? why it is more important than ever". *The Annals of Statistics*. 33 (1): 1–53. arXiv:math/0508526. doi:10.1214/009053604000001048.
- Gelman, A. and Hill, J. (2006). *Data Analysis Using Regression and Multilevel/Hierarchical Models*. Cambridge University Press. pp. 45–46. ISBN 978-0521867061.
- Gillies, M.T. & Coetzee, M. (1987). *A supplement of the African Anopheline Mosquitoes South of Sahara*. South African Institute for Medical Research, 55. DOI.org/10.1186/s12936-018-2189-5.
- Kass, R. E (2011). "Statistical inference: The big picture". *Statistical Science*. 26 (1): 1–9. arXiv:1106.2895. DOI:10.1214/10-sts337. PMC 3153074. PMID 21841892.
- Kleinbaum, D.G., Kupper, L.L. and Muller, K.E. (1988). *Applied Regression Analysis and Other Multivariable Methods*. 2nd ed.



Boston, Mass: PWS-Kent Publishing.

- Sit, V. (2007). Analyzing ANOVA Designs: Biometrics Information Handbook No. 5. Province of British Columbia, Ministry of Forests Research Program. Working paper 07/1995. Available at: <http://www.for.gov.bc.ca/hfd/pubs/docs/Wp/Wp07.pdf>.
- Winer, B. J., Brown, D. R. & Michels, K. M. (1991). Statistical Principles in Experimental Design, McGraw-Hill, New York, NY.
- World Health Organization, WHO (2015). World malaria report 2015. World Health Organization. ISBN: 9789241565158.
- World Health Organization, WHO (2018). World Malaria Report 2018. World malaria report 2018. World Health Organization. ISBN: 9789241565653
- World Health Organization, WHO (2019). World malaria report 2019. World Health Organization. ISBN: 9789241565721.
- Yates, F. (1934). The analysis of multiple classifications with unequal numbers in the different classes. Journal of the American Statistical Association. 29 (185): 51–66. doi:10.1080/01621459.1934.10502686. JSTOR 2278459.
- Zar, J.H. (1999). Biostatistical Analysis. Upper Saddle River, NJ: Prentice Hall. 20. BLAND, J. M. & ALTMAN, D. G. (1996b). Transforming data. British Medical Journal, 312: 770.



SMART FARMING - THE BACKBONE OF INDIAN ECONOMY

ESWARI CHANDRA AKANKSHA.CH.

R.M.K Engineering College, Kavaraipettai – 601206 , Thiruvallur Dist, Tamil Nadu , India

Dr. M. MEENA

R.M.K Engineering College, Kavaraipettai – 601206 , Thiruvallur Dist, Tamil Nadu , India

Ms. P. MALINI ANANDRAJ

R.M.K Engineering College, Kavaraipettai – 601206 , Thiruvallur Dist, Tamil Nadu , India

ABSTRACT

Agriculture is the broadest economic sector and plays a vital role in the overall economic development of a nation. Agriculture is the backbone of the Indian economy. Today agriculture routinely uses sophisticated technologies such as Robots, Moisture sensors, aerial images, and GPS technology. These advanced devices and precision agriculture and robotic systems allow businesses to be more profitable, efficient, safer, and environmentally friendly. Technological advancements in the arena of agriculture will ascertain to increase the competence of certain farming activities. For example, smart sensing and irrigation systems through wireless communications technology can be called smart farming. Novel and smart farming includes physical parameters such as soil moisture content, nutrient content, and mainly soil pH, vital in farming activity. The detailed modeling and control strategies of a smart irrigation and smart farming system are demonstrated

Keywords: Economic development, robots, aerial images, GPS technology.



SMART AGRICULTURE TECHNOLOGY USING IoT & RFID

Chenna Kesavan K.

R.M.K Engineering College, Kavaraipettai – 601206 , Thiruvallur Dist,Tamil Nadu , India

Dr. M. MEENA

R.M.K Engineering College, Kavaraipettai – 601206 , Thiruvallur Dist,Tamil Nadu , India

Dr. A. VIJAYALAKSHMI

R.M.K Engineering College, Kavaraipettai – 601206 , Thiruvallur Dist,Tamil Nadu , India

Dr. S.D. Uma MAGESWARI

R.M.K Engineering College, Kavaraipettai – 601206 , Thiruvallur Dist,Tamil Nadu , India

ABSTRACT

The goal of smart agriculture research is to ground a decision-making support system for farm management. In addition, smart farming deems it necessary to address the issues of population growth, climate change and labour that have gained a lot of technological attention, from planting and watering crops to health and harvesting.

Cloud computing is a major technique that can build massive data involved in agriculture production. IoT is a revolutionary technology that represents the future of agriculture and computing. RFID technologies can help develop plant factories and realize automatic control production of agriculture.

Climate-Smart Agriculture is an approach for guiding actions required to help stakeholders worldwide identify and develop strategies to make agriculture more productive and sustainable. A perfect combination of them can promote the fast development of agricultural modernization, realize smart agriculture and effectively solve the issues concerning agriculture, countryside, and farmers.

Keywords: Smart farming; cloud computing; IoT(Internet of things);RFID(Radio-frequency identification)



INFLUENCE OF GREEN MANURE FROM SPEAR GRASS ON SELECTED SOIL PHYSICAL PROPERTIES AND MAIZE GROWTH IN SOUTHERN GUINEA SAVANNA OF NIGERIA

***Ewetola E. A.**

Department of Crop Production and Soil Science, Ladoko Akintola University of Technology, Ogbomoso, Oyo State, Nigeria

Isola J. O.

Department of Soil Science, Forest Research Institute of Nigeria, Ibadan, Nigeria

Babatunde, I. E.

Department of Crop Production and Soil Science, Ladoko Akintola University of Technology, Ogbomoso, Oyo State, Nigeria

ABSTRACT

A field experiment was conducted in 2019 to determine the sole and combined effects of green manure from spear grass and NPK 15:15:15 fertilizer on selected soil physical properties and performance of maize (*Zea mays* L.). The treatments consisted of spear grass applied at, 5.0, 10.0 t ha⁻¹, NPK 15:15:15 at 120 kg N ha⁻¹, 2.5 t ha⁻¹ + 60 kg N ha⁻¹NPK and control (no amendment). The six treatments were arranged in a Randomized Complete Block Design with three replications. Green manure combined with NPK significantly reduced bulk density and increased total porosity compared to the control and sole NPK. Volumetric moisture content was significantly higher on 5 t ha⁻¹, 10 t ha⁻¹ and 2.5 t ha⁻¹ + 60 kg N ha⁻¹NPK compared to the control and NPK. Corresponding values of saturated hydraulic conductivity under 5 t ha⁻¹, 10 t ha⁻¹ and 2.5 t ha⁻¹ + 60 kg N ha⁻¹NPK were higher than the control and NPK although statistically similar. Sole application of NPK gave significantly taller plant, wider stem, higher number of leaves and larger leaf area compared with the control and other treatments. However, the order of growth parameter under the treatments were NPK > 2.5 t ha⁻¹ + 60 kg N ha⁻¹NPK > 5 t ha⁻¹ > 10 t ha⁻¹ > control. Soil physical condition was improved under sole application of organic amendment and combined application than sole NPK. Therefore, spear grass though regarded as noxious weed can serve as green manure applied either sole or combined with NPK to improve soil physical condition and maize production.

Keywords: Spear grass, green manure, NPK, Physical properties, maize growth



CLIMATE CHANGE AND ITS IMPACTS IN INDIAN HORTICULTURE

Assist. Prof. Dr. Arunkumar R.*

Department of Agricultural Extension, SRS Institute of Agriculture and Technology, Vedsandur, Tamil Nadu.

Senior Research Fellow, V. BALAMURUGAN

Department of Agricultural and Rural Management, Tamil Nadu Agricultural University, Coimbatore, Tamil Nadu.

ABSTRACT

Climate change and global warming is the largest concern of humankind in 21st century. The introduced commercial varieties of vegetables, fruits and flowers will perform ineffectively in an unpredictable way because of distortion of atmosphere. Ice cap melting in the Himalayan areas will diminishing chilling effect needed for the flowering of various horticultural plants such as Rhododendron, Saffron, Orchid, Apple etc. Commercial establishment of horticultural crops particularly cultivated under open field conditions will be affected severely. Because of high temperature physiological disorder of horticultural plants will be more pronounced. Some of the examples are Mango spongy tissue, litchi fruit cracking, etc. Air pollution mainly minimized the yield of various horticultural crops and improves the power of some physiological disorder mainly mango black tip. The most useful way is to follow conservation farming, using reforestation, water and forest conservation, renewable energy, etc. To support the productivity, alteration of recent horticultural practices and more usage of greenhouse technologies are the ways to minimize the impact of climate change. Advancement of new cultivars of horticultural plants tolerant to pests and disease resistance, high temperature, short duration and giving better yield under stress situations, as well as the adoption of hi-technology horticulture will be the main techniques to meet this difficulty.

Keywords: Climate change, global warming, horticultural crops and hi-technology horticulture.

KOYUNLARDA VERİMİ ETKİLEYEN BAZI ADAY GENLER

Arş. Gör. Ayşe Nur TANIŞ

Selçuk University, Faculty of Agriculture, Department of Animal Science, Konya, Türkiye
ORCID ID: 0000-0002-4369-0916

Dr. Öğr. Üyesi Fatma İLHAN

Selçuk University, Faculty of Agriculture, Department of Animal Science, Konya, Türkiye
ORCID ID: 0000-0002-9248-2056

Prof. Dr. İsmail KESKİN

Selçuk University, Faculty of Agriculture, Department of Animal Science, Konya, Türkiye
ORCID ID: 0000-0001-9358-7522

ÖZET

2020 Haziran sonu itibariyle Türkiye 42 milyon 713 bin baş koyun varlığına sahiptir. Çiftlik hayvanlarından biri olan koyun, ekonomik ve kültürel açıdan oldukça önemlidir. Çoğunlukla etleri, sütleri ve yünleri için yetiştirilmektedirler. Koyunlarda et verimi ve kalitesi, süt verimi ve kalitesi, yün verimi gibi verim özellikleri insanlar için önemlidir. Ayrıca büyüme ve üreme özellikleri de ekonomik açıdan önemlidir. Büyüme ve verim özelliklerinin genetik açıdan anlaşılması, bu hayvanlardan elde edilen verimi artırmaya olanak tanımaktadır. Gelişen teknoloji ve gen tanımlama yöntemleri ile ekonomik açıdan önemli fenotipik özelliklerle ilişkili aday genler tanımlanmıştır. Kantitatif özellik lokusu (QTL) ve genom çapında ilişkilendirme (GWAS) çalışmaları aday genlerin tanımlanmasında ve karakterize edilmesinde önemli bir role sahiptir. Büyüme ile ilgili genlerle yapılan çalışmalar sonucunda, büyüme hormonu geninin süttan kesim sonrası vücut ağırlığı artışını etkilediği tespit edilmiştir. LEP geni, karkas yağ ağırlığının artmasıyla ilişkilidir ve MSTN geni, karkas yağ ağırlığını azalttığı bildirilmiştir. β -LGB genotiplerinin laktasyon süresi ve laktasyon süt verimi üzerine etkileri istatistiksel olarak anlamlı bulunmuştur. Koyunlarda BMPRIB, BMPR ve BMP-15 genleri doğurganlık ile güçlü bir şekilde ilişkili bulunmuştur. FST geni, yapağı inceliği ve yün kıvrım özellikleri ile ilgili olarak tanımlanmıştır. Sıralama ve veri analizi teknolojilerindeki gelişmeler, farklı fenotipik özelliklerin genetik arka planlarını öğrenmede etkili olmuştur. Birden fazla özelliği etkileyen genlerin işlevini anlamaya yönelik çalışmaların daha fazla istatistiksel çalışma ve yeni genetik araçlar kullanılarak yapılması önemlidir. Bu araştırmada büyüme ve verim özelliklerini etkileyen bazı aday genler hakkında bilgiler bulunmaktadır. Bu çalışmalar koyunlarda et ve süt verimleri ile kalite, büyüme ve üreme faaliyetleri için faydalı olacaktır.

Anahtar Kelimeler: Aday gen, fenotipik özellik, gen bölgesi, koyun, *Ovis aries*, verim özellikleri

CANDIDATE GENES ASSOCIATED WITH YIELD TRAITS IN SHEEP

ABSTRACT

The end of June 2020, Turkey has 42 million 713 thousand head of sheep. Sheep, which is one of the farm animals, is very important economically and culturally. They are mostly grown for their meat, milk and wool. Yield traits such as meat yield and quality, milk yield and quality, wool yield from sheep are important for humans. In addition, growth and reproduction traits are also economically important. Understanding the growth and yield traits in terms of genetics allows to increase the yield from these animals. With the developing technology and gene identification methods, candidate genes associated with economically important phenotypic traits have been identified. Quantitative trait locus (QTL) and genome-wide association (GWAS) studies have an important role in identifying and characterizing candidate genes. As a result of studies with genes related to growth, it has been determined that the growth hormone gene affects the body weight gain after weaning. The LEP gene is associated with increase carcass fat weight and the MSTN gene reduce carcass fat weight. The effects of β -LGB genotypes on lactation period and lactation milk yield were found to be statistically significant. In sheep, the BMPRIB, BMPR and BMP-15 genes were strongly associated with fertility. The FST gene was characterized for wool fiber diameter and wool crimp traits. Advances in sequencing and data analysis technologies have been instrumental in learning the genetic backgrounds of different phenotypic traits. It is important to carry out studies to understand the function of genes that affect more than one trait, using more statistical studies and new genetic tools. In this research, there is information about some candidate genes that affect growth and yield traits. These studies will be beneficial for meat and milk yields and quality, growth and reproduction activities in sheep.

Keywords: Candidate genes; phenotype trait; genomic region; sheep; *Ovis aries*; yield traits

1. GİRİŞ

Ülkemiz, 2019 yılı Aralık ayına göre % 14.6 artan koyun sayısı ile 2020 yılı Haziran ayı sonunda 42 milyon 713 bin baş koyun varlığına sahiptir (TÜİK, 2020). Koyun (*Ovis aries*), hem kültürel hem de ekonomik olarak önemli çiftlik hayvanları arasında yer almaktadır. Koyunlar, çiftliklerde ve Türkiye’de çoğunlukla dar gelirli vatandaşlar tarafından yetiştirilmektedir. Daha çok insanlar için ekonomik öneme sahip olan et, süt, yapağı ve deri üretimi için yetiştirilmektedirler (Montossi ve ark., 2013).

Genetik ilerlemenin hızını artırmak ve suni tohumlama yöntemini kullanarak genetik olarak üstün olan hayvanlara öncelik vermek için araştırmalar yapılmıştır. Bu araştırmalar yerli ırkların korunması ve genetik çeşitliliğin artmasında önemli rol oynamaktadır. Yapılan seleksiyon sayesinde adaptasyon problemi olmayan, yaşadıkları bölgedeki hastalıklara kültür ırklarına göre daha dirençli olan, otlama ve sürü kabiliyeti yüksek yerli ırkların muhtemel potansiyelleri ortaya çıkarılabilecektir (Bayram, 2018). Yapılan araştırmalardan sonra,

kantitatif özellik lokuslarını (QTL) kullanmanın uygun olacağına karar verilmiştir. QTL analizi, kompleks özellikler için bir ya da birçok genomik bölge ve bir fenotipin birbiriyle ilişkili olup olmadığını göstermektedir (Miles ve ark., 2008). Ekonomik olarak önemli olan özelliklerin tanımlanmasında QTL kullanımı tercih edilmektedir. QTL ile yapılan çalışmaların genellikle çok geniş bir bölgeyi kapsamaması, gen tespitini zorlaştırmakta ve güven aralığını düşürmektedir. Bu nedenle, genom çapında ilişkilendirme çalışması (GWAS, Genome Wide Association Study) geliştirilmiştir. GWAS ile genomik bölgeler ve fenotipik özellikler arasındaki ilişkiler tanımlanmaktadır. Bu tanımlamalar tek nükleotit polimorfizmleri (SNP) baz alınarak yapılmaktadır (Xu ve ark., 2017). GWAS, farklı fenotipik özelliklerin, moleküler varyantlar ve aday genler ile ilişkisini belirlemek için önemli bir çalışmadır.

Bugüne kadar, çiftlik hayvanlarında ekonomik olarak önemli olan fenotipik özelliklere etki eden genleri belirlemek amacıyla farklı metotlar kullanılarak birçok çalışma yapılmıştır. Bu çalışmanın amacı, farklı koyun ırklarına ait verim özellikleri ile ilgili olarak tanımlanmış aday genleri özetlemektir.

2. KAYNAK ARAŞTIRMASI

2.1. Büyüme ile İlgili Genlerle Yapılan Çalışmalar

Büyüme özellikleri koyunlarda önemli ekonomik özelliklerdendir. Moleküler genetiğin ve genomik araçların gelişmesi, ekonomik özelliklerle ilişkili fonksiyonel genlerin tanımlanması ve açıklanmasını kolaylaştırmıştır. Büyüme, merkezi olarak hipofiz bezi tarafından düzenlense de, hipofiz bezinin gelişimini etkileyen genler de vardır. Örneğin LHX3 ve LHX4 genleri koyunlarda vücut büyümesi ve üreme süreçlerinde görev yapmaktadırlar (Park ve ark., 2013). MSTN geni, kaslanma ve büyüme ile ilişkili bulunmuştur (Broad ve ark., 2000; Sahu ve ark., 2017). Büyüme hormonu (GH) geninin süten kesme sonrası ağırlık kazancını etkilediğini tespit edilmiştir (Moradian ve ark., 2013). Glutamat metabotropik reseptör 1 (GRM1), metil-CpG bağlayıcı alan proteini 5 (MBD5), ubiquitin protein ligaz E3 bileşeni n-recogin 2 (UBR2), ribozomal protein L7 (RPL7) ve kromozom 2'nin yapısal bakımı (SMC2) aday genleri, kromozom düzeyinde süten kesim sonrası ağırlık artışı ile ilişkili olarak tanımlanmıştır (Zhang ve ark., 2013). Vücut kitle indeksini etkileyen yağ kütlesi ve obezite ile ilişkili protein (FTO) ve Apolipoprotein B Reseptörü (APOBR) genleri tanımlanmıştır (Wang ve ark., 2015). Miyosit güçlendirici bağlanma faktörü 2B (MEF2B) ve Tirotropin salgılayan hormon bozucu enzimin (TRHDE), koyunlarda vücut ağırlığını ve büyümesini etkileyen genler oldukları bildirilmiştir (Zhang ve ark. 2016). DRB1 * 2001 haplotipi süten kesim ağırlığı, yetişkin yaş ağırlığı ve ortalama günlük canlı ağırlık kazancı ile ilişkili bulunmuştur. Ovar-DRB1 genindeki varyasyonun, patojenlere karşı bağışıklık tepkilerini etkileyebildiği ve bu yüzden hastalık direncinde varyasyona yol açabileceği belirtilmiştir (Çınar ve ark., 2016). DNA bağlayıcı transkripsiyon faktörü aktivitesinde ve apoptotik süreçte önemli bir rol oynayan Tümör proteini p53 (TP53) geni, vücut büyüklüğü ile ilişkili olarak tanımlanmıştır (Kominakis ve ark., 2017).

Yukarıda bahsedilen genlerin hepsi de genel olarak vücut büyümesi, kas gelişimi, süttten kesim ağırlığı, canlı ağırlık kazancı gibi özelliklerle direkt ya da dolaylı yoldan ilgili bulunmuştur. Genler, özellikler ve koyun ırkları Çizelge 2.1.'de özetlenmiştir.

Çizelge 2.1. Vücut ağırlığı ve büyüme özellikleri ile ilişkili bazı aday genler.

Genler	Özellikler	Koyun Irkı	Yazar(lar)
LHX3	B	Hu, KKHK, LYKHK, TK	Zhao ve ark., 2017; Park ve ark., 2013
LHX4	B	Hu, KKHK, LYKHK, TK	Zhao ve ark., 2017; Park ve ark., 2013
MEF2B	CA, GÇ	Ujumqin koyunu	Zhang ve ark. (2016)
TRHDE	CA, GÇ	Ujumqin koyunu	Zhang ve ark. (2016)
FTO	VKİ	AMM, ÇMYK, ABD	Wang ve ark. (2015)
APOBR	VKİ	AMM, ÇMYK, ABD	Wang ve ark. (2015)
TP53	VÖ	Frizarta koyunu	Kominakis ve ark. (2017)
DRB*2001	SKA, YA	Rambouillet ve Columbia	Çınar ve ark. (2016)
	KB	MK, M ve T	Broad ve ark. (2000); Sahu ve ark. (2017)
MSTN	CA	Magra	Singh ve ark. (2020)
GH	SKSAK, B	Makui koyunu	Moradian ve ark. (2013)
GRM1	SKSAK	Sunit, Alman M., Dorper	Zhang ve ark. (2013)
MBD5	SKSAK	Sunit, Alman M., Dorper	Zhang ve ark. (2013)
UBR2	SKSAK	Sunit, Alman M., Dorper	Zhang ve ark. (2013)
RPL7	SKSAK	Sunit, Alman M., Dorper	Zhang ve ark. (2013)
SMC2	SKSAK	Sunit, Alman M., Dorper	Zhang ve ark. (2013)

B: Büyüme, CA: Canlı Ağırlık, GÇ: Göğüs Çevresi, VKİ: Vücut Kitle İndeksi, VÖ: Vücut Ölçüsü, SKA: Süttten Kesim Ağırlığı, YA: Yetişkin Ağırlık, KB: Kas Büyümesi, SKSAK: Süttten Kesim Sonrası Ağırlık Kazancı, KKHK: Küçük kuyruklu Han koyunu, LYKHK: Lanzhou yağlı kuyruklu Han koyunu, TK: Tong koyunu, AMM: Alman Mutton Merinosu, ÇMYK: Çin Moğol Yağlı Kuyruklu, ABD: Afrikalı Beyaz Dorper, MKMT: Madras Kırmızısı, Mercheri, Texel

2.2. Et Kalitesi ve Karkas ile İlgili Genlerle Yapılan Çalışmalar

Et, karkas, etin kalitesi ve karkas ağırlığı önemli fenotipik özelliklerdendir. Yağ asidi bileşimi, obezite, diyabet, nörolojik hastalıklar ve kanserler gibi insan hastalıklarını etkilemektedir. Bu nedenle et kalitesinin etkinliğini belirleyen faktörlerden biridir. Ayrıca yağ asidi bileşimi etin sertliğini, rengini ve etin raf ömrünü belirlemektedir. LEP geninin A113G varyantı tüm vücut yağ ağırlığı ile ilişkili bulunmuştur (Barzehkar ve ark., 2009). Myostatin geni et verimi ile ilişkili bulunmuştur (Hickford ve ark., 2010). DGAT1 ve UCP1 genlerinin, deri altı karkas yağ derinliği ile ilişkili bulunduğu bildirilmiştir (Mohammadi ve ark., 2013, Yang ve ark., 2014). CAST geninde et kalitesini ve yağ asidi kompozisyonunu etkileyen genetik varyantlar tespit edilmiştir (Aali ve ark., 2016).

Çizelge 2.2. Et kalitesi ve karkas ile ilişkili bazı aday genler.

Genler	Özellikler	Koyun Irkları	Yazar(lar)
LEP	KA	Kıvrıcık melezi kuzular	Kaplan ve ark. (2017)
	TVYA	Shal	Barzehkar ve ark. (2009)
	SKA	Zandi	

MSTN	EV	Romney	Hickford ve ark. (2010)
CAST	EK	Chall İnan koyunu	Aali ve ark. (2016)
	YAK	Zel İnan koyunu	Aali ve ark. (2016)
UCP1	DAKYD	NZ, Romney, Suffolk	Yang ve ark. (2014)
DGAT1	SYKA, DAKYD	Lori-Bakhtiari & Zel	Mohammadi ve ark. (2013)

KA: Karkas Ağırlığı, TVYA: Tüm Vücut Yağ Ağırlığı, SKA: Sütten Kesim Ağırlığı, EV: Et Verimi, EK: Et Kalitesi, YAK: Yağ Asidi Kompozisyonu, DAKYD: Deri Altı Karkas Yağ Derinliği, SYKA: Sırt Yağı Karkas Derinliği, NZ: New Zealand.

2.3. Süt Verimi ve Kalitesi ile İlgili Genlerle Yapılan Çalışmalar

Süt, insanlar için en önemli memeli kaynaklarından biridir. Süt verimi, süt proteini, süt yağı, kazein ve laktoz yüzdeleri en yaygın olarak bilinen süt özelliklerindedir. Bu özelliklerin üretim potansiyelleri esas olarak çevresel faktörler tarafından kontrol edilmektedir. Genetik olarak ise farklı genler tarafından kontrol edilmektedir. Polonya merinosunda süt proteinleri ve bunların verime etkilerini araştırmak amacıyla yapılan çalışmada kazein geninin α S1-CN genotipinin D alleli daha düşük yağ ve protein seviyesi ile, C alleli en yüksek süt verimi, protein ve yağ seviyesi ile ilişkili bulunmuştur (Mroczkowski ve ark., 2004). GH1 geninin Serrada Estrela koyun ırkında daha düşük süt verimi ile ilişkili bir gen olduğu tespit edilmiştir (do Rosário ve ark., 2006). Yok olma tehlikesi ile karşı karşıya olan Çine Çaparı koyunlarda β -LGB genotiplerinin (AA, AB, BB) laktasyon süresi ve laktasyon süt verimi üzerinde istatistik olarak önemli ($p < 0.05$), günlük ortalama süt verimi üzerinde ise önemsiz ($p > 0.05$) etkisi olduğu görülmüştür (Erdoğan, 2010). İtalyan Altamura koyunlarında palmdelphin (PALMD) ve yüzük parmağı proteini 145 (RFP145), İspanyol Churra koyunlarında alfa-laktalbumin (LALBA) genleri süt özellikleri ile ilgili genler olarak tanımlanmıştır (García-Gómez ve ark., 2012; Moioli ve ark., 2013). Büyüme hormonu ve prolaktin genlerinin fonksiyonunun düzenlenmesinde önemli rol oynayan POU1F1 geninin (Lan ve ark., 2009), süt üretimi üzerinde etkili olduğu bildirilmiştir (Özmen ve ark., 2014).

Yukarıda bahsedilen genlerin hepsi de genel olarak laktasyon süresi, laktasyon süt verimi, süt verimi, sütteki yağ ve protein oranı gibi özelliklerle direkt ya da dolaylı yoldan ilgili bulunmuştur. Genler, özellikler ve koyun ırkları Çizelge 2.3.'de özetlenmiştir.

Çizelge 2.3. Süt verimi ve kalitesi ile ilişkili bazı aday genler.

Genler	Özellikler	Koyun Irkları	Yazar(lar)
β -LGB	LS, LSV	Çine Çaparı	Erdoğan (2010)
		Kıvırcık	Almaz (2013)
POU1F1	SV	Sakız, Karaman, İvesi	Özmen ve ark. (2014)
PALMD	SV	İtalyan Altamura	García-Gómez ve ark., (2012); Moioli ve ark., (2013)

RFP145	SV	İtalyan Altamura	García-Gómez ve ark., (2012); Moioli ve ark., (2013)
LALBA	SV	İspanyol Churra	García-Gómez ve ark., (2012); Moioli ve ark., (2013)
GH1	SV	Serrada Estrela	do Rosário ve ark. (2006)
CSN2	SV, YO, PO	Polon Merinos	Mroczkowski ve ark. (2004)

LS: Laktasyon Süresi, LSV: Laktasyon Süt Verimi, SV: Süt Verimi YO: Yağ Oranı, PO: Protein Oranı.

2.4. Döl Verimi ile İlgili Genlerle Yapılan Çalışmalar

Yumurtlama oranı, bir batında doğan yavru sayısının çokluğu, toplam doğan kuzu sayısı, ilk kuzulama yaşı, ölü doğum ve erişkinlik yaşı gibi doğurganlığı etkileyen faktörler koyun endüstrisinde önemli etkiye sahiptirler. Özellikle yumurtlama oranı ve bir batında doğan yavru sayısının çokluğu, ekonomik değeri yüksek olan özelliklerdir. BMP15 geninin granüloza hücrelerini, teka hücrelerini ve oositi etkilediği, GDF9 geninin yumurtalık folikül gelişimini düzenlediği bildirilmiştir (Davis ve ark., 1982; McNatty ve ark., 2005). BMP15 geninin yumurtlama seviyesi ve yavrulama sayısını etkilediği, Cambridge ve Belcare ırkı koyunlarda BMP15 ve GDF9 birlikte folikül oluşumunda önemli bir rol oynadığı tespit edilmiştir (Galloway, 2000; Hanrahan, 2004). BMP15 ve BMP-15 genleri, doğurgan bir Çin ırkı olan Küçük Kuyruklu Han koyunlarında doğurganlıkla yüksek oranda ilişkili bulunmuştur (Chu ve ark., 2007). FecL lokusunun, Lacaune ırkı koyunlarda yumurtlama oranını etkilediği tespit edilmiştir (Doruillet ve ark., 2009). Çin Moğol Yağ Kuyruklu, Alman Merinosu ve Afrikalı Beyaz Dorper koyun ırklarında oosit gelişimi ile ilişkili Cyclin B2 (CCNB2) ve Solute Carrier Family 8A3 (SLC8A3) genlerinde moleküler varyantlar bildirilmiştir (Wang ve ark., 2015).

Yukarıda bahsedilen genlerin hepsi de genel olarak yumurtlama oranı, doğurganlık, folikül oluşumu ve gelişimi, üreme potansiyeli ve oosit gelişimi gibi özelliklerle direkt ya da dolaylı yoldan ilgili bulunmuştur. Genler, özellikler ve koyun ırkları Çizelge 2.4.'te özetlenmiştir.

Çizelge 2.4. Döl verimi ile ilişkili bazı aday genler.

Genler	Özellikler	Koyun Irkları	Yazar(lar)
BMP15	YO	Lacaune koyunu	Bodin ve ark. (2007)
	D	Küçük Kuyruklu Han	Chu ve ark. (2007)
BMP15	D	Küçük Kuyruklu Han	Chu ve ark. (2007)
	FO	Cambridge, Belcare	Galloway (2000); Hanrahan (2004)
GDF9	FO	Cambridge, Belcare	Galloway (2000); Hanrahan (2004)
	FG	Booroola	Davis ve ark. (1982); McNatty ve ark. (2005)

PRLR	ÜP	Sakız, Akkaraman, İvesi	Özmen (2010)
FecL	YO	Lacaune	Doruilhet ve ark. (2009)
TMEM154	LE	Rambouillet, Polypay, Columbia	Heaton ve ark. (2012); White ve ark. (2012)
CCNB2	OG	ÇMYK, Alman M, ABD	Wang ve ark. (2015)
SLC8A3	OG	ÇMYK, Alman M, ABD	Wang ve ark. (2015)

YS: Yumurta sayısı, D: Doğurganlık, FO: Folikül oluşumu, FG: Folikül gelişimi, ÜP: Üreme performansı, YO: Yumurtlama oranı, LE: Lentivirüs enfeksiyonu, OG: Oosit gelişimi.

2.5. Yapağı Kalitesi ve Yapağı Rengi ile İlgili Genlerle Yapılan Çalışmalar

Koyun yapağısı önemli ekonomik özelliklerden biridir. Ve küresel tarımda önemli bir rol oynamaktadır. İncelik, birörneklik (üniformite), uzunluk, elastikiyet, ondülasyon, direnç, parlaklık ve yapağı rengi, koyunlarda yapağı kalitesini belirleyen önemli yapağı özellikleri arasında yer almaktadır. Son yıllarda koyun yapağı özellikleri ile ilgili birkaç aday gen ve moleküler varyant bildirilmiştir. Yapılan çalışmalar sonucunda, FST, KAP ve KRT genleri yapağı kalitesi ile ilgili bulunmuştur. MC1R (melanocortin 1 receptor) geni, melanin sentezinde önemli rol oynamaktadır. ASIP (agouti signaling protein) ve MC1R, koyunlarda yapağı rengi varyasyonunun belirlenmesinde önemli rol oynar. ASIP, pigmentasyon oluşturma sürecinde MC1R ile antagonist bir ilişki içerisindedir. α -MSH reseptör etkileşimini bloke ederek pigmentasyon aktivitesini etkiler ve eumelanin pigmentinden pheomelanin pigmentine geçişe neden olur (Li ve ark., 2014). Dubian ve Privorian ırkı koyunlarda ASIP'in koyunlarda yün renklerini (beyaza karşı koyu renk) ve farklı benekli desenleri etkilemede diğer genetik faktörlerin veya mekanizmaların (diğer lokuslar veya diğer genlerle epistatik etkileşim) etkili olabileceğini göstermiştir (Fontanesi ve ark., 2012). FST geni, Xinjiang tipi Çin merinos koyunlarında (CMXT) yün lif çapı ve yün kıvrım özellikleri için ilişkili olarak tanımlanmıştır (Ma ve ark., 2017). Keratin ilişkili protein genlerinde (KAP6.1, KAP8.1, KAP8.2, KRTAP9-2 ve KAP16.4), yün kalitesi ile ilişkili genetik varyantlar bulunmuştur (Sulayman ve ark., 2017). KRT (keratin) genleri (KRT31, KRT36, KRT38, KRT85) yün kalitesi ile ilişkili bulunmuştur (Sulayman ve ark., 2018). MC1R geninde melanin sentezini düzenleyen ve bu ırk koyunlarda siyah cilt rengini geliştiren varyantlar bulunmuştur (Gebreselassie ve ark., 2020).

Yukarıda bahsedilen genlerin hepsi de genel olarak yapağı inceliği, yapağı kalitesi, kıl köklerinin gelişimi ve renk kalıtımı gibi özelliklerle direkt ya da dolaylı yoldan ilgili bulunmuştur. Genler, özellikler ve koyun ırkları Çizelge 2.5.'te özetlenmiştir.

Çizelge 2.5. Yapağı kalitesi ve rengi ile ilişkili bazı aday genler.

Genler	Özellikler	Koyun Irkları	Yazar(lar)
FST	Yİ, YK	CMXT	Ma ve ark. (2017)
KAP6.1	YK, KKG	CMXT	Sulayman ve ark. (2017)
KAP8.1	YK, KKG	CMXT	Sulayman ve ark. (2017)

KAP8.2	YK, KKG	CMXT	Sulayman ve ark. (2017)
KRTAP9-2	YK, KKG	CMXT	Sulayman ve ark. (2017)
KAP16.4	YK, KKG	CMXT	Sulayman ve ark. (2017)
MC1R	Renk	Dubian ve Privorian	Fontanesi ve ark. (2012)
		Çin Tan Koyunu	Gebreselassie ve ark. (2020)
ASIP	Renk	Dubian ve Privorian	Fontanesi ve ark. (2012)
		Fin Koyunu	Li ve ark. (2014)
KRT31	YK	CMXT	Sulayman ve ark. (2018)
KRT36	YK	CMXT	Sulayman ve ark. (2018)
KRT38	YK	CMXT	Sulayman ve ark. (2018)
KRT85	YK	CMXT	Sulayman ve ark. (2018)

Yİ: Yapağı inceliği, YK: Yapağı kalitesi, KKG: Kıl köklerinin gelişimi, CMXT: Chinese Merino (Xinjiang type).

3. SONUÇLAR

Dizileme ve veri analizi teknolojilerindeki gelişmeler, farklı fenotipik özelliklerin genetik arka planlarının öğrenilmesinde etkili olmuştur. İlgilenilen özelliklerle ilişkili tanımlanan genlerin ayrıntılı genetik bilgisi ile yapılan genetik iyileştirme programları, hayvanların üretim potansiyelini ve üreme etkinliğini artırmaya yardımcı olur. Bu da koyun üreticilerinin ve bu konuda çalışan endüstrinin üretim ve kârlılığının artmasına yardımcı olabilir. Bazıları birden fazla fenotipik özelliği etkileyen bir dizi gen ve moleküler varyant tespit edilmiştir. Birden fazla özelliği etkileyen genlerin, daha fazla istatistik çalışmalar ve yeni genetik araçlar kullanılarak fonksiyonunu anlama çalışmalarının yapılması önemlidir. Bu araştırmada, ekonomik açıdan önemli özelliklerle ilişkili genomik bölgeler ve ilgili genler ve ayrıca gen açıklamaları tartışılmakta ve özetlenmektedir. Bu çalışmalar, koyunlarda et ve süt verimleri ve kaliteleri, büyüme, üreme faaliyetleri için faydalı olacaktır.

KAYNAKLAR

- Aali, M.; Moradi-Shahrbabak, H.; Moradi-Shahrbabak, M.; Sadeghi, M.; Yousefi, A.R. Association of the calpastatin genotypes, haplotypes, and SNPs with meat quality and fatty acid composition in two Iranian fat-and thin-tailed sheep breeds. *Small Rumin. Res.* 2017, 149, 40–51.
- Almaz, E., 2013, Kıvrıkcık Koyunlarında Beta Laktoglobulin Polimorfizminin PCR-RFLP Yöntemiyle Belirlenmesi, Yüksek Lisans Tezi, *Namık Kemal Üniversitesi Fen Bilimleri Enstitüsü.*
- Amanda, W.; Thompson, VF.; Goll, DE., 2004, Interaction of calpastatin with calpain: a review, *Biol chem.* 385: 465-472.
- Arthur, P. F., 1995, Double muscling in cattle: a review, *Australian Journal of Agricultural Research*, 46: 1493-1515.
- Ata, N., 2012, Çine Çaparı ve Karya Koyunlarda Calpastatin Gen Polimorfizminin PCR-RFLP Yöntemi ile Belirlenmesi, Yüksek Lisans Tezi, *Adnan Menderes Üniversitesi Fen Bilimleri Enstitüsü Zootekni Anabilim Dalı*, 037.

- Balcıoğlu, M.S.; Karşlı, T.; Şahin, E.; Ulutaş, Z.; Aksoy, Y., 2014, Türkiye’de Yetiştirilen Bazı Yerli Koyun Irklarında Kalpastatin (CAST) Geni Polimorfizminin PCR-RFLP Yöntemiyle Belirlenmesi, Ankara, *Tarım Bilimleri Dergisi*.
- Barzehkar, R.; Salehi, A.; Mahjoubi, F., 2009, Polymorphisms of the ovine leptin gene and its association with growth and carcass traits in three Iranian sheep breeds, *J. Biotechnol*, Iran, 7, 24 1–246.
- Bayram, D., 2018, Türkiye Yerli Koyun Irklarından Akkaraman Irkında Canlı Ağırlık Artışı Üzerine Etkili Üç Aday Gen Yönünden Genetik Karakterizasyonları ve Genotip-Fenotip İlişkilerinin Araştırılması, Proje No: TSA-2016-6541, *Çok Disiplinli Araştırma Projesi*.
- Broad, T.; Glass, B.; Greer, G.; Robertson, T.; Bain, W.; Lord, E.; McEwan, J.; Peterson, S., 2000, Search for a locus near to myostatin that increases muscling in Texel sheep in New Zealand, Hamilton, New Zealand, *New Zealand Society of Animal Production*, 110–112.
- Bodin, L.; Di Pasquale, E.; Fabre, S.; Bontoux, M.; Monget, P.; Persani, L.; Mulsant, P., 2007, A novel mutation in the bone morphogenetic protein 15 gene causing defective protein secretion is associated with both increased ovulation rate and sterility in Lacaune sheep. *Endocrinology*, 148, 393–400.
- Cannon, B.; Nedergaard, J., 2004, Brown adipose tissue: Function and physiological significance, *Physiol. Rev.*, 84, 277–359.
- Choudhary, Vivek ve ark., DNA polymorphism of leptin gene in Bos indicus and Bos taurus cattle, 2005, *Genetics and Molecular Biology*, v. 28, n. 4, pp. 740-742.
- Chu, M.; Liu, Z.; Jiao, C.; He, Y.; Fang, L.; Ye, S.; Chen, G.; Wang, J., 2007, Mutations in BMPR-IB and BMP-15 genes are associated with litter size in Small Tailed Han sheep (*Ovis aries*), *J. Anim. Sci.*, 85, 598–603.
- Cinar, M.U.; Mousel, M.R.; Herrmann-Hoesing, L.M.; Taylor, J.B.; White, S.N., 2016, Ovar-DRB1 haplotypes * 2001 and * 0301 are associated with sheep growth and ewe lifetime prolificacy, *Gene*, 595, 187–192.
- Clop, A.; Marcq, F.; Takeda, H. Ve ark., 2006, A mutation creating a potential illegitimate microRNA target site in the myostatin gene affects muscularity in sheep, *Nat Genet*, 38, 813–818.
- Çelikeloğlu, K.; Erdoğan, M.; Hacan, Ö.; Koçak, S.; Bozkurt, Z.; Tekerli, M., 2018, Pırlak Koyunlarında BMPR1B, BMP15 ve GDF9 Genlerinde Olası Polimorfizmlerin Araştırılması, *Kocatepe Vet J*, 11(4): 356-362 DOI: 10.30607/kvj.428999.
- Davis, G.; Montgomery, G.; Allison, A.; Kelly, R.; Bray, A., 1982, Segregation of a major gene influencing fecundity in progeny of Booroola sheep, *N. Z. J*, 25, 525–529.
- do Rosário Marques, M.; Santos, I.C.; Carolino, N.; Belo, C.C.; Renaville, R.; Cravador, A., 2006, Effects of genetic polymorphisms at the growth hormone gene on milk yield in Serra da Estrela sheep, *J. Dairy Res.*, 73, 394–405.
- Drouilhet, L.; Lecerf, F.; Bodin, L.; Fabre, S.; Mulsant, P., 2009, Fine mapping of the FecL locus influencing prolificacy in Lacaune sheep, *Anim. Genet.*, 40, 804–812.
- Erdoğan, F., 2010, Yerli Gen Kaynağı Çine Çaparı Koyunların Süt Verim Özellikleri ve β -Laktoglobulin Gen Polimorfizmi, Yüksek Lisans Tezi, *Adnan Menderes Üniversitesi Fen Bilimleri Enstitüsü Zootekni Anabilim Dalı*, ZZO-YL-2010-0001.
- Fontanesi, L.; Rustempašić, A.; Brka, M.; Russo, V. Analysis of polymorphisms in the agouti signalling protein (ASIP) and melanocortin 1 receptor (MC1R) genes and association with coat colours in two Pramenka sheep types, 2012, *Small Rumin. Res.*, 105, 89–96.
- Galloway, S.M.; McNatty, K.P.; Cambridge, L.M.; Laitinen, M.P.; Juengel, J.L.; Jokiranta, T.S.; McLaren, R.J.; Luiro, K.; Dodds, K.G.; Montgomery, G.W., 2000, Mutations in an oocyte-derived growth factor gene (BMP15) cause increased ovulation rate and infertility in a dosage-sensitive manner, *Nat. Genet.*, 25, 279.
- García-Gámez, E.; Gutiérrez-Gil, B.; Sahana, G.; Sánchez, J.-P.; Bayón, Y.; Arranz, J.-J., 2012, GWA analysis for milk production traits in dairy sheep and genetic support for a QTN influencing milk protein percentage in the LALBA gene, 7, e47782.
- Gebreselassie, G.; Liang, B.; Berihulay, H.; Islam, R.; Abied, A.; Jiang, L., 2020, Genomic mapping identifies two genetic variants in the MC1R gene for coat colour variation in Chinese Tan sheep, *PLoS ONE* 15(8): e0235426.

- Grobet, L.; Poncelet, D.; Royo, L.J.; Brouwers, B.; Pirottin, D.; Michaux, C.F.; Ménéssier, M.; Zanotti, S.; Dunner, M., 1998, Molecular definition of an allelic series of mutations disrupting the myostatin function and causing double-muscling in cattle, *Mamm. Genome*, 9, pp. 210-213.
- Goll, D.E.; Thompson, V.F.; Li, H.; Wei, W.; Cong, J., 2003, The Calpain System, *Physiol Rev*, 83: 731–801.
- Govind, R.; Dhakad, S.; Gahlot, G.; Agrawal, V.K., Narula, H.K. and Pannu, U., 2018, Genetic variation in growth regulating myostatin gene in Magra sheep, *Journal of Entomology and Zoology Studies*, 6(4): 1875-187.
- Hajihosseino, A.; Chelongar, R.; Ajdary, M., 2014, The Effect of Igf-1 and Pit-1 Genes Polymorphisms on Fat-Tail Measurements (Fat-Tail Dimensions In Makooei Sheep.) *Adv. Environ. Biol.*, 8(4), 862-867.
- Hanrahan, J.P.; Gregan, S.M.; Mulsant, P.; Mullen, M.; Davis, G.H.; Powell, R.; Galloway, S.M., 2004, Mutations in the genes for oocyte-derived growth factors GDF9 and BMP15 are associated with both increased ovulation rate and sterility in Cambridge and Belclare sheep (*Ovis aries*), *Biol. Reprod.*, 70, 900–909.
- Heaton, M.P.; Clawson, M.L.; Chitko-Mckown, C.G.; Leymaster, K.A.; Smith, T.P.; Harhay, G.P.; White, S.N.; Herrmann-Hoesing, L.M.; Mousel, M.R.; Lewis, G.S., 2012, Reduced lentivirus susceptibility in sheep with TMEM154 mutations. *PLoS Genet.*, 8, e1002467.
- Hickford, J.G.; Forrest, R.H.; Zhou, H.; Fang, Q.; Han, J.; Frampton, C.M.; Horrell, A.L., 2010, Polymorphisms in the ovine myostatin gene (MSTN) and their association with growth and carcass traits in New Zealand Romney sheep, *Anim Genet.*, Feb; 41(1): 64-72.
- <https://data.tuik.gov.tr/Bulten/Index?p=Hayvansal-Uretim-Istatistikleri-Haziran-2020-33874>
- Kaplan, S.; Atalay, S., 2017, Kıvrıkcık Melezi Kuzularda Leptin, Kalpastatin ve İnsülin Benzeri Büyüme Hormonu 1 Gen Polimorfizmlerinin Araştırılması, NKUBAP.10.GA.17.117, *Namık Kemal Üniversitesi Bilimsel Araştırma Projesi*.
- Karim, L.; Coppieters, W.; Grobet, L.; Valentini, A.; Georges, M., 2000, Convenient genotyping of six myostatin mutations causing double-muscling in cattle using a multiplex oligonucleotide ligation assay, *Animal Genetics*, 31, 396-399.
- Kominakis, A.; Hager-Theodorides, A.L.; Zoidis, E.; Saridaki, A.; Antonakos, G.; Tsiamis, G., 2017, Combined GWAS and ‘guilt by association’-based prioritization analysis identifies functional candidate genes for body size in sheep, *Genet. Sel. Evol.*, 49, 41.
- Kumar, N.S.; Jayashankar, M.R.; Ramakrishnappa, N.; Nagaraja, C.S.; Fairoze, N.; Satyanarayana, K., 2015, Genetic polymorphism of ovine calpain gene in bandur sheep. *International Journal of Science, Environment and Technology*, 4(3): 804-812.
- Lan, X.; Li, M.; Chen, H.; Zhang, L.; Jing, Y.; Wei, T.; Ren, G.; Wang, X.; Fang, X.; Zhang, C., 2009, Analysis of caprine pituitary specific transcription factor-1 gene polymorphism in indigenous Chinese goats, *Mol. Biol. Rep.*, 36, 705–709.
- Li, M.H.; Tiirikka, T.; Kantanen, J., A genome-wide scan study identifies a single nucleotide substitution in *ASIP* associated with white versus non-white coat-colour variation in sheep (*Ovis aries*), 2014, *Heredity* 112, 122–131.
- Liu, H.-H., Wang, J.-W., Zhang, R.-P., Chen, X., Yu, H.-Y., Jin, H.-B., Li, L., Han, C.-C., Xu, F., Kang, B., He, H. and Xu, H.-Y., 2012, In ovo feeding of IGF-1 to ducks influences neonatal skeletal muscle hypertrophy and muscle mass growth upon satellite cell activation, *J. Cell. Physiol.*, 227: 1465-1475
- Ma, G.-W.; Chu, Y.-K.; Zhang, W.-J.; Qin, F.-Y.; Xu, S.-S.; Yang, H.; Rong, E.-G.; Du, Z.-Q.; Wang, S.-Z.; Li, H., 2017, Polymorphisms of *FST* gene and their association with wool quality traits in Chinese Merino sheep. *PLoS ONE*, 12, e0174868.
- Mahrous, K.; Hassanane, M.; Shafey, H.; Mordy, M.A.; Rushdi, H., 2016, Association between single nucleotide polymorphism in ovine Calpain gene and growth performance in three Egyptian sheep breeds, *J. Genet. Eng. Biotechnol.*, 14, 233–240.
- McNatty, K.P.; Galloway, S.M.; Wilson, T.; Smith, P.; Hudson, N.L.; O’Connell, A.; Bibby, A.H.; Heath, D.A.; Davis, G.H.; Hanrahan, J.P., 2005, Physiological Effects of Major Genes Affecting Ovulation Rate in Sheep; *Genetics Selection Evolution; BioMed Central*: London, UK, 25–38.

- Mroczkowski, S.; Korman, K.; Erhardt, G.; Piwczynski, D.; Borys, B., 2004, Sheep milk protein polymorphism and its effect on milk performance of Polish Merino, *Archiv fur Tierzucht*, 47:(6), 114-121.
- Mohammadi, H.; Shahrehabak, M.M.; Sadeghi, M., 2013 Association between single nucleotide polymorphism in the ovine DGAT1 gene and carcass traits in two Iranian sheep breeds, *Anim. Biotechnol.*, 24, 159–167.
- Moioli, B.; Scatà, M.C.; Steri, R.; Napolitano, F.; Catillo, G., 2013, Signatures of selection identify loci associated with milk yield in sheep, *BMC Genet.*, 14, 76.
- Moradian, C.; Mohamadi, N.; Sheshdeh, S.; Hajihosseini, A.; Ashrafi, F., 2013, Effects of genetic polymorphism at the growth hormone gene on growth traits in Makooei sheep, *Eur. J. Exp. Biol.*, 3, 101–105.
- Nikmard, M.; Molaee, V.; Eskandarinasab, M.P.; Djadid, N.D.; Vajhi, A.R., 2012, Calpastatin polymorphism in Afshari sheep and its possible correlation with growth and carcass traits, *Journal of Applied Animal Research*, 40:4, 346-350.
- Ozmen, O.; Kul, S.; Unal, E.O., 2014, Polymorphism of sheep POU1F1 gene exon 6 and 3'UTR region and their association with milk production traits, Iran, *Iran. J. Vet. Res.*, 15, 331.
- Özmen, Ö., 2010, Sakız akkaraman ve ivesi ırkı koyunlarda prolaktin PRLR reseptör geni polimorfizmlerinin belirlenmesi, Elazığ, *Yükseköğretim Kurumları tarafından destekli bilimsel araştırma projesi*.
- Polat, Y. Ö., 2006, Sakız koyun ırkında BMPR-IB geninde çoklu doğuma neden olabilecek FEC B alleli varlığının PCR-RFLP yöntemi ile araştırılması, Yayınlanmamış doktora tezi, *Uludağ Üniversitesi Sağlık Bilimleri Enstitüsü*.
- Sahu, A.R.; Jeichitra, V.; Rajendran, R.; Raja, A., Polymorphism in exon 3 of myostatin ,(MSTN) gene and its association with growth traits in Indian sheep breeds, *Small Rumin. Res.*, 149, 81–84.
- Siadkowska, E.; Zwierzchowski, L.; Oprzadek, J.; Strzałkowska, N.; Bagnicka, E.; Krzyzewski, J., 2006, Effect of polymorphism in IGF-1 gene on production traits in Polish Holstein-Friesian cattle, *Anim. Sci. Pap. Rep.*, 24(3): 225-237.
- Strunnikov, A.V.; Hogan, E.; Koshland, D., 1995, SMC2, a *Saccharomyces cerevisiae* gene essential for chromosome segregation and condensation, defines a subgroup within the SMC family, *Genes Dev.*, 9, 587–599.
- Sulayman, A.; Mamat, A.; Taurusun, M.; Huang, X.-X.; Tian, K.; Tian, Y.; Xu, X.; Fu, X., 2017, Identification of Polymorphisms and Association of Five KAP Genes with Sheep Wool Traits, *Asian Australas. J. Anim. Sci.*
- Sulayman, A.; Tursun, M.; Sulaiman, Y.; Huang, X.; Tian, K.; Tian, Y.; Xu, X.; Fu, X.; Mamat, A. and Tulafu, H., 2018, Association analysis of polymorphisms in six keratin genes with wool traits in sheep, *Asian-Australas J Anim Sci*, Vol. 31, No. 6:775-783.
- Wang, H.; Zhang, L.; Cao, J.; Wu, M.; Ma, X.; Liu, Z.; Liu, R.; Zhao, F.; Wei, C.; Du, L., 2015, Genome-wide specific selection in three domestic sheep breeds, *PLoS ONE*, 10, e0128688.
- White, S.N.; Mousel, M.R.; Herrmann-Hoesing, L.M.; Reynolds, J.O.; Leymaster, K.A.; Neiberghs, H.L.; Lewis, G.S.; Knowles, D.P., 2012, Genome-wide association identifies multiple genomic regions associated with susceptibility to and control of ovine lentivirus, *PLoS ONE*, 7, e47829.
- Yang, G.; Forrest, R.; Zhou, H.; Hodge, S.; Hickford, J., 2014, Genetic variation in the ovine uncoupling protein 1 gene: association with carcass traits in New Zealand (NZ) Romney sheep, but no association with growth traits in either NZ Romney or NZ Suffolk sheep., *J Anim Breed Genet.* Dec;131(6):437-44.
- Zhang, L.; Liu, J.; Zhao, F.; Ren, H.; Xu, L.; Lu, J.; Zhang, S.; Zhang, X.; Wei, C.; Lu, G., 2013, Genome-wide association studies for growth and meat production traits in sheep, *PLoS ONE*, 8, e66569.
- Zhang, L.; Ma, X.; Xuan, J.; Wang, H.; Yuan, Z.; Wu, M., 2016, Identification of MEF2B and TRHDE Gene Polymorphisms Related to Growth Traits in a New Ujumqin Sheep Population, *PLoS ONE*, 11(7): e0159504.
- Zhou, H.; Hickford, J.G.H.; Gong, H., 2009, Identification of Allelic Polymorphism in the Ovine Leptin Gene, *Mol Biotechnol*, 41, 22–25.

NİĞDE İLİNDE ISLAH ÇALIŞMALARINI YAPILAN BAZI RENKLİ PATATES KLONLARININ KALİTE ÖZELLİKLERİNİN BELİRLENMESİ

Havva Aybüke GÜVEN
Nevşehir Hacı Bektaş Veli University, Faculty of Engineering-Architecture, Department of Food Engineering
ORCID ID:0000-0001-6889-9268

Dr. Öğr. Üyesi Feyza KIROĞLU ZORLUGENÇ
Nevşehir Hacı Bektaş Veli University, Faculty of Engineering, Architecture, Department of Food Engineering
ORCID ID:0000-0001-8313-8459

ÖZET

Patates (*Solanum tuberosum* L.), çeşitli iklim bölgelerine kolaylıkla uyum sağlayabilen ve dünyanın hemen her yerinde tarımı yapılabilen bir bitkidir. İçerdiği karbonhidrat, protein, mineral maddeler, vitaminler ve antioksidan maddelerle insan beslenmesinde önemli bir yeri vardır. Patates yumrularının kabuk rengi sarı, kahverengi, mor, kırmızı veya mavi olabilmektedir. Antosiyaninler ve karotenoidler farklı renklerde patates oluşmasını sağlayan temel pigmentlerdir. Genellikle ülkemizde üretilen patatesler beyaz ve sarı renklidir. Diğer renklerdeki patatesler, beyaz ve sarı patatese göre daha fazla antioksidan madde içermeleri ve daha uzun süre depolanabilmeleri gibi bazı üstün özelliklere sahiptirler. Patateslerin kabuk ve etli kısımlarının rengine göre tüketim şekli ve miktarları değişim göstermektedir. Bu çalışmada materyal olarak, Tarım ve Orman Bakanlığı Patates Araştırma Enstitüsü'nce geliştirilen bazı renkli patates klonları kullanılmıştır.

Renkli patateslerin en ve boy ölçümleri yapılmış, ortalama ağırlık ve yoğunluk değerleri ile renk değerleri belirlenmiştir. Ayrıca patates örneklerinde suda çözünür kuru madde, pH, titrasyon asitliği, toplam ve indirgen şeker, toplam karbonhidrat, protein, nişasta, toplam fenolik madde, toplam antosiyanin, antioksidan aktivite ve mineral madde analizleri gerçekleştirilmiştir. Analiz sonuçları istatistiksel olarak değerlendirilmiştir. Bu araştırmadan elde edilen sonuçların, ıslah çalışmalarına ve literatüre katkı sağlaması hedeflenmiştir.

Anahtar Kelimeler: Renkli patates, Antioksidan, Antosiyanin, Fenolik madde

DETERMINATION OF QUALITY CHARACTERISTICS OF SOME COLOR POTATO CLONES WHICH WERE BREEDING IN NIGDE PROVINCE

ABSTRACT

Potato (*Solanum tuberosum* L.) is a plant that can easily adapt to various climatic region and can be cultivated almost anywhere in the world. It has an important place in human nutrition with the carbohydrates, protein, mineral substances, vitamins and antioxidant contents. The skin color of potato tubers can be yellow, brown, purple, red or blue. Anthocyanins and carotenoids are the basic pigments that provide the formation of potatoes of different colors. Generally, potatoes produced in our country are white and yellow. Colored potatoes have



some superior properties, such as containing more antioxidants and longer storage than white and yellow potatoes. Depending on the color of the skin and flesh of the potatoes, the consumption patterns and amounts vary. In this study, some colored potato clones developed by the Ministry of Agriculture and Forestry Potato Research Institute were used.

Width and length measurements of colored potatoes were made. The average weight, density and color values were determined. In addition, water-soluble dry matter, pH, titration acidity, total and reducing sugar, total carbohydrate, protein, starch, total phenolic substance, total anthocyanin, antioxidant activity and mineral substance analyzes were performed in potato samples. Data were evaluated statistically. It is aimed that the results obtained from this research will contribute to breeding studies and literature.

Keywords: Colored potato, Antioxidant, Anthocyanin, Phenolic substance



SATELLITE CROP MONITORING

K. GOMATHY

R.M.K. Engineering College, Kavaraipettai, Tiruvallur District, India

S. Devisri MAHALAKSHMI

R.M.K. Engineering College, Kavaraipettai, Tiruvallur District, India

Dr. G. Nixon Samuel VIJAYAKUMAR

R.M.K. Engineering College, Kavaraipettai, Tiruvallur District, India

Ms. M. G. Meedphin ARASI

R.M.K. Engineering College, Kavaraipettai, Tiruvallur District, India

ABSTRACT

Nowadays agriculture and food security have become a serious issue all over the world. New ways of crop monitoring should be introduced in order to meet food demand in the future. Satellite crop monitoring is the technology which promotes crop real time crop vegetative index monitoring via spectral analysis of high resolution satellite images for different fields and crops. It enables to track positive and negative dynamics of crop development. It belongs to precision agriculture methods. It allows to perform online crop monitoring on different fields worldwide. Satellite crop monitoring technology users are agronomists and agriculture companies' management, business owners, investors and investment analyser, insurance brokers, agriculture machinery producers. We have to understand how promising the land is and that's why satellite crop monitoring come in and provides many solutions for analyzing the state of agricultural fields, both national and at local level. The technology's advantage is a high automation level of sown area condition and its interpretation in an interactive map which can be read by different groups of users, save budget using effective VRA tool and saves time. Its greatest applications are Improved cloud mask, Water stress detection, Monitoring peanuts using AVHRR Satellite, predicting winter wheat multi-temporal EnviSat-ASAR and LANDsat TM satellite and so on. The unavoidable disadvantage of this technique is it leads to soil degradation.

Keywords: Satellite crop monitoring, Precision agriculture, VRA Toll, Soil degradation.

ISOLATION AND IDENTIFICATION OF BACTERIA CAPABLE OF PRODUCING BACTERIAL CELLULOSE FROM VINEGARS PRODUCED FROM DIFFERENT FRUITS

Melih GÜZEL

Gümüşhane University

ORCID ID: 0000-0001-5374-8838

Özlem AKPINAR

Gaziosmanpasa University

ORCID ID: 0000-0001-6593-8495

ABSTRACT

In this study, it was aimed to isolate and identify bacteria capable of producing bacterial cellulose (BC), from vinegar samples produced by traditional methods from different fruits, to determine the BC production capacity of these bacteria and to investigate the properties of the obtained BCs. BC production was carried out with bacteria isolated from rosehip, pear and hawthorn (yellow) vinegars, and it was determined that the bacteria which had the highest BC production amount was isolated from hawthorn vinegar. It was found that BCs produced by bacteria isolated from hawthorn (yellow) vinegar had higher thermal stability, while BC produced by bacteria isolated from pear vinegar had higher crystallinity and finer fiber diameter compared to other BCs. All produced BCs had superior properties such as high crystallinity, thermal stability and fine fiber. As a result of the study, it was concluded that different bacteria capable of producing BC from different vinegars could be isolated and the BCs produced by these bacteria would had different characters.

Keywords: Bacterial cellulose, vinegar, isolation, identification.



ROLE OF ARTIFICIAL INTELLIGENCE IN SMART AGRICULTURE

G. RĪTHANYA

RMK Engineering College, Kavaraipettai, Tiruvallur district

Dr. G. Nixon Samuel VĪJAYKUMAR

RMK Engineering College, Kavaraipettai, Tiruvallur district

Dr. A. JAGADESAN

RMK Engineering College, Kavaraipettai, Tiruvallur district

Ms. V. NĪRMALA

RMK Engineering College, Kavaraipettai, Tiruvallur district

ABSTRACT

Agriculture is the fundamental source of national prosperity. It is an age old process and indeed it is improving boundlessly through sophisticated technological developments. The advancements of modern technology in agriculture cannot be overtired. A great example of this is Crop sensor. Proper application of fertilizers and pesticides is a huge issue in agriculture. The use of crop sensors makes it easier for farmers to apply chemicals in the right place, at the right time. Scientists have discovered solar powered Internet Of Things (IOT) sensor which helps in building modern greenhouse. IOT participates in automatic and sustainable irrigation and also keeps a check on light, humidity, pressure and temperature. It has made our greenhouse smart by allowing weather stations to automatically adjust climatic conditions by using a set of instructions. In precision agriculture, Artificial Intelligence (AI) helps in detecting poor nutrition and diseases in plants. AI sensors can analyze weeds and decide which herbicide to apply within the field, without harming the actual produce. Developments like AI vacuum apparatus helps in harvesting mature apples from trees, which in turn helps in picking the right fruits. A recently developed multi-lingual plant disease and diagnostic app uses images of plants to detect diseases and also provides accurate diagnosis for that particular disease. These advancements favor in increased and supportable crop productivity ensuring overall well-being of the society.

Keywords: Crop sensors, Internet Of Things (IOT), smart greenhouse, precision agriculture, artificial intelligence (AI).



NANOTECHNOLOGY IN FOOD SAFETY

A. ASWINI

RMK Engineering College, Kavaraipettai, Tiruvallur District.

Aishwarya S.

RMK Engineering College, Kavaraipettai, Tiruvallur District.

Dr. A. VIJAYALAKSHMI

RMK Engineering College, Kavaraipettai, Tiruvallur District.

Dr. G. Nixon Samuel VIJAYAKUMAR

RMK Engineering College, Kavaraipettai, Tiruvallur District.

ABSTRACT

Nanotechnology is an emerging technology which play an eminent role in food processing, food packaging, food safety, functional food development, detection of foodborne pathogens and shelf-life extension of food or food products. The research in nanotechnology showed a great potential to improve packaging materials than a conventional packaging. Packaging has as main functions in the transportation and storage of foods, while protecting it from microorganisms, chemicals, oxygen, moisture, and light aiming at maintaining its quality and safety, and thus increasing shelf life. Polymers are the main materials used in food packaging. These properties of these materials can be improved by incorporating other compounds in the polymer matrix. The incorporation of nanomaterials in packaging materials is supported by their influence in the mechanical (high strength and stiffness) and barrier (low permeability) properties. This paper gives an overview of the role of nano technology and nano materials in food safety.

Keywords: Nanotechnology; food safety; foodborne pathogens



BAMBOO SHOOTS AND ITS BENEFITS

Assist. Prof. Dr. Sanjaikannan A.*

Department of Agricultural Engineering, SRS Institute of Agriculture and Technology, Veda sandur, Tamil Nadu.

Assist. Prof. Dr. R. LEENASREE

Department of Agricultural Engineering, SRS Institute of Agriculture and Technology, Veda sandur, Tamil Nadu.

ABSTRACT

Bamboo shoots are considered to be one of the useful nutritional foods. Their rich contents of carbohydrates, proteins, fibres, vitamins, and minerals and fat. Bamboo shoots also named as bamboo sprouts and are a culinary must-have in several dishes and soups, in Southeast Asian countries and in few parts in Indian country. Bamboo shoots that grow across China, Japan, Taiwan and are harvested during summer. In India, these delicious bamboo shoots are a staple of sorts in states like Arunachal Pradesh, Assam, Nagaland, Jharkhand, Manipur, Karnataka and Odisha. These shoots are very low on fat and sugar making it an ideal snack for the diabetics. The presence of fiber in large quantities and it helps in dealing with gut issues. Bamboo is known for having an earthy taste with hints of nuttiness. The subtle flavor will bring out the natural flavors in your dish by adding crunch, texture, and sweetness to any meal. One can consume bamboo shoots guilt-free as the calorie count does not exceed 20 calories for every 100 grams. These shoots are cardiac patient-friendly, as they contain unsaturated fats that help in fighting against bad cholesterol. Bamboo shoots are rich in vitamins and minerals that can help improve body's immune system. Various antioxidants present in bamboo shoots are important for stronger immunity.

Keywords: Bamboo shoots, Vitamins, immune system, antioxidants.



INVESTIGATIONS ON SOME IMPORTANT FACTORS THAT CAN INFLUENCE MAIZE GRAIN RESISTANCE TO MAIZE WEEVIL PEST IN STORAGE

Irene Adaeze KENNETH

Department of Crop and Soil Science, University of Port Harcourt, Nigeria

Luke Chinaru NWOSU*

Department of Crop and Soil Science, University of Port Harcourt, Nigeria

ABSTRACT

The use of resistant variety has been recognized as a key strategy to save maize (*Zea mays* L.) production in Africa against the maize weevil, *Sitophilus zeamais* Motschulsky (Coleoptera: Curculionidae). Most studies evaluate resistance in maize for short periods of time and studies under long storage duration have been recently advised. Therefore, ten improved maize varieties and one local variety were studied in the laboratory under long storage conditions using standard methods. Four varieties (36%) were resistant to *S. zeamais* attack whereas, 64% were moderately resistant. Moderate resistance in the local maize variety included as a check matched resistance in 60% of the improved maize varieties. The growing of resistant varieties identified will permit the postharvest storage of maize for long duration and minimize other problems linked to maize weevil infestation. Seed hardness, tannin and phytate did not contribute significantly to grain resistance to *S. zeamais* attack. Phenol was however identified as the basis for maize grain resistance to damage by *S. zeamais*. Majority of the improved maize varieties resisted colour change, mould infection and dampness during long storage and these provide the rationale for their selection for long storage.

Keywords: Resistant variety, postharvest storage, weevil infestation, phenol, long storage.



RESCUE FROM FOOD ADULTERATION BY SENSORS AND NANOTECHNOLOGY

R. Amara DEEPIKA

RMK Engineering College, Kavaraipettai, Tiruvallur District.

Dr. A. VIJAYALAKSHMI

RMK Engineering College, Kavaraipettai, Tiruvallur District.

Dr. G. Nixon Samuel VIJAYAKUMAR

RMK Engineering College, Kavaraipettai, Tiruvallur District.

ABSTRACT

In the present day to day life, everyone in the world experience food adulteration. What does food adulteration exactly mean? It is an intentional act that reduces the quality of food offered for sale by substitution of inferior components. Adulterated food is toxic and it could reduce the essential nutrients. So, it will affect growth and development of the body. Consumption of adulterated food causes serious health problems. It is something which happens worldwide. It is something which cannot be eradicated. Therefore, it's better for us to rescue ourselves. In olden days, the food adulteration can be identified by several traditional methods such as spectroscopy, chromatography, ELISA methods are used to identify these adulterant materials. But last few years, metal nanoparticles such as gold nano particles, silver nano particles, etc., are used to identify the adulterant in several food products. Similarly, carbon nano tubes, carbon nanofibers also used to detect food adulterants. These materials also used in the form of biosensors, nano sensors, and immunosensors which can help to detect at very sensitive levels toxic contaminants. This paper gives an insight view of various types of food adulterants added to food, ill effects of these materials, identification of these contaminants by using nano technology.

Keywords: Food adulteration; traditional methods; nano technology; biosensor



OVERVIEW OF BAMBOO DIVERSITY OF INDIA

Assist. Prof. Dr. Suyog A. BAGADE *

SRS Institute of Agriculture & Technology, Vedsandur (Affiliated to Tamil Nadu Agricultural University), Dist. Dindigul,
Tamil Nadu State (India)

M.Sc. (Forestry) Scholar, Aditi A. BAGADE

College of Forestry, Dr. B. S. Konkan Krishi Vidyapeeth, Dapoli, Dist. Ratnagiri, Maharashtra State (India)

ABSTRACT

Bamboos are one of earth's oldest and most precious plant materials and very important non-wood forest resources found in forest as well as non-forest areas. Bamboos are one of the fastest growing perennial plants which belong to the family Poaceae and are found in the tropical, sub-tropical and mild temperate regions of the world. Bamboos are distributed naturally in abundance East and Southeast Asia and Islands of Pacific and Indian Oceans. Bamboo has a rich history and a promising future as part of the solution to 21 st century challenges of meeting multifarious needs of the rural people for house construction, thatching, roofing, basket making, bows, food, furniture, fodder, pulp and paper and so on. Among the bamboo growing countries China stands first in the species diversity in position with 33 genera and 450 species. India is second largest diversity centre; comprises 148 species in 29 genera of bamboos are currently thought. The maximum concentration of species is found in the deciduous and semi evergreen regions of North-east and the tropical moist deciduous forests of North and South India except in Kashmir region. The North-eastern hilly States of India nearly 90 species of bamboos, 41 of which are endemic to that region. There are 3 large genera (Bambusa, Dendrocalamus and Ochlandra) of bamboos in India with more than 10 species each. Together, these three genera represent about 45% of the total bamboo species found in India. More than 50 per cent of the bamboo species occur in Eastern India.

Keywords: Bamboo, poaceae, perennial plants, diversity, forest.



AUTOMATED CULTIVATING AND HABITAT STABILIZER

T. Mohamed NADHIM

R.M.K. Engineering College, Kavaraipettai, Thiruvallur District.

Dr. M. MEENA

R.M.K. Engineering College, Kavaraipettai, Thiruvallur District.

Dr. Santhi M. GEORGE

R.M.K. Engineering College, Kavaraipettai, Thiruvallur District.

Dr. A. VIJAYALAKSHMI

R.M.K. Engineering College, Kavaraipettai, Thiruvallur District.

ABSTRACT

Today, we live in a world where technology has revolutionized the entire human race. This also paves a robust path for many multi-functional devices and innovations to appear in the present and near-future. Keeping this in mind a proportionate growth should also be contributed to the field of agriculture and land management. This project upholds the responsibility of “Cultivation” technically. This project has the proficiency to:

- Enable plants to grow in any habitat
- Conserve water in a large scale.
- Stabilize the fertility of the soil and the health of the plant
- Completely analyze the physical condition of the crops and update it live
- Reduce the workload farmer/gardener
- Reduce the cost of maintenance

This idea could completely change the perspective of farming/gardening. The prototype of this model uses moisture and other mineral sensors which constantly checks for the humidity and fertility of the soil. The current condition of the soil is continually updated to the controller board. Any set-back detected in the condition of the soil rather than the appropriate pre-set function triggers certain programs embedded in the controller board to rectify the defect using appropriate supply systems connected to the board. This way, the suitable conditions for the growth of the plants are maintained, ensuring the plants to grow beyond their natural habitat efficiently!

Keywords: Soil Fertility, Sensors, IoT, Water Conservation, Farming/Gardening,



NANOTECHNOLOGY IN AGRICULTURE

AL. SAKTHI

RMK Engineering College, Kavaraipeetai, Tiruvallur District.

Dr. A. VIJAYALAKSHMI

RMK Engineering College, Kavaraipeetai, Tiruvallur District.

Dr. G. Nixon Samuel VIJAYAKUMAR

RMK Engineering College, Kavaraipeetai, Tiruvallur District.

ABSTRACT

Nanotechnology is an emerging technology which plays an eminent role in versatile fields already. Researches made in nanotechnology has revealed that it has immense potential to resolve the many challenges faced by the agricultural field and its conventional methods. Agriculture involves usage of high levels of agrochemicals which contaminates the nature of the soil and tends to pollute nearby water bodies and groundwater. Also, usage of agrochemicals contaminates the crops and leaves chemical residues in it making it harmful for human consumption. Therefore, alternative usage of nanotechnology in agriculture helps us resolve such environment threatening factors involved in conventional agriculture. The significant interests of nanotech in agriculture includes specific applications like nano-fertilizers and nano-pesticides to trail products and nutrient levels to increase the crop productivity without causing any contamination of soil, water and protection against several pathogens and microbial diseases. The incorporation of nanotechnology in agriculture in the form of nano-fertilizers improves the absorption level of nutrients in the crops unlike the chemical fertilizers which tends to wear off due to external stimuli. Usage of these nanomaterials increases the crop yields by increasing the fertilizer nutrient availability in soil and nutrient uptake by the crops. Nano-pesticides suppresses crop diseases by acting directly on the phytopathogens through various mechanisms, including the production of reactive oxygen species. This paper gives an overview of the role of nanotechnology and nanomaterials in agriculture.

Keywords: Nanotechnology; Nano-fertilizers; Nano-pesticides



NANO MATERIALS IN ANCIENT AND CURRENT SCENARIO – AN OVERVIEW

B. KIRTHIKA

RMK Engineering College, Kavaraipettai, Tiruvallur District.

Dr. A. VIJAYALAKSHMI

RMK Engineering College, Kavaraipettai, Tiruvallur District.

Dr. G. Nixon Samuel VIJAYAKUMAR

RMK Engineering College, Kavaraipettai, Tiruvallur District.

ABSTRACT

Nano science and Nano technology play a crucial role in the present scenario. But using of nanomaterials is not a new one. There is a numerous example of ancient artefacts which were created using nano composites. The Lycurgus cup is a dazzling decorative Roman treasure from about AD400; it is made of a glass that changes color when light is shone through it. The glass contains gold-silver alloyed nano particles, which are distributed in such a way to make the glass look green in reflected light but, when light passes through the cup, it reveals a brilliant red. In the antiquities, nano particles were used by the Damascans to create swords with exceptionally sharp edges and the Romans to craft iridescent glassware. A corrosion resistant azure pigment known as Maya Blue, first produced in AD800, was discovered in the pre-columbian Mayan city of Chichen Itza. At present many nano materials like CNT play a vital role in all the industries such as medical, electronic, automobile, food safety, military etc. This paper gives an overview of the role and usage of nanomaterials in ancient and present scenario.

Keywords: Nanomaterials, Ancient nano materials, CNT, industries

SONLU ELEMANLAR METHODU İLE KAZICI YÜKLEYİCİ MAKİNEYE AİT STİK SİLİNDİRİN YAPISAL ANALİZİNİN İNCELENMESİ VE TASARIM İYİLEŞTİRME ÇALIŞMASI

Mert LÜYE

Çukurova Makine İmalat Ve Ticaret A.Ş.
ORCID ID: 0000-0001-9933-3144

Taner ERDOĞAN

Çukurova Makine İmalat Ve Ticaret A.Ş.

Ümit KARAHAAN

Çukurova Makine İmalat Ve Ticaret A.Ş.

ÖZET

Kazıcı yükleyici makinelerde stik grubu tasarımı çok büyük önem arz etmektedir. Kazı sırasında motor devrine bağlı ani ivmelenmeler sonucu hidrolik sistemde oluşan anlık yüksek basınçlar silindirlere ve montaj elemanlarını kritik gerilmelere maruz bırakmaktadır. Bu zorlu çalışma şartları göz önünde bulundurularak mevcut stik silindiri tasarımı, saha testlerine tabi tutularak sonlu elemanlar metodu ile yapısal olarak incelenecektir. Test ve yapısal analiz sonuçları doğrultusunda daha mukavim bir tasarım yapılması amaçlanmıştır. Prototip kazıcı yükleyicinin saha testlerinde 18000 çevrim ömür süresi sonucu stik silindiri tasarımında bağlantı elemanı olarak kullanılan 10.9 kaliteye sahip 8 adet M12x1,5x60-38s civatanın deformeye uğradığı ve tasarımın çalışamaz duruma geldiği tespit edilmiştir. Aynı çalışma şartlarında modellenerek gerçekleştirilen yapısal analiz sonucuna göre 14597 çevrim ömür süresi sonunda civataların deformeye uğradığı tespit edilmiştir. Saha testi ile yapısal analiz sonuçları arasındaki farkın, saha testinde makine operatörünün aralıklarla çalışmak zorunda olmasının sebep olduğu düşünülmektedir. Bu veriler doğrultusunda sürekli mukavim bir stik silindiri tasarımı yapılması hedeflenmiştir. Yapılan yeni tasarımda silindir ile silindir başı arasındaki bağlantıyı sağlayan 10.9 kalitede 8 adet M12x1,5x60-38s civatalar kaldırılmıştır. Bağlantı, silindir içine klavuz ve silindir başına dış açılarak doğrudan sağlanmıştır. Yeni stik silindiri tasarımı aynı çalışma koşullarında modellenerek sonlu elemanlar yöntemiyle analiz edilmiştir ve analiz sonuçlarına göre 521440 çevrim ömür süresine sahip, eski tasarıma göre 35,72 kat daha büyük ömür süresine sahip bir tasarım elde edildiği tespit edilmiştir.

Anahtar Kelimeler: Mukavim, Sonlu Elemanlar Methodu, Yapısal Analiz, Ömür Süresi



INVESTIGATION OF THE STRUCTURAL ANALYSIS OF THE STICK CYLINDER OF THE BACKHOE LOADER MACHINE WITH THE FINE ELEMENT METHOD AND THE DESIGN IMPROVEMENT STUDY

ABSTRACT

Stick group design is great importance in backhoe loader machines. The instantaneous high pressures that occur in the hydraulic system as a result of sudden accelerations due to engine speed during excavation expose the cylinders and assembly elements to critical stresses. Considering these difficult operating conditions, the current stick cylinder design will be subjected to field tests and structurally examined by the finite element method. It is aimed to make a more durable design in line with the test and structural analysis results. In the field tests of the prototype backhoe loader, it was determined that 8 bolts M12x1.5x60-38s of 10.9 quality, which are used as fasteners in the stick cylinder design, were deformed and the design became inoperable, as a result of a lifetime of 18000 cycles. According to the results of the structural analysis carried out by modeling under the same operating conditions, it was determined that the bolts were deformed at the end of 14597 cycle life. It is thought that the difference between the results of the field test and the structural analysis is due to the fact that the machine operator has to work at intervals in the field test. In line with these data, it is aimed to design a continuous resistant stick cylinder. In the new design, 8 bolts M12x1.5x60-38s of 10.9 quality, which provide the connection between the cylinder and the cylinder head, have been removed. The connection is made directly by tapping into the cylinder and threading the cylinder head. The new stick cylinder design was modeled under the same operating conditions and analyzed using the finite element method, and according to the results of the analysis, it was determined that a design with a 521440 cycle life time, 35.72 times longer than the old design, was obtained.

Keywords: Strength, Finite Element Method, Structural Analysis, Life Cycle



CHROMIUM INSERTION INTO ZIRCONIUM WAFER SURFACE

Hassan GUENDOZ

Mechanics Research Center (CRM), BP N73B, Ain El Bey, 25021 Constantine, Algeria.

ORCID ID: 0000-0001-5013-1429

ABSTRACT

Chromium ions were inserted into zirconium target with different bombardment energies using the SRIM software. In fact, the introduction of chromium ions improves the corrosion resistance of the implanted zirconium surface. The depth of the doped zone in the zirconium target is related to the incident energy where the mean thicknesses were 313, 552, and 1056 Å for the energies 50, 100, and 200 KeV, respectively. Chromium ion implantation creates damage in the zirconium wafer. The quantity of the displaced Zr atoms from their original sites due to the collision with Cr ions is proportional to the ion beam energy. Moreover, the phonons amount increases when the ion beam energy increases. The sputtering yield of Zr atoms attains its maximum value for the energy 100 KeV. Then, the sputtering yield diminishes as the acceleration energy keep increasing because some ejected zirconium atoms are located inside the target and the kinetic energy is insufficient to bring them to the surface.

Keywords: Chromium, Zirconium, Ion implantation, SRIM.

REAKTİF KONTROLLÜ SIKIŞTIRMA İLE ATEŞLEMELİ BİR MOTORDA LPG-DİZEL YANMASININ DENEYSSEL İNCELENMESİ

Selin UĞURAL

Erciyes University, Faculty of Engineering, Department of Mechanical Engineering
ORCID ID: 0000-0003-1626-8127

Prof. Dr. Bilge ALBAYRAK ÇEPER

Erciyes University, Faculty of Aeronautics and Astronautics, Department of Aerospace Engineering
ORCID ID: 0000-0001-5556-5170

ÖZET

Günümüzde otomobil kullanımının artmasıyla birlikte oluşan ciddi enerji ve çevre sorunları ile birlikte hızla artmakta olan katı emisyon standartları, içten yanmalı motorların performansının artırılmasına yönelik çalışmaların önem kazanmasına neden olmuştur. Araştırmacılar tüm bu sorunlara çözüm olabilecek alternatif yakıt kullanımı üzerinde uzun yıllardır çalışma yapmaktadırlar. Konvansiyonel yanma türlerinin dışında farklı yanma türleri üzerinde yapılan çalışmalar alternatif yanma modları arasında homojen dolgulu sıkıştırma ile ateşlemeli (HCCI), kısmi ön karışimli yanma (PPC) ve Reaktif Kontrollü Sıkıştırma ile Ateşlemeli (RCCI) yanma modlarının araştırılmasını zorunlu hale getirmiştir. RCCI yanması, emme manifoldundan enjekte edilen düşük reaktiviteli yakıtın (LRF) giriş stroku sırasında silindirdeki hava ile karıştırıldıktan sonra yüksek reaktiviteli yakıtın (HRF) direkt enjektör (DI) yardımıyla enjekte edilmesiyle gerçekleşir. Bu çalışmada bir dizel motorun RCCI yanma modunda benzin-dizel ve LPG-dizel yakıtlarının deneysel incelemesi gerçekleştirilmiştir. Alternatif yakıt kullanımına uygun hale getirilen LD820 motorunda yakıt karışımı olarak direkt silindir içerisine püskürtülen yüksek reaktiviteli dizel yakıt ve emme portuna püskürtülen düşük reaktiviteli LPG, Benzin yakıtları ele alınmıştır. Elde edilen sonuçlara bakıldığında LPG yakıtının deneylerde kullanılması ile yüksek verim elde edilmiştir. Ayrıca LPG ilavesinin güç değerini benzin ilavesine göre daha fazla artırdığı görülmüş, NO ve is emisyonları açısından LPG ile yapılan deneyde %30-%40 oranında maximum seviyeye çıkan emisyonlar LPG oranının artırılması ile azalmıştır. Benzin-dizel ile yapılan deneylerde LPG-dizele göre daha düşük seviyelerde emisyon elde edilmiştir.

Anahtar Kelimeler: RCCI, LPG-Dizel, Benzin-dizel, Emisyon, Performans

EXPERIMENTAL INVESTIGATION OF LPG-DIESEL COMBUSTION AT AN IGNITION ENGINE WITH REAGENT CONTROLLED COMPRESSION

ABSTRACT

Today, strict emission standards which are increasing rapidly with the serious energy-environmental problems caused by the increase in the use of automobiles have led to the importance of studies to increase the performance of internal combustion engines. Researchers have been working for many years on the use of

alternative fuels, which can be a solution to all these problems. Studies on different combustion modes include the investigation of homogeneous filled compression ignition (HCCI), partial premixed combustion (PPC) and reactive controlled compression ignition (RCCI) combustion modes among alternative combustion modes made it necessary except for conventional combustion types. RCCI “which is a fuel technology that provides an opportunity to control burning stage, time and reactivity of two different fuel to get a fuel mixture inside the cylinder”, occurs after low reactivity fuel that is injected from intake manifold, is mixed with air in the cylinder during entrance stroke and high reactivity fuel is injected with the help of a direct injector. Experimental investigation of gasoline-diesel and LPG-diesel fuels in RCCI combustion mode of a diesel engine was carried out at this work. High reactivity diesel fuel sprayed directly into the cylinder as fuel mixture and low reactivity LPG-Gasoline fuels sprayed into the intake port focused on in the LD 820 engine made suitable for alternative fuel use. According to the results obtained, high efficiency was acquired with the usage of LPG fuel in the experiments. Also it was observed that LPG addition has increased the power value more than gasoline addition. Emission that go up to the maximum level with the rate of %30 and %40, decreased with the usage of LPG, in terms NO and soot emissions in the experiments that is conducted with LPG. But lower levels of emissions were observed in the experiments conducted with gasoline-diesel experiments than gasoline-LPG experiment.

Keywords: RCCI, LPG-Diesel, Gasoline-Diesel, Emission, Performance

1 GİRİŞ

Günümüzde artan taşıt kullanımı ile birlikte hava kirliliği standartlarını zorlayan bir kirlilik sorunu öne çıkmaktadır. İnsan sağlığını tehdit eden bu sorun üzerinde yoğunlaşan araştırmacılar çalışmaları sonucunda alternatif yakıt kullanımına ilişkin bazı tezler ortaya koymuşlardır. Bu tezlere yönelik olarak alternatif yakıt kullanımının artan çevre sorunlarına çözüm olacağı gibi azalan yakıt rezerv sorununa da çözüm olabilmesi amaçlanmıştır.

Dizel motorlar yüksek verim ve moment, artan devir sayıları, dayanıklılık sağlayan ve benzin motorlarına kıyasla daha düşük karbon monoksit (CO) ve hidrokarbon (HC) emisyonu salınımı gibi üstünlükleri sebebiyle özellikle hafif karayolu taşıtlarında son yıllarda daha yaygın kullanılmaya başlanmıştır. Ancak dizel motorlarda özellikle petrol köklü yakıtlar kullanıldığı takdirde yüksek oranda azot oksit (NO_x), is ve partikül madde (PM) emisyonu üretirler. Dizel motorlarında yakıt ekonomisi sağlamak ve zararlı egzoz emisyonlarını azaltmak için çeşitli yöntemler uygulanmaktadır[1].

Dizel motorlarda karışımın homojen olmaması sebebi ile lokal zengin fakir karışımı bölgeleri oluşmakta ve yanma odasında yüksek sıcaklıkta gerçekleşen yanma sonucu NO_x ve is emisyonları ortaya çıkmaktadır. Düşük sıcaklıklarda oluşturulan yanma NO_x oluşumunu engellemektedir. Bununla birlikte yanma odasında tutuşma gecikmesi süresi uzamış olduğundan dolayı daha homojen bir karışım oluşturulabilmesi için zaman tanımış

olacaktır.

Reaktivite Kontrollü Sıkıştırma Ateşleme (RCCI), kontrol edilemeyen düşük sıcaklıktaki yanmayı çözmek için kullanılan bir yöntemdir. Düşük sıcaklıklarda meydana gelen RCCI yanması emme havası basıncının artırılmasına ve egzoz gazı resirkülasyonu (EGR) uygulanarak karışımın seyreltilmesine imkan tanımaktadır[2].

RCCI yanması düşük sıcaklıklarda meydana geldiğinden özellikle düşük motor yüklerinde CO ve HC emisyonları artmaktadır. Farklı reaktif özelliklerde yakıtlar kullanılarak ve emme havası giriş sıcaklığı artırılarak CO ve HC emisyonları azaltılabilmekte ve yanma kontrol edilebilmektedir[3]. Çift yakıt kullanımının motor üzerindeki etkileri farklı parametreler kullanılarak araştırılmıştır. Yapılan araştırmalar sonucunda kullanılan alternatif yakıtlardan biri de LPG-dizel yakıt karışımı olmaktadır.

Bu çalışmada LPG yakıtının düşük maliyet kolay bulunabilirlik ve diğer yakıtlara göre çevreyi daha az kirleten etkilerinden dolayı yakıt karışımında kullanılma sebebi olmuştur. Uygulanacak stratejiler ile çalışmada RCCI yanma modlu bir dizel motorda LPG-dizel yakıtlarının kullanılması ile düşük emisyon ve yakıt tüketimli motor teknolojisi geliştirilmesi üzerine çalışmalar yapılmıştır. Karşılaştırmalı bulgular elde edilmesi amacıyla benzin dizel karışımli deney dataları çalışmada kullanılmıştır.

2 YÖNTEM

Deneyel çalışma için motor modifikasyonu ile sisteme EGR hattı ve tüp bağlantıları gerçekleştirilmiştir. Deney aşamalarında, deney motoru saf dizel yakıtı ile çalıştırılmış veriler kaydedilmiştir, akabinde benzin-dizel ve LPG dizel yakıtları ile testler gerçekleştirilmiştir. Deney motoruna Benzin ve LPG yakıtının motor içerisine verilmesini sağlamak için emme manifoldu üzerine yakıt enjektörü monte edilmiştir. Enjektörün pulse miktarını ayarlayabilmek için sistem üzerine kontrol kartı takılmıştır. Deneyde kullanılacak tek silindirli dört zamanlı motor saf dizel yakıt ile yapılan deneyler haricinde saf LPG yakıtı ile farklı devirlerde çalıştırılarak veriler toplanmıştır. Deneyler sabit devirde 2000 d/d için tekrar edilmiştir. Silindir içerisinde oluşan basınç değerleri osiloskop ve enkoder yardımıyla Picoscope 6 programı içerisine aktararak veriler bilgisayar ortamına aktarılmıştır. Özgül yakıt sarfiyatı, efektif verim, ön karışım oranı (rp) gibi değerler yakıt alt ısı değeri ve deney verilerine bağlı olarak formüller yardımıyla hesaplanmıştır. Deneylerde test motoru olarak tek silindirli dört zamanlı Antor marka 4LD820 model dizel motor kullanılmıştır. Tablo 1’de motora ait özellikler verilmiştir. Egzoz gazı emisyon cihazı yardımıyla deneylerde elde edilen emisyonlar değerlendirilmiştir (Tablo 2).

Tablo 1. Deney Motoru Özellikleri

Tip	4LD 820
Silindir Sayısı (Adet)	1
Silindir Hacmi (cm ³)	817
Silindir Çapı (mm)	102
Strok (mm)	100

Tablo 2. Emisyon Cihazı Ölçüm Aralıkları [4]

CO	0...10 %Vol
CO ₂	0...20 %Vol
HC	0...20000 ppmVol
O ₂	0...21 %Vol
NO _x	0...5000 ppm
Lambda	0...5

Sıkıştırma Oranı	17:1
Motor Devri (d/d)	2600 (3000)
Motor Gücü (BG)	15/(17)

Deneyel çalışmada 50 kW'lık bir hidrolik dinamometre kullanılmış ve dinamometrenin ölçtüğü değerler ise PC 101BMS kontrol panosu yardımıyla okunmuştur. Deneylerde kullanılan yakıtlara ait özellikler Tablo 3'de verilmiştir.

Tablo 3. Deney Yakıt Özellikleri[5-6-7]

Özellik	Birim	Benzin	Dizel	LPG
Yoğunluk(15°C ta)	K g/m ³	740	840	2,78
Alt ısıl değeri	K j/kg	43500	42700	45812

Deneyel sisteme ait görüntü şekil 1'de verilmektedir.



Şekil 1. Deney Düzenegi

RCCI yanmasında ön karışım oranının etkisini gözlemlemek için gerçekleştirilen deneylerde r_p hesabı için eşitlik (1) den faydalanılmıştır.

$$r_p = \frac{m_{LPG} \times H_{uLPG}}{m_{LPG} \times H_{uLPG} + m_{dizel} \times H_{udizel}} \times 100 \quad (1)$$

r_p : LPG yakıtının karışımında bulunma oranı [%]

m_{LPG} : LPG kütleli debisi (g/s)

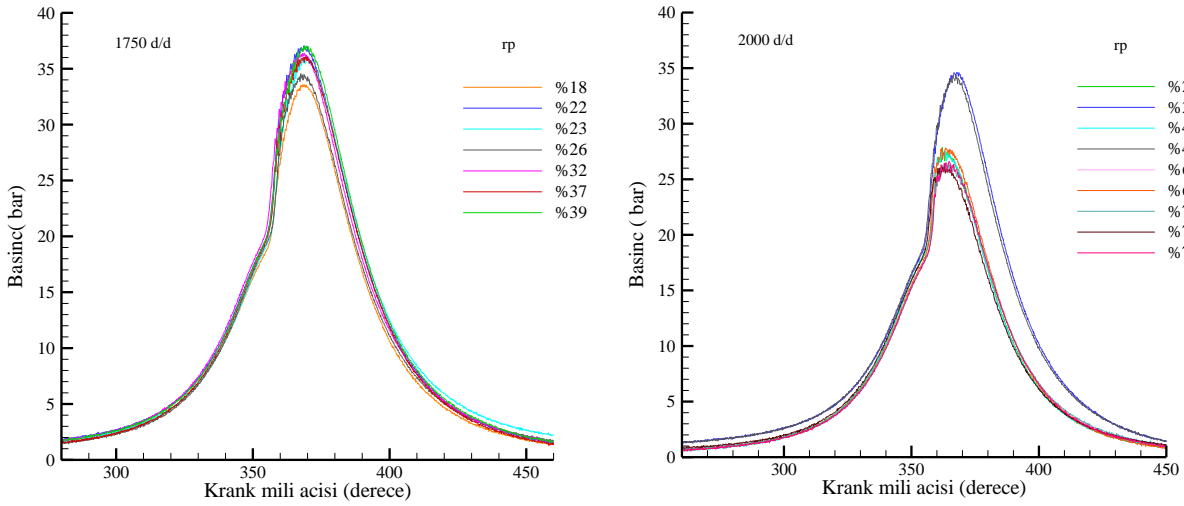
m_{dizel} : dizel yakıtın kütleli debisi (g/s)

H_{uLPG} : LPG alt ısıl değeri (kJ/kg)

H_{udizel} : dizel alt ısıl değeri (kJ/kg)

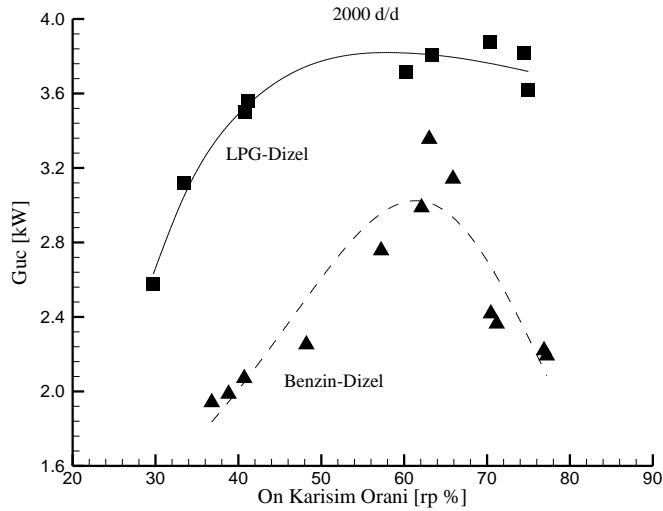
3 Bulgular

Deneysel çalışmada sabit devir sayısında (2000d/d) benzin-dizel ve LPG-Dizel karışımları farklı r_p değerleri için test edilmiştir. Şekil 2’de 1750 d/d ve 2000 d/d devir sayılarındaki krank mili açısı ile Basınç değişimleri LPG-Dizel karışımı için verilmektedir. R_p oranının artması ile basınç değerlerinde azalmalar olduğu görülmüştür. Maksimum basınç değerleri %39 r_p ve %33 r_p değerlerinde sırasıyla 1750 ve 2000 d/d ‘da elde edilmiştir. 2000 d/d incelendiğinde ön karışım oranının artması %75 ile basınç değerlerinde azalma olduğu görülmektedir. Bunun sebebinin artan LPG oranının yanmayı olumsuz yönde etkilediği düşünülmektedir.



Şekil 2. Farklı r_p Değerlerinde 1750 d/d Ve 2000 d/d İçin Silindir İçi Basınç Değişimleri

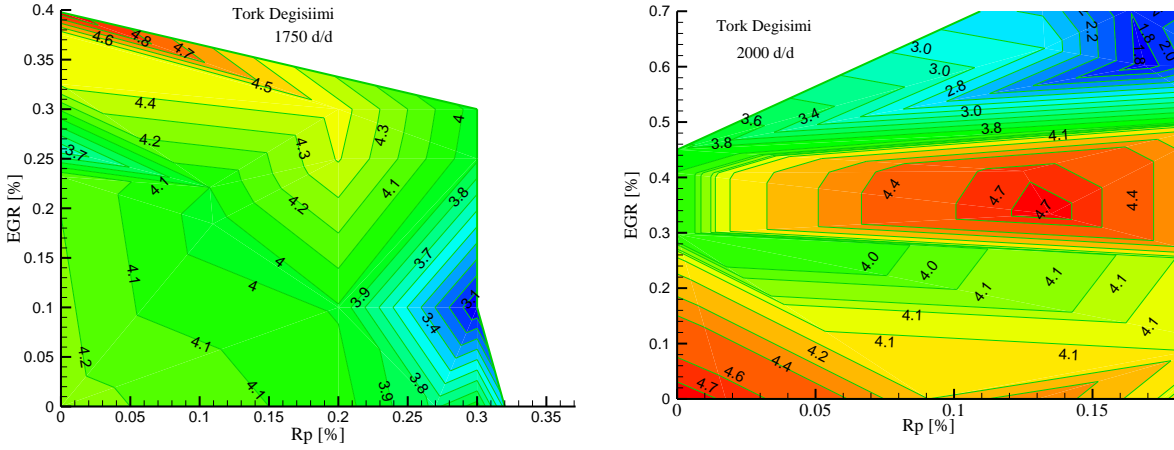
2000 d/d devir değerinde elde edilen efektif güç grafiği Şekil 3’de görülmektedir. LPG-dizel karışımlarında elde edilen güç değerlerinde artış gözlenmektedir. Ön karışım oranının artması ile güç değerleri yaklaşık %50 r_p değerine kadar artmış akabinde azlama şeklinde değişim göstermiştir. Maksimum güç değerleri yaklaşık 3.8 ve 3 civarında sırasıyla LPG-dizel ve Benzin-dizel karışımları için elde edilmiştir.



Şekil 3. Değişken r_p Değerlerine Göre Güç Değişimi

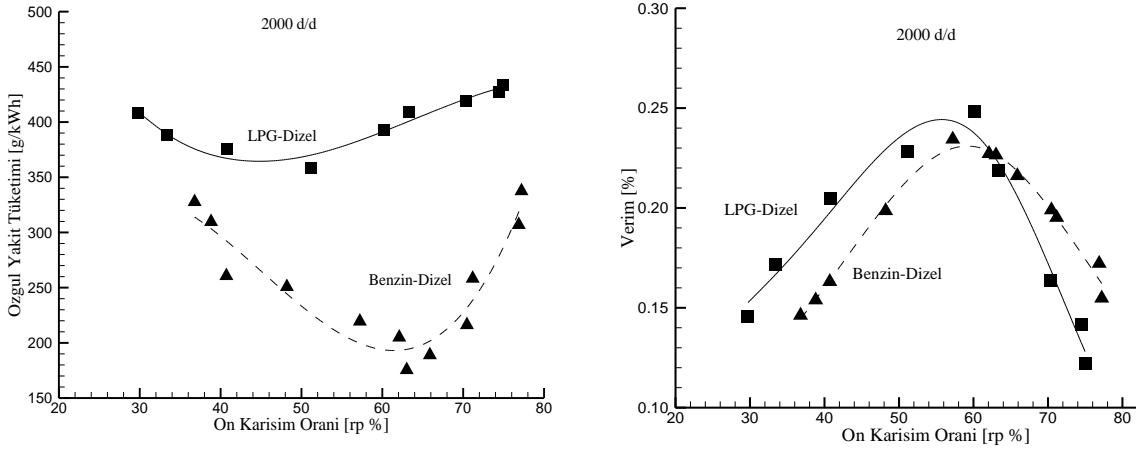
Şekil 4’de 1750d/d ve 2000 d/d devirlerdeki tork değişimleri r_p ve r_p oranlarına bağlı olarak sunulmuştur.

1750 d/d devir sayısında yüksek EGR oranı düşük rp oranlarında yüksek tork değerleri görülmektedir. Artan LPG oranı ve azalan EGR değerlerine göre tork değişimi azalma eğilimi göstermektedir. Torkun yüksek seviyelerden sonra azalma göstermesinin sebebi düşük motor hızlarında silindir içerisine giren hava hızı düşmesi ve karışım oranının bozulması olarak gösterilebilir. Bunun yanı sıra 2000 d/d artan tork değişimi doğru oranlarda yakıt karışımı elde edildiğini göstermektedir. Uygun EGR oranı ve rp değerleri ile max tork elde etmek mümkündür.



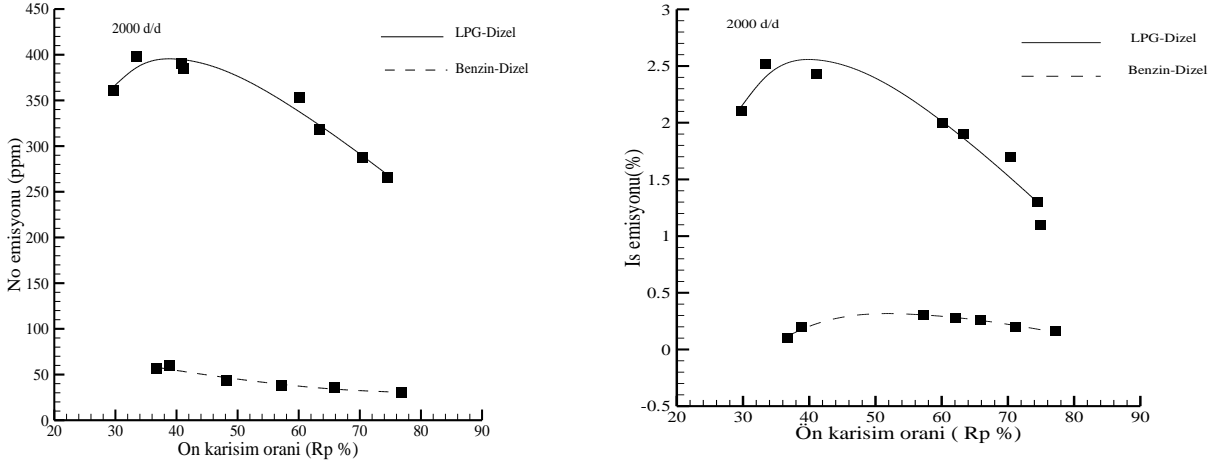
Şekil 4. Farklı rp ve EGR Oranlarına Göre Tork Değişimi

Motorun stabil çalışma durumunda kWh'lik iş başına tüketmesi gereken yakıtın gram cinsinden değeri özgül yakıt tüketimini vermektedir. LPG-dizel yakıtına ait öyt değerleri benzin-dizel karışımına nazaran daha yüksek elde edilmiştir (Şekil 5). Max değerler rp'nin artması ile artmış ve 450 g/kWh civarında elde edilmiştir. rp değerinin 45-50 olduğu aralıkta ise minimum ÖYT değerleri elde edilmiştir. Benzin –dizel karışımı için daha düşük değerler elde edilmiştir. Minimum ÖYT değeri yaklaşık 60-70 rp aralığında elde edilmiştir. Maksimum ÖYT değeri olarak ise 350g/kWh civarında değerler elde edilmiştir. Motor milinden alınan işin toplam enerjiye oranı efektif verim değerini vermektedir. Motorların LPG-dizel karışımı ile yapılan deneylerde verim benzin-dizel karışımlarına nazaran daha yüksek elde edilmiştir. Bunun sebebi LPG' nin ısıl değerinin daha yüksek olması ve homojen karışım oluşturmaya elverişli özelliği sebebiyle daha verimli bir yanma elde edilebildiği söylenebilir. LPG-Dizel ve Benzin-Dizel çift yakıtlarının karşılaştırılması olarak verildiği Şekil 5'de ön karışım oranının %50-60 seviyelerinde maksimum değere ulaştığı ve sonra düşüşe geçtiği görülmektedir. Maksimum verim değerleri %25 ile LPG-dizel karışımında elde edilirken yaklaşık %23 civarında benzin-dizel karışımları için elde edildiği görülmektedir.



Şekil 5. Değişken rp Değerlerine Bağlı Özgül Yakıt Tüketimi ve Verim Değişimleri

Emisyon değerlerinin ön karışım oranına bağlı değişimleri NO ve is emisyonları açısından Şekil 6'da sunulmuştur. İs oluşumunun başlıca nedeni dizel yakıtın silindir içinde yeterli hava bulamaması ve zamanında hava ile hızlı bir şekilde karışmaması ve buharlaşmaması olarak ifade edilebilir. LPG oranı arttıkça is oluşumuna daha çok sebep olan, hava ile daha zor karışan ve daha zor buharlaşan dizel yakıtı azalacağı için is emisyonları önemli ölçüde azalmaktadır. Her iki deney verileri de göz önüne alındığında ön karışım oranı %30 seviyelerinde iken ciddi oranda artış gözlenmiştir. Daha sonra LPG oranı arttıkça emisyon özellikleri düzenli azalma göstermiştir.



Şekil 6. Değişken rp Değerlerinde NO ve İs Emisyon Değişimleri

4 SONUÇ

Bu çalışmada tek silindirli bir dizel motor Antor LD820 deneylerde kullanılmıştır. RCCI yanma modunda LPG-dizel özellikle ele alınmış, 2000d/d sabit devirde benzin-dizel karışımları ile karşılaştırmalı olarak sunulmuştur. Deneylerde rp oranının verim, özgül yakıt tüketimi, emisyonlar üzerine etkisi araştırılmıştır. Deneysel çalışma sonucu elde edilen veriler kısaca özetlenecek olur ise:

- 2000 d/d değerinde en yüksek silindir basıncı 35 bar olarak %33,5 LPG bulunduğu durumda elde edilmiş ve LPG oranı arttıkça silindir içi basınç düşmüştür. %75,08 LPG oranında ise minimum 25 bar basınç değeri elde edilmiştir.
- 1750 d/d değerinde en yüksek silindir basıncı ise % 39,9 LPG oranında 38 bar olarak bulunmuştur. LPG oranı %18,5 değerine düştüğünde ise silindir içi basınç değeri 33 bar olarak ölçülmüştür.
- LPG-dizel karışımli deneyde %54 LPG oranında 2000 d/d değerinde en yüksek güç değerine 3,8 kW'a ulaşılmış, benzin-dizel karışımli deneyde %62 benzin oranında ise en yüksek güç değeri 3 kW olarak bulunmuştur. Dolayısıyla bu iki deney karşılaştırıldığında aynı devir sayısında LPG ilavesinin güç değerini benzine göre daha fazla artırdığı sonucuna ulaşılmıştır.
- 2000 d/d değerinde yapılan LPG-dizel ve benzin-dizel karışımli deneyler kıyaslandığında en az yakıt tüketimi en çok verim elde edilen LPG oranının %50, benzin oranının ise %60 olduğu görülmüştür. Bir diğer durum ise LPG ilavesi yakıt tüketimi açısından benzine göre daha fazla olurken efektif verim benzine göre daha yüksek olmaktadır.
- NO ve is emisyonları açısından LPG ile yapılan deneyde %30-%40 oranında maximum seviyeye çıkan emisyonlar LPG oranının artırılması ile azalmıştır. Fakat benzin-dizel ile yapılan deneylerde LPG-dizele göre daha düşük seviyelerde emisyon gözlenmiştir.

5 KAYNAK

1. Hoçur, A., 2015.Yenilenebilir Alternatif Yakıtların Dizel Motorlarda Kullanımının Performans Ve Emisyonlar Üzerindeki Etkilerinin İncelenmesi. Gümüşhane Üniversitesi Fen Bilimleri Enstitüsü, Yüksek Lisans Tezi, Gümüşhane, 91 s.
2. Pachiannan, T., Zhong, W., Rajkumar, S., He, Z., Leng, X., Wang, Q., 2019. A Literature Review Of Fuel Effects On Performance And Emission Characteristics Of Low-Temperature Combustion Strategies. Applied Energy 251:113380
3. Krishnamoorthi, M., Malayalamurthi, R., He, Z., Kandasamy, S., 2019. A review on low temperature combustion engines: Performance, combustion and emission characteristics. Renewable And Sustainable Energy Reviews 116:109404
4. Web sayfası : <https://silo.tips/download/girne-mah-kkyal-merkezi-b-blok-no-maltepe-stanbul-t-pbx-f-e> (Erişim tarihi: Temmuz 2021)
5. Web sayfası: <http://www.hanaenerji.com.tr/docs/TEP.pdf> (Erişim tarihi: Temmuz 2021)
6. Web sayfası: <http://www.opet.com.tr/ultra-force-urunleri> (Erişim tarihi: Temmuz 2021)
7. Web sayfası: https://www.kmo.org.tr/resimler/ekler/473ee1e407b6a82_ek.pdf (Erişim tarihi: Temmuz 2021)



MÉCANIQUES DES COMPOSITES TIC-NI FABRIQUÉS PAR LA MÉTALLURGIE DES POUDRE (FRITTAGE EN PHASE SOLIDE)

Lahcene MEBARKI

Centre de Recherche en Mécanique BPN ° 73B, 25021 Constantine, Algeria.

Lamine GHALMI

Université A/MIRA Bejaia laboratoire de technologie des matériaux et du génie des 2procédés Algerie

Kamel FEDAOUI

ISTA, University of Constantine1, Algeria

Mosbah ZIDANI

Faculty of Technology, University of Batna 2; Batna, Algeria

ORCID ID: 0000-0002-4716-5924

ABSTRACT

The influence of Ni content (5,20,50) on the microstructure and mechanical properties of TiC, Ni alloys developed by powder metallurgy (solid phase sintering) of TiC, Ni samples was studied. It was found that coherent boundaries between TiC and Ni were formed after sintering because Ni was attached to TiC in powder form. The particle growth by dissolution and precipitation of TiC in Ni was limited during sintering at 1350 °C, below the melting point of Ni. Therefore, the TiC particle size did not change with increasing Ni percentage. However, the TiC grain size increased with increasing Ni content (above the melting point of Ni) because dissolution and precipitation of TiC was promoted in the molten Ni. The flexural strength (~1400N/ mm²) of the sintered TiC-20Ni alloy at 1450 °C in this study was higher than that (5 and 50) of the TiC-Ni composite in the previous 50Ni study due to the effect of enlarged grains. The hardness was also improved by decreasing the Ni content (20). As a result, it was found that the microstructure and mechanical properties of TiC-Ni composites were customized by controlling the Ni content and sintering temperature in the process suggested in this study.

Keywords: composite carbide TiC,Ni, microstructure, mechanical properties density



3-D QUANTITATIVE STRUCTURE INVESTIGATION OF GREY CAST IRON FOAMS BY MICRO-CT IMAGES

Ali Can KAYA

Mechatronic Systems Engineering, Turkish-German University, Beykoz, İstanbul

ABSTRACT

Gray cast iron foams are cellular complex structures possessing a great potential to be used as sound absorber, thermal insulator, catalyst carrier, vibration damper and electrodes in rechargeable batteries. Characterization of those complex structures can be succeeded by 3D quantitative assessment of the micro-CT data for various applications. Here micro-CT data of the investment cast grey cast open cell iron foams was evaluated. Pores were segmented by distance transform and watershed algorithms. Afterwards labeling of the gray values was carried out and border labels were removed. Parameters including tortuosity, pore surface area, pore volume, sphericity and Euler number were determined from the labeled slices. Those parameters are of great importance for conductivity in a lithium-ion battery and tortuosity value of cast iron foams is favorable for this application. Further significant factors related with heat transfer such as strut thickness, connectivity and surface area to volume ratio were measured from binary CT slices. According to results, manufacturing method does not lead to a significant defect or irregularities impairing structural integrity and permeability of foam. Besides geometrical properties of grey cast iron foams are favorable for functional applications. Further investigations and experiments must be carried out to understand the applicability of foams for functional applications.

Keywords: micro-CT, tortuosity, foams, image processing



MECHANICAL, STRUCTURAL AND CORROSION CHARACTERISATIONS OF ALUMINIUM MATRIX COMPOSITE AMCs Al-X m.% (α -Fe₂O₃) ELABORATED BY LIQUID PHASE SINTERING

BOUTOUTA Aziza *

Mechanics Research Center, BP N73B, Constantine, Algeria.

NAOUAL Handel

Department of Civil Engineering, University of Mouhamed Cherif Messadia, Souk-Ahras, ALGERIA.

GANDOUZ Hassen

Mechanics Research Center, BP N73B, Constantine, Algeria.

ABSTRACT

The aim of this work is to contribute to the understanding of the effects of crystalline structures on the hardness and corrosion characteristics aluminium–hematite composites. So, a series of nominal Al–2, 4, 16 and, 40 wt% α -Fe₂O₃ compositions was developed by a liquid phase sintering process (700°C) from a compacted blend of high-purity powders of aluminum and hematite. The composites thus obtained were heat treated (500°C, 1 h) and characterized by means of x-ray diffraction and optical observation analyses as well as Vickers indentation testing and electrochemical measures.

Keywords: AMCs, Intermetallic compounds, DRX, Rietveld refinement, Optical observations, micro hardness Vickers and Taffel curves.



STUDY OF THE GRAIN KINETIC DURING ISOTHERMAL HEATING IN WELD REGION OF PIPELINE STEEL X70

BOUTOUTA Aziza *

Mechanics Research Center, BP N73B, Constantine, Algeria.

BLAOUÏ Mohamed Mossaab

Mechanics Research Center, BP N73B, Constantine, Algeria.

HANDEL Naoual

Department of Civil Engineering, University of Mouhamed Cherif Messadia, Souk-Ahras, ALGERIA.

BOUARÏCHA Amor

Department of Mechanical Engineering, Industrial Mechanical Laboratory. University of Badji Mokhtar, Annaba, ALGERIA.

ABSTRACT

In order to understand the growth behavior of the high frequency induction welded region of X70 pipeline steel under different conditions, the effects of austenitisation temperature and holding time during normalization processing have been experimentally determined. Samples were normalized at temperatures ranging from 900 °C to 1100 °C in increments of 50 °C for 30, 60, 100, 150 and 200 minutes. The welding process has been realized by industrial arc welding with circular weld seams ($F = 1400\text{Hz}$, $U = 15\text{KV}$). Optical micrographs were taken to measure the grain size using Jefferies Planimetric Method. The results show that the increase in heating temperature and holding time causes grain growth. With increasing time, the growth rate decreases. Conversely, the grain grows at a faster speed with the increase of heating temperature. The proportionality constant, K , and initial grain size D_0 were determined where $K = 2.26 [\mu\text{m}^2 / \text{min}]$ and $D_0 = 25.09 [\mu\text{m}]$ at 950 °C.

Keywords: Grain Growth Kinetic, Jefferies Planimetric Method, Austenitization Temperature, Holding Time, Ideal Grain Growth.

ALÜMİNYUM PROFİL ÖLÇÜM CİHAZI TASARIMI

Mehmet Ali TUNALI

KBE Mühendislik AR-GE Merkezi, Nilüfer Organize Sanayi Bölgesi, Bursa

Sercan KAYGISIZ

KBE Mühendislik AR-GE Merkezi, Nilüfer Organize Sanayi Bölgesi, Bursa

ÖZET

Günümüzde görüntü işleme teknolojileri kalite kontrol süreçlerinde birçok cihazda kullanılmaktadır. İlgili süreçlerde bu yaklaşımla hem doğruluk hem hız olarak birçok iyileşme sağlanabilmiştir. Süreçte uygun şekle ve boyuta sahip parçalar referans parça görüntüleri ile hızlı şekilde karşılaştırılmakta ve cihaz tarafından karar verilmektedir. Geleneksel kalite kontrol süreçlerinde olan gözle kontrol, ölçü aletleri ile boyutsal ölçümler gibi yaklaşımlar görüntü işleme teknikleri ile yer değiştirmektedir. Endüstriyel uygulamaların donanım sistemlerindeki maliyet düşüşleri ve matematiksel yaklaşımların gelişmesi ile birlikte bu değişimin daha da hızlanacağı tahmin edilmektedir. Bu bildiri; Alüminyum profil ölçüm cihazının (Nexus™) ve yazılımının geliştirilmesi süreci açıklanmaktadır. Cihazın ilk sürümü başarı ile geliştirilmiş ve ticarileşmiş olup ilk satışlar sonrasında müşteri geri bildirimleri ve saha gözlemleri neticesinde elde edilen deneyimlerle mevcut yapısı ergonomik kurallar doğrultusunda komple yeniden ele alınarak yenilikçi şekilde tasarlanmıştır. Cihazın dış görünüm ve yapısı ile birlikte insan-makine arakesitinde ergonomik tasarım yaklaşımı ile önemli iyileşmeler sağlanırken yazılım tarafında da Windows işletim sisteminden Java alt yapısına geçilerek IOS, Android, Linux, Windows tabanlı her türlü yapıda sistem ayırt etmeksizin çalışabilme özelliği katılmaktadır. Yazılım gelişiminde müşteri isteklerine bağlı olarak kalıp tespiti, makine yüklemesi gibi ilave modüller de geliştirilmeye devam edilmektedir. Bildiri içeriğinde cihazın geliştirme süreci, bu süreçte elde edilen tecrübeler, görüntü işleme süreçleri ile ilgili kazanımlar açıklanarak gelecek çalışmalar da vurgulanmıştır. Açıklanan çalışmanın bu alanda çalışan mühendisler için yol gösterici olacağı düşünülmektedir.

Anahtar Kelimeler: Alüminyum Profil, Profil Ölçümü, Görüntü İşleme, Ergonomi, Yazılım Geliştirme

DESIGN OF ALUMINUM PROFILE MEASURING DEVICE

ABSTRACT

Nowadays, image processing technologies are used in many devices in quality control processes. Many improvements in both accuracy and speed have been achieved with this approach in related processes. In the process, the parts with the appropriate shape and size are quickly compared with the reference part images, and the decision is made by the device. Approaches such as visual inspection, measuring instruments, and dimensional measurements in traditional quality control processes are being replaced by image processing techniques. It is estimated that this change will accelerate with the cost reductions in hardware systems of industrial applications and the development of mathematical approaches. In this paper, the development process of the Aluminum profile measuring device (Nexus™) and its software is explained. The first version of the device was successfully developed and commercialized. After the sales, it was designed innovatively by completely reconsidering its existing structure in line with ergonomic rules, with the experience gained from customer feedback and field observations. In addition to the external appearance and structure of the device, significant improvements have been achieved in the human-machine interface with the ergonomic design approach. On the software side, by switching from the Windows operating system to the Java infrastructure, the device can work in all kinds of systems based on IOS, Android, Linux, Windows without distinguishing the system. Additional modules such as mold detection and machine loading continue to be developed in software development depending on customer requests. In the paper's content, the development process of the device, the experiences gained in this process, the acquisitions related to the image processing processes were explained, and future studies were also emphasized. The study described is intended to be a guide for engineers working in this field.

Keywords: Aluminum Profile, Profile Measurement, Image Processing, Ergonomics, Software Development

GERÇEK ZAMANLI VERİLERLE ÜRETİM YÖNETİMİ YAZILIMI VE TASARIM VERİLERİNİN ENTEGRASYONU

Mehmet Ali TUNALI

KBE Mühendislik AR-GE Merkezi, Nilüfer Organize Sanayi Bölgesi, Bursa

Rafet Emir BİRCAN

KBE Mühendislik AR-GE Merkezi, Nilüfer Organize Sanayi Bölgesi, Bursa

ÖZET

İşletmelerin anlık verilerle yönetimi, günümüzün maliyet odaklı ve yüksek rekabet içeren ortamında zorunluluk haline gelmiştir. Özellikle imalat işletmelerinde birim zamanda çok sayıda ve farklı türde veri aynı anda üretilmektedir. Geleneksel yöntemde veriler çeşitli türde kâğıt formlarında bir yerden bir yere iletilirken, veri doğruluğunun teyit edilmesi de oldukça zaman alıcı ve çoğunlukla ihmal edilen bir işlemdir. Oysa verilerin anlamlandırılması ve etkili kararlar oluşturulması açısından hız ve doğruluk vazgeçilmez ölçütlerdir. Üretim yürütme sistem (Manufacturing Execution System, MES) yazılımları, süreçlerin izlenmesi ve yönetilmesinde önemli bir rol oynamaktadır. Bu bildiride; Prosüreç (PRS) üretim yönetim yazılımı ve bu yazılımın tasarım verileri entegrasyonu yönünde geliştirilmesi süreci açıklanmaktadır. PRS yazılımının ilk sürümü, küçük ve orta ölçekli firmaların üretim süreçlerinin kontrolüne ve izlenmesine yönelik olarak kullanıma sunulmuştur. Yazılım ayrıca, görsel yönetim araçlarının kullanıldığı üretim alanlarında bulunan bilgilendirme ekranlarına veri iletimi sağlamaktadır. PRS, genel üretim ve stok bilgilerinin raporlanmasına imkân vermektedir. Yazılım üzerinde yapılan geliştirme çalışmalarıyla tasarım resimleri, ürün ağaçları ve parça özelliklerinin de PRS üzerinden erişilebilir ve tanımlamaların değiştirilebilir olması sağlanmıştır. Bildiride geliştirilen yazılıma yönelik detaylar, geliştirme sürecinde elde edilen bilgi ve deneyimler ve gelecekte yapılması planlanan ileri düzey geliştirme hedefleri paylaşılmıştır. Bildirinin, akıllı fabrika veya karanlık fabrika da denilen geleceğin üretim yapılarına ait yazılımların geliştirilmesi açısından önemli bir deneyim paylaşımı olduğu öngörülmüştür.

Anahtar Kelimeler: Üretim Yürütme Sistemi (MES), Yazılım Geliştirme, Tasarım Verileri, Tasarım Verileri Entegrasyonu

PRODUCTION MANAGEMENT SOFTWARE WITH REAL-TIME DATA AND INTEGRATION OF DESIGN DATA

ABSTRACT

The management of businesses with instant data has become necessary in today's cost-oriented and highly competitive environment. Especially in manufacturing plants, many and different types of data are produced at the same time. In the traditional method, data was transferred from one place to another in various paper forms; verifying data accuracy was also a time-consuming and often neglected process. However, speed and accuracy

are essential criteria for making sense of data and generating efficient decisions. Manufacturing Execution System (MES) software plays a vital role in monitoring and managing processes.

In this paper, Prosüreç (PRS) production management software and its development process for design data integration are described. The first version of the PRS software is available to control and monitor the production processes of small and medium-sized companies. The software also provides data transmission to information screens in production areas where visual management tools are used. PRS allows reporting of general production and stock information. With the development studies on the software, design images, product trees, and part features can be accessed via PRS, and the definitions can be changed. The details of the software developed, the knowledge and experience gained during the development process, and the advanced development goals planned for the future were explained in the paper. It is foreseen that the paper is a critical experience sharing in terms of the development of software for the production structures of the future, which is also called the smart factory or the dark (lights-out manufacturing) factory.

Keywords: Manufacturing Execution System (MES), Software Development, Design Data, Design Data Integration



MODELING AND OPTIMIZATION OF THE SURFACE ROUGHNESS AND MACHINING TIME WHEN MILLING THE PA6

Aissa LAOUISSI

Mechanics Research Centre. Po, Box 73B, 25000 CONSTANTINE, ALGERIA.

ABSTRACT

The main objective of this work is to study the impact of the cutting parameters (a_p , f_z and V_c) on the evolution of the surface roughness (R_a) and the machining time during the milling of polyamid PA in using carbide inserts. The ANOVA was established in order to define the contribution of each cutting parameter on the factors studied, the approach of artificial neural networks "ANN" was then adopted to generate mathematical models of prediction, the latter were exploited in optimization of cutting parameters using genetic algorithms. In addition, the results obtained qualify the ANN and GA for monitoring the milling process.

GEMİ PERSONELİ KAYNAKLI GEMİ DİZEL MOTORU KRANKŞAFT HASARLARININ SEBEPSEL FAKTÖRLERİNİN DEĞERLENDİRİLMESİ

Şevki KUTAY

Recep Tayyip Erdogan University, Turgut Kıran Maritime Faculty, Marine Engineering
Department

ORCID ID: 0000-0002-1590-2918

Bünyamin KAMAL

Recep Tayyip Erdogan University, Turgut Kıran Maritime Faculty, Maritime Transportation
and Management Engineering Department

ORCID ID: 0000-0002-9885-114X

ÖZET

Krankşaft, geminin ana makinesinin en önemli parçalarından biridir. Büyük bir deniz kargo gemisi için ana makinenin krankşaftının arızalanması önemli bir operasyonel ve mekanik sorundur. Bir geminin ana makinesinin krankşaftı ömrü boyunca az sayıda hasar görse de maliyeti çok ağır olur. Bir geminin ana makinenin krankşaftının hasar görmesine neden olan bazı sebepsel faktörler vardır ve bunlar arasında gemi mürettebatından kaynaklanan faktörler en büyük sebepsel faktörlerden biri olarak karşımıza çıkmaktadır. Tekne ve makine (H& M) sigorta şirketleri ve armatörler için mali yük göz önüne alındığında, bir geminin gemi mürettebatı hatasından kaynaklanan ana makine krankşaft hasarının sebepsel mekanizmasının incelenmesi önleme açısından hayati önem taşımaktadır. Bu nedenle, bu çalışma, gemi mürettebatı hatasından kaynaklanan krankşaft hasarının nedensel mekanizmasına odaklanmaktadır. Bu hususta, bu makale, Bulanık Bayes Ağı yöntemi kullanılarak niteliksel ve niceliksel olarak açıklanan gemi mürettebatı kaynaklı nedensel faktörlerin olasılıksal ilişkilerini incelemektedir. Bunu takiben, sonuçların doğruluğunu artırmak için duyarlılık analizi ve aksiyom testleri icra edilmiştir. Gemi mürettebatı kaynaklı faktörler arasında, bakım ve onarımda meydana gelen personel kusurunun, mürettebat kaynaklı nedenlerin meydana gelmesini açıklayan en yüksek faktör olarak ortaya çıktığı ortaya çıkmıştır. Deniz sigortacılığı ekosistemindeki paydaşlar, gemi mürettebatından kaynaklanan riskleri azaltmak için bu araştırmanın sonuçlarından istifade edebilir.

Anahtar sözcükler: Deniz Dizel Motoru, Ana Makine Krankşaft Hasarı, Mürettebat kaynaklı sebepsel faktörler, Bulanık Bayes Metodu

EVALUATION OF CAUSAL FACTORS OF MARINE DIESEL ENGINE CRANKSHAFT DAMAGES STEMMING FROM VESSEL CREW

ABSTRACT

The crankshaft is one of the most important parts of the ship's main engine. For a large marine cargo vessel, the failure of the main engine's crankshaft is a significant operational and mechanical disaster. Although the crankshaft of a ship's main engine is damaged a few times during its lifetime, the cost becomes very heavy.

There have been some causal factors that lead to the damaging of a vessel's main engine crankshaft and among them, vessel crew-sourced factors appear as one of the largest causal factors. Considering the financial burden for hull & machinery (H&M) insurance firms and shipowners, it is vital to evaluate the causal mechanism of a ship's main engine crankshaft damage stemming from vessel crew fault for prevention. Therefore, this study concentrates on the causal mechanism of the crankshaft damage arising from vessel crew fault. In this regard, this paper examines probabilistic relationships of the vessel crew-sourced causal factors which are disclosed qualitatively and quantitatively using the Fuzzy Bayesian Network method. Following that sensitivity analysis and axiom tests are conducted to improve the accuracy of the results. Among the vessel crew originated factors, it is revealed that personel fault on repair and maintenance appears as the highest factor to explain the occurrence of the crew-sourced causes. Stakeholders in the marine insurance ecosystem can exploit the results of this research to decrease the risks arising from vessel crew.

Keywords: Marine Diesel Engine, Main Engine Crankshaft Damage, Crew-sourced causal factors, Fuzzy Bayesian Method

YENİ NESİL ARAÇLARDA KULLANILAN DOKUNMATİK KONTROL PANELİ VE MULTİMEDYA SİSTEMİNİN ELEKTRONİK PERFORMANSININ ISIL YÖNDEN SONLU HACİMLER METODUYLA İNCELENMESİ

Kemal Furkan SÖKMEN

Bursa Technical University, Faculty of Engineering and Natural Sciences, Department of Mechanical Engineering, Yildirim
Bayezid Campus

ORCID: 0000-0001-8647-4861

Emrah YÜRÜKLÜ

Daiichi Electronics R&D Center, Uludag University Technology Development Zone

ORCID: 0000-0002-7174-9321

Osman Bedrettin KARATAŞ

Bursa Technical University, Faculty of Engineering and Natural Sciences, Department of Mechanical Engineering, Yildirim
Bayezid Campus

ORCID: 0000-0003-4468-8778

ÖZET

Son yıllarda araçlarda dokunmatik panelli multimedya sistemi ve kontrol sistemlerinin kullanımı yaygınlaşmıştır. Dokunmatik panel üzerinde elektronik entegrelerin artması, panel ve tuş aydınlatmasında kullanılan LED'lerin kritik sıcaklık değerleri ve ses sistemini kontrol eden Amplifikatörün dayanım sıcaklıkları aşılması gereken mühendislik problemlerinin başında gelmektedir. Bu çalışmada örnek bir araç ön kontrol panel ve ses sistemi içinde bulunan elektronik bileşenler sıcaklık yönünden incelenmiştir. Panel aydınlatmasında kritik görev yapan LED'lerin ve ses sisteminde elektriksel olarak fazla güç çeken amplifikatörün kritik sıcaklık değerleri hesaplamalı akışkanlar dinamiği (HAD) ile incelenmiştir. Sistemin ürettiği ısı enerjisinin çevre plastik parçalara yansıttığı sıcaklık değeri ayrıca önem arz etmektedir. Çalışmada tasarım CATIA V5 R19 ticari yazılım programında Daiichi Ar-Ge birimi tarafından yapılmıştır. Isıl Analizler FloEFD ticari yazılımında eleman sayısından bağımsız çözüm elde edilerek gerçekleştirilmiştir. Analizler Steady State (Kararlı durum) şartlarında, 60 °C çevre sıcaklığında, ışıyım ile ısı transferi ve buoyancy (yer çekimi) etkileri dikkate alınarak yapılmıştır. Araç üreticisi firmanın standartlarına uygun olarak yapılan analizlerde, amplifikatör katalog bilgisine göre izin verilen maksimum jonksiyon sıcaklığı $T_j = 150$ °C'dir. Analiz sonucunda bu değer amplifikatör için $T_j=131$ °C olduğu ve sıcaklık problemi yaşanmayacağı tespit edilmiştir. Aynı şekilde panel, çerçeve ve ekran aydınlatması için kullanılan LED'lerin katalogta izin verilen maksimum sıcaklık değeri $T_j=125$ °C'dir. Analiz sonuçlarında hesaplanan LED T_j değeri 71,38 °C olarak elde edilmiştir. Sistemin herhangi bir ısıl probleminin bulunmadığı tespit edilmiştir. Isı üreten bileşenlerin çevresindeki plastik parçaların analiz sonucunda kritik sıcaklıklara ulaşmadığı görülmüştür.

Anahtar Kelimeler: Hesaplamalı Akışkanlar Dinamiği, Amplifikatör, Isı Transferi, Elektronik Soğutma, LED, Dokunmatik Panel

INVESTIGATION OF THE ELECTRONIC PERFORMANCE OF THE TOUCH CONTROL PANEL AND MULTIMEDIA SYSTEM USED IN THE NEW GENERATION VEHICLES WITH THE FINITE VOLUME METHOD IN THE THERMAL DIRECTION

ABSTRACT

In recent years, the use of touch panel multimedia and control systems in vehicles has increased. The increase in electronic integrations on the touch panel, the critical temperature values of the LEDs used in the panel and key lighting, and the withstand temperatures of the amplifier controlling the sound system are among the engineering problems that need to be overcome. In this study, electronic components in a sample vehicle front control panel and audio system were examined in terms of temperature. The critical temperature values of the LEDs, which play a critical role in panel lighting, and the amplifier, which draws more electrical power in the sound system, were investigated by computational fluid dynamics. The effect of the heat generated by the system on the surrounding plastic parts is also important. The design in the study was made by Daiichi R&D unit using commercial software CATIA V5 R19. Thermal analyzes were performed by obtaining a solution independent of the number of elements in the commercial software FLOEFD. The analyzes were carried out under steady state conditions, at an ambient temperature of 60 °C, taking into account the effects of radiation heat transfer and buoyancy. In the analyzes made in accordance with the standards of the vehicle manufacturer, the maximum allowable junction temperature $T_j = 150$ °C according to the amplifier catalog information. As a result of the analysis, this value was $T_j=131$ °C for the amplifier and it was determined that there was no temperature problem. The maximum temperature allowed in the catalog of LEDs used for panel, frame and screen lighting is $T_j=125$ °C. In the analysis results, this value was obtained as $T_j = 71.38$ °C for LED. It has been determined that the system does not have any thermal problems. As a result of the thermal analysis of the plastic parts around the heat generating components, it was observed that they did not reach critical temperatures.

Keywords: Computational Fluid Dynamics, Amplifier, Heat Transfer, Electronic Cooling, LED, Touch Panel

ON THE CHARACTERIZATION OF SPHERICAL CURVES

Ahmet YÜCESAN

Department of Mathematics, Süleyman Demirel University, Isparta, Turkey

ORCID ID: 0000-0002-5419-925X

ABSTRACT

We know that in differential geometry a curve is characterized with the help of an orthonormal moving frame adapted along the curve and its derivatives. If the curve can be continuously differentiable at least three times, then the Frenet frame is usually used. But if the curvature of the curve is zero at some points on the curve, then parallel frame which is an alternative frame is used. In this study, we derive a system of differential equations satisfied by the distance function of the curve to characterize curves with non-zero principal curvatures using the parallel frame in Euclidean 3 –space. As a consequence of this system of differential equations, we give a necessary and sufficient condition for the curve to be a spherical curve.

Keywords: Distance function, Parallel frame, Spherical curve.

1. INTRODUCTION

A curve in Euclidean 3 –space R^3 is studied by assigning at each point a certain frame, that is, a set of three orthogonal vectors. If the curve can be continuously differentiable at least three times, choosing frame along the curve is usually the Frenet frame $\{T, N, B\}$. Then the ratio of changes of the three vectors T, N and B along the curve is expressed in terms of the vectors themselves by the celebrated Frenet formulas (Theorem 3.2 in O’Neill, 2006). With this understanding, the theory of curves in R^3 is only a consequence of these fundamental formulas. So, the uniqueness and the ease of geometrical interpretation of the Frenet invariants will clearly make them retain their favored position. Therefore, the curves in R^3 are characterized according to these invariants. For instance, the condition for a curve to be a spherical curve, i.e. for it to lie on a sphere, is usually given in the form

$$\left(\left(\frac{1}{\tau} \right) \left(\frac{1}{\kappa} \right)' \right)' + \frac{\tau}{\kappa} = 0 \tag{1.1}$$

(see, page 32 in Struik, 1950). Their existence, the curve γ is required to be C^3 and γ', γ'' must be linearly independent. If the curve is only C^2 then the Frenet frame is not used along the curve. In this case, an alternative frame is used for the regular curve. To construct this alternative frame, the tangent vector T and two relatively parallel vector fields N_1 and N_2 whose derivatives along the curve are tangent are used. This frame is called a parallel frame along T . The reason for the name parallel is that the normal component of the derivatives of the normal vector fields are zero. For more on the parallel frame, see Bishop (1975), Hanson and Ma (1995).

As we mentioned above, the basic concept of this frame is to take the unique tangent vector $T(s)$ and choose

any convenient basis $\{N_1(s), N_2(s)\}$ in the plane perpendicular to $T(s)$ at each point such that the derivatives of $\{N_1(s), N_2(s)\}$ depend on only $T(s)$ and not each other. A parallel frame is not unique, in contrast to a Frenet frame. The parallel frame equations in R^3 are

$$\begin{pmatrix} T' \\ N_1' \\ N_2' \end{pmatrix} = \begin{pmatrix} 0 & k_1 & k_2 \\ -k_1 & 0 & 0 \\ -k_2 & 0 & 0 \end{pmatrix} \begin{pmatrix} T \\ N_1 \\ N_2 \end{pmatrix}. \quad (1.2)$$

for curve parametrized with arc length s . The relation between Frenet frame and relatively parallel frame is as follows:

$$\begin{pmatrix} T \\ N \\ B \end{pmatrix} = \begin{pmatrix} 1 & 0 & 0 \\ 0 & \cos\theta & \sin\theta \\ 0 & -\sin\theta & \cos\theta \end{pmatrix} \begin{pmatrix} T \\ N_1 \\ N_2 \end{pmatrix}$$

such that $\sin\theta(s) = \frac{k_1(s)}{\kappa(s)}$ and $\cos\theta(s) = \frac{k_2(s)}{\kappa(s)}$, where $k_1(s)$ and $k_2(s)$ are the principal curvature along $N_1(s)$ and $N_2(s)$, respectively. Also,

$$\kappa(s) = \sqrt{k_1^2(s) + k_2^2(s)}, \quad \theta(s) = \arctan\left(\frac{k_2(s)}{k_1(s)}\right) \quad \text{and} \quad \tau(s) = \theta'(s) \quad (1.3)$$

so that $k_1(s)$ and $k_2(s)$ correspond to a Cartesian coordinate system for the polar coordinates κ, θ with $\theta(s) = \int \tau(s) ds$.

Bishop (1975) introduced the relatively parallel frame and after giving the formulas of the relatively parallel frame, he characterized the spherical curves according to this frame as follows:

A C^2 regular curve is spherical if and only if (k_1, k_2) is on a line not through the origin. The distance of this line from the origin and the radius of the sphere are reciprocals.

Later, Okullu et al. (2019) gave a relationship between the principal curvatures if the curve is spherical.

In this work, we derive a system of differential equations characterizing regular curves which have non-zero the principal curvatures with respect to the parallel frame. Then, as an application of this system of differential equations, we give a necessary and sufficient condition for a curve to be a spherical curve.

2. A SYSTEM OF DIFFERENTIAL EQUATIONS FOR A REGULAR CURVE IN EUCLIDEAN 3-SPACE

We derive a general system of differential equations satisfied by distance function for a unit speed curve in Euclidean 3 –space R^3 . As a result of this system of differential equations we characterize spherical curves.

Let $\gamma = \gamma(s)$ be a unit speed curve with non-zero the principal curvatures with respect to the parallel frame in R^3 . The square distance function of γ is

$$d^2(s) = \langle \gamma(s), \gamma(s) \rangle.$$

We begin with the derivative of the square distance function with respect to s . Then

$$d(s)d'(s) = \langle \gamma(s), \gamma'(s) \rangle. \quad (2.1)$$

Substituting $h(s) = d(s)d'(s)$ and $\gamma'(s) = T(s)$ in (2.1), we write

$$h(s) = \langle \gamma(s), T(s) \rangle. \quad (2.2)$$

Differentiation of (2.2) with respect to s and using (1.2), we obtain

$$(h'(s) - 1) = \frac{1}{\rho_1} \langle \gamma(s), N_1 \rangle + \frac{1}{\rho_2} \langle \gamma(s), N_2 \rangle. \quad (2.3)$$

First, we leave $\langle \gamma(s), N_2 \rangle$ alone on the right-hand side of Eq. (2.3). So we get

$$\rho_1(h'(s) - 1) - \langle \gamma(s), N_1 \rangle = \frac{\rho_1}{\rho_2} \langle \gamma(s), N_2 \rangle, \quad (2.4)$$

where $\rho_1 = \frac{1}{k_1(s)}$ and $\rho_2 = \frac{1}{k_2(s)}$. Similarly, we differentiate (2.4) with respect to s and using (1.2) and (2.2), we have

$$\begin{aligned} \frac{\rho_1 \rho_2^2}{\rho_1' \rho_2 - \rho_1 \rho_2'} h''(s) + \frac{\rho_1' \rho_2^2}{\rho_1' \rho_2 - \rho_1 \rho_2'} h'(s) + \frac{\rho_2^2}{\rho_1' \rho_2 - \rho_1 \rho_2'} \left(\frac{1}{\rho_1} + \frac{\rho_1}{\rho_2^2} \right) h(s) \\ - \frac{\rho_1' \rho_2^2}{\rho_1' \rho_2 - \rho_1 \rho_2'} = \langle \gamma(s), N_2 \rangle. \end{aligned} \quad (2.5)$$

By differentiating (2.5) with respect to s and using (1.2) and (2.2), we find

$$\begin{aligned} \frac{\rho_1 \rho_2^2}{\rho_1' \rho_2 - \rho_1 \rho_2'} h'''(s) + \left(\left(\frac{\rho_1 \rho_2^2}{\rho_1' \rho_2 - \rho_1 \rho_2'} \right)' + \frac{\rho_1' \rho_2^2}{\rho_1' \rho_2 - \rho_1 \rho_2'} \right) h''(s) \\ + \left(\left(\frac{\rho_1' \rho_2^2}{\rho_1' \rho_2 - \rho_1 \rho_2'} \right)' + \frac{\rho_2^2}{\rho_1' \rho_2 - \rho_1 \rho_2'} \left(\frac{1}{\rho_1} + \frac{\rho_1}{\rho_2^2} \right) \right) h'(s) \\ + \left(\left(\frac{\rho_2^2}{\rho_1' \rho_2 - \rho_1 \rho_2'} \left(\frac{1}{\rho_1} + \frac{\rho_1}{\rho_2^2} \right) \right)' + \frac{1}{\rho_2} \right) h(s) - \left(\frac{\rho_1' \rho_2^2}{\rho_1' \rho_2 - \rho_1 \rho_2'} \right)' = 0. \end{aligned} \quad (2.6)$$

Second, we leave $\langle \gamma(s), N_1 \rangle$ alone on the right-hand side of Eq. (2.3). So we get

$$\rho_2(h'(s) - 1) - \langle \gamma(s), N_2 \rangle = \frac{\rho_2}{\rho_1} \langle \gamma(s), N_1 \rangle, \quad (2.7)$$

Considering Eq. (1.2) and taking the derivative of (2.7), we get

$$\rho_2 h''(s) + \rho_2' h'(s) + \left(\frac{1}{\rho_2} + \frac{\rho_2}{\rho_1^2} \right) h(s) - \rho_2' = \left(\frac{\rho_2}{\rho_1} \right)' \langle \gamma(s), N_1 \rangle \quad (2.8)$$

By differentiating (2.8) with respect to s and using (1.2) and (2.2), we find

$$\begin{aligned} \frac{\rho_1^2 \rho_2}{\rho_1' \rho_2 - \rho_1 \rho_2'} h'''(s) + \left(\left(\frac{\rho_1^2 \rho_2}{\rho_1' \rho_2 - \rho_1 \rho_2'} \right)' + \frac{\rho_1^2 \rho_2'}{\rho_1' \rho_2 - \rho_1 \rho_2'} \right) h''(s) \\ + \left(\left(\frac{\rho_1^2 \rho_2'}{\rho_1' \rho_2 - \rho_1 \rho_2'} \right)' + \frac{\rho_1^2}{\rho_1' \rho_2 - \rho_1 \rho_2'} \left(\frac{1}{\rho_2} + \frac{\rho_2}{\rho_1^2} \right) \right) h'(s) \\ + \left(\left(\frac{\rho_1^2}{\rho_1' \rho_2 - \rho_1 \rho_2'} \left(\frac{1}{\rho_2} + \frac{\rho_2}{\rho_1^2} \right) \right)' - \frac{1}{\rho_1} \right) h(s) - \left(\frac{\rho_1^2 \rho_2'}{\rho_1' \rho_2 - \rho_1 \rho_2'} \right)' = 0 \end{aligned} \quad (2.9)$$

Then we can give the following theorem.

Theorem 2.1 Let $\gamma = \gamma(s)$ be a unit speed curve with non-zero the principal curvatures with respect to the parallel frame in Euclidean 3 –space R^3 . Then $\gamma(s)$ satisfies the system of differential equations given by (2.6) and (2.9).

Now, we can give the following a consequence of Theorem 2.1 for characterization of spherical curve.

Corollary 2.2. If a unit speed curve γ in Euclidean 3 –space R^3 is a spherical curve, then γ satisfies the system of differential equations

$$\begin{cases} \frac{\rho_1' \rho_2^2}{\rho_1' \rho_2 - \rho_1 \rho_2'} = constant, \\ \frac{\rho_1^2 \rho_2'}{\rho_1' \rho_2 - \rho_1 \rho_2'} = constant. \end{cases} \quad (2.10)$$

Conversely, if the curve γ satisfies at least one of the differential equations in the system of differential equations (2.10), then γ is a spherical curve.

Proof. Let $\gamma = \gamma(s)$ be a unit speed spherical curve that is $\gamma = \gamma(s)$ lies on the sphere of radius r . Then

$$\langle \gamma(s), \gamma(s) \rangle = r^2$$

which implies the square distance function $d^2 = r^2$. So we see that $h = dd' = 0$. Substituting $h = 0$ and $h' = h'' = h''' = 0$ in the system of differential equations given by (2.6) and (2.9), we find the system of differential equations (2.10).

Conversely, let $\gamma = \gamma(s)$ be a unit speed Frenet curve which satisfies at least one of the differential equations in the system of differential equations (2.10). From Eqs. in (1.3) and the derivative of at least one of Eqs. in (2.10), we see that Eq. (1.1) is satisfied. Therefore $\gamma = \gamma(s)$ is a spherical curve.

REFERENCES

- Bishop, R. L. (1975). There is more than one way to frame a curve. Amer. Math. Monthly, 82, 246-251. <https://doi.org/10.2307/2319846>.
- Deshmukh S., Chen B.Y., Turki N.B. (2018). A differential equation for frenet curves in Euclidean 3-space and its applications. Romanian J. Math. Comp. Sci. 8(1), 1-6.
- Hanson, A. J., Ma, H. (1995). Parallel transport approach to curve framing. Tech. Rep. 425, Indiana University Computer Science Department.
- Okullu, P. B., Kocayigit, H., Aydın, T. A. (2019). An explicit characterization of spherical curves according to Bishop Frame and an approximately solution. Thermal Science, 23(1), 361-370. <https://doi.org/10.2298/TSCI181101049B>.
- O'Neill, B. (2006). Elementary differential geometry revised second edition. Elsevier Inc.
- Özdemir, M., Ergin, A. A. (2008). Parallel frames of non-lightlike curves, Missouri J. Math. Sci. 20(2), 127-137. <https://doi.org/10.35834/mjms/1316032813>.
- Struik, D.J. (1950). Lectures on classical differential geometry. Addison-Wesley, Reading, Mass.



MACHINE LEARNING GOOGLE AS A TOOL IN THE EVALUATION PROCESS IN MATHEMATICS “AN EXPERIENCE IN THE AMAZON - NORTHERN BRAZIL”

Prof. Dr. Aldemir MALVEIRA DE OLIVEIRA
Amazon Education Media Center (CEMEAM)

ABSTRACT

This investigation had as an experiment Google's machine learning as a tool to measure the cognitive skills of high school students in the state of Amazonas in the Mathematics curriculum component. Machine learning is an online Google App that the teacher uses as a form and/or assessment. In the case of this research, it was used as an evaluation where, it served to measure the percentage of hits and errors in proposed items in relation to certain mathematics contents and having their feedback in real time. In this way, the teacher optimized the feedback for students in real time and promoted the redefinition of the object of knowledge taught in a more punctual way, in terms of teaching and learning mathematics. This tool can be used in person or at a distance by students through smartphones, tablets, iPads and/or computers. After having access to the tool via a link sent by the teacher, students can work offline, needing only access to the network to send the respective activity. For this investigation, an evaluation was carried out considering the following objects of knowledge: properties of potentiation in R, Exponential and Logarithm. The feedbacks from this experiment enabled the teacher to re-signify the aforementioned objects of knowledge in a more punctual way. This, in turn, enhanced the real-time teaching and learning of knowledge objects for its students.

Keywords: Machine Learning; Google; Cognitive skills; Knowledge Object; Math.



FREE AND FORCED VIBRATION ANALYSIS OF SOLID STRUCTURES BY USING STRAIN BASED APPROACH

Rebiai CHERIF

University of Batna2, Faculty of Technology, Mechanical Engineering Department, Batna, Algeria.

ORCID ID: 0000-0001-7271-5011

Saidani NOUREDDINE

University of Batna2, Faculty of Technology, Mechanical Engineering Department, Batna, Algeria.

ABSTRACT

This paper deals with the development of a new strain based membrane element for static and dynamic analysis. This finite element has the two degrees of freedom at each of the four nodes and the displacement functions of the developed element satisfy the exact representation of the rigid body modes. The displacements field of this element is based on the assumed functions for the various components of strain which satisfy the compatibility equations. In static case some selected benchmarks problems are considered. For dynamic analysis both free and forced vibration analysis are considered, and Numerical computations show the good effectiveness of this developed element.

Keywords: Strain approach, dynamic analysis, finite element, linear analysis, free and forced vibration analysis.



ASSOCIATED PSEUDO-HYPERBOLIC SPACE PARTNER OF A SPACELIKE CURVE WITH TIMELIKE PRINCIPAL NORMAL

Tunahan TURHAN

Division of Elementary Mathematics Education, Süleyman Demirel University, Isparta, Turkey
ORCID ID: 0000-0002-9632-2180

Gözde ÖZKAN TÜKEL

Engineering Basic Sciences, Isparta University of Applied Sciences, Isparta, Turkey
ORCID ID: 0000-0003-1800-5718

Ahmet YÜCESAN

Department of Mathematics, Süleyman Demirel University, Isparta, Turkey
ORCID ID: 0000-0002-5419-925X

ABSTRACT

We present associated pseudo-hyperbolic space partner, radial function and radial pseudo-spherical function for a spacelike curve with timelike principal normal which does not lie on the pseudo-hyperbolic space in three dimensional Minkowski space. We get some relations between Frenet apparatus of a spacelike curve with timelike principal normal and Darboux apparatus of the associated pseudo-hyperbolic space partner of the curve in three dimensional Minkowski space. Using these relations, we obtain new results for curvature, torsion, radial function and radial pseudo-spherical function of a spacelike curve with timelike principal normal with respect to some special cases.

Keywords: Associated curve, Geodesic curvature, Pseudo-hyperbolic space, Radial function.

1. INTRODUCTION

Nowadays, the geometry and characterization of space curves in Euclidean 3-space and Minkowski 3-space are important study field for mathematicians. So, there are many literatures dealing with curvature theory and characterization of space curves. Especially, some curves have attracted the attention of many researchers because of their geometric properties. For example, rectifying curve is a space curve, where position vector always lies in its rectifying plane. The position vector of a rectifying curve is always in the direction of the Darboux vector. Therefore, rectifying curves can be interpreted kinematically as those curves whose position vector field determines the axis of instantaneous rotation at each point of the curve (Chen, 2003). This paper deals with the associated pseudo-hyperbolic space partner of the curve in Minkowski 3-space. The relations between the space curve and its associated pseudo-hyperbolic space partner are very interesting and important problem.

In Euclidean 3-space, for any regular space curve $r(s)$ with Frenet frame $\{\alpha(s), \beta(s), \gamma(s)\}$, we can write

$$\bar{r}(s) = r(s) + \lambda(s)\alpha(s) + \mu(s)\beta(s) + \nu(s)\gamma(s).$$

The curve $\bar{r}(s)$ is known generalized associated partner of $r(s)$. For the curve $\bar{r}(s)$, we have

$$\begin{aligned}\lambda'(s) &= \kappa(s)\mu(s) - 1, \\ \mu'(s) &= -\kappa(s)\lambda(s) + \tau(s)\nu(s), \\ \nu'(s) &= -\tau(s)\mu(s),\end{aligned}$$

where $\kappa(s)$ is the curvature and $\tau(s)$ is the torsion of $r(s)$ at s (Carmo,1976; Su et al., 1986).

Liu et al. (2019) study associated spherical partner, radial function and radial spherical function for space curve which doesn't lie on the sphere in Euclidean 3-space. Then, they give some relations for special curves and their associated spherical partners. Lastly, they get a new necessary and sufficient condition for the rectifying curves. Also, Turhan et al. (2021) present concept of associated pseudo-spherical partner, radial function and radial pseudo-spherical function for a non-null Lorentzian space curve which does not lie on the pseudo-sphere and get some relation between Frenet apparatus of a non-null Lorentzian space curve and pseudo-spherical Frenet apparatus of the associated pseudo-spherical partner of the curve in Minkowski 3-space.

In this work, we give concept of associated pseudo-hyperbolic space partner, radial function and radial pseudo-spherical function for a spacelike curve with timelike principal normal which does not lie on the pseudo-hyperbolic space in Minkowski 3-space. Then, we present some relations between Frenet apparatus of a spacelike curve with timelike principal normal and Darboux apparatus of the associated pseudo-hyperbolic space partner of the curve in Minkowski 3-space. Lastly, using these relations, we obtain new results for curvature, torsion, radial function and radial pseudo-spherical function of a spacelike curve with timelike principal normal with respect to some special cases.

2. PRELIMINARIES

We first briefly recall some general notions needed throughout the paper about non-null Lorentzian space curves, pseudo-spherical curves and Minkowski 3-space.

Let E_1^3 be Minkowski 3-space with the pseudo-scalar product

$$\langle u, v \rangle = u_1v_1 + u_2v_2 - u_3v_3,$$

where $u = (u_1, u_2, u_3)$, $v = (v_1, v_2, v_3) \in E_1^3$. A vector u in E_1^3 is said to be spacelike if $\langle u, u \rangle > 0$, or $u = 0$, timelike if $\langle u, u \rangle < 0$, lightlike (null) if $\langle u, u \rangle = 0$ and $u \neq 0$. Similarly, an arbitrary curve $r = r(s)$ can be spacelike, timelike or lightlike (null), if its velocity vector $r'(s)$ are spacelike, timelike or lightlike (null), respectively (Lopez, 2014).

Let $r: I \rightarrow E_1^3$, be a regular and non-null curve. The arc length parameter s of r is determined such that $\|r'(s)\| = 1$, $r'(s) = \frac{dr(s)}{ds}$. At a point $r(s)$ of r , let $\alpha(s) = r'(s)$ denote the unit tangent vector, $\beta(s)$ the unit principle normal vector and $\varepsilon_2\gamma(s) = \alpha(s) \times \beta(s)$ the unit binormal vector of r such that $\varepsilon_2 = \langle \gamma(s), \gamma(s) \rangle$. The

Frenet formulas of the frame $\{\alpha(s), \beta(s), \gamma(s)\}$ are given by

$$\begin{aligned}\alpha'(s) &= \varepsilon_1 \kappa(s) \beta(s), \\ \beta'(s) &= -\varepsilon_0 \kappa(s) \alpha(s) + \varepsilon_2 \tau(s) \gamma(s), \\ \gamma'(s) &= -\varepsilon_1 \tau(s) \beta(s),\end{aligned}\tag{1}$$

where $\varepsilon_0 = \langle \alpha(s), \alpha(s) \rangle$, $\varepsilon_1 = \langle \beta(s), \beta(s) \rangle$, $\kappa(s)$ is the curvature and $\tau(s)$ is the torsion of r at s .

We define the following notation given in (Liu, 2014) for Minkowski 3-space.

Definition 2.1. The non-null curve lying on one of the hyperquadrics (pseudo-sphere or pseudo-hyperbolic space)

$$\bar{r}(s) = \frac{1}{\sqrt{|\langle \ddot{r}(s), \ddot{r}(s) \rangle|}} \ddot{r}(s) = \beta(s)$$

is called associated curve of the curve $r(s)$ in E_1^3 .

Remark 2.1. For the special case if the curve $r(s)$ is a pseudo-spherical curve lying on one of the hyperquadrics, we don't use above definition as the notation of associated curve of the pseudo-spherical curve in E_1^3 . In the next section, we will give a new definition of associated curve for the curve lying on a hyperquadric in E_1^3 .

2.1 Pseudo-Hyperbolic Space Curves in Minkowski 3-space

Let $H_0^2(r) = \{u \in E_1^3 : \langle u, u \rangle = -d^2, d > 0\}$ be a two dimensional pseudo-hyperbolic space which is also known as two dimensional anti de-Sitter space. If $x(s)$ is a pseudo-hyperbolic space curve, then we have $\langle x(s), x(s) \rangle = -d^2$ and $x(s)$ is only a spacelike curve. We assume that $d = 1$. For a spacelike curve on pseudo-hyperbolic space, we have the Darboux frame $\{\alpha_0(s), x(s), y(s)\}$ with formulas as follows

$$\begin{aligned}\alpha_0'(s) &= \kappa_g(s) y(s) + x(s), \\ x'(s) &= \alpha_0(s), \\ y'(s) &= -\kappa_g(s) \alpha_0(s),\end{aligned}\tag{2}$$

where $\kappa_g(s)$ is the geodesic curvature.

In the following we call the unit spacelike pseudo-hyperbolic space curve simply as the pseudo-hyperbolic space curve. From Darboux formula, we have

$$y(s) = \frac{1}{\sqrt{1 + \langle x''(s), x''(s) \rangle}} [x''(s) - x(s)].\tag{3}$$

Definition 2.2. The pseudo-hyperbolic space curve $y(s)$ defined by (3) is called associated curve of the pseudo-hyperbolic space curve.

3. ASSOCIATED PSEUDO-HYPERBOLIC SPACE PARTNER OF A SPACELIKE CURVE WITH TIMELIKE PRINCIPAL NORMAL

As it is known, the non-null Lorentzian space curve in Minkowski 3-space have various causal characters. So, we consider only the a spacelike curve with timelike principal normal.

Assume that $r(\bar{s}): I \rightarrow E_1^3$ is a non-null Lorentzian space curve in Minkowski 3-space and

$$\begin{cases} f(\bar{s}) = \sqrt{|\langle r(\bar{s}), r(\bar{s}) \rangle|}, \\ r(\bar{s}) = \bar{f}(\bar{s})x(\bar{s}) = f(s)x(s) \end{cases} \quad (4)$$

where $x(s)$ is the pseudo-hyperbolic space curve with arc length parameter s .

Definition 3.1. The pseudo-hyperbolic space curve $x(s)$ defined by (4) is called associated spherical partner of the spacelike space curve $\bar{r}(s)$ with timelike principal normal in Minkowski 3-space. The function $\bar{f}(\bar{s}) = f(s)$ is called radial function of the curve $r(\bar{s})$. The geodesic curvature function κ_g of a pseudo-hyperbolic space curve $x(s)$ is called radial pseudo-spherical function of the curve $r(\bar{s})$.

Let the spacelike curve $x(s)$ be the associated pseudo-hyperbolic space partner of the spacelike curve $r(\bar{s})$ with timelike principal normal with the arc length parameter s . We assume that the curve $r(\bar{s})$ is not a pseudo-spherical curve so the function $f(s)$ is not a constant. Then, we have from (4)

$$\alpha(\bar{s}) \frac{d\bar{s}}{ds} = f(s)\alpha_0(s) + f'(s)x(s). \quad (5)$$

Considering (5), we can write

$$\alpha(\bar{s}) = \alpha_0(s)\cosh\vartheta + x(s)\sinh\vartheta \quad (6)$$

where ϑ is hyperbolic angel between the spacelike vector $\alpha(\bar{s})$ and the spacelike vector $\alpha_0(s)$. The hyperbolic angle is used here because the plane spanned by the spacelike vector $\alpha_0(s)$ and the timelike vector $x(s)$ is Lorentzian.

If we compare (5) and (6), we get

$$\frac{d\bar{s}}{ds} = \frac{f}{\cosh\vartheta} = \frac{f'}{\sinh\vartheta} = \sqrt{f^2 - f'^2}, \quad (7)$$

$$\tanh\vartheta = \frac{f'}{f} \quad (8)$$

and

$$\vartheta' = \frac{f''f - f'^2}{f^2 - f'^2}. \quad (9)$$

By using (6), we obtain

$$\kappa\beta \frac{d\bar{s}}{ds} = (\vartheta' + 1)(\alpha_0\sinh\vartheta + x\cosh\vartheta) + \kappa_g y\cosh\vartheta. \quad (10)$$

Taking into consideration (10), we can write

$$\begin{aligned} \beta &= (\alpha_0\sinh\vartheta + x\cosh\vartheta)\cosh\phi + y\sinh\phi \\ &= \alpha_0\sinh\vartheta\cosh\phi + x\cosh\vartheta\cosh\phi + y\sinh\phi. \end{aligned} \quad (11)$$

Comparing (10) and (11), we have

$$\kappa \frac{d\bar{s}}{ds} = -\frac{\vartheta'+1}{\cosh\theta} = -\frac{\kappa_g\cosh\vartheta}{\sinh\phi}, \quad (12)$$

$$\kappa \frac{d\bar{s}}{ds} = -(\vartheta' + 1)\cosh\phi + \kappa_g\cosh\vartheta\sinh\phi \quad (13)$$

and

$$\tanh\phi = \frac{\kappa_g\cosh\vartheta}{\vartheta'+1}. \quad (14)$$

Combining (6) and (11), we derive

$$\gamma = \alpha \times \beta = -(\alpha_0 \sinh \vartheta + x \cosh \vartheta) \sinh \phi - \cosh \phi y. \quad (15)$$

On the other hand, if we get derivative of (11), we get

$$\begin{aligned} (-\kappa\alpha + \tau\gamma) \frac{d\bar{s}}{ds} &= (\sinh \vartheta \cosh \phi)' \alpha_0 + (\cosh \vartheta \cosh \phi) x + (\sinh \phi)' y \\ &+ \sinh \vartheta \cosh \phi (x + \kappa_g y) + \cosh \vartheta \cosh \phi \alpha_0 - \sinh \phi \kappa_g \alpha_0. \end{aligned} \quad (16)$$

Then from (15) and (16), we arrive at

$$\tau \frac{d\bar{s}}{ds} = -(\phi' + \kappa_g \sinh \vartheta). \quad (17)$$

If we use (13) and (17) with (7), we have

$$\begin{cases} \kappa = \frac{-(\vartheta' + 1) \cosh \phi + \kappa_g \cosh \vartheta \sinh \phi}{\sqrt{f^2 - f'^2}}, \\ \tau = -\frac{\phi' + \kappa_g \sinh \vartheta}{\sqrt{f^2 - f'^2}}. \end{cases}$$

By using (12), we obtain

$$\begin{cases} \kappa = \frac{-(\vartheta' + 1) \cosh \phi + \kappa_g \cosh \vartheta \sinh \phi}{\sqrt{f^2 - f'^2}} = -\frac{\vartheta' + 1}{\sqrt{f^2 - f'^2} \cosh \phi} = -\frac{\kappa_g \cosh \vartheta}{\sqrt{f^2 - f'^2} \sinh \phi}, \\ \tau = -\frac{\phi' + \kappa_g \sinh \vartheta}{\sqrt{f^2 - f'^2}}. \end{cases} \quad (18)$$

Multiplying (11) with $\sinh \phi$ and (15) with $\cosh \phi$, we obtain

$$y = -\cosh \phi \gamma - \sinh \phi \beta$$

and multiplying (11) with $\cosh \phi$ and (15) with $\sinh \phi$, we have

$$\cosh \phi \beta + \sinh \phi \gamma = \sinh \vartheta \alpha_0 + \cosh \vartheta x. \quad (19)$$

From (6) and (19), we arrive at

$$\alpha_0 = \cosh \vartheta \alpha - \sinh \vartheta (\cosh \phi \beta + \sinh \phi \gamma)$$

and

$$x = -\sinh \vartheta \alpha + \cosh \vartheta (\cosh \phi \beta + \sinh \phi \gamma).$$

So, we give following proposition for summarize the above formulas and relations.

Proposition 3.1. Let $r(\bar{s}): I \rightarrow E_1^3$ be a spacelike space curve with timelike principal normal with Frenet frame $\{\alpha(\bar{s}), \beta(\bar{s}), \gamma(\bar{s})\}$ and $x(s)$ the associated pseudo-hyperbolic space partner of $r(\bar{s})$ with Darboux frame $\{\alpha_0(s), x(s), y(s)\}$ in Minkowski 3-space. So, we have following equalities,

$$\begin{cases} \alpha = \alpha_0 \cosh \vartheta + x \sinh \vartheta, \\ \beta = \alpha_0 \sinh \vartheta \cosh \phi + x \cosh \vartheta \cosh \phi + y \sinh \phi, \\ \gamma = -(\alpha_0 \sinh \vartheta + x \cosh \vartheta) \sinh \phi - \cosh \phi y, \end{cases} \quad (20)$$

$$\begin{cases} \alpha_0 = \cosh \vartheta \alpha - \sinh \vartheta (\cosh \phi \beta + \sinh \phi \gamma), \\ x = -\sinh \vartheta \alpha + \cosh \vartheta (\cosh \phi \beta + \sinh \phi \gamma), \\ y = -\cosh \phi \gamma - \sinh \phi \beta, \end{cases} \quad (21)$$

$$\left\{ \begin{array}{l} \frac{d\bar{s}}{ds} = \frac{f}{\cosh\vartheta} = \frac{f'}{\sinh\vartheta} = \sqrt{f^2 - f'^2}, \\ \tanh\vartheta = \frac{f'}{f}, \\ \tan\theta = \frac{\kappa_g \cosh\vartheta}{\vartheta' + 1}, \\ \kappa = \frac{-(\vartheta' + 1)\cosh\phi + \kappa_g \cosh\vartheta \sinh\phi}{\sqrt{f^2 - f'^2}} = -\frac{\vartheta' + 1}{\sqrt{f^2 - f'^2} \cosh\phi} = -\frac{\kappa_g \cosh\vartheta}{\sqrt{f^2 - f'^2} \sinh\phi}, \\ \tau = -\frac{\phi' + \kappa_g \sinh\vartheta}{\sqrt{f^2 - f'^2}}. \end{array} \right. \quad (22)$$

Remark 3.1. If $\phi \equiv 0 \pmod{\pi}$, from (14) we have $\kappa_g \equiv 0$, because of $\cosh\vartheta \neq 0$. So, from (15) and (2), $\gamma = -y$ is constant vector and the curve $r(\bar{s})$ is a planar curve.

4. CURVES WITH SPECIAL ASSOCIATED PSEUDO-HYPERBOLIC SPACE PARTNER

In this section we take into consideration the above relations of some special spacelike curves with timelike principal normal and their associated pseudo-hyperbolic space partners. By using these relations, we give some characterizations for these curves.

Theorem 4.1. If the arc length parameter of a spacelike curve with timelike principal normal is the same as its associated pseudo-hyperbolic space partner, the curve can be written as

$$r(s) = \cosh(s + b) x(s) \quad (23)$$

where b is constant and $x(s)$ is the associated pseudo-hyperbolic space partner of $r(s)$. The curvature function $\kappa(s)$, the torsion function $\tau(s)$ and the radial pseudo-spherical function $\kappa_g(s)$ of $r(s)$ satisfy

$$\left\{ \begin{array}{l} \kappa_g^2 = 4 - \kappa^2 - (\tau + \theta')^2, \\ \phi' = -\frac{2\kappa'}{\kappa\sqrt{4-\kappa^2}}. \end{array} \right. \quad (24)$$

Proof. Assume that the arc length parameter of the spacelike curve $r(s)$ with timelike principal normal is the same as its associated pseudo-hyperbolic space partner $x(s)$. So, from (7) or the first equation of (22), we arrive at

$$f^2 - f'^2 = 1.$$

So, $f(s)$ can be given as

$$f(s) = \cosh(s + b)$$

and we get (23). Taking into consideration $f(s)$ and (9), we get $\vartheta' = 1$. Thus we have from (18),

$$\left\{ \begin{array}{l} \kappa = -2\cosh\phi + \kappa_g \cosh\vartheta \sinh\phi = -\frac{2}{\cosh\phi} = -\frac{\kappa_g \cosh\vartheta}{\sinh\phi}, \\ \tau = -(\phi' + \kappa_g \sinh\vartheta). \end{array} \right.$$

These means that

$$\left\{ \begin{array}{l} \cosh^2\phi \kappa^2 = 4, \\ \sinh^2\phi \kappa^2 = \kappa_g^2 \cosh^2\vartheta \end{array} \right.$$

and

$$\kappa_g^2 = 4 - \kappa^2 - (\tau + \phi')^2.$$

If we get derivative of $\kappa \cosh \phi = -2$, we obtain

$$\phi' = -\frac{2\kappa'}{\kappa\sqrt{4-\kappa^2}}.$$

Theorem 4.2. Assume that the tangent vector field of a spacelike curve $r(\bar{s})$ with timelike principal normal and arc length parameter \bar{s} in Minkowski 3-space make a constant angle with the tangent vector field of its associated pseudo-hyperbolic space partner $x(s)$ with arc length parameter s . Then, the curve $r(\bar{s})$ can be given as

$$r(\bar{s}) = a\bar{s}x(\bar{s}) = e^{bs}x(s)$$

where a and b are constants and satisfy $a\sqrt{1-b^2} = b$. Also for the curvature function $\kappa(s)$, the torsion function $\tau(s)$ and the radial pseudo-spherical function $\kappa_g(s)$ of $r(s)$, we can give

$$\begin{cases} \kappa_g^2 = 1 - (1-b^2)e^{2b(s+c)}\kappa^2 - \left(b\sqrt{1-(1-b^2)e^{2b(s+c)}\kappa^2}\right)^2, \\ \tau = -\left(\frac{\theta'}{\sqrt{1-b^2}e^{b(s+c)}} + \frac{b\sqrt{1-(1-b^2)e^{2b(s+c)}\kappa^2}}{\sqrt{1-b^2}e^{b(s+c)}}\right), \\ \phi' = \frac{\kappa' - b\kappa}{\kappa\sqrt{1-(1-b^2)e^{2b(s+c)}\kappa^2}}. \end{cases}$$

Proof. Since the angle between the tangent of the curve and the tangent of its associated pseudo-hyperbolic space partner is constant, from (8), we have

$$\frac{f'}{f} = b$$

and it means that

$$f(s) = e^{b(s+c_1)}$$

where b and c_1 are constants. Then, we get $\sqrt{f^2 - f'^2} = \sqrt{1-b^2}e^{b(s+c)}$. Also, from

$$\frac{d\bar{s}}{ds} = \frac{f}{\cosh \vartheta}$$

we obtain

$$\bar{s} = \frac{1}{\cosh \vartheta} \int e^{b(s+c_1)} ds$$

and

$$\bar{s} = \frac{e^{b(s+c_1)}}{b \cosh \vartheta} + c_2$$

where $b = \tanh \vartheta$ and c_1, c_2 are constants. If we put $a = b \cosh \vartheta$, then we get $a\sqrt{1-b^2} = b$.

By using (18), we obtain

$$\begin{cases} \kappa = \frac{-\cosh\phi + \kappa_g \cosh\vartheta \sinh\phi}{\sqrt{1-b^2}e^{b(s+c)}} = -\frac{1}{\sqrt{1-b^2}e^{b(s+c)}\cosh\phi} = -\frac{\kappa_g \cosh\vartheta}{\sqrt{1-b^2}e^{b(s+c)}\sinh\phi}, \\ \tau = -\frac{\phi' + \kappa_g \sinh\vartheta}{\sqrt{1-b^2}e^{b(s+c)}}. \end{cases}$$

Hence we conclude that

$$\begin{cases} \kappa_g^2 = 1 - (1-b^2)e^{2b(s+c)}\kappa^2 - (b\sqrt{1-(1-b^2)e^{2b(s+c)}\kappa^2})^2, \\ \tau = -\left(\frac{\theta'}{\sqrt{1-b^2}e^{b(s+c)}} + \frac{b\sqrt{1-(1-b^2)e^{2b(s+c)}\kappa^2}}{\sqrt{1-b^2}e^{b(s+c)}}\right), \\ \phi' = \frac{\kappa' - b\kappa}{\kappa\sqrt{1-(1-b^2)e^{2b(s+c)}\kappa^2}}. \end{cases}$$

Theorem 4.3. Let $r(\bar{s}): I \rightarrow E_1^3$ be a spacelike space curve with timelike principal normal and the arc length parameter \bar{s} and $x(s)$ the associated pseudo-hyperbolic space partner of $r(\bar{s})$ with arc length parameter s in Minkowski 3-space. Then the position vector field of the associated curve β of $r(\bar{s})$ make a constant angle ϕ with the position vector field y of the associated curve of $x(s)$ if and only if the curvature function κ , the torsion function τ , radial function f and the radial pseudo-spherical function κ_g of $r(\bar{s})$ satisfy

$$\frac{\tau}{\kappa} = \sinh\phi \frac{f'}{f},$$

or

$$\kappa_g^2 = (f^2 - f'^2)(\sinh^2\phi\kappa^2 - \Gamma^2).$$

Proof. By using

$$\Gamma = \tau + \frac{\phi'}{\sqrt{f^2 - f'^2}},$$

then (18) is rewrite as below

$$\begin{cases} \kappa = \frac{-(\vartheta'+1)\cosh\phi + \kappa_g \cosh\vartheta \sinh\phi}{\sqrt{f^2 - f'^2}} = -\frac{\vartheta'+1}{\sqrt{f^2 - f'^2}\cosh\phi} = -\frac{\kappa_g \cosh\vartheta}{\sqrt{f^2 - f'^2}\sinh\phi}, \\ \Gamma = -\frac{\kappa_g \sinh\vartheta}{\sqrt{f^2 - f'^2}}. \end{cases} \quad (25)$$

From (25), by direct computation, we get

$$(f^2 - f'^2)(\sinh^2\phi\kappa^2) = \kappa_g^2 \cosh^2\vartheta,$$

$$\Gamma^2(f^2 - f'^2) = \kappa_g^2 \sinh^2\vartheta.$$

If we subtract the second equation from the first equation, we obtain

$$\kappa_g^2 = (f^2 - f'^2)(\sinh^2\phi\kappa^2 - \Gamma^2).$$

Combining (8) and (25), we derive

$$\frac{\Gamma}{\kappa} = \sinh\phi \frac{f'}{f}.$$

Since ϕ is constant, we get desired equality.

Theorem 4.4. Let $r(\bar{s}): I \rightarrow E_1^3$ be a spacelike space curve with timelike principal normal and the arc length parameter \bar{s} , Frenet frame $\{\alpha(\bar{s}), \beta(\bar{s}), \gamma(\bar{s})\}$ and $x(s)$ the associated pseudo-hyperbolic space partner of $r(\bar{s})$ with arc length parameter s , Darboux frame $\{\alpha_0(s), x(s), y(s)\}$ in Minkowski 3-space. If $\beta(\bar{s})$ is parallel with respect to $y(s)$, the curve $r(\bar{s})$ can be written as

$$r(\bar{s}) = r(s) = \frac{1}{\text{acosh}(-s+c)} x(s), \quad (26)$$

and the curvature function κ , the torsion function τ and the radial pseudo-spherical function κ_g of $r(\bar{s})$ satisfy

$$\begin{cases} a^2 \kappa^4 \kappa_g^2 = (\kappa^2 - \tau^2)^3, \\ \frac{\tau(\bar{s})}{\kappa(\bar{s})} = a\bar{s} + b = -\tanh(-s+c) \end{cases}$$

where $a \neq 0, b$ and c are constants.

Proof. Because β is parallel with respect to y , we have $\vartheta' + 1 = 0$. So, $\vartheta' = -1$ and $\vartheta = -s + c$, c is integral constant. From (8) or the first equation of (22), we obtain

$$\tanh \vartheta = \frac{f'}{f} = \frac{\sinh \vartheta}{\cosh \vartheta} = \frac{\sinh(-s+c)}{\cosh(-s+c)}$$

So,

$$f(s) = \frac{1}{\text{acosh}(-s+c)}$$

and

$$\frac{d\bar{s}}{ds} = \frac{1}{\text{acosh}^2(-s+c)}$$

From last equality, we get

$$a\bar{s} + b = -\tanh(-s+c)$$

where b is integral constant. Finally, (18) becomes

$$\begin{cases} \kappa = \frac{\kappa_g \cosh \vartheta}{a^{-1} \cosh^{-2}(-s+c)}, \\ \tau = -\frac{\kappa_g \sinh \vartheta}{a^{-1} \cosh^{-2}(-s+c)}. \end{cases}$$

Then by a direct calculation, we get the desired results.

With the aid of above theorem and notions of associated curve of a spacelike curve and pseudo-hyperbolic space curve, we can give following corollary for new characterization of the rectifying curves in Minkowski 3-space. İlarıslan et al. (2003) have studied geometric properties and characterization of the rectifying curve in Minkowski 3-space.

Corollary 4.5. A spacelike curve with timelike principal normal in Minkowski 3-space is rectifying curve if and only if its associated curve is coincide with the associated curve of its spacelike associated pseudo-hyperbolic space partner.

REFERENCES

Chen, B.Y. (2005). When does the position vector of a space curve always lie in its rectifying plane. *American Mathematical Monthly*, 110, 147-152.

Do Carmo, M.P. (1976). *Differential geometry of curves and surfaces*, Pearson Education.

İlarslan, K., Nevsovic, E., Petrovic, M.T. (2003). Some characterizations of rectifying curves in the Minkowski 3-space. *Novi Sad Journal of Mathematics*, 33(2), 23-32.

Liu, H. (2014). Curves in three dimensional Riemannian space forms. *Results in Mathematics*, 66, 469-480.

Liu, H., Liu, Y., Jung, S.D. (2019). Associated spherical partner of space curve in Euclidean 3-space. *Topology and its Applications*, 264, 79-88.

Lopez, R. (2014). Differential geometry of curves and surfaces in Lorentz-Minkowski space, *International Electronic Journal of Geometry*, 7-1, 44-107.

Su, B., Hua, X., Xin, Y. (1986). *Introduction to functional differential geometry*. Science Press.

Turhan T., Yücesan A., Özkan T. G. (2021). Associated pseudo spherical partner of a non-null Lorentzian space curve. *International Blacksea Coastline Countries Symposium*, April 28-30, Giresun.

SYNTHESES, ETUDES STRUCTURALES ET CARACTERISATIONS PHYSICO-CHIMIQUES DE DEUX NOUVEAUX COMPOSES ORGANOMETALLIQUES A BASE DE COBALT

W. JBELI

Université de Tunis El Manar, Faculté des Sciences de Tunis, Laboratoire de Matériaux, Cristallographie et Thermodynamique Appliquée, 2092 El Manar II, Tunis, Tunisie

M. F. ZID

Université de Tunis El Manar, Faculté des Sciences de Tunis, Laboratoire de Matériaux, Cristallographie et Thermodynamique Appliquée, 2092 El Manar II, Tunis, Tunisie

Les deux nouveaux composés organométalliques de formules $[\text{Co}(\text{C}_5\text{H}_6\text{N}_2)_2]\text{Cl}_2$ et $[\text{Co}(\text{C}_5\text{H}_6\text{N}_2)]\text{Cl}_3$, ($\text{C}_5\text{H}_7\text{N}_2$) notés respectivement **(1)** et **(2)** ont été synthétisés par la méthode d'évaporation lente à température ambiante et caractérisés par diffraction des rayons-X sur monocristal et par spectroscopie d'absorption IR. Le composé **(1)** cristallise dans le système orthorhombique avec le groupe d'espace $P2_1cb$ et avec les paramètres de maille : $a=7.742(2) \text{ \AA}$, $b=12.050(2) \text{ \AA}$, $c=6.873(2) \text{ \AA}$, $\alpha=\beta=\gamma=90^\circ$. Alors que le composé **(2)** cristallise dans le système monoclinique avec le groupe d'espace Cc et avec les paramètres de maille : $a=13.233(2) \text{ \AA}$, $b=8.111(3) \text{ \AA}$, $c=14.066(2) \text{ \AA}$, $\alpha=90^\circ$, $\beta=106.329^\circ$, $\gamma=90^\circ$. Dans ces deux composés, le cobalt occupe un environnement tétraédrique formé par les atomes de cobalt, chlore et azote. La cohésion de ses deux structures cristallines est assurée par des interactions hydrogène intermoléculaires de type $\text{N}-\text{H}\cdots\text{Cl}$, reliant des entités ioniques et les dimères adjacents et des interactions de type $\pi-\pi$ [1] entre les cycles des cations 2-aminopyridine. Dans le but de déterminer les pourcentages des interactions hydrogène intermoléculaires présents dans les deux complexes, des calculs de surfaces d'Hirshfeld et de vide cristallin ont été réalisés.

Mots clés: diffraction des rayons-X, complexes, interactions hydrogène.

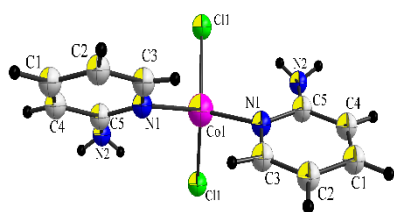


Fig.1. l'unité asymétrique de $[\text{Co}(\text{C}_5\text{H}_6\text{N}_2)_2]\text{Cl}_2$

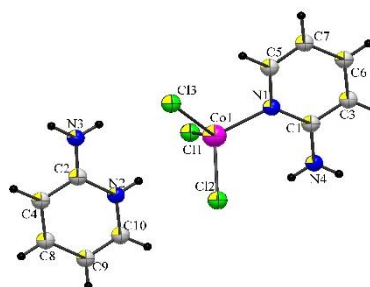


Fig.2. l'unité asymétrique de $[\text{Co}(\text{C}_5\text{H}_6\text{N}_2)]\text{Cl}_3$, ($\text{C}_5\text{H}_7\text{N}_2$)

Références

[1] C. Zhao, K. R. Ma, Y. Zhang, Y. H. Kan, R. Q. Li, H. Y. Hu, Spectrosc. Acta A, 153 (2015) 171



ORTHOGONAL BLOCK STRUCTURE, U-MATRICES AND UNIFORMLY BEST LINEAR UNBIASED ESTIMATORS

Carla Maria Lopes da Silva AFONSO DOS SANTOS

Polytechnic Institute of Beja, CMA- Center for Mathematics and Applications, FCT, New University of Lisbon, Portugal
ORCID ID: 0000-0002-0077-1249

Cristina Paula da SILVA DÍAS

Polytechnic Institute of Portalegre, CMA- Center for Mathematics and Applications, FCT, New University of Lisbon, Portugal
ORCID ID: 0000-0001-6350-5610

Célia Maria PÍNTO NUNES

Department of Mathematics and Center for Mathematics and Applications of University of Beira Interior, Portugal
ORCID ID: 0000-0003-0167-4851

João Tiago Praça NUNES MEXIA

Department of Mathematics and CMA- Center for Mathematics and Applications, FCT- New University of Lisbon, Portugal
ORCID ID: 0000-0001-8620-0721

ABSTRACT

Linear mixed models are suitable for correlated data, due to, for example, repeated measurements in experiments in agricultural research, medical research, and others. In this work we consider two successively more restricted classes of linear mixed models. The first class, that took a central role in the theory of randomized block designs, are models with orthogonal block structure, OBS. OBS are mixed models whose covariance matrix are the positive definite linear combinations of known pairwise orthogonal orthogonal projection matrices that add up to the identity matrix. An even more restricted class of mixed models, those of models with commutative orthogonal block structure, COBS, is reached by taking OBS and imposing a commutativity condition between the orthogonal projection matrix, on the space spanned by the mean vector, and the pairwise orthogonal orthogonal projection matrices, belonging to the principal basis of the commutative Jordan algebra of symmetric matrices, associated to the model. Equivalently, the commutativity occurs between the orthogonal projection matrix on the space spanned by the mean vector and the covariance matrix. According to Zmyslony's version of the Gauss-Markov theorem, this commutativity condition is a necessary and sufficient condition for least squares estimators for estimable vectors to be best linear unbiased estimators.

In the approach to the models with commutative orthogonal block structure, adopted in this work, we use the algebraic structure of the models, since this leads to interesting results on the estimation of variance components and on the building up of models, and we resort to U-matrices to express a general condition for commutativity.

Keywords: Best linear unbiased estimators, mixed models, models with orthogonal block structure, U-matrices.

Acknowledgements

This work was partially supported by the Fundação para a Ciência e a Tecnologia (Portuguese Foundation for Science and Technology) through the project UIDB/00297/2020 (Centro de Matemática e Aplicações) and UIDB/00212/2020

SİKLOBÜTİL SÜBSTİTÜYE EDİLMİŞ BİR YENİ BENZİMİDAZOLYUM TUZUNUN SENTEZİ VE KARAKTERİZASYONU

Neslihan ŞAHİN

Cumhuriyet University, Faculty of Education, Department of Basic Education

ORCID ID: 0000-0003-1498-4170

Elvan ÜSTÜN

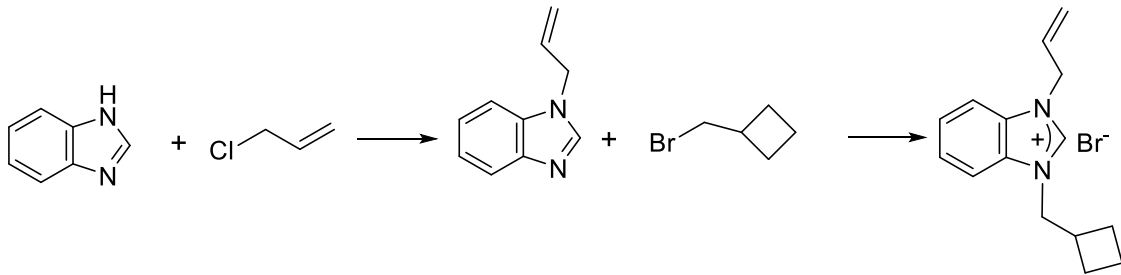
Ordu University, Faculty of Science and Arts, Chemistry Department, Cumhuriyet Campus

ORCID ID: 0000-0002-0587-7261

ÖZET

N-Heterosiklik karben (NHC) ligandlarının karakteristik özelliği, hacimli olmaları ve güçlü elektron verme özelliklerinden kaynaklanan yüksek koordinasyon yetenekleridir. Bu özellikleri ile NHC ligandları bazı metallerle güçlü bir şekilde kararlı kompleksler oluştururlar. Kararlı olan bu komplekslerin tekrar tekrar kullanılabilme özelliğinde olması ise bu bileşiklere ilgiyi arttırmaktadır. Bu yüzden literatüre yeni NHC ligantları kazandırmak ve bu ligantlardan yeni kompleksler elde ederek çeşitli özelliklerini incelemek oldukça önemlidir. N-Heterosiklik karben (NHC) ligandlarını içeren çok sayıda güçlü katalitik sistem tanımlanmış olsa da, bunları sentezleme yöntemleri daha yavaş ilerlemiştir. Ancak son zamanlarda bu bileşiklerin sentez yöntemleri oldukça geliştirilmiştir.

Bu çalışmada, yeni bir N-heterosiklik karben bileşiği olan 1-allil-3-siklobütil-benzimidazolyum bromür ligandı sentezlenmiştir. Sentezlenen bu yeni bileşiğin yapısı FT-IR, ¹H NMR ve ¹³C NMR spektroskopileri aydınlatılmıştır.



Anahtar Kelimeler: N-Heterosiklik karbenler, siklobütil, NMR, FT-IR.

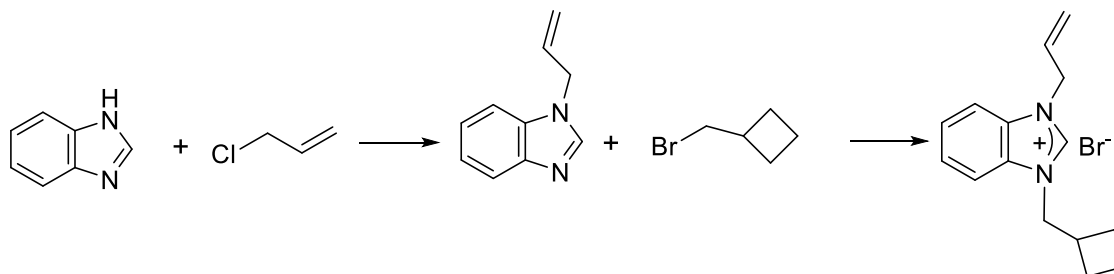
SYNTHESIS AND CHARACTERIZATION OF A NEW CYCLOBUTYL SUBSTITUTED BENZIMIDAZOLIUM SALT

ABSTRACT

A characteristic property of NHC (N-heterocyclic carbene) ligands is their high coordinating ability caused by their bulkiness and strong electron-donating property. With these properties, NHC ligands constitute strongly stable complexes with some metals. The fact that these stable complexes can be used fairly increases the interest

in these compounds. Therefore, it is important to introduce new NHC ligands to the literature and to examine their various properties by obtaining new complexes from these ligands. While numerous powerful catalytic systems incorporating NHC ligands have been described, methods of synthesizing them have advanced more slowly. However, recently, the synthesis methods of these compounds have been greatly improved.

In this study, 1-allyl-3-cyclobutyl-benzimidazolium bromide which a new N-heterocyclic carbene salt was synthesized. The structure of this novel compound was characterized by FT-IR, ^1H NMR and ^{13}C NMR spectroscopies.



Keywords: N-Heterocyclic carbenes, cyclobutyl, NMR, FT-IR.

1. INTRODUCTION

Since the discovery of the first N-heterocyclic carbene complexes by Öfele and Wanzlick in 1968 (Wanzlick and Schönherr, 1968; Öfele, 1968) and the first stable free carbene isolation by Arduengo in 1991 (Arduengo, 1991), N-Heterocyclic carbene precursor (NHCs) have been increasingly play an important role in many fields such as organometallic, organic synthesis, pharmaceutical and polymer chemistry. Although many powerful catalytic systems involving NHC ligands have been described, methods for synthesizing them have progressed more slowly (Wanzhi, 2010).

The most important property of NHC (N-heterocyclic carbene) ligands is high coordinating capability had by their bulkiness and strong electron-donating property. Its effects are stronger than those of trialkylphosphines and allow the formation of metal-NHC complexes by ligand exchange reactions of metal-phosphine complexes with NHC ligands (Nolan, 2006; Hartwig, 2009). In this way, NHC ligands form complexes strongly with some metals and also generate coordinated unsaturation species by pushing out a coordinated trans position ligand with the metal center. Therefore, metal complexes coordinated by NHC ligands are highly active species, chemically stable, and easy to handle, so they are expected to have a high turnover frequency.

Metal complexes of N-heterocyclic carbene precursors show catalytic activity in various reactions such as hydrogenation (Bernier and Merola, 2021), hydroformylation (Gil and Trzeciak, 2011), C-C coupling (Wass et al., 2007), olefin metathesis (Yoon, et al., 2020), hydrosilylation (Hamdi et al., 2021), and biological properties such as antimicrobial and anticancer activity (Üstün et al., 2021; Şahin et al., 2019). Synthesis of different metal complexes of each new NHC ligand will make a contribution to the literature.

With this viewpoint, a new N-heterocyclic carbene ligand, 1-allyl-3-cyclobutyl-benzimidazolium bromide, was synthesized (Figure 1). The structure of this new obtained compound was clarified by FT-IR, ^1H NMR, and $^{13}\text{C}\{^1\text{H}\}$ NMR spectroscopies.

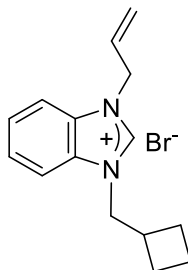


Figure 1. Structure of 1-allyl-3-cyclobutyl-benzimidazolium bromide.

2. EXPERIMENTAL

2.1. Materials and Method

Schlenk technique was used to synthesis of the N-heterocyclic carbene ligand under the argon gas. All chemicals and solvents were obtained from commercial sources. The solvents used were purified by distillation over the drying agents indicated and were transferred under Argon. Melting points were determined using Electrothermal 9100 melting point detection apparatus in capillary tubes and melting points are uncorrected values. Fourier transform infrared (FT-IR) spectra were recorded in the range $400\text{--}4000\text{ cm}^{-1}$ on Perkin Elmer Spectrum 100 FT-IR. ^1H NMR and $^{13}\text{C}\{^1\text{H}\}$ NMR spectra were taken using a Bruker As 400 Mercury spectrometer operating at 400 MHz (^1H), 100 MHz (^{13}C) in CDCl_3 with tetramethylsilane as the internal reference.

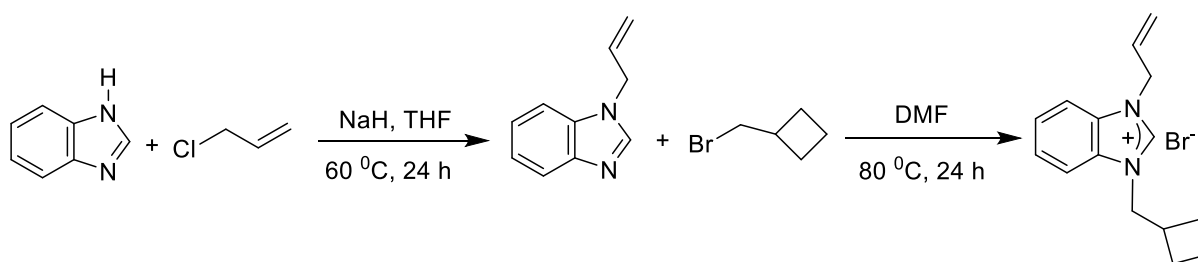
Synthesis of 1-allyl-3-cyclobutyl-benzimidazolium bromide

1-Allyl-3-cyclobutyl-benzimidazolium bromide was synthesized as described in the previous study by the current authors (Üstün et al, 2016). Benzimidazole (10 mmol) was added to a solution of NaH (10 mmol) in dry THF (30 mL) and the mixture was stirred for 1 h at room temperature. The allyl bromide (10.1 mmol) was added dropwise to the obtained solution and heated for 24 h at $60\text{ }^\circ\text{C}$. Then, the solvent was removed under the vacuum. Dichloromethane (50 mL) was added to the solid. The mixture was filtered and the obtained clear solution was concentrated under vacuum. The last solution was distilled and 1-allylbenzimidazole was obtained. The 1-allylbenzimidazole (1 mmol) and cyclobutylmethyl bromide (1 mmol) were stirred in DMF (5 mL) for 24 h at $80\text{ }^\circ\text{C}$ and the product was precipitated. After the solution was filtered, the solid was rinsed out with diethyl ether and dried under vacuum. The crude product was recrystallized from dichloromethane/diethyl ether. Yield: 76%, mp $101\text{--}102\text{ }^\circ\text{C}$, $\nu_{(\text{CN})}$: 1556 cm^{-1} . ^1H NMR (400 MHz, CDCl_3) δ (ppm): 1.94-2.03 (m, 4H, $\text{CH}_2(\text{CHC}_3\text{H}_6)$), 2.13-2.19 (m, 2H, $\text{CH}_2(\text{CHC}_3\text{H}_6)$), 3.07 (hept, 1H, $\text{CH}_2(\text{CHC}_3\text{H}_6)$), $J = 8\text{ Hz}$), 4.64 (d, 2H, $\text{CH}_2(\text{CHC}_3\text{H}_6)$), $J = 8\text{ Hz}$), 5.39 (d, 2H, $\text{NCH}_2\text{CHCH}_2$, $J = 8\text{ Hz}$), 5.45-5.51 (m, 2H, $\text{NCH}_2\text{CHCH}_2$), 6.15 (quint, 1H, $\text{NCH}_2\text{CHCH}_2$,

$J = 4$ Hz), 7.64-7.67 (m, 2H, Ar-*H*), 7.75-7.77 (m, 2H, Ar-*H*), 11.17 (s, 1H, NCHN). $^{13}\text{C}\{^1\text{H}\}$ NMR (100 MHz, CDCl_3): $\delta = 18.0$ $\text{CH}_2(\text{CHC}_3\text{H}_6)$, 25.9 $\text{CH}_2(\text{CHC}_3\text{H}_6)$, 34.5 $\text{CH}_2(\text{CHC}_3\text{H}_6)$, 50.1 (NCH₂CHCH₂), 52.3 $\text{CH}_2(\text{CHC}_3\text{H}_6)$, 121.6 (NCH₂CHCH₂), 129.8 (NCH₂CHCH₂), 113.1, 113.8, 127.2, 131.3, 131.5 (Ar-C), 142.4 (NCHN).

RESULT AND DISCUSSION

Functionalized N-heterocyclic carbene ligands containing classical donor groups have attracted much attention in synthesis chemistry. In this study, 1-allyl-3-cyclobutyl-benzimidazolium bromide was synthesized by the reaction of 1-allylbenzimidazole with cyclobutylmethyl bromide in DMF at 80 °C for 24 h. The reaction pathway was shown in Scheme 1.



Scheme 1. Synthesis of the N-heterocyclic carbene ligand

The structure of this novel N-heterocyclic carbene precursor was clarified by FT-IR, ^1H NMR, and $^{13}\text{C}\{^1\text{H}\}$ NMR spectroscopies. NMR measurement of the compound was taken in $d\text{-CDCl}_3$. According to the analysis results, in the ^1H NMR spectrum, the acidic proton (NHCN) of the compound gave peak at 11.17 ppm. The aromatic protons of the benzimidazole ring of the compound were seen in the range of 7.64-7.77 ppm as multiplets. At the allyl group in the compound, NCH₂CHCH₂ proton peaked at 6.15 ppm as quintet, NCH₂CHCH₂ protons peaked in the range of 5.45-5.51 ppm as multiplet, and NCH₂CHCH₂ protons peaked at 5.39 ppm as doublet. At the cyclobutyl group, $\text{CH}_2(\text{CHC}_3\text{H}_6)$ protons were seen at 4.64 ppm as doublet, $\text{CH}_2(\text{CHC}_3\text{H}_6)$ proton was seen at 3.07 ppm as heptet and $\text{CH}_2(\text{CHC}_3\text{H}_6)$ protons were seen at in the 1.94-2.19 ppm (Figure 2). In the $^{13}\text{C}\{^1\text{H}\}$ NMR spectrum of the NHC precursor, the NHCN carbene peak was seen at 142.4 ppm. Aromatic carbons of the compound were seen in the range of 113.1-131.5 ppm. NCH₂CHCH₂ carbon peaked at 50.1 ppm. $\text{CH}_2(\text{CHC}_3\text{H}_6)$ carbon peak was seen at 52.3 ppm and $\text{CH}_2(\text{CHC}_3\text{H}_6)$ carbons gave peak at 18.0 ppm and 25.9 ppm in (Figure 3). And $\text{CH}_2(\text{CHC}_3\text{H}_6)$ carbon gave at peak 34.5 ppm.

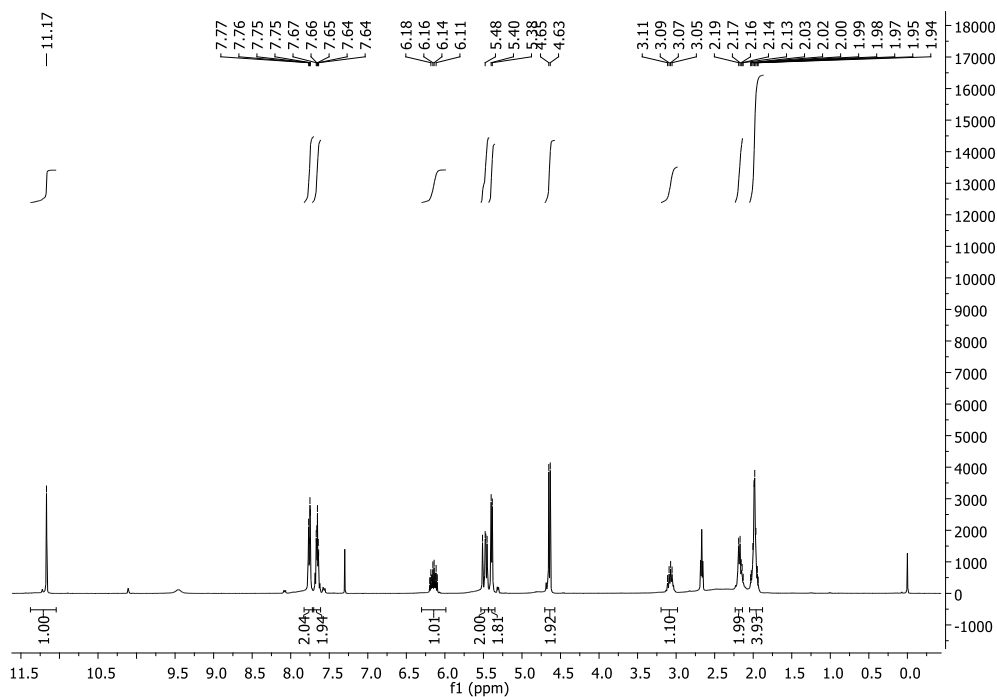


Figure 2. ^1H NMR spectra of the N-heterocyclic carbene precursor

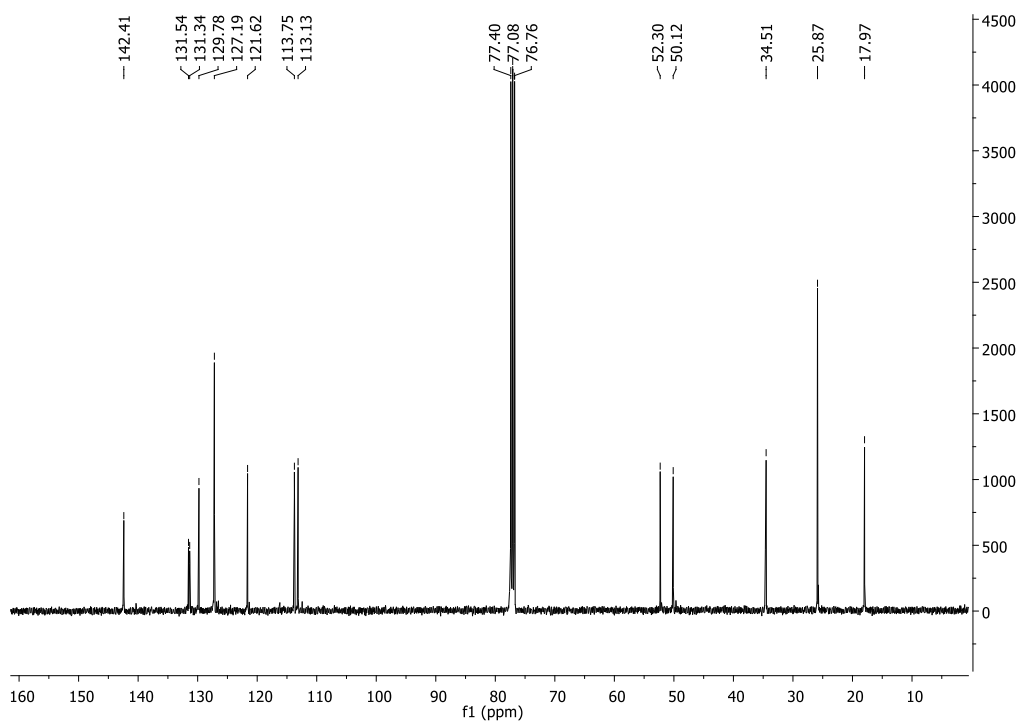


Figure 3. $^{13}\text{C}\{^1\text{H}\}$ NMR spectra of the N-heterocyclic carbene precursor

The FT-IR spectrum of the compound contains characteristic bands of stretching vibrations of C=N, C-N, C-H, and C=C groups. The FT-IR spectra for NHC precursor showed the aliphatic and aromatic C-H stretching vibrational bands in the range of 2770–3430 cm^{-1} . The C=N vibration in the benzimidazole ring of the NHC precursor was seen at 1556 cm^{-1} (Figure 4). The results are supported by previous similar studies (Çevik-Yıldız,

Şahin and Şahin-Bölükbaşı, 2020).

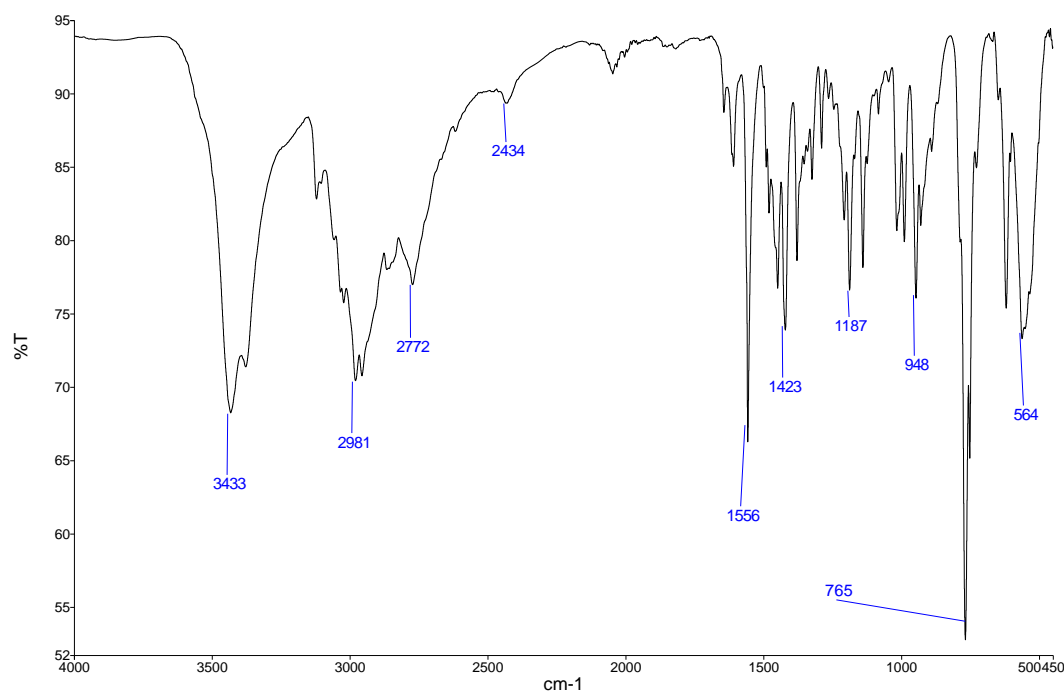


Figure 4. FT-IR spectra of the N-heterocyclic carbene ligand

4. CONCLUSIONS

In this study, a new NHC precursor that can be used in the synthesis of various metal complexes was synthesized and its structure was clarified by FT-IR, ^1H NMR and $^{13}\text{C}\{^1\text{H}\}$ NMR spectroscopies. The results of the analysis are in agreement with the literature. In future studies, it is planned to synthesize complexes of this compound with palladium, ruthenium and silver metals.

REFERENCES

- Arduengo, A.J., Harlow, R.L., & Kline, M. (1991) A Stable Crystalline Carbene. *Journal of the American Chemical Society*, 113(1), 361-363.
- Bernier, C. M., & Merola, J. S. (2021). Design of Iridium N-Heterocyclic Carbene Amino Acid Catalysts for Asymmetric Transfer Hydrogenation of Aryl Ketones. *Catalysts*, 11(6), 671.
- Çevik-Yıldız, E., Şahin, N., & Şahin-Bölükbaşı, S. (2020). Synthesis, characterization, and investigation of antiproliferative activity of novel Ag (I)-N-Heterocyclic Carbene (NHC) compounds. *Journal of Molecular Structure*, 1199, 126987.
- Gil, W., & Trzeciak, A. M. (2011). N-Heterocyclic carbene–rhodium complexes as catalysts for hydroformylation and related reactions. *Coordination Chemistry Reviews*, 255(3-4), 473-483.
- Hamdi, N., Slimani, I., Mansour, L., Alresheedi, F., Özdemir, I., & Gürbüz, N. (2021). Rhodium (I) complexes with N-heterocyclic carbene ligands: synthesis, biological properties and catalytic activity in the hydrosilylation of aromatic ketones. *Journal of Coordination Chemistry*, 1-22.
- Hartwig, J. F. (2009). *Organotransition Metal Chemistry: From Bonding to Catalysis*; University Science Book: Sausalito, CA, 2010.
- Nolan, S. P. (Ed.). (2006). *N-Heterocyclic carbenes in synthesis*. John Wiley & Sons.
- Öfele, K. (1968). 1,3-Dimethyl-4-imidazolinylden-(2)-pentacarbonylchrom ein neuer Übergangsmetall-carben-komplex. *Journal of Organometallic Chemistry*, 12(3), P42-P43.
- Şahin, N., Şahin-Bölükbaşı, S., Tahir, M. N., Arıcı, C., Çevik, E., Gürbüz, N., ... & Cummings, B. S. (2019). Synthesis, characterization and anticancer activity of allyl substituted N-Heterocyclic carbene silver (I) complexes. *Journal of Molecular Structure*, 1179, 92-99.
- Üstün, E., Ayvaz, M. C., Çelebi, M. S., Aşçı, G., Demir, S., & Özdemir, İ. (2016). Structure, CO-releasing property, electrochemistry, DFT calculation, and antioxidant activity of benzimidazole derivative substituted $[\text{Mn}(\text{CO})_3(\text{bpy})\text{L}]\text{PF}_6$ type novel



- manganese complexes. *Inorganica Chimica Acta*, 450, 182-189.
- Üstün, E., Şahin, N., Çelik, C., Tutar, U., Özdemir, N., Gürbüz, N., & Özdemir, İ. (2021). Synthesis, characterization, antimicrobial and antibiofilm activity, and molecular docking analysis of NHC precursors and their Ag-NHC complexes. *Dalton Transactions*, 50(42), 15400-15412.
- Wanzhi, L. B. Z. N. C. (2010). Synthesis of Metal N-Heterocyclic Carbene Complexes. *Progress in Chemistry*, 11.
- Wanzlick, H. W., & Schönherr, H. J. (1968). Direct synthesis of a mercury salt-carbene complex. *Angewandte Chemie International Edition*, 7(2), 141-142.
- Wass, D. F., Haddow, M. F., Hey, T. W., Orpen, A. G., Russell, C. A., Wingad, R. L., & Green, M. (2007). Cyclopropenylidene carbene ligands in palladium C–C coupling catalysis. *Chemical communications*, (26), 2704-2706.
- Yoon, J. S., Cena, N., & Schrodi, Y. (2020). Robust Olefin Metathesis Catalyst Bearing a Tridentate Hemilabile NHC Ligand. *Organometallics*, 39(5), 631-635.



STATISTICAL INVESTIGATIONS ON DISPARITY IN SPENDING HABITS OF ACADEMIC AND NON-TEACHING STAFF OF TERTIARY INSTITUTIONS IN IMO STATE, NIGERIA

Ugochinyere Ihuoma NWOSU*

Department of Statistics, Federal University of Technology Owerri, Nigeria

Chukwudi Paul OBÌTE

Department of Statistics, Federal University of Technology Owerri, Nigeria

Daniel Chinemeze OKOLÌE

Department of Statistics, Federal University of Technology Owerri, Nigeria

ABSTRACT

This study investigated the disparity in spending habits of academic and non-teaching staff of tertiary institutions in Imo State Nigeria during 2021. A total of 384 responses were obtained from sampled population. Data were analyzed using Chi-square and Mann-Whitney U tests with the aid of Statistical Package for the Social Sciences. The result revealed a significant disparity in the amount of money the academic and non-teaching staff spent on food items and transportation, but there was no significant disparity in the amount of money spent on utility bills monthly. Disparity occurred in the choice of having monthly budget for spending. Mann Whitney test revealed no disparity in the motives that influenced spending habits in the two categories of workers in Imo State, Nigeria.

Keywords: Chi-square, Mann-Whitney, food items, utility bills, budget.



PREPARATION, STRUCTURE ELUCIDATION, AND ANTIOXIDANT ACTIVITY OF NEW ISATIN DERIVATIVES INCLUDING SCHIFF BASES

Hasan YAKAN

Ondokuz Mayıs University, Faculty of Education, Department of Mathematics and Science Education,
Samsun, Turkey

ORCID ID: 0000-0002-4428-4696

ABSTRACT

New bis-isatins hydrazones including Schiff bases were obtained from terephthalaldehyde bis-hydrazone and 5-substituted isatins in the presence of a drop of hydrochloric acid under reflux in ethanol. Terephthalaldehyde bis-hydrazones were prepared by the reaction of hydrazide and terephthalaldehyde under reflux in ethanol. All the products were defined by using IR, ^{13}C NMR, ^1H NMR, spectroscopy and elemental analysis. They were tested *in vitro* antioxidant activity with free radical scavenging method using by the 1,1-diphenyl-2-picrylhydrazyl (DPPH $^{\cdot}$). The results were given with calculated IC_{50} values. Compound **2** (5-F) showed the strongest antioxidant activity among the synthesized compounds.

INTRODUCTION

Isatins are significant compounds in organic chemistry owing to many fields of application in pharmacological chemistry and their biological properties these results from possessing an indole nucleus with a ketone and a γ -lactam fused to the benzene ring [1-3]. They have anti-microbial [3], anti-tubercular [4], anti-oxidant [5], anti-convulsant [6], and anti-HIV [7]. Schiff bases of including isatins are known to have an extensive range of pharmacological and biological properties. They were reported as anticonvulsant [8], antibacterial, antiviral [9,10], antioxidant [1], anti-HIV and antifungal activity [11,12].

The significance of free radicals and reactive oxygen species (ROS) in the pathogenicity of various diseases such as metabolic disorders, reperfusion damage, inflammatory diseases, cellular aging, and cancer has attracted substantial consideration [13,14]. Many of these diseases were occurred with the bulking of free radicals in human bodies. Therefore, antioxidants have been noted to play a key role in preserving humans from many potentially serious diseases.

In this work, new isatins based on Schiff bases were prepared two stages. First, hydrazine and 5-substituted isatins react with to give intermediate product under reflux in ethanol. Second, intermediate product and terephthalaldehyde react with to give isatins based on Schiff bases in the presence of a drop of HCl under reflux in ethanol. FT-IR, ^1H NMR, ^{13}C NMR spectroscopy and elemental analysis were used to characterize the structures of the compounds. All the structures were determined *in vitro* antioxidant activity by the DPPH $^{\cdot}$ free radical scavenging method. The results were given with calculated IC_{50} values.

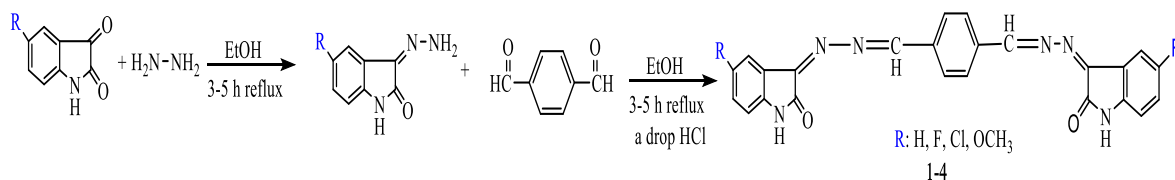
MATERIALS AND METHODS

Measurement and Reagents

All the substances were used without further purification and bought from Merck, Sigma, or Aldrich Chemical Company. Spectroscopic grade was used the solvent. The elemental analysis was measured on Eurovector EA3000-Single. Melting points were recorded with a Stuart SMP30 melting point apparatus and were not corrected. A Bruker Alpha FT-IR spectrometer was used for IR spectra. A JEOL ECX-400 (400 MHz) in DMSO- d_6 spectrophotometer was used for 1H and ^{13}C NMR spectra. A Shimadzu Pharmaspec 1700 UV-visible spectrophotometer was used for absorption measurements.

Synthesis 5-Substituted Isatin-Hydrazones Based on Schiff Bases (1-4)

5-Substituted isatins (3 mmol) and hydrazine (3 mmol) in ethanol-water mixture (3:1, 24 mL) were stirred and refluxed for 3-5 h. Then, the reaction mixture reacts with terephthalaldehyde in a drop of HCl as catalyst in the presence of ethanol (24 mL) for 3-5 h. After finishing reaction, the mixture was filtered and three times washed with ethanol. The formed solid was isolated and dried to give products (1-4) as shown in Scheme 1.



Scheme 1. Synthesis

of 5-substituted isatin based on Schiff bases

Antioxidant Activity

For this, DPPH was used in ethanol at a concentration of 55 μM . Stock solutions of the new compounds were prepared in DMSO to 250 μM . To the earlier prepared (4 mL) DPPH solution was added compound solutions of different concentrations (0.25, 0.50, 1.00, 2.50, 5.00 μM) and enough ethanol to a total of 5 mL. This mixture could stand in a dark room at ambient temperature for 30 minutes and then read at 517 nm against a blank [15].

For the sample compounds were calculated percentage inhibition of the free radical concentration and subsequently compared to the standard Trolox. The percentage of inhibition of radical scavenging activity was calculated by using the formula shown below:

$$\text{Radical scavenging activity (\%)} = [(A_c - A) / A_c \times 100]$$

Where A_c is the absorbance of the control and A is the absorbance of the test compound or standard [16].

In addition, IC_{50} values were calculated from the calibration curve. The IC_{50} value is determined as the

concentration of the all compounds required obtaining half maximum inhibition, and the low IC₅₀ value shows more antioxidant activity [17,18].

RESULTS AND DISCUSSION

Physical Data

The synthesized compounds were new. The current experimental results for the physical data, melting points, yields, and elemental analyses are presented in Tables 1 and 2.

Table 1. The physical data for the synthesized compounds

Comp.	M.P. (°C)	Solubility	Yield (%)
1	>350	DMSO (+)	83
2	>350	DMSO (+)	78
3	>350	DMSO (+)	95
4	>350	DMSO (+)	93

Table 2. The results for elemental analysis for the synthesized compounds

Comp.	Molecular Formula	Molecular Weight, g/mol	Calculated			Experimental		
			C%	H%	N%	C%	H%	N%
1	C ₂₄ H ₁₆ N ₆ O ₂	420.43	68.56	3.84	19.99	67.91	3.78	19.61
2	C ₂₄ H ₁₄ F ₂ N ₆ O ₂	456.41	63.16	3.09	18.41	62.88	2.98	18.21
3	C ₂₄ H ₁₄ Cl ₂ N ₆ O ₂	489.32	58.91	2.88	17.18	58.87	2.81	16.99
4	C ₂₆ H ₂₀ N ₆ O ₄	480.48	64.99	4.20	17.49	64.35	4.11	17.24

Vibrational Frequencies

In the FT-IR spectrum of the synthesized compounds, the aldehyde group (-CHO, two bands) signal of the starting material was not observed near 2750-2650 cm⁻¹. Besides, the amino (-NH₂) group's symmetric and asymmetric stretching bands did not observe at 3600-3200 cm⁻¹. These evidences supported an accomplished reaction as expected. In compound **1**, the -NH stretching vibration of isatin ring was observed at between 3275 cm⁻¹; the C=O signal of isatin ring was observed at 1719 cm⁻¹, the -C=N stretching vibration was appeared at 1591 cm⁻¹; the -C-N stretching vibration was appeared at 1173 cm⁻¹ as shown in Table 3. These frequencies of the compounds are highly consistent with the similar compounds [12,19,20].

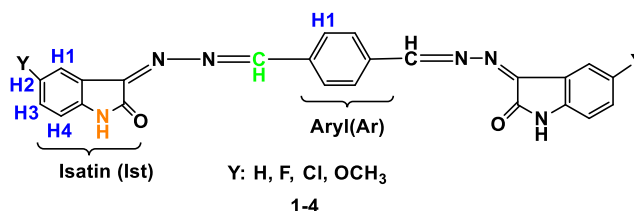
Table 3. FT-IR data of the products (cm⁻¹)

Comp.	-NH	Ar CH	C=O	C=N	C-N
1	3275	3051-3020	1719	1591	1173
2	3245	3108-3013	1735	1604	1205

3	3157	3104-3000	1732	1532	1193
4	3173	3101-2995	1731	1616	1179

¹H NMR Spectral Interpretation

The ¹H NMR spectra of the synthesized compounds were detected in DMSO-d₆ as solvent and showed general scheme for ¹H NMR spectral interpretations in Scheme 2.



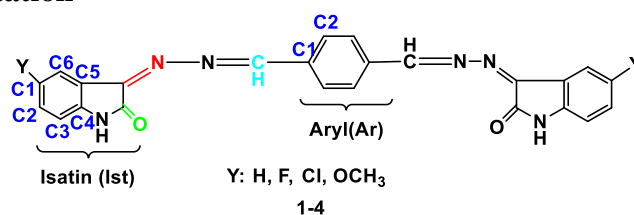
Scheme 2. General scheme for ¹H NMR spectral interpretations

For compound **1**, the H1 aromatic proton signal of aryl ring was observed as a doublet at 7.70-7.72 ppm. The signal of imin (-CH=N) was observed as a singlet at 8.13 ppm. The signal of isatin (-NH) was observed as a singlet at 10.97 ppm. The aromatic protons signals of isatin ring (H1-H4) were observed between 6.86 and 7.47 ppm. The H1 proton coupled to the H2 proton and showed doublet peaks at 6.88-6.86 ppm. The H2 proton coupled to the H1 and H3 proton and observed triplet peaks at 6.99-6.95 ppm. The H3 proton coupled to the H2 and H4 proton and observed triplet peaks at 7.40-7.36 ppm. The H4 proton coupled to the H3 proton and showed doublet peaks at 7.47-7.45 ppm. These results are agreement with the values for similar compounds [12,19,20]. For all the compounds, proton chemical shift values are presented in the Table 4.

Table 4. ¹H NMR (δ, ppm, in DMSO-d₆) values of the compounds

Comp.	CH=N	Ar H1	Ist NH	Ist H1	Ist H3	Ist H4
1	8.13	7.72-7.70	10.97	6.88-6.86	7.40-7.36	7.47-7.45
2	8.15	7.62-7.61	10.99	6.90-6.86	7.30-7.26	
3	8.13	7.78	11.10	6.90-6.89	7.47-7.44	7.50-7.48
4	8.60	7.42-7.41	10.77	6.82-6.79	7.01-6.98	7.10-7.09

¹³C NMR Spectral Interpretation



Scheme 3. General scheme for ¹³C NMR spectral interpretations

The ^{13}C NMR spectra of the products were detected in DMSO-d_6 and showed general scheme the spectral interpretations in Scheme 3. For compound **1**, the $-\text{C}=\text{O}$ signal of isatin region was detected at 163.9 ppm. The characteristic $-\text{CH}=\text{N}$ (imin) peak was observed at 145.2 ppm. The characteristic $-\text{C}=\text{N}$ peak of isatin ring was observed at 145.7 ppm. The aromatic carbons (C1-C2) of aryl ring were observed at 128.7 and 123.1 ppm, respectively. The aromatic carbons (C1-C6) of isatin region were also observed at 134.1, 133.9, 111.7, 134.9, 127.0, and 111.7 ppm, respectively. For compound **4**, the methoxy ($-\text{OCH}_3$) peak were detected at 56.5 ppm. For compounds **2-4**, the resonances of the C1 carbon atoms of isatin ring shifted down-field (high values of δ) due to the presence of electron-withdrawing groups $-\text{F}$, $-\text{Cl}$ and $-\text{OCH}_3$, respectively. These data are consistent with similar compounds [12,19,20]. For all the products, carbon chemical shift values are presented in the Table 5. Furthermore, the C1-C6 atoms were also split into doublets caused by interacting with the atomic nucleus of F for compound **2** and showed 17 different resonances in good agreement with the proposed structure.

Table 5. ^{13}C NMR values related to the compounds (δ , ppm, in DMSO-d_6)

Comp.	Ist C1-C6	Ist C=N	Ist C=O	CH=N	Ar C1	Ar C2
1	134.9-111.7	145.7	163.9	145.2	128.7	123.1
2	149.8-111.4	159.3	164.1	156.9	142.4	130.4
3	137.9-112.1	146.7	163.9	144.9	128.5	126.4
4	155.3-103.4	146.2	163.3	139.3	130.0	119.7

Antioxidant Activity Evaluation

Antioxidants are a material that significantly retarding inhibiting or preventing oxidation of a substrate at low concentrations and have various physiological roles in the body [21,22]. In this study, IC_{50} values were calculated at the end of DPPH analysis for the synthesized compounds and Trolox as shown in Table 6.

Antioxidant molecules can react with DPPH free radicals by giving hydrogen atoms or by electron donation via a free radical attack on these molecules [23,24]. According to this reaction ($\text{DPPH}^{\bullet} + \text{R-NH} \rightarrow \text{DPPH-H} + \text{R-N}^{\bullet}$), weaker hydrogen bonds are essential for higher antioxidant activity in a compound. The strength of these hydrogen bonds is proportional to electron density. Therefore, the structure of the tested compounds and electronic effects of groups/substituents in structures plays an important role for antioxidant activity [25,26]. Consequently, antioxidant activity based on two things: the first being the capacity/skill of compounds to lose hydrogen atoms, and the second being the stability of the formed radical [25-27].

The IC_{50} values of all synthetic test products were between 30.42 and 42.19 μM . The compounds exhibited low activity compared to a standard Trolox in Figure 1. Compound **2** had the strongest antioxidant activity among the synthesized compounds and followed the order Trolox > **2** > **4** > **1** > **3**. Compound **2** is possessed a fluorine atom

(-F) which had strong electron-withdrawing through inductive effect, decreasing electron density in the structure, which causes easier loss of the hydrogen atom.

Although compound **4** has an electron-donating group, it is higher activity than compound **3** due to it increased the stability of the formed radical. As for compounds **1** and **3**, compound **3** has lower activity than compound **1** due to diminishing the stability of the formed radical because of it has a chlorine atom and strong electron-withdrawing.

Table 6. IC₅₀ values for the compounds **1-4**

Compounds	DPPH activity IC ₅₀ (μM)*
1	37.09
2	30.42
3	42.19
4	34.24
Trolox	16.09

*IC₅₀ = the concentration (μM) exhibiting 50% inhibition of DPPH radical.
Values are expressed as means (n = 3).

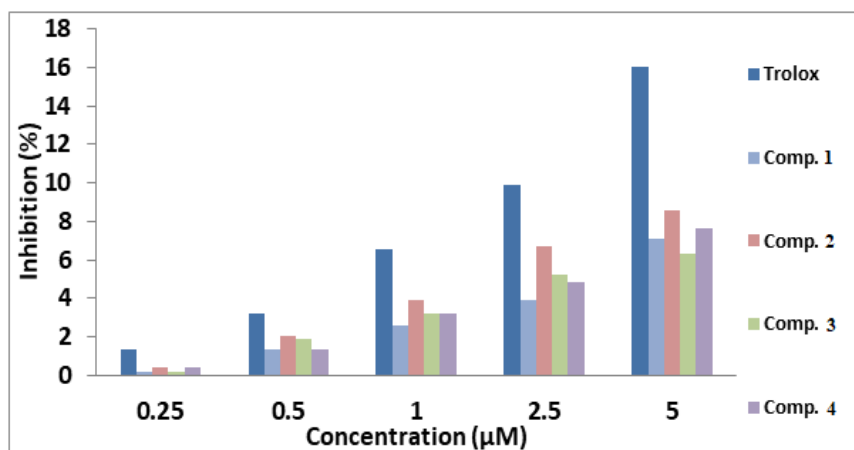


Figure 1. Variation of percent inhibition calculated by the DPPH method for Trolox and the compounds at different concentrations.

CONCLUSION

In this study, new isatin derivatives based on Schiff base have been obtained with excellent yields of 78-95%. All the synthesized compounds were elucidated by ¹H NMR, ¹³C NMR, IR, and elemental analyses. The *in vitro* antioxidant activities of the compounds were determined by the DPPH free radical scavenging method. IC₅₀ values of the new compounds ranged from 30.42 to 42.19 μM. Compound **2** of among the test compounds, showed the most acceptable antioxidant activity against the DPPH radical.

REFERENCES

- [1] Kiran, G., Sarangapani, M., Gouthami, T., & Narsimha reddy, A. R. (2013). Synthesis, characterization, and antimicrobial and antioxidant activities of novel bis-isatin carbohydrazone derivatives. *Toxicological & Environmental Chemistry*, 95(3), 367-378.
- [2] Pakravan, P., Kashanian, S., Khodaei, M. M., & Harding, F. J. (2013). Biochemical and pharmacological characterization of isatin and its derivatives: from structure to activity. *Pharmacological Reports*, 65(2), 313-335.
- [3] Patel, A., Bari, S., Talele, G., Patel, J., & Sarangapani, M. (2006). Synthesis and antimicrobial activity of some new isatin derivatives. *Iranian Journal of Pharmaceutical Sciences*, 5(4), 249-254.
- [4] Aboul-Fadl, T., & Bin-Jubair, F. A. (2010). Anti-tubercular activity of isatin derivatives. *International Journal of Research in Pharmaceutical Sciences*, 1(2), 113-126.
- [5] Haribabu, J., Subhashree, G. R., Saranya, S., Gomathi, K., Karvembu, R., & Gayathri, D. (2016). Isatin based thiosemicarbazone derivatives as potential bioactive agents: Anti-oxidant and molecular docking studies. *Journal of Molecular Structure*, 1110, 185-195.
- [6] Pandeya, S. N., Raja, A. S., & Stables, J. P. (2002). Synthesis of isatin semicarbazones as novel anticonvulsants-role of hydrogen bonding. *J Pharm Pharm Sci*, 5(3), 266-271.
- [7] Bal, T. R., Anand, B., Yogeewari, P., & Sriram, D. (2005). Synthesis and evaluation of anti-HIV activity of isatin β -thiosemicarbazone derivatives. *Bioorganic & Medicinal Chemistry Letters*, 15(20), 4451-4455.
- [8] Verma, M., Pandeya, S. N., Singh, K. N., & Stables, J. P. (2004). Anticonvulsant activity of Schiff bases of isatin derivatives. *Acta Pharmaceutica*, 54(1), 49-56.
- [9] Pandeya, S. N., Sriram, D., Nath, G., & DeClercq, E. (1999). Synthesis, antibacterial, antifungal and anti-HIV activities of Schiff and Mannich bases derived from isatin derivatives and N-[4-(4'-chlorophenyl) thiazol-2-yl] thiosemicarbazide. *European Journal of Pharmaceutical Sciences*, 9(1), 25-31.
- [10] Jarrahpour, A., Sheikh, J., El Mounsi, I., Juneja, H., & Hadda, T. B. (2013). Computational evaluation and experimental in vitro antibacterial, antifungal and antiviral activity of bis-Schiff bases of isatin and its derivatives. *Medicinal Chemistry Research*, 22(3), 1203-1211.
- [11] Pandeya, S. N., Sriram, D., Nath, G., & De Clercq, E. (2000). Synthesis, antibacterial, antifungal and anti-HIV evaluation of Schiff and Mannich bases of isatin and its derivatives with triazole. *Arzneimittelforschung*, 50(01), 55-59.
- [12] Jarrahpour, A., Khalili, D., De Clercq, E., Salmi, C., & Brunel, J. M. (2007). Synthesis, antibacterial, antifungal and antiviral activity evaluation of some new bis-Schiff bases of isatin and their derivatives. *Molecules*, 12(8), 1720-1730.
- [13] Halliwell, B., & Gutteridge, J. M. (2015). *Free radicals in biology and medicine*. Oxford university press, USA.
- [14] Tyagi, Y. K., Kumar, A., Raj, H. G., Vohra, P., Gupta, G., Kumari, R., & Gupta, R. K. (2005). Synthesis of novel amino and acetyl amino-4-methylcoumarins and evaluation of their antioxidant activity. *European Journal of Medicinal Chemistry*, 40(4), 413-420.
- [15] Sindhi, V., Gupta, V., Sharma, K., Bhatnagar, S., Kumari, R., & Dhaka, N. (2013). Potential applications of antioxidants—A review. *Journal of Pharmacy Research*, 7(9), 828-835.
- [16] Naik, N., Vijay Kumar, H., & Vidyashree, P. B. (2011). Synthesis and evaluation of antioxidant potential of novel isatin analogues. *Journal of Pharmacy Research*, 4(8), 2686-2689.
- [17] Frankel, E. N., & Meyer, A. S. (2000). The problems of using one-dimensional methods to evaluate multifunctional food and biological antioxidants. *Journal of the Science of Food and Agriculture*, 80(13), 1925-1941.
- [18] Yakan, H., Çavuş, M. S., Güzel, E., Arslan, B. S., Bakır, T., & Muğlu, H. (2020). Phthalocyanines including 2-mercaptobenzimidazole analogs: Synthesis, spectroscopic characteristics, quantum-chemical studies on the relationship between electronic and antioxidant properties. *Journal of Molecular Structure*, 1202, 127259.
- [19] Chinnasamy, R. P., Sundararajan, R., & Govindaraj, S. (2010). Synthesis, characterization, and analgesic activity of novel schiff base of isatin derivatives. *Journal of Advanced Pharmaceutical Technology & Research*, 1(3), 342.
- [20] Muğlu, H., Çavuş, M. S., Bakır, T., & Yakan, H. (2019). Synthesis, characterization, quantum chemical calculations and antioxidant activity of new bis-isatin carbohydrazone and thiocarbohydrazone derivatives. *Journal of Molecular Structure*, 1196, 819-827.
- [21] Wanasundara, P. K. J. P. D., & Shahidi, F. J. B. S. I. O. (2005). Antioxidants: science, technology, and applications. *Bailey's industrial oil and fat products*.
- [22] Shahidi, F. (2015). Antioxidants: Principles and applications. In *Handbook of Antioxidants for Food Preservation* (pp. 1-14). Woodhead Publishing.
- [23] N.F. Santos-Sánchez, R. Salas-Coronado, C. Villanueva-Cañongo, B. Hernández-Carlos, "Antioxidants. In: Emad Shalaby (editor). Antioxidant compounds and their antioxidant mechanism." *IntechOpen* 2019. doi: 10.5772/intechopen.85270

- [24] Mohammadpour, M., Sadeghi, A., Fassihi, A., Saghaei, L., Movahedian, A., & Rostami, M. (2012). Synthesis and antioxidant evaluation of some novel ortho-hydroxypyridine-4-one iron chelators. *Research in Pharmaceutical Sciences*, 7(3), 171.
- [25] Božić, A. R., Filipovic, N. R., Novaković, I., Bjelogrić, S. K., Nikolić, J. B., Drmanić, S. Ž., & Marinković, A. D. (2017). Synthesis, antioxidant and antimicrobial activity of carbohydrazones. *Journal of the Serbian Chemical Society*, 82(5), 495-508.
- [26] Bendary, E., Francis, R. R., Ali, H. M. G., Sarwat, M. I., & El Hady, S. (2013). Antioxidant and structure–activity relationships (SARs) of some phenolic and anilines compounds. *Annals of Agricultural Sciences*, 58(2), 173-181.
- [27] Queiroz, M. J. R., Ferreira, I. C., Calhelha, R. C., & Estevinho, L. M. (2007). Synthesis and antioxidant activity evaluation of new 7-aryl or 7-heteroaryl amino-2, 3-dimethylbenzo [b] thiophenes obtained by Buchwald–Hartwig C–N cross-coupling. *Bioorganic & Medicinal Chemistry*, 15(4), 1788-1794.



JOB MANAGER FOR JOB GROUPING ON COMPUTATIONAL GRIDS

Sr. Assist. Prof. Dr. Mrs.Y. SUREKHA

Department of Computer Science and Engineering,PVP Siddhartha Institute of Institute of Technology, Vijayawada, India

Assoc. Prof. Dr. K. Koteswara RAO

Department of Computer Science and Engineering,PVP Siddhartha Institute of Institute of Technology, Vijayawada, India

Sr. Assist. Prof. Dr. G. Lalitha KUMARI

B.Tech, Department of Computer Science and Engineering, PVPSIT

Mr. A. Srinath REDDY

B.Tech, Department of Computer Science and Engineering, PVPSIT

Ms. Kadiyala PUJITHA

Department of Computer Science and Engineering,PVP Siddhartha Institute of Institute of Technology, Vijayawada, India

Assist. Prof. Dr. Mr. N. Ramesh BABU

RGKUT, Srikakulam, Andhra Pradesh, INDIA

ABSTRACT

Grid Computing is a new and inevitable technology in the fields of Scientific and engineering, as well as in commercial and industrial enterprises. This growing technology facilitates the conduct of virtual organization by bringing together appropriate, and effective human, information, and computing resources for tackling complex, and multidisciplinary projects. Scheduling strategy plays an important role in the Grid environment to schedule the user jobs, and dispatch them to appropriate Grid resources. A good job scheduling method is needed to reduce the total time taken for the job execution in the Grid. This project focuses on the scheduling strategies for coarse-grained Grid applications. GridSim Toolkit has been used to model coarse-grained Grid applications by developing an efficient and effective job scheduling method. The proposed work deals with a job grouping-based scheduling system that dynamically assembles the individual fine-grained jobs of an application into a group of jobs, and sends these coarse-grained jobs to the Grid resources. This dynamic grouping should be done based on the processing requirements of each application, Grid resources availability and their processing capability. The granularity size of job processing is introduced to facilitate the job grouping activity in determining the total amount of jobs that can be processed in a resource within a specified time. The job grouping method decreases the total processing time and cost.

Keywords: Grid, job, toolkit, Gridsim



THE IMPACT OF CUSTOMER EXPECTED PERFORMANCE ON ONLINE WORD OF MOUTH WITH TRUST MEDIATOR

Alireza MOGHADDASI

Faculty Member of Imamreza International University, Mashhad, Iran

Ramuna MİRHAJIANMOGHADDAM

Ph. D. Candidate of Industrial Management, Yazd University, Yazd, Iran

ABSTRACT

The purpose of this study was to study the impact of customer-expected performance dimensions on online WOM of e-commerce websites with the role of trust mediator. This research is applied purpose and in terms of descriptive-survey nature. The statistical population of this study is all users of ebusiness websites in Mashhad, Iran. The sampling method is available in this non-probability research and the sample size is determined based on the number of explicit variables of the research. Finally, 175 samples were analyzed. The tool for collecting the standardized questionnaire was Loureiro et al. (2018) whose reliability was assessed by Cronbach's alpha and its construct validity by confirmatory factor analysis. Hypotheses were tested using structural equation modeling with the help of Smart PLS software. The results show that customer's expected performance influences customer satisfaction, trust and online WOM. Customer satisfaction also influenced the trust and online WOM and the effect of trust on online WOM was also confirmed. In this study, the mediating role of trust was confirmed.

Keywords: Customer Expected Performance, Customer Satisfaction, Trust, Online Word of mouth



HUMAN AUGMENTATION- AN OVERVIEW

Talapaneni GEETHIKA

RMK Engineering College, Kavaraipettai, Tiruvallur District. Tamil Nadu, India.

Dr. M. MEENA

RMK Engineering College, Kavaraipettai, Tiruvallur District. Tamil Nadu, India.

Dr. Santhi M. GEORGE

RMK Engineering College, Kavaraipettai, Tiruvallur District. Tamil Nadu, India.

Dr. A. VIJAYALAKSHMI

RMK Engineering College, Kavaraipettai, Tiruvallur District. Tamil Nadu, India.

ABSTRACT

Technologies that enhance human productivity and improve or restore capabilities of the human body or mind are an area of computing refer to “HUMAN AUGMENTATION”. It improves and restores the human body and mental capabilities. Its goal is to improve the human experience in both cognitive and physical ways. Other types of human augmentation technologies work with specific IT resources including the cloud, big data and mobile computing. These include wearable devices such as watches or bracelets that link the human body to external sources of information that are visual, audio or text bases. Some of the players in the human augmentation market include Google Inc, Samsung Electronics, Esko Bionics Holdings, Garmin, Fossil Group and others. There are many types in Human Augmentation like Bionics and Prosthetics, Brain computer interfaces, Neurotechnology, Nootropics, Gene Editing etc. Notable efforts in Human Augmentation are driven by the interconnected internet of Things (IoT) devices, including wearable electronics, personal drones, on-body and in-body nanonetworks. Non-invasive augmentation is possible with augmented reality and wearable technology. We’ve been editing our bodies cosmetically for a long time. Tattoos have been around for an estimated 12,000 years. Even Plastic Surgery is 100 years old, invented as we know it today to reconstruct soldiers faces after the first World war. Human Augmentation benefits are support or improve human capabilities and performance, alleviate social Inequalities, reduce social injustice, Improvement of overall physical and mental health, ensure human well-being and enhance bodily integrity.

Keywords: Human augmentation, IoT, Neurotechnology, human capabilities.

TÜRKİYE MOBİLYA SEKTÖRÜNÜN YILLARA GÖRE DIŞ TİCARET ANALİZİ

Hasan SERİN*

Kahramanmaraş Sütçü İmam Üniversitesi, Orman Fakültesi, Orman Endüstri Mühendisliği Bölümü, Kahramanmaraş, Türkiye

Ferhat ÖZDEMİR

Kahramanmaraş Sütçü İmam Üniversitesi, Orman Fakültesi, Orman Endüstri Mühendisliği Bölümü, Kahramanmaraş, Türkiye

Özet

Ülkelerin ekonomik yapıları içerisinde dış ticaret önemli bir yer tutmaktadır. Dış ticaret malların ulusal sınırların dışında alım satımı ile ilgili olarak, ithalat ve ihracat işlemlerinden oluşur. Gelişmiş ve gelişmekte olan ülkeler de dış ticaret döviz sağlamada ve ülkenin cari dengelerinde önemli bir etkiye sahiptir. Mobilya ürünlerinin de son yıllarda dış ticarete payı artmaktadır.

Bu çalışmamızda TUIK verileri ve bakanlıkların yayınladığı mobilya sektör raporları incelenerek 2011-2020 yıllar arasındaki mobilya sektörünün ihracat ve ithalat değerleri belirlenmiştir. 2011 yılında mobilya ürünlerinde yaklaşık 1.607 bin \$ ihracat gerçekleştirilir iken, 2020 yılında yaklaşık 2.396 milyon \$ ihracata ulaşılmıştır. Diğer taraftan, 2011 yılında yaklaşık 749 milyon \$ ithalat gerçekleşir iken, 2020 yılında 498 milyon \$ ithalat gerçekleşmiştir. Mobilya sektörü dış ticarete Türkiye ekonomisine pozitif yönlü bir katkı sağlamıştır.

Anahtar Kelimeler: Mobilya, İhracat, İthalat, Dış Ticaret

FOREIGN TRADE ANALYSIS OF THE TURKISH FURNITURE INDUSTRY BY YEARS

Abstract

Foreign trade has an important place in the economic structures of countries. Foreign trade consists of import and export transactions related to the buying and selling of goods outside national borders. Developed and developing countries also have a significant impact on foreign trade, foreign exchange and the country's current account balance. The share of furniture products in foreign trade has been increasing in recent years.

In this study, the export and import amounts of the furniture industry between 2011 and 2020 were determined by examining the TUIK data and the furniture sector reports published by the ministries. While approximately 1.607 thousand \$ export was realized in furniture products in 2011, approximately 2.396 million \$ export was reached in 2020.

On the other hand, while approximately 749 million dollars of imports were realized in 2011, 498 million dollars of imports were realized in 2020. As a result, the furniture industry has made a positive contribution to the Turkish economy in foreign trade.

Keywords: Furniture, Export, Import, Foreign Trade

Giriş

Ülkelerin gelişmesine ve refah düzeylerinin artmasına dış ticaret önem bir katkı vermektedir. Ülkelerin temel amaçlarından biri ekonomik büyümedir (Kesgingöz ve Karamelikli, 2015). Ticaret, mal ve hizmetleri belirli bir bedel karşılığı kullanıcılara ulaştıran alım-satım faaliyetidir. Ticaret, iç ve dış ticaret olmak üzere ikiye ayrılır. (Kaya ve Turguttopbaş 2012). Dış ticaret kavramı, uluslararası mal ticaretini kapsamaktadır (Utkulu, 2008). Dış ticaret, ithalat ve ihracat işlemlerinden oluşmaktadır. Ülkelerde ihracatlarını artırmak ve ithalatlarını azaltarak dünya ticaretinde önemli konumlara gelmeyi hedeflemektedir. Bu hedeflere ulaşmak için ülkelerin kendi ticaret potansiyelini arttıracak kararlar dış ticaret politikalarını oluşturmaktadır (Şerefli, 2016). İhracatın ülke ekonomisi ve kuruluşlar yönünden büyük bir öneme sahip olduğu somut bir gerçektir. İhracat, ülke ekonomisinin gelişmesinde ve kalkınmasında önemli rol oynar (Kendirli ve ark., 2003; Bedük ve İnce, 2005). Türkiye'nin dış ticaret ve ekonomik büyüme ilişkisini araştıran birçok çalışma yapılmıştır (Yapraklı, 2006; Koçat, 2008; Aktaş,2009; Korkmaz, 2014; Aksu, 2004).

Ülkemizde imalat sanayi içerisinde yer alan mobilya sektörü (Nemli ve ark., 2007; Serin ve Andaç, 2012) Türkiye'nin dış ticaretine katkılar vermektedir. İmalat sanayi içerisinde ihracatta aldığı pay %1,4-1,8, ithalat içerisinde aldığı pay ise, %0,28-2,9 arasında değişmektedir. Genel ihracat ve ithalat içerisinde aldığı pay ise sırasıyla %1,3-1,7, %0,23-2,2 arasında değişmektedir (Anonim 2020)

Türkiye'deki Mobilya sektörünü ekonomiye katkısını özet olarak; işyeri sayısı 2006 yılında 35.854 iken, bu sayı 2012 yılında 39.036'ya, 2019 yılında ise 39.042'ye yükselmiştir. Ücretli çalışan sayısı ise 2006 yılında 106.807 iken, 2012 yılında 159.246'ya, 2019 yılında ise 197.733 kişiye ulaşmıştır. Üretim değeri aynı dönemde iki katından fazla büyüyerek 2012 yılında 16 milyar TL'ye ve 2019 yılında ise 44 milyar TL'yi geçmiştir. Katma değerdeki artış daha hızlı gelişmiştir. 2006 yılında yaratılan katma değer 1,5 milyar TL iken, 2012 yılında 3,5 milyar ve 2019 yılında ise 10 milyar TL olarak gerçekleşmiştir (Anonim 2015; Anonim 2020).

Türkiye mobilya sektörü, Dünya mobilya üretiminin yaklaşık %1,3'ünü gerçekleştirmektedir. Türkiye mobilya sektörü, 2016 yılı itibarıyla 230 ülkeye 2,234 milyar dolar mobilya ihraç etmiş ve Dünya sıralamasında 14. Avrupa ülkeleri sıralamasında ise 6. sırada yer almıştır. 2012 değerlerine göre Dünya sıralamasında 5, Avrupa sıralamasında ise 10 kademe ilerlemiştir. İthalat verilerine göre, 125 ülkeden 60 milyon dolar değerinde mobilya ithal etmiş ve Dünya sıralamasında 27. Avrupa ülkeleri sıralamasında ise 12. sırada yer almıştır (TOBB, 2017).

Dünya dış ticaretinde mobilya sektörü önemli bir konumda yer almaktadır. Mobilya üretiminin yaklaşık 473 milyar dolar olduğu tahmin edilmektedir. 197 milyar dolarlık bölümü ihracat, 190 milyar dolarlık bölümünü ithalat oluşturmaktadır. Dünya mobilya ticaretini ağırlıklı gelişmiş ve gelişmekte olan ülkeler

gerçekleştirmektedir (Anonim, 2020).

Bu çalışmamızda imalat sanayi içerisinde yer alan ve orman ürünleri sektöründe önemli bir konuma sahip olan mobilya sanayisinin dış ticaretteki durumu yıllara bağlı olarak incelenmiştir.

Materyal ve Yöntem

Materyal

Bu çalışmamızda Türkiye mobilya sektörünün dış ticaretini araştırmak için Türkiye İstatistik Kurumu (TÜİK) verileri, bakanlıkların ve odaların yayınladığı mobilya sektör raporları materyal olarak seçilmiştir. Türkiye mobilya sektörünün 2011-2020 yılları arasındaki dış ticaretini oluşturmak için;

- TÜİK verileri,
- T.C. Kalkınma Bakanlığı Onuncu Kalkınma Planı Mobilya Çalışma Grubu 2018
- T.C. SANAYİ VE TEKNOLOJİ BAKANLIĞI, Mobilya Sektör Raporu, 2020
- T.C. Ticaret Bakanlığı Mobilya Sektör Raporu, 2021

incelenmiştir.

Yöntem

Mobilya sektör rapor verileri Microsoft Excel programında tablo ve grafik haline dönüştürülmüştür. 2011-2020 yıllar arasındaki mobilya sektörünün ihracat ve ithalat değerleri,

Mobilya ihracatının ithalatı karşılama oranı ve ticaret hacmi değerleri belirlenmiştir

Bulgular

Değişik sektör raporlarından elde edilen veriler kullanılarak 2011-2020 yılı arasında Türkiye mobilya sektörünün dış ticaret durumu Tablo 1’de gösterilmiştir. Türkiye Mobilya ihracatı 2011 yılında yaklaşık 1.606 milyon dolar, 2015 yılında yaklaşık 2.166 milyon dolar ve 2019 yılında ise yaklaşık 3.067 dolar olarak gerçekleşmiştir. 2020 yılında dünyada yaşanan korona virüs nedeniyle yaşanan pandemi nedeniyle yaklaşık 2.396 milyon dolar ihracat yapılabilmektedir.

Tablo 1. Türkiye'nin 2011-2020 yılları arasında mobilya sektörü dış ticareti

Yıllar	İhracat (000 \$)	İthalat (000 \$)	Dış Ticaret Dengesi (000 \$)	Karşılama Oranı (Export/Import)X100	Hacim (000 \$)
2011*	1.606.993	857.018	749.975	188	2.464.011
2012*	1.898.602	821.357	1.077.245	231	2.719.959
2013**	2.130.500	839.542	1.290.958	254	2.970.042
2014	2.319.311	854.212	1.465.099	272	3.173.523
2015	2.166.546	747.880	1.418.666	290	2.914.426
2016	2.141.524	529.813	1.611.711	404	2.671.337
2017	2.067.251	521.580	1.545.671	396	2.588.831
2018	2.345.094	505.012	1.840.082	464	2.850.106
2019	3.067.611	472.740	2.594.871	649	3.540.351
2020***	2.396.069	498.092	1.897.977	481	2.894.161

*T.C. Kalkınma Bakanlığı Onuncu Kalkınma Planı Mobilya Çalışma Grubu2018

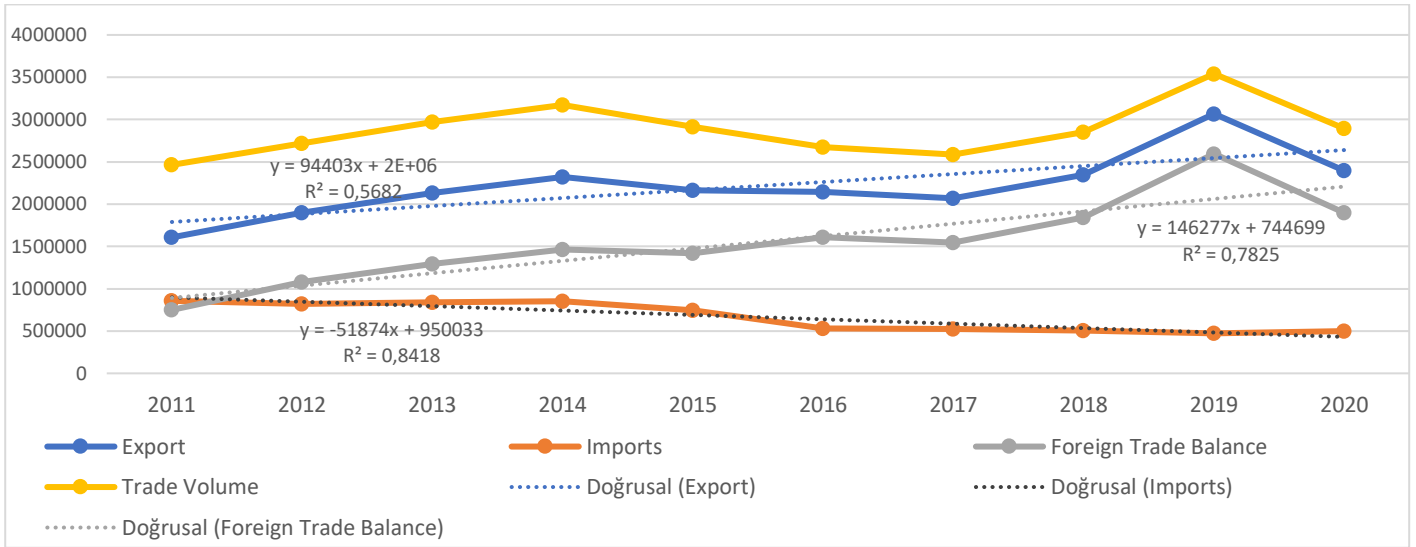
** T.C. SANAYİ VE TEKNOLOJİ BAKANLIĞI, Mobilya Sektör Raporu, 2020

*** T.C. Ticaret Bakanlığı Mobilya Sektör Raporu, 2021

Tablo 1'e göre Türkiye'nin ithalat oranı incelendiğinde, 2011 yılında yaklaşık 857 milyon dolar, 2015 yılında yaklaşık 747 milyon dolar ve 2019 yılında yaklaşık 472 milyon dolar olarak gerçekleşmiştir. Ayrıca, Türkiye'nin mobilya sektörü dış ticaret hacmi 2011 yılında yaklaşık 2.464 milyon dolar, 2015 yılında yaklaşık 2.914 milyon dolar, 2019 yılında yaklaşık 3.540 milyon dolar ve 2020 yılında ise yaklaşık 2.849 milyon dolar olarak gerçekleşmiştir.

Türkiye'nin mobilya dış ticaretinde ihracatın ithalatı karşılama oranı pozitif yönde değerler vermiştir. İhracatın ithalatı karşılama oranları 2011 yılında %188, 2015 yılında %290 ve 2020 yılında ise %481 olarak hesaplanmıştır.

Tablo 1'deki veriler kullanılarak 2011-2020 yılları arasında Türkiye mobilya sektörünün dış ticaretteki ihracat, ithalat, dış ticaret dengesi ve ticaret hacmi değerlerine bağlı olarak eğilim durumları ve regresyon denklemi Şekil 1' de verilmiştir. Elde edilen regresyon denklemleri Türkiye mobilya dış ticaret değerlerinin tahminlerinde kullanılması için R² değerleri uygun olduğunu göstermektedir.



Şekil 1. Türkiye Mobilya Sektörünün 2011-2021 yılları arasındaki eğilimleri

Dış ticaret eğilimleri Şekil 1'e göre incelendiğinde Türkiye'nin mobilya ihracatında olumlu yönde artış olduğu, ithalat eğiliminde ise bir azalma olduğu görülmektedir. Özellikle son yıllarda ithalat eğiliminde büyük bir azalma olduğu anlaşılmaktadır.

Sonuçlar

Yapılan değerlendirmeler sonucunda;

- Türkiye'nin mobilya ihracat değeri 2011 yılında 1.606 milyon dolardan 2020 yılına yaklaşık %149 artarak 2.396 milyon dolara çıkmıştır.
- Türkiye'nin mobilya ithalat değeri 2011 yılında 857 milyon dolardan 2020 yılına yaklaşık %58 azalarak 498 milyon dolara inmiştir.
- Türkiye mobilya sektörü dış ticarete 2011-2020 yılları arasında değer olarak pozitiftir.
- Mobilya sektörü ihracatı 2018 yılında 2,65 milyar dolar olarak gerçekleşmiş olup, 2019 yılında bir önceki yıla göre %15,7 oranında artarak 3,06 milyar dolar olmuştur. Mobilya sektörü ithalatı 2018 yılında 516 milyon dolar olarak gerçekleşmiş olup, 2019 yılında ise bir önceki yıla göre %8,5 azalarak 472 milyon dolar olmuştur.

Türkiye imalat sanayi içerisinde yer alan ve dış ticarete katkı veren mobilya sektörü, dış ticaret dengesi artı olan sektörlerimizdendir. Türkiye'nin coğrafi konumu ve lojistik avantajından dolayı son yıllarda yurtdışı pazarlara doğrudan kendi dağıtım kanallarını açan firma sayılarında önemli artışlar olmuştur. Diğer taraftan, yurt dışında inşaat sektöründe faaliyet gösteren Türk şirketlerin sayılarının artması ve kullanılan mobilyaların Türkiye'den sağlanması ihracatın artmasına olumlu katkılar yapmıştır.

Kaynaklar

- Aksu, L., (2014). "Türkiye'de 1960-2009 Yıllarını Kapsayan Dış Ticaret Politikalarının İktisadi Büyüme Üzerindeki Etkilerinin Ekonometrik Analizi", *Trakya Üniversitesi Sosyal Bilimler Dergisi*, 16(1): 363-408
- Aktaş, C., (2009). "Türkiye'nin İhracat, İthalat ve Ekonomik Büyüme Arasındaki Nedensellik Analizi", *Kocaeli Üniversitesi Sosyal Bilimler Enstitüsü Dergisi*, 18(2): 35-47
- Anonim, (2015). *Mobilya İmalatı Sanayi, Küresel Rekabette İstanbul Sanayi Odası Meslek Komiteleri Sektör Stratejileri Projesi*, ISBN: 978-605-137-432-1, 70s.
- Anonim, (2020). *Mobilya Sektör Raporu, Sanayi Genel Müdürlüğü, Sektörel Raporlar ve Analizler Serisi*, Ankara. 21s.
- Bedük, A., İnce, M., (2005). *Türkiye'de İhracatın Geliştirilmesinde Sektörel Dış Ticaret Şirketlerinin Önemi, Öneri Dergisi, Volume 6, Issue 23, 169- 179*
- Kaya, F. ve Turguttopbaş, N., (2012). *Dış Ticaret İşlemleri, T.C. Anadolu Üniversitesi Yayını No: 2526*.
- Kesgingöz, H., ve Karamelikli, H., (2015). "Dış Ticaret-Enerji Tüketimi ve Ekonomik Büyümenin CO2 Emisyonu Üzerine Etkisi", *Kastamonu Üniversitesi İktisadi ve İdari Bilimler Dergisi*, Sayı:9.
- Kendirli, S., Kılıç, S., Çağırın, H. (2003). *Türkiye'deki Küçük ve Orta Ölçekli İşletmelerin İhracat Durumlarına Yeni Bir Çözüm: Elektronik Ticaret ve Çorum'da Faaliyet Gösteren KOBİ'lere Yönelik Araştırma. Ekonomik ve Teknik Dergi Standart*, 504, s.47.
- Koççat, H., (2008), "Exchange Rates, Exports and Economic Growth in Turkey: Evidence from Johansen Cointegration Tests", *International Journal of Economic Perspectives*, 2(1): 5-11
- Korkmaz, S., (2014). "Türkiye Ekonomisinde İhracat ve Ekonomik Büyüme Arasındaki Nedensellik İlişkisi", *Business and Economics Research Journal*, 5(4): 119-128.
- Nemli, G., Hızıroğlu, S., Serin, H., Akyüz, K.C., Akyüz, İ., Toksoy, D., (2007). *A Perspective from furniture and cabinet manufacturers in Turkey, Building and Environment* 42 1699-1706.
- Serin, H., Andaç, T., (2012). *An investigation of the preferences of furniture consumers depending on education and age factors in Turkey, African Journal of Business Management* Vol. 6(22), pp. 6658-6666.
- Şerefli, M., (2016). *Dış Ticaretin Ekonomik Büyüme Üzerine Etkisi: Türkiye Örneği, Kastamonu Üniversitesi İktisadi ve İdari Bilimler Fakültesi Dergisi* 13: 136-143
- Utkulu, U., (2008), "Türkiye'de Dış Ticaretin Gelişimi ve Yapısal Değişim", *Dokuz Eylül Üniversitesi, İktisadi ve İdari Bilimler Fakültesi, İktisat Bölümü*.
- TOBB, (2017). *Türkiye Mobilya Ürünleri Meclisi Sektör Raporu, TOBB Yayın No: 2018/304*
ISBN: 978-605-137-684-4, Gökçe Ofset, Ankara, 96s.
- Yapraklı, S., (2007). *İhracat ile Ekonomik Büyüme Arasındaki Nedensellik: Türkiye Üzerine Ekonometrik Bir Analiz, ODTÜ Gelişme Dergisi*, 34: 97-112.

PANDEMİ DÖNEMİNDE TÜRKİYE MOBİLYA SEKTÖRÜNÜN GZFT ANALİZİ İLE DEĞERLENDİRİLMESİ

Hasan SERİN*

Kahramanmaraş Sütçü İmam Üniversitesi, Orman Fakültesi, Orman Endüstri Mühendisliği Bölümü, Kahramanmaraş, Türkiye

Ferhat ÖZDEMİR

Kahramanmaraş Sütçü İmam Üniversitesi, Orman Fakültesi, Orman Endüstri Mühendisliği Bölümü, Kahramanmaraş, Türkiye

ÖZET

İşletmelerin gelecek ile ilgili doğru politika ve strateji belirlemede içerisindedir bulunduđu durumu dikkate alarak güçlü yönlerini, zayıf yönlerini, fırsatlarını ve tehditlerini (GZFT) tarafsız ve doğru biçimde belirlemelidir. GZFT analizi mevcut durumu ortaya koymak için kullanılan yöntemlerden birisidir. Bu bildiri, pandemi döneminde ülkemizin mobilya sektörünün durumu, sektörde çalışan mühendisler, iş yeri sahipleri ve konu uzmanı akademisyenlerden görüş alınarak, beyin fırtınası tekniđi ile GZFT analizi yapılarak ortaya konulmuştur. Mobilya sektörünün pandemi döneminde en önemli güçlü yönleri; ülkemizin ihracat için cođrafi konumu ve ürün çeşitliliđi, zayıf yönleri ise; finans yetersizliđi, profesyonel yönetici eksikliđi, fırsatlar; iç ve dış pazarda artan talep, Avrupa ve Orta Dođu pazarına yakınlık, tehditler olarak da; Çin ürünleri, sektörde taklit ürünlerin fazlalığı ve küçük işletmelerin rekabet edememe gücü olarak belirlenmiştir.

Anahtar Kelimeler: Mobilya, Pandemi, GZFT analizi

EVALUATION OF THE TURKISH FURNITURE INDUSTRY WITH SWOT ANALYSIS DURING THE PANDEMIC PERIOD

ABSTRACT

Considering the situation in which businesses determine the right policy and strategy for the future, they should determine their strengths, weaknesses, opportunities and threats (SWOT) impartially and accurately. SWOT analysis is one of the methods used to reveal the current situation. In this paper, the situation of the furniture sector in our country during the pandemic period was revealed by taking the opinions of the engineers, business owners and academicians working in the sector, and SWOT analysis using the brainstorming technique. The most important strengths of the furniture industry during the pandemic period were determined as the geographical location and product variety of our country for export, and the weaknesses were identified as lack of finance and lack of professional managers. On the other hand, increasing demand in the domestic and foreign markets as opportunities for the sector, proximity to the European and Middle East market, and Chinese products, the excess of imitation products in the sector and the inability of small enterprises to compete are determined as threats.

Keywords: Furniture, Pandemic, SWOT analysis,

Giriş

Türkiye Mobilya sektörü küçük ve orta ölçekli işletme yapısına sahip gelişen sektörlerinden biridir, 2000’li yıllarda sonra büyük ölçekli uluslararası rekabette üretim yapan ve kümeleme olarak belirli bölgelerde kurulmuş işletmeler bulunmaktadır. Türkiye mobilya sektörü her geçen yıl pazar şartlarına uygun ürün çeşitliliği ve standartlarını artırmaktadır.

Mobilya sektöründe TÜİK verilerine göre; 39.042 işyeri sayısı, 197.733 çalışan sayısı ile imalat sanayisi içerisinde önemli bir konumdadır. Ayrıca, mobilya ile ilgili perakende sektöründe de 100.000 çalışan sayısının olduğu tahmin edilmektedir. Mobilya sanayi katma değer açısından da ülkemizin önde gelen sektörlerinden birisi olup, ihracatta yerli kaynakları en çok kullanan ve ithal ürünlere bağımlılığı en az olan sektörlerden biri olarak ekonomiye katkısını artarak devam ettirmektedir (Anonim, 2020).

Diğer taraftan, Dünya mobilya üretimi 2004 yılında yaklaşık 220 milyar dolar değerinde iken 2013 yılında 437 milyar dolara kadar ulaşmıştır. Dünya mobilya üretiminin 150 milyar dolarlık bölümü üretici ülkelerde tüketiciye arz edilir iken, 70 milyar doları aşan bölümü uluslararası dış ticarete değerlendirilmiştir. Mobilya pazarının 2050 yılında 1 trilyon doları geçeceği tahmin edilmektedir (Sarıkaya ve Doğan, 2016).

Mobilya sektörünün dünya mobilya pazarında rekabette dahi güçlü hale gelmesi, kendini geliştirmesi, gelecekle ilgili doğru kararlar alması, ulusal ve uluslararası değişen çevre şartlarına uyması ve sürdürülebilir olarak yönetilmesi için stratejik analizler yapması gerekmektedir

İşletmeler çalışma konuları, yapıları, misyon ve vizyonlarını dikkate alarak yönetilmektedir. İşletmeler alacakları kararlarda, içinde bulunduğu konumu ve çevresini incelemeli, değişim verilerini planlama ve uygulamalarında kullanmalıdır (Dinçer 2007). İşletme, ulusal ve uluslararası çevreyi incelediğinde güçlü ve zayıf yönlerini, oluşan yeni fırsatlar ve tehditlerin farkında olacaktır (Eren 2013; Erol ve ark. 2013; Serin, ve Özdemir, 2018). İşletmeler güçlü yanlarını geliştirmek ve zayıf yanlarını azaltmak, fırsatlardan yararlanmak ve tehditlere karşı önlem alarak işletmelerin dahi yönetilmesini sağlayacaktır (Şahin ve Serin, 2018). Ancak, işletmenin bunları yapabilmesi için, mevcut durumunu tespit etmesi gerekmektedir. İşletme mevcut durumunu GZFT analizi ile tespit edebilir ve buna bağlı olarak stratejisini belirleyebilir (Tetik, 2019).

Bu çalışmada, Türkiye mobilya sektörünün pandemi durumunda yaşadıkları zorluklar, fırsatlar ve tehditler ortaya konulması amaçlanmıştır. Yapılan çalışma sonucunda sektöre yardımcı olacak öneriler verilmiştir.

Materyal ve Metot

Materyal olarak ülkemizdeki mobilya sanayi seçilmiştir. Pandemi döneminde Türkiye mobilya sektörünün durumu ortaya koymak için, sektörde çalışan mühendisler, iş yeri sahipleri ve konu uzmanı akademisyenlerden görüş alınarak, beyin fırtınası tekniği ile GZFT analizi yapılarak ortaya konulmuştur

Beyin fırtınası, belirli bir konuda belirli sayıdaki konu uzmanının çözüm arayışına yönelik grup tartışması sırasında farklı görüşler ile çözüm yollarını artırmak için kullanılan yöntemlerden biridir (Osborn, 1961). Bu teknik, belirli sayıda bir katılımcı ile gerçekleştirilir. Belirli kurallar uygulanır ve katılımcıların yeni ve yaratıcı fikirler üretmesi hedeflenir. Beyin fırtınası tekniğinde, herkesin katılımı eşit ve takımın birliğini sağlar (Hardingam, 1997; Tuckman, 2001).

GZFT Analizi: Bir ürünün rakiplerine göre avantajlarının ve dezavantajlarının tespit edilip, işletmenin ürünle ilgili karşılaşılabileceği fırsatların ve tehditlerin önceden saptanarak stratejik pazarlama planlaması yapmasında elde ettiği verileri kullanması yöntemidir (Güngör ve Arslan, 2004, Serin 2011).



Şekil 1. GZFT Analizi (<http://sbpturkiye.com/swot-analizi.html>)

Şekil 1’de görüldüğü gibi, GZFT, Güçler (Strengths), Zaafiyetler (Weaknesses), Fırsatlar (Opportunities) ve Tehditler (Threats) kelimelerinin ilk harflerinden oluşmaktadır (Kahraman ve ark., 2007). GZFT sonucunun değerlendirilmesi ile alınacak kararlar ilişkin stratejik bir görüş ortaya konulmaktadır (Uçar ve Doğru, 2005).

Bulgular

Beyin fırtınası sonucunda mobilya sektörü ile ilgili bir çok fikir üretilmesine rağmen sadece pandemi döneminde ön plana çıkan Türkiye mobilya sektörünün güçlü yönler, zayıf yönler, fırsatlar ve tehditler ele alınmıştır.

Güçlü yönler

- Son yıllarda kurulan ve seri, markalı üretim yapan modern üretim tesislerinin varlığı,

- Üretimde oluşan yoğun kümelenme, makineleşmenin artması ve buna bağlı olarak yüksek üretim teknolojisinin kullanılması,
- Avrupa'daki gelişmiş ülkelere göre daha ucuz olan işgücü maliyetleri,
- Sanayinin teknoloji kullanımına yönelik artan isteği ve uyumu ile ürün ve malzeme çeşitliliğinin arttırması,
- Potansiyel pazarlara yakınlık ile lojistik avantajlar ve genel itibari ile önemli pazarlar karşısındaki coğrafi konum,
- Pandemi döneminde siparişlere göre esnek üretim imkanlarının bulunması.

Zayıf Yönler

- Pandemiden dolayı, mesleki uygulamalı eğitim yetersizliği ve nitel ve nicel olarak kalifiye eleman bulunmaması,
- Pandemiden dolayı hammadde ve yardımcı malzeme tedarikinde yaşanan kısıtlamalar,
- Pandemiden dolayı yüksek hammadde maliyetleri,
- Pandemiden dolayı fuar ve organizasyonların ertelenmesi ve tanıtım faaliyetlerinin yetersizliği,
- Türkiye mobilya sektörünün büyük çoğunluğunun düşük sermayeli küçük ve orta boy işletmelerden oluşması,
- Markalaşma, kalite ve yönetim eksikleri,
- Pandemi döneminde devlet desteğinin istenen seviyede olmaması,
- Pandemi döneminde artan girdi maliyetleri

Fırsatlar

- Pandemi döneminde uzun süreli evde kalınması nedeniyle müşteri odaklı ürün ve çeşitlilik talebi,
- Avrupa'daki artan tüketim nüfusu,
- Dünya mobilya tüketiminde artış ve inşaat sektöründeki artan yatırımlar,
- Sektörde, inovasyon, tasarım ve marka bilincinin her geçen gün artıyor olması,
- Türkiye'nin coğrafi konumu nedeniyle değişik pazarlara yakınlık,
- Müşterilerin çevre ve iklim değişikliği ile ilgili bilinç düzeyinin artması nedeniyle çevre uyumunu gözeten yeşil mobilyaların talebinin artması,

- Bilgi Teknolojisi ve elektronik cihazların gelişmesi ile birlikte akıllı mobilyalara artan ihtiyaç,

Zayıf yönler

- Pandemi döneminde yurt dışından sağlanan hammadde ve yardımcı malzeme tedarikinde yaşanan engeller,
- Mobilya sektörü için yetersiz yurtiçi hammadde kaynakları,
- Mobilya sektöründe üretim teknolojisinde dışa bağımlılığın sürmesi,
- Pandemi nedeniyle tanıtım ve pazarlama faaliyetlerinin sınırlı olması,
- Pandemi nedeniyle yaşanan karantinalar ve alınan tedbirlerden dolayı kalifiye işgücü açığının artması,
- Sektörde yaygın olarak yaşanan model ve tasarım taklidi ve kopyacılığın sürmesi,
- Çin ile rekabet

Sonuç ve Öneriler

Beyin fırtınası tekniği ile yapılan GZFT analizi sonucunda;

- Mobilya sektörünün pandemi döneminde en önemli güçlü yönleri; ülkemizin ihracat için coğrafi konumu ve ürün çeşitliliği,
- Zayıf yönleri ise; finans yetersizliği, profesyonel yönetici eksikliği,
- Fırsatlar; iç ve dış pazarda artan talep, Avrupa ve Orta Doğu pazarına yakınlık,
- Tehditler olarak da; Çin ürünleri, sektörde taklit ürünlerin fazlalığı ve küçük işletmelerin rekabet edememe gücü olarak belirlenmiştir.

Öneriler olarak;

- Yaşanan gelişmeler pandemi döneminin devam edeceğini göstermektedir. Bu ortamda işletmelerin pazarlama ve tanıtım faaliyetlerini arttırması için internet ortamında sanal fuarlar ve tanıtım imkanlarını geliştirmelidirler.
- İşletmelerin pandemi döneminde hayatta kalmaları için finansman ve sermaye olanaklarının artırılması yolları araştırılmalı, maliyetleri azaltacak destekler (enerji, hammadde vb.) verilmelidir.
- Avrupa ve Orta Doğu pazarına yakınlık dikkate alınarak pazara dönük müşteri istek ve beklentilerini karşılayacak esnek üretimler yapılmalıdır.
- Pandemi döneminde iş gücü temininde yaşanan olumsuzlukları gidermek ve rekabet gücünü arttırmak için teknolojik (otomasyon, smart production) yatırımlara destek verilmelidir.

- Pandeminin hammadde, yardımcı malzeme kaynakları ve lojistik sektörünü etkisi sonucu yaşanan hammadde sorunlarını aşmak için yerli hammadde ve yardımcı malzeme üretim olanaklarının geliştirilmesi,
- Türk mobilya sektörü yurtiçi, yurtdışı geniş bayi ve mağazalaşma, potansiyel pazarlara yakınlık ile lojistik avantajını, önemli pazarlar karşısındaki coğrafi konumu değerlendirmelidir.

Kaynaklar

- Anonim, (2020). Mobilya Sektör Raporu, Sanayi Genel Müdürlüğü, Sektörel Raporlar ve Analizler Serisi, Ankara. 21s.
- Diñçer, Ö. (2007). Stratejik Yönetim ve İşletme Politikası, 8. Baskı, Alfa Yayınevi, İstanbul.
- Eren, E., (2013). Stratejik Yönetim ve İşletme Politikası, 9. Baskı, Beta Basım A.Ş., İstanbul.
- Erol, Y., İnce, A., Aras, M., (2013). “Türk Sanayi Sektöründe Stratejik Yönetim Yaklaşımları Tercih: ISO 1000 Firmalarında Bir Araştırma”, Business and Economics Research Journal, 4 (3)
- Hardingham, A., (1997). Takım Çalışması (A. Bora ve O. Cankoçak, Çev.). İlkaynak Kültür ve Sanat Ürünleri LTD.ŞTİ.
- Kahraman, C., Çetin Demirel, N., Demirel, T., (2007). Prioritization of e-Government strategies using a SWOT-AHP analysis: the case of Turkey. European Journal of Information Systems, 16, 284-298.
- Sarıkaya, S., Doğan, Ö., (2016). Mobilya Sektör Raporu, Orta Anadolu İhracatçı Birlikleri Genel Sekreterliği, Ankara, 36s.
- Serin, H., (2011). Orman Endüstri Mühendislerinin Sorunları ve Fırsatları. 2023'e Doğru 1. Doğa ve Ormancılık Sempozyum bildiri kitapçığı, 2023'e Doğru 1. Doğa ve Ormancılık Sempozyumu Konferansı, 21-27 Kasım, 117-127 s., Antalya, Türkiye.
- Serin, H., Özdemir, F., (2018). Artvin İlinin Orman Ürünleri Bakımından GZFT Analizi İle Değerlendirilmesi. Uluslararası Artvin Sempozyumu 18-20 Ekim 2018.
- Şahin, Y., Serin H., (2018). Diyarbakir İli Mobilya Sanayisinin GZFT Analizi İle Değerlendirilmesi, Turkish Journal of Forest Science 2 (1): 83 – 90
- Tetik, M., (2019). GZFT Analizi, İşletmenin Stratejisinin Belirlenmesi ve Dengeli Ölçüm Kartının Oluşturulması: Antalya'daki Bir Alkollü İçecek İşletmesinde Uygulama, Muhasebe Bilim Dünyası Dergisi, 21(2); 393-426
- Tuckman, B.W., (1965). Developmental sequence in small groups. Psychological Bulletin, 63(6), 384-399.
- Uçar, D., Doğru, A. Ö., (2005). CDB Projelerinin Stratejik Planlaması ve SWOT Analizi. TMMOB Harita ve Kadastro Mühendisleri Odası, 10. Türkiye Harita Bilimsel ve Teknik Kurultayı 28 Mart-1 Nisan 2005, Ankara.

A REAL TIME FALL DETECTION OF ELDERLY PEOPLE IN INDOOR ENVIRONMENTS

Mustafa Hussain RAFEEQ
Gaziantep University

Serkan OZBAY
Gaziantep University

ABSTRACT

Human fall detection can help physiotherapists not only lessen after-fall consequences also even save lives by establishing sensor-based alarm systems. Typically, elderly individuals suffer from a variety of ailments, and falling is a fairly common occurrence for them at this time. In this light, this research serves as a framework for distinguishing fall event from other indoor natural human activities. In this research, we present a modified DenseNet 121 approach that relies on the deletion of some layers and the addition of others for fall detection. Losses are reduced and network variables like weights and learning rate are updated using the binary cross-entropy loss function. Finally, the sigmoid classifier is employed to identify human falls using binary classification. The suggested project achieves a precision of 98.83% in experiments, outperforming existing modern models.

Introduction

In this study, a fall is defined as an occurrence in which a person falls from a standing posture and is unable to support himself.

Elder people, especially those who live alone and unassisted, suffer from sudden falls due to the fragility of older people's bodies, as well as possible fall dangers (slippery floors, inadequate lighting, unstable furniture, obstructed paths, etc.). That is why a human fall detection system is very mandatory for many people.

In recent years, certain countries have seen a significant increase in their old population. According to statistics on human fall detection, falls are a major cause of injurious mortality in people over the age of 79 [1]. According to a study conducted by the National Institutes of Health in the United States, around 1.6 million elderly persons in United States suffer from fall-related injuries each year [2]. Furthermore, China is experiencing the greatest society ageing in Earth history, with the number of citizens expected to climb to almost 35% by 2050 from 2020 [2]. According to research [3], 93% of the elderly live alone in their homes, with 29% of them living alone in a house. Even if they do not have any physical injuries, it has been proven that nearly half of the elderly persons who are laying on the floor for more than an hour due to a fall would die within six months [4]. As a result, it is critical to implement a penetration monitoring system for elderly people that can identify fall behaviors inside the room quickly and automatically, alerting caregivers.

A deep learning and vision-based framework for human fall detection and classification are proposed in this

paper, which can monitor elderly persons in the interior environment. We modified a transfer learning DenseNet 121 model to detect person drop behavior. In addition, we tested our proposed model against the most well-known dataset, the UR fall detection dataset. In comparison to other current models, our suggested model performs admirably on these datasets.

Related Work

Various types of deep learning models have been developed throughout this decade. Convolutional neural networks (CNNs) have done enormous hits in areas such as image segmentation, object recognition, natural language processing, image processing, and machine translation, all of which necessitate a large training dataset.

According to research by Stone, Erik E., and Marjorie S., elderly individuals at the house fall majority of the time in low light settings [5]. By reducing occlusion effects, Sowmya K. and Kang-Hyun Jo [6] categorize fall occurrences in a congested internal setting. In [7], deep bidirectional LSTM (DB-LSTM) and convolutional neural network are used to create a real-world action recognition system. The deeper-cut method is used to extract the 2D skeleton from RGB sequences in [8], and long short-term memory (LSTM) is used to distinguish five different events. In [9], they use the faster R-CNN approach, which yields a 95.5% accuracy because it could not effectively assort fall cases while an individual is sitting down on a sofa or chair. In [10], they propose a two-stage human fall categorization model with 97.34 % accuracy. Chen et al. [11] use OpenPose to detect person fall cases using the skeleton of a person details with 97 percentage points.

Dataset

The UR fall detection dataset [12] is among the most widely used benchmarks, consisting of 70 indoor videos, 30 of which are fall occurrences and 40 of which are regular living activities. Two Kinect cameras are used to record fall actions, while only one camera is used to record daily life activities. There are 30 frames per video in this collection. Every movie has a resolution of 640×240 pixels.

Proposed Architecture

DenseNet [13] is a network architecture in which each layer is feed-forward connected to each other (within each dense block). All previous layers' feature maps are handled as distinct inputs for each layer, while their own feature maps are transferred on to whole following levels as inputs. DenseNet 121 consists of 4 dense blocks. The Table 1 shows the details of DenseNet 121 architecture.

Table 1: DenseNet 121 architecture

Layers	DenseNet 121
Convolution	7 x 7 conv, stride 2
Pooling	3 x 3 max pool, stride 2

Dense Block 1	$\begin{bmatrix} 1 \times 1 \text{ Conv} \\ 3 \times 3 \text{ Conve} \end{bmatrix} \times 6$
Transition Layer 1	1 x 1 conv
	2 x 2 average pool, stride 2
Dense Block 2	$\begin{bmatrix} 1 \times 1 \text{ Conv} \\ 3 \times 3 \text{ Conve} \end{bmatrix} \times 12$
Transition Layer 2	1 x 1 conv
	2 x 2 average pool, stride 2
Dense Block 3	$\begin{bmatrix} 1 \times 1 \text{ Conv} \\ 3 \times 3 \text{ Conve} \end{bmatrix} \times 24$
Transition Layer 3	1 x 1 conv
	2 x 2 average pool, stride 2
Dense Block 4	$\begin{bmatrix} 1 \times 1 \text{ Conv} \\ 3 \times 3 \text{ Conve} \end{bmatrix} \times 16$
Classification Layer	7 x 7 global average pool
	1000D fully-connected, SoftMax

The modifications made to this architecture are by deleting the SoftMax layer and adding some layers instead of it as shown in Table 2.

Table 2: DenseNet 121 Modified

Layers	DenseNet 121Modified
Pooling	average pool
Dense	units: 256 activation function: leaky relu
Dropout	0.4
Dense	units: 1 activation function: sigmoid

Evaluation Metrics

The accuracy, precision, recall, and F1-score of the suggested design are also assessed. The following equation [14] shows the rate of correctly identified data accuracy:

$$\text{Accuracy} = (TP + TN) / (TP + TN + FP + FN) \quad (1)$$

where TP stands for true positive rate, which means the detected outcome is a fall, which is in fact a fall case, TN stands for true negative rate, which means the detected state is a non-fall, which is indeed a non-fall event, FP stands for false-positive rate, which means the detected status is a fall, which is truly a non-fall event in real-time, and FN stands for false negative, which means the detected produce is a non-fall, which is really.

In binary classification, a precision score of 100% means that each item in the positive category is related to the positive item, as determined on the formula [14]:

$$\text{Precision} = \text{TP} / (\text{TP} + \text{FP}) \quad (2)$$

Sensitivity is defined as the likelihood of a positive test outcome using the equation [14]:

$$\text{Sensitivity} = \text{TP} / (\text{TP} + \text{FN}) \quad (3)$$

The formula for calculating specificity [14] is presented below, which gives the possibility of a negative test outcome.

$$\text{Specificity} = \text{TN} / (\text{TN} + \text{FP}) \quad (4)$$

The harmonic mean of precision and sensitivity is represented by the F1-score. The F1-score of the test data is calculated using the equation [14].

$$\text{F1 - score} = 2 * (\text{Precision} * \text{Sensitivity}) / (\text{Precision} + \text{Sensitivity}) \quad (5)$$

Proposed Architecture Process

A recording camera will be set in the house to monitor the elderly. Despite certain privacy worries, it will provide us with knowledge about our setting in the event of a fall cases. Video having a resolution of 224 x 224 are used to create sequential frames. Figure 2 illustrates the example of the process with the extraction of essential properties from frames. The output is sent to a sigmoid classifier to determine the category. The planned network is depicted in Figure 1 as an overview.

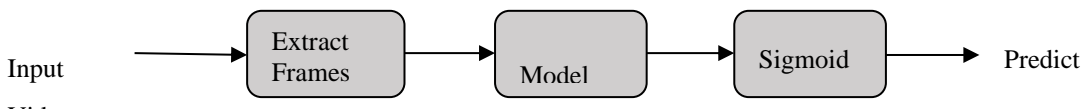


Figure 1. Proposed human fall classification model.



Figure 2. Detect human fall process.

Results

To execute this model, we conducted various tests on the proportion of training and validation datasets in order to improve accuracy, and we achieved 98.83% accuracy in the UR fall detection dataset. The model obtains good training and validation accuracy for 80% training, 10% validation, and 10% for testing data in the 20th

epoch as illustrated in Figure 3. Preprocessing was achieved in two steps: scaling and augmentation. Images are scaled to 224 x 224 to reduce computational costs. Augmentation is applied to the scaled image, which modifies images before the training. We used brightness, horizontal flip, saturation, and clip to enhance the image. This facilitates the model's generalization.

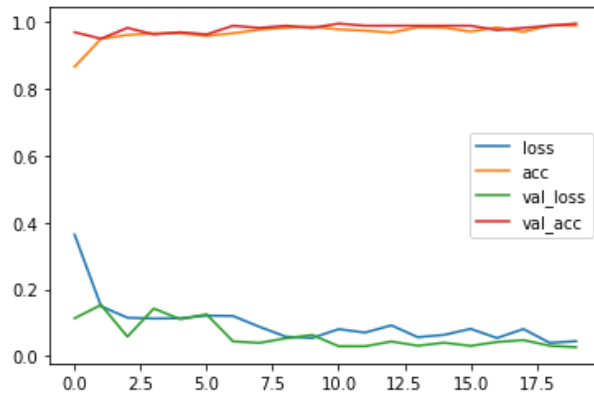


Figure 3. Performance of model for 80% training and 10% validation data.

Our suggested model achieves good accuracy with fewer training epochs. The confusion matrix in Figure 4 explains it. The grey boxes 84 and 86 refer to the true positive and true negative respectively. It means that the proposed method achieves accurate classification of 170 images out of 172 images. Between all, two non-fall images are incorrectly labelled as a fall event.

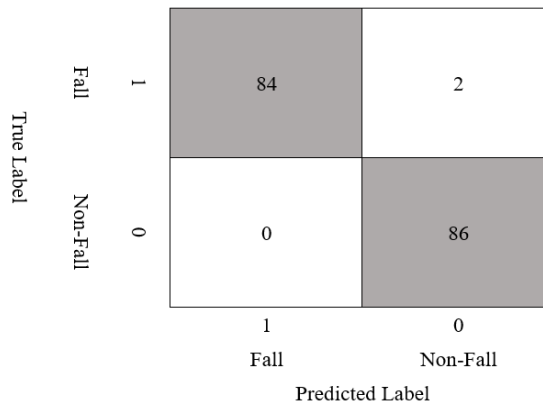


Figure 4. The output of the confusion matrix on the test dataset.

Table 3 shows the comparative classification results of our proposed technique and five other deep learning methods on the UR Fall Detection Dataset. The data reveal that our method outperforms other methods even in terms of overall accuracy, precision, and F-score. This means that, when it comes to fall detection, our system can more accurately detect the probability of a fall while reducing the chance of mistaking other everyday activities for fall out.

Table 3: Results between our method and some approaches on the same dataset.

Method	Accuracy %	Precision %	F-Score
Dai et al. [15]	97.33	97.78	97.78
Harrou et al. [16]	96.66	94	96.91
Kwolek and Kepski [17]	90	83.30	90.89
Kasturi et al. [18]	96.34	-----	-----
Wang et al. [19]	96.91	97.65	97.08
Our method	98.83	97.72	98.85

Conclusions

The research discussed in this article focuses on using machine learning techniques to investigate fall detection that is a precise and effective system for elderly. We adopted the fall classification of the person or not by modifying the DenseNet121 algorithm by deleting and adding some layers.

The proposed method is applicable, according to the findings of the experiments. On the UR Fall Detection Dataset, the method obtains 98.83 % accuracy. This finding demonstrates the importance of the combination of falling-state and fallen-state properties. The falling-state characteristics aid in detecting abrupt changes in the human body's form. The fallen-state features can detect the state of a human body lying on the ground and lessen the likelihood of similar motions, such as bending and being misjudged.

References

1. Mubashir, M., Shao, L., & Seed, L. (2013). A survey on fall detection: Principles and approaches. *Neurocomputing*, 100, 144-152.
2. Yang, L., Ren, Y., Hu, H., & Tian, B. (2015). New fast fall detection method based on spatio-temporal context tracking of head by using depth images. *Sensors*, 15(9), 23004-23019.
3. Rougier, C., Meunier, J., St-Arnaud, A., & Rousseau, J. (2011). Robust video surveillance for fall detection based on human shape deformation. *IEEE Transactions on circuits and systems for video Technology*, 21(5), 611-622.
4. Lord, S. R., Smith, S. T., & Menant, J. C. (2010). Vision and falls in older people: risk factors and intervention strategies. *Clinics in geriatric medicine*, 26(4), 569-581.
5. Stone, E. E., & Skubic, M. (2014). Fall detection in homes of older adults using the Microsoft Kinect. *IEEE journal of biomedical and health informatics*, 19(1), 290-301.
6. Kasturi, S., & Jo, K. H. (2017, July). Classification of human fall in top Viewed kinect depth images using binary support vector machine. In *2017 10th International Conference on Human System Interactions (HSI)* (pp. 144-147). IEEE.
7. Ullah, A., Ahmad, J., Muhammad, K., Sajjad, M., & Baik, S. W. (2017). Action recognition in video sequences using deep bi-directional LSTM with CNN features. *IEEE access*, 6, 1155-1166.
8. Lie, W. N., Le, A. T., & Lin, G. H. (2018, January). Human fall-down event detection based on 2D skeletons and deep learning approach. In *2018 International Workshop on Advanced Image Technology (IWAIT)* (pp. 1-4). IEEE.

9. Min, W., Cui, H., Rao, H., Li, Z., & Yao, L. (2018). Detection of human falls on furniture using scene analysis based on deep learning and activity characteristics. *IEEE Access*, 6, 9324-9335.
10. Han, K., Yang, Q., & Huang, Z. (2020). A two-stage fall recognition algorithm based on human posture features. *Sensors*, 20(23), 6966.
11. Chen, W., Jiang, Z., Guo, H., & Ni, X. (2020). Fall detection based on key points of human-skeleton using openpose. *Symmetry*, 12(5), 744.
12. Kwolek, B., & Kepski, M. (2014). Human fall detection on embedded platform using depth maps and wireless accelerometer. *Computer methods and programs in biomedicine*, 117(3), 489-501.
13. Huang, G., Liu, Z., Van Der Maaten, L., & Weinberger, K. Q. (2017). Densely connected convolutional networks. In *Proceedings of the IEEE conference on computer vision and pattern recognition* (pp. 4700-4708).
14. Ghoneim(2021), S. Accuracy, Recall, Precision, F-Score & Specificity, Which to Optimize on Available online:<https://towardsdatascience.com/accuracy-recall-precision-f-score-specificity-which-to-optimize-on867d3f11124>.
15. Dai, B., Yang, D., Ai, L., & Zhang, P. (2018, October). A novel video-surveillance-based algorithm of fall detection. In *2018 11th International Congress on Image and Signal Processing, BioMedical Engineering and Informatics (CISP-BMEI)* (pp. 1-6). IEEE.
16. Harrou, F., Zerrouki, N., Sun, Y., & Houacine, A. (2019). An integrated vision-based approach for efficient human fall detection in a home environment. *IEEE Access*, 7, 114966-114974.
17. Kwolek, B., & Kepski, M. (2014). Human fall detection on embedded platform using depth maps and wireless accelerometer. *Computer methods and programs in biomedicine*, 117(3), 489-501.
18. Kasturi, S., & Jo, K. H. (2017, July). Classification of human fall in top Viewed kinect depth images using binary support vector machine. In *2017 10th International Conference on Human System Interactions (HSI)* (pp. 144-147). IEEE.
19. Wang, B. H., Yu, J., Wang, K., Bao, X. Y., & Mao, K. M. (2020). Fall detection based on dual-channel feature integration. *IEEE Access*, 8, 103443-103453.



PLM ENHANCEMENT DEVELOPMENT PORTAL

Aman MISHRA

Alumni, Army Institute of Technology, Pune

Assoc. Prof. Dr. Rahul DESAI

Department of Information Technology, Army Institute of Technology, Pune

Assist. Prof. Dr. Mr. G. M. WALUNJKAR

Department of Information Technology, Army Institute of Technology, Pune

ABSTRACT

In Industry, Product Life Cycle Management (PLM) is the process of managing the entire lifecycle from its conception, through design and manufacture, to service and disposal. PLM integrates people, data, processes and business systems and provides a product information backbone for companies and their extended enterprise. During each Implementation the customizations of different PLM objects are done from scratch. It can be avoided by using other customization as reference and modify accordingly. In this, each code is segregated based upon few criterion namely, Object type, Module type and Tool. The idea of developing a code portal is to create a central repository of all the codes that are developed over a period of time. The code maintained in this repository will be modularized, standardized, factored, tested and documented in order to facilitate quick search and reference. As a developer, it is often observed that similar codes are rewritten over and over again for different customers or for different customizations pertaining to same customer. Each time, it requires putting same degree of effort as the developer starts coding from the scratch. The repository viz. the code portal would provide a point of reference to start. At the same time it would save on the time spent on developing the code. Thus various features includes reduced development time, creation of knowledge base repository, reduces dependency of developer on other members for help, collaboration among team members through discussion and reusability of code.

Keywords: PLM, Code Portal, Documentation, Modules, Customization



CONTRIBUTION TO THE VALORIZATION OF CRYSTALLIZED AND GRANULATED SLAG IN CONCRETE MAKING

Naoual HANDEL

Department of Civil Engineering, Laboratory InfraRES, University of Mouhamed Cherif Messadia, Souk-Ahras, Algeria
ORCID ID: 0000-0002-5711-9999

Aziza BOUTOUTA

Mechanics Research Center (CRM), Constantine, Algeria
ORCID ID: 0000-0002-5711-9999

Khalil BOUCHOUK

Department of Civil Engineering, Laboratory INFRARES, University of Mouhamed Cherif Messadia, Souk-Ahras, Algeria

ABSTRACT

Within the framework of the valorization of the waste of blast furnace, an experimental study was carried out on concretes made by the crystallized and granulated slag to terminate their physical-mechanical behaviors. Four types of concrete mixtures were prepared, one ordinary concrete, one slag concrete where gravel was replaced by crystallized slag, and two other all-slag concrete where gravel and sand were substituted by crystallized slag and the second by granulated slag sand.

The characterization of these concretes was made from their mechanical properties: compressive strength, tensile strength and longitudinal Young's modulus as well as their durability: capillarity, mass water absorption and shrinkage. The experimental results showed that the concretes with crystallized slag allow to obtain a significant improvement of their behavior in comparison with the ordinary concretes and prepared by the granulated slag.

Keywords: Concrete, Slag concrete, Crystallized slag, Granulated slag, Behaviors, mechanical characteristic.

YONGA LEVHA FABRİKASINDA RİSK ANALİZ ÖRNEĞİ

Ferhat ÖZDEMİR*

Kahramanmaraş Sütçü İmam Üniversitesi, Orman Fakültesi, Orman Endüstri Mühendisliği Bölümü, Kahramanmaraş, Türkiye

Hasan SERİN

Kahramanmaraş Sütçü İmam Üniversitesi, Orman Fakültesi, Orman Endüstri Mühendisliği Bölümü, Kahramanmaraş, Türkiye

Özet

Risk analizi iş kazalarının en aza indirilmesi için iş yerlerinde tehlikeleri belirlemek ve gerekli koruyucu önlemleri almak için önemlidir. Bu çalışmanın amacı işçi sağlığı ve iş güvenliği açısından yonga levha fabrikası çalışanlarının, çalışma ortamlarında karşılaşılabilecekleri tehlike, risk ve bu risklere karşı alınması gereken tedbirleri belirlemektir. Çalışma yerleri içerisinde iş kazalarına yol açabilecek olan potansiyel tehlike ve riskler L Tipi Matris (5x5 Matris) yöntemi ile olayın şiddeti ve risk olasılıkları kullanılarak tespit edilmiştir. İş kazalarına yol açabilecek risk ve tehlikelerin kabul edilemez seviyede olduğu bazı tespitler belirlenmiştir. Elde edilen risk matrisi sonucuna göre, yonga levha fabrikasında kabul edilemez risk faktörleri olarak, siloda bulunan korkulukları olmayan yüksek merdivenler, silo bandı rollerinin açıkta olması ve değirmenlerde koruyucu korkulukların bulunmaması olarak belirlenmiştir.

Anahtar Kelimeler: Yonga levha, Risk analizi, İş sağlığı ve güvenliği, L matris

RISK ANALYSIS EXAMPLE IN PARTICLEBOARD FACTORY

Abstract

Risk analysis is important to identify hazards and take necessary protective measures in order to minimize occupational accidents. The aim of this study is to determine the dangers and risks that the employees of the particle board factory may encounter in their working environment and the precautions to be taken against these risks in terms of occupational health and safety. Potential hazards and risks that may cause work accidents in workplaces were determined using the L Type Matrix (5x5 Matrix) method, using the severity of the event and the risk probabilities. Some determinations have been made that the risks and hazards that may lead to occupational accidents are at an unacceptable level. According to the obtained risk matrix result, unacceptable risk factors in the particle board factory were determined as high stairs without guardrails in the silo, the absence of protective silo belt rollers and the absence of protective guardrails in the mills.

Keywords: Particleboard, Risk analysis, Occupational health and safety, L matrix

Giriş

Üretim ve hizmet sektörü başta olmak üzere tüm sektörlerde ve hatta günlük hayatımız içerisinde insan faktörünün olduğu her yerde iş sağlığı ve güvenliği kavramının olması kaçınılmaz bir gerçektir. Bütün çalışanları dahil olmak üzere bir kurum ya da kuruluşun yaptığı işe bağlı olarak çalışanlarının sağlık ve güvenliğine etki eden faktör ile şartların tamamına iş sağlığı ve güvenliği denilmektedir (Ofluoğlu ve Sarıkaya, 2013). İş sağlığı ve iş güvenliği terimi hiçbir yerde ayrı olarak değerlendirilmemektedir (Fişek ve Piyal, 1989). Bunlar bir bütünü oluşturan kavramlardır. Çalışma hayatında iş kazası ve meslek hastalıklarının olması olağan bir durumdur. İş kazalarının olmasının temel sebebi çalışma ortamındaki tehlikeli durum, tehlikeli davranış ve kaçınılmaz sebep dediğimiz olağan üstü durumları ifade eden doğal felaketlerdir. İş kazasının önlenmesi %98 mümkün iken, meslek hastalıkları ise %100 önlenebilmektedir. Bu sebeplerden dolayı gerçekleşen iş kazası ve meslek hastalıklarından dolayı insan hayatı kaybolmakta, işgücü kaybı artmakta ve üretim miktarı azalmaktadır.

İş kazaları ve meslek hastalıklarının bir kısmı çalışan bir kısmı ise işveren kaynaklı olabilmektedir. Çalışanların tehlikeli davranışlarda bulunması ve işverenin çalışanlar için gerekli olan alet, araç-gereç, kişisel koruyucu vb. konularda yükümlülüklerini yerine getirmemesi iş kazalarının temel sebebidir. Ancak iş kazalarının ve meslek hastalıklarının sorumluluğu kanuni ve vicdani açıdan işverene aittir. Bu nedenle çalışma ortamlarında işverenler tarafından iş kazası ve meslek hastalığının önlenmesine yönelik tedbir açısından risk analizi yapılması gerekir. İşletmelerin faaliyetleri esnasında olması muhtemel risklerin önceden belirlenmesi, tanımlanması, değerlendirilmesi ve bunların sonuçlarının en aza indirilmesi ya da tamamen yok edilmesi için alınması gereken önlemlerin belirlenmesine risk analizi denmektedir (URL-1). Bu amaçla uygulanan Fine-Kinley, Tehlike ve İşletmebilme (HAZOP), L Tipi Matris, Neden-Sonuç, İş Güvenlik, Ön Tehlike, X Tipi Matris, Hata Ağacı, Olay Ağacı, Hata Türleri- Etki ve Olursa Ne Olur Analiz Metodu gibi birçok risk analiz yöntemi bulunmaktadır (URL-2). Çalışmamızda bu metotlardan L tipi matris analiz yöntemini kullanılmıştır. L tipi matris analiz yöntemi risk analizi tek kişi tarafından yapılacak ve basit bir şekilde yapılabilecekse tercih edilir. Tehlikelere acil önlem alınması gereken durumlarda tehlikenin türü ve boyutunun tespitinde kullanılır. Bu yöntemde risk belirlenmesi tehlikenin olasılık ve etki (şiddet) miktarına bağlı olarak elde edilir. Risk analizi yapılması sonucu iş kazalarının ve meslek hastalıklarının azalması ile güvenli bir ortam sağlanarak işçi açısından sağlık, işveren açısından ekonomik bakımından daha avantajlı bir durum oluşur (Demir, 2010).

Yonga levha fabrikaları birçok bölümden oluştuğu için her bölümde yapılan işe bağlı olarak işçilerin güvenliğinin sağlanması açısından ilgili iş sahasına ait işçiler tarafından kullanılan malzeme, makine ve çalışma ortamında meydana gelebilecek tehlike-risklerinin belirlenmesi ve buna uygun önlemlerin alınması gereklidir. Bu çalışmada yonga levha fabrikası çalışanlarının iş sağlığı ve güvenliği açısından ortaya çıkabilecek risk ve bu risklere karşı alınması gereken tedbirlerin belirlenmesi amaçlanmıştır.

Materyal ve Yöntem

Bu çalışmada, yonga levha fabrikasında çalışan teknik personel ve işçilerin İSG kapsamında güvenli bir şekilde çalışabilecekleri sağlık ve güvenliği ile ilgili karşılaşması olası tehlikeler belirlenmiştir. Çalışmada L Tipi Matris (5x5) metodu kullanılmıştır.

L tipi matris (5x5) metodu

Kullanılmasının basit olması sebebiyle L Tipi Matris (5x5) Metodu genelde en çok tercih edilen risk analiz metodudur. İki ya da daha fazla değişken arasındaki ilişkinin belirlenmesinde değerlendirme metodu olarak kullanılır (Anonim, 2000, Özkılıç, 2005). Sebep-sonuç ilişkisinin ortaya konulmasında kullanılır. Bu metotla herhangi bir olayın vuku bulma olasılığı veya bunun gerçekleşmesi durumunda ortaya çıkabilecek sonucun ne olacağı hakkında değerlendirme ve ölçüm değerlerini içerir. Risk değeri “olasılık x etki derecesinin çarpımına eşittir (Eker, 2013).

İş kazalarının meydana gelme olasılık skalasının L Tipi Matris (5x5) Metodunda ki açıklaması (Tablo 1) ile risk belirleme formülü (1) aşağıda verilmiştir.

$$\text{Risk} = \text{Olasılık} \times \text{Etki (Şiddet)} \quad (1)$$

İş kazalarının ihtimal (olasılık) skalası Tablo 1’ de, iş kazalarının etki/zarar-sonuç açıklaması Tablo 2’ de, iş kazalarının risk matrisi Tablo 3’ de ve önlem sırasına göre alınacak karar ve yapılacak eylemler ise Tablo 4 ‘de verilmiştir

Tablo 1. İş kazalarının ihtimal (olasılık) skalası (Turgut, 2014)

Değer	Açıklama	Kategori
1. Çok düşük	Hemen hemen hiç	Oluşması beklenmiyor
2. Düşük	Düşük	Birkaç yılda bir
3. Orta	Orta	Yılda bir veya iki kez
4. Yüksek	Yüksek	Ayda bir
5. Çok yüksek	Çok yüksek	Haftada bir/her gün

(İhtimal: Zarar – hasar durumunun zamana bağlı olarak gerçekleşme olasılığını ifade etmektedir.)

Tablo 2. İş kazalarının etki/ zarar-sonuç tablosu (Turgut, 2014)

Değer	Açıklama	Kategori
1.Çok düşük	Dikkate alınmalı	İş kaybı olmayan, ilk yardım gerektirmeyen
2.Düşük	Önemli	İlk yardım gerektirebilecek durumlar, ayakta tedavi
3.Orta	Ciddi	Tedavi gerektiren yaralanmalar, yatarak tedavi, kısa süreli iş göremezlik
4.Yüksek	Çok ciddi	Ciddi yaralanma, uzuv kaybı, meslek hastalığı, sürekli iş göremezlik
5.Çok yüksek	Katlanılmaz	Ölüm

Değer	Açıklama	Kategori
1.Çok düşük	kate alınmalı	İş kaybı olmayan, ilk yardım gerektirmeyen
2.Düşük	Önemli	İlk yardım gerektirebilecek durumlar, ayakta tedavi
3.Orta	Ciddi	Tedavi gerektiren yaralanmalar, yatarak tedavi, kısa süreli iş göremezlik
4.Yüksek	Çok ciddi	Ciddi yaralanma, uzuv kaybı, meslek hastalığı, sürekli iş göremezlik
5.Çok yüksek	Katlanılamaz	Ölüm

(Değer, var olan tehlikenin gerçekleşmesi ile insan, iş alanı ve çevre üzerinde meydana getireceği zarar ya da hasarın şiddetini göstermektedir)

Tablo 3. İş kazalarının risk matrisi (Atay, 2014).

OLASILIK	ETKİ (ŞİDDET)				
	1 (çok hafif)	2 (hafif)	3 (orta)	4 (ciddi)	5 (çok ciddi)
1 (çok düşük)	1 Önemsiz Riskler	2 Düşük	3 Düşük	4 Düşük	5 Orta
2 (düşük)	2 Düşük	4 Düşük	6 Orta	8 Orta	10 Yüksek
3 (orta)	3 Düşük	6 Orta	9 Orta	12 Yüksek	15 Yüksek
4 (yüksek)	4 Düşük	8 Orta	12 Yüksek	16 Çok Yüksek	20 Çok Yüksek
5 (çok yüksek)	5 Orta	10 Yüksek	15 Yüksek	20 Çok Yüksek	25 Katlanılamaz

Tablo 4. Önlem sırasına göre alınacak karar ve yapılacak eylemler (Atay, 2014).

Önlem Sırası	Risk Değeri	Karar	Eylem
5	1<R<4	Kabul edilebilir risk	Acil tedbir gerektirmeyebilir.
4	5<R<9	Dikkate değer risk	Bu risklere kontrol tedbirleri geliştirilmeli ve planlama yapılmalı
3	10<R<15	Kayda değer önemli risk	Bu risklere mümkün olduğu kadar çabuk müdahale edilmeli
2	16<R<25	Kabul edilemez risk	Bu risklerle ilgili hemen çalışma yapılmalı
1	25<R	Katlanılamaz risk	Yapılan iş durdurulmalı ve acil önlem alınmalı

Bulgular

Yonga levha fabrikasında çalışanların maruz kalabileceği iş kazalarına neden olacak tehlike potansiyeli ve riskler belirlenmiştir. Bu verilerin elde edilmesi L Tipi Matris (5x5 Matris) Yöntemi ile yapılmıştır. Farklı renkler ile de mevcut risk ile ilişkili etki/zarar potansiyeli gösterilmiştir.

Tablo 5. Fabrika bölümlerindeki tehlike, risk, olasılık- şiddet miktarları

TEHLİKE ALANI	TEHLİKE TANIMI	TEHLİKENİN ADI VE RİSKİ	ŞİDDET OLASILIĞI	ŞİDDET RİSKİ	RİSK (SONUÇ)	AZALTICI VE ÖNLEYİCİ FALİYETLER
Beton Silo Altı Uzun Bant	Silo bandı roleleri açıkta olması	Personelin uzuv kaptırma riski	4	4	16	Bant altına korkuluk tesis edilmesi
Beton silo altı uzun banttaki miktatsız	Silo bandının miktatsız yerinde açıkta döner aksam	Personelin uzuv kaptırma riski	4	2	8	Izgara korkuluklu muhafaza yapılması
Arabalı bandı besleyen, uzun bant	Açıkta döner aksam	Uzuv kaptırma riski	4	3	12	Korkuluk yapılması
Bunker altı değirmen besleme helozyonu	Açıkta kablo	Kablolar üzerine basılması ve elektriğe çarpılma riski	4	3	12	Kablo kanalının ısla edilmesi
Değirmen	Merdiven korkuluğu ve platform korkuluğu yok	Personelin düzme ve yaralanma riski	4	4	16	Merdiven korkuluğu ve platform korkuluğu yapılması
Yaş yonga silosu boşaltma helozyonu	Elektrik motorlarına müdahale zor.	Yüksekte çalışma var korkuluk ve platform olmadığından düşme riski	4	3	12	Motora ulaşımın kolay olması
Yangından korunma silosu üstü	Yan yüzeylerinde büyük açıklık	Personelin aşağıya düşme riski	5	3	15	Yan korkulukların aralarına payanda atılması
CL silosu üst platformu merdiveni	Merdiven yatay çemberleri eksik, Merdiven sonu korkuluk eksik	Personelin düşme riski	4	5	20	Merdiven yatay çemberlerinin çoğaltılması ve korkuluk yapılması
CL ısıtmalı helazon	Platform kenarı korkuluk eksik	Personelin düşme riski	3	4	12	Korkuluk tamamlanacak
Blendırın bulunduğu platform	Zemin platformunda tekmelik eksik	Malzeme düşürme riski	2	2	4	Tekmeliğin yapılması
Form istasyonu SL alt kısa bant	SL kısa bant motoru zincir değişimi için platform yok	Personelin düşme riski	4	3	12	Kısa bant motoruna ulaşmak için platform yapılması
Kalınlık ölçen ve patlak ayırıcı bölgesi başlangıcı bant altından geçiş yolu son kenarı	Kalınlık ölçerlerin altına geçilme riski	Personelin yaralanma riski	3	3	9	Geçiş yolunun sol tarafının çitle kapatılması
Bor yağ tankına çıkma merdiveni	Merdiven korkuluğunun çemberlerinin eksik olması	Personelin düşme riski	3	2	6	Merdiven korkuluğu eksik ve çemberlerinin artırılması

Tablo 5 incelendiğinde olasılık ve şiddete bağlı olarak elde edilen sonuç miktarı belirlenmiş ve Tablo 3' de verilen iş kazalarının risk matrisine göre sonuçlandırılmıştır. Her bir aralık farklı renklerle ifade edilmiştir. Tabloda dört farklı aralık ve renkte sonuçlar elde edilmiştir. Yeşil renk ile ifade edilen zemin platformunda tekmelik eksik olması ile malzeme düşürme riskinin olduğu çalışma alanı risk açısından acil tedbir

gerektirmeyen kabul edilebilir risk grubundadır.

Mavi renk ile gösterilen beton silo altı uzun banttaki bölümde mıknaş silo bandının mıknaşlı yerinde açıkta döner aksamın olduğu ve çalışan kişilerin uzuv kaybına uğrayabileceği, kalınlık ölçen ve patlak ayırıcı bölgesi başlangıcı bant altından geçiş yolu son kenarı bölümünde, kalınlık ölçerlerin altına geçilme riski nedeniyle yaralanma riskinin olduğu ve bor yağ tankına çıkma merdiveninin olduğu kısımda merdiven korkuluğunun çemberlerinin eksik olması nedeni ile çalışanların düşme riskinin olduğu belirlenmiştir. Bunlar dikkate değer risk gruba girmektedir. Bu sebeple bu risklere kontrol tedbirleri geliştirilmeli ve planlama yapılmalıdır.

Turuncu renklerle gösterilen arabalı bandı besleyen, uzun bantta, açıkta döner aksam nedeni ile uzuv kaptırma riski, bunker altı değirmen besleme helozyonu bölümünde, açıkta kablo olması çalışanların kablolar üzerine basması ve elektriğe çarpılma riskinin olduğu, Yaş yonga silosu boşaltma helozyonu kısmında elektrik motorlarına müdahalenin zorluğu sebebiyle yüksekte çalışma olduğu için korkuluk ve platform olmadığından düşme riskinin bulunduğu belirlenmiştir. Ayrıca yangından korunma silosu üstünde yan yüzeylerinde büyük açıklık olmasından dolayı çalışanların düşme riskinin belirlendiği, CL ısıtmalı helazon kısmında Platform kenarında yine korkuluğun eksik olması yüzünden düşme riskinin olduğu, form istasyonu SL alt kısa bant bölümünde SL kısa bant motoru zincir değişimi için platformunun olmaması yüzünden kişilerin düşme riskinin olduğu tespit edilmiştir. Bu tespitler dikkate değer risk grubunda olup bunlarla ilgili olarak bu risklere kontrol tedbirleri geliştirilmeli ve planlamaları yapılmalıdır.

Kırmızı renk ile gösterilen beton silo altı uzun bant kısmında silo bandı röleleri açıkta olmasından dolayı personelin uzuv kaptırma riski, değirmen bölümünde merdiven korkuluğu ve platform korkuluğunun olmaması nedeni ile çalışanların düşme ve yaralanma riskinin olduğu, CL silosu üst platformu merdiveninin olduğu bölümde, merdiven yatay çemberlerinin eksik, merdiven sonu korkulukların yine olmaması yüzünden çalışanların düşme riskinin olduğu belirlenmiştir. Kırmızı renkli grup kabul edilemez risk grubunda yer aldığı için bu risklerle ilgili hemen çalışma yapılmalıdır. Fabrikadaki incelemede hiçbir bölümde yapılan işin durdurulmasını ve acil önlem alınmasını gerektiren katlanılmaz risk grubuna giren bir bölüm bulunmamaktadır.

Yapılan incelemede elde verilen göre yonga levha fabrikasında: çalışanlara eğitim ve bilgilendirme yapılmalı, bant altına korkuluk tesis edilmesi, ızgara korkuluklu muhafaza yapılması, korkuluk yapılması, kablo kanalının ısla edilmesi merdiven korkuluğu ve platform korkuluğu yapılması, motora ulaşımın kolay olması, yan korkulukların aralarına payanda atılması, merdiven yatay çemberlerinin çoğaltılması, tekmeliğin yapılması, kısa bant motoruna ulaşmak için platform yapılması, geçiş yolunun sol tarafının çitle kapatılması ile önleyici tedbirler alınabilir.

Sonuç

6331 Sayılı İş Sağlığı ve Güvenliği Kanununda belirtildiği gibi çalışma yerleri çalışma ortamına uygun şekilde dizayn edilmelidir. İş kazalarına neden olabilecek tehlikeler L Tipi Matris yöntemi kullanılarak irdelenmiş ve buna bağlı olarak da alınması gerekli olan önleyici tedbirler tespit edilmiştir.

Yonga levha fabrikasında 13 bölüm incelenmiş ve elde edilen bulgulara göre “Kabul edilebilir risk “grubunda 1 bölüm, “Dikkate değer risk “taşıyan 3 bölüm, “Kayda değer önemli risk taşıyan” 6 bölüm, “Kabul edilemez risk” grubunda 3 bölümde belirlenmiş olan risklerle ilgili çalışma yapılarak risk oranları düşürülmelidir yada mümkün ise tamamen yok edilmelidir. Fabrikada “Katlanılamaz” risk grubunda bulunan hiçbir bölüme rahatlanmamıştır. Tespit edilen eksikliklerin yapılması ve uygulanması ile yonga levha fabrikasındaki çalışma ortamının çalışanlar açısından sağlıklı ve daha güvenli bir iş yeri haline geleceği öngörülmektedir.

Kaynaklar

- Ofluoğlu, G. ve Sarıkaya, G., (2013). OHSAS 18001 İş Sağlığı ve İş Güvenliği Yönetim Sistemi, www.kamu-is.org.tr/pdf/835.pdf.
- Fişek, G. ve Piyal, B., (1989). İşçi Sağlığı Kılavuzu, TTB Yayıncılık, Ankara.
- URL-1: [https://www.taksimosg.net/risk-analizi-nedir/\(2021\)](https://www.taksimosg.net/risk-analizi-nedir/(2021)).
- URL-2: <https://multinet.com.tr/blog/inovasyon-girisimcilik/risk-analizi-nedir-ve-nasil-yapilir>. 19.11.(2021)
- Demir, S., (2010). Tehlikeli kimyasal maddelerin iş sağlığı ve güvenliği yönetimi, Yüksek Lisans Tezi, İstanbul Teknik Üniversitesi Fen Bilimleri Enstitüsü,
- Anonim, (2000). Department Of Defense Standard Practice for System Safety, MIL-STD-882D USA, (10 Feb. 2000).
- Özkılıç, Ö., (2005). İş Sağlığı ve Güvenliği Yönetim Sistemleri ve Risk Değerlendirme Metodolojileri, Ankara: Ajans Türk Basımevi, 28.
- Eker, T., (2013). İş Sağlığı ve Güvenliği Kapsamında Risk Analizi ve Metal Sektöründe Bir Uygulama, Yüksek Lisans Tezi, Fen Bilimleri Enstitüsü, İstanbul.

MOBİLYA ÜRETİMİNDE KULLANILAN TİCARİ MDF LEVHALARIN YÜZEY PÜRÜZLÜLÜKLERİNİN ARAŞTIRILMASI

Ferhat ÖZDEMİR*

Kahramanmaraş Sütçü İmam Üniversitesi, Orman Fakültesi, Orman Endüstri Mühendisliği Bölümü, Kahramanmaraş, Türkiye

Hasan SERİN

Kahramanmaraş Sütçü İmam Üniversitesi, Orman Fakültesi, Orman Endüstri Mühendisliği Bölümü, Kahramanmaraş, Türkiye

Özet

Bu çalışmanın amacı mobilya üretiminde çok fazla miktarda kullanılan orta yoğunluklu lif levhaların (MDF) yüzey pürüzlülüğü özelliklerinin belirlenmesidir. Piyasada ticari olarak satılan farklı dört firmanın ürettiği 18mm kalınlığındaki MDF levhalar kullanılmıştır. Levhaların yüzey pürüzlülükleri ölçülmüş, daha sonra 185 °C de 20 dakika ısıtılma işlemi uygulanmış ve tekrar yüzey pürüzlülükleri ölçülmüştür. Bu firmalara ait levhalardan elde edilen test numunelerinin yüzey pürüzlülüğü testleri ISO 4287' ye göre ölçülmüştür. Ölçümler Marsurf M300 cihazı ile iğne taramalı yöntem yoluyla gerçekleştirilmiştir. Numunelerin yüzey pürüzlülüğü kalitesini belirlemek için ortalama pürüzlülük (Ra), on nokta pürüzlülük ortalama değeri (Rz) ve en büyük pürüzlülük değeri (Rmax) parametreleri ölçülmüştür. Elde edilen verilere göre tüm firmalara ait sonuçlar arasında farklılıklar tespit edilmiştir. Sonuçta C kodlu firma tarafından üretilen MDF levhaların yüzey pürüzlülük değerlerinin diğer firmalara kıyasla daha iyi yüzey kalitesine sahip olduğu belirlenmiştir.

Anahtar kelimeler: MDF levha, Yüzey pürüzlülüğü, Mobilya, Isıl işlem

INVESTIGATION OF THE SURFACE ROUGHNESS OF COMMERCIAL MDF BOARDS USED IN FURNITURE MANUFACTURING

Abstract

The aim of this study is to determine the surface roughness properties of medium density fiberboards (MDF), which are used in large amounts in furniture production. 18mm thick MDF boards produced by four different companies sold commercially in the market were used. The surface roughness of the boards was measured, then heat treatment was applied at 185 oC for 20 minutes and the surface roughness was measured again. The surface roughness tests of the test samples obtained from the boards of these companies were measured according to ISO 4287. Measurements were made with the Marsurf M300 device using the needle scanning method. Average roughness (Ra), ten-point roughness average value (Rz) and maximum roughness value (Rmax) parameters were measured to determine the surface roughness quality of the samples. According to the data obtained, differences were determined between the results of all companies. As a result, it was determined that the surface roughness values of the MDF boards produced by the C-coded company had better surface quality compared to other companies.

Keywords: MDF board, Surface roughness, Furniture, Heat treatment

Giriş

MDF levhalar mobilya üretiminde, kapı ve doğramacılık gibi birçok alanda bol miktarda kullanılmaktadır (Nicewicz ve Matejak, 2000, Proszyk 1999). Dış mekânda kullanımından ziyade genellikle iç mekânlarda kullanılmaktadır. Özellikle dolap vb. birçok mobilya üretiminin temel hammaddesidir. MDF levhaların özellikleri üzerine ağaç türü, lif uzunluğu, kullanılan reçinenin türü ve miktarı, varsa katkı maddeleri ve miktarları, lif kuruluğu ve levha pres sıcaklığı, süresi ve miktarı gibi birçok faktör etki etmektedir. Bu nedenle hammadde olarak uygun ağaç seçimi önemlidir (Akbulut ve diğerleri 2000, Koç 2002). MDF levha üretiminde yapraklı ve iğne yapraklı ağaçların düşük kalitedeki kısımları ve fabrikalarda atık olarak kalan kısımların kullanılması bir avantaj olarak kabul edilmektedir. İç mekândan ziyade dış mekânda kullanılma özelliğinin geliştirilmesi ile ilgili bazı çalışmalar yapılmaktadır.

Özellikle dış mekânlarda MDF ve yonga levha gibi ahşap esaslı kompozit malzemelerin kullanım alanlarının artırılmasına yönelik olarak ısıtma işlemi veya yüzey işlemleri uygulanması mümkündür. Ahşap esaslı levhalarda ısıtma işlemi rutubet alma-verme özelliğini azaltmak, mikro organizmalara karşı korumak ve denge rutubet miktarını azaltmak için uygulanır (Yıldız, 2002).

Isıtma işlemi sayesinde ahşap esaslı levhaların yüzeyi estetik açıdan geliştirilebilir ve bu ekonomik bir şekilde tüketiciye yansıtılabilir. Yüzeyin kaplanması, yüzeyin boyanması ve vernik için yüzey pürüzlülüğü büyük önem arz eder. Yüzey pürüzlülüğünü etkileyen en önemli faktörler hammadde özellikleri ve üretim şartları ile sonraki işlemlerdir. Kullanılan lifin boyutu ve şeklinin yanı sıra kullanılan reçine türü, pres şartları ve uygulanan zımparalama işlemi ile ilgili olarak birçok değişken söz konusudur. Üretilen MDF levhaların yüzeyleri birçok malzeme ile kaplanabilir. Bunların arasında en çok tercih edilen ise melamin emdirilmiş kâğıt, vinil, boya ve verniktir. Levhaların yüzeyleri kaplanırken yüzeydeki pürüzlülük derecesi yapışma esnasında malzeme kalitesi üzerine etki edecektir (Hızıroğlu 1996). Levha yoğunluğu da yüzey pürüzlülüğü ve işlenmesi için önemli bir faktördür. Levha yoğunluğu arttıkça liflerin daha fazla sıkıştırılmış olması nedeniyle hem işlenmesi hem boyanması hem de yüzeyinin kaplanması esnasında yapışma özelliklerini olumlu etkileyecektir. Özellikle yoğunluğu biraz yüksek MDF levhalar yatak odası ve mutfak kapısı gibi taşıyıcı özellik göstermesi gereken malzeme üretiminde kullanılmaktadır (Wang ve ark., 2001).

Yüzeyi kaplanacak malzemelerin yüzey kaplamasından sonra yüzey kalitesinin iyi olması için yüzeyinin düzgün ve sağlam olması gerekmektedir. Bu nedenle yapılan çalışmada piyasada satılan ticari firmaların ürettiği levhaların yüzey pürüzlülüğü ve ısıtma işlemi sonrası yüzey pürüzlülüğündeki değişimleri araştırılacaktır.

Materyal ve Yöntem

Materyal

Piyasa ticari olarak satılan, yoğunlukları 0,75-0,80 g/cm³ arasında olan dört farklı firmaya ait MDF levhalardan 100x100x180 mm ebatlarında test numuneleri elde edilmiştir.

Metot

MDF levhalara 200 °C de 20 dakika süre ile Nüve oven KD 400 markalı kurutma fırının kullanılarak ısıl işlem uygulanmıştır. 20±2 °C sıcaklık ve 65±5% bağıl nemde rutubet derecesi %12 ulaşılıncaya kadar test numuneleri klimatize edilmiştir. Yüzey pürüzlülük ölçümleri X ile yapılmıştır. Testler yüzey pürüzlülüğü ölçüm standardına bağlı kalınarak yapılmıştır (ISO 4287, 1997). Ölçümlerde Ra (profil girinti-çıkıntıları ortalama pürüzlülük değeri), Rz (on nokta pürüzlülüğü ortalama değeri), Rmax (en büyük pürüzlülük değeri) ve Rq (aritmetik ortalamanın karekökü) parametreleri ölçülmüştür. Her bir ticari firmaya ait MDF levha için 6 adet test numunesi hazırlanmış ve her bir numune üzerinde ise 4 adet ölçüm gerçekleştirilmiştir (Şekil 1).



Şekil 1. Marsurf M300 yüzey pürüzlülük cihazı

Bulgular ve Tartışma

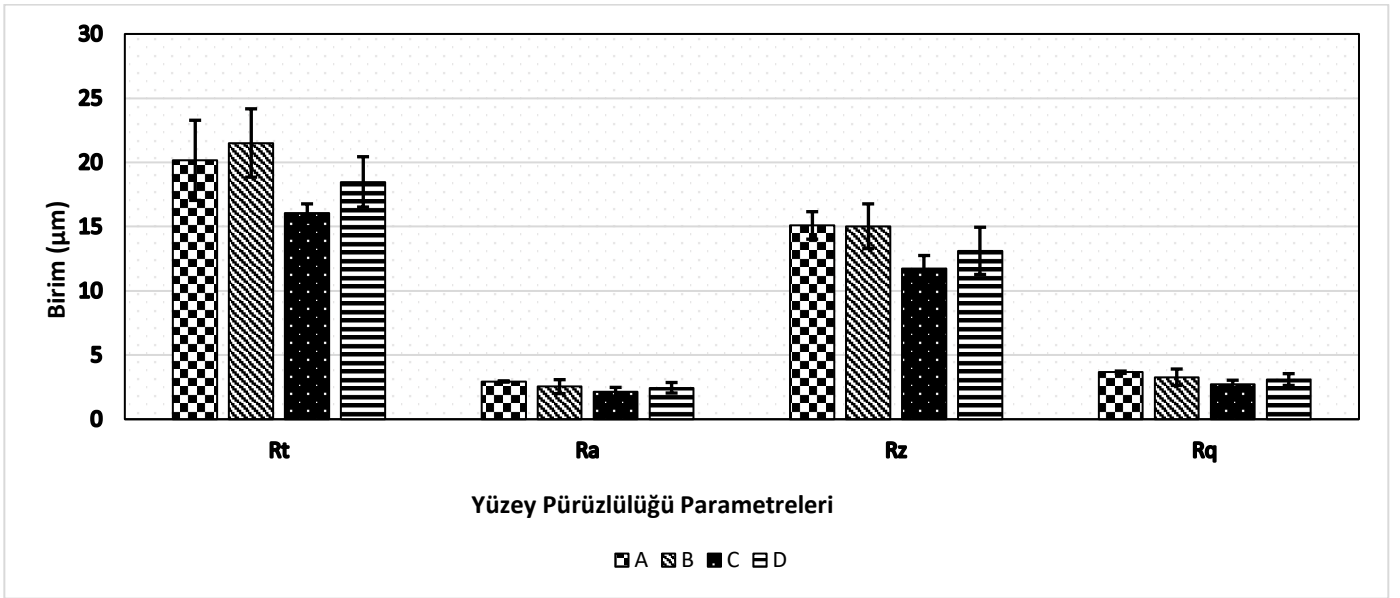
Piyasadan temin edilen ticari firmalara ait MDF levha test numunelerinden elde edilen yüzey pürüzlülük ölçüm değerleri Tablo 1' de verilmiştir.

Tablo.1. Firmalara ait MDF levhaların yüzey pürüzlülüğü ölçüm değerleri

Firma	Rmax (µm)	Ra (µm)	Rz (µm)	Rq (µm)
A	20,16 (3,24)	2,94 (0,05)	15,09 (1,07)	3,66 (0,09)
B	21,51 (1,80)	2,54 (0,54)	15,03 (1,74)	3,27 (0,64)
C	16,06 (0,94)	2,14 (0,34)	11,72 (1,03)	2,71 (0,33)
D	18,48 (1,55)	2,45 (0,41)	13,11 (1,84)	3,09 (0,46)

* Parantez içerisindeki değerler standart sapma, değerleridir

Tablo 1’ de firmalara ait yüzey pürüzlülüğü Rmax, Ra, Rz ve Rq değerleri belirlenmiştir. Tablo incelendiğinde A kodlu firma MDF levhasının Rmax, Ra, Rz ve Rq değerlerinin sırasıyla 20.16, 2.94, 15.09 ve 3.66 μm olduğu belirlenmiştir. B kodlu firma MDF levhasının ise Ra değerinin (21,51 μm) yüksek olduğu diğer değerlerin ise düşük olduğu görülmektedir. D kodlu firma MDF değerleri ise A ve B firmasının değerlerine yakın olmakla birlikte tüm parametre değerlerinde yine de her iki firmaya göre daha düşük veriler elde edilmiştir. Firmalar içerisinde en iyi değerler C kodlu firmaya ait levhalar da tespit edilmiştir. C kodlu firma Rmax, Ra, Rz ve Rq ölçüm değerleri sırasıyla 15.5, 11.74, 10.72 ve 2,34 μm olarak belirlenmiştir. Tüm firmalar içerisinde en düşük yüzey parametre değerlerine sahiptir. Yüzey pürüzlülüğü ölçüm değerlerine ait grafik Şekil 2’ de verilmiştir.



Şekil 2. Farklı firmalara ait MDF levhaların yüzey pürüzlülüğü ölçüm değerleri grafiği

Dört farklı firmaya ait ısıtılmış MDF levha test numunelerinin yüzey pürüzlülüğü ölçüm değerleri Tablo 2’ de verilmiştir.

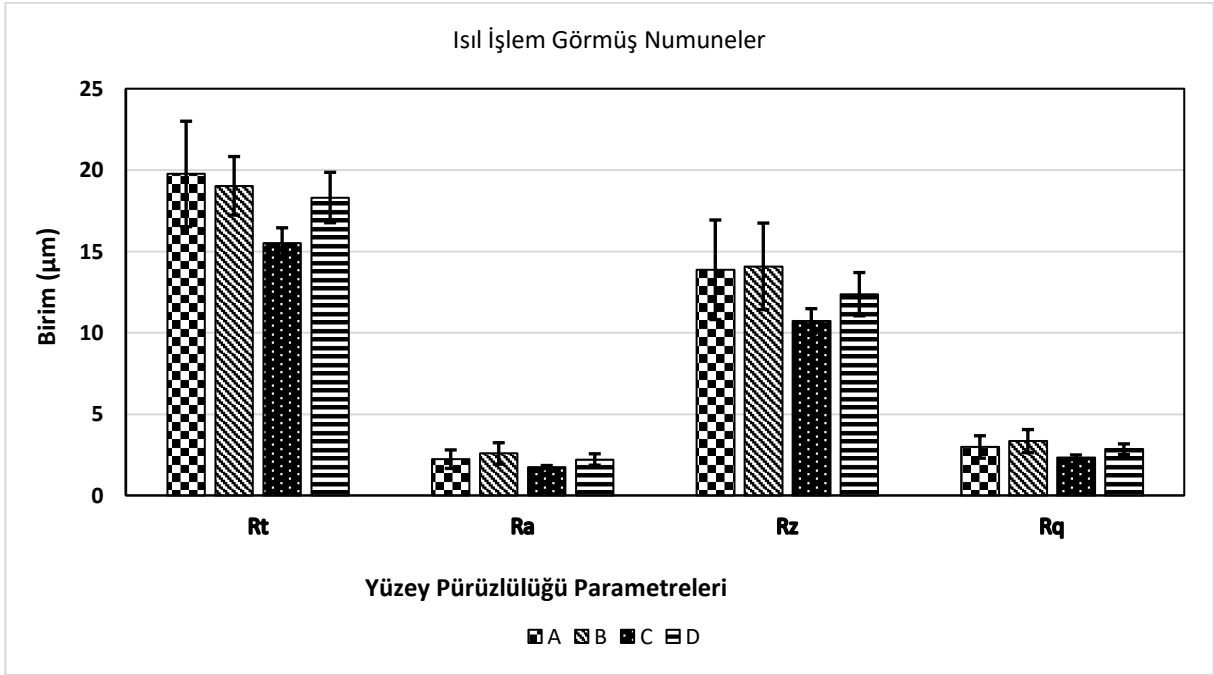
Tablo 2. Firmalara ait ısıtılmış MDF levhaların yüzey pürüzlülüğü ölçüm değerleri

Firma	Rmax (μm)	Ra (μm)	Rz (μm)	Rq (μm)
A	19,76 (3,12)	2,23 (0,57)	13,87 (3,06)	2,98 (0,69)
B	19,03 (2,66)	2,58 (0,66)	14,08 (2,66)	3,34 (0,71)
C	15,51 (0,71)	1,74 (0,10)	10,72 (0,76)	2,34 (0,15)
D	18,31 (1,96)	2,21 (0,35)	12,37 (1,33)	2,84 (0,33)

* Parantez içerisindeki değerler standart sapma, değerleridir

Tablo incelendiğinde A kodlu firmanın test numuneleri yüzey pürüzlülüğü ölçüm değerlerinin B kodlu firmaya yakın olduğunu ancak sadece Rmax değerinin yüksek olduğu belirlenmiştir. B kodlu firmanın MDF numunelerinin Rmax, Ra, Rz ve Rq değerleri sırasıyla 19.03, 2.58, 14.08 ve 3,34 μm ’ tır. En düşük veriler ise yine C kodlu firmaya ait numunelerde tespit edilmiştir. Rmax, Ra, Rz ve Rq değerleri sırasıyla 15.51, 1.74, 10.72 ve 2.34 μm olarak belirlenmiştir. Isıtılmış uygulama ile tüm levhaların yüzey parametre değerlerinde

olumlu etki yaptığı ancak en az etkiyi ise B kodlu levhada yaptığı tespit edilmiştir. Isıl işlem uygulanmış firmalara ait test numunelerinin ölçüm parametre değerlerinin grafiği Şekil 3' verilmiştir.



Şekil 3. Isıl işlem uygulanmış test numuneleri yüzey pürüzlülük ölçüm değerleri

Ahşap ve ahşap esaslı levhalarda ısıl işlemin etkisinin araştırıldığı ve yüzey pürüzlülüğü ile ilgili birçok çalışma bulunmaktadır. Ayrılmış ve Winandy (2009) MDF levhalar farklı süre ve sıcaklıklarda ısıl işlem uygulamışlar ve yüzey pürüzlülüğünün bu işlemde olumlu etkilendiğini sonucuna ulaşmışlardır. Bu sonuçların Özdemir ve Yıldırım (2017), Aydın ve ark., (2002), Ünsal ve ark., (2011) ile Korkut ve ark., (2008) yapmış olduğu çalışmalar ile uyumlu olduğu belirlenmiştir. Ahşap esaslı levhalara uygulanan ısıl işlem malzemenin mekanik, fiziksel özelliklerinin yanı sıra kimyasal yapısında ve yüzey kalitesi üzerinde de etkili olmaktadır. Isıl işlem yapılan malzemelerin yüzeylerinde uygulanan ısı etkisi ile plastikleşme oluşmakta ve yüzey daha düzgün hale gelmektedir. Ayrıca yüzeyde ısının pres ile uygulanması durumunda yoğunlukta bir artış da görülmektedir. Yüzey pürüzlülüğü iyileştirilmesi için yapılan zımparalama ve planya işlemindeki kayıp oranı da yine yüzey pürüzlülüğü ile ilgilidir. Yüzey yapılacak yapıdırma işlemlerinde yüzeyin mümkün olduğu kadar pürüzsüz olması istenmektedir.

Sonuçlar

Farklı firmalara ait MDF levha test numunelerinden elde edilen bulgulara göre:

1. C kodlu firmanın ürettiği MDF levha diğer MDF levhalara kıyasla daha iyi yüzey özelliklerine sahiptir.
2. Isıl işlem yapılması ile tüm firmalara ait MDF levhaların yüzey özellikleri iyileşmiştir.
3. Isıl işlem ile levhaların yüzey kalitesinde iyileşme etkisinin firmalara göre farklılık arz ettiği belirlenmiştir.
4. Isıl işlem uygulaması ile en iyi sonuç yine C kodlu firmaya ait levhalarda tespit edilmiştir.

Kaynakça

- Nicewicz, D., Matejak, M., (2000). *Technologia półtwardych płyt pilśniowych*. Wyd. SGGW, Warszawa.
- Proszyk, S., (1999). *Technologia tworzyw drzewnych. Wykończanie powierzchni. Część 2*. WSiP, Warszawa, 376 pp.
- Akbulut, T., Hızıroğlu, S., N., (2000). Surface absorption, surface roughness, and formaldehyde medium density fiberboard. *Forest Prod. J.* 50 (6): 45-48
- Koç, E., 2002: Effects of some factors on appearance properties of profiled MDF surface in covering. M.Sc. Thesis. Istanbul University, Institute of Science and Technology Second Freeman Publications, Inc., San Francisco, California, USA
- Yıldız, S., (2002). Physical, mechanical, technological and chemical properties of beech and spruce wood treated by heating, Ph.D. Thesis, Black Sea Technical University, Trabzon, Turkey.
- Hızıroğlu, S., (1996) Surface roughness analysis of wood composites: A stylus method. *Forest Prod. J.* 46 (7/8):67-72
- Wang, S., Winistorfer, P. M., Young, T. M., Helton, C., 2001: Step-closing pressing of Part I: Influence on the vertical density profile. *Holz als Roh- und Werkstoff* (59): pp. 19-26.
- Ayrılmış, N., Winandy, J. E., (2009). “Effects of post heat-treatments on surface characteristics and adhesive bonding performance of medium density fiberboard”, *Materials and Manufacturing Processes*, 24, 594-599.
- Özdemir, F., Yıldırım, S. (2017). Isıl İşlem Uygulanmış Orta Yoğunluklu Lif Levhanın (MDF) Yüzey Pürüzlülüğü Üzerine Araştırma, *Turkish Journal of Forest Science* 1(1), 85-92
- Aydın, İ., Çolakoğlu, G., (2002). The effects of veneer drying temperature on wettability, Surface roughness and some properties of plywood, 6th European Panel Products Symposium. In *Proceedings of the Sixth European Panel Products Symposium*, North Wales Conference Centre, Llandudno, October 9–11, North Wales, UK, 60–69.
- Ünsal. Ö., Candan. Z., Korkut. S., (2011). Wettability and roughness characteristics of modified wood boards using a hot-press, *Industrial Crops and Products*. 34, 1455- 1457.
- Korkut, D.S., Korkut, S., Bekar, İ., Budakçı, M., Dilik, T., Çakıcıer, N., (2008). The effects of heat treatment on the physical properties and surface roughness of Turkish Hazel (*Corylus Colurna L.*) Wood, *Int. J. Mol. Sci.*, 9(9), 1772-178.



MONITORING AND ASSESSMENT OF WATER QUALITY IN THE GUENITRA DAM, ALGERIA USING PHYSICOCHEMICAL PARAMERTS AND POLLUTION ORGANIC INDEX

Dounia KEDDARI

Territory Planning Research Center, Constantine, Algeria.
Laboratory of Biology and Environment, University of Constantine 1, Constantine, Algeria.

Farah BOUTOUATOU

Territory Planning Research Center, Constantine, Algeria.
Territorial Sciences, Natural Resources and Environment Laboratory, University of Constantine 1, Constantine, Algeria.

ABSTRACT

Surface water is subject to strong anthropogenic pressures caused by the development and extension of agricultural, industrial and domestic activities. Pollution is a serious problem for the environment due to discharges dumped into rivers and excessive use of agricultural fertilizers. The objective of this study is to assess the quality and state of organic pollution in surface water in Guenitra dam, Algeria, based on the organic pollution index (IPO) for 10 years (2010 to 2020) by monitoring 10 parameters. The results obtained show highly significant increases were observed at the output ($p < 0.001$) for pH and dissolved oxygen; very significant ($p < 0.01$) for nitrites, COD and BOD5; significant ($p < 0.05$) for dry residues and organic matter. The nitrates, phosphates and ammonium showed no significant differences ($p > 0.05$). The OPI highlighted waters with low-to-moderate pollution, essentially due to high levels of nitrites. The COD/BOD5 ratio highlighted a wastewater sometimes difficultly biodegradable (ratio > 3). In conclusion, often throughout all the study period, the waters indicate bad quality and non-negligible risks to human health according to the Algerian standards recommended by the National Agency for Hydric Resources (ANRH); it is thus strongly advocated that these waters must undergo appropriate treatment to improve its physicochemical quality.

Keywords: Water quality, Monitoring, Organic Pollution Index (OPI), *Guenitra* dam, East Algeria.



STUDY OF NOISE LEVEL DURING DIWALI FESTIVAL 2021 AT SELECTED RESIDENTIAL AREAS IN NASHIK CITY OF INDIA

R. A. DALVI

Department of Environmental Science, K.R.T. Arts, B.H. Commerce & A.M. Science (KTHM) College, Gangapur Road,
Nashik – 422002, Maharashtra, India

D. B. MORE

Department of Environmental Science, K.R.T. Arts, B.H. Commerce & A.M. Science (KTHM) College, Gangapur Road,
Nashik – 422002, Maharashtra, India

S. S. NIPHADÉ

Department of Environmental Science, K.R.T. Arts, B.H. Commerce & A.M. Science (KTHM) College, Gangapur Road,
Nashik – 422002, Maharashtra, India

K. D. AHIRE *

Department of Environmental Science, K.R.T. Arts, B.H. Commerce & A.M. Science (KTHM) College, Gangapur Road,
Nashik – 422002, Maharashtra, India

ABSTRACT

Diwali is a festival of lights and one of the major festivals celebrated in India. People enjoy this festival with verity of activities and blasting of fire crackers. The present work has been carried out to study noise level during Diwali Festival at selected residential areas of Nashik City in the month of November 2021. This study tried to understand the noise level differences between non-Diwali session and Diwali Session. Shanti Nagar, Vidya Nagar and Sai Nagar residential areas in Nashik City have selected for monitoring the noise level during Diwali Festival. Noise has measured in equivalent sound level (Leq) in decibel (dB) unit with the help of Sound Level Meter SL-100 Leutron during 2nd November 2021 to 5th November 2021. Everyday total 180 reading were taken from 7 PM to 10 PM at one minute interval at every selected residential area. This study stated that noise level during Diwali Festival 2021 at all three residential places were higher compared to non-Diwali session. Calculated noise limits have also compared with limits prescribed by the Central Pollution Control Board (CPCB). Noise pollution due to firecrackers during Diwali has been identified as one of the major sources of noise pollution in the city.

Key Words: Noise Pollution, Diwali Festival 2021, Residential Areas, Nashik etc.



SIX SIGMA APPROACH TO ACHIEV THE STATISTICAL QUALITY ASSURANCE

Assoc. Professor, K. Koteswara RAO

Department of Computer Science and Engineering, PVP Siddhartha Institute of Institute of Technology, Vijayawada, India

Sr . Assist. Prof. Dr. G. Lalitha KUMARI

Department of Computer Science and Engineering, PVP Siddhartha Institute of Institute of Technology, Vijayawada, India

Assist. Prof. Dr. Mrs. Y. SUREKHA

B.Tech, Department of Computer Science and Engineering, PVPSIT

Ms . B. Kanaka APARNA

B.Tech, Department of Computer Science and Engineering, PVPSIT

Mukkapati ROHITH

Department of Computer Science and Engineering, PVP Siddhartha Institute of Institute of Technology, Vijayawada, India

Assist. Prof. Dr. Mr. N Ramesh BABU

RGKUT, Srikakulam, Andhra Pradesh, INDIA

ABSTRACT

Today software is experiencing the renaissance and six sigma plays crucial role. The blooms of size 250*320sqmm size which are being produced at steel melt shop are kept at bloom storage yard. Accordingly these blooms are charged into the furnaces and rolled into the billets of size 125*125sqmm. The bloom is converted into billets when drawn through seven stands of variable speeds. Later the billet is passed through the shear to get cut into three pieces for passing to the Wire Rod Mill (WRM) feeding. The material passing from stand-1 is continuous and passes through the stand-7 where it gets the cross section of 125*125sqmm. Whenever a problem arises due power failure or any other malfunctioning; the material struck up and is twisted in between the stands which is known as COBBLE. Removing the cobble takes minimum three to four hours which hampers the production and is a direct loss to the company.

Thus the problem needs to be looked into and the solution aroused in the form of Six Sigma tools. Six Sigma is widely recognized as a business that employs statistical and non-statistical tools and techniques, change management tools, project management skills, team work skills and a powerful roadmap (DMAIC) to maximize an organization's return on investment (ROI) through the elimination of defects in processes. DMAIC methodology provides with a data-driven methodology for achieving sustained process improvements by reducing defects. This methodology is used to identify inadequacies in the existing process and to make lasting and controllable changes to products and processes that improve product quality, customer satisfaction and the company's profitability.

Thus, with the help of proper tools and techniques of this procedure the problem had been handled. Sufficient data was collected and the various factors that affect the process and lead to failure were analyzed. The Six Sigma roadmap enabled to identify the potential causes of the failure and provided effective methods to eliminate them or minimize them. The project is all about the way the problem was tackled and the process was improved.



ARTIFICIAL VISION - MADE POSSIBLE BY MICRO MEDICAL ELECTRONICS

Assoc. Professor, K. Koteswara RAO

Department of Computer Science and Engineering, PVP Siddhartha Institute of Institute of Technology, Vijayawada, India

Sr . Assist. Prof. Dr. G. Lalitha KUMARI

Department of Computer Science and Engineering, PVP Siddhartha Institute of Institute of Technology, Vijayawada, India

Assist. Prof. Dr. Mrs. Y. SUREKHA

B.Tech, Department of Computer Science and Engineering, PVPSIT

Mr. CH. Rajesh CHANDRA

B.Tech, Department of Computer Science and Engineering, PVPSIT

Mounisha RAAVI

Department of Computer Science and Engineering, PVP Siddhartha Institute of Institute of Technology, Vijayawada, India

Assist. Prof. Dr. Mr. N. Ramesh BABU

RGKUT, Srikakulam, Andhra Pradesh, INDIA

ABSTRACT

Blindness is more feared by the public than any other ailment. Artificial vision for the blind was once the stuff of science fiction. But now, a limited form of artificial vision is a reality .Now we are at the beginning of the end of blindness with this type of technology. In an effort to illuminate the perpetually dark world of the blind, researchers are turning to technology. They are investigating several electronic-based strategies designed to bypass various defects or missing links along the brain's image processing pathway and provide some form of artificial sight.

Linking electronics and biotechnology, the scientists has made the commitment to the development of technology that will provide or restore vision for the visually impaired around the world. Our paper describes the development of artificial vision system, which cures blindness to some extent. Our paper explains the process involved in it and explains the concepts of artificial silicon retina, cortical implants etc. The roadblocks that are created are also elucidated clearly. Finally the advancements made in this system and scope of this in the future is also presented clearly.

Key words: silicon retina, cortical implants, road blocks, retina.



SENSOR TECHNOLOGY IN FOOD INDUSTRY

GOPIKA A.

RMK Engineering College, Kavaraipettai, Tiruvallur District.Tamil Nadu, India

Dr. A. VIJAYALAKSHMI

RMK Engineering College, Kavaraipettai, Tiruvallur District.Tamil Nadu, India

Dr. G. Nixon Samuel VIJAYAKUMAR

RMK Engineering College, Kavaraipettai, Tiruvallur District.Tamil Nadu, India

ABSTRACT

In the modern technology sensors play a key role in all the industries to enhance the quality of the products. In food industry, chemical or bio sensors are used throughout the manufacturing process for the detection and identification of contaminants such as heavy metals, residual agrochemicals, toxic metabolites, food borne pathogen, food adulterants etc. The food quality and food safety can be identified by using sensors. In addition to that, it plays a vital role in food package (i.e) smart package/intelligent package also. This smart package includes many components such as Time Temperature Indicators (TTIs), Radio Frequency Identification (RFID) systems, ripeness indicators. RFID tag with variety of sensors used to identify the freshness of meat, packaged milk etc. In future software play a crucial role in sensors by analyzing process data, detecting events that need intervention, optimizing their processes and gathering insights about the factory processes. This paper gives an overview of various types of sensors used in food industry and food packaging and scope of future in the field.

Keywords: sensor; food processing; intelligent package; RFID; software



EXPERIMENTAL AND EFFICIENT USAGE OF DATA MINING PRIMITIVES

Sr . Assist. Prof. Dr. G. Lalitha KUMARI

Department of Computer Science and Engineering, PVP Siddhartha Institute of Institute of Technology, Vijayawada, India

Assoc. Professor, K. Koteswara RAO

Department of Computer Science and Engineering, PVP Siddhartha Institute of Institute of Technology, Vijayawada, India

Assist. Prof. Dr. Mrs. Y. SUREKHA

B.Tech, Department of Computer Science and Engineering, PVPSIT

Ms. B. Chaitanya SREYA

B.Tech, Department of Computer Science and Engineering, PVPSIT

Kolli Pooja SRI

Department of Computer Science and Engineering, PVP Siddhartha Institute of Institute of Technology, Vijayawada, India

Assist. Prof. Dr. Mr. N. Ramesh BABU

RGKUT, Srikakulam, Andhra Pradesh, INDIA

ABSTRACT

In today's world of computing software is experiencing the renaissance. In this software renaissance World computerized record keeping system plays a crucial role. In traditional systems sometimes there is a chance to acquire irrelevant data, which leads to the concept called Data Mining where all the users can get the necessary, useful and relevant data. This paper mainly encompasses what defines data mining tasks various types of knowledge to be mined, how the data is relevant to the task, how data can be mined and other concept hierarchies which can conclude as overview of Data Mining primitives .



EFFICIENT MONITORING OF THE PROJECTS THROUGH THE PERT AND MILESTONES

Assist. Prof. Dr. Mr. N. Ramesh BABU
RGKUT, Srikakulam, Andhra Pradesh, INDIA

Assist. Prof. Dr. Mrs. Y. SUREKHA
B.Tech, Department of Computer Science and Engineering, PVPSIT

Assoc. Professor, K. Koteswara RAO
Department of Computer Science and Engineering, PVP Siddhartha Institute of Institute of Technology, Vijayawada, India

Sr . Assist. Prof. Dr. G. Lalitha KUMARI
Department of Computer Science and Engineering, PVP Siddhartha Institute of Institute of Technology, Vijayawada, India

Mr. G. Bhargav RAMUDU
B.Tech, Department of Computer Science and Engineering, PVPSIT

Monika Sai PINNINTI
Department of Computer Science and Engineering, PVP Siddhartha Institute of Institute of Technology, Vijayawada, India

ABSTRACT

This paper concentrates on monitoring projects through the PERT and MILESTONES using soft computing techniques. Complex, multilayered and distributed projects require a series of activities, some of which must be preferred sequentially and others parallelly. This collection of series and parallel tasks can be modeled as a network. PERT is statistical technique applied to such a networks. In this paper we attempted to simulate the PERT networks and graphically represented the tasks along with their inter dependencies. Here project identifies the critical and non-critical tasks and evaluates the critical path to determine which tasks have an impact on the schedule.

Once a project has advanced to the phase of performance, the focus shifts from the discovery to tracking and reviewing it. MILESTONES are used to track the progress of the project at different stages and the PERT chart, on continual basis. This paper integrated both these techniques for an efficient and easier monitoring. In order to reap the results of the project sooner, we gave a provision to reduce the scheduled completion time with minimum cost burden. This can be achieved by assigning more labor and resources to the various activities.



INFLUENCE of OXYGEN PRESSURE on OPTICAL PROPERTIES of RF MAGNETRON SPUTTERING Ga₂O₃ THIN FILMS

Hicret HOPOĞLU

Sivas Cumhuriyet University, Faculty of Technology, Department of Optical Engineering
ORCID ID: 0000-0003-4797-0840

Hafize Seda AYDINOĞLU

Sivas Cumhuriyet University, Department of Medical Services and Techniques, Program of Opticianry, Vocational School of
Healthcare
ORCID ID: 0000-0003-0416-8276

Ebru Şenadım TÜZEMEN

Sivas Cumhuriyet University, Nanophotonics Research and Application Center
Sivas Cumhuriyet University, Department of Physics, Faculty of Science
ORCID ID: 0000-0001-9166-7422

ABSTRACT

In recent years, a great deal of research has been carried out on the development of oxide semiconductor devices for practical applications in various industries, and the promising advantages of wide energy band gap semiconductor oxides have attracted attention. Gallium is an element in group 3A of the periodic table. It has many important compounds such as GaAs, GaN, InGaN. These compounds are semiconductors. Due to their electronic and optical properties, they are used in many fields and are the subject of many researches. GaN and InGaN can be used in areas such as light emitting diodes. Another important compound of gallium is gallium oxide (Ga₂O₃). Gallium oxide is a semiconductor material with high chemical and thermal stability, wide band gap (~4.9 eV). It is used in many fields depending on its optical, physical and chemical properties, especially as a sensing material in luminescent materials and gas sensors. Gallium oxide is a material with 5 different crystal structures: α , β , γ , δ and ϵ . In these phases, α and β phases can be obtained as stable. The β phase is the most thermally and chemically stable phase among all structures. In addition, the β phase has an energy band gap of 4.7-4.9 eV. Because of these properties, studies on gallium oxide have focused on the β phase. In this study, Ga₂O₃ semiconductor films were produced on sapphire substrate using the RF magnetron sputtering technique. The films were produced at 60 W power and at 0, 2% and 4% oxygen. The thickness of the films was 200 nm and the rate was 0.7 Å/s. Then the films were annealed at 900 degrees in air. Finally, the optical properties of the produced thin films were investigated and the energy band gaps were calculated.

Keywords: Ga₂O₃, magnetron sputtering, optical properties



OPTICAL PROPERTIES OF NiO_x THIN FILMS PRODUCED BY MAGNETRON SPUTTERING AT DIFFERENT PRESSURES

Hicret HOPOĞLU

Sivas Cumhuriyet University, Faculty of Technology, Department of Optical Engineering
ORCID ID: 0000-0003-4797-0840

Ebru Şenadım TÜZEMEN

Sivas Cumhuriyet University, Nanophotonics Research and Application Center
Sivas Cumhuriyet University, Department of Physics, Faculty of Science
ORCID ID: 0000-0001-9166-7422

ABSTRACT

Metal oxide gas sensors have recently attracted much attention due to their higher sensitivity, fast response and recovery times, low power consumption and low production costs. One of the metal oxide materials obtained from the metal with these properties is nickel, which is a ferromagnetic transition metal. Nickel is oxidized to a chemically stable nickel oxide (NiO), which has a cubic rock salt type structure, intrinsic p-type semiconductor behavior. Nickel is an easily available material and is abundant in the world. This metal also has good conductivity only after metals such as Cu, Au, Ag and Pt. The very good adhesion of nickel to the glass results in a very uniform surface of the grown thin films. Nickel oxide (NiO_x), a p-type oxide semiconductor, has attracted great attention due to its versatile and tunable properties. It is one of the critical materials in a wide variety of electronics applications. Due to its wide energy band gap (NiO or Ni(II) oxide has high resistivity, a wide energy band gap of 3.6 – 4.0 eV), NiO_x is widely used in studies in optoelectronics and p-n heterojunctions. The properties of NiO_x thin films are highly dependent on the deposition method and conditions. In this study, NiO_x thin films were deposited on glass substrate using a NiO target with a purity of 99.999% and a thickness of 0.250 inches by magnetron sputtering method at different RF pressure. The transmittance and energy band gap of the films were investigated.

Keywords: NiO_x, magnetron sputtering, optical properties This research was supported by Scientific Research Project Fund of Sivas Cumhuriyet University under the project number F-2021-640.



INVESTIGATION OF THE STATISTICAL RELATIONSHIP BETWEEN POROSITY, SCHMIDT HARDNESS AND WATER ABSORPTION RATES IN VOLCANIC ROCKS USING SPSS PROGRAM

Gökhan KÜLEKÇİ

Gumushane University, Faculty of Engineering and Natural Sciences, Department of Mining Engineering
ORCID ID: 0000-0002-2971-4045

ABSTRACT

Volcanic rocks, also called igneous rocks, are formed by the solidification of magma under the earth's crust at different depths. Volcanic rocks are divided into 3 groups as surface (volcanic), semi-deep (vein) and depth (plutonic) rocks according to the depth at which they solidify. These rocks make up about 65% of the earth's crust. This rock structure, which forms more than half of the earth's crust, is used in many basic areas from the marble sector to the aggregate sector. In determining the usage areas of volcanic rocks, primarily physical properties should be determined. In field studies, values such as Schmidt hardness value, porosity and water absorption rate are often used to identify the rock and measure its physical properties. Intense experimental processes and long field studies are required to determine these values.

The branch of science that examines whether the collected data has a significant effect on each other and produces solutions is called statistical science. SPSS is one of the programs used in this science. The SPSS program is an application that establishes a statistical relationship between dependent or independent data and reveals whether this relationship is significant or not.

In this study, experimental values on volcanic rocks were used. It was investigated whether there is a statistical relationship between the experimentally determined schmidt hardness value, porosity and water absorption rates in previous studies. T-tests were performed using the numerical values obtained in the study using the SPSS program, and the statistical relationship of these values, which were found experimentally before, was examined.

Keywords: Statistical relationship, Porosity, Schmidt Hardness, SPSS Program, Water Absorption Rate, Volcanic rocks,

SPSS PROGRAMI KULLANILARAK, VOLKANİK KAYAÇLARDA POROZİTE, SCHMIDT SERTLİK DERECELERİ VE SU EMME ORANLARI ARASINDAKİ İSTATİKSEL İLİŞKİNİN İNCELENMESİ

ÖZET

Magmatik kayaç olarak da adlandırılan volkanik kayaçlar, yer kabuğunun altında bulunan magmanın farklı derinliklerde katılaşması ile oluşurlar. Volkanik kayaçlar katılaştıkları derinliklere göre yüzey (volkanik), yarı derinlik (damar) ve derinlik (Plütonik) kayaçları diye 3 gruba ayrılırlar. Bu kayaçlar yer kabuğunun yaklaşık %65'ni oluştururlar. Yer kabuğunun yarısından fazlasını oluşturan bu kayaç yapısı, mermer sektöründen agrega sektörüne kadar birçok temel alanda kullanılır. Volkanik kayaçların kullanım alanlarının belirlenmesinde öncelikli olarak fiziksel özellikler saptanması gerekmektedir. Saha çalışmalarında, kayacın tanınması ve fiziksel özelliklerin ölçülmesi için sıklıkla Schmidt sertlik değeri, içsel boşluk (porozite) ve su emme oranı gibi değerler kullanılmaktadır. Bu değerlerin saptanması için yoğun deney süreçleri ve uzun saha çalışmaları gerekmektedir. Toplanan verilerin birbiri üzerinde anlamlı bir etkisinin olup olmadığını inceleyen ve çözüm üreten bilim dalına istatistik bilimi denir. SPSS bu bilim de kullanılan programlardan biridir. SPSS programı bağımlı ya da bağımsız veriler arasında istatistiksel ilişki kurmaya ve bu ilişkinin anlamlı olup olmadığını ortaya koyan bir uygulamadır.

Yapılan bu çalışmada, volkanik kayaçlar üzerinde deneysel olarak ortaya konmuş değerler kullanılmıştır. Önceki çalışmalarda deneysel olarak saptanan schmidt sertlik değeri, porozite ve su emme oranları arasında istatistiksel bir bağ olup olmadığı incelenmiştir. Çalışmada elde edilmiş sayısal değerler SPSS programı kullanılarak T-testi yapılmış ve önceden deneysel olarak bulunan bu değerlerin istatistiksel olarak ilişkisi incelenmiştir.

Anahtar kelimeler: İstatistiksel ilişki, Porozite, Schmidt Sertlik, SPSS Programı, Su Emme Oranı, Volkanik kayaçlar,

1. INFORMATION

Volcanic rocks have been used by humans for thousands of years due to their formation process and durability. Volcanics have been used by people in various parts of buildings and for architectural decorative purposes. Generally, the usage areas are outdoors; It is used as wall covering and flooring material, as stair step, paving slab, cobblestone, curb stone, and as flooring and covering material indoors, in bathroom and kitchen applications (Karsli *vd.*, 2013; Külekçi ve Yılmaz, 2016, 2017). The main function of using natural stones as exterior wall cladding is to protect the building from external environmental factors, especially rain, rather than creating the external appearance of the building. For this reason, it is very important that the natural stones to be used as exterior cladding comply with the standards (Külekçi ve Yılmaz, 2016; Külekçi ve Yılmaz, 2017a;

Gökhan Külekçi, 2019). It is necessary to know the resistance of the rocks used in many sectors against chemical and mechanical degradation. Weathering is the process of breaking down rock and soil materials by chemical weathering or physical disintegration of surfaces where rocks interact with climatic changes (Külekçi ve Yılmaz, 2017b; Aliyazicioğlu ve Külekçi, 2018; Külekçi ve Yılmaz, 2018; G. Külekçi, 2019). The fragmentation process depends on the external environmental factors triggered by the geographical structure of the rock (climate, plant growth, etc.) and the rock material and rock mass properties. The resistance of formations to weathering and rock fragmentation determines the mineralogical structure of the rock, its water absorption rate, grain size and porosity (Kahraman, Fener ve Gunaydin, 2016). Volcanic rocks are used in many fields. especially in mining and underground filling (Külekçi 2018, Külekçi vd. 2016, Külekçi 2021).

Meteoric waters, which are a very effective element in the deterioration of the rock under the influence of the atmosphere, can cause weathering in the cavities of the rock (cracks and intergranular spaces) due to seasonal effects due to freezing and thawing, as well as wetting the rock surface due to precipitation, the penetration of water into the rock and the kneading of these surfaces by the effect of the wind. Therefore, it causes the physicomaterial properties of the rock to change with the effect of water. There are many different studies on the weathering of rocks in the literature. The susceptibility of rocks to degradability is determined by stability parameters such as the dispersion stability index (SDI). Although SDI is particularly used in cementitious or weak rocks, there are application examples for all types of rocks.

In this study, it was investigated whether there is a statistical relationship between the Schmidt hardness value, porosity and water absorption rates, which were determined experimentally in previous studies on volcanic rocks. The numerical values obtained in the study were T-tested using the SPSS program and the statistical relationship of these previously experimental values was examined.

1.1. Working Area

The Eastern Black Sea region is a region where Cretaceous and Tertiary magmatism is most common. However, despite this intense magmatism, very well-preserved Jurassic-Tertiary aged sedimentary successions crop out in the region. The Akçaabat-Düzköy (SW Trabzon) region attracts attention with the presence of successions that characterize all Pontides from the Jurassic to the end of the Tertiary. In addition, this region is among the places where Jurassic-Lower Cretaceous aged successions can be observed geographically in the Eastern Pontides. (Yılmaz ve Korkmaz, 1999; Vural, 2018; Külekçi ve Vural, 2021; Vural ve Kaygusuz, 2021, Vural ve Külekçi, 2021)(**Figure 1.1**).



Figure 1.1 Geological map of the study area

The study area is the volcanic rocks located in the Center of Gümüşhane Province in the Eastern Black Sea Region of Turkey.

2. RESEARCH AND FINDINGS

In order to determine the usability of Gümüşhane Granite as marble and to what extent it can be used, samples from magmatic granites were taken from 7 different points in the center of Gümüşhane province. These samples were brought to Karadeniz Technical University Mining Engineering laboratory to conduct experimental studies. Here, the core samples extracted from the rock blocks using a laboratory type drilling machine and the cubic samples cut from the rock blocks with a stone cutting machine were prepared in accordance with the standards.

2.1. Apparent porosity test

It was observed that the average porosity of Gümüşhane Granites was 2.11%. Findings When the classification of the rocks according to the porosity according to the Tarhan (1989) classification is examined, it is seen that the granites are in the "small void" rock class with 2.11% (Table 2.1).

Table 2.1. Rock classification table (Tarhan 1989).

Rock grade	Porosity %
Very Compact	<1
Less Space	1-2,5
Mid-Space	2,5-5
Pretty Spaced	5-10
Multi-Cavity	10-15
Too Much Space	>20

As can be seen from the analysis, the mean porosity and standard deviation of the samples in the study were

found to be 2.11 and 0.21. As a result of the applied one sample t-test, Sig. (2-tailed) value was found to be 0.66. Since $p > 0.05$, statistically, the prosies of the sample samples are considered to have few voids.

Table 2.2. Porosity t-test tables

One-Sample Statistics						
	N	Mean	Std. Deviation	Std. Error		
Mean						
Prosity	7	2,1086	,55264	,20888		

One-Sample Test						
Test Value = 2						
	t	df	Sig. (2-tailed)	Mean Difference	95% Confidence Interval of the Difference	
					Lower	Upper
Prosity	,520	6	,622	,10857	-,4025	,6197

2.2. Water absorption rate

According to TS 2513, the weight water absorption rate of natural building blocks should not be greater than 1.8%. When the statistical analysis of the obtained results was made, the average water absorption rate of the samples was found to be 0.80 and the standard deviation was 0.01. As a result of the applied single sample t-test, Sig. (2-tailed) value was found to be 0.00. Since $p < 0.01$, it can be said that the water absorption rates of the samples are statistically in accordance with the standard.

Table 2.3. Water absorption rates (Küleççi ve Yılmaz, 2017b)

	<i>Water abs. %</i>
<i>1</i>	0.55
<i>2</i>	0.85
<i>3</i>	1.10
<i>4</i>	1.15
<i>5</i>	0.56
<i>6</i>	0.84
<i>7</i>	0.54
<i>Mean</i>	0.80±0,01

Table 2.4. Water absorption t-test tables

One-Sample Statistics						
	N	Mean	Std. Deviation	Std. Error Mean		
Water abd.	7	,7986	,25958	,09811		

One-Sample Test						
	Test Value = 1.8					
	t	df	Sig. (2-tailed)	Mean Difference	95% Confidence Interval of the Difference	
					Lower	Upper
Water abd.	-10,207	6	,000	-1,00143	-1,2415	-,7614

2.3. Schmidt hammer test results

The average hardness and standard deviation of the samples were found to be 53 and 2.86 according to the rock measurements. As a result of the applied single sample t-test, Sig. (2-tailed) value was found to be 0.511. Since $p > 0.05$, it has been shown that the hardness of the specimens is close to 55 statistically and can be included in this class. With these results, it can be said that the Gümüşhane volcanics are quite hard.

Table 2.5. Rock hardness classification according to Schmidt hammer rebound number (Küleççi ve Yılmaz, 2017b).

Rock grade	Schmidt Hammer recoil number	Average number of rebounds of Gumushane Volcanite
Soft	0-10	
Little soft	10-20	
Less harsh	20-40	
Hard	40-50	
Pretty tough	50-60	53±2,9
Too hard	>60	

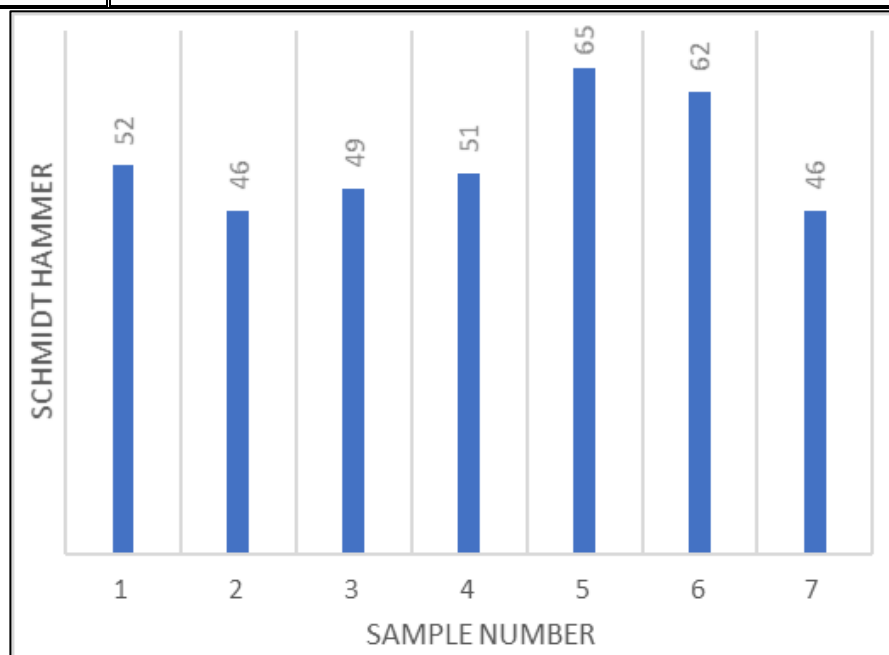


Figure 2.1. Schmidt Hammer recoil number

Table 2.6. Schmidt Hammer t-test tables

One-Sample Statistics						
	N	Mean	Std. Deviation	Std. Error Mean		
Schmidt Hammer	7	53,0000	7,57188	2,86190		

One-Sample Test						
Test Value = 55						
	t	df	Sig. (2-tailed)	Mean Difference	95% Confidence Interval of the Difference	
					Lower	Upper
Schmidt Hammer	-,699	6	,511	-2,00000	-9,0028	5,0028

3. RESULTS

In the study, the physical properties of the "Gümüşhane volcanics" were examined. Samples were taken from the field, some parameters of the physical properties were determined, and statistical evaluation of them was made.

In the study, it is seen that the volcanics are in the "little void" rock class with 2.11%.

In addition, it has been shown that volcanics provide statistically the condition of "water absorption rate of natural building stones should not be greater than 1.8% according to TS 2513". The water absorption rate of the samples was found to be 0.80%.

It was determined that the hardness of the specimens used in the study was close to 55 and could be included in this class. With these results, it can be said that the Gümüşhane volcanics are quite hard.

REFERENCES

- Aliyazicioğlu, Ş. ve Külekçi, G. (2018). Investigation of usability of limestone and basalt type rocks as road infrastructure filling, Trabzon Çatak case, *II. Cappadocian geosciences symposium 24-26*, ss. 207–211.
- Kahraman, S., Fener, M. ve Gunaydin, O. (2016). "Estimating the uniaxial compressive strength of pyroclastic rocks from the slake durability index", *Bulletin of Engineering Geology and Environment*. doi: 10.1007/s10064-016 0893-3.
- Karsli, O. vd. (2013) "Geochemical modelling of early Eocene adakitic magmatism in the Eastern Pontides, NE Anatolia: continental crust or subducted oceanic slab origin?", *International Geology Review*, 55(16), ss. 2083–2095. doi: Doi 10.1080/01431161.2013.819958.
- Külekçi, G. (2021). Comparison of Field and Laboratory Result of Fiber Reinforced Shotcrete Application, *Periodica Polytechnica Civil Engineering*, 65(2), ss. 463–473. doi: 10.3311/PPci.17033.
- Külekçi, Gökhan (2019). Slake durability of the volcanites of Artvin region, *4. International conference on Civil and Environmental Geology and Mining Engineering*, ss. 1132–1139.
- Külekçi, G. (2019). The distribution of water in Artvin region volcanites, *ICOCEM 2019*. Giresun, Turkey.
- Külekçi, G. ve Vural, A. (2021). Determination of excavatorability in a quarry and comparison with the applied method, *International Halich Congress*. İstanbul, Türkiye, ss. 299–307.
- Külekçi, G. ve Yilmaz, A. O. (2017a). Investigation of Trabzon volcanilities usable as external covering, *MSU journal of science*, 5(2), ss. 459–464.
- Külekçi, G. ve Yilmaz, A. O. (2017b). The investigation of some physical properties of granitoids: case study from Gümüşhane, Turkey, *IMCET2017*, ss. 175–181.

- Külekçi, G. ve Yılmaz, A. O. (2016). The Investigation of Usage of Trabzon (Düzköy) Region Volcanites as Filling Material for Roads, *8th International Aggregates Symposium*, ss. 13–14.
- Külekçi, G., Erçikdi, B. ve Aliyazicioğlu, Ş. (2016). Effect of Waste Brick as Mineral Admixture on the Mechanical Performance of Cemented Paste Backfill, *IOP Conference Series: Earth and Environmental Science*, 44(4), s. 042039. doi: 10.1088/1755-1315/44/4/042039.
- Külekçi, G. (2018). *Investigation of the utilization areas of construction and demolition wastes in the Black Sea region instead of aggregate and their areas of usage in the mining industry*. Karadeniz Technical universty.
- Külekçi, G. ve Yılmaz, A. O. (2018). Roadway tunnel construction with drilling-blasting method; Gümüşhane environment road example, *International Journal on Mathematic, Engineering and Natural Sciences*, 4, ss. 34–39.
- Tarhan, F., (1989). Mühendislik Jeolojisi Prensipleri, K.T.Ü. Basımevi, Trabzon.
- Vural, A. (2018) “Evaluation of soil geochemistry data of Canca Area (Gümüşhane, Turkey) by means of Inverse Distance Weighting (IDW) and Kriging methods-preliminary findings”, *Bulletin Of The Mineral Research and Exploration*, 158, ss. 10–20. doi: 10.19111/bulletinofmre.430531.
- Vural, A. ve Kaygusuz, A. (2021) Geochronology, petrogenesis and tectonic importance of Eocene I-type magmatism in the Eastern Pontides, NE Turkey, *Arabian Journal of Geosciences*, 14(6), s. 467. doi: 10.1007/s12517-021-06884-z.
- Vural, A. ve Külekçi, G. (2021). Bahçecik (Gümüşhane) ve Yakın Civarı Zenginleştirilmiş Jeoturizm Güzergahı, *UMTEB 11. Uluslararası Mesleki ve Teknik Bilimler Kongresi*. Ankara, Türkiye, ss. 251–268.
- Yılmaz, C. ve Korkmaz, S. (1999) “Basin development in the eastern Pontides, Jurassic to Cretaceous, NE Turkey”, *Zentralblatt für Geologie und Paläontologie*, 1, ss. 1485–1494.

THE STATISTICAL RELATIONSHIP OF CURE TIME AND COMPRESSIVE STRENGTH IN PASTE BACKFILLING

Gökhan KÜLEKÇİ

Gumushane University, Faculty of Engineering and Natural Sciences, Department of Mining Engineering
ORCID ID: 0000-0002-2971-4045

ABSTRACT

In the developing world conditions, protecting the environment has become one of the biggest goals. The wastes generated as a result of mining operations pose numerous economic, environmental and ecological problems. Safe storage of mine wastes is very important in order to eliminate these problems. For this reason, the most preferred storage method in mining enterprises recently is the cement paste filling method. The homogeneous filling material, which is formed as a result of mixing the plant waste after the mining production by adding water and cement in certain proportions in the paste filling plant, and which serves to fill the underground cavities, is called paste filling.

The branch of science that examines whether the collected data has a significant effect on each other and produces solutions is called statistical science. SPSS is one of the programs used in this science. The SPSS program is an application that establishes a statistical relationship between dependent or independent data and reveals whether this relationship is significant or not.

In this study, the statistical accuracy of the strength results depending on the curing time experimentally found in the laboratory environment will be tested. T-test and one-way manova test were performed using the SPSS program to the results of the curing time and the increase in compressive strength as the curing time progressed, which were found in previous studies, and the statistical relationship of these previously experimental values was investigated.

Keywords: Compressive strength, Statistical relationship, Paste backfill, SPSS Program,

MACUN DOLGUDA KÜR SÜRESİ İLE BASINÇ DAYANIMININ İSTATİKSEL İLİŞKİSİ

ÖZET

Gelişen dünya şartlarında çevrenin korunması en büyük hedeflerden biri haline gelmiştir. Madencilik işlemleri sonucu ortaya çıkan atıklar ekonomik, çevresel ve ekolojik olarak sayısız problem oluşturmaktadır. Bu problemlerin giderilmesi açısından maden atıklarının güvenli bir şekilde depolanması çok önemlidir. Bu nedenle maden işletmelerinde son zamanlarda en fazla tercih edilen depolama yöntemi çimentolu macun dolgu yöntemidir. Maden üretimi sonrasında tesis atığının, macun dolgu tesisinde belirli oranlarda su ve çimento eklenerek karıştırılması sonucu oluşan ve yeraltı boşluklarını doldurmaya yarayan homojen dolgu malzemesine

macun dolgu adı verilir.

Toplanan verilerin birbiri üzerinde anlamlı bir etkisinin olup olmadığını inceleyen ve çözüm üreten bilim dalına istatistik bilimi denir. SPSS bu bilim de kullanılan programlardan biridir. SPSS programı bağımlı ya da bağımsız veriler arasında istatistiksel ilişki kurmaya ve bu ilişkinin anlamlı olup olmadığını ortaya koyan bir uygulamadır.

Yapılan bu çalışmada, laboratuvar ortamında deneysel olarak bulunan kür süresine bağlı dayanım sonuçlarının istatistiksel olarak doğruluğu test edilecektir. Daha önceki çalışmalarda bulunan kür süresi ve kür süresi geçtikçe basınç dayanımında oluşan artış sonuçlarına SPSS programı kullanılarak T-testi ve tek yönlü manova testi yapılmış ve önceden deneysel olarak bulunan bu değerlerin istatistiksel olarak ilişkisi incelenmiştir.

Anahtar kelimeler: Basınç dayanımı, İstatistiksel ilişki, Macun dolgu, SPSS Programı,

1. INFORMATION

Filling the cavities formed as a result of ore production in underground mines, using a suitable filling material, for the purpose of fortification and/or storage of wastes is called filling. The filling process is the process of placing the worthless part extracted from the mine and/or the aggregate of different sizes brought from outside to fill the voids formed after production, using cement as a binder or without binder. The use of binder, the type/ratio of binder, the type of filling material/grain size range, the conditions for placing the filling and the resulting void structure are the main parameters affecting the filling strength (Yılmaz vd., 2014; Külekçi ve Çullu, 2019, 2021).



Figure 1.1. Cemented/non-cemented rock fill, Cemented Paste Backfill, Hydraulic fill

According to the results of the particle size distribution analysis performed on the waste material with Malvern Mastersizer, the amount of material below 20 μm was determined as 58.42% for dam waste (Ercikdi, Külekçi ve Yılmaz, 2015; Külekçi ve Aliyazicioğlu, 2018).

In this study, the effect of ground marble waste on the short and long term mechanical performance of sulfide paste filler and the statistical quality of this effect were evaluated.

2. RESEARCH AND FINDINGS

2.1. Experimental Studies

In this study, copper mine facility waste, cement and marble waste were used (Figure 2.1).

5-9% Portland cement is used as the binder in the putty filling, depending on the solid ratio and the underground production conditions. The binder used constitutes 42% of the putty filling operating costs (for 2008) (Külekçi, Ercikdi ve Yılmaz, 2016; Külekçi, Çullu ve Yılmaz, 2018; G. Külekçi, 2021).

According to the results of the particle size distribution analysis performed on the waste material with Malvern Mastersizer, the amount of material below 20 μm was determined as 58.42% for dam waste.

Marble is formed as a result of metamorphism or recrystallization of rocks, the main component of which is calcium carbonate, under heat and pressure, containing at least 95% calcium carbonate (CaCO_3) in its composition, usually with a density of 2550-2800 kg / m^3 , due to the secondary minerals in it. It is called a rock that can be in various colors and can be cut and polished (Külekçi, Ercikdi ve Yılmaz, 2016; Külekçi, Çullu ve Yılmaz, 2018; Gökhan Külekçi, 2021).



Figure 2.1. Materials used in the study (facility waste,cement/ binder, marble waste)(Külekçi, 2013)

In order to see the contribution of the marble waste to the strength, a total of 90 samples, 72 samples and 18 control samples containing only binder, were prepared by adding 10-30% to the standard binder. Each of these samples was subjected to uniaxial compressive strength test (Figure 2.2.).



Figure 2.2. Sample casting, curing processes and compressive strength in paste backfilling (Külekçi, 2013)

2.2. Findings and Discussion

Compressive strength tests were carried out on the prepared paste filler samples at the end of 7-14-28-56-90 and 180 days. It was observed that the strengths increased graphically (Figure 2.3).

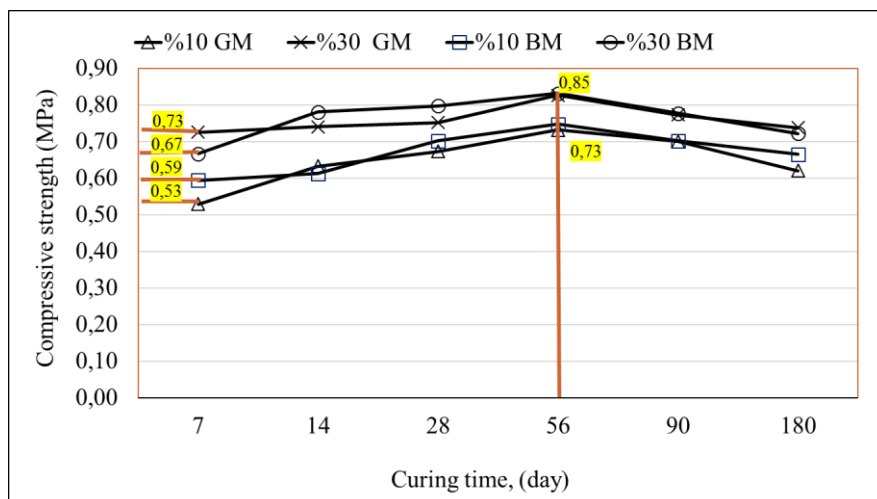


Figure 2.3. Compressive strengths depending on curing time (Külekçi, 2013)

Table 2.1. Compressive strengths on the 7th, 28th and 180th days

Kür süresi/ Curing time, Gün/Day	7. gün	28. gün	180. gün
	0,5	0,68	0,57
Dayanım/ Strength, (MPa)	0,56	0,59	0,67
	0,46	0,73	0,65
	0,48	0,64	0,63
	0,63	0,67	0,6

Strength tests were carried out on the cement paste samples. The results show that the strength increases depending on the curing time. To confirm this increase statistically, paired samples t-tests were performed on 5 different samples that were broken for each cure time (Table 2.1).

2.3. Examination of 7th and 28th day strengths

Looking at the strength table, there is a statistical difference between the average strength at the end of the 7th day and the strength at the end of 28 days. And this difference is in the direction of increase (table 2.2-3).

Table 2.2. The paired samples t-test relationship of the curing times on the 7th and 28th days.

Paired Samples Statistics					
Pair 1	Mean	N	Std. Deviation	Std. Error Mean	
	Kür7	,5260	5	,06914	,03092
	Kür28	,6620	5	,05167	,02311

Paired Samples Test						
Pair 1	Paired Differences Mean	Std. Deviation	t	df	Sig. (2-tailed)	
					95% Confidence Interval of the Difference Lower	Upper
	Kür7 - Kür28	-,13600	,10114	4	,04523	-,26159
						-,01041

Table 2.3. Average strength increase of the 7th and 28th days

Curing time, Day	7.	28.
Strength, (MPa)	0.53 ±0,031	0,66 ±0,023*
*p<0,05		

When the increase on the 7th and 180th days was compared statistically, the mean strength at the end of 180 days was found to be 0.62±0.018 MPa. There was no statistical difference between the strengths on the 7th and 180th days (p>0.05).

Table 2.4. The paired samples t-test relationship of the curing times on the 7th and 180th days.

Paired Samples Correlations									
		N		Correlation		Sig.			
Pair 1	Kür7 & Kür180	5		-,138		,825			

Paired Samples Statistics					
		Mean	N	Std. Deviation	Std. Error Mean
Pair 1	Kür7	,5260	5	,06914	,03092
	Kür180	,6240	5	,03975	,01778

Paired Samples Test									
		Paired Differences					t	df	Sig. (2-tailed)
		Mean	Std. Deviation	Std. Error Mean	95% Confidence Interval of the Difference				
					Lower	Upper			
Pair 1	Kür7 - Kür180	-,09800	,08438	,03774	-,20277	,00677	-2,597	4	,060

3. RESULTS

As a result of the study,

- The compressive strength of the cement paste filling samples increased from the first day and reached the maximum level at the end of 56 days.
- At the end of 56 days, there was a serious decrease in strength,
- It is possible that the strength increases at the end of 7 and 28 days are statistically significant, but since the correlation number is very low, these values may be a coincidence, and there may not be an increase in strength in all paste filling samples.
- As a result of the statistical analysis between 7 days and 180 days, it was revealed that the increase was not real.

REFERENCES

- Ercikdi, B., Külekçi, G. ve Yılmaz, T. (2015). Utilization of granulated marble wastes and waste bricks as mineral admixture in cemented paste backfill of sulphide-rich tailings, *Construction and Building Materials*, 93, ss. 573–583. doi: 10.1016/j.conbuildmat.2015.06.042.
- Külekçi, G. (2013). *Investigation of the utility of the waste brick and marble powders on the paste backfill*. Karadeniz Technical University.
- Külekçi, Gökhan (2021). The Effect of Pozzolans and Mineral Wastes on Alkali-silica Reaction in Recycled Aggregated Mortar, *Periodica Polytechnica Civil Engineering*, 65(3), ss. 741–750. doi: 10.3311/PPci.17355.
- Külekçi, G. ve Aliyazicioğlu, Ş. (2018). Comparison of backfill methods in underground mining, *International refereed & indexed journal on mathematic, engineering and natural sciences*, 5, ss. 76–82.
- Külekçi, G. ve Çullu, M. (2019). The Effect of Polypropylene Fibers , Used in Different Proportions , on Paste Filling, *3. International*



Conference on Advanced Engineering Technologies, ss. 313–320.

- Külekçi, G. ve Çullu, M. (2021). The Investigation of Mechanical Properties of Polypropylene Fiber-Reinforced Composites Produced With the Use of Alternative Wastes, *Journal of Polytechnic*. doi: 10.2339/politeknik.777832.
- Külekçi, G., Çullu, M. ve Yılmaz, A. O. (2018). Environmental problems to be created in mining procedures and measures to be taken; quarry an example of dust emissions, *EurAsia waste management symposium*, ss. 319–327.
- Külekçi, G., Ercikdi, B. ve Yılmaz, T. (2016). Effect of Marble Wastes on Paste Backfill Strength”, *International Black Sea Mining & Tunnelling Symposium*, ss. 297–304.
- Yılmaz, T. vd. (2014). Effect of sample size on the strength and ultrasonic properties of paste backfill included mineral admixture, *XIth Regional Rock Mechanics Symposium*, ss. 193–203.

ON THE TRIVIALITY OF IWASAWA MODULE OF THE CYCLOTOMIC \mathbb{Z}_2 -EXTENSIONS OF CERTAIN REAL BIQUADRATIC

ABDELKADER EL MAHI

ACSA Laboratory, Department of Mathematics, Faculty of Sciences, Mohammed
First University, Oujda, Morocco.

Email address: elmahi.abdelkader@yahoo.fr

M'HAMMED ZIANE

ACSA Laboratory, Department of Mathematics, Faculty of Sciences, Mohammed
First University, Oujda, Morocco.

Email address: ziane12001@yahoo.fr

Abstract

Let p be a prime number and k a finite extension of the field \mathbb{Q} of rational numbers. The \mathbb{Z}_p -extension k_∞/k is an infinite Galois extension with the Galois group $\Gamma = \text{Gal}(k_\infty/k)$ topologically isomorphic to the additive group of the ring \mathbb{Z}_p of p -adic integers. Especially, for any prime number p and number field k , there exists a cyclotomic \mathbb{Z}_p -extension k_∞/k obtained by the compositum $k_\infty = k\mathbb{Q}_\infty$, where \mathbb{Q}_∞ is the cyclotomic \mathbb{Z}_p -extension k_∞/k which is contained in a field $k(\mu^\infty)$ constituted by all elements of k and the group μ^∞ of the p^{th} power roots of unity. For each positive integer n , there is unique cyclic extension k_n/k of degree p^n contained in k_∞ , which is called the n^{th} layer of k_∞/k . Thus, a \mathbb{Z}_p -extension can be regarded as a tower

$$k = k_0 \subset k_1 \subset k_2 \subset \dots \subset k_n \subset \dots \subset k_\infty.$$

Let $X = X(k_\infty) = \varprojlim A(k_n)$ be the projective limit of the p -Sylow subgroups $A(k_n)$ of ideal class groups of k_n with respect to the norm maps. By the natural action of Γ , X becomes a module over the completed group ring $\mathbb{Z}_p[[\Gamma]]$ and is called Iwasawa module of k_∞/k [2]. Let λ , μ and ν be the Iwasawa invariants, then the order $|A(k_n)|$ of $A(k_n)$ satisfies.

Iwasawa's class number formula. $|A(k_n)| = p^{\lambda n + \mu p^n + \nu}$.

Let L be the maximal unramified abelian p -extension of k and similarly $L(k_n)$ be the maximal unramified abelian p -extension of k_n . We denote by $L(k_\infty)$ the maximal unramified abelian pro- p -extension of k_∞ . The Galois group $X_\infty = \text{Gal}(L(k_\infty)/k_\infty)$ is isomorphic to the inverse limit of the Galois groups $\text{Gal}(L(k_n)/k_n)$ with respect to the restriction maps. By the class field theory we have

$$X_\infty = \text{Gal}(L(k_\infty)/k_\infty) \simeq \varprojlim A(k_n).$$

For each positive integer n , let $\zeta_{2^{n+2}}$, a primitive 2^{n+2} -th roots of unity in the complex number field. Then the n^{th} layer \mathbb{Q}_n of the cyclotomic \mathbb{Z}_2 -extension $\mathbb{Q}_\infty/\mathbb{Q}$ is the field $\mathbb{Q}(\zeta_{2^{n+2}} + \zeta_{2^{n+2}}^{-1})$. Especially, the first layer \mathbb{Q}_1 is the real quadratic field $\mathbb{Q}(\sqrt{2})$. Therefore if $\sqrt{2} \notin k$, the first layer k_1 of the cyclotomic \mathbb{Z}_2 -extension of a number field k is $k_1 = k(\sqrt{2})$.

In this paper, we prove the existence of infinitely many real biquadratic fields k , with the Iwasawa λ , μ - and ν -invariants of the cyclotomic \mathbb{Z}_2 -extension of k are zeros. Our main theorem is the following.

Theorem 0.1. *Let p , q and s be distinct prime numbers with*

$$p \equiv q \equiv s \equiv 3 \pmod{8}$$

k one of the following biquadratic fields

2010 *Mathematics Subject Classification.* 11R23, 11R37, 11S25. *Key words and phrases.* Iwasawa theory, Class field theory, Class group, Units.

$$\mathbb{Q}(\sqrt{pq}, \sqrt{ps}), \quad \mathbb{Q}(\sqrt{2pq}, \sqrt{ps}) \quad \text{or} \quad \mathbb{Q}(\sqrt{pq}, \sqrt{2ps}).$$

Then the Iwasawa module X_∞ is trivial. Consequently $\lambda = \mu = \nu = 0$.

References

- [1] R. GREENBERG, *On the Iwasawa invariants of totally real number fields*, Amer.J. Math. 98 , 263284(1976).
- [2] L. C. WASHINGTON, *Introduction to Cyclotomic Fields*(2nd. Edition),Graduate Texts in Math. vol. 83, Springer (1997).



isarc
INTERNATIONAL SCIENCE AND ART RESEARCH CENTER
<https://www.isarcconference.org/>



ISBN: 978-625-8007-78-7